

VOLUME 36

JANUARY 1958

NUMBER 1

# Canadian Journal of Chemistry

*Editor:* LÉO MARION

*Associate Editors:*

- HERBERT C. BROWN, *Purdue University*  
A. R. GORDON, *University of Toronto*  
C. B. PURVES, *McGill University*  
Sir ERIC RIDEAL, *Imperial College, University of London*  
J. W. T. SPINKS, *University of Saskatchewan*  
E. W. R. STEACIE, *National Research Council of Canada*  
H. G. THODE, *McMaster University*  
A. E. VAN ARKEL, *University of Leiden*

*Published by THE NATIONAL RESEARCH COUNCIL*

OTTAWA

CANADA

# CANADIAN JOURNAL OF CHEMISTRY

(Formerly Section B, Canadian Journal of Research)

Under the authority of the Chairman of the Committee of the Privy Council on Scientific and Industrial Research, the National Research Council issues THE CANADIAN JOURNAL OF CHEMISTRY and five other journals devoted to the publication, in English or French, of the results of original scientific research. Matters of general policy concerning these journals are the responsibility of a joint Editorial Board consisting of: members representing the National Research Council of Canada; the Editors of the Journals; and members representing the Royal Society of Canada and four other scientific societies.

The Chemical Institute of Canada has chosen the Canadian Journal of Chemistry as its medium of publication for scientific papers.

## EDITORIAL BOARD

### Representatives of the National Research Council

R. B. Miller, *University of Alberta*  
H. G. Thode, *McMaster University*

D. L. Thomson, *McGill University*  
W. H. Watson (Chairman), *University of Toronto*

### Editors of the Journals

D. L. Bailey, *University of Toronto*  
T. W. M. Cameron, *Macdonald College*  
H. E. Duckworth, *McMaster University*

K. A. C. Elliott, *Montreal Neurological Institute*  
Léo Marion, *National Research Council*  
R. G. E. Murray, *University of Western Ontario*

### Representatives of Societies

D. L. Bailey, *University of Toronto*  
Royal Society of Canada  
T. W. M. Cameron, *Macdonald College*  
Royal Society of Canada  
H. E. Duckworth, *McMaster University*  
Royal Society of Canada  
Canadian Association of Physicists  
T. Thorvaldson, *University of Saskatchewan*, Royal Society of Canada

K. A. C. Elliott, *Montreal Neurological Institute*  
Canadian Physiological Society  
R. G. E. Murray, *University of Western Ontario*  
Canadian Society of Microbiologists  
H. G. Thode, *McMaster University*  
Chemical Institute of Canada

### Ex officio

Léo Marion (Editor-in-Chief), *National Research Council*  
J. B. Marshall (Administration and Awards), *National Research Council*

---

*Manuscripts* for publication should be submitted to Dr. Léo Marion, Editor-in-Chief, Canadian Journal of Chemistry, National Research Council, Ottawa 2, Canada.  
(For instructions on preparation of copy, see Notes to Contributors (inside back cover).)

*Proof, correspondence concerning proof, and orders for reprints* should be sent to the Manager, Editorial Office (Research Journals), Division of Administration and Awards, National Research Council, Ottawa 2, Canada.

*Subscriptions, renewals, requests for single or back numbers, and all remittances* should be sent to Division of Administration and Awards, National Research Council, Ottawa 2, Canada. Remittances should be made payable to the Receiver General of Canada, credit National Research Council.

The journals published, frequency of publication, and prices are:

Canadian Journal of Biochemistry and Physiology	Monthly	\$3.00 a year
Canadian Journal of Botany	Bi-monthly	\$4.00 a year
Canadian Journal of Chemistry	Monthly	\$5.00 a year
Canadian Journal of Microbiology	Bi-monthly	\$3.00 a year
Canadian Journal of Physics	Monthly	\$4.00 a year
Canadian Journal of Zoology	Bi-monthly	\$3.00 a year

The price of regular single numbers of all journals is 75 cents.

# Canadian Journal of Chemistry

*Issued by THE NATIONAL RESEARCH COUNCIL OF CANADA*

VOLUME 36

JANUARY 1958

NUMBER 1

## Symposium on The Structure and Reactivity of Electronically-Excited Species

### A REPORT ON A SYMPOSIUM HELD BY THE PHYSICAL CHEMISTRY DIVISION OF THE CHEMICAL INSTITUTE OF CANADA<sup>1</sup>

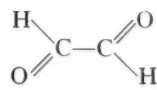
K. J. LAIDLER AND D. A. RAMSAY

A symposium on the structure and reactivity of electronically-excited species was held at the University of Ottawa under the auspices of the Physical Chemistry Division of the Chemical Institute of Canada on September 5th and 6th, 1957. A number of invited papers were presented, most of these having previously been printed in full and distributed to the participants in advance of the meeting. The sessions were devoted to brief presentations of these invited papers, to presentations of additional work, and to general discussions. A number of the invited papers are being published in the present issue of the Canadian Journal of Chemistry; in this paper we give a general account of the meeting, emphasizing the main matters that were discussed and the main conclusions that were drawn. The papers will be discussed under two main headings, the first dealing with the structures of electronically-excited species and the second with their reactivities.

#### THE STRUCTURES OF ELECTRONICALLY-EXCITED SPECIES

During recent years considerable efforts have been devoted to the detailed study of the electronic spectra of simple polyatomic molecules. The rapid development of the subject may be seen from the following chronological list of molecules, ions, and free radicals for which rotational and vibrational analyses have been carried out:

Prior to 1940	H <sub>2</sub> CO, CO <sub>2</sub> <sup>+</sup>
1940 to 1950	CS <sub>2</sub> , CO <sub>2</sub> <sup>+</sup> , SO <sub>2</sub> , NO <sub>2</sub> , ClO <sub>2</sub>
1950 to 1957	C <sub>2</sub> H <sub>2</sub> , HCN, CS <sub>2</sub> , H <sub>2</sub> CO, CS <sub>2</sub> <sup>+</sup> , C <sub>4</sub> H <sub>2</sub> <sup>+</sup> NH <sub>2</sub> , HCO, CH <sub>3</sub> , HNO



<sup>1</sup>Manuscript received October 3, 1957.

Contribution from the Department of Chemistry, University of Ottawa, and the Division of Pure Physics, National Research Council, Ottawa, Canada.  
Issued as N.R.C. No. 4538.

There is therefore available at the present time fairly detailed knowledge of the structures of these species in their ground and excited states, and a number of them were discussed at the symposium.

#### *Shapes of Excited Species*

An introductory paper dealing with the structures of electronically-excited species was presented by G. Herzberg (National Research Council, Ottawa), who pointed out that the symmetry species and shapes of molecules in electronically-excited states are often considerably different from the corresponding properties in the ground states. For example,  $C_2H_2$ , HCN, and  $CS_2$  are linear in their ground states but non-linear in their first electronically-excited states. The free radicals  $NH_2$  and  $HCO$  are non-linear in their ground states and linear in their low-lying excited states.

Additional examples of changes of molecular shape or molecular symmetry accompanying an electronic transition were afforded by subsequent papers presented at the meeting. G. W. Robinson and V. E. DiGiorgio (Johns Hopkins University, Baltimore, Md.) presented conclusive evidence that formaldehyde is non-planar in its low-lying excited state, and K. Allison and A. D. Walsh (Queen's College, Dundee) showed that a similar deviation from planar symmetry may occur in one or two of the electronic states involved in Rydberg transitions of formaldehyde. G. W. King (McMaster University, Hamilton, Ont.) discussed the absorption spectrum of glyoxal, and showed that while there is probably very little change in molecular geometry during the transition there is a change of molecular symmetry. In the general discussion period Walsh advanced the idea that  $NH_2$  may not be quite linear in its low-lying excited state. The potential-energy curve may have a small potential maximum in the  $180^\circ$  configuration, and this may account for the negative anharmonicity in the bending vibrations.

The experimental data which have accumulated on the shapes of molecules in electronically-excited states have provided striking support for the general accuracy of the extensive predictions made by Walsh in 1953. The general usefulness of these predictions was underlined by the discussions at the meeting.

#### *Theoretical Treatments of Excited States*

R. S. Mulliken (University of Chicago) dealt with the molecular orbital method for computing the energies of electronically-excited states. He suggested that we may be at the dawn of a new era of structural chemistry in which it will be possible to make detailed and reliable calculations of energies and other properties. He presented the results of some recent calculations on CO,  $N_2$ ,  $C_2H_2$ , and several molecules of the  $AB_2$  type, and compared the results with experimental data wherever available. The possibility that certain excited states of  $AB_2$  molecules may have unsymmetrical configurations was discussed, and supporting evidence was cited in the case of the  $ClO_2$  molecule, in which the antisymmetric stretching vibration appears to be excited with considerable intensity in the absorption spectrum.

J. W. Linnett (Oxford University) discussed an apparent discrepancy in viewpoint between simple molecular orbital theories as developed by Walsh and hybridized orbital theories as developed by Pauling. According to the former viewpoint the simplest electronic transition may be regarded as due to the transfer of an electron from one orbital to another, and may be accompanied by a considerable change in molecular geometry. According to the latter viewpoint the shapes of molecules are determined by hybridized groups of electrons, e.g.  $sp^2$ ,  $sp^3$ , rather than by individual electrons. The change of

shape that may accompany an electronic transition should therefore be regarded as indicating a change of hybridization. By considering possible electron distributions in simple molecules such as N<sub>2</sub>, CO, and C<sub>2</sub>H<sub>2</sub>, Linnett showed that the two methods of approach may differ merely in viewpoint rather than in fundamental concepts.

#### *Multiplicities of Excited States*

Considerable discussion centered on the question of the multiplicities of the excited states of various molecules. A. E. Douglas (National Research Council, Ottawa) presented some preliminary results on Zeeman effects which strongly suggested that the excited state of the near ultraviolet bands of CS<sub>2</sub> is a triplet and not a singlet as had previously been assumed. G. W. Robinson and V. E. DiGiorgio discussed some very weak bands of formaldehyde which showed a doublet spacing that does not change appreciably with either vibrational excitation or isotopic substitution. They assigned these bands to a singlet-triplet system and suggested that the rather large doublet spacing may be due to a coupling between the electron spin and residual unquenched orbital angular momentum in the molecule. Further work is clearly required, both theoretically and experimentally, on (1) the Zeeman effect in polyatomic molecules, and (2) spin-orbit coupling in polyatomic molecules.

In connection with the multiplicity problem mentioned above some headway might be made if the theoreticians were to form a more definite view about the *f* values to be expected for "allowed" and "forbidden" transitions, and if the experimentalists were to begin to measure the integrated intensities of various band systems. It would be valuable to have order of magnitude *f* values from both points of view.

Theoretical work on the intensity of the  $^1A_2 \leftarrow ^1A_1$  bands of formaldehyde was presented by J. A. Pople and J. W. Sidman\* (Cambridge University). The bands are forbidden by the electronic selection rules, and electronic-vibration interaction is usually invoked to explain the existence of the perpendicular bands. This explanation, however, cannot account for the appearance of parallel bands, and Pople and Sidman suggested that the intensity of these bands may be due to an electronic-rotational interaction. They calculated an approximate *f* value, and thus provided a challenge to the experimentalists to obtain the measured value.

#### *Excited States of Ions*

An interesting method for obtaining information regarding the excited states of molecular ions was described in a paper by D. C. Frost and C. A. McDowell (University of British Columbia, Vancouver, B.C.). An essentially monoenergetic source was used in a mass spectrometer, and discontinuities in the curves of ion current *versus* electron energy were observed; these discontinuities yielded information concerning the energies of the excited states of the ions. This approach provides a valuable complement to the usual spectroscopic methods, there being very little spectroscopic information available on the electronic spectra of polyatomic ions. The only spectra obtained so far have been in emission, and the only ions for which detailed analyses have been carried out are CO<sub>2</sub><sup>+</sup>, CS<sub>2</sub><sup>+</sup>, and C<sub>4</sub>H<sub>2</sub><sup>+</sup>. No absorption spectrum of a molecular ion, whether diatomic or polyatomic, has yet been observed in the gas phase.

The spectra of molecular ions have frequently been investigated in the solid phase, and a paper was presented by J. W. Sidman on the emission and absorption spectra of the nitrite ion in the crystalline state at low temperatures. Information was derived

\*Now at Department of Chemistry, Cornell University, Ithaca, N.Y.

concerning the vibrational and lattice frequencies for both the ground and excited states, and the results were compared with the predictions made by Walsh for 18-electron  $AB_2$  systems.

#### *Interaction between Electronic and Vibrational Motions*

Two of the papers at the symposium described the rather complex interaction between electronic and vibrational motions in polyatomic molecules. M. H. L. Pryce and U. Öpik (Bristol University) and H. C. Longuet-Higgins and R. A. Sack (Cambridge University) dealt with the dynamical Jahn-Teller effect; this paper was concerned with the vibronic energy levels of a non-linear molecule in a doubly-degenerate electronic state which is split in first order by a doubly-degenerate vibrational mode. Theoretical patterns were presented showing the vibrational structures and intensity distributions expected for bands involved in transitions between a Jahn-Teller distorted state and a non-degenerate electronic state. These predictions should prompt experimentalists to obtain data on transitions of this type.

The second paper along these lines was presented by K. Dressler and D. A. Ramsay (National Research Council, Ottawa) and dealt with the Renner effect in linear polyatomic molecules. This work was concerned with the complex vibronic patterns that may arise as the result of the interaction between electronic orbital angular momentum in a linear polyatomic molecule and the angular momentum associated with the bending vibrations. The analysis of the spectrum of  $NH_2$  suggests that the vibronic levels of a hypothetical  $\Pi$  state split into two groups, half of the levels correlating with the vibronic levels observed in the excited state and the other half with vibrational and rotational levels of the ground state. The interpretation of the experimental results involves a considerable extrapolation of the theory originally developed by Renner, and necessitates further theoretical investigations.

The problem of the transfer of electronic and vibrational energies in weakly coupled systems was discussed both theoretically and experimentally in papers by J. N. Murrell (Cambridge University and University of Chicago) and by D. S. McClure (R.C.A. Laboratories, Princeton, N.J.). The general problem of energy transfer is now being attacked using a variety of experimental techniques, such as ultrasonics, flash photolysis, shock waves, and fluorescence quenching, and information is being obtained concerning the probabilities for the conversion of energy from one form to another.

An important problem of interest to spectroscopists, photochemists, and theoreticians concerns the probability of predissociation in polyatomic molecules. Recent spectroscopic work has shown that the probability of predissociation in a polyatomic molecule depends not only on energy and symmetry considerations, as in a diatomic molecule, but on additional quantum numbers that have no counterpart in a diatomic molecule. Recent work on the ultraviolet spectrum of HCN has shown that the probability of predissociation in the non-linear excited state increases with the quantum number for rotation about the axis of least inertia of the molecule. In the linear excited state of HCO the  $\Sigma$  vibronic levels associated with the various vibrational modes have been found to be stable; the  $\Pi$ ,  $\Delta$ , . . . vibronic levels, on the other hand, are predissociated. Theoretical investigation of these new empirical rules is needed.

#### THE REACTIVITY OF ELECTRONICALLY-EXCITED SPECIES

The section of the symposium devoted to reactivity was introduced by E. W. R. Steacie (National Research Council, Ottawa), who outlined the role played by electronically-excited species in reaction mechanisms, and gave a brief history of the subject

of reaction mechanisms with special reference to excited states. He pointed out that in the early days of chain reactions excited species, or 'hot' molecules, were introduced in order to explain certain features of the mechanisms, and that in some cases their introduction was without basis. As time goes on, however, we are learning more and more about the detailed nature of the reactions involving these excited species, and in some cases can make reliable identifications of the species. On the whole rather more is known about the part played by electronically-excited species in flames, but knowledge of their role in thermal, photochemical, and photosensitized reactions is rapidly being gained.

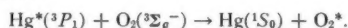
H. Eyring (University of Utah, Salt Lake City) gave a broad review of the subject of reactions of electronically-excited species, and emphasized the importance of treating the reactions theoretically in terms of potential-energy surfaces. He discussed from a theoretical standpoint certain processes involving argon ions, and also the interpretation of the mass spectrum of propane.

#### *Theoretical Treatments*

Several papers in the symposium were devoted to the theoretical treatment of reactions involving electronically-excited species. R. A. Marcus (Polytechnic Institute of Brooklyn) presented a theory of unimolecular reactions of electronically-excited molecules. He dealt with the process of excitation of a molecule in its ground state to vibrationally-excited states of the electronically-excited molecule, and also the unimolecular breakdown of the molecule formed. The course of this reaction is represented by a motion on a potential-energy surface, the reaction being the passage over a saddle point. Marcus's final expression for the rate of the reaction involves an activation energy that is independent of the frequency of the absorbing light, and a frequency factor that depends on the frequency of the light. The frequency factor for the unimolecular decomposition of an electronically-excited species will in general be smaller than  $10^{13}$  sec.<sup>-1</sup>, the value typical for molecules in their ground states. A second paper by Marcus dealt with the potentialities and limitations of the flash photolysis method for studying the chemical reactions of excited states.

The decomposition of an electronically-excited molecule was also treated by B. Stevens\* (Princeton University). It has been concluded by Sponer and Teller that whereas an optical transition in a symmetrical molecule excites the totally symmetric vibrations, it is the non-totally symmetric vibrations that are usually responsible for the dissociation processes. The unimolecular breakdown of an electronically-excited molecule therefore involves an internal redistribution of vibrational energy, and the rate depends on the magnitude of coupling of the optically active (symmetrical) and dissociative (non-symmetrical) vibrations; this coupling will be a function of the anharmonicity and hence of the energy. The implications of this were worked out in some detail by Stevens, who pointed out that the rate of the dissociation process will vary very considerably with the amount of optical energy given to the molecule. If the amount of energy is small there will be little coupling between the two types of vibration, and therefore a low probability of unimolecular dissociation; as the energy is increased the probability of transfer from the optically active to the dissociative vibrations becomes greater, and the rate of reaction is therefore greater.

A paper by E. K. Gill and K. J. Laidler (University of Ottawa) dealt for the most part with the nature of the reaction



In the past there has been some discussion as to the electronic nature of the oxygen

\*Now at Esso Research and Engineering Co., Linden, N.J.

formed in this reaction. Gill and Laidler considered both the experimental evidence and the potential-energy surfaces, and showed that both lead to the conclusion that the oxygen formed is in the  $^3\Sigma_u^+$  state. This is the highest electronically-excited state of oxygen for which there is enough energy available in the excited mercury, so that in the reaction there has been a minimal transfer of electronic to vibrational energy. The experimental evidence for this conclusion is that inert gases increase the rate of ozone production in this reaction, which they could hardly do if the excitational energy of the oxygen were to a considerable extent vibrational energy; the inert gases would then readily bring about deactivation. The theoretical treatment of the reaction involves the use of the potential-energy surfaces, and when these are constructed it is seen that there is an easy path for the formation of the  $^3\Sigma_u^+$  oxygen.

#### *Experimental Studies of Simple Systems*

A number of the papers presented at the symposium dealt with experimental studies of reactions of a very simple type; many of them dealt with reactions involving three atoms, reactions that are very simple to treat theoretically. H. E. Gunning\* (Illinois Institute of Technology, Chicago) presented the results of a number of experiments on photosensitization by isotopic mercury atoms. The procedure was to excite  $Hg^{202}$  ( $^3P_1$ ) atoms in natural mercury vapor, and to cause them to react with substrates that form solid mercury compounds when the photosensitization process occurs. The solid mercury compounds formed were examined to see whether they were enriched in the  $Hg^{202}$  isotope. Such enrichment is evidence for the primary formation of the mercury compound. One group of substances used consisted of halides such as hydrogen chloride, methyl chloride, and carbon tetrachloride; these formed  $Hg_2Cl_2$  on photoexcitation, and there was enrichment of the isotope in every case. It therefore follows that the excited mercury reacts directly with the abstraction of a halogen atom. Three substances which form  $HgO$  were studied: water vapor, nitrous oxide, and oxygen. There was very slight isotope enrichment in the case of  $H_2O$ , but no enrichment at all with nitrous oxide and oxygen.

During the presentation of his paper Gunning referred to the fact that his more recent results had indicated quite different quenching cross-sections for  $Hg^{198}$  and  $Hg^{202}$  in their  $^3P_1$  states. In the discussion period Shuler pointed out that this was a very surprising result since isotopes would be expected to react at approximately the same rate. There was considerable discussion on this point, but no definite conclusions were drawn.

The chemiluminescence in the system atomic sodium plus atomic hydrogen was discussed in a paper by J. D. McKinley, Jr.,† and J. C. Polanyi‡ (Princeton University), the procedure being to allow atomic sodium to diffuse into a mixture of atomic and molecular hydrogen. The results indicated that the reaction giving rise to luminescence is either  $Na + Na + H \rightarrow NaH + Na^*$  or  $Na + H + H \rightarrow H_2 + Na^*$ . In the former case the collision yield is  $4 \times 10^{-3}$ , in the latter case  $1 \times 10^{-5}$ ; these figures are based on Bodenstein's method of calculating rates of termolecular collisions.

Two papers dealt with the quenching of the iodine fluorescence spectrum, one by C. L. Arnot and C. A. McDowell (University of British Columbia) and the other by J. C. Polanyi (University of Toronto). When iodine vapor is excited by the green mercury line at 5461 Å there is produced a  $^3\Pi$  electronically-excited state of iodine in the 26th vibrational level. On collision with foreign molecules these excited iodine molecules may undergo a transition to the 25th and the 27th vibrational levels, and new fluorescence

\*Now at Department of Chemistry, University of Alberta, Edmonton, Alta.

†Now at the National Bureau of Standards, Washington, D.C.

‡Now at the Department of Chemistry, University of Toronto.

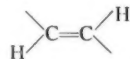
bands appear corresponding to transitions from these levels to ground electronic states. In addition there is the possibility of a direct fluorescence of the electronically-excited molecule in the 26th vibrational state, and it is possible to compare the rate constants for vibrational energy transfer ( $k_t$ ) with those for fluorescence ( $k_f$ ), for various added gases. Some ratios of rate constants obtained by Arnot and McDowell are as follows:

Added gas	He	Ne	A	O <sub>2</sub>
$k_t/k_f$ (liter mole <sup>-1</sup> )	$5.31 \times 10^4$	$2.69 \times 10^4$	$1.64 \times 10^4$	$1.5 \times 10^4$

On the assumption that the fluorescence lifetime for the excited iodine is  $10^{-8}$  second, these ratios are approximately ten times as great as would be calculated using the collision theory. There are two possible reasons for this discrepancy: the lifetime of the excited iodine may be less by a factor of ten or so, or the rate constants for the transfer processes may indeed be ten times greater than the collision frequencies. In the discussion of this paper Mulliken pointed out that data are probably available for making a calculation of the lifetime of the excited iodine molecule, so that it should be possible to resolve this problem. In Polanyi's investigation of the system the results were somewhat different; transfer in the case of hydrogen molecules, for example, occurred in one out of every four collisions.

Work on the reaction between nitric oxide and oxygen atoms was described by T. M. Sugden and E. M. Bulewicz (Cambridge University) and by F. Kaufman (Aberdeen Proving Ground, Maryland). When small amounts of nitric oxide are added to a system containing oxygen atoms, such as a flame, a greenish continuum is emitted, and this was studied by Sugden and Bulewicz over a range of temperatures and compositions. It has for some time been believed that the continuum is due solely to the process  $\text{NO} + \text{O} \rightarrow \text{NO}_2 + h\nu$ , and that the intensity of the continuum may be used as a measure of the oxygen-atom concentration in a flame. However, the results of Sugden and Bulewicz showed that nitric oxide catalyzed the combinations of free radicals in flames, and that the intensity of the continuum is determined by more complicated processes than a simple combination of NO and O. The intensity may therefore not be used as a measure of oxygen atom concentrations. Various other reactions giving rise to the formation of  $\text{NO}_2^*$  were considered. Kaufman's work provided rate constants for the reaction  $\text{O} + \text{NO} + \text{M} \rightarrow \text{NO}_2 + \text{M}$ .

G. J. Minkoff (Imperial College, London) dealt with the mechanism of the thermal decomposition of acetylene, with special references to the role played by electronically-excited states of acetylene. It was pointed out that the relatively large reaction rates observed at the beginning of the induction period are not consistent with previous mechanisms involving the intervention of stable dimers, and that in order to explain the kinetics it is necessary to postulate that a diradical is produced on the surface; this diradical then undergoes a polymerization in the gas phase, with some chain ending occurring on the surface. Minkoff postulated that at lower temperatures the triplet diradical formed is in the *trans* configuration



and that this readily undergoes polymerization. At higher temperatures the *cis* form is produced to a greater extent and, owing to the proximity of the hydrogen atoms, readily undergoes dehydrogenation. There was considerable discussion about the nature of the excited states of acetylene, and G. W. King indicated that his work with Ingold showed

the triplet state of acetylene to be normally in the *trans* form. Mulliken pointed out that the *cis* and *trans* forms should not differ very much in energy.

#### *Elementary Processes in Flames*

In addition to that of Sugden and Bulewicz, referred to above, there were two papers dealing with reactions in flames. A paper by H. P. Broida and K. E. Shuler (National Bureau of Standards, Washington) described additional work by these authors on the study of flame temperatures and energy distributions. Their work involved the addition of iron to various flames and a study of the electronic states of the iron, a number of iron lines being examined. The general conclusion was that iron is a good thermometer in that if there is equilibrium in the flame the iron lines provide a reliable temperature for the flame; if on the other hand there is not equilibrium this fact is readily revealed.

T. Carrington (National Bureau of Standards, Washington) described investigations on the electronically-excited ( $^2\Sigma^+$ ) OH radicals in oxyacetylene flames burning at atmospheric and reduced pressures. The results indicate that these electronically-excited radicals are quenched at practically every collision. This is of some interest since non-equilibrium populations of rotational levels of the excited radicals had been observed spectroscopically in certain flames and discharges, and the results have often been assumed to indicate a persistence of the initial rotational distribution. It has been assumed that the OH radicals remain in the excited state for the normal radiative lifetime of the electronic transitions ( $6 \times 10^{-6}$  second), and therefore undergo at atmospheric pressure about a thousand collisions before radiating. Carrington's discovery that the quenching efficiency is very high indicates, however, that this cannot be so: the electronically-excited radicals have no chance to undergo a series of collisions. The non-equilibrium distribution cannot therefore be due to the persistence of the rotational levels, and must correspond to the distribution existing when the OH radicals are initially formed. A possible mechanism for the production of abnormal populations of OH\* in flames and in discharges through water vapor was suggested by Broida; his explanation is based on the idea, due originally to Niira, that electronically-excited H<sub>2</sub>O\* dissociates into OH\* ( $^2\Sigma^+$ ) with excess rotational energy. In flames, according to Broida, the excited H<sub>2</sub>O is produced in the reaction



#### *Reactions of More Complex Molecules*

Several papers dealt with reactions involving polyatomic molecules, including the one by Stevens discussed above. J. Heicklen and W. A. Noyes, Jr., (University of Rochester) and H. Okabe (National Research Council, Ottawa) dealt with reactions involving electronically-excited ketone molecules. Heicklen and Noyes showed that the primary processes for simple ketones, such as acetone, are essentially as follows:

- (1) The initial absorption of radiation gives rise to a singlet-excited ketone, the vibrational energy of which depends upon the wave length.
- (2) Some of the initially excited molecules dissociate, the number depending upon the wave length and the pressure. Others lose vibrational energy by collision to reach the lowest vibrational level of the upper singlet state.
- (3) Molecules in the lowest vibrational level in the singlet state may either fluoresce or be converted into a triplet state which rapidly passes into its lowest vibrational level.
- (4) Phosphorescence may occur from the lowest vibrational level of the triplet state, but dissociation may occur if molecules are raised to higher vibrational levels of this state.

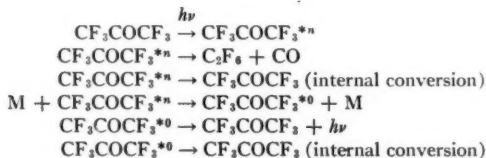
There are therefore two methods of dissociation, one of which depends on wave length but only slightly on temperature, the other only slightly on wave length but greatly on temperature. Some work with biacetyl,  $\text{CH}_3\text{COCOCH}_3$ , was described, and it was shown that at 4358 Å the decomposition is due to collision between two triplet-excited biacetyl molecules:



When a mixture of acetone and biacetyl is irradiated at 3130 Å the light is absorbed solely by the acetone, but fluorescence of biacetyl has been observed. This is attributed to reactions involving transfer of electronic energy on collision, as follows:



A paper on the fluorescence and photolysis of hexafluoroacetone,  $\text{CF}_3\text{COCF}_3$ , was presented by H. Okabe (National Research Council). The excitation of hexafluoroacetone vapor by light of wave length 3130 Å gives rise to strong fluorescence. The variation of the fluorescence efficiency with pressure and the addition of foreign gases suggest that the fluorescence may be principally from the lowest vibrational level of the short-lived singlet-excited state. It is proposed that the molecule is raised to the upper vibrational levels of a singlet-excited state, and subsequently deactivated to the lowest vibrational level of that state, from which it fluoresces. The molecule in the higher vibrational level can dissociate into  $\text{C}_2\text{F}_6$  and CO. The over-all reaction scheme proposed to explain the results is as follows:



Here  $*n$  denotes the  $n$ th vibrational level of the singlet excited state,  $*0$  the lowest vibrational level.

In the discussion period the possibility that the singlet-excited state may pass into a triplet-excited state by internal conversion was discussed in some detail.

# THE LOWER EXCITED STATES OF SOME SIMPLE MOLECULES<sup>1</sup>

R. S. MULLIKEN

## ABSTRACT

The present and prospective rapidly increasing usefulness of good LCAO-MO calculations on the electronic states of simple molecules in the interpretation of observed excited states is pointed out. As examples, the observed and predicted states of, in particular, the  $\pi^3\pi$  configurations of N<sub>2</sub> and CO are compared with those of C<sub>2</sub>H<sub>2</sub> and HCN and with those of CO<sub>2</sub> and CS<sub>2</sub>. Further, the results of LCAO-SCF calculations on CO<sub>2</sub> and on O<sub>3</sub> are surveyed, and it is shown how these can be helpful in interpreting and understanding the ground and excited states of AB<sub>2</sub> (especially AO<sub>2</sub>) molecules in general. A new interpretation of the so-called  $d^3\Pi$  state of CO as a case  $b\pi_u\pi_g$ ,  $^3\Delta_u$  state is proposed. Tentative interpretations of some of the ultraviolet absorption spectra of C<sub>2</sub>H<sub>2</sub>, HCN, and of a number of AB<sub>2</sub> molecules are reviewed or suggested, including some discussion of the shapes of excited states. The AB<sub>2</sub> discussion is a revision of one given earlier. Finally, following up a suggestion of Coon, it is pointed out that there exists strong evidence for slightly unequal Å—O distances in certain excited states of ClO<sub>2</sub> and SO<sub>2</sub>.

## INTRODUCTION

Experience shows that any antibonding MO is much stronger in its effects than its corresponding bonding MO. For example, two H atoms in the  $\sigma_g 1s$   $\sigma_u 1s$  state repel, two He atoms ( $\sigma_g 1s^2$   $\sigma_u 1s^2$ ) repel, and two coplanar CH<sub>2</sub> groups in C<sub>2</sub>H<sub>4</sub> in its first excited states (configuration . . . (x+x)(x-x) in LCAO symbolism) twist to become perpendicular.<sup>2</sup> Further examples are found in molecules AB<sub>2</sub>, where as soon as all bonding (and non-bonding) MOs are filled (as in CO<sub>2</sub>, NO<sub>2</sub><sup>+</sup>, N<sub>3</sub><sup>-</sup>, etc.), addition of further electrons causes bending (as in NO<sub>2</sub>, O<sub>3</sub>, SO<sub>2</sub>, ClO<sub>2</sub>, excited CS<sub>2</sub>, etc.); this gives relief (with energy-lowering) from otherwise strong antibonding. The writer has discussed the double-bond case (8) and the AB<sub>2</sub> cases (9),<sup>3</sup> and A. D. Walsh (16) has treated the AB<sub>2</sub> and a variety of other cases in a comprehensive series of papers which have given marked impetus to the study of the shapes of excited molecules.

Meanwhile new spectroscopic and other data and theoretical LCAO-MO electronic structure computations provide a basis for increased (though not yet thorough) insight into this field. Some of the new evidence and conclusions are reviewed below, in a discussion of some simple linear molecules, and of AB<sub>2</sub> molecules in general. Emphasis is placed first on observed and computed excited electronic states of the prototype molecules CO, N<sub>2</sub>, C<sub>2</sub>H<sub>2</sub>, and CO<sub>2</sub> all of which if or when linear have a lowest or second-lowest excited configuration of the type . . .  $\pi^3\pi$ . Attention is then given to the low excited states and non-Rydberg spectra of CO<sub>2</sub> and C<sub>2</sub>H<sub>2</sub>. Finally, a comparison between theoretical computations on the forms and energies of the LCAO-MOs of CO<sub>2</sub> (180°) and O<sub>3</sub> (120°) throws light on the energies and shapes of the spectroscopically known excited states of CO<sub>2</sub>, NO<sub>2</sub>, and so on. In some excited states of AB<sub>2</sub> molecules, there is evidence of further loss of symmetry ( $C_{2v} \rightarrow C_s$ ) in addition to bending; this can be understood as giving additional relief from antibonding.

<sup>1</sup>Manuscript received August 16, 1957.

Contribution from the Laboratory of Molecular Structure and Spectra, Department of Physics, The University of Chicago, Chicago 37, Illinois. This paper was presented at the Symposium on the Structure and Reactivity of Electronically-Excited Species held at the University of Ottawa, Ottawa, Canada, September 5 and 6, 1957.

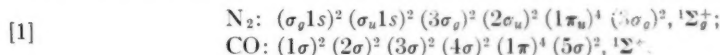
This work was assisted by the Office of Ordnance Research under Project TB2-0001(505) of Contract DA-11-022-ORD-1002 with the University of Chicago.

<sup>2</sup>See Mulliken (8). In C<sub>2</sub>H<sub>4</sub>, the twisting is distinctly assisted by hyperconjugation in the twisted form. This is strong enough so that C<sub>2</sub>H<sub>4</sub><sup>\*</sup>, even though no antibonding electron is present, probably is only barely or not quite stable toward twisting (10, 17).

<sup>3</sup>The acute-angled O<sub>3</sub> model reluctantly adopted there was forced by the then available knowledge of the infrared spectrum. It does not affect the essential features of the paper.

THE LOW EXCITED ELECTRONIC LEVELS OF CO, N<sub>2</sub>, AND CO<sub>2</sub>

To begin, let us consider theory and experiment for the lowest excited configurations of CO and N<sub>2</sub>, then of CO<sub>2</sub>. The ground states of N<sub>2</sub> and CO may be described as:



Leaving aside the four inner electrons, the theoretically computed forms and energies (i.e. ionization energies or term values) of the ground-state MOs and of the two atomic-valence-shell excited MOs are described in LCAO approximation in Table I. Especially notable are the considerable hybridization in the σ MOs and the resulting strength of bonding in the lowest energy of these, with corresponding weakness of bonding in the last occupied MO, and great strength of antibonding in the excited σ MO. Similar characteristics are found for all other molecules on which theoretical LCAO-MO SCF computations have been made (e.g. CO<sub>2</sub> and O<sub>3</sub>, Table V).

TABLE I  
FORMS OF N<sub>2</sub> AND CO MOLECULAR ORBITALS\*

Nitrogen				Carbon monoxide			
MO	Form†	ε (ev.)		MO	Form†	ε (ev.)	
		Obs.	Calc.			Obs.	Calc.
3σ <sub>u</sub>	h, -h	(A)		6σ	h, -h	(A)	
1π <sub>g</sub>	{x, -x} z, -z	(A)	7‡	6‡	2π	{X, -x} Z, -z	(A)
3σ <sub>g</sub>	h', h'	(b)	15.6	14.8	5σ	H', h'	(a)
1π <sub>u</sub>	{x, x} z, z	(B)	17.1	15.8	1π	{x, X} z, Z	(B)
2σ <sub>u</sub>	sh', -s-h'	(a)	18.7	19.9	4σ	sh, H'	(b)§
2σ <sub>g</sub>	sh, sh	(B)	—	39.5	3σ	h, sh	(B)

\*Based on: C. W. Scherr (J. Chem. Phys. **23**, 569 (1955)) for N<sub>2</sub>, R. C. Sahni (Trans. Faraday Soc. **49**, 1 (1953)) for CO.

†The symbols s; h; h' mean 2s; a 2s, 2pσ hybrid with strong end toward the other atom and positive; and a 2s, 2pσ hybrid with weak end toward the other atom and positive (cf. Fig. 1); x and z refer to 2px and 2pz, together comprising 2pπ. The symbols B and b mean strongly or weakly bonding, A and a mean strongly or weakly antibonding.

‡Rough weighted average term values based on excitation energies to various states.

§Observed; calc. is (a).

Theoretically computed energies (N<sub>2</sub>), and observed energies and other data (CO, N<sub>2</sub>), are given in Table II for the various states of the two lowest excited configurations. It should be noted that this table incorporates the most recent spectroscopic results and their interpretation, and includes a new identification of the d state of CO as a <sup>3</sup>Δ<sub>u</sub> state (cf. Table II footnote). A study of Table II gives confidence that LCAO-MO computations on simple molecules can predict correctly the energy order of the various states of a π<sup>3</sup>π configuration, and even roughly quantitatively the positions of the lower-energy excited states. However, the predicted energy of the π<sub>u</sub><sup>3</sup>π<sub>g</sub>, <sup>1</sup>Σ<sub>u</sub><sup>+</sup> state of N<sub>2</sub> is certainly too high, since the actual energy can surely not exceed the (vertical) 17.5 ev. required to remove a 1π<sub>u</sub> electron entirely. We may nevertheless reasonably conclude from the very high computed value that the vertical energy of the actual state must be rather close to the π<sub>u</sub> ionization limit. This is true for the observed state b' identified in Table II as π<sub>u</sub><sup>3</sup>π<sub>g</sub>, <sup>1</sup>Σ<sub>u</sub><sup>+</sup>; its vertical energy is roughly 14 or 15 ev. The theory also shows that this one

TABLE II  
COMPARISON OF SOME CARBON MONOXIDE AND NITROGEN MOLECULE STATES

Confign.	Carbon monoxide*				Nitrogen†				
	State	Energy (ev.)	$\omega_e$ (cm. <sup>-1</sup> )	$r_e$ (Å)	State	Energy (ev.)	$\omega_e$ (cm. <sup>-1</sup> )	$r_e$ (Å)	
$\pi^{-1}\pi^*$	Near $e^3\Sigma^-$				$b' ^1\Sigma_u^+$	12.85	(24.9)	752	1.44
					$w ^1\Delta_u$	9.26 (+?)	(9.8)	1548	1.26
					$a' ^1\Sigma_u^-$	8.76 (+?)	(9.0)	1530	1.27
		8.11	1094	1.39	$^3\Sigma_u^-$	[8.76]	(9.0)		
$\sigma^{-1}\pi^*$	$d ^3\Delta^*$	7.72*	1138*	1.39*	$^3\Delta_u$	[7.47]	(7.7)		
	$a' ^3\Sigma^+$	6.92	1231	1.35	$A ^3\Sigma_g^+$	6.17	(6.5)	1460	1.29
Ground	$A ^1\Pi$	8.07	1516	1.24	$a ^1\Pi_g$	8.55	(9.1)	1694	1.22
	$a ^3\Pi$	6.04	1739	1.21	$B ^3\Pi_g$	7.35	(8.1)	1734	1.21
Ground	$X ^1\Sigma^+$	0.00	2170	1.128	$X ^1\Sigma_g^+$	0.00		2358	1.094

\*The CO state  $d$  here identified as  $^3\Delta$  (Hund's case b) has hitherto been called  $d ^3\Pi$  (Hund's case a), following an analysis by Gerö and Szabo (*Ann. Physik*, **35**, 597 (1939)) of the  $d \rightarrow a$  emission bands. Although their data are not adequate for a conclusive judgment, the reported structure seems to be entirely compatible with  $^3\Delta(b) \rightarrow ^3\Pi(a)$ , and not with  $^3\Pi(a) \rightarrow ^3\Pi(a)$ . See G. Herzberg and T. J. Hugo (*Can. J. Phys.*, **33**, 757 (1955)) and Tanaka, Jursa, and Leblanc (*J. Chem. Phys.*, **26**, 862 (1957)), and references there given, for sources of the above data on CO. Because of some uncertainty in the vibrational numbering,  $\omega_e$  may be somewhat larger, and  $r_e$  and the energy somewhat smaller, for  $d ^3\Delta$ .

†For sources of the data on  $N_2$ , see R. S. Mulliken, in *Proceedings of the Conference on Aeronomy* (held at Cambridge, Mass., in June, 1966), (Pergamon Press, Ltd., London, 1967), and references there given. Values in brackets are estimated (not observed). Energy values in parentheses are vertical values from LCAO-MO theoretical computations by C. W. Scherr (*J. Chem. Phys.*, **23**, 569 (1955)). Observed energy values are non-vertical; the vertical values would be about 0.5 ev. higher for the  $\sigma^{-1}\pi^*$  states, about 1.5 ev. higher for the  $\pi^{-1}\pi^*$  states.

state must be much more ionic in character than all the other  $\pi_u^3 \pi_g$  states, justifying the identification in Table II with an observed state of much larger  $r_e$  and smaller  $\omega_e$  than the others. Further, the theory shows that this  $^1\Sigma_g^+$  state is the only one of the  $\pi_u^3 \pi_g$  states to which spectroscopic transition from the ground state is allowed by the selection rules (analogously for  $\pi^3 \pi^*$ ,  $^1\Sigma^+$  of CO), but that this one transition should be intense ( $V, N$  type). The state identified in Table II with  $^1\Sigma_g^+$  is the lowest-energy  $^1\Sigma^+$  state of  $N_2$  to which an intense transition occurs.<sup>4</sup>

The good agreement of theory and experiment for CO and  $N_2$  lends strong credence to the LCAO-MO theoretically predicted energy order and rough quantitative locations of the states of the excited configurations . . .  $1\pi_g^3 2\pi_u$ , . . .  $1\pi_g^3 3\sigma_g$ , and . . .  $1\pi_g^3 3\sigma_u$  for linear  $CO_2$  (cf. Table III). The negative computed  $\epsilon$  values (term values) for  $3\sigma_g$  and  $3\sigma_u$  (see Table V) of course cannot be taken literally. They may, however, reasonably be interpreted to mean that the actual (necessarily positive)  $\epsilon$  values for these MOs are small. The computed negative values probably signal a characteristic breakdown of the usual LCAO-MO approximation, based on free-atom Slater AOs, for high-energy LCAO-MOs. Further, such small- $\epsilon$  LCAO-MOs should probably be, as it were, dissolved and replaced by Rydberg MOs. Borderline cases between LCAO and Rydberg MOs are known. For example, the LCAO-MO  $\sigma_u 1s$  (i.e.,  $1s_a - 1s_b$ ) of  $H_2$  is nearly identical in form and

<sup>4</sup>There should also be another high-energy  $^1\Sigma_g^+$  state of (approximately)  $V$  type, corresponding to the configuration  $\sigma_g^{-1} \sigma_u^3$ . Presumably this is present at somewhat higher energies, but possibly the  $b'$  state is  $\sigma_g^{-1} \sigma_u^3$  and the  $\pi_u^{-1} \pi_g$   $V$  state is at higher energies, or possibly the situation is more complicated and involves mixing of two or more  $^1\Sigma_g^+$  states.

TABLE III  
CARBON DIOXIDE STATES

Linear CO <sub>2</sub> ( $D_{\infty h}$ )		Bent CO <sub>2</sub> ( $C_{2v}$ )	Probable form	Observed†
Confign. and state	Energy (ev.)*	Confign., state, polzn.**		
$\pi_g^3 \sigma_g$	${}^1\Pi_g$ (14.6)	$a_2 b_2^2 a_1, {}^3A_2, {}^1A_2(f)$	Linear‡	
	${}^3\Pi_g$ (14.6)	$a_2^2 b_2 a_1, {}^3B_2, {}^1B_2(y)$	Linear‡	
	${}^1\Sigma_u^+$ (22.1)	$a_2 b_2^2 b_1, {}^1B_2(y)$	Linear‡	
	${}^1\Delta_u$ (9.5)	$a_2^2 b_2 b_1, {}^1A_2(f)$ $a_2^2 b_2 a_1, {}^1B_2(y)$	Linear‡ Bent	Band systems with maxima at $\lambda 1475$ (8.2 ev.), $f = 0.004$ , bands to at least $\lambda 1810$ ; $\lambda 1330$ (9.4 ev.), $f = 0.005$ ; $\lambda 1100$ , $f = 0.12$ . Identify $\lambda 1475$ upper state with ${}^1\Delta_u$ ${}^1B_2$ , $\lambda 1100$ level with a Rydberg state or states.
	${}^3\Sigma_u^-$ (9.2)	$a_2^2 b_2 b_1, {}^3A_2$	Linear‡	
	${}^1\Sigma_u^-$ (9.2)	$a_2 b_2^2 a_1, {}^1A_2(f)$	Bent	
	${}^3\Delta_u$ (case b) (8.4)	$a_2 b_2^2 b_1, {}^3B_2$ $a_2 b_2^2 a_1, {}^3A_2$	Linear‡ Bent	
	${}^3\Sigma_u^+$ (7.6)	$a_2^2 b_2 a_1, {}^3B_2$	Bent	
	${}^1\Sigma_g^+$ 0.00	$a_2^2 b_2^2, {}^1A_1$	Linear	

\*Calculated vertical energies (in parentheses): J. F. Mulligan (J. Chem. Phys. **19**, 1428 (1951)).

†P. G. Wilkinson and H. L. Johnston (J. Chem. Phys. **18**, 190 (1950)), E. C. Y. Inn, K. Watanabe, and M. Zelikoff (J. Chem. Phys. **21**, 1648 (1953)). Unpublished photographs by Dr. P. G. Wilkinson of this laboratory show definite band structure in the  $\lambda 1475$  system.

‡But perhaps slightly unsymmetrical.

\*\*Polarization expected for absorption transition from ground state ( $f$  means forbidden).

must be identified with the Rydberg (or united-atom) MO  $2p\sigma_u$ . Again, the C—H antibonding  $a_1$  excited LCAO-MO for CH<sub>4</sub> (or NH<sub>3</sub>, or H<sub>2</sub>O) strongly resembles and must be identified with the Rydberg MO 3s.

We may now conclude that: (1) the  ${}^1\Sigma_u^+$  state of  $\pi_g^3 \pi_u$  for linear excited CO<sub>2</sub> is to be expected only at much higher energies than the others of this configuration, and (2) the  ${}^3\Pi_g$  and  ${}^1\Pi_g$  states of  $\pi_g^3 \sigma_g$  and the  ${}^3\Pi_u$  and  ${}^1\Pi_u$  states of  $\pi_g^3 \sigma_u$  are to be expected only at high energies close to the  $\pi_g$  ionization limit (13.8 ev.), and well above all the  $\pi_g^3 \pi_u$  states except the  ${}^1\Sigma_u^+$ . Point (2) makes it fairly certain that Walsh (16) was right in assuming the  $3\sigma_g$  MO of CO<sub>2</sub> to be less firmly bound than the  $2\pi_u$ , reversing the order assumed by the present writer (9) in his 1942 diagram of the orbital energies of AB<sub>2</sub> molecules for apex angle 180°.<sup>5</sup>

Let us next consider the predicted levels of linear and bent CO<sub>2</sub> (Table III) in relation to the observed absorption spectra above 1000 Å. For bent CO<sub>2</sub> ( $C_{2v}$  symmetry), the  $\pi_g$  MO of  $\pi_g^3 \pi_u$  must split into an  $a_2$  and a  $b_2$  MO, and the  $\pi_u$  into an  $a_1$  and a  $b_1$ .<sup>6</sup> The partial configuration  $\pi_g^3 \pi_u$  thus gives rise to four partial configurations yielding four singlet and four triplet states. The latter must be correlated with the several linear-molecule  $\pi_g^3 \pi_u$  states in the manner shown in Table III if we assume that the  $a_1$  excited MO becomes rapidly lower than  $b_1$  on bending, as is indicated by both empirical (9, 16) and now also theoretical (cf. Table V) evidence. It can then be predicted that some of

<sup>5</sup>The writer in 1942 thought  $3\sigma_g$  might be lower because of the large amount of 2s in it, if strongly antibonding; but Mulligan's LCAO-MO computations show it to be nevertheless of high energy.

<sup>6</sup>The orbital notation follows the internationally approved recommendations (J. Chem. Phys. **23**, 1997 (1955)).

these states should be bent, others linear (Table III). There seems to be little doubt that the observed rather weak absorption system with maximum near  $\lambda 1475$  (cf. Table III) represents a transition to a bent  $^1\Delta_u B_2$  state, as proposed by Walsh.

The interpretation of the observed second rather weak  $\text{CO}_2$  system with maximum near  $\lambda 1330$  then presents a puzzle; Walsh has identified it as the transition to the  $^1\Sigma_g^+$  of  $\pi_g^3 \pi_u$  or to the corresponding  $^1B_2$  state, but this identification must apparently be rejected because (a) the transition is too weak, and (b) its upper state should surely be considerably higher in energy in view of Point (1) in the second preceding paragraph. The state in question might conceivably be identified with  $^1\Pi_g$  of  $\pi_g^3 \sigma_g$ , but this seems to be excluded by (a) Point 2 of the second preceding paragraph, and (b) the fact that the molecule in this state is expected to be linear, in which case there should be only one relatively strong band in the system, instead of the large number actually observed. A rather plausible identification would be with a transition to a strongly bent  $b_1 a_1^2 a_1$ ,  $^1B_1$  or  $b_1^2 a_1 a_1$ ,  $^1A_1$  upper state corresponding to a  $^1\Sigma_g^-$  or  $^1\Delta_g$  state of the linear-molecule configuration  $1\pi_u^3 2\pi_u$ , although one would have expected such a state to be distinctly higher in energy, since the ionization potential of  $1\pi_u$  is 3.6 volts higher than that of  $1\pi_g$  (cf. Table V).

In the doubtless analogous case of the weak near-ultraviolet  $\text{CS}_2$  absorption spectrum, rotational and vibrational analysis seems to show conclusively that the lowest excited singlet level is a bent  $^1B_2$  (equilibrium angle about  $140^\circ$  according to Dr. B. Kleman), with rotational perturbations attributable to the predicted (cf. Table III) nearby  $^1A_2$  state. Direct transitions to the latter state, being electronically forbidden, should be weaker than to the  $^1B_2$ . According to a private communication from Dr. Kleman, the bands at the high-frequency end of the near-ultraviolet  $\text{CS}_2$  absorption look like a separate system; if so, this might be analogous to the  $\lambda 1330$   $\text{CO}_2$  system.

[*Added after the conference.*—Dr. A. E. Douglas reported at the conference that the low-frequency end of the near-ultraviolet  $\text{CS}_2$  spectrum shows a pronounced Zeeman effect, indicating that the excited state is a triplet state. The high-frequency end, which shows no definite evidence of a Zeeman effect, might then have a singlet upper state. These results can be understood without radical revision of the preceding discussion if the upper state of the weak low-frequency bands is the lowest  $^3A_2$  of Table III, related to  $^3\Delta_u$  of the linear case; its rotational perturbations would be attributed to the second (or possibly both) of the low  $^3B_2$  states of Table III. The stronger high-frequency region could then be explained by transitions to the bent  $^1B_2$  state related to  $^1\Delta_u$  of the linear case. Additional weak transitions to other states listed in Table III might possibly also be present in the observed structure. This revision of the earlier interpretation of the near-ultraviolet  $\text{CS}_2$  absorption spectrum is not unreasonable in view of the relatively strong spin-orbit coupling in the sulphur atom (analogous singlet-triplet transitions should be very much weaker and very difficult to observe in  $\text{CO}_2$ ). However, the fact that no indication whatever of the presence of triplet fine structure has been noted in any of the band lines by Liebermann or by Kleman, in spite of the use of high resolution, seems difficult to reconcile with a triplet state for the upper state of the low-frequency near-ultraviolet bands.]

On the basis of the preceding discussion and Table III, it seems fairly safe to conclude (a) that the lowest singlet excited states of  $\text{CO}_2$  are a bent  $^1B_2$  and  $^1A_2$  with vibrational zero levels near 7 ev., and (b) that the lowest triplet states are corresponding bent  $^3B_2$  and  $^3A_2$  states near 5–5.5. ev. (Walsh (16) attributes a well-known emission system observed in carbon monoxide flames to a transition from a higher triplet level to one of

TABLE IV  
COMPARISON OF SOME NITROGEN AND ACETYLENE STATES

Config. and state	N <sub>2</sub> energy (ev.)*	Linear C <sub>2</sub> H <sub>2</sub> energy (ev.)*		Non-linear C <sub>2</sub> H <sub>2</sub>	
		If <i>trans</i> (C <sub>2h</sub> )	If <i>cis</i> (C <sub>2v</sub> )	Config., state, polzn.†	Probable form
$\sigma_g \pi_g$	{ $^1\Pi_g$ $^3\Pi_g$ }	8.35	(9.1)	(High?)	
		7.35	(8.1)	(High?)	
$^1\Sigma_u^+$	12.85(?)	(24.9)	(19.98)	$a_u b_u^2 b_g, ^1B_u (y, z)$	Linear,‡ high energy
		9.26	(9.8)	{ $a_u^2 b_u b_g, ^1A_u (x)$ $a_u^2 b_u a_g, ^1B_u (y, z)$ }	$b_1 a_1^2 a_3, ^1B_2 (y)$ Linear‡
$^1\Delta_u$	[8.76]	(9.0)	(8.02)	$b_1^2 a_1 b_3, ^1B_2 (y)$	Bent, stably planar
		8.76	(9.0)	$b_1^2 a_1 a_2, ^3A_2$	Linear‡
$\pi_u^3 \pi_g$	$^1\Sigma_u^-$	[7.47]	(7.7)	$b_1 a_1^2 b_g, ^1A_u (x)$	Bent, easy to twist
		6.17	(6.5)	$b_1 a_1^2 b_g, ^3B_u$	Trans
$^3\Sigma_u^+$	$\pi_u^4 \sigma_g^2$	$\nu = 2330$	$\nu_{CC} = 1974$	$b_1 a_1^2 a_3, ^3B_2$	Linear‡
		$r = 1.09 \text{ \AA}$	$\nu_{CC} = 612$	$b_1 a_1^2 b_3, ^3A_2$	Bent, easy to twist
$^1\Sigma_g^+$	$\pi_u^4 \sigma_g^2$	$\nu = 2330$	$\nu_{CC} = 1.20$	$b_1^2 a_1 b_3, ^3B_2$	Bent, stably planar
		$r = 1.09 \text{ \AA}$			

\*Calculated (vertical) values in parentheses. For N<sub>2</sub>, C. W. Scherr (*J. Chem. Phys.* **23**, 569 (1955)). For linear C<sub>2</sub>H<sub>2</sub>, I. G. Ross (*Trans. Faraday Soc.* **48**, 973 (1952)). In both cases, without allowance for configuration interaction. For some additional possibilities in the case of C<sub>2</sub>H<sub>2</sub>, see text "Added after the meeting".

†The MO configurations given of course neglect configuration interaction. Polarization of absorbed light for transition to state is indicated in parentheses (f, forbidden; x, perpendicular to plane; y, parallel to CC line for *cis*, along least axis of inertia for *trans*).  
‡Or possibly bent and twisted.

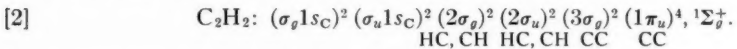
§C. K. Ingold and G. W. King (*J. Chem. Soc.* 2708 (1953)), K. K. Innes (*J. Chem. Phys.* **22**, 863 (1954)), and references given there. The transition to the 5.23 ev. state is x-polarized, with an oscillator strength f of about 10<sup>-4</sup>. See also Ref. 10, and text "Added after the meeting".

$\nu_{CC} = 1389$   
 $\nu_{CH} = 1048$   
 $r_{CC} = 1.39 \text{ \AA}$   
 $\theta = 120^\circ$

these.) With respect to the higher excited levels, the present survey suggests that considerably more study, both experimental and theoretical, is needed. Similar remarks apply to  $\text{CS}_2$ .

### THE LOW EXCITED LEVELS OF ACETYLENE

The ground-state electron configuration of  $\text{C}_2\text{H}_2$  should be closely analogous to that of  $\text{N}_2$  (cf. [1]) except for the C—H bonding properties of the  $\sigma$  MOs:



The capital letters under the last four MOs indicate their probable major bonding characteristics. For spectroscopic purposes, the major difference from  $\text{N}_2$  is that  $3\sigma_g$ , because of its strong C—C bonding function, must be less easily excited than  $1\pi_u$ , the reverse of what is true for  $\text{N}_2$ .<sup>7</sup> Hence for linear excited  $\text{C}_2\text{H}_2$ , the  $(3\sigma_g)(1\pi_u)^4 1\pi_g$  states, unlike  $\text{N}_2$  (Table II), are doubtless definitely above all except perhaps the highest ( $1\Sigma_g^+$ ) of the  $(3\sigma_g)^2 (1\pi_u)^3 1\pi_g$  states, so that we need consider only the latter. In Table IV, the observed and computed  $\pi_u^3 \pi_g$  states of  $\text{N}_2$ , and the corresponding computed states for linear  $\text{C}_2\text{H}_2$  (14),<sup>8</sup> are compared. From our experience on CO and  $\text{N}_2$  as discussed above, we may place confidence in these computed values for linear  $\text{C}_2\text{H}_2$  so far as the energy order of the states is concerned, and also very roughly quantitatively. The foregoing considerations furnish a basis for the correlations given in Table IV of these linear-molecule with bent-molecule states of excited  $\text{C}_2\text{H}_2$ , and give some guidance as to the energy order for the bent-molecule states.

Now let us assume, with Walsh (16), that  $1\pi_u$  splits into two MOs differing little in energy, namely  $a_1$  and  $b_1$  for  $C_{2v}$  (*cis*) symmetry, or  $b_u$  and  $a_u$  for  $C_{2h}$  (*trans*) symmetry, and that  $1\pi_g$  splits into one MO whose energy does not change with bending ( $a_2$  for *cis*,  $b_g$  for *trans*) and another whose energy decreases strongly with bending ( $b_2$  for *cis*,  $a_g$  for *trans*).<sup>9</sup> This assumed behavior on bending is analogous to what happens in  $\text{AB}_2$  molecules, where it is definitely known that the low-energy  $\pi$  MOs  $1\pi_u$  (bonding) and  $1\pi_g$  (non-bonding) split only slightly with bending, while the high-energy antibonding  $2\pi_u$  splits very strongly (cf. Table V). The MOs  $a_2$  or  $b_g$  from  $\pi_g$  and  $b_1$  or  $a_u$  from  $\pi_u$  are antisymmetric to the plane of bent  $\text{C}_2\text{H}_2$  and necessarily remain strongly bonding and antibonding, respectively, during bending. For  $C_{2v}$  (*cis*-bent)  $\text{C}_2\text{H}_2$ , the correlations in Table IV are formally identical with those for  $\text{CO}_2$  (Table III) except for the MO labels ( $a_2$  replaces  $b_2$ ,  $a_1$  replaces  $b_1$ , and vice versa, because the configuration here is  $\pi_u^3 \pi_g$  instead of  $\pi_g^3 \pi_u$ ). For  $C_{2h}$  (*trans*-bent)  $\text{C}_2\text{H}_2$ , which has no analogue for  $\text{CO}_2$ , the correlations are similar, but the selection-polarization rules for allowed spectroscopic transitions from the ground state are distinctly altered. Ingold and King, and Innes, in their thorough analyses of the observed weak absorption band system near  $\lambda 2200$ , find transitions only to *trans*-bent  ${}^1A_u$  excited molecules (see Table IV) (4, 5). The absence of transitions to *cis*-bent molecules can be explained by the spectroscopic forbiddenness of  ${}^1A_2 \leftarrow {}^1\Sigma_g^+$ , but there is

<sup>7</sup>The writer estimates that the ionization potential of  $3\sigma_g$  is 20–21 volts, whereas the observed minimum ionization potential of  $\text{C}_2\text{H}_2$ , which must belong to  $1\pi_u$ , is only 11.3 volts.

<sup>8</sup>For further calculations, see Serre (15) and references given there.

<sup>9</sup>Ingold and King, on the other hand, assume that  $\pi_u b_1$  and  $\pi_g a_g$  (or  $\pi_u b_1$  and  $\pi_g a_2$ ) both become nearly non-bonding and nearly equal in energy in bent  $\text{C}_2\text{H}_4$ . This results in a very different pattern of predicted excited levels. A consequence is that the lowest  ${}^1B_u$  of bent  $\text{C}_2\text{H}_2$  should be rather far (perhaps 3 ev.) below the lowest  ${}^1A_u$  (cf. Fig. 3 on p. 2715 of their papers (4)). Since the transition to this state should then lie in the visible, and be relatively strong, their assumption about the nature of these MOs seems improbable (but see below). However, they are in agreement with Table IV and with Walsh that the configuration of the  ${}^1A_u$  upper level of the  $\lambda 2200$  system is  $a_u b_u^2 a_g$ .

TABLE V  
MOLECULAR ORBITALS OF OZONE AND CARBON DIOXIDE\*

MO	Form	$\epsilon$ (ev.)	$\epsilon$ (ev.)		Form	MO
			Compd.	Obs.		
$4b_1$	$-h, y, h$ (A)		(-4.8)	[2est]	$-h, Y, h$ (A)	$3\sigma_u$
$5a_1$	$-h, h, -h$ (A)		(-3.1)	[2est]	$-h, S, -h$ (A)	$3\sigma_g$
$2b_1$	$-x, x, -x$ (A)		- - - - (2.5)	(5appr)	$\{ -x, X, -x \}$ (A)	$2\pi_u$
$1a_2$	$x, 0, -x$ (N)	13.7	11.5	13.73	$\{ x, 0, -x \}$ (N)	$1\pi_u$
$4a_1$	$-p, zh', -p$ (a)	14.8				
$3b_1$	$p, v, -p$ (a)	15.6				
$1b_1$	$x, X, z$ (B)	21.3	18.8	17.30	$\{ x, z, p \}$ (B)	$1\pi_u$
$3a_1$	$p-s, Zh', p-s$ (b)	22.8				
$2b_2$	$h', y, -h'$ (a)	25.2	17.9	18.07	$-s+h', y, s-h'$ (a)	$2\sigma_u$
$2a_1$	$-s, s-h', -s$ (A)	32.6	19.4	19.38	$H', s, H'$ (a)	$2\sigma_g$
$1b_2$	$Sh, y, -S-h$ (B)	41.0	42.4		$sh, y, -s-h$ (B)	$1\sigma_u$
$1a_1$	$sh, Sh, sh$ (B)	47.3	44.9		$hs, s, hs$ (B)	$1\sigma_g$

\*See Fig. 1 for explanation of atomic orbital symbols describing the form of each MO. The symbols B, b, N, a, A respectively mean strongly bonding, weakly bonding, essentially non-bonding, weakly antibonding, and strongly antibonding. Computed quantities based on I. Fischer-Hjalmars (*Arkiv. för Fysik*, **II**, 529 (1957)) for O<sub>3</sub>, and J. F. Mulligan (*J. Chem. Phys.* **19**, 947, 1428 (1951)) for CO<sub>2</sub>. The "observed"  $\epsilon$  values for the occupied MOs of CO<sub>2</sub> are ionization potentials based on Rydberg series (including the latest unpublished results of Y. Tanaka on 2 $\sigma_g$ ) and the CO<sub>2</sub><sup>+</sup> spectrum (for 1 $\pi_u$ ). For the unoccupied MOs of CO<sub>2</sub>, the  $\epsilon$  values are approximate average term values appropriate to excited states. Ozone is at the left, carbon dioxide at the right.

no reason to suppose that *cis*-bent  $^1A_2$  molecules cannot exist, although perhaps (4) they may have somewhat higher energy.

Comparing with CO<sub>2</sub>, it seems relevant that the intensity of  $^1A_u$  (*trans*)  $\leftarrow$   $^1\Sigma_g^+$  in acetylene ( $f = 10^{-4}$ , cf. Table IV footnote), whose analogue  $^1A_2 \leftarrow ^1\Sigma_g^+$  in CO<sub>2</sub> is forbidden, is much less than that of the observed  $^1B_2 \leftarrow ^1\Sigma_g^+$   $\lambda 1475$  system of CO<sub>2</sub> ( $f = 0.004$ ). This seems reasonable, since  $^1A_u \leftarrow ^1\Sigma_g^+$  of C<sub>2</sub>H<sub>2</sub> must acquire its intensity from  $^1\Pi_u A_u \leftarrow ^1\Sigma_g^+$  transitions (through some weak mixing of higher-configuration  $^1\Pi_u A_u$  states with our  $^1\Sigma_u^- A_u$ ), while  $^1B_2 \leftarrow ^1\Sigma_g^+$  of CO<sub>2</sub> can acquire its intensity mainly from the predicted very intense ( $\pi^3\pi$ ,  $^1\Sigma_u^+$ )  $^1B_2 \leftarrow ^1\Sigma_g^+$  transition (by admixture of ( $\pi^3\pi$ ,  $^1\Sigma_u^+$ )  $^1B_2$  into ( $\pi^3\pi$ ,  $^1\Delta_u$ )  $^1B_2$  on bending).

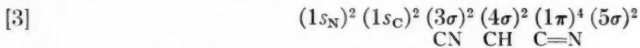
It can now be predicted that there should be absorption transitions  $^1B_z$  (*cis*)  $\leftarrow$   $^1\Sigma_g^+$  and  $^1B_u$  (*trans*)  $\leftarrow$   $^1\Sigma_g^+$  for C<sub>2</sub>H<sub>2</sub>, and that these should be much stronger than the  $^1A_u$  (*trans*)  $\leftarrow$   $^1\Sigma_g^+$   $\lambda 2200$  system. It seems likely that these predicted transitions can be identified with the rather plentiful confusion of bands, which are relatively weak but stronger than the  $\lambda 2200$  system, extending from near  $\lambda 2000$  for a few hundred angstroms toward shorter wavelengths.<sup>10</sup> A detailed study of these bands, if feasible, would be of great interest. Comparisons with recent work of Herzberg and Innes (3) on HCN will also be valuable; here again, the linear-molecule predicted states of  $\pi^3\pi$  configuration should be similar to those of N<sub>2</sub> or CO.

[Added after the meeting.—At  $\lambda 1520$  occurs the origin of the first Rydberg transition

<sup>10</sup>See the extensive discussion in Walsh's paper (16). Further, on the basis of unpublished results, Dr. P. G. Wilkinson estimates a total  $f$  value of very roughly  $10^{-3}$  for the bands between  $\lambda 1900$  and  $\lambda 1550$ . But Dr. T. M. Dunn of University College, London (private communication), estimates an  $f$  value five or ten times larger for these bands. He also estimates a larger  $f$  value for the " $\lambda 2200$ " system, and furthermore estimates that the intensity maximum of this system is near  $\lambda 1900$  rather than  $\lambda 2200$ .

of  $C_2H_2$ . This is an intense transition ( $f = 0.13$  according to Moe and Duncan (7)). On the basis of the vibrational structure (essentially only two or three quanta of the C—C stretching vibration) and the appearance of the bands, the excited state here, hence presumably the  $^2\Pi_u$  ground state of  $C_2H_2^+$ , is definitely linear. A report on this transition and on the next group of strong bands near  $\lambda 1340$ , going beyond previous work of W. C. Price (12), is in course of preparation by Dr. P. G. Wilkinson. Wilkinson's analysis indicates the presence of a very close group of three upper electronic states for the  $\lambda 1340$  group, of which two seem to be Rydberg states with a nearly but not quite linear configuration, while the third appears to be a non-Rydberg state in which the molecule is *trans*-bent, perhaps to  $120^\circ$ , and *twisted*. (Price assigned this whole group of bands to a single Rydberg transition.) The most likely identification of this bent and twisted state is with the transition to the high-energy  $^1B_u$  state of Table IV which corresponds to the linear-molecule  $\pi_u^3 \pi_g, ^1\Sigma_u^+$  state. The high intensity ( $f$  about 0.17 according to Moe and Duncan for the group of three electronic transitions near  $\lambda 1340$ ; more or less equally shared by all three) and the energy (9.25 ev., as compared with 12.85 ev. for the supposedly analogous  $^1\Sigma_u^+$  of  $N_2$ —cf. Table IV) tend to support this identification. However, it is evident that our theoretical understanding is still incomplete. A possibility not considered in Table IV, which perhaps may be important, is that for linear acetylene there exist low excited  $^3\Pi_u$  and  $^1\Pi_u$  states of configuration  $\pi_u^3 \sigma_u$  involving a strongly antibonding  $\sigma_u$  MO analogous to  $3\sigma_u$  of  $N_2$  (cf. Table I) but lower in energy, to which might correspond bent states one of which could be (or could be mixed into) the  $\lambda 1340$  bent upper state. Final conclusions must await further experimental and theoretical study.

In seeking to interpret the four electronic absorption systems of HCN and DCN which Herzberg and Innes (3) observe below  $\lambda 2000$ , a qualitative theoretical consideration indicates an electron configuration



in which the last  $\sigma$  MO ( $5\sigma$ ) and the  $\pi$  MO may have about equal ionization potentials, or the  $5\sigma$  even somewhat less than the  $1\pi$ . This is in marked contrast to acetylene (cf. [2] and text above) where there seems to be no doubt that the last  $\sigma$  MO ( $3\sigma_g$ ) is very much more tightly bound than the  $1\pi_u$  MO. The excited states of HCN for the molecule if it were linear should then resemble closely those of  $N_2$  and CO (cf. Table II) in that the configuration  $\sigma^{-1}\pi^*$  would be involved in giving rise to the lowest excited states. On this basis, the bent upper state of Herzberg and Innes'  $\alpha$  system might be identified with the  $^1A''$  state corresponding to the linear-molecule  $\sigma^{-1}\pi^*, ^1\Pi$  state, while the  $\beta$ ,  $\gamma$ , and  $\delta$  system upper states could be correlated with some of the other states corresponding to  $\sigma^{-1}\pi^*$  and  $\pi^{-1}\pi^*$ . In favor of this identification is the fact that Herzberg and Innes find a considerable increase in the C—H distance in the  $\alpha$  upper level, which does not seem to be understandable (and is not found in the  $\lambda 2200$  system of  $C_2H_2$ ) in terms of any state correlated with a pure  $\pi^{-1}\pi^*$  linear-molecule configuration. In  $\sigma^{-1}\pi^*$ , the C—H distance could be increased if the  $5\sigma$  MO is somewhat C—H bonding. The interpretation suggested here is open to objections, but may at least point toward some possibilities which should be explored.]

Because of the definite conclusions as to the energy order and other characteristics of the  $\pi_u^3 \pi_g$  states of linear  $C_2H_2$ , the correlations and interpretations proposed here are somewhat different from those of Walsh. They also differ considerably from those of

Ingold and King (4). The present interpretation is in harmony with the observation of a  $^1A_u$  lowest excited state of moderately high energy. It does not, however, offer any explanation as to why the molecule is bent to just  $120^\circ$  in this state. Complete LCAO-MO theoretical calculations on  $C_2H_2$  and HCN, for various geometrical forms and electronic states, should be exceedingly helpful in giving better answers and increased understanding.

#### THE LOWER-ENERGY EXCITED LEVELS AND SPECTRA OF BENT $AB_2$ MOLECULES

As is well known,  $AB_2$  molecules with up to 16 valence-shell electrons ( $CO_2$ , etc.) are linear in their ground states, but those with more are bent. Recent microwave and other spectroscopic work now affords reliable information on angles and internuclear distances for many of these (cf. Table VI). The bent form of the 17-19 electron molecules can be explained if (a) the linear form is stabilized by the net effect of the predominantly bonding and non-bonding MOs occupied by the first 16 electrons, (b) the next two electrons go into an MO ( $4a_1$ ) whose energy decreases rapidly with bending, (c) the next electron goes into an MO which is little affected by bending (cf.  $ClO_2$ ). The increased bending in 20-electron molecules like  $F_2O$  and  $Cl_2O$  may presumably be attributed to decreased  $s-p$  hybridization in the halogen outer atoms and other quantitative changes. Recent LCAO-MO theoretical calculations on the electronic structures of  $CO_2$  and  $O_3$ , for the experimentally known internuclear distances in each case, throw a great deal of light on the forms of all the MOs involved. A survey of the results, including a simplified rough description of the computed form and energy of each MO occupied in the ground state, as well as of the forms of all valence-shell-AO excited MOs, is presented in Table V (see also Fig. 1). The table has a number of points of interest. In studying it, however, one should keep in mind that the computed results, while good, are only approximate.<sup>11</sup> The reliability of the computed  $\epsilon$  values can be judged by a comparison of observed and computed values for  $CO_2$ —see also Tables II and III. The approximate forms of the MOs are probably fairly reliable in most cases.

The following points are especially relevant here. (1) The linear-molecule  $1\pi_u$  and  $1\pi_g$  MOs split and change in energy relatively little as a result of bending. (In comparing  $\epsilon$  values of bent  $O_3$  and linear  $CO_2$  in Table V, it should be kept in mind that the larger nuclear charge on the central atom in  $O_3$  causes a general increase in  $\epsilon$  values.) (2) The first excited MO  $2\pi_u$  of  $CO_2$  splits very strongly to give a  $4a_1$  MO whose  $\epsilon$  in  $O_3$  is as large as the MOs corresponding to  $1\pi_g$ , and a  $2b_1$  MO whose  $\epsilon$  should not change on bending. We have thus a theoretical explanation of the highly angle-sensitive  $4a_1$  MO which is known empirically. One notes that, although the  $2\pi_u$  MO is strongly antibonding, and the  $2b_1$  remains so, the  $4a_1$  for a  $120^\circ$  angle is only weakly antibonding. The very large  $\epsilon$  of  $4a_1$  at  $120^\circ$  is a result which comes out of the theoretical calculation and which perhaps cannot be fully explained in qualitative terms, although it can be partially attributed to the decreased antibonding. (3) The linear-molecule MOs  $3\sigma_g$  and  $3\sigma_u$  are very high in energy, and go over into even higher energy (at least for the  $3\sigma_g$ ) bent-molecule MOs  $5a_1$  and  $4b_2$ . The thus-indicated  $\epsilon$  values are so small that, contrary to earlier assumptions (9), these MOs probably may be left out of consideration in the explanation of observed absorption spectra except perhaps at short wavelengths in the vacuum ultraviolet.

The theoretical computations permit considerable improvements in both the writer's and Walsh's  $AB_2$  diagrams with respect to the energies of the various MOs, and give new

<sup>11</sup>Besides the approximations inherent in the LCAO-MO SCF method, the computations on  $O_3$  and  $CO_2$  did not specifically take into account the  $1s$  electrons. Further, many of the integrals involved were approximated. On the other hand, the results for  $N_2$  in Table I are based on a complete exact LCAO-MO SCF computation.

TABLE VI. SOME IDENTIFICATIONS OF OBSERVED WITH PREDICTED NON-INTERSYSTEM SPECTRA OF NON-LINEAR AB<sub>2</sub> MOLECULES

Transition	Polzn. and strength	Predictions*		Observed data, <sup>†</sup> in the following order for each molecule with the column heading, $\alpha$ and $r$ ( $\text{\AA}$ ) for ground state; below, $\Delta E_{\text{rot}}$ in ev. (and $\lambda_{\text{max}}$ in $\text{\AA}$ ); polarization; $f$ value (or strength); $\alpha' - \alpha''$ ; $r' - r''$ ; $\Delta v_g > 0$ ; $x_{3a} (\text{cm}^{-1})$	
		No <sub>2</sub> <sup>-</sup> (134°, 1.19)	O <sub>2</sub> <sup>-</sup> (116°, 1.23)		
2b <sub>1</sub> ← 4a <sub>1</sub>	x, w	+ +	3 (λ4000); ?; 0.003; to 180° (?); ?; ?	3.54 (λ3500); x; 2.1 (λ6000); ?; 0.6×10 <sup>-4</sup>	Possibly λ3500 +0.06 Å; 2.4 (or 1.2); +9
4a <sub>1</sub> ← 4b <sub>2</sub>	y, s?	—	~0 5.3 (λ2550); y; 0.0007; to 116°; +	(4a <sub>1</sub> full) 4.27 (λ2900); ?; 0.0004	(4a <sub>1</sub> full) large?; 1?; 2.4 none
2b <sub>1</sub> ← 3b <sub>2</sub>	f	~0	+	(calc. $f = 10^{-4}$ ) 4.86 (λ2550); y? 0.086	4.2 (λ2900); y? 0.006; —? large?; 1?; 2.4 none
2b <sub>1</sub> ← 1a <sub>2</sub>	y, s	~0	+	8.7 (λ1450); y? 5	5 (λ2450); y; small;

\*See Table V (ozone) for approximate forms of MOs. The symbols x, y, f respectively refer to transitions polarized perpendicular to the molecule plane, parallel to the B-B axis, or forbidden; w means weak, s, strong. The predicted changes in apex angle  $\alpha$  and A-B distance  $r$  are based on the bending and bonding properties of the MOs involved.

<sup>†</sup>Ground-state data for NO<sub>2</sub>, cf. G. E. Moore *J. Opt. Soc. Am.* **43**, 1045 (1953) and G. R. Bird *J. Chem. Phys.* **25**, 1040 (1956); for NO<sub>2</sub><sup>-</sup> (in crystal), M. R. Trueler (*Acta Cryst.* **5**, 132 (1952)); for O<sub>3</sub>, cf. R. H. Hughes *J. Chem. Phys.* **24**, 1313 (1956); for SO<sub>2</sub>, S. R. Polo and M. K. Wilson *J. Chem. Phys.* **22**, 900 (1954); for ClO<sub>3</sub>, J. D. Dunits and K. Hedberg *J. Am. Chem. Soc.* **72**, 3108 (1950). Spectroscopic data: NO<sub>2</sub> absorption, L. Harris and G. W. King (*J. Chem. Phys.* **21**, 1934) and G. Wilse Robinson (*report at Ohio State University Spectroscopic Conference (1957)*); for NO<sub>2</sub> absorption intensities, T. C. Hall and F. E. Blacet (*J. Chem. Phys.* **20**, 1745 (1952)) and Harris and King (*loc. cit.*); for NO<sub>2</sub> fluorescence spectrum (probably 2b<sub>1</sub> → 4a<sub>1</sub>; smaller f longer lifetime) in emission may be explained by lower transition probability at larger angle), D. Neuberger and A. B. F. Duncan (*J. Chem. Phys.* **22**, 1633 (1954)). Note that here 2b<sub>1</sub> → 1a<sub>2</sub> in NO<sub>2</sub> should give rise to two non-inter-system transitions of which an identification is given here for one. For NO<sub>2</sub><sup>-</sup> in Na<sup>+</sup>NO<sub>2</sub><sup>-</sup> crystal; see W. G. Travick and W. H. Eberhardt (*J. Chem. Phys.* **22**, 462 (1954)), J. W. Sidman (*J. Am. Chem. Soc.* **79**, 2869, 2875 (1957)); Sidman's work shows that the N≡N<sub>200</sub> system is an allowed one in spite of its weakness and confirms the x polarization found by Travick and Eberhardt. The f values for NO<sub>2</sub><sup>-</sup> are based on aqueous solution data of H. L. Friedman (*J. Chem. Phys.* **21**, 319 (1953)); the N≡N<sub>200</sub> solution band is apparently much weaker or possibly absent in the crystal, while the N≡N<sub>100</sub> solution band shows a double peak, and possibly part or most of the f value may belong to a different (charge-transfer) transition. O<sub>3</sub>: calculated frequencies (not given above) and  $f$  values, I. Fischer-Hjalmars (*loc. cit. Table V*); absorption bands, cf. survey by H. Spomer and E. Teller (*Rev. Modern Phys.* **13**, 76 (1941)) and more recent literature. It is here assumed that the very weak reported infrared system is due to impurities (perhaps O<sub>2</sub>) or is an inter-system transition. Evidence that the bands near λ3500 form a system distinct from the stronger region near λ2550 has also been disregarded. CF<sub>3</sub> emission, P. Venkateswarlu (*Phys. Rev.* **77**, 676 (1950)), absorption, R. K. Laird, E. B. Andrews, and R. F. Barrow (*Trans. Faraday Soc.* **46**, 803 (1950)), SO<sub>2</sub>, λ3800 system, Russell et al. (*ASTIA AD81060, CGFMN et al. (ASTIA AD95806)*), with J. B. Conn, N-3000 system, N. C. Metropolis (*Phys. Rev.* **60**, 215 (1941)) and see P. A. de Maine (*J. Chem. Phys.* **26**, 1036 (1957)) for CCl<sub>4</sub> solution data from which f value has been computed. The N≡N<sub>200</sub> system and a stronger absorption region near λ3800 also appear in fluorescence. ClO<sub>2</sub>, J. B. Conn and E. Ortiz (*J. Molecular Spectroscopy* (In press, 1957) and *Phys. Rev.* **96**, 845A (1954)). In a private communication, J. B. Conn gives  $f = 1.7 \times 10^{-7}$  and  $4.3 \times 10^{-3}$  respectively for the SO<sub>2</sub> λ3800 and λ3600 systems. See also text added after the meeting.

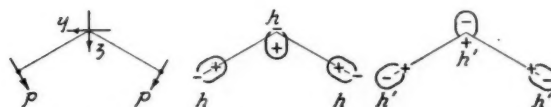


FIG. 1. Schematic diagram to indicate forms of atomic orbitals used in describing  $O_2$  molecular orbitals in LCAO approximation. For any atom,  $s$  means  $2s$  and  $x$  means  $2px$ , while  $h$  and  $h'$  respectively refer to various in-plane  $sp$  hybrids directed more or less toward or away from the center but whose exact forms and orientations vary from case to case. For the middle atom,  $y$  and  $z$  mean  $2py$  and  $2pz$  with positive end in the direction shown. For the outer atoms,  $p$  means an in-plane  $2p$  AO directed approximately perpendicular to an  $O-O$  bond. The  $x$  AO's are antisymmetric to the molecular plane, while all others are symmetric. Double symbols in the descriptions (e.g.  $sh$  or  $p-s$ ) are used where hybridization is somewhat minor in importance (e.g.  $sh$  means a mixture of  $s$  and  $h$ ,  $p-s$  a mixture of  $p$  and  $-s$ ). Capital letters are used in a few cases to indicate rather strong predominance in the total LCAO-MO.

Fig. 1 applies also to  $CO_2$  if the apex angle is increased from  $120^\circ$  to  $180^\circ$  with the O atom orbitals retaining their orientations to the CO axes; the  $x$  and the  $p_0$  and  $z_0$  AOs now become  $\pi$  AOs.

insight into the forms of the MOs. In combination with new experimental data of the last few years, they have led the writer to review earlier attempts to interpret the electronic absorption spectra of triatomic oxides, and to propose, in Table VI, identifications of known spectra above about  $\lambda 2000$ . In this effort, he is indebted to Professors G. W. Robinson, J. B. Coon, and W. H. Eberhardt for suggestions and for information on their current work.

The assignments of observed band systems to MO transitions for the several molecules are to a large extent mutually consistent and consistent with theoretical requirements and expectations (listed under "Predictions"). However, there seem to be some discrepancies which are difficult to explain, and the identifications must therefore still be considered provisional. These difficulties will now be mentioned and commented on briefly.

(1) The  $SO_2 \lambda 3800$  system is so weak that one is tempted to attribute it to a singlet-triplet transition, but if this is correct, the corresponding singlet-singlet transition should be nearby at somewhat shorter wavelengths. Although the  $\lambda 2900$  system fulfills this specification, its  $\Delta\alpha$ ,  $\Delta\tau$  characteristics are so different as to rule out such a relation. The much stronger bands near  $\lambda 2000$  are too far away. Thus one is left with the assignments in the table. The low intensities of the assigned  $SO_2$  bands, and the fact that we have ignored the strong bands near  $\lambda 2000$  whereas for  $NO_2$  and  $NO_2^-$  we have included strong bands at short wavelengths in the assignments, are not entirely satisfactory.

[*Added after the meeting.*—Dr. A. E. Douglas reported at the meeting that the  $SO_2 \lambda 3800$  system shows a pronounced Zeeman effect. This supports its interpretation as a singlet-triplet transition rejected above, but does not answer the contrary argument given above. Douglas finds no Zeeman effect in the  $\lambda 2900$  system; if  $\lambda 3800$  is actually a singlet-triplet transition,  $\lambda 2900$  is probably  $2b_1 \leftarrow 4a_1$  (it will be noted that the experimental data in Table VI which would contradict this appear with a ?) and  $2b_1 \leftarrow 1a_2$  is probably represented by strong bands near  $\lambda 2000$ .]

In the case of ozone, the assignments are definitely tentative and need further study (see footnote on  $O_3$  in Table VI). For all the molecules, additional non-Rydberg transitions besides those considered in Table VI, involving excitation from the deeper occupied MOs (and possibly also to higher excited MOs), are of course to be expected at shorter wavelengths, and a number of such transitions have certainly been observed. There seems, however, to be no reason why  $d$  hybridization for S and Cl in  $SO_2$  and  $ClO_2$  should markedly affect the long wavelength spectra. It should make the MOs  $1a_2$  and  $3b_2$  somewhat bonding, and strengthen the bonding MOs on the whole.

(2) The identification of the visible  $\text{NO}_2$  bands as  $2b_1 \leftarrow 4a_1$  seems to be supported by the work of Robinson (13) and of Eberhardt, but the observed intensity ( $f = 0.003$ ) is higher than expected, and also higher than for the transition identified as  $4a_1 \leftarrow 3b_2$ , which one might expect to be rather strong. An *alternative identification* would be to attribute the visible bands to  $4a_1 \leftarrow 3b_2$ , the bands with  $\lambda_{\max}$  at about 2350 to  $2b_1 \leftarrow 1a_2$ , and to suppose that the  $2b_1 \leftarrow 4a_1$  bands are present among the visible bands but too weak to be noticed. It should be noted that  $4a_1 \leftarrow 3b_2$  is possible only for  $\text{NO}_2$  among the molecules in Table VI, since in the others the  $4a_1$  shell is filled in the ground state.

(3) While  $4a_1$  in  $\text{NO}_2$  should be more or less halfway down from  $2b_1$  toward  $3b_2$  and  $1a_2$ , as one sees by interpolation between  $\text{CO}_2$  and  $\text{O}_3$  in Table V, it should in the other molecules (judging from the  $\text{O}_3$  calculated results in Table V) be close to  $1a_2$  and  $3b_2$ , and the latter should have  $\epsilon$  values near 15 ev., while  $2b_1$  is expected to have  $\epsilon$  near 5 ev. Hence the  $2b_1 \leftarrow 4a_1$  and  $2b_1 \leftarrow 1a_2$  spectra of  $\text{NO}_2^-$ ,  $\text{O}_3$ ,  $\text{SO}_2$ , and  $\text{ClO}_2$  might be expected to have frequencies corresponding to about 10 ev., instead of being in the range 3–6 ev. as observed according to Table VI. However, since an examination of Table V excludes any possibility of alternative MOs which could give smaller predicted excitation energies, we must apparently conclude that the MO identifications are not essentially at fault.

Granting this, it would seem that theoretical calculations based more directly on *electronic states* may be needed to account for the observed spectra. In general, the energies of electronic states can be estimated only roughly by the assumption of a definite fixed orbital energy  $\epsilon$  for each excited MO. "Configuration interaction" often strongly affects excitation energies. Reorganization when excitation from one to another particular MO involves a large change in charge distribution can also cause energy lowering. When *degenerate* MOs are involved, there are often a number of states covering a wide energy spread, as for example in the  $\pi^3\pi$  states of Tables II–IV. While it is true that in bent  $\text{AB}_2$  molecules there are no degenerate MOs, one may expect a partial persistence of the widely spread groupings of states that would exist for the degenerate-MO configurations of these molecules if linear. In fact the discussion given above of the excited states as a point of departure was based on this premise. In applying the same approach to the excited states of, say,  $\text{NO}_2$  and  $\text{O}_3$ , one would first compute the energies of the linear-molecule states, then consider what happens on bending. For  $\text{NO}_2$ ,  $\pi_g^4 \pi_u^2$ ,  $^2\Pi$  would yield the ground state . . .  $1a_2^2 3b_2^2 4a_1$ ,  $^2A_1$  and the low excited state . . .  $1a_2^2 3b_2^2 2b_1$ ,  $^2B_1$ , while the several states  $^4\Pi_g$ ,  $^2\Pi_g$ ,  $^2\Pi_g$ ,  $^2\Phi_g$ , and  $^2\Pi_g$  of  $\pi_g^3 \pi_u^2$  would give a number of other excited states. For  $\text{O}_3$ , one would start with the states of  $\pi_g^4 \pi_u^2$  and  $\pi_g^3 \pi_u^3$ . In general, *it is important to consider states as well as orbitals*.

A final point of considerable interest which emerges from some of the data on  $\text{SO}_2$  and  $\text{ClO}_2$  is the probability that these molecules become slightly unsymmetrical ( $C_s$  instead of  $C_{2v}$  symmetry) when excitation to a  $2b_1$  MO occurs. This MO (cf. Table VI) is inescapably antibonding, but its antibonding effect would be expected to be smaller for an unsymmetrical structure—just as, conversely, a bonding electron in a delocalized MO can give stronger total bonding than one localized between two nuclei. The evidence for an unsymmetrical upper state for the  $\text{ClO}_2$  band system, first brought to the writer's attention by J. B. Coon (2),<sup>12</sup> and for the  $\lambda 3800$  and  $\lambda 2900$   $\text{SO}_2$  systems, consists in the fact that the (for  $C_{2v}$  antisymmetric) frequency  $\nu_3$  is more strongly excited in the upper state than could otherwise reasonably be understood; further, that this frequency shows an

<sup>12</sup>Earlier, Lotmar (6) gave evidence for an unsymmetrical upper state (cf. p. 780) for the  $\text{SO}_2$  bands near  $\lambda 2000$ , in the fact that  $\Delta\nu_3 > 0$  seems to occur in fluorescence. However, later work raises some questions as to this evidence (1).

exceptionally large positive anharmonicity (cf.  $x_{33}$  values in Table VI). If we assume that these upper states are unsymmetrical, then in terms of the coordinate  $Q_3$  associated with  $\nu_3$  under  $C_2$  symmetry, one has a double minimum problem.<sup>13</sup> If the asymmetry is only slight, so that the hump between the two minima is very low, the  $\nu_3$  vibration levels should still be fairly evenly spaced, as for  $C_{2v}$  symmetry. However, the resulting broadened potential curve should result in (a) diminishing the effective force constant for small  $\nu_3$  vibrations but introducing strong positive anharmonicity, (b) permitting transitions  $\Delta\nu_3 = 2, 4 \dots$  to occur much more strongly than would be possible by Franck-Condon considerations if there were a single minimum. (Also,  $\Delta\nu_3 = 1, \dots$  can now occur if the transition is  $y$  or  $z$  polarized, but probably only very weakly.) The expected results agree with what is observed. For larger asymmetry, the situation would change to resemble ordinary inversion doubling as in  $\text{NH}_3$ ; one should then observe strong negative anharmonicity, but  $\Delta\nu_3 > 0$  should still occur readily.

One is tempted to connect unsymmetry of an  $\text{AB}_2$  excited state with photodissociation into  $\text{AB} + \text{B}$ . Minimum-energy dissociation of  $\text{AB}_2$  into  $\text{AB} + \text{B}$  may be effected, with or without initial asymmetry, by suitable simultaneous excitation of the vibrational coordinates  $Q_1$  and  $Q_3$  (and in general also  $Q_2$ ). The main importance of initial asymmetry for direct photodissociation would be in softening the usual Franck-Condon inhibitions against  $\Delta\nu_3 > 0$ . The diffuseness of the high-frequency regions of some  $\text{AB}_2$  absorption systems (e.g. the  $\text{ClO}_2$  system) may well be due to direct dissociation of this sort at a saddle-point or a saddle-asymptote of the vibrational energy and/or to vibrational predissociation of vibrational levels near and above such a saddle-point, or above such a saddle-asymptote. In other cases, predissociation into a different electronic state having a lower vibrational saddle-point or saddle-asymptote may occur.

#### REFERENCES

1. CHOW, T. C. Phys. Rev. **44**, 638 (1938).
2. COON, J. B. Bull. Am. Phys. Soc. **2**, 100 (1957).
3. HERZBERG, G. and INNES, K. K. Can. J. Phys. **35**, 842 (1957).
4. INGOLD, C. K. and KING, G. W. J. Chem. Soc. 2708 (1953).
5. INNES, K. K. J. Chem. Phys. **22**, 863 (1954).
6. LOTMAR, W. Z. Physik, **83**, 765 (1933).
7. MOE, G. and DUNCAN, A. B. F. J. Am. Chem. Soc. **74**, 3136 (1952).
8. MULLIKEN, R. S. Phys. Rev. **41**, 751 (1932); **43**, 279 (1933).
9. MULLIKEN, R. S. Phys. Rev. **60**, 512 (1941); Revs. Modern Phys. **14**, 204 (1942).
10. MULLIKEN, R. S. and ROOTHAN, C. C. J. Chem. Revs. **41**, 219 (1947).
11. ÖPIK, U. and PRYCE, M. H. L. Proc. Roy. Soc. A, **238**, 427 (1957).
12. PRICE, W. C. Phys. Rev. **47**, 444 (1935).
13. ROBINSON, G. W., McCARTY, M., and KEELTY, M. C. J. Chem. Phys. **27**, 972 (1957), and unpublished work.
14. ROSS, I. G. Trans. Faraday Soc. **48**, 973 (1952).
15. SERRE, J. Compt. rend. **242**, 1469 (1956).
16. WALSH, A. D. J. Chem. Soc. **2260** (1953).
17. WILKINSON, P. G. Can. J. Phys. **34**, 651 (1956).

<sup>13</sup>Öpik and Pryce (11) have discussed a related situation for a linear  $\text{AB}_2$  molecule.

# EQUIVALENT ORBITALS AND THE SHAPES OF EXCITED SPECIES<sup>1</sup>

J. W. LINNETT

## ABSTRACT

The electron distributions in the ground states of  $C_2H_2$ ,  $HCO$ , and  $NH_2$ , and in one excited state of each species, have been considered by transforming the simple molecular orbitals into equivalent ones. In the light of these considerations, the shapes and dimensions of the above species in these states have been discussed. It is found that a considerable degree of understanding can be achieved though there is uncertainty in the interpretation in some cases.

## INTRODUCTION

The object of this paper is to discuss some ways in which the shapes of molecules and radicals in their ground and excited states are decided by their electronic structures. The molecule  $C_2H_2$  and the radicals  $HCO$  and  $NH_2$  will be considered as examples. An extensive treatment of this type of problem has been given by Walsh (10), his approach being that of *simple* molecular orbital (M.O.) theory. This method, in its simple form, implies that the total energy can be represented to a satisfactory approximation by the sum of a number of one-electron energies of values corresponding to the orbitals that are occupied. Clearly this is an overapproximation, for interelectronic effects arising both from their charge and from the consequences of the Pauli principle (i.e. effects of multiplicity) are ignored. To some extent, of course, in drawing diagrams in his papers, Walsh has taken account of these effects, for the graphs of energy against angle are not computed from a number of one-electron calculations but are derived on a more empirical basis.

Simple M.O. theory, because interelectronic effects are ignored, is clearly an oversimplification. This may be particularly serious in the discussion of shapes, for these are, to a large extent, decided by the mutual effects of electrons on one another. For example, methane is tetrahedral because the Pauli principle requires that four electrons with parallel spins in the  $2s$  and three  $2p$  orbitals of carbon will be, with greatest probability, at the corners of a regular tetrahedron (11). Moreover charge effects favor this shape also. Also  $NH_3$  is pyramidal because of the presence of the lone pair and of the interaction of this with the bonding pairs (7). Consideration of shapes should therefore include interelectron effects as well as one-electron effects, and consequently the simple M.O. procedure is not wholly satisfactory.

The approach used in this paper will be that based on the representation of the molecular wave function in terms of equivalent orbitals which are linear combinations of the basic one-electron molecular orbitals, for these allow an easier appreciation of the electron distribution, and a more reasonable assessment of the effects of electron interactions. This procedure has been used previously by the author to discuss the bonding in the ground and some excited states of the diatomic molecules and ions formed by carbon, nitrogen, and oxygen (5). Equivalent orbitals of this type are to be preferred when electron distributions are being considered (4). It was found that the force constants and bond lengths correlated well with the number of electrons concentrated in the internuclear region, providing the types of orbitals that were occupied were taken into account.

For the diatomic molecules it was shown (5) that the wave function could be transformed in part from an M.O. description to an equal equivalent orbital description, the

<sup>1</sup>Manuscript received August 16, 1957.

Contribution from Inorganic Chemistry Laboratory and Queen's College, Oxford University, Oxford, England.  
This paper was presented at the Symposium on the Structure and Reactivity of Electronically-Excited Species held at the University of Ottawa, Ottawa, Canada, September 5 and 6, 1957.

equivalent orbitals being atomic orbitals if the L.C.A.O. (linear combination of atomic orbitals) approximation was being used for the molecular orbitals. Let us consider a diatomic molecule AB and the orbitals  $\pi_1$  (bonding) and  $\pi_2$  (antibonding). There are two degenerate  $\pi_1$  orbitals, which may be designated  $\pi_1^+$  and  $\pi_1^-$ , involving  $e^{+i\phi}$  and  $e^{-i\phi}$  respectively where  $\phi$  is the azimuthal angle. To a first approximation one may write for the molecular orbitals expressions of the type

$$\begin{aligned} [1] \quad \pi_1^+ &= a \cdot 2p_{\pi_A}^+ + b \cdot 2p_{\pi_B}^+, \\ \pi_2^+ &= a' \cdot 2p_{\pi_A}^+ - b' \cdot 2p_{\pi_B}^+, \end{aligned}$$

where  $a$ ,  $b$ ,  $a'$ , and  $b'$  are all positive. Suppose that two electrons having parallel spins occupy  $\pi_1^+$  and  $\pi_2^+$ , and, for the moment, that these are the only two electrons in the molecule. To satisfy the Pauli principle the wave function must be

$$[2] \quad \begin{vmatrix} \pi_1^+(1) \cdot \alpha(1) & \pi_2^+(1) \cdot \alpha(1) \\ \pi_1^+(2) \cdot \alpha(2) & \pi_2^+(2) \cdot \alpha(2) \end{vmatrix},$$

where  $\alpha$  is the spin function. The above function can easily be shown to be identical with

$$[3] \quad \begin{vmatrix} 2p_{\pi_A}^+(1) \cdot \alpha(1) & 2p_{\pi_B}^+(1) \cdot \alpha(1) \\ 2p_{\pi_A}^+(2) \cdot \alpha(2) & 2p_{\pi_B}^+(2) \cdot \alpha(2) \end{vmatrix}.$$

So one may equally describe the electrons as being in the atomic orbitals  $2p_{\pi_A}^+$  and  $2p_{\pi_B}^+$  or as being in  $\pi_1^+$  and  $\pi_2^+$ . On this basis one may describe the ground state (G.S.) of O<sub>2</sub> either as  $\sigma_g^2 \cdot \sigma_u^2 \cdot \pi_u^4 \cdot \sigma_g^2 \cdot \pi_g^2$  or as  $2s_A \cdot \bar{2}s_A \cdot 2s_B \cdot \bar{2}s_B \cdot 2p_{\pi_A}^+ \cdot 2p_{\pi_B}^+ \cdot 2p_{\pi_A}^- \cdot 2p_{\pi_B}^-$ . ( $\pi_u^+ \cdot \pi_u^- \cdot \sigma_g \cdot \sigma_g$ ). In the second of these the presence of an electron with a  $\beta$  spin function in the orbital  $2s_A$  is represented by  $\bar{2}s_A$ , while, if the spin wave function is  $\alpha$ , the bar sign is omitted (5). This type of procedure will now be used to consider the shape and binding in some polyatomic molecules and radicals in both ground and excited states.

#### THE GROUND AND EXCITED STATES OF ACETYLENE

Ingold and King (3) have shown that the absorption band system of acetylene in the neighborhood of 2200 Å is due to a transition to an excited state in which the acetylene molecule is bent, having a *trans* configuration and a center of symmetry. They also bring forward good evidence for believing that the bond between the two carbon atoms is probably a three-electron bond and that the symmetry of the state is  $^1A_u$ .

The electronic structure of the ground state of acetylene is analogous to that of nitrogen, which may be represented by  $\sigma_g^2 \cdot \sigma_u^2 \cdot \pi_u^4 \cdot \sigma_g^2$ . This is equivalent to  $2s_A \cdot \bar{2}s_A \cdot 2s_B \cdot \bar{2}s_B$ . ( $\pi_u^+ \cdot \pi_u^- \cdot \sigma_g^- \cdot \sigma_g$ ) and corresponds to a configuration of maximum probability in which each nitrogen nucleus and  $K$ -electron core is surrounded by two approximately tetrahedral sets of electrons, there being five in each set, three in the bond region and two on the internuclear axis, both these being outside the bond region and at opposite ends of the molecule (5). The configuration of maximum probability is therefore reminiscent of Baeyer's interpretation of the triple bond. In acetylene the first four electrons of the set  $\sigma_g^2 \cdot \sigma_u^2 \cdot \pi_u^4 \cdot \sigma_g^2$  serve to bond the hydrogen atoms to the carbon, and the remaining six the two carbon atoms to one another, the spatial configuration of the electrons being satisfactory for doing this with a linear arrangement of the four nuclei. For N<sub>2</sub>, a relatively small excitation of this system can be achieved by transferring one electron from the  $\pi_u$  to a  $\pi_g$  molecular orbital. Only singlet states will be considered here since it is certain that the excited state observed by Ingold and King is a singlet. There are several singlet states described by  $\sigma_g^2 \cdot \sigma_u^2 \cdot \pi_u^3 \cdot \sigma_g^2 \cdot \pi_g$ . They are:

$$\begin{aligned}
 & \text{or } \frac{\sigma_g \cdot \overline{\sigma_g} \cdot \overline{\sigma_u} \cdot \overline{\sigma_u} \cdot \overline{\pi_u^+} \cdot \overline{\pi_u^-} \cdot \sigma_g \cdot \overline{\sigma_g} \cdot \overline{\pi_g^+}}{2s_A \cdot 2s_A \cdot 2s_B \cdot 2s_B \cdot 2p\pi_A^+ \cdot 2p\pi_B^+ \cdot (\pi_u^+ \cdot \pi_u^- \cdot \sigma_g \cdot \overline{\sigma_g})} \quad \left. \right\} {}^1\Delta_u \\
 [4] \quad & \text{or } \frac{\sigma_g \cdot \overline{\sigma_g} \cdot \overline{\sigma_u} \cdot \overline{\sigma_u} \cdot \overline{\pi_u^+} \cdot \overline{\pi_u^-} \cdot (\overline{\pi_u^+} \cdot \overline{\pi_g^-} + \overline{\pi_u^-} \cdot \overline{\pi_g^+}) \cdot \sigma_g \cdot \overline{\sigma_g}}{2s_A \cdot 2s_A \cdot 2s_B \cdot 2s_B \cdot (\pi_u^+ \cdot \pi_g^- + \pi_u^- \cdot \pi_g^+) \cdot (\pi_u^+ \cdot \pi_u^- \cdot \sigma_g \cdot \overline{\sigma_g})} \quad \left. \right\} {}^1\Sigma_u^- \\
 & \text{or } \frac{\sigma_g \cdot \overline{\sigma_g} \cdot \overline{\sigma_u} \cdot \overline{\sigma_u} \cdot \overline{\pi_u^+} \cdot \overline{\pi_u^-} \cdot (\overline{\pi_u^+} \cdot \overline{\pi_g^-} - \overline{\pi_u^-} \cdot \overline{\pi_g^+}) \cdot \sigma_g \cdot \overline{\sigma_g}}{2s_A \cdot 2s_A \cdot 2s_B \cdot 2s_B \cdot (\pi_u^+ \cdot \pi_g^- - \pi_u^- \cdot \pi_g^+) \cdot (\pi_u^+ \cdot \pi_u^- \cdot \sigma_g \cdot \overline{\sigma_g})} \quad \left. \right\} {}^1\Sigma_u^+
 \end{aligned}$$

For all these the bonding group is  $(\pi_u^+ \cdot \pi_u^- \cdot \sigma_g \cdot \overline{\sigma_g})$  so that the bond length would be expected to be about  $0.92 \times 1.40 = 1.29 \text{ \AA}$  (cf. Linnett (5), Table 3 (1.40) and Figure 1 (0.92)). No  ${}^1\Delta_u$  state has been identified for  $\text{N}_2$  but the state designated  $j$  (Herzberg (1)) is described as  ${}^1\Sigma_u^+$  (about 100,000 cm.<sup>-1</sup> above the G.S.) and the state  $a'$  (probably 60,000 cm.<sup>-1</sup> above the G.S.) is probably  ${}^1\Sigma_u^-$ . The first of these ( $j$ ) has  $r_0 = 1.28 \text{ \AA}$  while the second ( $a'$ ) has  $r_e = 1.28 \text{ \AA}$ . It seems possible therefore that  $j$  and  $a'$  are to be identified with the corresponding two states described just above.

The three states just described differ in the non-bonding group of two electrons with parallel spins, one in a  $\pi_u$  (bonding) and one in a  $\pi_g$  (antibonding) orbital. The differing groups are:

$$\begin{aligned}
 [5] \quad & {}^1\Delta_u: \quad \pi_u^+ \cdot \pi_g^+ \quad (\text{and } \pi_u^- \cdot \pi_g^-) \\
 & {}^1\Sigma_u^-: (\pi_u^+ \cdot \pi_g^- + \pi_u^- \cdot \pi_g^+) \\
 & {}^1\Sigma_u^+: (\pi_u^+ \cdot \pi_g^- - \pi_u^- \cdot \pi_g^+)
 \end{aligned}$$

For the situation in which electrons 1 and 2 occupy the above orbitals the above become, using  $\pi_u^+ = \pi_u \cdot e^{+i\phi}$  and  $\pi_g^- = \pi_g \cdot e^{-i\phi}$ , etc.:

$$\begin{aligned}
 [6] \quad & {}^1\Delta_u : \{ \pi_u(1) \cdot \pi_g(2) - \pi_u(2) \cdot \pi_g(1) \} \{ \cos(\phi_1 + \phi_2) \pm i \sin(\phi_1 + \phi_2) \} \\
 & \text{or } \{ 2p\pi_A(1) \cdot 2p\pi_B(2) - 2p\pi_A(2) \cdot 2p\pi_B(1) \} \{ \cos(\phi_1 + \phi_2) \pm i \sin(\phi_1 + \phi_2) \} \\
 & {}^1\Sigma_u^- : \{ \pi_u(1) \cdot \pi_g(2) - \pi_u(2) \cdot \pi_g(1) \} \{ \cos(\phi_1 - \phi_2) \} \\
 & \text{or } \{ 2p\pi_A(1) \cdot 2p\pi_B(2) - 2p\pi_A(2) \cdot 2p\pi_B(1) \} \{ \cos(\phi_1 - \phi_2) \} \\
 & {}^1\Sigma_u^+ : \{ \pi_u(1) \cdot \pi_g(2) + \pi_u(2) \cdot \pi_g(1) \} \{ \sin(\phi_1 - \phi_2) \} \\
 & \text{or } \{ 2p\pi_A(1) \cdot 2p\pi_B(2) - 2p\pi_A(2) \cdot 2p\pi_B(1) \} \{ \sin(\phi_1 - \phi_2) \}
 \end{aligned}$$

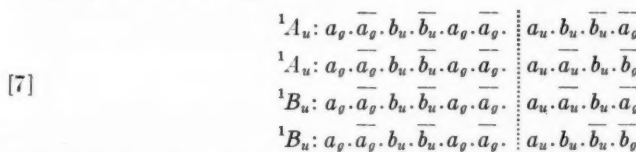
(When considering the symmetry of these last expressions it must be remembered that the bonding group  $\pi_u^+ \cdot \pi_u^-$  has the symmetry represented by a negative sign so that the symmetry of the whole group of electrons is the reverse of the symmetry of the pair considered in the expressions [6].) The probability distribution for this non-bonding group in the  ${}^1\Delta_u$  state is independent of  $\phi_1$  and  $\phi_2$ , one electron being on each nitrogen atom. For the  ${}^1\Sigma_u^-$  state there is one electron on each atom so placed that the highest probability is when the two are in the same plane (i.e.  $(\phi_1 - \phi_2) = 0$  or  $\pi$ ). The  ${}^1\Sigma_u^+$  state is an ionic state, there being a high probability of both electrons being simultaneously on A or on B. This means that the electron pattern of the  ${}^1\Delta_u$  state may be summarized as  $sp^3(\sigma\pi^2); sp^2(\sigma)$ .\* The first group,  $sp^3(\sigma\pi^2)$ , forms a set like that for a conventional

\*The symbolism used here has been described by the author elsewhere (5) and signifies a set of one spin which employs an  $sp^3$  group of orbitals from each atom, the bonding group consisting of three electrons in a  $\sigma$  and two  $\pi$  orbitals, and a second set of the other spin which employs an  $sp^2$  group of orbitals from each atom, the bonding group consisting of one electron in a  $\sigma$  orbital. The atomic orbitals used are given outside the brackets and the bonding orbitals inside the brackets. In addition the orbitals occupied by electrons of one spin are given before the semicolon and those occupied by electrons of the other spin are given after the semicolon.

triple bond, which has been described above. The second group,  $sp^2(\sigma)$ , of five electrons involves in the configuration of maximum probability a triangular arrangement round each atom, one electron being between the nuclei (5). In the  $^1\Delta_u$  state the plane of the triangular group round one atom is independent of the plane of the group round the other atom (probability independent of  $\phi_1$  and  $\phi_2$ ). For the  $^1\Sigma^-$  state the electron pattern is also  $sp^3(\sigma\pi^2)$ ;  $sp^2(\sigma)$ , but the triangular planes of the electrons of the  $sp^2(\sigma)$  set tend to lie in the same plane (maximum when  $(\phi_1 - \phi_2) = 0$  or  $\pi$ ). For the  $^1\Sigma^+$  state the electron pattern is  $sp^3(\sigma\pi^2)$ ;  $sp(p^2)^{\frac{1}{2}}(\sigma)$ , this being an ionic state.

Consideration of acetylene differs from that of nitrogen in that the location of the protons must also be examined. These protons will be in a particular spatial relation to one another and to the rest of the molecule. For this reason the electronic pattern of the  $^1\Delta_u$  states will not be well suited to holding the protons since the electrons of the  $sp^2(\sigma)$  set on the two atoms do not tend to have any particular spatial relation with respect to one another with the result that the electron cloud will tend to be too diffuse for binding. In the  $^1\Sigma^-$  state the two sets are separately well suited to bonding the protons but in different places. The  $sp^3(\sigma\pi^2)$  set would tend to bind them in a linear form on the CC axis, but the  $sp^2(\sigma)$  set will tend to bind them in a non-linear planar form, either *cis* or *trans*. So this state unmodified is not suited to binding the two protons. However if the electrons of the  $sp^3(\sigma\pi^2)$  set, which are outside the central bond region, are displaced towards the directions of the electrons of the  $sp^2(\sigma)$  set, two electron pair CH bonds could be formed. But, if this happened without any modification of the  $\sigma\pi^2$  group in the central bond region, the electron configuration round each carbon atom would become very unbalanced and this is improbable on the grounds of both charge and spin correlation. The unevenness of the distribution can be remedied to some extent by moving an electron out of the bond region so that the  $sp^3(\sigma\pi^2)$  set becomes  $sp^3p^{\frac{1}{2}}(\sigma\pi)$ , one tetrahedral position on each carbon atom being occupied by only one electron. On this basis, this excited state of acetylene would be expected to be planar and non-linear (probably *trans* because of charge repulsion effects), involving an ordinary electron pair CH bond and a CC bond having three electrons in the bond region (even though it is derived from a state of N<sub>2</sub> having four electrons in the bond region). All these features are observed by Ingold and King, the CC and CH bond lengths being 1.383 and 1.09 Å respectively, the corresponding vibration frequencies being consistent with these values. Moreover, the bending frequency for the excited state is higher than that in the ground state, which would be anticipated for this structure (cf. Walsh (10)). This is the electronic structure suggested by Ingold and King for the excited state, for the  $^1\Sigma^-$  state of the linear molecule correlates with the  $^1A_u$  state of the bent one and the orbital occupation would also be that expected. The orbitals of *trans* HCCH will now be considered briefly.

The possible molecular orbitals of *trans* HCCH are of the symmetries represented by  $a_g$ ,  $a_u$ ,  $b_g$ , and  $b_u$ ;  $a$  and  $b$  represent orbitals symmetric and antisymmetric to the twofold symmetry axis, and  $g$  and  $u$  those that are symmetric and antisymmetric to the center respectively. The four singlet excited states which correlate with the  $^1\Delta_u$  ( $^1A_u$  and  $^1B_u$ ),  $^1\Sigma^-$  ( $^1A_u$ ), and  $^1\Sigma^+$  ( $^1B_u$ ) states are:



[7] The orbitals to the right of the dotted line correlate with the  $\pi_u^3 \cdot \pi_g$  group of the linear

molecule. The two derived from the  $\pi_u^+.$  $\pi_u^-$  group of two electrons with the same spin are in all cases the  $a_u.b_u$  pair. The pair derived from the  $\pi_u.\pi_g$  set with the other spin differs in the four cases. In the first  ${}^1A_u$  state it is a  $b_u.a_g$  and both these orbitals are concentrated in the plane of the molecule. For the second  ${}^1A_u$  state both the orbitals ( $a_u.b_g$ ) are concentrated out of the plane of the molecule, the molecular plane being a node. Electrons in these two orbitals are clearly not suited to binding the protons in the molecular plane. With the two  ${}^1B_u$  states the orbital pairs are  $a_u.a_g$  and  $b_u.b_g$ . In both cases one orbital is concentrated in the molecular plane and the other has that plane as a node. This group will not be suited for binding the atoms in a planar arrangement. So the only state of this set of four which would be expected to provide strong binding for the atoms in a planar arrangement is the first  ${}^1A_u$  state. This correlates with the  ${}^1\Sigma^-$  state, which has just been discussed as providing a suitable basis for the binding, if a modification occurs which leads to the molecule becoming non-linear. The whole interpretation is therefore entirely self-consistent as between the electronic structures of the linear and bent forms (9), and also as between the electronic structure and the observed shape and dimensions.

#### THE NH<sub>2</sub> RADICAL

The lowest state of a linear NH<sub>2</sub> radical would be expected to be a  ${}^2\Pi$  state having the orbital occupation  $\sigma_g.\sigma_g.\sigma_u.\sigma_u.\pi_u^+.\pi_u^+.\pi_u^-$ . The orbitals occupied by the electrons of one spin form the set  $\sigma_g.\sigma_u.\pi_u^+.\pi_u^-$ , which will involve contributions from the 2s and three 2p orbitals of the nitrogen atom. Therefore it will be expected that there will be a tetrahedral group of four electrons round the nitrogen atom. The orbitals occupied by electrons of the other spin form the set  $\sigma_g.\sigma_u.\pi_u^+$ , which will involve contributions from the 2s and two 2p orbitals of the nitrogen atom. Therefore it will be expected that there will tend to be a triangular group of three electrons round the nitrogen atom. Neither of these sets is in fact suitable for binding the atoms in a straight line. However they are both well suited to binding the two protons in directions which are at about 110° with respect to one another. A suitable mutual orientation of the triangle and the tetrahedron can achieve this simultaneously. In fact, NH<sub>2</sub>, in the ground state, is found to be non-linear (8), though the angle (103½°) is smaller than would be expected from the above arguments. Presumably the explanation for this lies in the polarization of the electron cloud round the nitrogen atom as a result of the presence of the protons. Such polarization always tends to cause a reduction in interbond angles (6). The electronic structure then becomes  $a_1.\bar{a}_1.b_2.\bar{b}_2.a_1.\bar{a}_1.b_1$  (cf. Walsh (10)).

The two members of the degenerate pair of the  ${}^2\Pi$  ground state of linear NH<sub>2</sub> pass, on bending the molecule in a particular plane, into the configurations  $a_1.\bar{a}_1.b_2.\bar{b}_2.a_1.\bar{a}_1.b_1$  and  $a_1.\bar{a}_1.b_2.\bar{b}_2.a_1.b_1.\bar{b}_1$ . As has been said, the consequence of this, for the ground state, is that the set of four of one spin and the set of three of the other both tend to cause the HNH angle to be about 110°. Moreover, in the ground state, these effects operate in the same plane for both spin sets. In the excited state, the set of four electrons is similar, but the set of three would here tend to bend the molecule in a plane at right angles to that in which the set of four would tend to bend it. The experimental data indicate that the best compromise between these two effects results in the molecule having the lowest energy when it is linear.

#### THE HCO RADICAL

This is isoelectronic with the NO molecule, which, in the ground state, has the structure  $\sigma_1.\bar{\sigma}_1.\sigma_2.\bar{\sigma}_2.\pi_1^+.\pi_1^+.\pi_1^-.\pi_1^-.\sigma_3.\bar{\sigma}_3.\pi_2^+$ . One group of orbitals ( $\sigma_1.\sigma_2.\pi_1^+.\pi_1^-.\sigma_3.\pi_2^+$ ) is

that characteristic of an ordinary double bond,  $sp^3(\sigma\pi)$ , and the other group ( $\overline{\sigma_1}, \overline{\sigma_2}, \overline{\pi_1^+}, \overline{\pi_1^-}, \overline{\sigma_3}$ ) is that characteristic of an ordinary triple bond,  $sp^3(\sigma\pi^2)$ . On passing to a consideration of HCO it is clear that there is no direction from the carbon atom in which two electrons, one from each set, tend to be concentrated. An electron pair CH bond can however be achieved in the same manner as that discussed for the excited state of HCCH, namely by modifying the  $sp^3(\sigma\pi^2)$  group to one of  $sp^3p^\frac{1}{2}(\sigma\pi)$  so that the electrons not in the CO bond region are concentrated off the CO axis. However it would seem that, as with acetylene, this can only be done at the expense of weakening the CO bond; in this case, from a five-electron to a four-electron one. The observed length is 1.20 Å(2), which may be compared with 1.23 for  $H_2CO$ , 1.16 for  $CO_2$  and  $COS$ , and 1.13 for  $CO$ . It is not clear just how the observed lengths should be interpreted. The length is nearer to that in  $H_2CO$  than that in  $CO$  but it is not certain what allowance should be made for the absence of one proton and one electron compared with  $H_2CO$ . A possibility is that the electronic structure is intermediate between that in which the CH bond is an electron pair bond and the CO a four-electron one, and that in which the CH is essentially a one-electron bond and the CO a five-electron bond. This would explain why the CO bond is somewhat shorter than that in  $H_2CO$ , why the molecule is bent, but it would suggest that the CH might be somewhat weak. Information on this is not available.

Of the excited state observed by Herzberg and Ramsay (2) three structural features are known: (a) the molecule appears to be linear; (b) the CO bond length (1.18) is a little smaller than that in the ground state, though still considerably longer than that in  $CO$ ; (c) the CH valence vibration suggests a strong CH bond analogous to those in the ground states of  $HCN$  and  $HCCH$ .

The lowest state of linear HCO is a II state and therefore doubly degenerate. If the molecule is bent in a particular plane, these members of the doubly degenerate pair pass into the states  $a_1'^2.a_2'^2.a_3'^2.a_1''^2.a_4'^2.a_5'$  and  $a_1'^2.a_2'^2.a_3'^2.a_1''^2.a_4'^2.a_2''$  since the degenerate members of the II pair of orbitals pass into an  $a'$  and an  $a''$  orbital (cf. Walsh (10)). The situation appears to be somewhat similar to that in  $NH_2$ . That is, for the ground state, both sets of electrons have configurations tending to cause the molecule to bend in the same plane, while, for the excited state, the two sets have configurations tending to cause the molecule to bend in different planes, with the result that the best compromise (i.e. lowest energy) is achieved when the molecule is linear. In this linear configuration the structure of the set of five electrons having the same spin will probably be  $sp^3(\sigma\pi^2)$ , since this tends to concentrate an electron on the OC axis for binding the hydrogen atom. The other set must remain  $sp^3(\sigma\pi)$ . However, this will mean that, in the linear excited state, there will be a greater concentration of electrons in the CO bond region than in the bent ground state. This accounts for the CO bond being shorter in the excited than in the ground state, as is observed. However, the strength of the CH bond is surprising.

#### SUMMARY

From the above discussion it can be seen that considerations of the above kind, which involve transforming the molecular orbitals into orbitals more localized in particular, and if possible separate, regions of space, enable one to draw conclusions about the electron distribution in different states. As a consequence, certain properties of the ground and excited states can be understood. The application of these ideas has been most successful for the states of acetylene involved in the transition observed by Ingold and King. The interpretation of the states of  $NH_2$  and  $HCO$  is however less certain in the present state of our understanding of electron configurations.

## ACKNOWLEDGMENT

I wish to thank Dr. D. A. Ramsay for the conversation we had recently in Oxford about his work on HCO and NH<sub>2</sub>.

## REFERENCES

1. HERZBERG, G. Molecular spectra and molecular structure of diatomic molecules. D. Van Nostrand Co. Inc., New York. 1950. p. 553.
2. HERZBERG, G. and RAMSAY, D. A. Proc. Roy. Soc. (London), A, **233**, 34 (1956).
3. INGOLD, C. K. and KING, G. W. J. Chem. Soc. 2702, 2704, 2708, 2725, 2745 (1953).
4. LENNARD-JONES, J. E. J. Chem. Phys. **20**, 1024 (1952).
5. LINNETT, J. W. J. Chem. Soc. 275 (1956).
6. LINNETT, J. W. and MELLISH, C. E. Trans. Faraday Soc. **50**, 657 (1954).
7. LINNETT, J. W. and POE, A. J. Trans. Faraday Soc. **47**, 1033 (1951).
8. RAMSAY, D. A. J. Chem. Phys. **25**, 188 (1956).
9. ROSS, I. G. Trans. Faraday Soc. **48**, 973 (1952).
10. WALSH, A. D. J. Chem. Soc. 2260, 2266, 2288, 2296, 2301, 2306, 2318, 2321, 2325, 2330 (1953).
11. ZIMMERMANN, H. K. and VAN RYSELBERGHE, P. J. Chem. Phys. **17**, 598 (1949).

# THE NATURE OF FORMALDEHYDE IN ITS LOW-LYING EXCITED STATES<sup>1</sup>

G. W. ROBINSON AND V. ERDMANIS DiGIORGIO

## ABSTRACT

Long path length, high resolution spectra in the near ultraviolet of H<sub>2</sub>CO and D<sub>2</sub>CO at -78°C. have been obtained, and further strong evidence in support of a non-planar excited state is presented. The double-headed bands to the long wavelength side of the singlet-singlet system are shown to belong to the singlet-triplet transition. A vibrational analysis and partial rotational analysis shows the excited triplet state to be very similar to the excited singlet state. The larger C—O stretching frequency in the triplet state may characterize the multiplicity of these states in the simple aliphatic aldehydes and ketones. It is found that the C—O bond order in both states is very nearly 1.5, and striking similarities between the bonding in these states and the C—O bonding in formic acid are pointed out. The similarity between the singlet and triplet excited states may not extend to chemical behavior because of spin correlation rules, but there are no general reasons why the triplet state should be more reactive than the singlet.

## INTRODUCTION

Recently an extensive body of experimental evidence has indicated that a rather large difference in geometry exists between the ground and excited state structures of most simple polyatomic molecules. In many instances, even the symmetry properties of the equilibrium configurations are different. For example, acetylene, while linear in its ground state, has a non-linear *trans* configuration in its low-lying excited state (15). Ethylene has a planar structure in the ground state with a very high barrier for internal rotation, but in its low-lying <sup>1</sup>B<sub>1u</sub> state, as well as in its Rydberg states, the molecule exhibits an equilibrium configuration in which the CH<sub>2</sub> groups are no longer coplanar, and the barrier for internal rotation is more nearly that expected for a carbon-carbon single bond (37, 38). The molecules NH<sub>2</sub> (9, 29), HCO (14), and probably NO<sub>2</sub> (31) are bent in the ground state but linear in their low-lying excited states, while for CS<sub>2</sub> (16) and quite likely HCN and CO<sub>2</sub> (34, 35), the opposite holds true. The ammonia molecule has a low-lying electronic state which has a planar configuration (1), and formaldehyde, the topic of this paper, is non-planar in its low-lying excited states (3, 30).

Such changes in geometry are to be expected if the *bonding* electron configuration is changed by the electronic transition. For similar reasons, chemical properties are expected to be quite different in the ground as compared with the excited states of such molecules.

The formaldehyde molecule is an excellent testing ground for the study of these effects. An intimate knowledge concerning the low-lying excited states has intrinsic interest since the molecule is a simple example of a group of molecules on which a considerable number of photochemical investigations have been made (27). Furthermore, the long wavelength system is a prototype of *n*-π\* transitions which have attracted a great deal of theoretical and experimental interest. Finally, evidence presented here indicates that certain of the long wavelength absorption bands are associated with a singlet-triplet transition in the molecule, so that now the possibility exists of studying in detail the rotational-vibrational structure of a triplet state in a polyatomic molecule.

The first part of the paper discusses in a qualitative way the electronic, structural, and chemical properties of the low-lying excited states of formaldehyde based on the

<sup>1</sup>Manuscript received August 16, 1957.

Contribution from Department of Chemistry, The Johns Hopkins University, Baltimore, Maryland. This paper was presented at the Symposium on the Structure and Reactivity of Electronically-Excited Species held at the University of Ottawa, Ottawa, Canada, September 5 and 6, 1957.

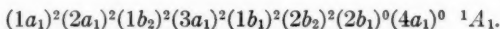
Work supported in part by the Office of Ordnance Research, U.S. Army, under Project No. TB2-0001 of Contract No. DA-36-034-ORD-2169.

results of recent spectroscopic investigations. The second part treats briefly the experimental techniques and gives some details concerning the more recent investigations of the singlet-singlet as well as the singlet-triplet systems.

#### THE GROUND STATE

The absence of inversion doubling in addition to the observed statistical weights of the rotational sublevels definitely shows that the ground state has the well-known planar Y-shaped structure of point group  $C_{2v}$  (12). In spite of the large amount of work on formaldehyde and its isotopically substituted species, zero-point vibrations cause some uncertainty to exist in the structural determination (7).

The electronic structure of the ground state has been discussed by Mulliken (23), McMurry and Mulliken (22), and more recently by Walsh (36). The 12 valence electrons are situated in the six lowest-lying molecular orbitals which in approximate order of energy are\*



Roughly, the nature of these orbitals with respect to molecular bonding is

$1a_1$	2s oxygen, non-bonding
$2a_1$	$\text{CH}_2$ , bonding
$1b_2$	$\text{CH}_2$ , bonding
$3a_1$	CO, $\sigma$ bonding
$1b_1$	CO, $\pi$ bonding
$2b_2$	$2p_y$ oxygen, lone pair non-bonding
$2b_1$	CO, $\pi$ antibonding
$4a_1$	CO, $\sigma$ antibonding.

The orbitals  $2b_1$  and  $4a_1$  are the first two excited orbitals.

Since the low-lying transitions in the molecule are localized in the CO bond, an alternative and fairly useful description regards formaldehyde as a perturbed linear molecule with symmetry axis along the CO direction. In the linear limit the  $a_1$  orbitals correlate with  $\sigma$ -orbitals as does  $1b_2$ . The pairs  $1b_1$  and  $2b_2$  as well as  $2b_1$  and  $3b_2$  (not listed) become degenerate in this limit to form  $\pi$ -orbitals. The correlation diagram will resemble very closely that given by Walsh (35) for HAB molecules except an additional low-lying  $\sigma$ -orbital must be added. The available electrons fill all orbitals up to and including the first  $\pi$ -orbital, which holds four electrons, and the electronic symmetry is thus  $^1\Sigma^+$  (perturbed).

#### THE NEAR ULTRAVIOLET TRANSITIONS

The lowest-lying electronic states in formaldehyde result from excitation of an electron from the non-bonding  $2b_2$  orbital into the  $2b_1$  excited orbital which is CO antibonding. A triplet state  $^3A_2$  and a singlet state  $^1A_2$  result. The presence of the antibonding  $\pi$ -electron in both states is expected to cancel approximately the bonding power of a bonding  $\pi$ -electron so that essentially a *three-electron bond results*. The CO linkage is expected to be about intermediate in length between a single and double bond. The HCH angle should be smaller† while the C—H distance should be larger than these same parameters in the ground state. The force constants and vibrational frequencies are well known to change in a similar way (3).

\*The notation throughout is that suggested by Mulliken (25).

†The opposite is actually observed.

The most interesting effect of the decreased bond order is the lack of stability of the planar equilibrium configuration in these excited states (3, 30), the out-of-plane angle lying about midway between zero degrees and the out-of-plane angle for a tetrahedral structure ( $55^\circ$ ). Thus, strictly speaking, the electronic wave functions do not transform as representations of  $C_{2v}$ , but this is still a good approximation since the molecular orbitals do not feel very strong perturbative effects of the hydrogens. For this reason and for simplicity of discussion we prefer to retain the  $C_{2v}$  nomenclature throughout. In those instances where effects arise owing to the slight deviation from  $C_{2v}$  symmetry, the appropriate  $C_s$  description will be given in parentheses.

Because of the non-planar equilibrium configuration of the excited states, inversion doubling occurs (3, 30). The extremely low observed barriers for inversion indicate that a very small amount of energy stabilization is gained through mixing of carbon  $2s$  and  $2p_z$  orbitals in the non-planar molecule. The doubling of vibrational levels, many of which are not observed, introduces some uncertainty into the determination of excited state fundamentals.

The chemical properties of these states are quite different from those of the ground state, but *there are no general reasons why the triplet state should be more reactive than the singlet* since both exhibit nearly identical electronic structures. Both have two free valences and may be appropriately described as diradicals. The conservation of electron spin angular momentum (13) may under certain conditions allow one species to be more reactive than the other. For example, it would be predicted that the triplet states, but not the excited singlet states, of aldehydes and ketones would react very rapidly with  $O_2$  ( $^3\Sigma_g^-$  ground state), since in the latter case the reaction intermediate can not be produced in its singlet ground state. Such reactions of excited polyatomic molecules have not been discussed to a great extent in the past, but may in certain cases be important as evidenced from recent work (28).

Transitions to the  ${}^1, {}^3A_2$  excited states can be observed in absorption, while emission has been observed only for the singlet-singlet transition. These transitions are formally forbidden under the strict  $C_{2v}$  selection rules but occur through mixing with nearby electronic states. The strong type-*B* ( $\perp$ ) bands are actually allowed by the non-planar selection rules (3) but could gain intensity through mixing with the  ${}^1B_2$  state at  $\sim 7$  ev.

The weaker type-*A* ( $||$ ) bands are of a kind  ${}^1A_1({}^1A') \rightarrow {}^1A_2({}^1A'')$  in the total vibronic sense and are strictly forbidden under the  $C_{2v}$  as well as the  $C_s$  selection rules. These transitions may gain intensity through mixing with a neighboring  $A_1$  state (3), but there is an alternative way of understanding this apparent anomaly.\* In the perturbed linear description of formaldehyde, three excited states would result from excitation of an electron to the first excited  $\pi$ -orbital,  $\Sigma^+$ ,  $\Sigma^-$ , and  $\Delta$ , the last probably lying lowest.

\*NOTE ADDED IN PROOF.—According to a paper soon to be published by J. A. Pople and J. W. Sidman, the mixing of  $A_1$  and  $A_2$  electronic states arises through a rotational-electronic interaction. That vibrationally-induced mixing does not occur to give a  $||$ -type zero-zero band is clear, since there is no fundamental with  $a_2$  symmetry. The viewpoint taken by us that formaldehyde can be considered a perturbed linear molecule with inherent mixing of the originally degenerate electronic states is exactly equivalent to the theory of Pople and Sidman. This was pointed out to us by Professor H. C. Longuet-Higgins in a private discussion. The interaction is the electronic analogue of the coriolis-type rotational-vibrational interactions which cause mixing of approximately degenerate vibrational states of different symmetries in polyatomic molecules. The mixing gives rise to vibrational angular momentum which can interact with the rotational angular momentum to produce anomalies in the subband positions and intensities. In the present problem, electronic orbital angular momentum about the C—O axis arises from the interaction. In the absence of spin the perturbation can be detected through intensity anomalies, but in the triplet state, Hund's case-a coupling can occur, and subband positions as well as intensities are affected. The as yet incomplete experimental observations seem to bear out these concepts quite well, but it should be remembered that the observed  $||$ -type bands could occur in an electric quadrupole transition.

The  ${}^1\Delta$  state correlates with the  ${}^1A_2$  state in the non-linear molecule, and the long wavelength spectrum could be described as a highly perturbed  ${}^1\Sigma^+ \leftrightarrow {}^1\Delta$  transition for which  $\Delta K = 0, \pm 1$ . Type-C ( $\perp$ ) bands were not observed even though some effort was made to find them. These would be Franck-Condon forbidden since they require excitation of  $b_2$  vibrations in the excited state.

The singlet-triplet transition becomes allowed probably through a spin-orbit perturbation. The orbital part of the perturbation operator transforms as representations of the rotational subgroup  $C_2$ , and because of symmetry, matrix elements are non-zero only for certain pairs of interacting electronic states (20). According to these selection rules, the  ${}^3A_2$  state can mix with  ${}^1B_1$ ,  ${}^1B_2$ , and  ${}^1A_1$  states through perturbations by the  $x$ ,  $y$ , and  $z$  components, respectively, of the spin-orbit operator. The observed bands resemble double-headed parallel bands having an irregular subband structure (see Fig. 3). Until a complete rotational analysis of these bands is obtained, however, the exact nature of the perturbing state will not be known. At present, it would appear that the  $z$  component of the perturbation operator is the one responsible for the mixing. This result is in disagreement with previous theoretical and experimental investigations (21).

#### EMISSION SPECTRUM

In formaldehyde, as in the higher aldehydes and ketones, the fluorescence and discharge emission spectra are identical (32), and their existence indicates the presence of relatively stable excited states in these molecules. It is well established (3, 30) that the triplet state is not involved to an observable extent in emission, and all observed bands have now been explained solely on the basis of the  ${}^1A_2 \rightarrow {}^1A_1$  transition. A good reproduction of the very sharp electrodeless discharge spectrum can be found in the literature (30). As in most polyatomic systems, transitions occur from only a few of the lowest-lying vibrational levels in the excited electronic state. In  $H_2CO$ , under the conditions of discharge tube excitation, emission occurs strongly from the vibronic ground level and also from the level in which one quantum of  $\nu_2'$  has been excited. Much weaker transitions occur from  $2\nu_2'$  and also from the  $0^-$  member of the first inversion doublet. The only ground state fundamentals which are involved are  $\nu_1''$  and  $\nu_2''$ , this being in qualitative agreement with the predictions of the Franck-Condon principle.

The vanishingly small emission intensity from the  $1^\pm$  inversion doublet in  $H_2CO$  is strong evidence in favor of predissociation in this region of the potential energy surface (4). This would set an upper limit to the dissociation energy,



A few remarks about the photolysis of  $H_2CO$  at 3650 Å (10) should be made. At dry ice temperature the absorption coefficient is negligible, the 3650 Å Hg line falling between two singlet-triplet bands. However, at temperatures where photochemical experiments must be performed to avoid polymerization, i.e.  $T > 100^\circ C.$ , there is considerable hot band structure from the  ${}^1A_1 \rightarrow {}^1A_2$  transition in this region. The analysis of the spectrum shows that the primary photochemical process would populate high rotational sublevels of  $0^+$  or  $0^+ + \nu_2'$ , these final states lying somewhat higher than 82 kcal./mole. It is therefore probable that the previously reported upper limit of 78 kcal./mole is slightly low. It should be mentioned that in these low-lying regions of the excited state

\*The  ${}^2A'$  state is probably the electronic ground state of CHO (35). The minimum additional energy needed to produce electronically excited CHO is about 10,000 cm.<sup>-1</sup> (14). See, however, Refs. (4) and (14).

potential energy surface, the predissociation is so relatively weak that the rotational fine structure in absorption can be resolved to at least  $0.1 \text{ cm}^{-1}$ . Even so, the transition probability for predissociation may still be a factor of  $10^4$  greater than that for the radiative transition. The intermediate dissociative state through which these predissociation processes occur is no doubt the first excited C—H antibonding triplet state since this state would correlate with the correct dissociation products.

The report (11) of two emitting levels, presumably  ${}^1A_2$  as well as  ${}^3A_2$ , in acetone is puzzling and may indicate that the complex nature of the potential surfaces in the larger molecules is more advantageous to triplet state population prior to emission.

#### THE ABSORPTION SPECTRUM

In order to resolve the rotational structure in the weak singlet-triplet transition, collision broadening and hot band overlapping must be reduced to a minimum. To accomplish this, multiple pass techniques at  $-78^\circ \text{ C}$ . were employed both for  $\text{H}_2\text{CO}$  and for  $\text{D}_2\text{CO}$ . The gain in resolution above that obtained under ordinary conditions is striking, the limitation apparently being instrumental resolving power, in this case 250,000.

A multiple pass cell similar to the one described by Bernstein and Herzberg (2) was capable of giving path lengths of up to about 50 meters. The cell was cooled with dry ice, and at this temperature, formaldehyde pressures of 30 mm. Hg could be used. This pressure furnishes more than the necessary meter-atmosphere absorbing path for observation of the singlet-triplet bands. The procedure is also the most convenient for observation of the singlet-singlet system, since it was found that the vapor pressure of the gas over the polymer kept at room temperature is adequate. The rate of polymerization on the mirror surfaces was finite yet sufficiently slow so as not to cause difficulties.

The lack of hot band structure not only aids in the rotational analysis but also permits an unambiguous vibrational analysis to be made. For example, the photographs shown in Fig. 1 leave no doubt as to the hot band nature of the  $\alpha$ -band at  $27021 \text{ cm}^{-1}$ , and also they conclusively show the singlet-triplet bands to be temperature insensitive.

#### *The Singlet-Singlet System*

The very nice work of Brand (3) on the vibrational analysis of the emission and absorption systems quite strongly indicates a non-planar excited state. At about the same time, the rotational analysis of the  $\alpha$ -band in emission was completed (30, 33) and showed a negative inertial defect,  $\Delta = I_C - I_A - I_B$ , in the excited state, proving beyond doubt the non-planar structure. The analysis will be published elsewhere (33), but the results are listed in Table I. The structural parameters, except for the HCH

TABLE I  
 $\text{H}_2\text{CO}$  PARAMETERS, GROUND AND  ${}^1A_2$  ELECTRONIC STATES

	Ground state (7, 17)	${}^1A_2$ state
$I_A$	1.792 a.m.u.- $\text{\AA}^2$	1.881 a.m.u.- $\text{\AA}^2$
$I_B$	13.015	14.985
$I_C$	14.864	16.767
$\Delta$	+0.057	-0.099
$\angle \text{HCH}$	$120^\circ$	$122^\circ$
$\text{C}=\text{O}$	$1.22 \text{ \AA}$	$1.32 \text{ \AA}$
$\text{C}-\text{H}$	$1.08 \text{ \AA}$	$1.09 \text{ \AA}$ (assumed)
Out-of-plane angle	$0^\circ$	$20^\circ$

angle and possibly the C—H distance, do lie about midway between  $Sp^2$  and  $Sp^3$  structures, but these must be considered tentative because of the lack of  $CD_2O$  data as well as the effect of zero-point vibrations.

The once puzzling  $127\text{ cm.}^{-1}$  spacing in the excited state is simply a result of inversion through a very low potential barrier. The first two intense  $\perp$ -bands of the absorption system are transitions from the ground vibronic state to the  $0^-$  and  $1^-$  members of the inversion doublets, and Brand assigned the weak  $\parallel$ -bands in this region to similar transitions involving  $0^+$  and  $1^+$ . Since high dispersion plates taken of the gas at  $T > 100^\circ\text{ C.}$  did not show clearly the presence of  $0^+$ , there was some doubt about this interpretation (30), but the validity of Brand's assignment is completely borne out by a study of the spectrum at  $T = -78^\circ\text{ C.}$  (see Fig. 2). The band marked  $0^+$ , highly overlapped by the  ${}^3P$ -branches of the  $A$ -band ( $0^-$ ), should have the same lower state as the  $A$ -band and the same excited state as the  $\alpha$ -band. A partial rotational analysis (19) shows that this is indeed the case. Incidentally, from these analyses an improved value of the out-of-plane bending fundamental in the ground state can be obtained (Table II). The barrier for inversion can be calculated to be  $\sim 650\text{ cm.}^{-1}$  (3) from the positions

TABLE II  
FUNDAMENTAL FREQUENCIES ( $\text{cm.}^{-1}$ ) IN THE GROUND AND EXCITED STATES OF  $H_2CO$  AND  $D_2CO$

	$H_2CO$			$D_2CO$		
	${}^1A_1$	${}^1A_2$	${}^3A_2$	${}^1A_1$	${}^1A_2$	${}^3A_2$
$0^-$	—	127	30	—	69	
$1^+$	—	530	537	—	387	
$1^-$	—	951	779	—	669	448
$2^+$	—		1171	—		889
$2^-$	—			—		
$\nu_1$	2780	2851		2056	2077	
$\nu_2$	1738	1177	1251	1700	1174	1249
$\nu_3$	1503	1321		1106		1086
$\nu_4$	1164.7	683	643	938		
$\nu_5$	2874			2160		
$\nu_6$	1280	899		990	735	

of the doublets, but the value is expected to be very approximate because of the inadequacies of the simple theories for low barriers. This is evidenced by the lack of agreement between barriers computed from  $CH_2O$  and  $CD_2O$  data. The absence of higher inversion doublets than  $1^\pm$  in both  $H_2CO$  and  $D_2CO$  is caused by the fact that above the barrier the vibrational wave functions are approximately orthogonal with those in the ground electronic state.

In addition to  $\nu_2'$  and the inversion doublets, the frequencies  $\nu_1'$ ,  $\nu_3'$ , and  $\nu_4'$  also occur weakly in combinations with these. Therefore all fundamentals except  $\nu_5'$  may be approximately obtained and these are given in Table II along with the ground state values. The C—O stretching frequency  $1177\text{ cm.}^{-1}$  is very nearly the same as that observed for C—O in carboxylic acids, and may indicate similar three-electron bonding configurations in the two cases. The otherwise unexplained large value of  $\nu_1'$  gives further evidence of this.\*

\*The similarity between the properties of the CHO bonding in the  ${}^1A_2$  state of formaldehyde and the ground state of formic acid is quite striking:

	$H_2CO\ ({}^1A_2)$	$HCOOH$
C—H stretch	$2855\text{ cm.}^{-1}$	$2943\text{ cm.}^{-1}$
C—O stretch	$1177\text{ cm.}^{-1}$	$1180\text{ cm.}^{-1}$
C—O bond length	$1.32\text{ \AA}$	$1.312\text{ \AA}$

The "three-electron" nature of the C—O bond in  $HCOOH$  is further evidenced by recent microwave work (18).

PLATE I

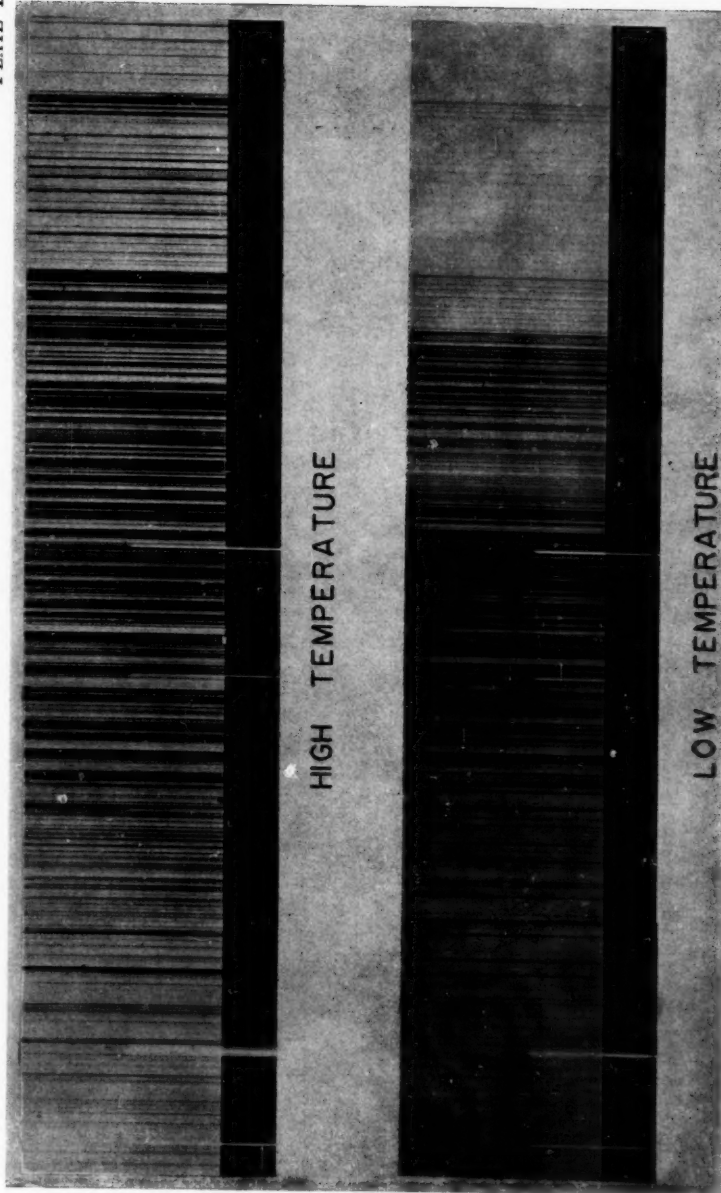


FIG. 1.  $\text{H}_2\text{CO}$  bands at  $\lambda 3700$ . (a) Spectrum taken at  $120^\circ \text{C}.$ ,  $0.1$  meter-atm. path. (b) Spectrum taken at  $-78^\circ \text{C}.$ ,  $0.8$  meter-atm. path. Notice that the fairly strong  $\perp$ -band ( $\alpha$ -band) has lost much of its intensity at  $-78^\circ \text{C}.$  Directly beneath it is found a weak, temperature insensitive singlet-triplet band.

PLATE II

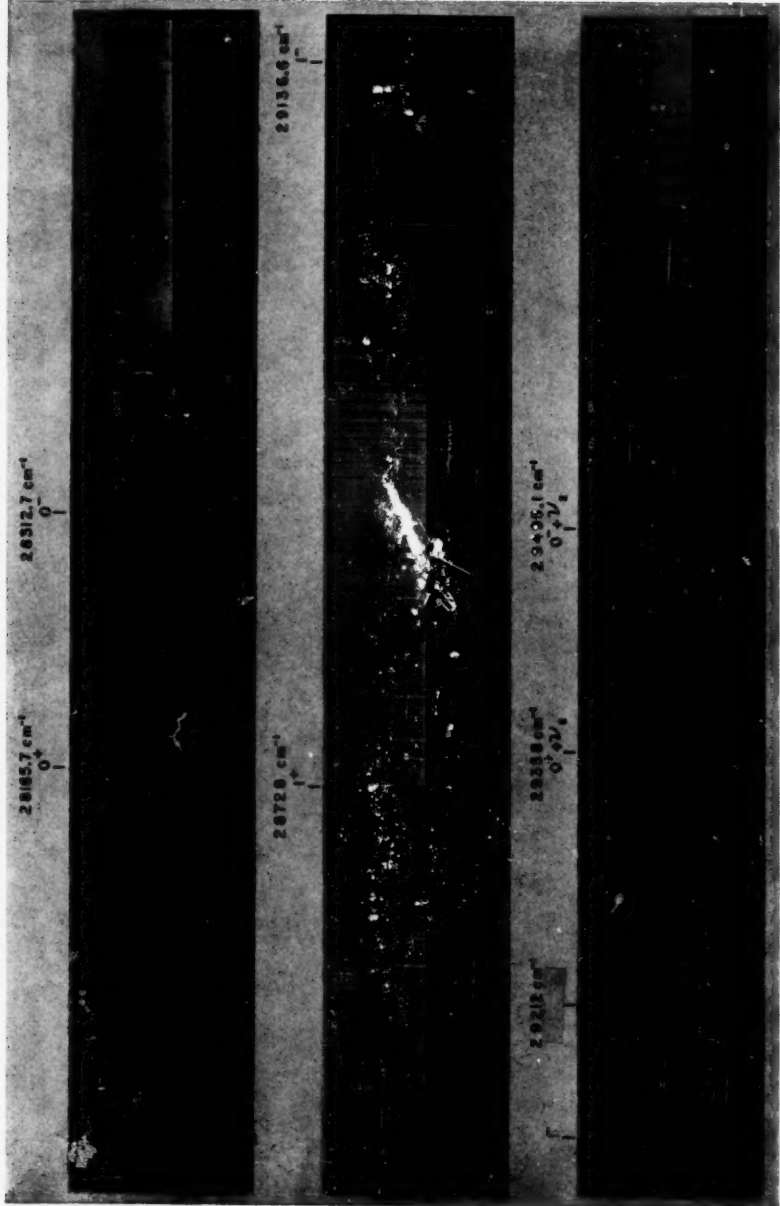


FIG. 2. Inversion doubling in the  ${}^1\text{A}_2$  state of  $\text{H}_2\text{CO}$ . The spectrum was obtained at  $-78^\circ\text{C}$ , 0.2 meter-atm. path. The unmarked parallel band at  $29212 \text{ cm}^{-1}$  probably involves excitation of the  $\nu_6$  fundamental in the excited state.

PLATE III

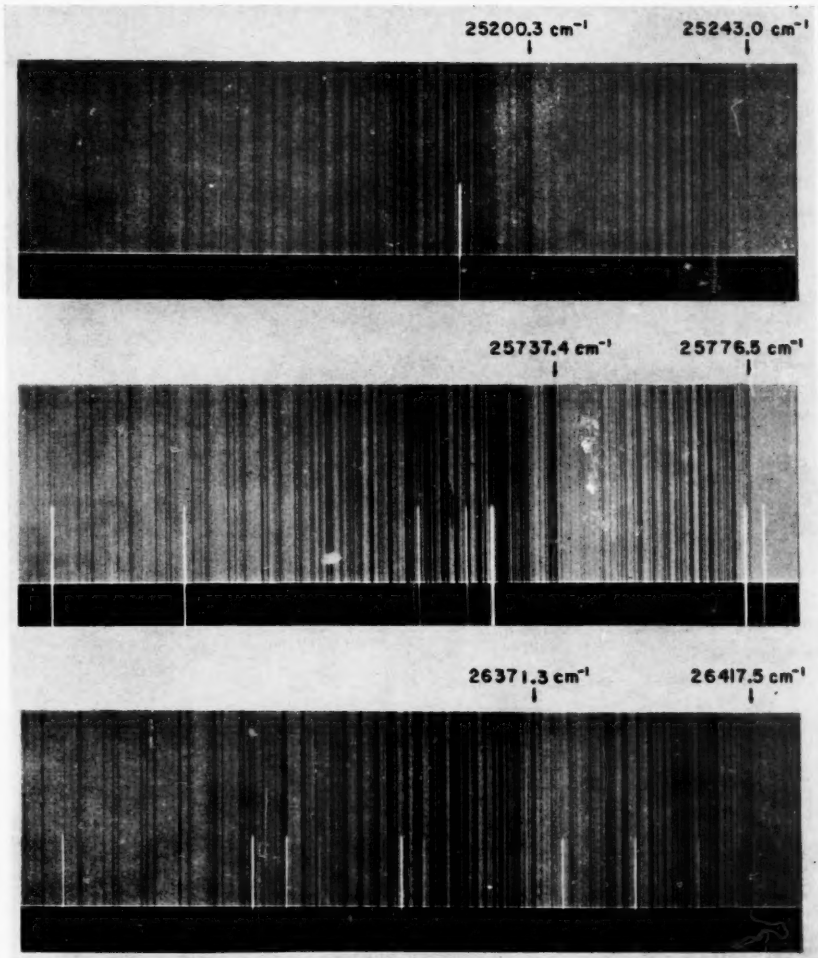


FIG. 3. Some singlet-triplet bands of H<sub>2</sub>CO. Spectra taken at -78° C., 0.8 meter-atm. path. The doublet spacing does not change with vibrational excitation nor with isotopic substitution.

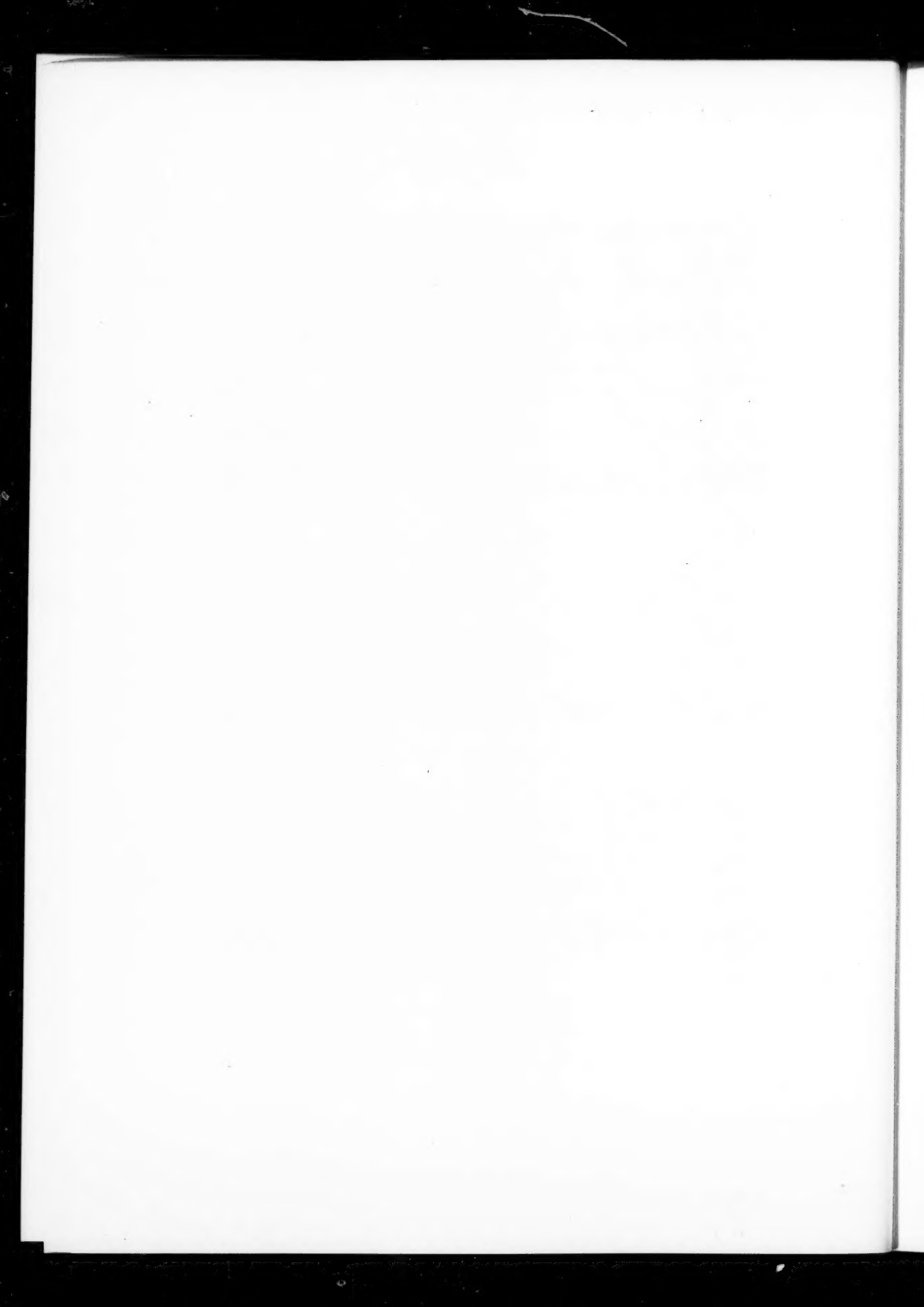


Table III lists all bands and their assignments. Since the vibrational pattern can be easily followed down to  $\lambda = 2500 \text{ \AA}$  it is safe to say that *the spectrum in the region  $2500 \text{ \AA} < \lambda < 3700 \text{ \AA}$  is caused by a single electronic transition.*

TABLE III  
VIBRONIC BANDS OF SINGLET-TRIPLET TRANSITIONS OF H<sub>2</sub>CO AND D<sub>2</sub>CO

Assignment	H <sub>2</sub> CO			D <sub>2</sub> CO		
	$\lambda_{\text{air}}$	$\nu_{\text{vac}}$	Int.	$\lambda_{\text{air}}$	$\nu_{\text{vac}}$	Int.
0 <sup>+</sup>	3967.10	25200.2	m	3948.11	25321.4	w
1 <sup>+</sup>	3884.32	25737.3	s	3879.53	25769.0	s
2 <sup>+</sup>	3790.94	26371.2	m	3814.14	26210.8	m
0 <sup>+</sup> + $\nu_2$	3775.15	26481.5	w	3762.47	26570.7	w
1 <sup>+</sup> + $\nu_3$				3722.60	26855.3	w
1 <sup>+</sup> + $\nu_2$	3704.56	26986.1	m	3700.43	27016.2	s
4 <sup>+</sup>				3689.06	27099.5	ww
2 <sup>+</sup> + $\nu_2$	3618.98	27624.2	w	3641.32	27454.7	s
0 <sup>+</sup> +2 $\nu_2$	3604.52	27735	w	3597.52	27789.0	w
1 <sup>+</sup> + $\nu_2$ + $\nu_3$				3558.22	28095.9	w

#### The Singlet-Triplet Transition

The singlet-triplet bands with origins at approximately 3950 Å in H<sub>2</sub>CO and D<sub>2</sub>CO have been known for some time, being observed independently by Brand (3), Cohen and Reid (5), Coon (6), and Robinson (30). A reproduction of three of these bands in the H<sub>2</sub>CO spectrum is given in Fig. 3. The bands are temperature insensitive (Fig. 1), are different in appearance from the usual parallel or perpendicular bands (compare Fig. 2), and do not fit into the established vibronic pattern of the 3650 Å system. These facts indicate that the bands belong to another electronic system, almost certainly to  ${}^1A_1 \rightarrow {}^3A_2$  since they are weak and lie to the long wave-length side of the *lowest predicted singlet-singlet transition*.

High resolution (resolving power = 250,000) photographs were obtained of the H<sub>2</sub>CO and D<sub>2</sub>CO systems at high and low temperatures. In all, nine D<sub>2</sub>CO and eight H<sub>2</sub>CO bands were found, many of which lay under hot band structure on the high temperature plates. The bands are "double-headed", *the doublet spacing being about  $40 \pm 3 \text{ cm}^{-1}$  in all bands of both isotopic species*. Since the magnitude of the spacing does not change on isotopic substitution, and is not highly dependent on vibrational excitation, this is strong evidence that it arises from an electronic, and not a rotational or vibrational origin. The doubling probably is caused by "case-a" coupling (13) of electron spin and partially quenched electron orbital angular momentum along the "symmetric top" axis. The electronic angular momentum then couples with the component of rotational angular momentum in this direction to give the observed irregular subband structure. The rotational analysis of the bands is in progress and thus far it has been possible to establish that the constant  $\frac{1}{2}(B+C)$  for the  ${}^3A_2$  state is very nearly identical but slightly larger than that of the  ${}^1A_2$  state. This shows, as expected, that the C—O bond distance is quite similar in the two states.

The observed bands measured from the low frequency member of the doublet are listed, together with their vibrational assignments, in Table III. Some temperature sensitive bands of H<sub>2</sub>CO, have been observed by Coon (6) at very long path-lengths and moderate dispersion. The observed effects of inversion doubling show that the excited state is non-planar, and from Coon's bands, some of which are analogous to the  $\alpha$ -band in the singlet-singlet system, one can calculate the inversion splitting to be

$$\begin{array}{ll} 0^+ - 0^- & 30 \text{ cm.}^{-1} \\ 1^+ - 1^- & 242 \text{ cm.}^{-1} \end{array}$$

which means that the barrier for inversion is somewhat higher in the triplet state than in the singlet state.

The triplet state fundamentals which have been observed are tabulated in Table II along with the singlet state values. The C—O stretching fundamental  $\nu_2'$  is about 75  $\text{cm.}^{-1}$  larger than  $\nu_2'$  in the excited singlet state. Since this difference is expected to remain fairly constant among the aliphatic aldehydes and ketones, it may provide a good check as to the multiplicity of the excited state in the many instances where only the coarse structure of the spectrum can be resolved.

In conclusion we would like to thank Professor G. H. Dieke for the use of the 21-ft. grating spectrograph on which much of this work was done. We also wish to extend our appreciation to Mr. Maclyn McCarty for helping with the calculations.

#### REFERENCES

1. BENEDICT, W. S. *Phys. Rev.* **47**, 641 (1935).
2. BERNSTEIN, H. J. and HERZBERG, G. *J. Chem. Phys.* **16**, 30 (1948).
3. BRAND, J. C. D. *J. Chem. Soc.* 858 (1956).
4. BRAND, J. C. D. and REED, R. I. *J. Chem. Soc.* 2386 (1957).
5. COHEN, A. D. and REID, C. *J. Chem. Phys.* **24**, 85 (1956).
6. COON, J. B. Symposium on Molecular Structure and Spectroscopy, Columbus, Ohio. 1957.
7. DAVIDSON, D. W., STOICHEFF, B. P., and BERNSTEIN, H. J. *J. Chem. Phys.* **22**, 289 (1954).
8. DIEKE, G. H. and KISTIAKOWSKY, G. B. *Phys. Rev.* **45**, 4 (1934).
9. DRESSLER, K. and RAMSAY, D. A. Symposium on Molecular Structure and Spectroscopy, Columbus, Ohio. 1957.
10. GORIN, E. J. *J. Chem. Phys.* **7**, 256 (1939).
11. GROH, H. J., JR., LUCKEY, G. W., and NOYES, W. A., JR. *J. Chem. Phys.* **21**, 115 (1953).
12. HERZBERG, G. Infrared and Raman spectra of polyatomic molecules. D. Van Nostrand Co., Inc., New York. 1945.
13. HERZBERG, G. Spectra of diatomic molecules. D. Van Nostrand Co., Inc., New York. 1950.
14. HERZBERG, G. and RAMSAY, D. A. *Proc. Roy. Soc. (London)*, A, **233**, 34 (1955).
15. INGOLD, C. K. and KING, G. W. *J. Chem. Soc. (London)*, 2702 (1953).
16. KLEMAN, B. Symposium on Molecular Structure and Spectroscopy, Columbus, Ohio. 1956.
17. LAWRENCE, R. B. and STRANDBERG, M. W. P. *Phys. Rev.* **83**, 363 (1951).
18. LERNER, R. G., DAILEY, B. P., and FRIEND, J. P. *J. Chem. Phys.* **26**, 680 (1957).
19. McCARTY, M., JR. Unpublished work.
20. MCCLURE, D. S. *J. Chem. Phys.* **17**, 665 (1949).
21. MCCLURE, D. S. *J. Chem. Phys.* **17**, 905 (1949).
22. McMURRY, H. L. and MULLIKEN, R. S. *Proc. Natl. Acad. Sci.* **26**, 312 (1940).
23. MULLIKEN, R. S. *J. Chem. Phys.* **3**, 564 (1935).
24. MULLIKEN, R. S. *Revs. Modern Phys.* **14**, 204 (1942).
25. MULLIKEN, R. S. *J. Chem. Phys.* **23**, 1997 (1955).
26. NOYES, W. A., JR. Unpublished work.
27. NOYES, W. A., JR., PORTER, G. B., and JOLLEY, J. E. *Chem. Revs.* **56**, 49 (1956).
28. PORTER, G. B. *J. Am. Chem. Soc.* **79**, 1878 (1957).
29. RAMSAY, D. A. *J. Chem. Phys.* **25**, 188 (1956).
30. ROBINSON, G. W. *Can. J. Phys.* **34**, 699 (1956).
31. ROBINSON, G. W. Symposium on Molecular Structure and Spectroscopy, Columbus, Ohio. 1957.
32. ROBINSON, G. W. Unpublished work.
33. ROBINSON, G. W. and BENEDICT, W. S. Manuscript in preparation.
34. WALSH, A. D. *J. Chem. Soc.* 2266 (1953).
35. WALSH, A. D. *J. Chem. Soc.* 2288 (1953).
36. WALSH, A. D. *J. Chem. Soc.* 2306 (1953).
37. WILKINSON, P. G. *Can. J. Phys.* **34**, 643 (1956).
38. WILKINSON, P. G. and MULLIKEN, R. S. *J. Chem. Phys.* **23**, 1895 (1955).

# EXCITED STATES OF THE MOLECULAR IONS OF HYDROGEN FLUORIDE, HYDROGEN IODIDE, WATER, HYDROGEN SULPHIDE, AND AMMONIA<sup>1</sup>

D. C. FROST AND C. A. McDOWELL

## ABSTRACT

The ionization of the molecules of hydrogen fluoride, hydrogen iodide, water, hydrogen sulphide, and ammonia, by essentially monoenergetic electrons, has been studied in a mass spectrometer. The various excited states of the molecular ions of these compounds have been observed and the corresponding energy levels of the ions have been measured. The results are interpreted in terms of the electronic structures of these molecules as given by molecular orbital theory.

## INTRODUCTION

The analysis of visible or ultraviolet spectra yields information about the excited states of molecules and free radicals. Almost all of our present data have been obtained in this way. And though a vast amount of such information is available, little of this refers to saturated molecules. There are obvious reasons why this is so, and it will undoubtedly be some time before sufficient spectroscopic data are available to permit the excited states of many saturated molecules to be evaluated. It is now possible, however, to use electron impact methods to obtain some of this much desired information. Recently a new electron impact technique (5, 6) has been used to study the ionization of molecules. This method utilizes essentially monoenergetic electrons with an energy spread of  $\sim 0.1$  ev., and so it is now possible to determine accurately the energies of the excited states of many molecular ions. These data are now available for molecular ions of nitrogen (6), methane (7), the alkyl halides (7), and several other molecules. In this paper we shall describe some new results for the molecular ions of hydrogen fluoride, hydrogen iodide, water, hydrogen sulphide, and ammonia.

Besides yielding values for the energy levels of the excited states of the various molecular ions, the present studies are of interest for other reasons. They enable the molecular orbital theories of the electronic structures of these molecules to be assessed. Furthermore, it is known from self-consistent field molecular orbital theories (8, 13, 14, 17, 21), that Koopmans' theorem indicates to a good approximation that the energy of an electron in a given molecular orbital is equal to minus the ionization potential referring to the removal of an electron from that orbital; and it follows that once the several ionization potentials of a molecule are known, the energies of the various molecular orbitals are likewise known. The determination of the energies of the molecular orbitals of molecules is important, for by this means there are available further data for the more detailed assessment of the reliability of self-consistent field molecular orbital calculations. As was mentioned earlier, optical spectroscopic studies have not so far yielded much of the desirable information for saturated compounds, and it is perhaps for such molecules that the present studies are particularly important in that now there have become available data which cannot as yet be provided by any other experimental method.

## EXPERIMENTAL

The Metropolitan-Vickers M.S.I. mass spectrometer, modified as previously described (6, 7), was used to determine the ionization potentials. As the tube of this instru-

<sup>1</sup>Manuscript received October 8, 1957.

Contribution from the Department of Chemistry, University of British Columbia, Vancouver 8, B.C., Canada.  
This paper was presented at the Symposium on the Structure and Reactivity of Electronically-Excited Species held at the University of Ottawa, Ottawa, Canada, September 5 and 6, 1957.

ment and the inlet system are largely made of glass, a new gas introduction system had to be provided so that we could study hydrogen fluoride. The new inlet system was made from copper and it extended through a metal-glass seal down into the ionization chamber. At the extremity of the copper inlet tube a small teflon tube was added to provide insulation between the inlet tube and the ion source. A diagram of the inlet system is shown in Fig. 1. It will be noted that only metal gas valves with teflon diaphragms were used.

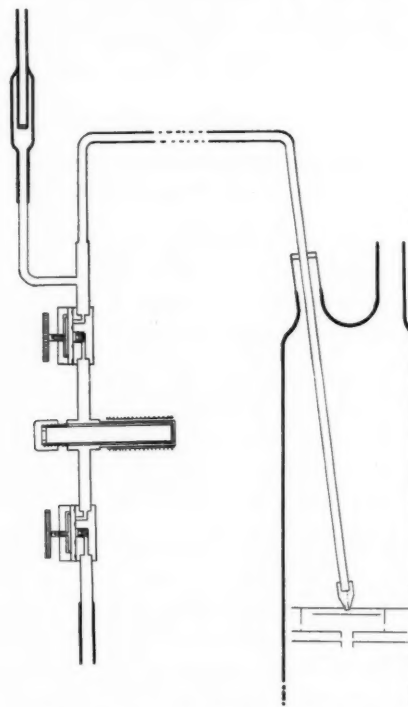


FIG. 1. All-metal inlet system for introducing hydrogen fluoride into mass spectrometer.

The hydrogen fluoride was prepared by heating a dry sample of potassium hydrogen fluoride. The reaction vessel was a copper-lined brass cylinder which could be heated electrically (see Fig. 1).

The hydrogen iodide was prepared by the combination of hydrogen and iodine vapor over a platinized asbestos catalyst in a high vacuum system, the gas being purified by repeated fractionation.

The other compounds used were prepared by normal chemical methods and highly purified before use.

Krypton was used as a calibration gas for all the studies. The ionization potential of krypton was taken as  $112914.5 \text{ cm}^{-1}$  (1) or  $13.997 \text{ v.}$ , taking  $8066.83 \text{ cm}^{-1}$  equal to  $1 \text{ v.}$  (2).

#### EXPERIMENTAL RESULTS

The ionization efficiency curve for hydrogen fluoride is shown in Fig. 2. This shows clearly that there are two ionization processes, one producing the  $\text{HF}^+$  ion in its ground

state, and the other the ion in its first excited state. The averages of many determinations of the two ionization potentials with their standard deviations are given in Table I. Fig. 3 shows the ionization efficiency curve for the formations of the  $\text{HI}^+$  ion from hydro-

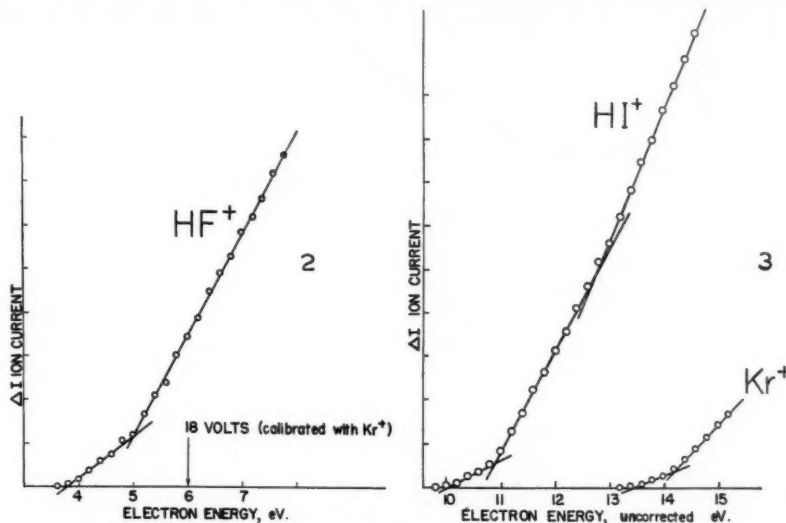


FIG. 2. The ionization efficiency curve for the formation of the  $\text{HF}^+$  ion.  
 FIG. 3. The ionization efficiency curve for the formation of the  $\text{HI}^+$  ion.

TABLE I  
 VERTICAL IONIZATION POTENTIALS OF HYDRIDES

Compound	Ionization potential (v.)	Electronic state of ion
Hydrogen fluoride	$15.77 \pm 0.02$	${}^3\Pi_{g/2,1/2}$
	$16.91 \pm 0.10$	${}^3\Sigma$
Hydrogen iodide	$10.44 \pm 0.04$	${}^3\Pi_{g/2}$
	$11.14 \pm 0.04$	${}^3\Pi_{1/2}$
	$13.27 \pm 0.10$	${}^3\Sigma$
Water	$12.60 \pm 0.01$	${}^2B_1$
	$14.35 \pm 0.03$	${}^2A_1$
	$16.34 \pm 0.06$	${}^2B_2$
Hydrogen sulphide	$10.45 \pm 0.03$	${}^2B_1$
	$12.46 \pm 0.03$	${}^2A_1$
	$14.18 \pm 0.04$	${}^2B_2$
	$16.07 \pm 0.05$	?
Ammonia	$10.40 \pm 0.02$	${}^2A_1$
	$15.31 \pm 0.04$	${}^2E_{g/2,1/2}$

gen iodide. Here it is evident that there are three ionization processes. We shall show later that the first two are observed because the spin-orbital components of the  ${}^3\Pi$  ground state of the  $\text{HI}^+$  ion have been resolved. The other process refers to the formation of the  ${}^3\Sigma$  first excited state of the  $\text{HI}^+$  ion. The values of the ionization potentials for hydrogen iodide are given in Table I. Fig. 4 shows the ionization efficiency curve for the water molecule. The three ionization processes result from the formation of the  $\text{H}_2\text{O}^+$  ion in its ground  ${}^2B_1$  state, and its two excited states, the  ${}^2A_1$  and  ${}^2B_2$  states. The corresponding ionization potentials are given in Table I. In the case of hydrogen sulphide,

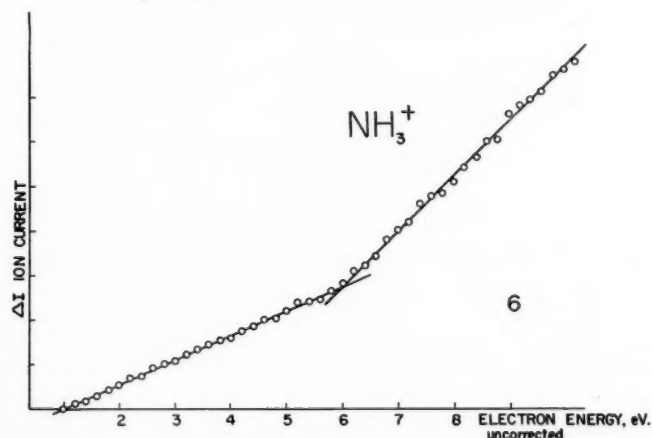
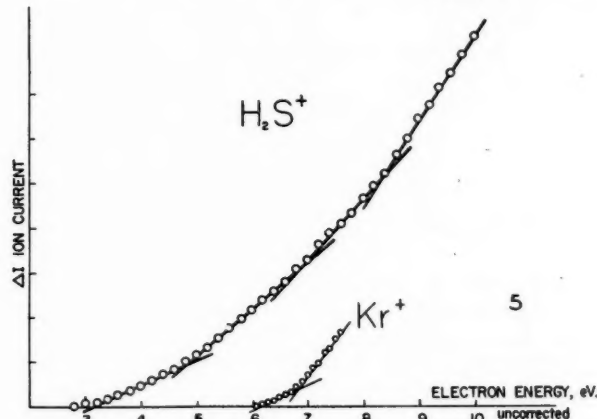
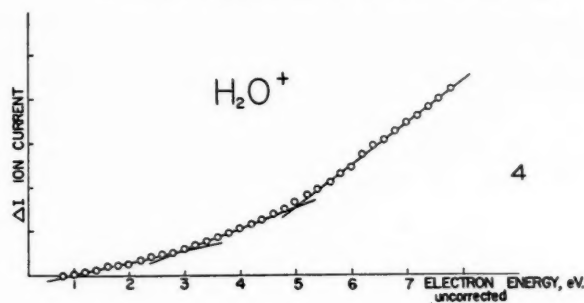


FIG. 4. The ionization efficiency curve for the formation of the  $\text{H}_2\text{O}^+$  ion.  
 FIG. 5. The ionization efficiency curve for the formation of the  $\text{H}_2\text{S}^+$  ion.  
 FIG. 6. The ionization efficiency curve for the formation of the  $\text{NH}_3^+$  ion.

for which the ionization efficiency curve is shown in Fig. 5, besides the processes due to the formation of the  $\text{H}_2\text{S}^+$  ion in its  ${}^2\text{B}_1$  ground state and its  ${}^2\text{A}_1$  and  ${}^2\text{B}_2$  excited states, an extra ionization process is observed. The origin of this is not clear. The four observed

ionization potentials are listed in Table I. Fig. 6 shows the ionization efficiency curve for ammonia. Here there are clearly two ionization processes. The first refers to the formation of the  $\text{NH}_3^+$  ion in its  ${}^2A_1$  ground state, and the second to the formation of the  $\text{NH}_3^+$  ion in its first excited  ${}^2E$  state. The corresponding ionization potentials are listed in Table I.

## DISCUSSION

### *Hydrogen Fluoride*

The electronic structure of hydrogen fluoride can be represented by the molecular orbital formula



in which the orbitals are written in order of decreasing ionization energy from left to right. The first ionization potential which we have observed to occur at 15.77 ev. will refer to the removal of an electron from the  $(2p\pi)$  orbital to form an  $\text{HF}^+$  ion in its  ${}^2\Pi_1$  state. This state has two components,  ${}^2\Pi_{3/2}$  and  ${}^2\Pi_{1/2}$ , but for fluorine compounds our apparatus cannot resolve these (3). The first excited state of the  $\text{HF}^+$  ion will be formed by the removal of an electron from the  $(2p\sigma)$  orbital of equation (1) to yield the  ${}^2\Sigma$  state of the ion. The process which we have observed to occur at 16.91 ev. obviously is due to the formation of the  $\text{HF}^+$  ion in its first  ${}^2\Sigma$  excited state.

Recently Johns and Barrow (12) reported the observation of the ultraviolet spectra of the  $\text{DF}^+$  and  $\text{HF}^+$  ions. They concluded that the observed bands were due to transitions between a lower *A*-state and an upper *B*-state. The *A*-state was assumed to arise from the combination  $\text{H}^+$  (or  $\text{D}^+$ ) +  $\text{F}(^2P)$  and was assumed to be the  $A \ {}^2\Sigma^+$ -state. These spectroscopic studies indicate that the  $A \ {}^2\Sigma^+$ -state of the  $\text{HF}^+$  ion is 16.88 ev. above the ground  ${}^1\Sigma_g^+$  state of hydrogen fluoride. Our results indicate clearly that the ionization potential which we observe at 16.91 v. is due to the formation of the  $\text{HF}^+$  ion in its first excited state, i.e. the  $A \ {}^2\Sigma^+$  state, and the ionization potential due to the formation of the  $\text{HF}^+$  ion in its ground state is 15.77 v. The ground state we take to be the  ${}^2\Pi_1$  state in agreement with the molecular orbital formula [1] and with the spectroscopic data for the molecular ions  $\text{HCl}^+$ ,  $\text{HI}^+$ , and  $\text{HBr}^+$ , all of which are known (10) to have  ${}^2\Pi_1$  ground states. It follows, therefore, that bands due to the transitions  $A \ {}^2\Sigma^+ - X \ {}^2\Pi_1$  and  $B \ {}^2\Sigma^+ - X \ {}^2\Pi_1$  are still to be found for the  $\text{DF}^+$  and  $\text{HF}^+$  ions. Our results indicate that the former bands should be found in the near infrared.

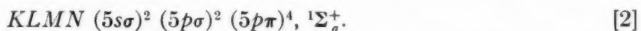
Hydrogen fluoride, being a simple molecule with only 10 electrons, has recently been the subject of several extensive theoretical studies. Mueller (16) has reported the results of both a molecular and an atomic orbital treatment, while Kastler (13) has made a very detailed study of this compound from the valence bond standpoint. A self-consistent field molecular orbital treatment using Roothaan's (21) method has been carried out by Duncan (3), and more recently by Hamano (9). Hurley (11) has recently given a detailed discussion of the ground state of this molecule using the method of "atoms in molecules".

With the exception of Duncan's work, nearly all the other authors have chosen either the dissociation energy of the hydrogen fluoride molecule or its dipole moment as data for assessing the accuracy of their calculations. Above, we have mentioned that ionization potentials may be more useful data for comparing the validity of theoretical calculations. Duncan calculated that the first ionization potential of hydrogen fluoride should be 11.3 v. This is very much less than our experimentally determined value of 15.77 v. An examination of Duncan's calculation shows that the method used is probably

not the best one, and a detailed treatment of the hydrogen fluoride molecule recently carried out by Dr. J. A. R. Cope of this laboratory, using a method analogous to Hurley's "atoms in molecules" treatment, leads to a theoretical value for the first ionization potential which is in very good agreement with the experimental one.

### *Hydrogen Iodide*

The hydrogen iodide molecule may be represented by the molecular orbital equation



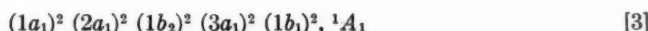
From this equation it follows that it would require least energy to remove an electron from the non-bonding ( $5p\sigma$ ) orbital, thus forming an ion with the structure . . . ( $5p\sigma$ ) ( $5p\pi$ )<sup>3</sup> and so presumably in a  $^2\Pi_4$  state with spin-orbital components  $^2\Pi_{3/2}$  and  $^2\Pi_{1/2}$ . Some years ago Price (19) obtained spectroscopic evidence to substantiate this, and also the fact that of the two spin-orbital components, the  $^2\Pi_{1/2}$  was the upper one. Price observed a Rydberg series for hydrogen iodide with a limit at 89,130 cm.<sup>-1</sup>, i.e. there is an ionization potential at 11.049 v. This limit Price assigned to the  $^2\Pi_{1/2}$  level of the  $\text{HI}^+$  ion. From considerations of the magnitude of the spin-orbital coupling separations of halogen atoms, Price concluded that the  $^2\Pi_{3/2}$  level of the  $\text{HI}^+$  ion should lie about 0.66 ev. below the  $^2\Pi_{1/2}$  level, i.e. the ionization potential referred to this level should be  $11.049 - 0.66 = 10.39$  v. Price was unable to find any Rydberg series which could be satisfactorily established as going to this limit. Our experimental results, shown as the ionization efficiency curve for the  $\text{HI}^+$  ion in Fig. 3, do, however, clearly indicate the formation of the  $\text{HI}^+$  ion in both the  $^2\Pi_{3/2}$  and the  $^2\Pi_{1/2}$  states, as well as an excited state above these. The separation of the spin-orbital components,  $^2\Pi_{3/2}$  and  $^2\Pi_{1/2}$ , of the ground state of the  $\text{HI}^+$  ion we find to be 0.70 ev., a value which is in excellent agreement with that estimated by Price (19), and also with the value we observed earlier for the separation of the spin-orbital components  $^2E_{3/2}$  and  $^2E_{1/2}$  of the ground state of the  $\text{CH}_3\text{I}^+$  ion (3). That this interpretation of the first two processes in the ionization efficiency curve of the  $\text{HI}^+$  ion is correct is supported by the photoionization studies of Watanabe (24), who found the first ionization potential of HI to be  $10.38 \pm 0.02$  v. The value which we observed in our experiments is  $10.44 \pm 0.04$  v.

The third ionization process observed at 13.27 v. for the  $\text{HI}^+$  ion is obviously to be ascribed to the formation of this ion in its  $^2\Sigma$  excited state. This state would arise by the removal of an electron from the ( $5p\sigma$ ) orbital of HI to form the  $\text{HI}^+$  ion with the electronic structure . . . ( $5p\sigma$ )<sup>1</sup> ( $5p\pi$ )<sup>4</sup>. It will be recalled that we observed the formation of the  $\text{HF}^+$  ion in the corresponding state. It is of interest to compare the value of 13.27 v. for the ionization potential of HI, referring to the production of the  $\text{HI}^+$  ion in its  $^2\Sigma$  excited state, with that of 11.22 v. observed for the formation of the  $\text{CH}_3\text{I}^+$  ion in its  $^2A_1$  excited state. Both these states arise by the removal of an electron from the  $\sigma$ -orbitals concentrated mainly along the X—I bond. It is, therefore, to be expected that the corresponding ionization potentials will vary as binding energies of the electrons in these X—I  $\sigma$ -orbitals. The dissociation energies of the X—I bonds can be taken as a rough measure of the binding energies of the electrons in the  $\sigma$ -type orbitals under discussion. The dissociation energy of the hydrogen iodide molecule is 70.44 kcal. mole<sup>-1</sup> (9), whereas the dissociation energy of the C—I bond in methyl iodide is 52.6 kcal. mole<sup>-1</sup> (15). This difference reflects that found for the ionization potentials referring to the removal of an electron from the  $\sigma$ -type orbitals along the X—I bonds in these two compounds.

### Water

The ionization efficiency curve for the water molecule is shown in Fig. 4. Here there are obviously three different ionization processes occurring at  $12.60 \pm 0.01$ ,  $14.35 \pm 0.03$ , and  $16.34 \pm 0.06$  v. It is interesting to note that in early experiments Sugden and Price (22), using a simple ionization tube, found evidence for ionization processes in water at similar voltages. These they attributed to the formation of the water molecule in various excited states. Their technique was, however, rather simple, and as they did not have any means of making mass analysis, they could not be certain that the different ionization processes observed did, in fact, refer wholly to the formation of excited states of the molecular ion species.

The electronic structure of the water molecule in terms of molecular orbital theory can be written as (18, 4):



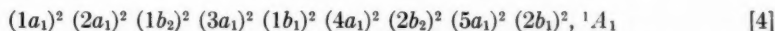
Recent self-consistent field molecular orbital calculations by Ellison and Shull (4) have shown that this is the correct order of the orbitals and that the  $(1b_1)$  is a pure  $2p_z$  orbital of oxygen, the main bonding orbitals being the  $(1b_2)$  and  $(3a_1)$  orbitals, though  $(2a_1)$  has some bonding character also.

This molecular orbital formula for water indicates that the first three states of the  $H_2O^+$  ion should be the  ${}^2B_1$ ,  ${}^2A_1$ , and  ${}^2B_2$  states. These we assume to be those associated with the ionization processes observed at 12.6, 14.35, and 16.34 v. This identification is supported by Ellison and Shull's calculations, which give the energies of the  $(1b_1)$ ,  $(3a_1)$ , and  $(1b_2)$  orbitals for a H—O—H valence angle of  $105^\circ$  as  $-11.79$ ,  $-13.20$ , and  $-18.35$  ev., values which are in reasonable agreement with those which we have determined experimentally. The present assignment agrees with that suggested earlier by Sugden and Price (22). It should perhaps be pointed out that there is no doubt about the accuracy of the identification of the ground state of the  $H_2O^+$  ion as a  ${}^2B_1$  state. It may also be noted that the presently reported value for the first ionization potential of the water molecule is in excellent agreement with the spectroscopic value of  $12.56 \pm 0.01$  v. obtained by Price (20) from a Rydberg series in the far ultraviolet spectrum of water.

### Hydrogen Sulphide

Hydrogen sulphide has the same symmetry, i.e.  $C_{2v}$ , as the water molecule and it was of interest to see if the excited states of the molecular ion bore any relation to those observed for the water molecule. The ionization efficiency curve for the formation of the  $H_2S^+$  ion is shown in Fig. 5. This curve is reminiscent of that for the water molecule, though the uppermost ionization process was not observed in that case.

The electronic structure of hydrogen sulphide can be represented by the following molecular orbital formula:



The first 10 electrons are in orbitals which approximate to the minor shell  $1s^2 2s^2 2p_z^2 2p_y^2 2p_z^2$  structure of the sulphur atom. The last eight, in valence shell molecular orbitals, correspond to the last eight electrons in the molecular orbital formula for the water molecule.

From this equation it follows that the first three ionization processes observed for the  $H_2S^+$  ion are due to the formations of the  ${}^2B_1$ ,  ${}^2A_1$ , and  ${}^2B_2$  states of the ion. These we

identify with the ionization potentials observed at  $10.45 \pm 0.03$ ,  $12.46 \pm 0.03$ , and  $14.18 \pm 0.04$  v. It is of interest to note that Sugden and Price (22) observed ionization processes in hydrogen sulphide at 10.5, 12.2, and 14.0 v. and gave a similar interpretation. Again there is no doubt about the accuracy of our identification of the first ionization potential. This refers to the removal of an electron from the  $2p_y$  orbital of the sulphur atom. Our value of 10.45 v. is to be compared with the spectroscopic value of 10.47 v. obtained by Price (20) and the result of 10.46 v. obtained by Watanabe (24) from photoionization experiments.

### Ammonia

The ionization efficiency for ammonia (Fig. 6) shows the presence of an excited state of the  $\text{NH}_3^+$  ion at 4.91 ev. above the first ionization potential. The identification of the two states of the  $\text{NH}_3^+$  ion is apparent from the molecular orbital formula for ammonia. Ammonia belongs to the symmetry group  $C_3$ , and so its molecular orbital formula is:



The first ionization potential observed at  $10.40 \pm 0.02$  v. obviously refers to the energy required to remove an electron from the non-bonding ( $3a_1$ ) orbital to form a  $\text{NH}_3^+$  ion in its  $^2A_1$  ground state, assuming that the  $C_3$  symmetry is retained in the ion. This value of 10.4 v. for the first ionization potential of ammonia is confirmed by the photoionization work of Watanabe (24), though Walker and Weissler (23) report that their photoionization studies showed that ionization set in at 10.07 v.

The second ionization process which we observed to occur at  $15.31 \pm 0.02$  v. is identified as being due to the formation of the first excited state of the  $\text{NH}_3^+$  ion, i.e. the  $^2E$  state, by the removal of an electron from the ( $1e$ ) degenerate orbital of the ammonia molecule. This ( $1e$ ) orbital of ammonia is the main bonding orbital and it spans the three N—H bonds. It is interesting to note that Walker and Weissler (23) found evidence for a second ionization process setting in a little above 15 ev. They were, of course, not able to identify the cause of this, but our results at least show that at this energy there lies the first excited state of the  $\text{NH}_3^+$  ion and so Walker and Weissler's observation is at least partly due to the formation of this excited state of the  $\text{NH}_3^+$  ion.

### ACKNOWLEDGMENT

We wish to thank the National Research Council of Canada for grants in support of this work.

### REFERENCES

1. BECKER, R. F. and GOUDSMIT, S. Atomic energy states. McGraw-Hill Book Co., Inc., New York. 1932.
2. DUMOND, J. W. M. and COHEN, E. R. Phys. Rev. **82**, 555 (1951).
3. DUNCAN, A. B. F. J. Am. Chem. Soc. **77**, 2107 (1955).
4. ELLISON, F. O. and SHULL, H. J. Chem. Phys. **23**, 2348 (1955).
5. FOX, R. E., HICKAM, W. M., KJELDAAS, T., JR., and GROVE, D. J. Phys. Rev. **84**, 859 (1951).
6. FROST, D. C. and McDOWELL, C. A. Proc. Roy. Soc. A, **232**, 227 (1955).
7. FROST, D. C. and McDOWELL, C. A. Proc. Roy. Soc. A, **241**, 194 (1957).
8. HALL, G. G. and LENNARD-JONES, Sir J. Proc. Roy. Soc. A, **202**, 155 (1950).
9. HAMANO, H. J. Chem. Soc. Japan, **77**, 985 (1956).
10. HERZBERG, G. Spectra of diatomic molecules. D. Van Nostrand Co. Inc., New York. 1950.
11. HURLEY, A. Proc. Phys. Soc. A, **69**, 301 (1956).
12. JOHNS, J. W. C. and BARROW, R. F. Nature, **179**, 374 (1957).
13. KASTLER, D. J. chim. phys. **50**, 556 (1953).
14. KOOPMANS, T. Physica, **1**, 104 (1933).
15. McDOWELL, C. A. and COX, B. C. J. Chem. Phys. **20**, 1496 (1952).
16. MUELLER, C. R. J. Chem. Phys. **19**, 1498 (1951).

17. MULLIKEN, R. A. J. Am. Chem. Soc. **77**, 887 (1955).
18. MULLIKEN, R. A. J. chim. phys. **46**, 497, 675 (1949).
19. PRICE, W. C. Proc. Roy. Soc. A, **167**, 216 (1938).
20. PRICE, W. C. J. Chem. Phys. **4**, 147 (1936).
21. ROOTHAN, C. C. J. Revs. Modern Phys. **23**, 69 (1951).
22. SUGDEN, T. M. and PRICE, W. C. Trans. Faraday Soc. **44**, 108 (1948).
23. WALKER, W. C. and WEISSLER, G. L. J. Chem. Phys. **23**, 1540 (1955).
24. WATANABE, K. J. Chem. Phys. **26**, 542 (1957).

# THE ELECTRONIC SPECTRA OF CRYSTALLINE TOLUENE, DIBENZYL, DIPHENYLMETHANE, AND BIPHENYL IN THE NEAR ULTRAVIOLET<sup>1</sup>

ROBERT COFFMAN<sup>2</sup> AND DONALD S. MCCLURE<sup>3</sup>

## ABSTRACT

The electronic absorption spectra of single crystals of toluene, dibenzyl, diphenylmethane, and biphenyl have been photographed at 20° K. using polarized light in the range 3000 to 2500 Å. The fluorescence spectrum of biphenyl has also been examined. This is the first time that the excited states of biphenyl analogous to the  $B_{2u}$  state of benzene have been observed. The main features of the spectra are similar for all four compounds, and the differences may be understood in terms of the weak coupling between the benzene rings of the "double molecules".

## I. INTRODUCTION

According to current theory the  $\pi$ -electronic states of the dibenzyl molecule should closely resemble those of the toluene molecule. Any slight differences would have to be ascribed to a mechanical or electronic coupling between the rings in dibenzyl. The electronic component of this coupling should be small because the  $-\text{CH}_2-\text{CH}_2-$  link between the benzene rings is not a conjugative link. Greater differences are expected between toluene and diphenylmethane since only one  $-\text{CH}_2$  group separates the rings in the latter. Finally with no intervening "insulating group", as in biphenyl, the spectra may differ greatly.

This series of molecules has been investigated before (2), but only with the aid of solution spectra, and no clear results have been obtained. We have obtained the spectra of single crystals at 20° K. with polarized light. Under these conditions a wealth of detail is observed. In the present article, the experimental results are described, and partial vibrational analyses of the spectra are given. One of us has interpreted further details of the spectra in terms of the electronic and vibrational coupling energies between the benzene rings. This work is reported in the article following this one (12).

An especially interesting discovery made during the course of this work is the existence of a weak, sharp transition in biphenyl. In previous studies of this molecule, only strong continuous absorption regions have been found.

## II. EXPERIMENTAL

The polarized spectra of single crystals were obtained using a large Hilger quartz prism instrument. The details have been described previously (10). The spectra were observed at 20° K. At 77° K. they are quite broad and very few details may be resolved. Helium temperatures would probably have given sharper lines than 20° K., and would permit a more precise analysis, which would have been advantageous in several cases.

The biphenyl crystals were flakes grown from the vapor. They had the cleavage plane, the *ab* plane, most fully developed. From the order of interference determined with a quartz wedge in the polarizing microscope, and the value  $\Delta n = 0.097$  for the birefringence on the *ab* plane (18), the thickness of the crystals was found. They were usually between

<sup>1</sup>Manuscript received August 16, 1957.

Contribution from the Department of Chemistry and Chemical Engineering, University of California, Berkeley, California. This paper was presented at the Symposium on the Structure and Reactivity of Electronically-Excited Species held at the University of Ottawa, Ottawa, Canada, September 5 and 6, 1957.

Work supported in part by the Office of Naval Research under contract N6-ori-211-III.

<sup>2</sup>Present address: General Electric Co., Electronic Park, Syracuse, New York.

<sup>3</sup>Present address: RCA Laboratories, Princeton, New Jersey.

2 and  $5 \mu$  thick, and several millimeters across. A complete structure analysis of the biphenyl crystal does not exist. It is known to have the space group  $C_{2h}^5$  with two molecules per unit cell, and to have the long molecular axis nearly coinciding with the *c* axis (3, 15). Since  $\beta = 94.5^\circ$ , the long axis is nearly perpendicular to the *ab* plane. We therefore expected to be able to observe only the short-axis polarized transitions. We found a polarization ratio of  $I_a/I_b = 1.0$  for short-axis transitions. The two molecules per unit cell must be nearly at right angles to each other if we are correct. Krishnan (9) and Dhar (4), using diamagnetic anisotropy and X-ray analysis respectively, obtained values for the molecular orientation parameters which would result in a polarization ratio  $I_a/I_b = 1/3.89$  for short-axis transitions and would give appreciable intensity along the *a* axis for long-axis transitions. Our results are in disagreement with theirs in both respects.

Dibenzyl crystals were grown by cooling a melt held between quartz plates pressed together. Large areas having many crystals all aligned in the same way could be made by remelting most of the crystal and letting it grow again from a small unmelted bit. The value of the birefringence was obtained as approximately 0.13 by measuring the retardation and thickness on some moderately thick crystals grown in the above manner. This number could then be used for the thinner crystals, whose thickness could not be measured directly. The crystal plane developed in these crystals is the *ab* plane. A very precise X-ray structural study has been made by Jeffrey (8). The theoretical polarization ratio for a short-axis transition in the molecule is  $I_a/I_b = 0.65$ . No large polarization effects were therefore expected, or found.

Crystals of toluene were grown by allowing the liquid to solidify between quartz plates in a temperature gradient established over a liquid nitrogen bath. Diphenylmethane crystals were grown by allowing the melt to solidify between quartz plates. Its melting point is  $26^\circ\text{C}$ ., but crystals grew well at  $20^\circ\text{C}$ . The diphenylmethane crystals were examined in the polarizing microscope and an area showing uniform orientation of the dielectric axes and low retardation was masked off and used for the experiments. The toluene crystals were examined in the dewar at  $77^\circ\text{K}$ . between crossed polaroids. A magnified image of the crystal mass was projected onto a white card, and a large uniformly oriented area was selected. The dielectric axes of this area were oriented vertically and horizontally and the image of the crystal was projected onto the slit of the spectrograph. The areas used were about one millimeter across.

The vapor spectra of these molecules are very complex. That of biphenyl is continuous (1). We examined the vapor spectrum in a 3 meter path after finding the sharp crystal spectrum, but could detect no sharp absorption bands. The spectrum of toluene vapor reported by Ginsburg and Robertson (7) was helpful in the analysis of the crystal spectrum. Robertson and Matsen (17) have reported the spectrum of diphenylmethane, but few details were given. No reports of the spectrum of dibenzyl vapor have been published to our knowledge.

### III. RESULTS AND INTERPRETATION

Microphotometer tracings of the absorption spectra obtained are shown in Figs. 1-4. There is no marked dichroism arising from intermolecular interactions, but in the cases of toluene and diphenylmethane there are strong differences between the oppositely polarized spectra arising from molecular orientation. Several plates of the biphenyl spectrum appeared to show a crystal dichroism in the first strong band amounting to  $4\text{ cm}^{-1}$ . This is probably real, but since the bands are about  $10\text{ cm}^{-1}$  wide it is hard to be certain of it.

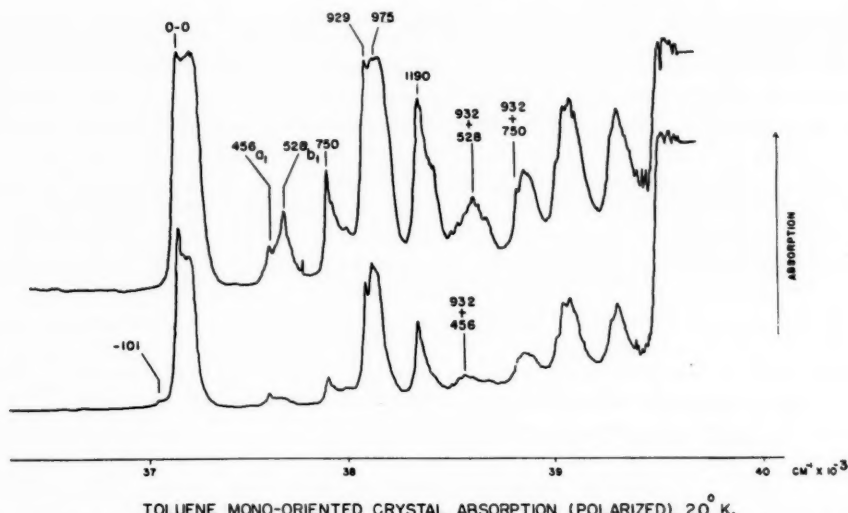


FIG. 1. Polarized absorption of oriented toluene crystals at 20° K. Some of the more important features are noted on the microphotometer tracing and others may be identified by reference to Table I.

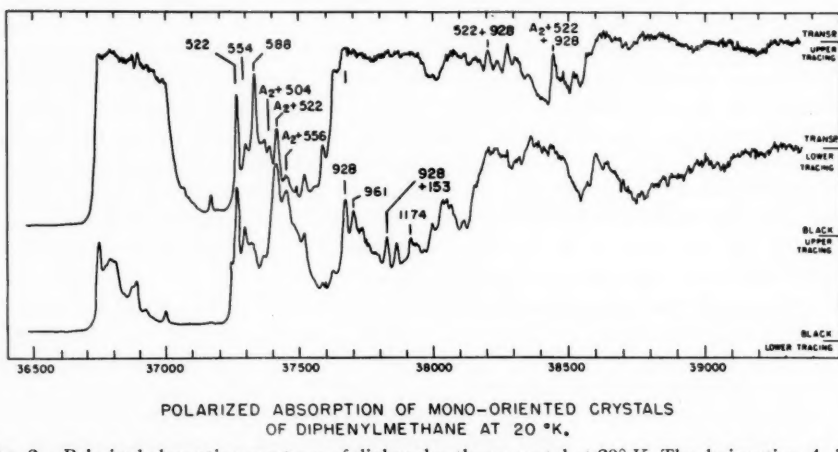


FIG. 2. Polarized absorption spectrum of diphenylmethane crystal at 20° K. The designation  $A_2$  in the figure is to be interpreted as  $2\Delta$ , and equals approximately  $150 \text{ cm}^{-1}$ .

#### A. Toluene

The observed lines and their interpretation are given in Table I and the spectrum is illustrated in Fig. 1. The agreement with Ginsburg's analysis of the vapor (7) is excellent if one takes the first strong band of the crystal spectrum,  $37155 \text{ cm}^{-1}$ , as the 0-0 band. This is  $322 \text{ cm}^{-1}$  to the red of the 0-0 band of the vapor. There is a weak band at  $37054$ ,  $101 \text{ cm}^{-1}$  to the red of the 0-0 band. This is undoubtedly the same sort of band as is found in crystalline benzene, naphthalene, phenanthrene, etc., and probably serves as the origin of fluorescence, although the fluorescence spectrum was not studied. Other than this, there

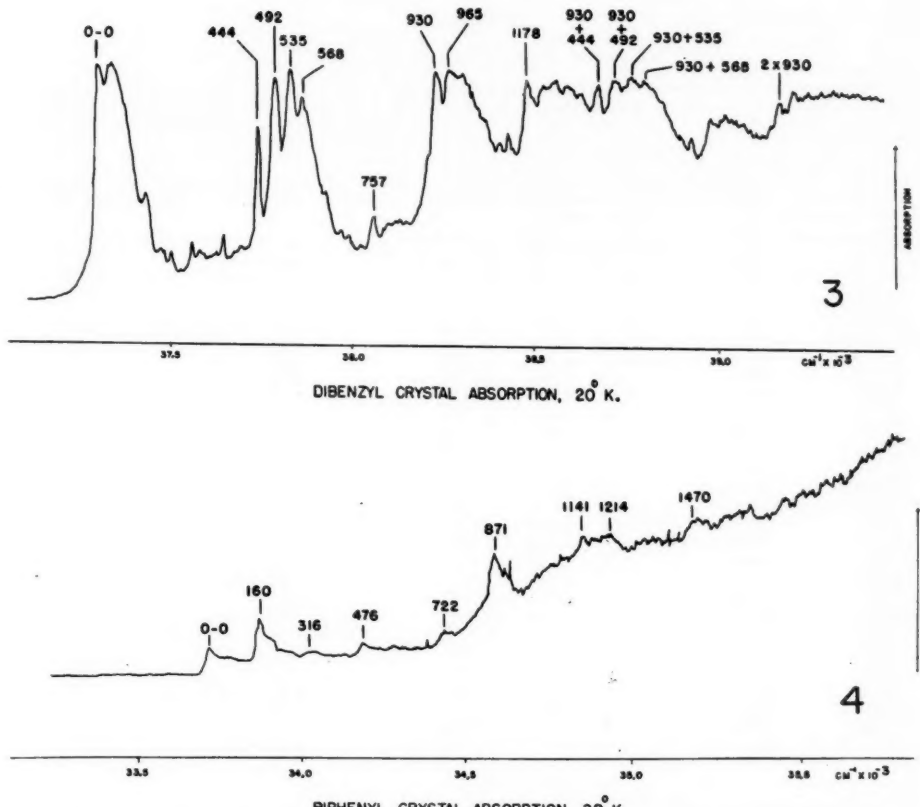


FIG. 3. Absorption spectrum of dibenzyl crystal at 20° K., *ab* plane. The polarized spectrum is the same along the *a* and *b* axes.

FIG. 4. Absorption spectrum of single biphenyl crystal, *ab* plane, at 20° K. The spectra are identical along the two axes except as noted in the text. The background appearing at higher frequencies is probably the long-axis transition giving rise to the well-known continuous absorption of this molecule.

are no distinct crystal effects. The 0-0 band components are at the same energy, so the intermolecular resonance energy is very small.

The most interesting feature of the spectrum is the region where the vibrations analogous to  $e_{2g}$  of benzene appear. The 456 and 528  $\text{cm}^{-1}$  peaks respectively represent the  $a_1$  and  $b_1$  components of this motion in point group  $C_{2v}$ . The  $a_1$  vibrational addition should be polarized in the same way as the 0-0 band, along the short axis in the molecular plane, while the  $b_1$  band should be polarized along the ring-methyl direction, or long axis. These facts enable one to determine approximately how the toluene molecules are oriented in the crystal. The oriented gas model (fixed, but non-interacting molecules) can be used with confidence here because of the demonstrated absence of strong intermolecular resonance. The polarization of the 528  $\text{cm}^{-1}$  band shows that the long axis is confined to one direction in the projection of the crystal plane we have studied. The polarization of the 456  $\text{cm}^{-1}$  band shows that the short axis prefers the same direction by a factor of about 2. At least two molecules and probably four are needed per unit cell.

TABLE I

## POLARIZED ABSORPTION SPECTRUM OF A TOLUENE CRYSTAL AT 20° K.

The frequency of each band is given, with a probable error of 3 cm.<sup>-1</sup>, in column 1. The intensity in column 2 is indicated by vs = very strong, s = strong, m = medium, w = weak, vw = very weak, sh = shoulder on a stronger band. Most bands are polarized about twice as strongly in one of the crystal directions as in the other. This is indicated by 0 in column 3. The departures from the 2:1 ratio are indicated by + and -. Frequency differences from the 37155 cm.<sup>-1</sup> band are given in column 4, and the analysis of these differences in column 5. The vibration frequencies used in column 5 are from Ginsburg's work (see Ref. 7). The error given in column 6 is positive if the assigned combination is greater than the observed frequency. Positive deviations could be caused by anharmonicity.

$\nu$ (cm. <sup>-1</sup> )	Int.	Pol.	$\Delta\nu$ (cm. <sup>-1</sup> )	Interpretation	Error
37054	vvw	—	-101	Crystal effect	
37155	vs	0	0	0-0, $^1A_1 \rightarrow ^1B_1$	
37209	vs	0	46	Lattice vib.	
37612	w	0	457	456 $a_1$ ( $e_{2g}$ )	-1
37682	m	+	527	528 $b_1$ ( $e_{2g}$ )	1
37907	m	0	750	751 $a_1$	1
37920	w(sh)	0	765		
37988	w(sh)	0	833		
38083	s	0	929	932 $a_1$	3
38130	s	0	975	965 $a_1$	-10
38345	ms	0	1190	1189 $a_1$	-1
38418	w(sh)	+	1263	528+751	16
38506	w(sh)	0	1350		
38540	w(sh)	0	1385	932+456	3
38575	w(sh)	0	1420	965+456	1
38622	m	+	1467	932+528	-7
38680	w	0	1525		
38835	w(sh)	0	1680	932+751	3
38870	m	0	1715	965+751, 1189+528	1, 2
38890	w(sh)	0	1735	751+528+456	0
39025	w(sh)	0	1870	2×932	-6
39060	w(sh)	0	1905	932+456+528	11
39090	m	0	1935	1189+751	5
39280	w(sh)	0	2125	1189+932	-4
39310	m	0	2155	1189+965	-1

Much fine structure appears on the plates, and also in the tracings. This may be evidence for excitation of the methyl group motions.

*B. Dibenzyl*

Of the three double molecules the spectrum of this one, illustrated in Fig. 3, should bear the most similarity to that of toluene, and should therefore be the easiest to understand. Table II shows the positions of the bands observed and the remarkable similarity of the prominent vibrational intervals to those of toluene. Since no dichroism was observed at the 0-0 band, 37296 cm.<sup>-1</sup>, there must be very little intermolecular resonance. The fluorescence of this crystal could not be observed, possibly because traces of stilbene could not be entirely removed. The stilbene absorption, however, is too weak to interfere with the dibenzyl absorption. A few very weak bands to the red of the 0-0 band remain uninterpreted. Again, of chief interest is the region from 450 to 600 cm.<sup>-1</sup> from the origin.

The appearance of four bands instead of two in this region is direct evidence for either vibrational or electronic coupling between the rings. The analysis of these bands appears in the following paper.

The totally symmetric frequencies in the rest of the spectrum are very close to those of toluene, as expected. There is evidence that some of these bands are doubled, an indication of vibrational coupling between rings. The 930 cm.<sup>-1</sup> peak is as sharp as the 929 peak in toluene, so there is probably very little interaction here. But the analogue of the toluene

TABLE II  
ABSORPTION SPECTRUM OF A DIBENZYL CRYSTAL AT 20° K.

The intensities are designated as in Table I. The frequency differences of column 3 are measured from 37296 cm.<sup>-1</sup>, and are analyzed in column 4. Frequencies in parentheses followed by t are toluene frequencies.

$\nu$ (cm. <sup>-1</sup> )	Int.	$\Delta\nu$ (cm. <sup>-1</sup> )	Interpretation	$\nu$ (cm. <sup>-1</sup> )	Int.	$\Delta\nu$ (cm. <sup>-1</sup> )	Interpretation
36870	VVV			38300	s	1004	
36895	VVV			38322	VW	1026	
37184	VVVW			38338	VW	1042	
37296	VS	0	0-0	38363	VW	1067	
37334	VS	38	0+38	38382	VW	1086	
37365	M	69		38398	VW	1102	
37426	M	130	0+130	38425	VW	1129	
37462	M	166	0+130+38	38435	VW	1139	
37500	M	204		38455	VW	1159	
37530	VW	234		38474	S	1178	$a_g$ (1189t)
37554	W	258		38492	W(sh)	1196	
37565	VW	269		38522	S	1226	
37598	VW	302		38556	S	1260	
37642	W	346		38590	S	1294	
37673	VW	377		38625	S	1329	
37684	VW	388		38675	S	1379	930+444
37698	VW	402		38720	S	1424	930+492
37740	S	444		38765	S	1469	930+535
37788	S	492	(456t)	38795	S	1499	930+568
37831	S	535		38872	M (sh)	1576	
37884	S	568	(528t)	38894	M	1598	
37926	M	630		38925	M	1629	
37970	VW	674		38970	M	1674	
37985	VW	689		39015	M	1719	
38020	VW	724		39032	M	1736	
38053	W	757	$a_g$ (751t)	39046	M	1750	
38087	VW	791		39062	M	1766	
38115	W	819		39082	M	1786	
38140	VW	844		39134	M	1838	
38200	M	904		39160	S	1864	2×930
38226	S	930	$a_g$ (932t)	39200	S	1904	930+959
38265	S	959	$a_g$ (965t)				

975 cm.<sup>-1</sup> peak appears to be split into 959 and 1004 cm.<sup>-1</sup>. The analogue of 1190 cm.<sup>-1</sup> in toluene appears to be 1178+1196 cm.<sup>-1</sup> in dibenzyl. The 750 cm.<sup>-1</sup> peak is sharp and not split in dibenzyl.

### C. Diphenylmethane

The spectrum of a diphenylmethane crystal is considerably more complex than those of toluene and dibenzyl (see Fig. 2). Table III gives the observed bands for two directions of polarization labelled *w* (weakly absorbing) and *s* (strongly absorbing). The crystals studied were in every case too thick to resolve the structure near the origin in the *s* polarization. In the *w* direction, structure could be resolved throughout the entire spectrum. The fact that great differences are observed in the spectra of the two polarizations is very fortunate, since it makes a detailed interpretation possible. We have not obtained accurate intensity measurements, however, and cannot take full advantage of this fact. In the following paper, it will be shown that both the molecular shape and an approximate crystal structure could be obtained from accurate spectral intensity data.

The spectrum may be analyzed, as shown in Table III, if one assumes that there are two origins separated by 150 cm.<sup>-1</sup>, and two superposed spectra nearly identical to dibenzyl spectra. The occurrence of two spectra is interpreted as a result of electronic resonance between the two rings. The details of this interpretation are given in the following paper.

TABLE III

## POLARIZED ABSORPTION SPECTRUM OF A DIPHENYLMETHANE CRYSTAL AT 20° K.

The intensity of each band is given for the weakly absorbing (*w*) component, and the strongly absorbing (*s*) component. Frequency differences are given in column 4, measured from 36742 cm.<sup>-1</sup>. Column 5 gives the interpretation of lines considered as combinations. See Table II of following paper for further details. Frequencies in parentheses designated by *t* are toluene frequencies.

$\nu$ (cm. <sup>-1</sup> )	<i>w</i>	<i>s</i>	$\Delta\nu$ (cm. <sup>-1</sup> )	Interpretation	Error
36742	m	vs—edge of	0	0-0 <i>A</i> → <i>A</i>	
36770	m (br)	broad band			
36788	m				
36800	m				
36840	vw				
36867	w				
36887	w		145	0-0 <i>A</i> → <i>B</i> (2Δ)	
36921	vw				
36996	vw				
37167	vvw	vw			
37246	m	0	504		
37264	s	s	522		
37296	m	m	554		
37320	m	0?	578?		
37330	0?	s	588		
37365	w	w	623		?
37386	0?	w	644	2Δ+504	
37415	s	m	673	2Δ+522	
37449	m	w	707	2Δ+556	
37480	w (sh)	0?	738	2Δ+588	
37516	w	w	774	<i>a</i> <sub>1</sub> (751t)	
37583	vvw	w	841		
37623	vw	s	881		
37670	m	vs—edge of	928	<i>a</i> <sub>1</sub> (932t)	
37703	m	broad band	961	<i>a</i> <sub>1</sub> (965t)	
37728	m		986		
37823	w		1081	928+153	
37862	w		1120	961+159	
37916	w		1174	<i>a</i> <sub>1</sub> (1189t)	
37993	m		1251		
38035	m		1293		
38049	m		1307		
38065	m		1323	1174+149	
38113	m		1371		
38155	s (sh)		1413		
38200	vs	vs	1458	522+928	-8
38230	vs	vs	1488	554+928	-6
38260	vs	vs	1518	588+928	-2
38310	vs	vs	1568	2Δ+504+928	15
38350	vs	s	1608	2Δ+522+928	-7
38385	s	s	1643	2Δ+556+928	-10
38440	s	vs	1698		
38480	s	s	1738		
38520	w	s	1778		
38560	m	s	1818		
38600	s	vs	1858	2×928	-2
38635	s	vs	1893	928+961	-4

*D. Biphenyl*

The biphenyl absorption spectrum observed on the *ab* plane of a crystal 5.0  $\mu$  thick at 20° K. is shown as a tracing in Fig. 4, and the observed features are listed in Table IV. As is well known, the solution and vapor spectra of biphenyl are entirely diffuse, but sharp bands appear in the crystal spectrum. They have the same strength in both the *a* and the *b* directions. These bands are very weak compared to the continuous absorption.

The order of magnitude of the *f*-number associated with the weak transition is about 0.001, whereas the solution spectrum of the strong absorption band yields an *f*-number of 0.44.

TABLE IV  
ABSORPTION SPECTRUM OF A SINGLE CRYSTAL OF BIPHENYL AT 20° K.

The interpretation of the frequency differences, measured from 33714 cm.<sup>-1</sup>, may have to be modified as mentioned in the text. Frequencies of polarized Raman lines are given when they are close to an excited state interval (Fruhling, Ref. 6). p = polarized.

$\nu$ (cm. <sup>-1</sup> )	Int.	$\Delta\nu$ (cm. <sup>-1</sup> )	Interpretation	Raman
33714	m	0	$^1A_g \rightarrow ^1B_{2g}$	
33874	s	160		161
33915	sh	201		
34030	w	316		
34190	m	476	316+160	324 p
34280	w	566		
34436	m	722		
34585	vs	871	722+160	731 p
34622	sh	918		
34855	m	1141		1157 p
34882	m	1168		
34928	m	1214		
35184	m	1470		1503 p?
35290	m	1576		1600 p?
35340	m	1726	1576+160	
35455	w	1741		

The first band which can be seen in the spectrum of the 5  $\mu$  crystal is as strong as the other bands of the spectrum; yet because of the high symmetry of the molecule, it is not necessarily the true electronic origin of the weak transition. Therefore we studied the absorption of thicker crystals and the fluorescence. In a 50  $\mu$  crystal at 77° K., broad absorption appears beginning at about 33200 cm.<sup>-1</sup>, 510 cm.<sup>-1</sup> to the red of the first sharp band. There is a diffuse maximum at 33310 cm.<sup>-1</sup>.

Pesteil (14) has reported the fluorescence spectrum of biphenyl crystal at 2° K. We studied the spectrum at 77° K. merely to be sure that impurities were not present in our samples and to verify the main features of Pesteil's data. He reports the first fluorescence band to lie at 33340 cm.<sup>-1</sup>. This coincides within the rather large limit of error with our 33310 cm.<sup>-1</sup> absorption maximum. The band which Pesteil calls the origin of the electronic system is at 32480 cm.<sup>-1</sup> and is a weak band. We found this to be the first strong band of the spectrum; this is our main disagreement with Pesteil, but the different crystallographic plane used by Pesteil (*ac* plane) and the difference in temperature may explain it. The intervals measured from the 32480 cm.<sup>-1</sup> band to the other fluorescence bands agree very well with the Raman bands (6), as Pesteil shows.

The origins of progressions in symmetric vibrations in absorption and fluorescence are 1232 cm.<sup>-1</sup> apart, and the band where weak absorption and weak fluorescence coincide lies 860 cm.<sup>-1</sup> above the fluorescence origin and 374 cm.<sup>-1</sup> below the absorption origin. The 860 cm.<sup>-1</sup> interval is very nearly equal to an infrared frequency (16). Furthermore, a weaker band reported by Pesteil at 32610 cm.<sup>-1</sup> in fluorescence is 730 cm.<sup>-1</sup> from the 33340 cm.<sup>-1</sup> band. The 730 cm.<sup>-1</sup> interval also appears in the infrared. It seems quite likely therefore that the fluorescence spectrum is a forbidden transition which appears principally through the action of the 860 cm.<sup>-1</sup> vibration. The forbidden 0-0 band at 33340 cm.<sup>-1</sup> appears weakly because of the perturbations from the crystal field. The

33714 cm.<sup>-1</sup> band is interpreted as the origin of an allowed transition. The 374 cm.<sup>-1</sup> difference between these two origins may be interpreted in terms of the interaction between the two benzene rings, as is done in the following paper. It would be difficult to call the 1232 cm.<sup>-1</sup> interval a 1-0+0-1 interval with 860 cm.<sup>-1</sup> the 1-0 band and 374 cm.<sup>-1</sup> the 0-1 band because these two frequencies are not comparable in magnitude. A difference of only 10-20% would be expected if this were to be the interpretation.

There is an alternative interpretation of the weak 33340 cm.<sup>-1</sup> band which must be considered. Similar weak absorption bands have been observed before in molecular crystals such as phenanthrene (11) and naphthalene (13). There is no possibility of interpreting these in terms of an intramolecular resonance. They must be interpreted as fluorescence from the same electronic state as the absorption. The energy separation has not been fully interpreted, but is only present in pure molecular crystals, not in diluted crystals or in other types of solution.

A rigorous experiment to decide between these alternatives would be to use a crystal which is transparent in the region where biphenyl absorbs, and to examine the polarized solid solution spectra of biphenyl in this solvent. We have not done this experiment but instead used a 3-methylpentane glass as the solvent for absorption and emission. The absorption at 77° K. in this glass is continuous, and the point where  $\epsilon = 100$  is at approximately 35600 cm.<sup>-1</sup>. The fluorescence bands are quite broad, and the onset of the first one was estimated to be at 34000 cm.<sup>-1</sup>. There is thus a difference of 1600 cm.<sup>-1</sup> between the onset of absorption and emission. It appears therefore that the gap is not less than in the crystal.

Another difference between biphenyl and the other crystals mentioned is that there is no strong emission beginning from the weak absorption band. As we have pointed out, only very faint emission occurs here, whereas in naphthalene and phenanthrene, the strong allowed band begins here. Therefore the emission observed from biphenyl must be coming from a state different from the state absorbing at 33714 cm.<sup>-1</sup>. We conclude that there is good evidence for the existence of two excited electronic levels, 33340 and 33714 cm.<sup>-1</sup>.

The analysis of the vibrational intervals in the absorption spectrum of biphenyl is given in Table IV. The interpretation of this analysis is not so obvious as in the case of the other molecules we have discussed. In the other cases, the vibrations which were excited in the transition were all analogous to the ones in the toluene spectrum. Even though the excited state of biphenyl can be considered to be derived from the  $B_{2u}$  state of benzene and is closely related to it, there must be enough differences to change the vibrational overlap integrals so as to favor other vibrations.

The spectrum may be understood if it is compared to the Raman spectrum (6). There is a line at 161 cm.<sup>-1</sup> which appears only in the solid and whose nature is not known. It is quite possible that the prominent 160 cm.<sup>-1</sup> band in the absorption spectrum corresponds to a vibration mode similar to the 161 cm.<sup>-1</sup> Raman line.

A polarized Raman line at 324 cm.<sup>-1</sup> corresponding to a totally symmetric vibration could well be the ground state counterpart of the 316 cm.<sup>-1</sup> interval seen in absorption. Another polarized line of 731 cm.<sup>-1</sup> could be the analogue of the 722 cm.<sup>-1</sup> absorption band. The strong 871 cm.<sup>-1</sup> absorption band has no analogue in the Raman spectrum, however. It is therefore interpreted as the combination 160+722. Other probable associations of Raman and absorption bands are noted in Table IV.

There is an interesting similarity between the types of vibrations excited in the biphenyl spectrum and those excited in the stilbene spectrum (5). These two molecules are similar in that their benzene rings are conjugated, while in dibenzyl and diphenylmethane they

are not. In both stilbene and dibenzyl the symmetric C—C stretching modes derived from  $\nu_{1g}$ ,  $e_{2g}$ , 1584 cm.<sup>-1</sup>, and  $\nu_{1g}$ ,  $e_{1u}$ , 1485 cm.<sup>-1</sup>, of benzene are excited while the frequencies in the neighborhood of 1000 cm.<sup>-1</sup> analogous to the  $\nu_2$ ,  $a_{1g}$ , 992 cm.<sup>-1</sup>, breathing mode of benzene are much less strongly excited. With the unconjugated molecules, exactly the opposite occurs. A simple explanation of this is that polar structures contribute more to the excited states of the conjugated molecules, and these structures, in order to exist, must shrink some bonds and expand others in just the way required to excite the symmetric partners of the degenerate vibrations.

Both stilbene and biphenyl have strongly excited low frequency vibrations. In stilbene these may be explained in terms of totally symmetric bending modes, but there are no such modes in biphenyl, and it does not seem possible to explain the 160 cm.<sup>-1</sup> interval as a totally symmetric molecular vibration. The lowest such mode should be the vibration of one ring against the other, and this could hardly be below 300 cm.<sup>-1</sup>. (Perhaps the polarized 324 cm.<sup>-1</sup> line is this mode.) Because the absorption intensity in this transition is very low, it may be that the 160 cm.<sup>-1</sup> interval represents a non-totally-symmetric vibration which mixes in some other electronic state. But, if our  $B_{1u}$  assignment of the 33714 cm.<sup>-1</sup> state is correct, the 160 cm.<sup>-1</sup> vibration must be *g* in order to induce such mixing, and no *g* vibration of biphenyl could be this low. A possibility is that it represents the addition of a  $374 + 160 = 534$  cm.<sup>-1</sup> frequency to the forbidden electronic origin at 33340 cm.<sup>-1</sup>. The value 534 cm.<sup>-1</sup> is in the range of the benzene-like  $e_{2g}$  vibration. It would have to be the antisymmetric  $a_1$  component since a short-axis transition must be produced (see following paper).

#### IV. CONCLUSIONS

In all four molecules studied the spectra are produced by transitions closely related to the  $^1A_{1g} \rightarrow ^1B_{2u}$  transition of benzene appearing at 2600 Å. In the spectra of toluene, dibenzyl, and diphenylmethane, the same types of ring vibrations are excited during the transitions. This fact is of importance in analyzing the spectra of the latter two molecules. Quite different types of vibrations are excited in the biphenyl transition. Some of these vibrations are the highest frequency C—C stretching vibrations of the rings, similar to those excited by electronic transitions in stilbene, anthracene, and other conjugated aromatic molecules.

The low temperature spectra under our conditions of high resolution have revealed several important details about the excited electronic states of four related molecules. In each case the magnitude of the electronic and vibrational interactions between the benzene rings of the double molecules may be deduced from the spectra. Details of these interactions are discussed in the following paper.

#### REFERENCES

1. ALMASY, F. and LAEMMEL, H. *Helv. Chim. Acta*, **33**, 2092 (1950).
2. BRAUDE, E. A. *J. Chem. Soc.* 1890, 1898, 1902 (1949).
3. CLARK, G. L. and PICKETT, L. *J. Am. Chem. Soc.* **53**, 167 (1931).
4. DHAR, J. *Indian J. Phys.* **7**, 43 (1932).
5. DYCK, R. and McCLURE, D. S. To be published.
6. FRUHLING, A. *Ann. Physik*, **6**, 401 (1951).
7. GINSBURG, N. and ROBERTSON, W. *J. Chem. Phys.* **14**, 511 (1946).
8. JEFFREY, G. A. *Proc. Roy. Soc. (London)*, A, **288** (1947).
9. KRISHNAN, K. S., GUHA, B. C., and BANERJEE, S. *Phil. Trans. Roy. Soc. London*, A, **231**, 235 (1933).
10. McCLURE, D. S. *J. Chem. Phys.* **22**, 1668 (1954).
11. McCLURE, D. S. *J. Chem. Phys.* **25**, 481 (1956).
12. McCLURE, D. S. *Can. J. Chem.* **36**, 59 (1958).
13. McCLURE, D. S. and SCHNEPP, O. *J. Chem. Phys.* **23**, 1575 (1955).
14. PESTEIL, P. and BARBARON, M. *J. phys. radium*, **15**, 92 (1954).

15. PICKETT, L. W. *Nature*, **131**, 513 (1933).
16. RICHARDS, R. E. and THOMPSON, H. W. *Proc. Roy. Soc. (London)*, A, **195**, 1 (1948).
17. ROBERTSON, W. W. and MATSEN, F. A. *J. Am. Chem. Soc.* **72**, 5250 (1950).
18. WINCHELL, A. N. *The optical properties of organic compounds*. 2nd ed. The University of Wisconsin Press, Madison, Wis. 1954.

# ENERGY TRANSFER IN MOLECULAR CRYSTALS AND IN DOUBLE MOLECULES<sup>1</sup>

DONALD S. MCCLURE<sup>2</sup>

## ABSTRACT

The theory of the transfer of electronic energy between two molecules, or between two parts of a "double molecule", is discussed for the case in which vibrational quanta are present. The results are obtained for two limiting cases of weak and strong electronic interaction. Some of the phenomena occurring in the intermediate region are discussed qualitatively. With the aid of these results the spectra of biphenyl, diphenylmethane, and dibenzyl have been analyzed, and the electronic energy exchange parameter has been determined for each. These data are compared with similar data on durene crystal and the paracyclophanes. The electronic energy exchange parameter is given approximately correctly by considering the interaction of electronic transition dipoles except for very close and for very distant molecules.

## I. INTRODUCTION

Two kinds of weakly coupled systems in which energy transfer processes have been observed are molecular crystals and "double molecules", i.e. molecules consisting of two identical parts coupled through a weakly conjugating linkage. Recently, high resolution single crystal spectra of several double molecules have been obtained (2). The spectral data are analyzed in this paper and compared with existing information on molecular crystals and other double molecules. Our main purpose is to show what the actual values of these energy transfer parameters are and to make them available for theoretical work.

Vibrational as well as electronic energy transfer has been observed. Effects of intermolecular coupling on vibrations have been observed in infrared spectra of single crystals as well as in electronic spectra. Our main interest in vibrational coupling in this paper will be in the way it interacts with the electronic coupling. This interaction may take any form from a minor splitting of vibrational levels to a major change in the geometry of the system.

Some of the theory of electronic states of weakly coupled systems has been reviewed by Craig (3), who applies it to molecular crystals. In this theory the interaction between the units of the molecular crystal occurs by way of an excitation transfer without necessarily any electron transfer. The intermolecular potential is usually expanded in a multipole series and the leading term is evaluated to determine the interaction energy. In this way Craig (3) calculated the spectrum of the anthracene crystal using the dipole-dipole term and Fox and Schnepp (5) calculated the spectrum of the benzene crystal using the octupole-octupole term. Longuet-Higgins and Murrell (6) have developed a theory which is applicable to "double molecules", since the potential for interaction between the parts is not expanded in a multipole series and allowance is made for electron transfer processes. The energy states of biphenyl, for example, were calculated.

## II. ELECTRONIC SPLITTING IN BIPHENYL, DIPHENYLMETHANE, AND DIBENZYL

Schematic representations of the spectra of toluene and the related double molecules are shown in Fig. 1, after the work of Coffman and McClure (2). The original spectra were taken at 20° K. with polarized light and single crystals. Only in the case of biphenyl

<sup>1</sup>Manuscript received August 16, 1957.

Contribution from the Department of Chemistry and Electrical Engineering, University of California, Berkeley, California. This paper was presented at the Symposium on the Structure and Reactivity of Electronically-Excited Species held at the University of Ottawa, Ottawa, Canada, September 5 and 6, 1957.

<sup>2</sup>Now at Radio Corporation of America Laboratories, Princeton, New Jersey.

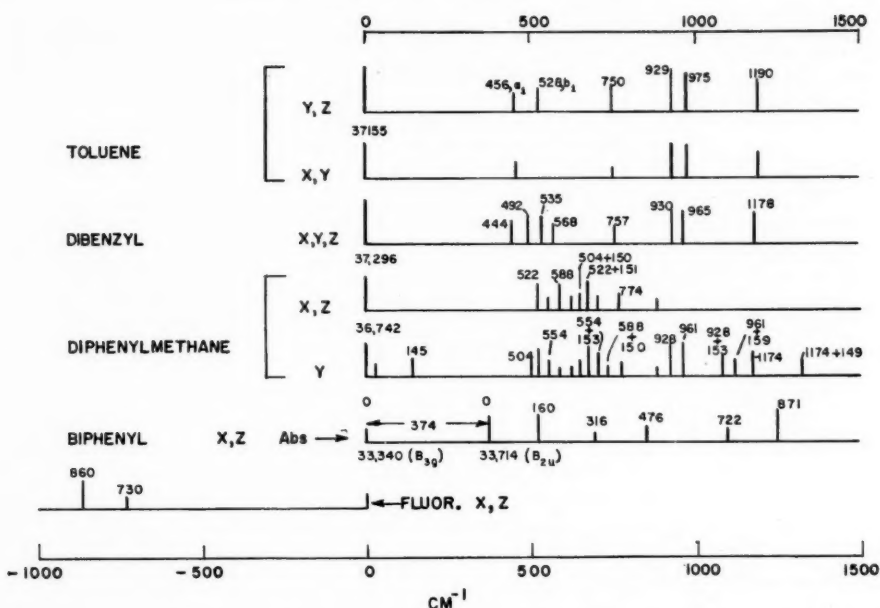


FIG. 1. Schematic drawings of the spectra of toluene and some related double molecules. Vibration frequencies measured from the electronic origins are given.

is it possible to observe the electronic splitting directly, as indicated in the analysis on Fig. 1. In the other two cases, it is possible with the aid of the toluene spectrum for comparison to find the approximate value of the electronic splitting. The molecular shapes and the coordinate systems to be used in the following discussion are shown in Fig. 2.

#### A. Analysis of the Spectra of Double Molecules

Some simple quantum mechanical problems must be considered first before proceeding to the spectroscopic data. The electronic and vibrational states of double molecules may be written to a first approximation as products of the wave functions of the separate parts. For the ground state  $\psi^n = \psi_1^0 \psi_2^0$ , and for the excited states, corresponding to the  $m$ th excited state of the parts,

$$[1] \quad \left. \begin{array}{l} \psi_S^m \\ \psi_A^m \end{array} \right\} = \frac{1}{\sqrt{2}} (\psi_1^0 \psi_2^m \pm \psi_1^m \psi_2^0).$$

The subscript  $S$  goes with the + sign and  $A$  with the - sign. The double molecules we are considering have symmetry elements, some of which interchange rings.  $\psi_S$  and  $\psi_A$  will behave oppositely under such symmetry operations, i.e. one will change sign and the other not. The  $\pm$  property itself may be considered as a symmetry element in the following general discussion.

In each case the excited state is like the  $B_{2u}$  state of benzene and therefore in the individual rings there is a node across the ring passing through the point of substitution. This transition is forbidden in benzene, but allowed in toluene. However the vibrational electronic interaction mechanism active in benzene still induces an appreciable transition moment in toluene as well as in the double molecules under consideration. Our most

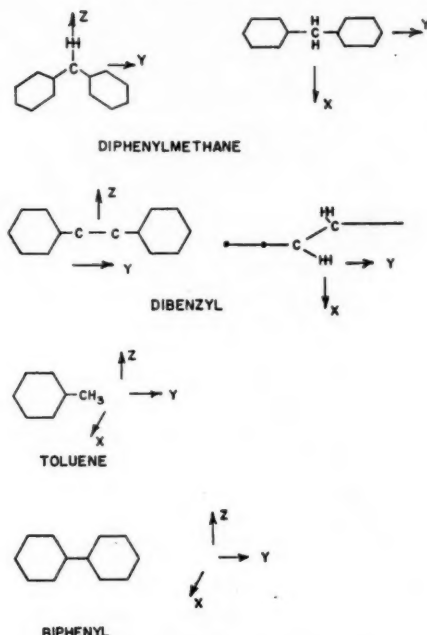


FIG. 2. Coordinate systems and symmetry properties of toluene, dibenzyl, diphenylmethane, and biphenyl. The rings of diphenylmethane are drawn to indicate the foreshortening due to rotation about the C—CH<sub>2</sub> bond.

interesting results will be obtained by analyzing the spectrum in the region where the perturbing vibration appears. In benzene this is an  $e_{2g}$  mode of 521 cm.<sup>-1</sup> which splits in toluene into an  $a_1$  at 456 cm.<sup>-1</sup> and a  $b_1$  at 528 cm.<sup>-1</sup> in the excited state. Note that the  $a_1$  mode is lower, since it involves motion of the attached methyl group, while in the  $b_1$  vibration there is a node at the methyl group.

The following problems must now be solved in order to interpret the spectra.

#### *1. Splitting of the Vibrationless Transition in Double Molecules.*

The hamiltonian for the double molecule may be written as  $H_1 + H_2 + H_{12}$ , where  $H_1$ ,  $H_2$  are the hamiltonian functions for toluene and  $H_{12}$  is an interaction potential. Using the wave functions given earlier, the energy of the  $S$  state is  $D + \Delta$ , and of the  $A$  state  $D - \Delta$ , relative to the unperturbed energy as zero. Here  $D$  is the displacement of the center of gravity due to the interaction potential, i.e.,

$$[2] \quad D = \int (\psi_1^0 \psi_2^m)^2 H_{12} d\tau$$

and  $\Delta$  is half the splitting, i.e.

$$[3] \quad \Delta = \int \psi_1^0 \psi_2^m H_{12} \psi_1^m \psi_2^0 d\tau.$$

The transition moment is

$$[4] \quad \frac{\mathbf{M}_S}{\mathbf{M}_A} = \frac{\mathbf{M}_1 \pm \mathbf{M}_2}{\sqrt{2}}$$

for the *S* and *A* states. The vector sum is zero for one of the states in the case of dibenzyl, since it corresponds to a *g*-state. In diphenylmethane both states may have non-zero components for certain geometries. The displacement, *D*, will be neglected in later calculations since it does not affect the spectrum.

## 2. Splitting of Symmetric Vibronic States

Vibrations which are totally symmetric in toluene form two vibrations in the double molecule. They will have different energies because of the mechanical and electronic coupling between the two rings. One can write four product-type vibronic wave functions corresponding to the presence of one vibrating ring and one electronically excited ring in the double molecule. It is important to realize that the ring containing the electronic excitation may or may not contain the vibrational excitation. Another important distinction, discussed in detail by Simpson and Peterson (9), is related to the first. One must distinguish two limiting cases: (1) the electronic interaction between the parts of the molecule results in a splitting which is small compared to the vibrational intervals, (2) the electronic interaction produces a splitting much larger than the vibrational intervals. These are called the weak and the strong coupling cases, respectively. We may now list the wave functions, the first order energies, and the transition probabilities from the ground state for these two limiting cases. This information is given in Table I. It has been assumed throughout that the electronic and vibrational wave functions of each part of the double molecule are exactly the same as those of the related single molecules.

TABLE I  
WAVE FUNCTIONS, ENERGIES, AND TRANSITION PROBABILITIES FOR WEAK AND STRONG COUPLING

State	Symm.	Wave function	First order energy	Transition probability
Ground	<i>S</i>	$\psi_1^0 \psi_2^0 X_1^{00} X_2^{00}$	0	—
<i>m</i> -Electronic	$\begin{cases} S \\ A \end{cases}$	$1/\sqrt{2} [\psi_1^m \psi_2^0 X_1^{m0} X_2^{00} \pm \psi_1^0 \psi_2^m X_1^{00} X_2^{m0}]$	$E_m \pm \Delta$	$(\mathbf{M}_1 \pm \mathbf{M}_2)/\sqrt{2}$
Weak coupling:				
<i>m</i> -elect.	$\begin{cases} S \\ A \end{cases}$	$1/\sqrt{2} [\psi_1^m \psi_2^0 X_1^{m0} X_2^{0a} \pm \psi_1^0 \psi_2^m X_1^{0a} X_2^{m0}]$	$E_m + V_a^0 \pm \Delta$	$\begin{cases} 0 \\ (\mathbf{M}_1 + \mathbf{M}_2)S_{1a} \end{cases}$
+ <i>a</i> -vibr.	$\begin{cases} S \\ A \end{cases}$	$1/\sqrt{2} [\psi_1^m \psi_2^0 X_1^{ma} X_2^{00} \pm \psi_1^0 \psi_2^m X_1^{00} X_2^{ma}]$	$E_m + V_a^m \pm \Delta$	$\begin{cases} (\mathbf{M}_1 \pm \mathbf{M}_2)S_{1a}/\sqrt{2} \\ 0 \end{cases}$
Strong coupling:				
<i>m</i> -elect.	$\begin{cases} S \\ A \end{cases}$	$1/2 [\psi_1^m \psi_2^0 + \psi_1^0 \psi_2^m] [X_1^{S0} X_2^{Sa} \pm X_1^{Sa} X_2^{S0}]$	$E_S + V_a^S \pm v$	$\begin{cases} (\mathbf{M}_1 + \mathbf{M}_2)S_{1a} \\ 0 \end{cases}$
+ <i>a</i> -vibr.	$\begin{cases} S \\ A \end{cases}$	$1/2 [\psi_1^m \psi_2^0 - \psi_1^0 \psi_2^m] [X_1^{A0} X_2^{Aa} \pm X_1^{Aa} X_2^{A0}]$	$E_A + V_a^A \pm v$	$\begin{cases} (\mathbf{M}_1 - \mathbf{M}_2)S_{1a} \\ 0 \end{cases}$

Notes to table:

*m* = *m*th excited electronic state of one ring.

*a* = *a*th vibrational mode.

$\psi_i^m$  = electronic wave function of ring *i* in state *m*.

$X_1^{ma}$  = vibrational wave function of ring 1 in electronic state *m* and vibrational state *a*.

$\Delta$  = electronic coupling energy.

*v* = vibrational coupling energy.

$V_a^m$  = vibrational energy of *a*th mode in *m*th electronic state.

*S* = Symmetric under ring interchange.

*A* = Antisymmetric under ring interchange.

$E_m$  = energy of *m*th electronic state.

$\mathbf{M}_1$  = transition moment of one ring from 0 to *m*.

$E_S = E_m + \Delta$ ,  $E_A = E_m - \Delta$ .

$S_{1a}$  = Franck-Condon overlap integral; a-vibr., ring 1.

The qualitative results are these. In the weak coupling limit, the electronic splitting  $\Delta$  is very small. If it is considered to be zero there are two vibronic states: one having a vibrational quantum in the unexcited ring with its ground state frequency,  $V_a^0$ ; and the other having a vibrational quantum in the excited ring, with the frequency  $V_a^m$ , determined by the force constants of the excited state. Only the second of these states has a non-vanishing transition probability from the ground state. This is a result of vibrational overlap. Two vibronic states separated by  $2\Delta$  arise from each one when the first order electronic energy coupling is added.

In the strong coupling limit, there are two widely separated electronic states of the double molecule. In this limit  $2\Delta$  is much larger than the vibrational energies. The vibration frequencies  $V_a^S$  and  $V_a^A$  are characteristic of the force constants of the excited states  $S$  and  $A$ . The mechanical coupling  $v$  between the rings is considered to be small and splits each vibration into a symmetric and an antisymmetric mode. The symmetry of each state is determined by the product of the vibrational and the electronic symmetry, since it is possible to separate the electronic and vibrational wave functions in the strong coupling limit. One of the  $A$  states,  $S \cdot A$ , and one of the  $S$  states,  $A \cdot A$ , have zero transition probability from the ground state because the vibrational overlap factor,  $S_{1a} - S_{2a}$ , is zero.

Real cases of course fall into the intermediate region. We will not attempt to solve the intermediate coupling problem here, but will only point out those features of it which are important for analyzing the spectra at hand. Intermediate coupling must begin to be considered when the two classes of weak coupling states interact appreciably. This occurs when the value of  $\Delta$  approaches  $V_a^0 - V_a^m$ , the difference in energy of a vibration in the ground state and in the  $m$ th excited state. These energy differences are of the order of  $100 \text{ cm}^{-1}$ . In the examples to be discussed later, values of  $\Delta$  less than and greater than this figure are found. We expect the vibrational intervals to become altered when  $\Delta$  is in the region of  $V_a^0 - V_a^m$ .

Simpson and Peterson pointed out that the splitting energy,  $\Delta$ , in the weak coupling region is proportional to the band intensity of the individual vibronic bands undergoing the interaction, while in the strong coupling limit  $\Delta$  is proportional to the full electronic band intensity. In the intermediate region the  $\Delta$  value depends upon matrix elements of electronic interaction between different vibronic states, and so will have a value larger than in the weak coupling limit. The  $\Delta$  value will begin to increase rapidly when the interacting systems are close enough so that these second order matrix elements become large, that is when  $\Delta$  is of the order of  $V_a^m$ .

Thus we may distinguish two important cases of the intermediate coupling region: (1)  $\Delta \approx V_a^0 - V_a^m$  and (2)  $\Delta \approx V_a^m$ .

In the first region in which  $\Delta \approx V_a^0 - V_a^m$ , mixing must occur between the two  $S$  states, and between the two  $A$  states. The transition probabilities are therefore no longer zero and finite respectively, but all four states must have a finite transition probability. The spectrum for small  $\Delta$  should appear as a lower doublet at  $E_m + V_a^m \pm \Delta$  and a weak doublet at higher energies  $E_m + V_a^0 \pm \Delta$ , since  $V_a^0$  is usually greater than  $V_a^m$ . By the time  $\Delta$  has reached  $V_a^0 - V_a^m$ , there should be four lines of roughly equal spacing, and having intensities determined only by the orientation of the vectors  $\mathbf{M}_1$  and  $\mathbf{M}_2$ . Thus if the molecular geometry permitted  $\mathbf{M}_1 + \mathbf{M}_2$  to equal  $\mathbf{M}_1 - \mathbf{M}_2$  all four lines would be of equal intensity.

As the second region is approached there should be no large changes in relative in-

tensity of the four vibronic lines. Somewhere between the second region and the strong field limit, the intensity of two of the lines must decrease. The spectrum now consists of a pair of widely spaced doublets, and one component of each must lose its intensity.

### 3. Degenerate Vibration in the Excited State

The degenerate vibration is split in the molecule even without energy exchange. One of its components acts like an ordinary totally symmetric vibration while the other induces a forbidden transition by vibrational-electronic interaction. The problem thus reduces to a treatment of the non-totally-symmetric vibration. This vibration induces a transition in the half-molecule, independent of energy transfer. The degenerate vibrations of most interest are derived from the benzene  $e_{2g}$  mode. In toluene this becomes  $a_1$  and  $b_1$  ( $C_{2v}$ ). We will continue to use  $a$  and  $b$  to designate the totally symmetric and non-symmetric components, respectively.

The energy levels are not appreciably affected by the vibrational mixing of excited states, and the transition probabilities are enhanced in the double molecule to the same extent as in the single molecule.

A possible effect could arise from the fact that vibrational mixing, if it is to produce any enhancement of intensity, must occur between states in weak coupling and states in strong coupling. The result is that the overlap factor, which causes two of the weak coupling states to have zero transition probability, is no longer as effective, and these two states could have a finite transition moment. The induced moment for this case is the moment induced in the single molecule times a vibrational overlap integral, ( $X_1^{0a} \cdot X_1^{S0}$ ). This is similar to the Franck-Condon overlap integral, and may sometimes have an appreciable value. It is probably not an important source of intensity, however, compared to the intermediate coupling effects discussed in Section 2. The conclusion is therefore that vibrationally induced transitions will act no differently from the direct transitions in the double molecules, and all the considerations of Section 2 apply equally to both.

We may now proceed to the analysis of the spectra.

### B. Dibenzyl

The important features of the spectrum of dibenzyl are shown in the diagram of Fig. 1. No splitting of the 0-0 band could be observed, and a direct measure of the coupling between the benzene rings cannot be made. The appearance of four bands related to the  $e_{2g}$  vibration of benzene is of considerable interest, however, and permits some estimate to be made of the ring-ring interaction. The interpretation of these bands as arising from the mode related to  $e_{2g}$  of benzene seems well justified if one compares the spectrum with that of toluene, diagrammed in Fig. 1 and shown in detail in the preceding paper (2).

The dibenzyl molecule in the crystal has the symmetry  $C_u$ , but it is very close to  $C_{2h}$ , and selection rules based on  $C_{2h}$  are found to be closely obeyed. If we let the ring-interchanging operation defining  $S$  and  $A$  be the  $C_2$  axis, then the pure electronic state related to  $B_{2u}$  of benzene, or  $A_1$  of toluene, will become  $A_u(S)$  and  $B_g(A)$ . Transitions to the  $A_u$  state are expected to be as strong as in toluene, and those to the  $B_g$  state are forbidden. If a dipole-dipole interaction potential is assumed (Sec. III), one predicts that the  $B_g$  state lies below the  $A_u$  state.

In the weak coupling limit we would expect to have a spectrum similar to that of toluene. Only two bands would appear in the  $e_{2g}$  region. These would correspond to the

$a_1$  and  $b_1$  vibrations observed in toluene. The vibronic state containing the  $a_1$  vibration would be  $S(A_u)$ , the same as the pure electronic transition, while the vibronic state containing the  $b_1$  vibration would be  $A(B_u)$ . The polarizations would be  $z$  and  $y$  respectively, in analogy with toluene.

The presence of four bands of comparable intensity can be interpreted by assuming an appreciable excursion into the intermediate coupling region where the vibronic states containing ground state vibrational quanta may gain intensity. If we refer to Table I, and let  $a$  and  $b$  represent the  $a_1$  and  $b_1$  toluene-type vibrations we would expect the following levels, whose total energies are given to the right, to appear with appreciable intensity:

$$\begin{array}{ll} S(A_u) & E_m + V_a^0 + \Delta, \\ A(B_u) & E_m + V_b^0 - \Delta, \end{array} \quad \begin{array}{ll} S(A_u) & E_m + V_a^m + \Delta, \\ A(B_u) & E_m + V_b^m - \Delta, \end{array}$$

where  $m$  represents the  $B_{2u}$  type excited state. We know the approximate values of the vibrational quanta to be close to the following values for toluene:

$$V_a^0 = 521 \text{ cm.}^{-1}, \quad V_a^m = 456 \text{ cm.}^{-1},$$

$$V_b^0 = 622 \text{ cm.}^{-1}, \quad V_b^m = 528 \text{ cm.}^{-1}.$$

The intervals are measured in the spectrum from the electronic  $S$  level at  $E_m + \Delta$ . If we subtract this from the energy formulas for the vibronic levels and substitute the vibrational quanta we obtain a set of theoretical intervals which must be compared to the measured ones. By making the band assignments which appear to be the most consistent we obtain the list of comparisons:

Theor.	Exptl.
521	→ 535
622 - 2Δ	→ 568
456	→ 444
528 - 2Δ	→ 492

The values for  $2\Delta$  are 54 and 36, with an uncertainty of about 14, considering the mismatch of the two intervals which do not involve  $\Delta$ . We will use  $2\Delta = 45 \pm 14 \text{ cm.}^{-1}$ .

### C. Diphenylmethane

Neither the true molecular shape nor the crystal structure of this compound is known. The single crystal spectra are strongly polarized, however, and some information about energy transfer within the molecule may therefore be obtained. The spectrum is diagrammed in Fig. 1.

One assumption which seems unlikely to be wrong is that diphenylmethane has a twofold symmetry axis bisecting the  $\text{C}-\text{CH}_2-\text{C}$  angle. The angle of rotation  $\phi$  of the phenyl groups about the  $\text{C}(\text{ar})-\text{CH}_2$  axis is unknown. The  $\text{C}-\text{CH}_2-\text{C}$  angle may be assumed to be close to  $112^\circ$ . The molecular geometry and the coordinate system to be used are shown in Fig. 2.

The spectrum in the  $e_{2g}$  region has the eight bands which would be predicted for a molecule having no more than  $C_2$  symmetry. Only four would be permitted for  $C_{2v}$  symmetry. In the two configurations corresponding to  $C_{2v}$ , the phenyl planes are perpendicular or parallel to the  $\text{C}-\text{CH}_2-\text{C}$  plane. It is clear then that the angle of rota-

tion,  $\phi$ , of the phenyl groups around the C—C bond is between  $0^\circ$  and  $90^\circ$  ( $\phi$  will be measured from the perpendicular position).

As in the case of dibenzyl there is no clear evidence for a forbidden electronic origin. In case  $\phi = 0$  ( $C_2$  geometry) the forbidden transition would be  $A_1 \rightarrow A_2$  and the allowed one  $A_1 \rightarrow B_2$  ( $x$ -polarized). In  $C_2$  geometry with  $0^\circ < \phi < 90^\circ$ , the  $A_2$  excited state becomes an  $A$  state having a transition moment along the  $z$ -axis. The  $B_2$  state becomes a  $B$  state and gradually loses its  $x$ -moment and gains a  $y$ -moment as  $\phi$  increases. If a dipole-dipole interaction between the two rings is assumed, the energy of the  $A$  and  $B$  states as a function of the angle  $\phi$  may be found. The energies are

$$[5] \quad E \begin{pmatrix} A \\ B \end{pmatrix} = \pm \frac{2M^2}{R^3} (2.308\sin^2\phi - 1),$$

where  $M$  is the transition moment in one ring. Both the energies and the transition moments of states  $A$  and  $B$  are plotted in Fig. 3 as a function of angle. It can be seen

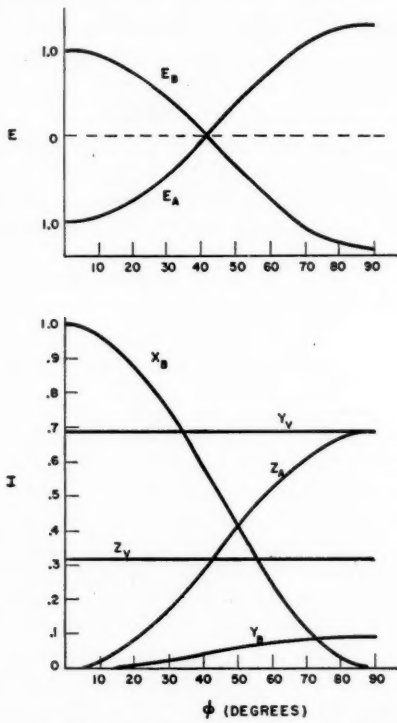


FIG. 3. Upper part: Energies of the  $A$  and  $B$  electronic states of diphenylmethane as a function of the angle of rotation  $\phi$ .

Lower part:  $X_B$ ,  $Y_B$ ,  $Z_A$ —probabilities of short-axis transitions in the rings of diphenylmethane along molecular axes (see Fig. 2).  $Y_V$ ,  $Z_V$ —probabilities of long-axis transitions (vibration-induced) along molecular axes.

that the higher state always has the higher transition moment, and that the two states coincide at  $\phi = 41^\circ$ . The transition moments for vibronic transitions of the  $a_1$ -type toluene vibrations have the same polarization properties as the electronic origins, and

may therefore be read from Fig. 3. The induced transition moments due to the  $b_1$ -type toluene vibrations have polarizations independent of the angle  $\phi$ . These are also plotted in Fig. 3. The intensity of the  $y$ -component of the vibrationally induced transition is the same as the vibration-induced intensity in toluene times  $\sin^2 56^\circ$ . That of the  $z$ -component is proportional to  $\cos^2 56^\circ$ . Further deductions from Fig. 3 may be made after examining the spectrum again.

The region of the spectrum corresponding to the  $e_{2g}$  vibration of benzene has its first band at  $504 \text{ cm}^{-1}$  from the allowed origin. This is somewhat higher than in toluene, where the first such band is at  $456 \text{ cm}^{-1}$ . This suggests that the vibration modes of diphenylmethane are not as strictly comparable to those of toluene and benzene as in the case of dibenzyl. Nevertheless we will proceed with a similar analysis since the other prominent vibration frequencies,  $928$ ,  $961$ , and  $1174 \text{ cm}^{-1}$ , are very close to the dibenzyl frequencies  $930$ ,  $965$ , and  $1178 \text{ cm}^{-1}$ .

The bands of the  $e_{2g}$  region fall into two groups:  $504$  to about  $580$ , and  $649$  to about  $700 \text{ cm}^{-1}$ . If the second group are to be interpreted as vibrations of a character similar to the first, they must contain an electronic component which results in an energy about  $150 \text{ cm}^{-1}$  higher than that of the first group.

This is true not only for the  $e_{2g}$  region, but the entire spectrum may be analyzed as a superposition of two nearly identical spectra displaced from each other by  $150 \text{ cm}^{-1}$ . The three totally symmetric frequencies,  $928$ ,  $961$ , and  $1174 \text{ cm}^{-1}$ , are found repeated at  $153$ ,  $159$ , and  $149 \text{ cm}^{-1}$  respectively. This is within experimental error of  $150 \text{ cm}^{-1}$  because the bands here are somewhat broad. The band analogous to the  $750 \text{ cm}^{-1}$  band of toluene seems to be present at  $774 \text{ cm}^{-1}$  in diphenylmethane but its high frequency counterpart would fall too close to  $928 \text{ cm}^{-1}$  to be distinguishable from it.

A detailed analysis of the vibrational structure in the  $e_{2g}$  region may be made. It appears necessary to assume  $\phi = 30^\circ$  (approximately) and that the energy of the  $A$  state lies below that of the  $B$  state. It is also reasonable to identify each vibronic state by means of its strong coupling symbol, because the electronic splitting is large enough to separate two groups of vibronic levels into the states which ultimately go over into strong coupling states. Thus the symmetric and antisymmetric electronic and vibrational wave functions are represented by  $\psi_S$ ,  $\psi_A$ ,  $X_S$ ,  $X_A$  respectively. The superscript  $a$  or  $b$  is added to  $X$  in order to indicate the type of vibrational mode. The analysis is shown in Table II.

The analysis is not entirely satisfactory because  $X_A^a$  must be assumed to lie above

TABLE II  
ANALYSIS OF DIPHENYLMETHANE SPECTRUM IN  $400\text{--}700 \text{ cm}^{-1}$  REGION

State	Symmetry	Intensity and polarization, calc.	Assignment	Polarization observed
$\psi_S X_S^a$	$B$	$x, \cos^2 \phi; y, 0.096 \sin^2 \phi M^2$	$556 + 2\Delta$	$x, y$
$\psi_S X_S^b$	$B$	$y, \sin^2 56 M_i^2$	$588 + 2\Delta$	$y$
$\psi_S X_A^a$	$A$	$z, 0.69 \sin^2 \phi M^2$	$522 + 2\Delta$	$x, y$
$\psi_S X_A^b$	$A$	$z, \cos^2 56 M_i^2$	$504 + 2\Delta$	$z$
$\psi_A X_S^a$	$A$	$z, 0.69 \sin^2 \phi M^2$	$554$	$x, y$
$\psi_A X_S^b$	$A$	$z, \cos^2 56 M_i^2$	$588$	$z$
$\psi_A X_A^a$	$B$	$x, \cos^2 \phi; y, 0.096 \sin^2 \phi M^2$	$522$	$x, y$
$\psi_A X_A^b$	$B$	$y, \sin^2 56 M_i^2$	$504$	$y$

Notes to table:  $M$  = direct vibronic transition moment,  
 $M_i$  = vibrationally induced moment.

It is assumed that intermediate coupling causes enough mixing of states that transitions forbidden in the limiting cases are as strong as the allowed transitions.

$X_A$ <sup>b</sup>. Also the states  $\psi_s X_A$ <sup>a</sup> and  $\psi_A X_s$ <sup>a</sup>, which are mixed in the intermediate region, do not have the correct polarization. The relationship between the polarization of a vibration in the first group of bands (superposed on the *A* origin) and the same frequency in the second group (superposed on the *B* origin) is correct in all cases, and the absolute polarizations, arising from the assumption that the *A* state is the lower one, are correct in three cases. Even though certain details do not seem entirely correct, it appears that the splitting between the *A* and *B* states,  $2\Delta$ , is almost certainly  $150 \text{ cm}^{-1}$ .

The higher frequency electronic origin could be the band at  $145 \text{ cm}^{-1}$  from the first origin. Both origins are much stronger in one component than the other, and in fact the spectrum in one polarization has not been resolved because the crystals used have been too thick.

The diagram of Fig. 3 shows that in order to obtain strong absorption to both the *A* and *B* electronic origins in one polarization for  $\phi$  between  $20^\circ$  and  $60^\circ$ , the molecular *y*-axis must be in the weakly absorbing direction of the crystal, and the *x* and *z* axes must both lie in the strongly absorbing direction. For values of  $\phi$  near  $80$ – $90^\circ$ , the *x* direction could be the weakly absorbing direction with *y* and *z* in the strong direction. We do not have good intensity measurements, so cannot say definitely what the molecular configuration is. It should be possible, however, to determine a molecular and a crystal structure from such measurements.

#### D. Biphenyl

In the experimental observations on the biphenyl crystal, the light was propagated parallel to the long molecular axis. Thus the only  $\pi$ – $\pi$  transitions which could be observed are along the short axis. This was advantageous in that interference from the very strong long-axis polarized transition  ${}^1A_{1g} \rightarrow {}^1B_{2u}$  was eliminated, and only the weak short-axis transitions could be seen. Using the diagram of Fig. 2 and Herzberg's notation for the group  $D_{2h}$ , the states of biphenyl derived from the  $B_{2u}$  state of benzene are  $B_{1u}$  and  $B_{3g}$ . Transitions are permitted from the ground state to the  $B_{1u}$  state, but not to the  $B_{3g}$  state. The allowed transition should have about the same intensity as the corresponding toluene transition. According to the intensity estimates made from the photographic plates they are approximately the same.

Both fluorescence and absorption have been observed, and direct observation of the two electronic states was therefore possible. The absorption beginning at  $33714 \text{ cm}^{-1}$  is interpreted as the  $A_g \rightarrow B_{1u}$  transition. According to Pesteil (7), the fluorescence begins at  $33340 \text{ cm}^{-1}$  with a series of weak bands, and a series of strong bands begins at  $32480 \text{ cm}^{-1}$ . The transition moment of the strong bands is along the long axis of the molecule. Our fluorescence experiments (2) essentially confirmed Pesteil's results but did not go as far as his. A broad band having its maximum at about  $33310 \text{ cm}^{-1}$  appeared in the absorption spectrum of a crystal  $50 \mu$  thick. We think that this is the absorption corresponding to the  $33340 \text{ cm}^{-1}$  fluorescence.

The interval between  $33340 \text{ cm}^{-1}$  and the strong fluorescence band  $32480 \text{ cm}^{-1}$  is  $860 \text{ cm}^{-1}$ . This is equal to a known infrared absorption band. Its symmetry properties are not known, however. The interpretation is that a  $860 \text{ cm}^{-1}$  vibration makes a forbidden transition, whose origin is  $33340 \text{ cm}^{-1}$ , allowed through vibrational-electronic interaction. The long-axis polarization of the fluorescence is reasonable, since the strongest nearby transitions which may be mixed in by vibration are long-axis polarized. The origin at  $33340 \text{ cm}^{-1}$  is interpreted as the  $A_g \rightarrow B_{3g}$  transition made allowed by the unsymmetrical crystal field. Since the corresponding allowed  $A_g \rightarrow B_{1u}$  transition is the  $33714 \text{ cm}^{-1}$  absorption, the  $B_{1u}$ – $B_{3g}$  separation is  $374 \text{ cm}^{-1}$ .

### E. Paracyclophanes

Cram, Allinger, and Steinberg (4) have published the solution spectra of the paracyclophanes, a series of molecules in which two benzene rings are linked together in both para positions by  $(\text{CH}_2)_n$  groups. The spectra look very similar to a *p*-xylene spectrum when the benzene rings are separated by at least  $(-\text{CH}_2-)_4$  at both positions. If the rings are any closer a new and weaker band appears to the red. Table III gives the energy difference between the two bands for the compounds studied. These values of  $\Delta E$  are only approximate because of the breadth of the bands.

TABLE III  
INTERACTION ENERGIES BETWEEN BENZENE RINGS

Paracyclophanes		$C_1-C_1'$	$C_4-C_4'$	$R$ (separation of ring centers)	$\Delta E$ (calc.)	$\Delta E$ (obs.)
<i>m</i>	<i>n</i>					
2	2	1.54	1.54	1.54	632	2400
2	3	1.80	2.26	2.03	278	2700
2	4	2.12	3.16	2.64	126	1600
3	3	2.52	2.52	2.52	142	2800
3	4	2.84	3.41	3.12	78	1950
3	6	3.50	5.27	4.39	28	~0
4	4	3.73	3.73	3.73	44	~0
Other molecules				$R_1$ (ring center)	$R_2$ (nearest points)	
Biphenyl				4.25	1.45	760
Diphenylmethane ( $\phi = 30^\circ$ )				4.88	2.56	120
Dibenzyl				6.66	3.94	37
Durene crystal				6.45	29.6	<5

The weaker absorption band to the red is most probably the forbidden transition of the two which would be expected in the 2600 Å region of the double molecules. If the benzene rings are exactly parallel, this transition is rigorously forbidden in the pure electronic spectrum. Since it is always quite broad, it is probable that it only appears through vibrational-electronic interaction.

Some of the energy differences given in Table III are very large compared to those found for the singly linked double molecules of the previous section. The total intensity of the absorption per ring to both upper states is about right for the  $A_g \rightarrow B_{2u}$  transition in *p*-xylene, so that the large splitting is not caused by admixtures of higher excited benzene-like  $\pi$  states. Cram, Allinger, and Steinberg have also calculated the ring-ring distances in these compounds assuming that the bond angles and distances are as nearly "normal" as possible. They point out that the large spectral changes only occur when the rings are closer than the Van der Waals packing distance of 3.40 Å. The distances between corresponding para and para-prime positions in some of these molecules are given in Table III.

### F. Molecular Crystals

Crystal structure data are available for benzene and durene, but for very few other crystals containing principally benzene rings. Fox and Schnepf (5) have published an interpretation of the benzene spectrum as observed by Broude, Medvedew, and Prikhotjko (1). The spectrum of the durene crystal in absorption and fluorescence has been studied by Schnepf and McClure (8). There are two molecules per unit cell in

this crystal and from its geometry some splitting is expected. No dichroism could be found, however, and the splitting must be under  $5 \text{ cm}^{-1}$ .

### III. INTERPRETATION OF THE DATA

A detailed interpretation of the data derived in this article would be of considerable value in learning about the outer parts of the wave functions of the systems considered. The energy transfer phenomena depend predominantly upon the shape of the wave functions in their outer regions. As our main purpose was to establish some valid numbers, only a rudimentary treatment based on the dipole-dipole interaction will be attempted here. An equation similar to eq. [5] is used.

All that is needed to carry out this treatment is a knowledge of the geometry, and the strength of the transition in the individual molecules, or parts of molecules. From the integrated absorption band one may obtain the magnitude of the transition moment (in cm.) through the equation

$$M^2 = 3.97 \times 10^{-20} \int \epsilon d\nu / \nu,$$

where  $\epsilon$  is the molar extinction coefficient to base 10. The value of  $M$  for toluene is found to be  $0.10 \text{ \AA}$ , and this number may be used in calculations on other compounds containing benzene rings. The full electronic transition moment has been used. The results of the calculations are shown in Table III.

Some of the paracyclophane splitting energies are greater by an order of magnitude than that predicted from the excitation exchange energy. In the two cases, the 3,6 and 4,4 compounds, where no splitting could be observed in the solution spectra, small splittings were calculated. The smallest splitting distinguishable in the solution spectra is roughly  $500 \text{ cm}^{-1}$ . In the spectrum of the 4,4 compound, some spreading out of the vibrational structure is observable in the solution spectra, and in the low-temperature polarized crystal spectra one expects to see clear evidence for the ring-ring interaction.

The paracyclophanes, which have the very large splittings, all have their benzene rings separated by less than the "packing thickness" of  $3.40 \text{ \AA}$ . Since below this distance there must be considerable  $\pi-\pi$  overlapping, it is reasonable to find that the dipole-dipole energy does not account for all of the splitting.

For the other double molecules, the dipole-dipole energy gives somewhat better values for the splitting. Taking the distance of separation from the nearest points of the benzene rings gives better values than using the separation of the ring centers. As pointed out by Schnepf and McClure (8), the durene crystal should have an observable dichroic splitting according to the dipole-dipole model. This is the one case in Table III where an overestimate of the interaction energy certainly occurs.

In the calculations for Table III the full electronic moment has been used. Simpson and Peterson (9) have recently shown that one must use only the individual vibronic band moments in the limit of very weak coupling, and the full electronic moment only in strong coupling. The overestimate of the durene energy is probably explainable in this way, as it is a very weakly coupled system.

In diphenylmethane the coupling seems to require use of the full electronic moment. The use of point dipoles is obviously a poor approximation for such closely coupled rings, and the full geometry of the system should be used. This statement also applies to the other molecules where large coupling energies are involved.

The numbers in Table III are believed to be well deserving of further theoretical study.

## REFERENCES

1. BROUDE, V. L., MEDVEDEV, V. C., and PRIKHOTJKO, A. F. *Zhur. Eksptl. i Teoret. Fiz.* **21**, 665 (1951).
2. COFFMAN, R. E. and McCCLURE, D. S. *Can. J. Chem.* **36**, 48 (1958). (Preceding paper).
3. CRAIG, D. P. *J. Chem. Soc.* 539 (1955).
4. CRAM, D. J., ALLINGER, N. L., and STEINBERG, H. *J. Am. Chem. Soc.* **76**, 6132 (1954).
5. FOX, D. and SCHNEPP, O. *J. Chem. Phys.* **23**, 767 (1955).
6. LONGUET-HIGGINS, H. C. and MURRELL, J. N. *Proc. Phys. Soc. (London)*, A, **58**, 601 (1955).
7. PESTEIL, P. and CABANNES, J. *Compt. rend.* **235**, 1384 (1952). PESTEIL, P. and BARBARON, M. *J. phys. radium*, **15**, 92 (1954).
8. SCHNEPP, O. and McCCLURE, D. S. To be published.
9. SIMPSON, W. T. and PETERSON, D. L. *J. Chem. Phys.* **26**, 588 (1957).

## DIABATIC REACTIONS<sup>1</sup>

HENRY EYRING, GEORGE STEWART, AND RANSOM B. PARLIN

### ABSTRACT

The fundamentals of diabatic reactions are briefly reviewed. The two important types of radiationless transitions at the crossover region of two potential surfaces are considered kinetically and rate formulations are given. The first type involves an appreciable activation energy in excess of the heat of reaction. The second does not. The reaction velocity is formulated using the absolute rate theory where the transmission coefficient is interpreted in terms of the Landau-Zener probability approximation. The over-all rate of a sequence of reactions is treated in accordance with the principle that resistances in series are additive. If the second in a sequence of two reaction steps involves a negative activation energy and is slow because of failure to cross to the new surface the resultant repeated passage through the crossover region requires a special formulation of the transmission coefficient, which is given. Whether this transmission coefficient influences the over-all rate or not depends on whether or not it belongs to the rate-determining step.

Quenching reactions are classified in terms of the number of free valences involved, an electron being excited from a saturated molecule conferring radical-like properties on the excited molecule. Excited odd-electron molecules will attract at considerable distances without appreciable activation energy.

The transmission coefficient is discussed in terms of recruitment factors for cases in which the products of a reaction are out of equilibrium.

Hot positive ions resulting from mass spectrographic reactions are indicated as another example of diabatic reactions, and a procedure for treating these by the activated complex theory is briefly mentioned.

Most chemical reactions at low temperatures proceed adiabatically, in the Ehrenfest sense, and so involve no crossing over from one potential energy surface to another (2). Diabatic reactions induced by radiation or by fast particles (2, 3) pass from one surface to another either by absorbing radiation or by a radiationless transition at the crossover region of two potential energy surfaces, or else by spontaneous emission of radiation (5). The Einstein transition probabilities are given by the well-known relations (1, 7)

$$[1] \quad A_{m \rightarrow n} = \frac{8\pi h\nu_{mn}^2}{C^3} B_{m \rightarrow n} = \frac{32\pi^3 \nu_{mn}^2}{3C^3 \hbar} \int \psi_m^* \sum_i e_i \mathbf{r}_i \psi_n d\tau,$$

where the symbols have their usual meaning. A most useful relation for the probability

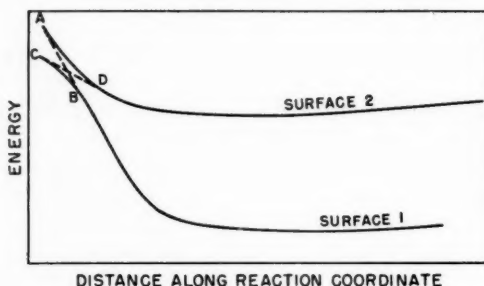


FIG. 1.

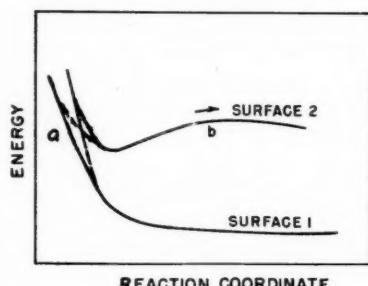


FIG. 2.

<sup>1</sup>Manuscript received October 3, 1957.

Contribution from the Department of Chemistry, University of Utah, Salt Lake City, Utah. This paper was presented at the Symposium on the Structure and Reactivity of Electronically-Excited Species held at the University of Ottawa, Ottawa, Canada, September 5 and 6, 1957.

of continuing along one of the dotted curves in Fig. 1 instead of following along a full curve is given by the approximate relationship

$$[2] \quad P = \exp(-4\pi^2\epsilon_{12}^2/\hbar v |S_1 - S_2|)$$

due to Landau (4) and Zener (11).

In equation [2],  $2\epsilon_{12}$  is the distance between the upper and lower full curves along a vertical line passing through the intersection of the dotted lines. The value of  $\epsilon_{12}$  is  $\int \psi_m^* H^{(1)} \psi_n d\tau$ , where  $\psi_m$  and  $\psi_n$  are the eigenfunctions of  $H_0$  corresponding to the crossing lines and  $H^{(1)}$  is the perturbation which shifts the system to the full-lined non-crossing energy surfaces;  $v$  is the velocity of approach along the reaction coordinate and  $S_1$  and  $S_2$  are the respective slopes of the two dotted lines. For complicated intersecting surfaces a more exact solution than [2] should be found, but in any case appropriate averages of the parameters in [2] are required to give a mean value for the probability  $\bar{P}$ . The reaction velocity for passing from surface 2 to surface 1 is

$$[3] \quad v = \prod_i C_i (\hbar k T / h) \exp(-\Delta F^\pm / RT).$$

We will write  $\mathfrak{H} = \mathfrak{H}_1 \mathfrak{H}_2$ , where

$$[4] \quad \mathfrak{H}_2 = 2\bar{P}(1-\bar{P})$$

and  $\mathfrak{H}_1$  will be discussed subsequently. The velocity of the back reaction is

$$[5] \quad v_b = \prod_b C_b (\hbar k T / K h) \exp(-\Delta F^\pm / RT),$$

where  $C_b$  is the concentration of the  $b$ th product molecule and  $K$  is the equilibrium constant. The other symbols have the same values as in [3].

In Fig. 2 we have a second common type of surface crossing. Here the crossover point is at a lower value of the energy than the final state on surface 2 (to the right of  $b$ ). In this case we have a specific rate constant at  $a$  which we call  $k_a$  and at  $b$  there is a specific rate constant  $k_b$ . The over-all rate is then

$$[6] \quad v = \prod_i C_i / (k_a^{-1} + k_b^{-1}) = \prod_i C_i k_a k_b / (k_a + k_b).$$

Again the velocity of the back reaction is

$$[7] \quad v_b = \prod_b (C_b / K) [k_a k_b / (k_a + k_b)].$$

The rate constants  $k_a$  and  $k_b$  are each to be calculated as if the other rate-limiting process were absent. More generally, a sequence of any number of reactions has an over-all rate constant equal to the reciprocal of the sum of the reciprocals of the individual rates each calculated as though it were the only rate-determining step. This result is in accordance with the principle that resistances in series are additive (6). In [7] we have  $k_b = \mathfrak{H}_b (\hbar k T / h) \exp(-\Delta F_b^\pm / RT)$ , where  $\mathfrak{H}_b \approx 1$  and  $k_a = \mathfrak{H}_a (\hbar k T / h) \exp(-\Delta F_a^\pm / RT)$ . We now take  $\mathfrak{H}_a = \mathfrak{H}_1 \mathfrak{H}_2$ , where

$$[8] \quad \mathfrak{H}_2 = \{1 - [1 - 2\bar{P}(1-\bar{P})]^\nu\} (\tau v)^{-1}.$$

Here  $\tau$  is the lifetime of the complex which vibrates  $\nu$  times per second along the reaction coordinate if the only escape of the complex is back to surface 2, that is,

$$[9] \quad 1/\tau = (\hbar k T / h) \exp[-(\Delta F_b^\pm - \Delta F_a^\pm) / RT].$$

The term in [8] which is raised to the power  $\nu\tau$  expresses the probability of not transi-

tioning in  $\nu\tau$  tries so that the quantity in brackets expresses the chance of transitioning in  $\nu\tau$  vibrations. Consequently  $\mathfrak{H}_2$  is the average chance of transitioning per vibration.  $\Delta F_a^\pm$  and  $\Delta F_b^\pm$  are the standard free energies in going from the initial state to the activated states *a* and *b*, respectively.  $\mathfrak{H}_1$  is the fraction of activated complexes moving from right to left, at equilibrium, which were formed from reactants.  $\mathfrak{H}_1$  is discussed subsequently.

#### TYPE REACTIONS

The reverse of each quenching process is an excitation so that by the principle of microscopic reversibility discussing one is equivalent to discussing the other. When molecules collide there is a tendency for the compressed electron orbits to be promoted as they are promoted in the united atom. Thus, at some interatomic distance one expects a crossing of the non-excited state with the corresponding excited state, as seen in Figs. 1 and 2. Our figures and discussion apply as well to quenching within a molecule as to quenching by collision. In internal quenching the lower surfaces, instead of being flat, turn up like a parabola. This only changes the detailed partition functions to be used but does not modify the above formal considerations.

It is convenient to classify the types of quenching reaction in terms of the number of free valences involved. When an excited saturated molecule is quenched by a second saturated molecule, we have the hole from which the electron was ejected conferring radical-like properties on the excited molecule. Thus the activation energy for collision of such a pair should not exceed a few calories in analogy to the radical reactions  $H + H_2 \rightarrow H_2 + H$  with 8 calories activation energy, or the reaction  $H + Cl_2$  with about 2 calories. The lowering of the activation energy due to the polar nature of the excited molecule leads us to expect low values approaching zero for the activation energy of barrier crossing leading to quenching. At room temperature each 1.3 calories activation energy yields a decrease in the apparent collision cross section by a factor of 10. Such a process is represented in Fig. 1. If the quencher or the excited molecule possesses an odd number of electrons in addition to being excited, two molecules will attract at considerable distance without appreciable activation energy, thus leading to large apparent cross sections. Fig. 2 exemplifies this situation.

#### THE CHEMICAL BOND AND ACTIVATION ENERGY

An electronic orbital behaves like a fluid sphere or rod of high surface tension which, like any fluid, seeks the lowest possible level of potential energy consistent with minimum surface area. Thus, if there are holes of low potential energy lying in two adjacent atoms and if in addition there is an available electron which by occupying the holes jointly can lower its energy, then the atoms will be drawn together by the electronic orbital, thus forming a chemical bond. Minimum curvature for the orbital means minimizing the kinetic energy, much as minimizing surface area lowers total surface energy for a fluid. Laidler (3) has compiled tables listing a variety of quenching cross sections and explained many of them in terms of the types of potential surfaces which cross. A crossing of surfaces with different multiplicities leads to slow reaction rates because of a small  $k_a$ . It is interesting that the observed cross sections are all near enough to ordinary kinetic theory values to preclude activation energies larger than a few calories. Since, however, with competing reactions only the fast reactions are exhibited, we naturally miss such quenching reactions as are relatively slow.

It is natural to expect that the rare gases would be poor quenchers of excited saturated

molecules or even of excited mercury, not being able to complex with them, whereas excited radicals such as O<sup>\*</sup>H, which can form coordination complexes even with saturated structures, should be quenched by most molecules including the rare gases. The efficiency of the rare earths and transition elements in picking up excitation in the carbon arc is understandable in terms of their unfilled shells, which when excited complex with even saturated molecules making  $k_a$  large. Even what Laidler (3) classifies as physical quenching where no new chemical species emerges might well be described as a chemical isomerization in which an excited isomer with its unsaturated valences by being quenched (or by emitting light) changes over into the completely or at least more completely saturated isomer. In this important sense all quenching processes are chemical reactions, each passing through its peculiar activated complex. The quenching molecule, when it emerges unchanged, has served like any other catalyst in providing a changed reaction path, in this case by yielding a crossing of potential surfaces.

Table I lists some of the quenching cross sections found in compilations such as those of Laidler (3). Gases like H<sub>2</sub> and D<sub>2</sub> have quenching cross sections larger than kinetic theory values if they react readily with Hg(<sup>3</sup>P<sub>1</sub>), thus avoiding a multiplicity change, or if they overcome the multiplicity restriction, by having a long lifetime,  $\tau$ , for the complex, as is probably true for Na(<sup>2</sup>P). Cd(<sup>3</sup>P<sub>1</sub>), in spite of reacting with the hydrogens, is probably slowed down by a slow multiplicity change.

TABLE I  
CROSS SECTIONS, Å<sup>2</sup>

	Hg( <sup>3</sup> P <sub>1</sub> )	Cd( <sup>3</sup> P <sub>1</sub> )	Na( <sup>2</sup> P)
H <sub>2</sub>	8.6, 6.0	0.67, 3.54	7.4
D <sub>2</sub>	8.4, 11.9	0.19, 1.80	
Unsaturated hydrocarbons			
C <sub>2</sub> H <sub>2</sub>	23	22	
C <sub>2</sub> H <sub>4</sub>	48, 26	24.9	44
C <sub>2</sub> H <sub>6</sub>	31	29	52
C <sub>4</sub> H <sub>8</sub> -1	33.5	35.2	58
C <sub>4</sub> H <sub>8</sub> -2	29	30.6	58
C <sub>6</sub> H <sub>6</sub>	41.9, 59.9	28.4	75
Saturated hydrocarbons			
CH <sub>4</sub>	0.059	0.012	0.11
C <sub>2</sub> H <sub>6</sub>	0.42	0.024	0.17
C <sub>2</sub> H <sub>8</sub>	1.6	0.012	0.2
n-C <sub>4</sub> H <sub>10</sub>	4.1	0.064	0.3
n-C <sub>6</sub> H <sub>12</sub>	8.6	—	—
n-C <sub>6</sub> H <sub>14</sub>	16	—	—
n-C <sub>8</sub> H <sub>16</sub>	24	—	—
Odd electron			
NO	24.7	—	—
Halogens			
I <sub>2</sub>	—	—	40
Br <sub>2</sub>	—	—	100

The unsaturated hydrocarbons with their  $\pi$  electrons attract at large distances and then complex strongly enough that  $k_a \gg k_b$  because of a long lifetime,  $\tau_1$ , of the complex or else by an increase in the transition per vibration,  $2\bar{P}(1-\bar{P})$ . It is interesting that for the quenching of Na(<sup>2</sup>P), where chemical changes in the unsaturated hydrocarbons

do not occur, the quenching cross sections are nevertheless greater than for  $\text{Hg}({}^3P_1)$  and  $\text{Cd}({}^3P_1)$ , where  $\text{H}_2$  is liberated. One must conclude that long lifetimes,  $\tau$ , contrive to make  $k_a \gg k_b$  and that this is independent of whether there are subsequent chemical changes or not. This indication that the rate-determining step is the "physical quenching" whether or not this is followed by a chemical reaction is interesting in connection with Zemansky's (10) evidence that oscillators which most nearly matched their quantum to the 5.03 kcal. for the change  $\text{Hg}({}^3P_1) \rightarrow \text{Hg}({}^3P_0)$  were most efficient in the quenching process.

Table I indicates also that for saturated hydrocarbons the rate-determining step for quenching seems to yield roughly similar cross sections whether chemical reactions follow as for  $\text{Hg}({}^3P_1)$  or  $\text{Cd}({}^3P_1)$  or whether they do not as for  $\text{Na}({}^3P)$ . This suggests again that the rate-determining step is low for methane because  $2\bar{P}(1-\bar{P})$  and/or  $\tau$  are low. Larger molecules would be expected to complex more readily with the excited atoms and so increase  $\tau$  and, therefore, the quenching cross section, as is observed. The remaining cases are also in accord with the view that in quenching the rate-determining step is usually without an activation energy and is governed by  $\tau$  and  $2\bar{P}(1-P)$  whether or not it is followed by a subsequent chemical reaction.

#### THE TRANSMISSION COEFFICIENT, THE CONNECTIVITY OF STATES, AND THE RECRUITMENT FACTORS

We have discussed at some length  $\mathfrak{H}_2$ , which we will call the diabatic factor in the transmission coefficient  $\mathfrak{H}_a = \mathfrak{H}_1 \mathfrak{H}_2$ . The factor  $\mathfrak{H}_1$  is the additional factor required to correct an equilibrium reaction rate expression for non-equilibrium conditions. Ideally we should consider every possible quantum state of a reacting system as a separate species and proceed by the methods made familiar in dealing with chain reactions. Such a procedure yields the set of equations

$$[10] \quad dc_i/dt = \sum_j (k_{j \rightarrow i} c_j - k_{i \rightarrow j} c_i),$$

where there are as many equations as there are quantum states. In the general case the  $k$ 's are functions of the concentrations of various species, the temperature, which isotope is involved, and the radiation density. At equilibrium we have  $dc_i/dt = 0$  for all species. In a steady state,  $dc_i/dt$  can be taken as zero to a good approximation only for certain intermediates which exist at very low concentrations in the reaction sequence. For those states considered to maintain an equilibrium distribution in spite of the reaction we assume

$$[11] \quad d \ln c_i/dt = d \ln \sum_k c_k/dt = -d \ln \sum_i c_i/dt.$$

This is, of course, a great simplification and never quite true. In [11]  $\sum_k c_k$  gives the total concentration of a particular reactant while  $\sum_i c_i$  is the concentration of a product;  $c_i$  is the concentration of the particular species in the  $i$ th quantum state. When one observes that the products of a reaction are out of equilibrium as chemiluminescent spectra often show, it follows by the principle of detailed balance that for the reverse reaction the reacting species would not be withdrawn from the reservoir of states in such a way as to maintain equilibrium exactly. To this extent a mean  $\mathfrak{H}_1$  is not exactly true but is still a useful approximation. However, molecular beam experiments such as those of Taylor and Datz (9) will require something better than a mean  $\mathfrak{H}_1$  and will be revealing the detailed structure of potential energy surfaces. The various isotopic reactions may have nearly equal mean values of  $\mathfrak{H}_1$ , in spite of markedly fluctuating transmission coefficients for various states of the activated complex.

As indicated in equation [10], a particular state recruits its occupants from all other states. We define the recruitment factor for the  $j$  to  $i$  state with reference to equation [10] as

$$[12] \quad f_{j \rightarrow i} = k_{j \rightarrow i} c_j^0 / \sum_j k_{j \rightarrow i} c_j^0,$$

where the zero subscript refers to the equilibrium concentration and  $\sum_j f_{j \rightarrow i} = 1$ . Clearly the  $f$ 's are expressible in terms of partition functions alone. In order that  $\mathfrak{H}_1$  should be unity, it is clear that every activated complex corresponding to crossing from reactant to product should recruit only from reactants, since  $\mathfrak{H}_1$  is the total recruitment from reactant over recruitments from both reactants and from products. However, if it recruits equally from reactants and products,  $\mathfrak{H}_1$  is still one-half. In pathological cases such as in the reaction  $H_2 \rightarrow 2H$ , the activated complex states moving in the direction reactants to products recruit largely from products. This yields a correspondingly low value for  $\mathfrak{H}_1$ .

#### MASS SPECTROGRAPHIC REACTIONS

The activated complex theory has been applied to reactions in the mass spectrograph (8). When an electron knocks another electron out of a molecule and makes a positive ion, this constitutes a Franck-Condon transition from the low potential surface for the molecule up to the surface corresponding to the ion. If the electron removed were completely localized in one bond in the ground state, and if there were no electronic reorganization in the positive ion, then only one bond length would be too short after the transition and the stored up energy would either break the weakened bond or would be insufficient to do so. Instead, the bonds finally broken bear little relation to the bond which must have been the source of the displaced electron. Another way of looking at the situation is that the equilibrium structure of the positive ion usually differs greatly from that of the neutral molecule in many bonds. The result is that, typically, ionization creates a positive ion with several electron volts of energy scattered over many degrees of freedom and only as the Lissajous motion of the mass point concentrates the dissociation energy in a bond does one get dissociation.

Thus, ionization creates a hot positive ion which usually has sufficient energy to break a variety of bonds each with a specific rate constant. The appearance potentials fix the activation energy for the corresponding reactions and the vibration frequencies can be estimated so that one can calculate a corresponding set of rate constants. Thus, for an assumed energy in the molecule, one can calculate the percentage of each of the possible products formed during the time the positive ion stays in the mass spectrograph. If the distribution function of number of ions against energy stored in the ion can be measured, or assumed, or calculated one can predict the mass spectra for a molecule. Much remains to be learned about such measurements and calculations, but enough success has been achieved to indicate that the outlined procedure is on the right track. Hot positive ions with their mobile structure and enormous reactivity seem to constitute one more diabatic province at least partly understood. Characteristically the energy left in electronically excited states crosses over and becomes available as vibrational energy promoting reaction on the lowest state of the positive ion. Molecules like the aromatic hydrocarbons which tend to fluoresce in solution possess groups of states which do not cross effectively with other states and, as would be expected, yield larger percentages of parent ions.

We wish to express our appreciation to the National Science Foundation for their support of this research.

## REFERENCES

1. EYRING, H., WALTER, J., and KIMBALL, G. E. Quantum chemistry. John Wiley and Sons, Inc., New York. 1944. p.115.
2. GLASSTONE, S., LAIDLER, K. J., and EYRING, H. The theory of rate processes. McGraw-Hill Book Company, Inc., New York. 1941.
3. LAIDLER, K. J. The chemical kinetics of excited states. Oxford Univ. Press, London. 1955.
4. LANDAU, L. Physik. Z. Sowjetunion, **46**, No. 2 (1932).
5. LUMRY, R. and EYRING, H. Radiation biology. Vol. 3. Edited by A. Hollaender. McGraw-Hill Book Company, Inc., New York. 1956. Chap. I.
6. PARLIN, R. B. and EYRING, H. Ion transport across membranes. Edited by H. T. Clarke. Academic Press Inc., New York. 1954. p. 103.
7. PAULING, L. and WILSON, E. B. Introduction to quantum mechanics. McGraw-Hill Book Company, Inc., New York. 1935.
8. ROSENSTOCK, H. M., WALLENSTEIN, M. B., WAHRHAFTIG, A. L., and EYRING, H. Proc. Natl. Acad. Sci. U.S. **38**, 667 (1952).
9. TAYLOR, E. H. and DATZ, S., JR. J. Chem. Phys. **23**, 1711 (1955).
10. ZEMANSKY, M. W. Phys. Rev. **36**, 1919 (1930).
11. ZENER, C. Proc. Roy. Soc. (London), A, **137**, 696; A, **140**, 660 (1933). See also Ref. 1, Chap. 16.

# REACTIONS INVOLVING ELECTRONICALLY-EXCITED OXYGEN<sup>1</sup>

E. KERRY GILL AND K. J. LAIDLER

## ABSTRACT

The various electronically-excited states of oxygen atoms and molecules are briefly considered. Certain reactions involving some of these electronically-excited species are then discussed with reference to the experimental evidence and to the potential-energy surfaces on which they occur. In the case of the mercury-photosensitized formation of ozone from oxygen it is concluded that both experimental evidence and theoretical arguments point to the fact that the oxygen molecule initially formed is in an excited  $^3\Sigma_u^+$  state. Consideration is also given to the mechanism of formation of  $O_2^*$  in the carbon monoxide flame and in other flames. The reactions



and



are also discussed briefly.

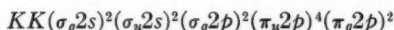
## INTRODUCTION

A considerable number of electronically-excited states of oxygen molecules and atoms are known to exist, and spectroscopic data have provided detailed information about many of them. Several of these excited species are known to be involved in chemical reactions, either as reactants or as products. The purpose of this paper is to refer to a few of the more common reactions of this type, to discuss the evidence for the nature of the species involved, and to consider detailed reaction mechanisms from the standpoint of the method of potential-energy surfaces.

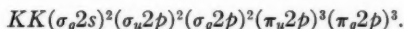
## ELECTRONIC STATES

The electronic states of O and  $O_2$  will be mentioned only very briefly, since this matter has been fully discussed elsewhere (14, 15). According to the Wigner-Witmer correlation rules two atoms of oxygen in their ground states ( $^3P_g$ ) can produce, on combination, 18 different electronic species of the molecule, while one ground state atom plus one in the first excited level ( $^1D_g$ ) can give an additional 18 species. Only a few of these are stable or relatively abundant, and Fig. 1 shows the potential-energy curves for those states of the molecule that have been observed spectroscopically. The  $^1\Sigma_u^-$  and  $^3\Delta_u$  states ( $^3\Delta_u$  not drawn) have been detected by Herzberg (16).

The ground state of  $O_2$  ( $^3\Sigma_g^-$ ) and the first two excited states ( $^1\Delta_g$  and  $^1\Sigma_g^+$ ) have the electronic configuration



and dissociate to normal  $^3P_g$  atoms as shown in the figure. Additional excited states are formed by the transfer of an electron from the bonding ( $\pi_u 2p$ ) orbital to the antibonding ( $\pi_g 2p$ ) orbital to give



This configuration could produce the states  $^1\Sigma_u^+$ ,  $^1\Sigma_u^-$ ,  $^1\Delta_u$ ,  $^3\Sigma_u^+$ ,  $^3\Sigma_u^-$ , and  $^3\Delta_u$ , of which  $^1\Sigma_u^-$ ,  $^3\Sigma_u^+$ ,  $^3\Sigma_u^-$ , and  $^3\Delta_u$  have been observed.  $^3\Sigma_u^-$  dissociates into  $O(^3P_g) + O(^1D_g)$ , the rest into ground-state  $O(^3P_g)$  atoms.

<sup>1</sup>Manuscript received August 16, 1957.

Contribution from the Department of Chemistry, University of Ottawa, Ottawa, Canada. This paper was presented at the Symposium on the Structure and Reactivity of Electronically-Excited Species held at the University of Ottawa, Ottawa, Canada, September 5 and 6, 1957.

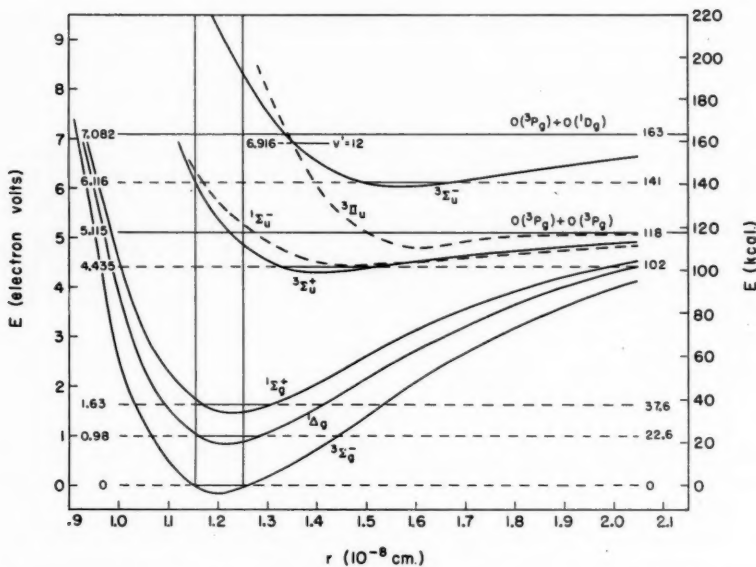


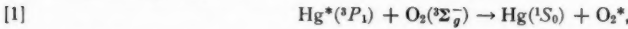
FIG. 1. Potential-energy curves for the ground and excited states of the oxygen molecule.

Fig. 1 also includes a  $^3\Pi_u$  curve recently proposed by Wilkinson and Mulliken (34) to account for the predissociation of  $O_2(^3\Sigma_g^-)$  into  $^3P_g$  atoms.

#### THE REACTION $Hg^*(^3P_1) + O_2(^3\Sigma_g^-) \rightarrow Hg(^1S_0) + O_2^*$

Molecular oxygen is an effective quencher for the 2537 Å mercury line, the quenching cross-section being very large (29, 35). This quenching process involves the transition from the  $^3P_1$  state of Hg to the  $^1S_0$  state, a transition that occurs with an energy liberation of 4.88 ev. or 112.5 kcal. Ozone is produced during the quenching, and it is of interest to consider the state of the oxygen after it has reacted with the excited mercury atom.

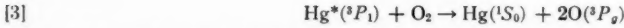
In the first place, there is abundant evidence that the reaction is



where  $O_2^*$  is an excited state of oxygen, the nature of which is discussed below. The reasons for preferring this reaction to



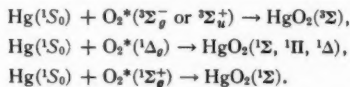
and



are briefly as follows. Reaction [2] is exothermic by at least 64 kcal. (32) and is therefore energetically possible; however if it were followed by  $O + O_2 \rightarrow O_3$  there would be one molecule of ozone formed from each Hg\* atom.† Experimentally at least seven molecules are formed (3, 32), and the reaction  $HgO + O_2 \rightarrow Hg + O_3$  is too endothermic to be useful. Reaction [3] can be excluded as being slightly endothermic.

†Since the Hg is converted into HgO there can be no re-excitation to Hg\*. If reaction [1] occurs re-excitation is possible and large yields can result.

According to the correlation rules  $Hg^*(^3P_1)$  and  $O_2(^3\Sigma_g^-)$  can combine to give the linear complex  $HgO_2$  in  $\Sigma$  and  $\Pi$  states with singlet, triplet, and quintet multiplicities. Energetically, since 4.88 ev. is available, the  $O_2^*$  could be in any one of the four lowest electronic states, namely  ${}^3\Sigma_g^-$  (ground),  ${}^1\Delta_g$ ,  ${}^1\Sigma_g^+$ , and  ${}^3\Sigma_u^+$ . All of these states are permitted by the correlation rules, as may be seen as follows:



The question now to be decided is which of these four electronic states of  $O_2$  is actually formed. Various suggestions have previously been made. Mitchell (25) suggested that, since the ground state of oxygen has a vibrational level at 4.86 ev., which corresponds closely to the energy released, this state will actually be formed; in other words, the electronic energy of the mercury will pass almost entirely into vibrational energy of the oxygen. However, recent work has indicated (23, p. 105) that this resonance factor, arising from the matching of energy levels, is not an important one. Volman (33), on the basis of his results (32) on the effect of foreign gases on ozone production, suggested that the oxygen produced was either vibrationally excited  ${}^3\Sigma_g^-$  or a singlet state, and argued against its being the  ${}^3\Sigma_u^+$  state. Finally one of us (see p. 101 of Ref. 23) has tentatively suggested that the most probable process is the one involving the least loss of electronic energy, and from this it follows that the  ${}^3\Sigma_u^+$  state is the one that should be produced.

In the following two subsections we re-examine this problem from both the experimental and theoretical points of view, and conclude that the  ${}^3\Sigma_u^+$  state is probably produced.

#### *Influence of Foreign Gases*

The reactions subsequent to reaction [1] and leading to ozone production are



and



where  $M$  is a third body required to carry off the excess energy. Volman's discussion (33) of the probable state of the  $O_2^*$  produced in reaction [1] is based on the effects of foreign gases added to the system. A number of such gases were found to increase the rate of ozone production in the mercury-photosensitized reaction, the order of effectiveness being



These gases play a role in reaction [5] as well as in the reactions

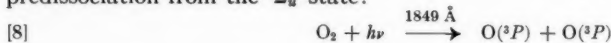


and



This behavior of foreign gases is to be contrasted with their effects on the unsensitized photochemical formation of ozone from oxygen at 1849 Å (32). The foreign gases were in this case found to reduce the role of ozone formation, their order of effectiveness as retarders being the same as above. At this wavelength oxygen dissociates into two normal

$^3P$  atoms (27, p. 246), either by a direct transition to a repulsive state of  $O_2$  or by a predissociation from the  $^3\Sigma_u^-$  state:



Subsequent processes are



and



The reactions occurring in the sensitized and unsensitized reactions may thus be compared as follows:

	Sensitized reaction (accelerated by foreign gases)	Unsensitized reaction (retarded by foreign gases)
I	$Hg^*(^3P_1) + O_2(^3\Sigma_g^-) \rightarrow Hg(^1S_0) + O_2^*$	
II	$O_2^* + O_2 \rightarrow O_3 + O$	$O_2 + h\nu \xrightarrow{1849 \text{ \AA}} O(^3P) + O(^3P)$
III	$O + O_2 + M \rightarrow O_3 + M$	$O + O_2 + M \rightarrow O_3 + M$
IV	$Hg^* + M \rightarrow Hg + M^*$	
V	$O_2^* + M \rightarrow O_2 + M^*$	$O + O + M \rightarrow O_2 + M$

It is to be noted that in the sensitized reaction M catalyzes the production of ozone as far as III is concerned and inhibits it in IV and V. In the unsensitized reaction M is a catalyst in VII and an inhibitor in VIII.

In the sensitized reaction the foreign gases catalyze the formation of ozone, the inert gases being the most effective. Evidently their effect on III overrides that on IV and V. But if, as Volman asserts, the energy of  $O_2^*$  is largely vibrational, these gases would readily bring about deactivation, and no over-all accelerating effect would result. In our view the simplest explanation of the facts is that the excitation energy of  $O_2^*$  is largely electronic in nature. If this is the case the quenching to lower electronic states will occur only with difficulty, and hardly at all with the inert gases (20). In order for the ozone-producing reaction II to occur readily the  $O_2^*$  must have at least 94 kcal. of energy. If this  $O_2^*$  is in the  $^3\Sigma_u^+$  state, even if it is in its ground vibrational level it still has more than this amount of energy. In the case of the three lower known electronic states, however, quenching by the foreign gases to the ground vibrational state would produce a molecule having insufficient energy to produce ozone. The facts are therefore completely explained if the  $^3\Sigma_u^+$  state is formed, but not if any of the lower states are formed.

We may now consider whether these ideas are also consistent with the facts regarding the unsensitized formation of ozone by 1849 Å radiation, the mechanism for which is given above. To explain the retardation by foreign gases it must be supposed that their effect on reaction VIII is more important than on VII. This is probably due to the relative rates of the reactions; reaction VIII presumably has no activation energy, while Dainton and Kimberley (2) by an indirect method have concluded that VII has an activation energy of 4.3 kcal. Furthermore, in the thermal decomposition of ozone, which probably occurs by the mechanism



Griffith and McKeown (10) found that He, A, N<sub>2</sub>, and CO<sub>2</sub> catalyzed the decomposition;

this indicates that the last reaction is influenced by M more than is VII. Reaction VIII has not been included in the scheme for the sensitized reaction since there will be a much smaller concentration of oxygen atoms than in the unsensitized process; the over-all rate is very much less.

Volman (33) based his conclusion that  $O_2^*$  is not in the  ${}^3\Sigma_u^+$  state upon the relative effects of the foreign gases, and made no mention of the important fact that increasing their concentration increases the rate. It is of interest that the results indicate the order of the effects of the gases to be the same on III as on VIII.

The conclusion of the present subsection is that the  $O_2^*$  produced in reaction [1] is in the  ${}^3\Sigma_u^+$  state, and it would be of interest to have direct spectroscopic evidence of this. In the meantime we will now show that the same conclusion is suggested by the theoretical considerations.

#### Potential-Energy Surfaces

It is instructive to discuss the mechanism of reaction [1] using the method of potential-energy surfaces. Fig. 2 shows a schematic representation of the surfaces, the method

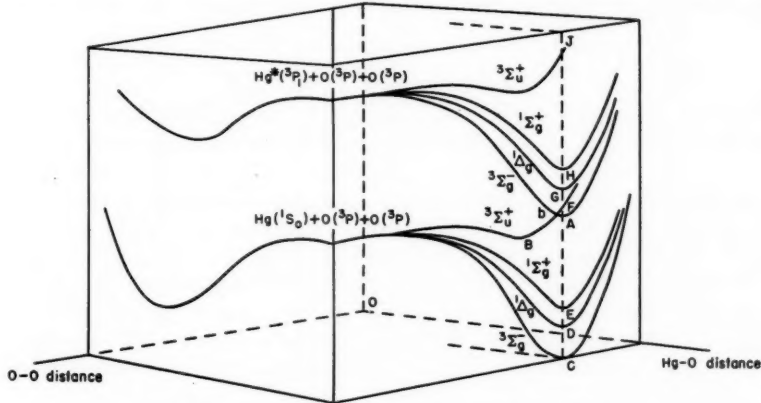
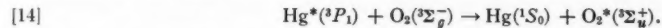


FIG. 2. Potential-energy surfaces for the Hg—O—O system.

employed being that previously used by one of us (20, 21, 22, 23, 24). Point A represents the initial state of the reaction, with  $Hg^*({}^3P_1)$  and  $O_2({}^3\Sigma_g^-)$  separated from one another. Points B, C, D, and E represent possible final states, corresponding to  $Hg({}^1S_0)$  together with  $O_2$  in its ground state (point C) or some excited state. Points A, B, C, D, and E are the entrances to valleys that proceed into the cube from the right-hand face.

Consider first the possibility of a transition from A to B, corresponding to the process



When the potential-energy curves are constructed accurately, using the spectroscopic data, the form of the curves in the region of the points A and B is as shown in Fig. 3. It is to be seen that the crossing point b lies at about the ground vibrational level of the  $O_2({}^3\Sigma_g^-)$  curve, so that the transition can easily occur even at considerable separations between  $Hg^*$  and  $O_2$ . The potential-energy surfaces therefore confirm our deductions from the experimental results that the  $O_2^*$  formed will be in the  ${}^3\Sigma_u^+$  state, corresponding to the least transfer of electronic energy into other forms. The fact that the transition

can occur at large separation is consistent with the very large quenching cross-section observed for the reaction (29, 35).

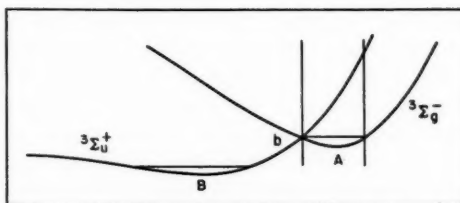


FIG. 3. Enlarged version of a portion of Fig. 2.

If for any reasons the transition to *B* did not occur, the conclusion from the surfaces is that the next most likely possibility is a transition to *E*; failing that, transitions to *D* and *C* could occur. In other words, the system "cascades" through the various electronic states. The evidence for this is as follows. Fig. 4 shows a schematic potential-energy profile through the line *CAJ* in Fig. 2. In this diagram the valley starting at *A*

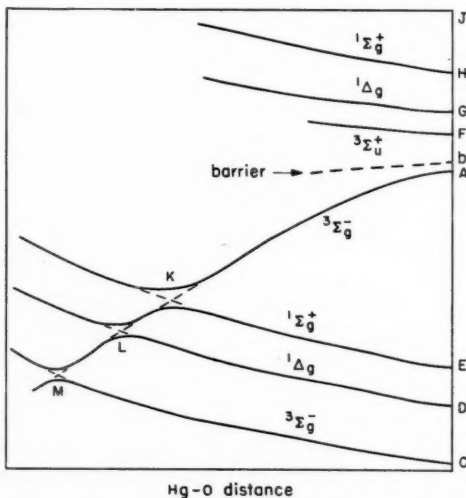


FIG. 4. Potential-energy profile through *CAJ* in Fig. 2. The designations refer to the state of the oxygen molecule.

is represented as going down as the Hg—O distance is decreased; this corresponds to attraction between Hg\* and O<sub>2</sub>. A number of valleys will start from the points *C*, *D*, *E*, *F*, *G*, and *H*; some of these will correspond to repulsive states and will therefore slope upwards. The dotted line starting at *b* represents the top of the barrier separating the valleys *A* and *B*; this line should not be in the plane of this profile but slightly above it (i.e. corresponding to larger O—O separations).

With regard to the valleys starting at *A*, *C*, *D*, and *E* there is some choice of multiplicities, and it will be assumed that those curves represented in Fig. 4 all correspond to the same multiplicity. The non-crossing rule then provides for resonance splittings, as

shown at *K*, *L*, and *M*. At the point *K* a system proceeding in the direction *AK* may undergo a transition and end up at *E*. Failing such a transition the next possibility is a transition at *L*, the system ending up at *D*. Failing that the oxygen will be in the ground state, at *C*. These latter possibilities, however, are very unlikely. Although the curves shown in Fig. 4 are only schematic it does not seem to be possible, by modifying the form of the curves, to arrive at conclusions other than those reached above.

To summarize, our conclusion from the potential-energy surfaces is that the order of probabilities for the formation of oxygen in reaction [1] is



The conclusion that the  $^3\Sigma_u^+$  state is the most likely confirms our deduction from the experimental evidence based on the effects of foreign gases on ozone production.

THE REACTIONS  $O(^3P) + CO(^1\Sigma_u^+) \rightarrow CO_2^*(^3\Pi)$   
AND  $CO_2^*(^3\Pi) + O_2 \rightarrow CO_2 + O_2^*$

The reactions



and



are believed to take place in the carbon monoxide flame. Since the mechanisms and other features of the reactions have recently been discussed (9, 23) only a brief discussion will be given here.

The luminosity of the carbon monoxide flame is too great to be attributed to thermal radiation alone, so that the presence of electronically excited species is to be expected. The ground state of  $CO_2$  is  $^1\Sigma_g^+$  (26) and the first excited states probably  $^3\Pi$  and  $^1\Pi$  in that order. Spectroscopic observation of the flame shows no evidence of any excited  $CO_2$ , and it is therefore believed that  $CO_2$  is formed as above. Since  $CO$  is a singlet in its ground state, reaction with a normal (triplet) oxygen atom will necessarily produce excited  $CO_2^*(^3\Pi)$ , whereas  $CO_2$  ( $X ^1\Sigma_g^+$ ) can be formed directly only from an atom in a singlet state:



The presence of  $O$  atoms in the reaction has been confirmed by Gaydon (6, 7). It is found (8, 11) that  $O(^3P)$  atoms do not react with  $CO$  on every collision, but the reaction between  $O(^1D)$  and  $CO$  is much more rapid (28).

If the  $CO_2$  formed in [15] were in the ground state, the process would be exothermic by 126.7 kcal., whereas the actual heat liberated is lower than this by the energy of excitation and is probably about zero (7). The spectral continuum of the flame has been attributed (7) to the association reaction



At the same time, the banded structure of the spectrum is due to the Schumann-Runge system

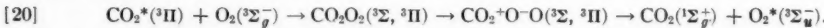


Hornbeck (17) observed that with increasing  $O_2/CO$  ratio, the intensity of the continuum decreased while that of the banded structure increased. This would be explained

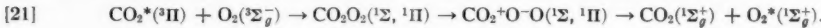
by the fact that an increase in  $O_2$  pressure will increase the amount of  $O_2^*$  formed in [16] and consequently the intensity of the Schumann-Runge bands. But also the  $CO_2^*$  ( $^3\text{II}$ ) is brought to the ground state by this radiationless transition and less will be at hand to give the continuum reaction [18] (23, p. 72).

The possibility of physical quenching in [16], with the oxygen remaining in its ground state, is not forbidden by the correlation rules, but consideration of the disposition of the potential-energy surfaces involved (9) shows that it is very unlikely since the  $^3\Sigma$  surface lies much below the others with no apparent connection between them.

Two excited electronic states of oxygen have been detected in the flame; one is the  $^3\Sigma_u^-$  state which, by passing to the lowest state, gives the Schumann-Runge bands. This state can be formed via triplet complexes, and if ionic surfaces are involved, the process would be (Ref. 23, p. 101):

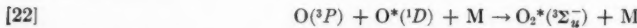


The other state is the  $^1\Sigma_g^+$ , which can be produced via singlet complexes:



#### THE REACTION $O(^3P) + O^*(^1D) + M \rightarrow O_2^*(^3\Sigma_u^-) + M$

The fact that the Schumann-Runge bands have been observed in the hydrogen (1, 5, 31), carbon monoxide (18), and ammonia (19) flames suggests that there may be a reaction such as



common to all of these flames, by which the  $O_2^*(^3\Sigma_u^-)$  is produced (Ref. 23, p. 75). The metastable  $O^*$  ( $^1D$ ) may be produced thermally, from the dissociation of one of the reaction intermediates such as  $OH^*(^2\Sigma^+)$ , or perhaps, in the case of the CO flame, from



#### THE REACTIONS $O + O_3 \rightarrow 2O_2^*$ AND $O_2^* + O_3 \rightarrow 2O_2 + O$

The reactions



and



are believed to occur in the photochemical decomposition of ozone. The primary process of the scheme must be

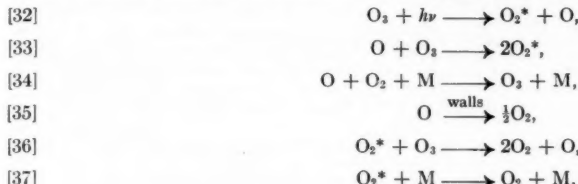


From thermal data,  $\Delta H$  for [26] is 24.1 kcal. corresponding to a wavelength of about 11,800 Å, which would be the infrared limit for a possible dissociation (Ref. 29, p. 144). Shorter wavelengths supply energy for the following reactions:

		$\Delta H$ (kcal.)	$\lambda$ (Å)	
[27]	$O_3 + h\nu \rightarrow O_2(^3\Sigma_g^-) + O(^3P)$	24.1	11,800	I.R. ↓
[28]	$O_3 + h\nu \rightarrow O_2^*(^1\Delta_g) + O(^3P)$	47.1	6,200	Visible ↑
[29]	$O_3 + h\nu \rightarrow O_2^*(^1\Sigma_g^+) + O(^3P)$	62	4,600	Visible ↓
[30]	$O_3 + h\nu \rightarrow O_2(^3\Sigma_g^-) + O^*(^1D)$	70	4,000	U.V. ↑
[31]	$O_3 + h\nu \rightarrow O_2^*(^1\Sigma_g^+) + O^*(^1D)$	108	2,600	U.V. ↓

Consequently, it has been suggested (30) that the O atom of [26] is  $^3P$  when absorption takes place in the visible region, and  $^1D$  when in the ultraviolet.

The experimental work of Forbes and Heidt (4, 12) showed a range of values for the quantum yield  $\phi$  and a complex dependence of  $\phi$  on ozone concentration, total pressure, light intensity, etc. Heidt (13) concluded that activated molecules must play a part in the reaction and found it necessary to postulate an energy chain:



The rather complicated expression for  $\phi$  that results gives the correct dependence of  $\phi$  on light intensity, pressure, and so forth.

Whether or not the  $\text{O}_2$  of [32] is electronically excited depends upon the wavelength used, as seen above.  $\Delta H$  for reaction [33] is  $(-92.3 + 2E_e)$  kcal. where  $E_e$  is the excitation energy of each  $\text{O}_2^*$  in [33]. Consequently, each oxygen molecule could be in the  ${}^1\Sigma_g^+$  state and the reaction still be exothermic. Now  $\Delta H$  for reaction [36] is  $(25.7 - E_e)$  kcal. so that in order for it to be exothermic,  $E_e > 25.7$  kcal. or 1.12 ev.; i.e.  $\text{O}_2^*$  is  ${}^1\Sigma_g^+$  or a vibrationally excited form of a lower state.

Ozone absorbs weakly in the visible and strongly in the ultraviolet region. The electronic term level of the  ${}^1\Sigma_g^+$  state of  $\text{O}_3$  is 38 kcal., which, according to Heidt, corresponds roughly to the difference in energy between the long wave limits of the ultraviolet and visible absorption spectra of  $\text{O}_3$ , 3500 and 6500 Å (Ref. 27, p. 396). If this also corresponds to the energy difference between two electronic levels of  $\text{O}_3$ , the upper one of which dissociates spontaneously to  $\text{O}_2 + \text{O}$ , then reaction [36] may be expected to be very efficient if the  $\text{O}_2^*$  is  ${}^1\Sigma_g^+$ . It is therefore assumed that this is the electronic state involved.

#### REFERENCES

1. BROIDA, H. P. and SHULER, K. E. *J. Chem. Phys.* **20**, 168 (1952).
2. DANTON, F. S. and KIMBERLEY, H. M. *Trans. Faraday Soc.* **46**, 629 (1950).
3. DICKINSON, R. G. and SHERRILL, M. S. *Proc. Natl. Acad. Sci. U.S.* **12**, 175 (1926).
4. FORBES, G. S. and HEIDT, L. J. *J. Am. Chem. Soc.* **56**, 1671 (1934).
5. GAYDON, A. G. *Nature*, **164**, 22 (1949).
6. GAYDON, A. G. *Proc. Roy. Soc. A*, **183**, 111 (1944).
7. GAYDON, A. G. *Trans. Faraday Soc.* **42**, 292 (1946).
8. GEIB, K. H. and HARTECK, P. *Ber.* **66**, 1815 (1932).
9. GRIFFING, V. and LAIDLER, K. J. *Third symposium on combustion, flame and explosion phenomena*. Williams and Wilkins Co., Baltimore, Md. 1949, p. 432.
10. GRIFFITH, R. O. and McKEOWN, A. *J. Chem. Soc.* **127**, 2087 (1925).
11. HARTECK, P. and KOPSCHE, V. *Z. physik. Chem. (Leipzig)*, B, **12**, 327 (1931).
12. HEIDT, L. J. and FORBES, G. S. *J. Am. Chem. Soc.* **56**, 2365 (1934).
13. HEIDT, L. J. *J. Am. Chem. Soc.* **57**, 1710 (1935).
14. HERZBERG, G. *Atomic spectra and atomic structure*. Prentice-Hall, Inc., New York. 1937.
15. HERZBERG, G. *Molecular spectra and molecular structure. Vol. I. Spectra of diatomic molecules*. D. Van Nostrand Co. Inc., New York. 1950.
16. HERZBERG, G. *Can. J. Phys.* **31**, 657 (1953).
17. HORNBECK, G. A. *J. Chem. Phys.* **16**, 845 (1948).
18. HORNBECK, G. A. and HOPFIELD, H. S. *J. Chem. Phys.* **17**, 982 (1949).
19. HORNBECK, G. A. See Ref. 23, p. 75.
20. LAIDLER, K. J. *J. Chem. Phys.* **10**, 34, 43 (1942).
21. LAIDLER, K. J. *J. Chem. Phys.* **15**, 712 (1947).
22. LAIDLER, K. J. *J. Chem. Phys.* **22**, 1740 (1954).
23. LAIDLER, K. J. *The chemical kinetics of excited states*. Clarendon Press, Oxford. 1955.
24. LAIDLER, K. J. and SHULER, K. E. *Chem. Revs.* **48**, 153 (1951).

25. MITCHELL, A. C. G. *J. Franklin Inst.* **206**, 817 (1928).
26. MULLIKEN, R. S. *J. Chem. Phys.* **7**, 14 (1939).
27. NOYES, W. A. and LEIGHTON, P. A. *The photochemistry of gases*. Reinhold Publishing Corporation, New York. 1941.
28. POPOV, B. *Acta Physicochim. U.R.S.S.* **3**, 223 (1935).
29. ROLLEFSON, G. K. and BURTON, M. *Photochemistry and the mechanism of chemical reactions*. Prentice-Hall, Inc., New York. 1939.
30. SCHUMACHER, H. J. *J. Am. Chem. Soc.* **52**, 2377 (1930).
31. SHULER, K. E. *J. Chem. Phys.* **19**, 888 (1951).
32. VOLMAN, D. H. *J. Am. Chem. Soc.* **76**, 6034 (1954).
33. VOLMAN, D. H. *J. Chem. Phys.* **24**, 122 (1956).
34. WILKINSON, P. G. and MULLIKEN, R. S. *Astrophys. J.* **125**, 594 (1957).
35. ZEMANSKY, M. W. *Phys. Rev.* **36**, 919 (1930).

# PRIMARY PROCESSES IN REACTIONS INITIATED BY PHOTOEXCITED MERCURY ISOTOPES<sup>1</sup>

HARRY E. GUNNING<sup>2</sup>

## ABSTRACT

A study has been made of the reaction of  $\text{Hg}^{202}(^3P_1)$  atoms, photoexcited in natural mercury vapor, with a number of substrates which form solid mercury compounds in mercury photosensitization. Some data are also given for reactions initiated by  $\text{Hg}^{196}(^3P_1)$  atoms. The solid mercury compounds formed were examined for enrichment in the isotope initiating the reaction. Such enrichment would be evidence for the primary formation of the mercury compound.

Three  $\text{HgO}$ -forming substrates were studied: water vapor, nitrous oxide, and oxygen. The  $\text{Hg}_2\text{Cl}_2$ -forming substrates studied included hydrogen chloride, methyl chloride, methylene chloride, chloroform, carbon tetrachloride, isopropyl chloride, and boron trichloride. One  $\text{Hg}_2\text{Br}_2$ -forming substrate was examined—isopropyl bromide.

Among the  $\text{HgO}$ -forming substrates only water vapor gave enrichment in  $\text{Hg}^{202}$  in the  $\text{HgO}$  product. The  $\text{Hg}^{202}$  content of the oxide was found to vary from 32 to 35%, depending on reaction conditions, compared to a natural abundance of 29.6%. With water vapor—butadiene mixtures, oxides containing as high as 90%  $\text{Hg}^{202}$  were obtained. Similar enrichment factors were obtained for  $\text{Hg}^{196}(^3P_1)$  reactions.

Hydrogen chloride and the alkyl chlorides yielded calomels containing a maximum of 45%  $\text{Hg}^{202}$ . Methyl chloride gave similar enrichment factors in  $\text{Hg}^{196}$  for the  $\text{Hg}^{196}(^3P_1)$  reaction. The calomel formed in the boron trichloride reaction showed no enrichment.

Addends such as butadiene and benzene, when added to hydrogen chloride, increased the  $\text{Hg}^{202}$  enrichment from 45% to 60%.

For those reactions which yield mercury compounds enriched in the initiating mercury isotope, evidence is presented for a single primary process. Failure to obtain pure isotopes is attributed to exchange reactions with adsorbed natural mercury during recovery of the enriched mercury from the product. It is postulated that the addends react with the mercury product and reduce chemisorption of natural mercury on the product.

The significance of these findings in the mechanisms of the reactions studied is discussed.

## INTRODUCTION

Mercury-6( $^3P_1$ ) photosensitization has been extensively employed as a photochemical technique for the study of free radical reactions in the gas phase. Little, however, is known about the nature of the primary process in such reactions. The situation is complicated by the fact that mercury is polyisotopic, consisting of an even-mass group of isotopes of zero nuclear spin,  $\text{Hg}^{196}$ ,  $\text{Hg}^{198}$ ,  $\text{Hg}^{200}$ ,  $\text{Hg}^{202}$ ,  $\text{Hg}^{204}$ , together with two odd-mass isotopes,  $\text{Hg}^{199}$  and  $\text{Hg}^{201}$ , of nuclear spin 1/2 and 3/2 respectively. These isotopes may differ markedly, one from another, in the efficiency of energy transfer in the collision of the photoexcited isotope with the substrate, and also in the nature of the primary reaction. The problem would clearly be simplified by studying the mechanism of reactions initiated by the 6( $^3P_1$ ) state of a single mercury isotope. Through a systematic investigation of monoisotopic mercury-photosensitization the importance of nuclear spin and related factors could be assessed.

In many mercury-photosensitized reactions solid compounds of mercury are formed. Thus  $\text{HgO}$  is a product in the reaction of Hg 6( $^3P_1$ ) atoms with  $\text{H}_2\text{O}$ ,  $\text{O}_2$ , and  $\text{N}_2\text{O}$ , while  $\text{Hg}_2\text{Cl}_2$  is formed with alkyl chlorides as substrates, and  $\text{Hg}_2\text{Br}_2$  with the alkyl bromides. If the solid mercury compound is formed exclusively in the primary process, the product

<sup>1</sup>Manuscript received August 16, 1957.

Contribution from the Department of Chemistry, Illinois Institute of Technology, Chicago 16, Illinois. This paper was presented at the Symposium on the Structure and Reactivity of Electronically-Excited Species held at the University of Ottawa, Ottawa, Canada, September 5 and 6, 1957.

This work was supported by the U.S. Atomic Energy Commission under Contract AT(11-1)-43.

<sup>2</sup>Present address: Department of Chemistry, University of Alberta, Edmonton, Alberta.

should contain only that mercury isotope which has been excited. If the isotope is photo-excited in natural mercury vapor ( $Hg^N$ ), any enrichment in that isotope in the solid mercury product will be evidence for primary formation of the product.

Experiments in monoisotopic mercury-photosensitization are performed in general by exposing the substrate gas, presaturated with  $Hg^N$ , to the resonance radiation from a quartz electrodeless discharge containing a trace of the mercury isotope to be studied. The even-mass isotopes will emit a single hyperfine component at 2537 Å, and this component will be absorbed by the same isotope in the  $Hg^N$  vapor in the reaction cell.

Owing to the small separation in the hyperfine components of the 2537 Å line, *ca.* 0.01 Å, the optical conditions for the unique excitation of a single mercury isotope in  $Hg^N$  vapor are very critical. Broadening effects in both emission and absorption must be minimized. An experimental and theoretical study of this problem has recently been made by Osborn, McDonald, and Gunning (3). These authors showed that the lamp must be operated at constant temperatures below 30° C., and that the substrate gas pressure in the reaction system must be kept low to reduce pressure-broadening effects in absorption. Under these conditions it was shown that the observed absorption could be calculated on the assumption that the emission line was a Doppler type, of width determined by the lamp wall temperature, modified by self-absorption, and that the absorption line was a pure Doppler line.

In this paper the results of a number of exploratory studies on various substrates will be presented. The majority of the photosensitizations have been carried out with  $Hg^{202}6(^3P_1)$  atoms. However, some data are reported for  $Hg^{198}6(^3P_1)$  atoms. Among the  $HgO$ -forming substrates,  $H_2O$ ,  $N_2O$ , and  $O_2$  have been studied. The results on a number of calomel-forming substrates will be reported. These include  $HCl$ ,  $CH_3Cl$ ,  $CH_2Cl_2$ ,  $CHCl_3$ ,  $CCl_4$ , *i*- $C_3H_7Cl$ , and  $BCl_3$ . Data on one  $Hg_2Br_2$ -forming substrate, *i*- $C_3H_7Br$ , will also be given.

#### EXPERIMENTAL

The details of the lamp assembly have already been described (2). The quartz electrodeless discharge tubes were 6 mm. I.D. and 25 cm. in length. The excitation was maintained by a 2450 Mc. oscillator. In all runs the lamps were maintained at constant temperature,  $\pm 0.1^\circ C.$ , by a sheath of thermostated cooling water. The lamp temperatures used varied slightly with various substrates, within the 25–30° C. range. A number of shapes and sizes of quartz cells were employed in the studies. It was shown that cell dimensions did not influence the enrichments obtained. Most of the data on  $HCl$  and the alkyl halides were obtained using ribbon-type quartz cells, with windows 0.1 cm. apart. The data on  $HgO$ -forming substrates were obtained with quartz spiral reaction cells with the lamp placed concentric with the coils of the cell. The cells were attached to the reaction system with spherical joints.

A conventional flow system was employed with manometers placed at exit and entrance points to measure the pressure drop across the cell. Flow rates were measured with calibrated capillary flow meters. The stream of substrate gas was presaturated with  $Hg^N$  by allowing it to pass through an operating, umbrella-type, mercury diffusion pump.

During the irradiation the solid mercury product deposited in and downstream from the radiation zone. At the end of the run, the product was removed by solution in hydrochloric acid. The acid solution was partially neutralized with sodium hydroxide, and the mercury recovered by deposition on gold wire. The isotopic composition of the mercury was determined *in vacuo* by resonance radiation absorbiometry. This method has already been described (2).

The particular experimental procedures employed with each substrate will be described in forthcoming publications.

## RESULTS

### *The Reaction of Water Vapor with Hg<sup>202</sup>(<sup>3</sup>P<sub>1</sub>) Atoms*

Separate studies on the Lorentz-broadening effect of added substrate gas on the contour of the absorption line indicated that total foreign gas pressures should not exceed 50 mm. (3). All runs were therefore performed below 50 mm. pressure.

A large number of runs was carried out with water vapor alone, and in the presence of nitrogen and helium as carrier gases. The percentage of Hg<sup>202</sup> found in the oxide product varied from 32 to 35%, compared to the natural abundance of 29.6%.

The addition of butadiene to the water vapor stream was found to have a remarkable effect on the enrichments obtained. Some of the preliminary data have already been published (6). Only the basic findings will be noted here. Thus with the progressive addition of higher mole percentages of butadiene to the water vapor, it was found that the enrichment increased markedly, reaching a maximum value of 90% Hg<sup>202</sup> with a 4:1 mole ratio of water vapor to butadiene.

### *The Reaction of Water Vapor with Hg<sup>198</sup>(<sup>3</sup>P<sub>1</sub>) Atoms*

Several experiments have been done on the irradiation of flowing butadiene - water vapor mixtures, presaturated with Hg<sup>N</sup>, with a Hg<sup>198</sup>-electrodeless discharge. Here the photoexcitation process is complicated (3) by the fact that the 201b component in absorption is separated from the 198 component by only 0.0011 Å. The Doppler half-width of the emission line is calculated to be 0.0024 Å. Hence the emission line from the Hg<sup>198</sup> source should simultaneously excite both Hg<sup>198</sup> and Hg<sup>201</sup> atoms. In the absorbiometric method of analysis (2), the Hg<sup>198</sup> source was operated under the same conditions as in the reaction. Hence the analytical data will yield the total enrichment in Hg<sup>198</sup>+Hg<sup>201</sup>.

For butadiene - water vapor mixtures over the range of 35-45 mole per cent butadiene, the fractional enrichment in Hg<sup>198</sup>+Hg<sup>201</sup> was found to vary from 3.21 to 3.13. If the emission line did not appreciably overlap the 201b component, these data would correspond to a change in Hg<sup>198</sup> concentration from the natural abundance of 10.0% to 31.3-32.1%. By analogy with the Hg<sup>202</sup> reaction, it is expected that high purity Hg<sup>198</sup> should be obtainable with lower concentrations of butadiene in the stream, using an Hg<sup>198</sup> source, operated at 0° C.

### *The Reaction of Hg<sup>202</sup>(<sup>3</sup>P<sub>1</sub>) Atoms with Nitrous Oxide and Oxygen*

Both nitrous oxide and oxygen form HgO in mercury photosensitization. Enrichment in Hg<sup>202</sup> in the oxide product would of course be evidence for formation of HgO in the primary process. A large number of runs have been made with these substrates over the pressure range from 0 to 100 mm. In all cases the HgO formed had the normal abundance of Hg<sup>202</sup>.

### *The Reaction of Hg<sup>202</sup>(<sup>3</sup>P<sub>1</sub>) Atoms with Hydrogen Chloride and the Alkyl Halides*

Hydrogen chloride and the alkyl chlorides were found to form deposits of calomel in mercury photosensitization. X-Ray examination of these deposits showed them to consist of Hg<sub>2</sub>Cl<sub>2</sub>, together with traces of HgCl<sub>2</sub>.

The calomel was removed from the reaction vessel by solution in concentrated hydrochloric acid. Repeated tests showed that mercury did not detectably dissolve under these conditions. The acid solution was neutralized with sodium hydroxide, and the mercury

was recovered by plating on gold. The isotope analysis was done as with the HgO-forming substrates.

Hydrogen chloride was found to form an enriched calomel, containing a maximum of 45% Hg<sup>202</sup>. The highest yields were obtained at substrate pressures less than 50 mm., and at high flow rates. The low pressures were necessary to eliminate Lorentz broadening effects. The effects of flow rate will be discussed in a later paper.

Free radical acceptor addends such as butadiene, propylene, and benzene were found to increase markedly the enrichment in Hg<sup>202</sup>. Benzene and butadiene were found to increase the enrichment to 60% Hg<sup>202</sup>. Propylene was somewhat less effective, yielding calomels containing a maximum of 52% Hg<sup>202</sup>.

Of the alkyl chlorides, methyl and isopropyl chlorides were the most thoroughly studied. These compounds behaved similarly to hydrogen chloride in that maximum enrichments of 45% were obtained for the pure substrates. The addition of butadiene was found to be almost ineffective in increasing the enrichment in contrast to the hydrogen chloride reaction.

Among the simple alkyl chlorides, it was found that increasing the length of the alkyl chain did not markedly change the enrichment.

The series CH<sub>3</sub>Cl, CH<sub>2</sub>Cl<sub>2</sub>, CHCl<sub>3</sub> and CCl<sub>4</sub> was studied in order to determine the effect of increasing chlorine substitution on the Hg<sup>202</sup> enrichment. The first three members of the series all gave maximum enrichments in the 43–45% range. In proceeding from CH<sub>3</sub>Cl to CHCl<sub>3</sub> progressively lower pressures had to be used since the Lorentz broadening cross section of the substrate molecule increased with increasing chlorine substitution. Carbon tetrachloride did not form measurable yields of calomel.

One Hg<sub>2</sub>Br<sub>2</sub>-forming substrate, isopropyl bromide, was studied in order to determine the influence of the type of halogen on the enrichment. The Hg<sub>2</sub>Br<sub>2</sub> was found to be enriched to a maximum of 35% Hg<sup>202</sup>—a markedly lower value than obtained with the chlorides.

Several experiments were done with boron trichloride as the calomel-forming substrate. While good yields of calomel were obtained, no enrichment was detected.

#### *The Reaction of Methyl Chloride with Hg<sup>198</sup>6(<sup>3</sup>P<sub>1</sub>) Atoms*

In this reaction a maximum enrichment factor of 1.5 was obtained, corresponding to an increase in Hg<sup>198</sup> concentration from 10.0 to 15.0%. As in the case of the reaction of water vapor with Hg<sup>198</sup>6(<sup>3</sup>P<sub>1</sub>) atoms, part of this enrichment could be attributed to Hg<sup>201</sup>.

#### *The Effect of Product Recovery Techniques on Enrichment*

It is well known that mercury vapor tends to adsorb readily on its own solid compounds. In the formation of HgO and Hg<sub>2</sub>Cl<sub>2</sub> during monoisotopic photosensitization, it was found that appreciable adsorption of Hg<sup>N</sup> occurred on the surface of the solid mercury product. It was therefore possible that exchange reactions could occur during the recovery of the product by solution in hydrochloric acid. The importance of exchange reactions was clearly demonstrated by the following experiment: An HgO, 88% enriched in Hg<sup>202</sup>, was prepared from the reaction of Hg<sup>202</sup>6(<sup>3</sup>P<sub>1</sub>) atoms with a water-butadiene mixture. The HgO was recovered by solution in 1:5 acid by volume. After analysis the mercury was dissolved in dilute nitric acid, the oxide was precipitated with base, and the oxide was redissolved in 1:5 acid. A tiny globule of natural mercury was added to the solution in hydrochloric acid and let stand for an hour. The mercury metal was removed by filtration, and the mercury in the solution was recovered by plating on gold. Analysis showed that the mercury contained only 42% Hg<sup>202</sup>. Several similar experi-

ments were performed with enriched mercury samples, and it was concluded that exchange was occurring between dissolved  $Hg^N$  and the  $Hg^{202++}$  ions present in the acid solution.

The exchange reaction between  $Hg^N$  (dissolved) and  $Hg^{202++}$  was found to increase in rate at higher acid concentrations. These exchange reactions are now being systematically studied.

#### DISCUSSION

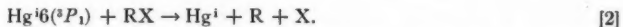
From the data presented here on the reactions of single isotopes, photoexcited in natural mercury vapor, with hydrogen chloride and some simple alkyl halides, it would appear likely that the primary reaction:



occurs to an appreciable extent. The fact that the mercury recovered in the  $Hg^i X$  product is not a pure isotope might be attributed to one or more of the following factors:

(a) The emission line is sufficiently broad to cause photoexcitation of more than one isotopic species.

(b) Two primary processes are operative: the isotopically-specific process [1] above, together with



The X atoms formed in [2] could form  $Hg^N X$  by reaction with the  $Hg^N$  always present in the reaction cell.

(c) Many secondary exchange reactions could occur which would reduce enrichment in the final product. Thus secondary gas-phase reactions of the type



could account for the observed enrichments.

(d) Exchange reactions could occur in the recovery of the mercury from the product, owing to the presence of adsorbed  $Hg^N$  in the product.

The fact that essentially pure  $Hg^{202}$  can be obtained from the water-butadiene reaction would indicate that only  $Hg^{202}$  isotopes are being photoexcited. This conclusion is further substantiated by the work of Osborn, McDonald, and Gunning (3), on the shapes of the emission and absorption lines.

Sufficient evidence is not yet available to determine the importance of factors (b) and (c). However, from the data now known, the fact that pure isotopes are not recovered in the mercury product can be reasonably explained by factor (d). Thus in the recovery of mercury from the  $HgX$  product, it is necessary to dissolve the product in concentrated hydrochloric acid. It has already been shown that  $Hg^{i+}$  ions exchange with dissolved  $Hg^N$  in acid solution. The rate of the exchange increased markedly with increased acid concentration. The high enrichments obtained in the water reaction were possible only because of the fact that the  $HgO$  can be dissolved in dilute acid. The extent to which the exchange reaction would be important would also depend upon the amount of adsorbed  $Hg^N$  on the mercury product. Semiquantitative data have now been obtained in this laboratory which indicate that  $Hg^N$  adsorbs much more strongly on  $Hg_2Cl_2$  than it does on  $HgO$ .

From the foregoing it can be seen that our findings can be explained on the assumption that (1) there is a single primary process and (2) exchange reactions in product recovery cause reduction in enrichment.

The lower maximum enrichment found for isopropyl bromide, compared to the alkyl

chlorides, may be due to differences in  $Hg^N$  adsorption in the product. A more reasonable explanation, however, would be that direct photolysis of the bromide is occurring, with the formation of  $Hg^NBr$  from the reaction of Br atoms with the  $Hg^N$  present.

The role of butadiene in increasing the enrichment in the hydrogen chloride reaction with photoexcited  $Hg^{202}$  and  $Hg^{198}$  atoms, an effect much more evident in the water reaction, was at first thought to arise from the suppression of secondary calomel formation. Thus if Cl atoms are formed in the primary process, they would be expected to add rapidly to butadiene, thereby reducing the formation of  $Hg^NCl$ . While this possibility has not been eliminated, an alternative explanation is that the butadiene polymer, formed by the interaction of butadiene with R radicals from the primary process, deposits on the calomel product, and protects it from  $Hg^N$  adsorption. It has been noted that a thin film of butadiene polymer does indeed form over the calomel (4).

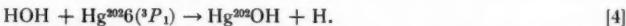
For hydrogen chloride and the alkyl halides studied, our data are consistent with the assumption that reaction [1] is the only primary process operative. The normal mercury-6( $^3P_1$ )-photosensitized decomposition of methyl chloride has been studied by Masson and Steacie (1). These authors conclude that reaction [2] is the primary process. It should be emphasized that their conclusions are not in disagreement with ours, since they investigated the reaction at 72–328° C., whereas our work was done at 25–30° C. It would be expected that higher temperatures would favor reaction [2] over reaction [1]. In the reaction of methyl chloride with  $Hg^{202}6(^3P_1)$  atoms (5), at 30° C., no hydrogen chloride was detected among the products. This is important evidence that reaction [2] does not occur to an appreciable extent under these conditions.

In the chlorinated methane series, no change of maximum enrichment was observed in methyl chloride through chloroform. In the carbon tetrachloride reaction the quantum yield of calomel formation is apparently very small, since the quantities of calomel obtained were insufficient for analysis, in the same exposure period used for the other chlorinated methanes.

The absence of enrichment in the boron trichloride reaction would indicate that the primary process involves scission into  $BCl_2 + Cl$ . This reaction is currently under study in this laboratory as a method for synthesizing  $B_2Cl_4$ .

Among the three  $HgO$ -forming substrates studied—water vapor, nitrous oxide, and oxygen—only water vapor was found to give enrichment. The absence of enrichment in the nitrous oxide reaction would be evidence in favor of the primary cleavage into  $N_2 + O$ . In the oxygen reaction  $HgO$  can be eliminated as a primary product.

A detailed study of the reaction of  $Hg^{202}6(^3P_1)$  atoms with water vapor and water vapor-butadiene mixtures will be published shortly (7). The data obtained would favor the primary process:



The marked effect of added butadiene on the enrichment may be due in part to a suppression of the reaction:



by virtue of the rapid reaction of H atoms with butadiene. It appears more likely, however, that the butadiene prevents the reduction of  $HgO$  by H atoms at the wall. The removal of H atoms should increase the over-all quantum yield of  $HgO$  formation, without changing the isotopic composition of the mercury. The butadiene must also serve to eliminate exchange reactions. In this connection it should be noted that  $HgOH$  has free radical character. Hence there may be a direct addition reaction between  $HgOH$

and butadiene. The resulting compound may protect the mercury compound from exchange reactions in product recovery.

#### CONCLUSIONS

In this paper it has been shown how the technique of monoisotopic photosensitization may be employed to give important information on the primary process in mercury-photosensitized reactions wherein solid mercury compounds are formed as products. Quantum yields are currently being measured for a number of the reactions discussed in this paper. From these data, taken in conjunction with the enrichment values, it should be possible to determine the absolute rate of the primary, isotopically-specific process.

Photosensitization with natural mercury is a complex process owing to the polyisotopic character of natural mercury. The odd-mass isotopes of finite nuclear spin probably differ markedly from the even-mass isotopes in their quenching reactions. Through detailed studies on monoisotopic photosensitization considerable information should be obtained on the factors which determine the nature and rate of primary processes in collisions of the second kind.

#### ACKNOWLEDGMENTS

The author is deeply indebted to a number of his present and former graduate students whose work is discussed here. He would especially like to thank Dr. C. Cameron McDonald, Dr. Kenton R. Osborn, Mr. Richard Pertel, Mr. John A. Poole, and Mr. John McDowell.

#### REFERENCES

1. MASSON, C. R. and STEACIE, E. W. R. *J. Chem. Phys.* **19**, 183 (1951).
2. OSBORN, K. R. and GUNNING, H. E. *J. Opt. Soc. Am.* **45**, 552 (1955).
3. OSBORN, K. R., McDONALD, C. C., and GUNNING, H. E. *J. Chem. Phys.* **26**, 124 (1957).
4. OSBORN, K. R., McDONALD, C. C., and GUNNING, H. E. To be published.
5. OSBORN, K. R., McDONALD, C. C., and GUNNING, H. E. To be published.
6. PERTEL, R. and GUNNING, H. E. *J. Chem. Phys.* **26**, 219 (1957).
7. PERTEL, R. and GUNNING, H. E. To be published.

# SOME EFFECTS OF INTRAMOLECULAR VIBRATIONAL ENERGY TRANSFER IN COMPLEX FLUORESCENT MOLECULES<sup>1</sup>

B. STEVENS<sup>2</sup>

## ABSTRACT

The effects of intramolecular redistribution of vibrational energy on both the fate of an excited complex molecule and the appearance of its electronic spectra are discussed in terms of a three-dimensional energy surface. It is suggested that continuous absorption be used as a criterion for the application of classical methods to intra- and inter-molecular vibrational energy transfer in those cases where fluorescence emission is observed.

## INTRODUCTION

The selection rules require that comparatively few vibrations of a polyatomic molecule are excited during an electronic transition (13) and that if the transition is allowed these are totally symmetric (8). Since totally symmetric vibrations lead to the simultaneous rupture of more than one bond if excited sufficiently, it is concluded that normal dissociation into two fragments is brought about by non-totally symmetric vibrations, the ground state energy of which is preserved during the electronic transition (25). If a forbidden transition to the fluorescent state is observed owing to the excitation of a non-totally symmetric vibration as in benzene (26) and naphthalene (24), this vibration is rarely excited sufficiently to cause direct dissociation. Thus the normal photodissociation of polyatomic molecules involves an internal transfer of energy from totally symmetric to non-totally symmetric vibrations.

## THE THREE-DIMENSIONAL ENERGY SURFACE

Let us make the generalization that the majority of vibrations of a complex molecule will not be excited during an electronic transition but will be associated with dissociation along one coordinate, whilst the few optically excited vibrations require a much higher energy for a dissociation which produces more than two fragments; these will be referred to as optically inert or dissociative vibrations and optically active vibrations respectively. The energy of the former will be related to the vapor temperature  $T$ , whilst that of the latter will be determined by the energy  $hc\nu$  of the absorbed quantum.

If the vibrations of the excited  $n$ -atomic molecule are assumed to be harmonic, its total vibrational energy  $V$  is given by

$$V = hc[\bar{\nu}_1(v_1 + \frac{1}{2}) + \bar{\nu}_2(v_2 + \frac{1}{2}) + \dots + \bar{\nu}_{3n-6}(v_{3n-6} + \frac{1}{2})] \\ = V_A + V_D,$$

where  $v_i$  and  $\bar{\nu}_i$  are the level and frequency of the  $i$ th vibration and  $V_A$  and  $V_D$  are the energy sums of optically active and optically inert vibrations respectively. If we now consider the molecule as a single harmonic oscillator we may write

$$V = k\alpha^2/2 = k(\alpha_A^2 + \alpha_D^2)/2,$$

<sup>1</sup>Manuscript received September 24, 1957.

Contribution from The James Forrestal Research Centre, Princeton University, Princeton, New Jersey, U.S.A. This paper was presented at the Symposium on the Structure and Reactivity of Electronically-Excited Species held at the University of Ottawa, Ottawa, Canada, September 5 and 6, 1957.

This research was supported by the United States Air Force under Contract No. AF 33(038)-23976 monitored by the Office of Scientific Research.

<sup>2</sup>Present address: Products Research Division, Esso Research and Engineering Co., Linden, New Jersey, U.S.A.

where  $k$  has the dimensions of a force constant and  $\alpha$  is a vibrational amplitude with optically active and dissociative components  $\alpha_A$  and  $\alpha_D$  related to  $V_A$  and  $V_D$  respectively; these components have the properties

$$V_A, \alpha_A = f(\bar{v}); \quad V_D, \alpha_D = f(T).$$

The energy surface of the excited  $n$ -atomic molecule may now be represented as a circular paraboloid of radius  $\alpha$  at height  $V$  above its minimum, with mutually perpendicular horizontal coordinates  $\alpha_A$  and  $\alpha_D$ . This is shown in Fig. 1 as a series of isoenergetic con-

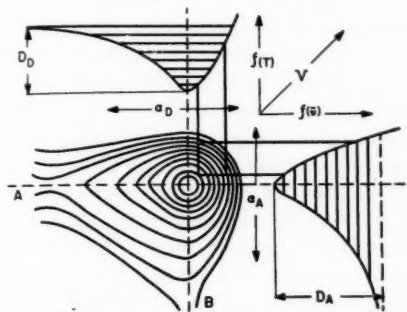


FIG. 1. Three-dimensional energy surface for a complex fluorescent molecule.

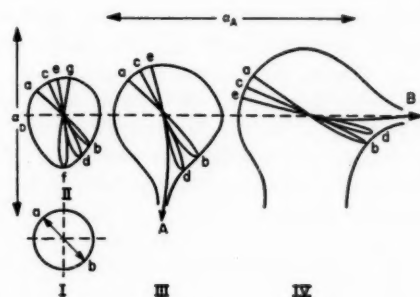


FIG. 2. Isoenergetic contours for four types of vibrational levels recognized in Fig. 1.

tours in which the effects of anharmonic forces are taken into consideration; cross sections showing the variation of surface energy along each coordinate are drawn at the top and to the right of the figure. The effects of anharmonic forces along the  $\alpha_D$  coordinate leading to normal dissociation at  $A$  when  $V \gg D_D$  may be expected to be more pronounced than those along the  $\alpha_A$  coordinate which requires that  $V \gg D_A \gg D_D$  for dissociation into several fragments to take place at  $B$ .

#### THE EFFECT OF INTRAMOLECULAR VIBRATIONAL ENERGY TRANSFER ON EMISSION AND PHOTODISSOCIATION

Four types of energy contour recognized in Fig. 1 are shown in Fig. 2. The behavior of the potentially fluorescent molecule in each of the corresponding vibrational levels at pressures so low that collisional perturbation is negligible is discussed below.

(a) The lowest vibrational levels produced by the absorption of a frequency  $\bar{v}$  close to the frequency  $\bar{v}_0$  of the 0,0 band at the lowest possible vapor temperatures (see Fig. 1) are comparatively free from anharmonic effects and may be represented by contour I of Fig. 2. If we may assume that both vibrational components are in phase at the instant of transition, the vibrational excursion is represented by the line  $ababa\dots$  and little or no redistribution of energy between the vibrational components takes place during the lifetime  $\tau$  of the excited molecule. Since  $V_A = hc(\bar{v} - \bar{v}_0) \sim 0$ , the characteristic fluorescence spectrum will be emitted.

In benzene the 0,0 band is not observed and higher vibrational levels are produced by the absorption of a frequency greater than  $\bar{v}_0$ . Owing to the high symmetry of this molecule these levels will also have the properties of contour I and the absence of vibrational energy redistribution results in the appearance of the well-known resonance emission (14, 16) originating from the level  $V_A = hc(\bar{v} - \bar{v}_0)$ . At higher pressures  $V_A$  is collisionally

reduced to a minimum and the simpler fluorescence spectrum is observed (7); in view of the discussion of contour II below, an increase in either  $T$  or  $\bar{v}$  should produce the same effect. Similar remarks apply to the naphthalene emission spectrum in which progressions from the vibrationally excited upper state are observed at low pressures (24).

(b) An increase in either  $\bar{v}$  or  $T$  produces intermediate vibrational levels (Fig. 1) with  $V < D_A$  which are represented by contour II of Fig. 2. These are characterized by an increased anharmonicity along the dissociative coordinate  $\alpha_D$ , and the initial vibrational excursion may be imagined to precess along  $abcde$  until it is stabilized along  $efgfe\dots$  with  $V_A \sim 0$  and  $V_D = CT + hc(\bar{v} - \bar{v}_0)$ , where  $C$  is the molecular heat capacity.<sup>3</sup> If this precession is stabilized within the time interval  $\tau$ , the virtual independence of the fluorescence spectrum of  $T$  and  $\bar{v}$  at low pressures where  $\tau < 1/Z$  is understood (21).

(c) Higher vibrational levels with  $D_D < V < D_A$  produced by a further increase in  $T$  or  $\bar{v}$  or both have the hypothetical contour III (Fig. 2). Here the precession  $abcde$  representing the transfer of optically excited vibrational energy allows dissociation at  $A$  to compete with fluorescence emission. The probability  $d$  of dissociation will depend on the speed of the precession and on the barrier width at  $A$ , both of which increase with the over-all energy  $V$ . Since  $V = f(\alpha_A, \alpha_D)$ , the equivalence of thermal and optical contributions to  $d$  is evident (19, 20).

(d) Contour IV of Fig. 2 corresponds to the highest vibrational levels of the excited molecule with  $V > D_A$ . Two dissociative possibilities exist and the path followed may be expected to depend on the relative magnitudes of the optically and thermally excited vibrational components. The production of more than two fragments at  $B$  requires that  $hc(\bar{v} - \bar{v}_0)$  be greater than  $CT$  for the precession to follow the direction  $abcde$  as shown, and in this respect it is interesting to note the production of  $C_2H_2$  when benzene vapor is photolyzed by the Al spark (1855–2000 Å) (32), whereas at longer wavelengths the principal non-condensable product is  $H_2$  (17, 23). A thermally induced dissociation into three or more fragments would not be expected owing to the much larger probability of normal dissociation at  $A$  as the molecule is collisionally activated in its ground state; the absorption of a sufficiently energetic quantum produces this type of level directly and allows both modes of disruption to compete. The variation of the primary photodissociation process with the frequency of absorbed radiation has been previously recognized (18); it appears from this discussion that the controlling factor is the relative magnitude of  $V_A(\bar{v})$  and  $V_D(T)$  rather than  $\bar{v}$  alone.

#### THE EFFECT OF INTRAMOLECULAR VIBRATIONAL ENERGY TRANSFER ON THE APPEARANCE OF ELECTRONIC SPECTRA

Beyond a certain frequency limit the discrete absorption spectrum of a diatomic molecule becomes diffuse owing to the onset of predissociation. The lifetime of the excited molecule is reduced by a transition to a dissociated state with the result that the corresponding line width  $b$  given by

$$b = h/2\pi\tau$$

is increased.  $b$  approaches the separation of vibrational levels as  $\tau$  is reduced to the order of a vibrational period and the spectrum becomes continuous at shorter wavelengths.

The absorption spectra of polyatomic gases exhibit similar characteristics ranging from sharp bands at long wavelengths, through a diffuse region, to a continuum in the

<sup>3</sup>It is not suggested that the energy is transferred to the inactive vibrations because these are anharmonic; the anharmonicity allows the internal redistribution of the energy  $hc(\bar{v} - \bar{v}_0)$  amongst all vibrations, of which those referred to as inactive are by far the more numerous.

direction of higher frequencies (12, 29, 30); the structure at longer wavelengths fades into a continuous background as the temperature is increased (2, 10, 11) and shows a tendency to disappear completely as the molecule becomes more complex. It has been suggested that continuous absorption is due to predissociation in this case also (1, 27), but whilst this is probably true for simpler molecules which cannot be excited to fluorescence in this region, the following arguments suggest that this is not a unique interpretation in the case of more complex systems.

(a) As the complexity of a conjugated molecule increases, its absorption spectrum shifts towards the red (5). Since an energy corresponding to approximately 4000 Å is required to break the weaker bonds, absorption in the visible region should be discrete if dissociation alone is responsible for continuous absorption. The structureless bands of organic dyes do not support this criterion.

(b) To produce the necessary line broadening  $\tau$  must be reduced to the order of a few vibrational periods in which case fluorescence emission would no longer be observed. A number of organic vapors can be excited to fluorescence by absorption in the continuous region (19, 29), which in several cases extends over the whole range; it is found moreover that the rate of dissociation is sufficiently slow to compete with emission when the wavelength of absorbed radiation varies by several hundred Å (18, 19).

(c) Fluorescence spectra in general exhibit less structure than the corresponding absorption spectra. Since the energy range of the observed emission rarely exceeds 20 kcal., dissociation of the ground state following emission is extremely unlikely (16).

It has been pointed out that the spacing of vibrational levels in polyatomic molecules decreases very rapidly with increasing vibrational energy (15); furthermore, as an increase in molecular complexity usually lowers molecular symmetry, a larger number of vibrations are electronically excited, which, together with a closer spacing of rotational levels due to larger moments of inertia, may well account for the appearance of continuous spectra in these cases (16). The remainder of this discussion will be concerned with the additional hypothesis that the diffuse and continuous spectra of complex molecules are due in part to line broadening.

To produce an appreciable effect, the broadening of vibration-rotational lines must be due to a process taking place within a few vibrational periods following the absorption act, yet allowing fluorescence emission to take place after an interval of approximately  $10^{-8}$  second. This process must be intramolecular since continuous spectra are observed at low pressures (7, 30), and to account for continuous emission it must also take place in the ground state. If we consider that the line width  $b$  is determined by the lifetime  $\theta$  of the individual vibronic states rather than by the lifetime  $\tau$  of the electronically excited molecule, then such a process could be the internal redistribution of vibrational energy (22). If  $\theta$  is of the order of 10 vibrational periods,  $b$  is approximately  $5 \text{ cm.}^{-1}$ , which, in view of the already close spacing of the numerous vibration-rotational lines, is sufficient to produce a continuous aspect.

A complex molecule has been defined as one in which the probability  $W$  of internal energy transfer exceeds  $1/\tau$  (22). Since  $\theta = 1/W$  and  $W$  increases both with molecular complexity and total vibrational energy  $V$ ,  $\theta$  has the range of values

$$\tau > \theta(T, v) > 10^{-13} \text{ second.}$$

Thus we may expect discrete absorption only if this produces vibrational levels with the properties of contour I (Fig. 2), i.e. for simpler molecules at low vapor temperatures in the long-wave region. At shorter wavelengths, higher temperatures, or for more complex

molecules with larger heat capacities, absorption produces vibrational levels with the contour II, the lifetime  $\theta$  of the initially formed vibronic state is reduced by internal energy redistribution, and the structure fades into a continuous background. This is the behavior observed.

The continuous nature of emission spectra is similarly explained if the surface in Fig. 1 is used to represent the molecular ground state. The energies of the vibrational components following emission are given by

$$V_A = hc(\bar{\nu}_0 - \bar{\nu}^*),$$

$$V_D = hc(\bar{\nu} - \bar{\nu}_0) + CT,$$

where  $\bar{\nu}^*$  is the frequency of emitted radiation. The dependence of  $V_D$  on the frequency  $\bar{\nu}$  of absorbed radiation arises from the transfer of the optically excited vibrational energy to this component prior to emission. Discrete fluorescence spectra will be observed only if the lowest vibrational levels of the ground state represented by contour I are produced. This requires that both  $V_A$  and  $V_D$  be small, as is the case at low temperatures for simple molecules with lower heat capacities when both the absorbed and emitted radiations have frequencies close to  $\bar{\nu}_0$ . These are the conditions under which the discrete emission spectra of benzene (14, 16), toluene (3), benzonitrile (3), fluorobenzene (4), aniline (30), naphthalene (24, 31), and anthracene (28) are observed. Since  $\bar{\nu}$  is usually greater than  $\bar{\nu}_0$ ,  $V_D$  is larger in the ground state following emission than in the upper state following absorption, with the result that fluorescence spectra are often less discrete than the corresponding absorption.

Thus diffuseness in the electronic spectra of polyatomic fluorescent molecules and of diatomic molecules may be considered as having a common origin if it is accepted that the lifetime of the vibronic states determines the width of vibration-rotational lines. In the former case intramolecular vibrational energy transfer reduces the lifetime of the initially formed vibronic state by changing the energies of the optically active and inactive components, but need not necessarily lead to dissociation. The internal energy transfer requires that a number of isoenergetic vibrational combinations be available for each vibrational level, in which case the levels themselves will be sufficiently closely spaced to account for the observed continuum. The criterion of continuity is largely one of resolution and its appearance may be due to both factors discussed, in which case there is some justification for the following conclusions:

(a) Where absorption in the continuous region excites fluorescence, the internal redistribution of vibrational energy is sufficiently rapid for thermal equilibrium to be established between the numerous oscillators within the interval  $\tau$  (9), and the concept of vibrational temperature (6) is valid.

(b) The spacing of vibrational levels in a molecule excited by absorption in its continuous region is sufficiently close for the collisional removal of vibrational energy to be treated as a process of accommodation (6, 20).

(c) This classical treatment of vibrational energies cannot be applied to polyatomic molecules excited by absorption in the discrete region.

#### REFERENCES

1. ALMASY, F. *Naturwiss.* **20**, 296 (1932).
2. ASUNDI, R. K. and PADHYE, M. R. *Indian J. Phys.* **23**, 237 (1949).
3. BASS, A. M. *J. Chem. Phys.* **18**, 1403 (1950).
4. BASS, A. M. and SPONER, H. *J. Opt. Soc. Am.* **40**, 380 (1950).
5. BAYLISS, N. S. *Quart. Revs.* **6**, 319 (1952).

6. BOUDART, M. and DUBOIS, J. T. *J. Chem. Phys.* **23**, 223 (1955).
7. CUTHERBERTSON, G. R. and KISTIAKOWSKY, G. B. *J. Chem. Phys.* **4**, 9 (1936).
8. DUNCAN, A. B. F. *J. Chem. Phys.* **3**, 384 (1935).
9. DUSCHINSKY, F. *Compt. rend. acad. sci. U.R.S.S.* **17**, 179 (1937).
10. HENRI, V. *Trans. Faraday Soc.* **25**, 765 (1929).
11. HENRI, V. and CARTWRIGHT, C. H. *Compt. rend.* **200**, 1532 (1935).
12. HENRI, V. and WURMSER, R. *J. phys. radium*, **8**, 289 (1927).
13. HERZBERG, G. and TELLER, E. *Z. physik. Chem. (Leipzig)*, B, **21**, 410 (1933).
14. INGOLD, C. K. and WILSON, C. L. *J. Chem. Soc.* 941, 955 (1936).
15. KASSEL, L. S. *J. Am. Chem. Soc.* **53**, 2143 (1931).
16. KISTIAKOWSKY, G. B. and NELLES, M. *Phys. Rev.* **41**, 595 (1932).
17. KRASSINA, G. I. *Acta Physicochim. U.R.S.S.* **10**, 189 (1939).
18. NEPORENT, B. S. *Zhur. Fiz. Khim.* **13**, 965 (1939).
19. NEPORENT, B. S. *Zhur. Fiz. Khim.* **21**, 1111 (1947).
20. NEPORENT, B. S. *Zhur. Fiz. Khim.* **24**, 1219 (1950).
21. NEPORENT, B. S. *Zhur. Eksp. i Teoret. Fiz.* **21**, 172 (1951).
22. NEPORENT, B. S. *Izvest. Akad. Nauk S.S.S.R. Ser. Fiz.* **15**, 533 (1951).
23. PRILESHAJEVA, N. A. *Acta Physicochim. U.R.S.S.* **10**, 193 (1939).
24. SCHNEPP, O. and McCCLURE, D. S. *J. Chem. Phys.* **20**, 1375 (1952).
25. SPONER, H. and TELLER, E. *Revs. Modern Phys.* **13**, 75 (1941).
26. SPONER, H., NORDHEIM, G., SKLAR, A. L., and TELLER, E. *J. Chem. Phys.* **7**, 207 (1939).
27. TERENIN, A. *Acta Phys. Polon.* **5**, 229 (1936).
28. TERENIN, A. *Acta Physicochim. U.R.S.S.* **18**, 210 (1943).
29. TERENIN, A., VARTANYAN, A., and NEPORENT, B. S. *Trans. Faraday Soc.* **35**, 39 (1939).
30. VARTANYAN, A. *Izvest. Akad. Nauk S.S.S.R. Ser. Fiz.* **3**, 341 (1938).
31. WEST, W. *Ann. N.Y. Acad. Sci.* **41**, 203 (1941).
32. WILSON, J. E. and NOYES, W. A., Jr. *J. Am. Chem. Soc.* **63**, 3025 (1941).

# STUDIES OF CHEMICAL REACTIONS OF EXCITED SPECIES USING INTENSE LIGHT SOURCES<sup>1</sup>

R. A. MARCUS

## ABSTRACT

The use of measurements of the products of flash photolysis as a means for studying the reactions of electronically-excited molecules is discussed. With intense light sources the problem of isolating these reactions from others involving free radicals is simplified. The flash sources also have their limitations, and misleading information which can result from the presence of inert gases is noted. A diagnostic test is proposed for detecting the effects (if any) of a possible adiabatic temperature rise of the flash.

Some recent studies in the author's laboratory are summarized. Evidence is presented that in the flash photolysis of acetone acetyl radicals arise from an excited molecule. Several deactivation processes are described and compared with results from fluorescence studies.

## INTRODUCTION

The study of the chemical products of photochemical systems using low light intensities has yielded a considerable body of knowledge about the reactions of free radicals and some information about the behavior of electronically-excited molecules (13, 18). The short-lived species are produced in these systems in a well-defined way at a definite temperature. At the usual wavelengths employed there is no formation of ions which result from many other sources of radiation, nor are there the high temperatures which accompany the use of shock waves for producing these intermediates. Various methods of production and observation of unstable chemical species have been the subject of a recent symposium (19) and survey (10).

A number of detailed investigations have served to point up some of the information which can be derived about the electronically-excited molecules by these low light intensity techniques and at the same time have revealed their limitations. The experimental results show that the problem of distinguishing between the reactions of excited states and reactions involving free radicals is frequently a matter of some difficulty. Several such examples will be discussed.

In the method of flash photolysis, an intense light source is used, such as a flash lamp (11, 12), a spark (7), or an exploding wire (14). In these systems the concentration of the free radicals is so high that radical-radical reactions are usually favored over all others unless the radical is "hot". The reaction products thus become a more direct measure of the primary photochemical steps and of the reactions of the resulting electronically-excited molecules. However, since low intensity light sources have certain compensating features, the two techniques provide complementary rather than alternative approaches for the investigation of the reactions of excited states.

The study of unstable species and their reactions, by spectroscopic observations of the flashed system, has been reviewed recently (12). We shall be principally concerned here, instead, with flash studies based on a determination of reaction products.

<sup>1</sup>Manuscript received August 16, 1957.

Contribution from the Department of Chemistry, Polytechnic Institute of Brooklyn, Brooklyn, New York. This paper was presented at the Symposium on the Structure and Reactivity of Electronically-Excited Species held at the University of Ottawa, Ottawa, Canada, September 5 and 6, 1957. A second paper presented at the Symposium, on the theory of internal conversion or dissociation of excited molecules, will be published elsewhere.

This research was supported by the United States Air Force under Contract No. AF 33 (616) 8887, monitored by WCRRC, Aeronautical Research Laboratory, Wright Air Development Center.

### EXAMPLES OF LOW LIGHT INTENSITY STUDIES—THEIR FINDINGS AND LIMITATIONS

In the photolysis of acetone, Noyes and his collaborators have shown that traces of oxygen (*ca.* 0.02 mm.) can quench the fluorescence of a long-lived electronically-excited acetone molecule (3) and can inhibit ethane formation at low light intensities (8, 9). A considerable amount of information was obtained about the latter process, but it is difficult to separate the reactions of oxygen with the excited molecules from those with the methyl radicals. However, from the rate constant estimated in the above study it can be computed that 10 mm. of oxygen will not react with methyl radicals under the usual flash photolysis conditions, thereby permitting the reaction with excited molecules to be studied in the absence of competing free radical processes.

Another important reaction of excited states is unimolecular dissociation. Some evidence described later suggests that acetyl radicals, but not carbon monoxide, may arise from the unimolecular dissociation of an excited acetone molecule which can be quenched by acetone at moderate pressures. This unimolecular reaction undoubtedly has some temperature coefficient, but its amount has not been definitely established. Complicating features occur, such as an increasing dissociation of acetyl radicals themselves with increasing temperature. The study of this system with intense light sources will serve to eliminate the latter reaction and permit an assessment of the temperature dependence of the former. Recently, flash experiments have provided some information on this process (17).

The photolysis of perfluoroacetone has been recently shown to result in the formation of carbon monoxide from an excited perfluoroacetone molecule (2). The unimolecular reaction rate constant was studied as a function of temperature. Since no perfluoroacetyl compound could be detected, it was not certain whether the dissociation first resulted in a short-lived perfluoroacetyl radical or whether there was a direct split into carbon monoxide. Supplementing this study by one employing flash photolysis could serve either to detect the radical or to place a lower limit on the latter's unimolecular rate constant, of the order of  $10^6 \text{ sec.}^{-1}$  or so (depending on the light intensity).

### SOME LIMITATIONS OF FLASH PHOTOLYSIS

While flash photolysis experiments have much to offer, they also have their limitations, whose importance depends upon the purpose for which they are being used. One problem is that of obtaining sufficiently monochromatic light by filters without reducing the intensity unduly and without having to use an inordinate number of flashes. Again, depending upon the flash time, there may be a more or less appreciable departure from steady-state conditions for the transient species. This situation will complicate the mathematical treatment of certain reaction schemes but not that of others. This problem will be analyzed in detail elsewhere.

Computation of variations in the light absorbed accompanying changes in the experimental conditions can be a difficult problem. It was not one in the present study, however, (except at wavelengths below 2000 Å where the absorption of acetone was not proportional to pressure at the pressures employed). The type of light source used in this study serves to alleviate the difficulty. Calculation of absolute quantum yields is a more formidable problem, partly because of the polychromatic nature of the light.

The reaction temperature may be uncertain because of some increase caused by the flash. Its amount can be reduced by increasing the heat capacity of the gaseous system, i.e. by adding large amounts of inert gas. This procedure, we shall see, has resulted in

misleading information when excited states are present. An alternative way is simply to investigate the effects of reducing the intensity and, thereby the temperature rise, of the flash. At these high light intensities, the quantum yields of products would probably not vary with light intensity if no temperature change occurs. Thus, when no intensity effect is found, this is evidence that either temperature changes do not occur or that if they do, their effect on the reaction products is negligible.

#### STUDIES IN THE FLASH PHOTOLYSIS OF ACETONE

The flash apparatus used in the present experiments (14) was of a standard type, but the customary flash lamp was replaced by an exploding wire. It proved to be convenient, cheap, and reproducible within several per cent. It was found that the light intensity could be easily varied in a known way merely by changing the distance from this line source, a long thin wire, to the axis of a parallel, cylindrical quartz reaction vessel (14). On the other hand, in any experimentation where an extremely large number of flashes is required, a flash lamp is preferable since it can be automatically flashed many times. In most of the experiments reported below the number of flashes varied between one and three, and the total per cent decomposition was about 0.1%. The flash period was fairly long, about 300  $\mu$ sec.

##### *Preliminary Studies with Unfiltered Light*

In some preliminary experiments (15) using light containing radiation of wavelengths near 1900 Å, ethane, carbon monoxide, and methane were measured. No hydrogen was formed. The ratio of ethane to carbon monoxide was greater than one, averaging about 1.25 and indicating the presence of biacetyl.

Using 400 mm. carbon dioxide, the ethane to carbon monoxide ratio fell to about 0.95. Traces of biacetyl (0.1 to 0.7 mm.) also reduced the ratio to slightly below unity, even though they were present in too small an amount to absorb the radiation. When the 1900 Å light was removed by interposing a cellophane filter, these amounts of biacetyl had no effect at all on the products, showing that the electronically-excited molecule which it quenched arises from light in the 1900 Å region.

In the experiments in this and in the following sections the ratio of methane to carbon monoxide was about 0.1. There is evidence from these studies that this methane is not formed from a disproportionation between methyl and acetyl radicals. For example, the acetyl radicals could be reduced to zero concentration by addition of carbon dioxide, without appreciably affecting the methane to carbon monoxide ratio. Instead, the methane appears to arise either from a primary photochemical act or from the collision of a hot methyl radical with acetone. If the primary photochemical step is indeed the origin of the methane at high light intensities, the photolysis of mixtures of acetone and acetone-*d*<sub>6</sub> should result in the formation of methane and methane-*d*<sub>4</sub>, but not any other deuterated methanes. Such experiments are in progress.

A methane to carbon monoxide ratio of 0.1 has also been obtained in experiments made with a fairly intense light source (1). These authors detected ketene.

In an earlier flash photolysis study using unfiltered radiation (5), Khan, Norrish, and Porter photolyzed acetone to high conversions and in the presence of 480 mm. carbon dioxide. This gas was added to reduce the temperature rise. Their ratio of methane to carbon monoxide was the same as ours but their ethane to carbon monoxide ratio was about 0.9. This is quite consistent with our subsequent results on the deactivating effects of carbon dioxide and of traces of biacetyl. It also serves to indicate the limitations of using inert gases to reduce the temperature rise when excited states are present.

### *Studies with Filtered Light*

In these experiments (16), a cylindrical cellophane filter was employed. It surrounded the reaction vessel and was protected from the exploding wire by a concentric close-fitting quartz tube. The quantum yields of carbon monoxide and ethane, or more precisely the ratios of each of these products to the acetone pressure, were independent of light intensity when it was varied by a factor of five. The quantum yield of carbon monoxide was constant over a range of acetone pressures varying from 7 to 160 mm. (though there may be a 15% drop at high pressures, ~220 mm.). The yield of ethane decreased markedly with increasing acetone pressure, as in Fig. 1. This curve lies approximately between the curve found by Herr and Noyes at 3130 Å and their curve at 2537 Å.

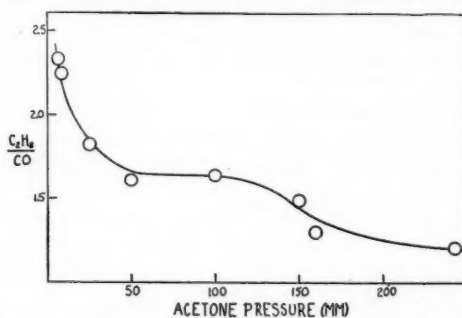


FIG. 1. Plot of ethane to carbon monoxide ratio vs. acetone pressure at room temperature. The point at 100 mm. is the mean of 1.62, 1.65, 1.66.

(4). These authors used low light intensities and worked at constant absorbed intensity to reduce the effects of changing the relative amounts of the secondary free radical reactions as the radical concentration varies. The shape of our curve suggests the presence of two excited acetone states.

Since our yields were independent of the light intensity, either the temperature of the system in these experiments is that of the room or temperature effects can be neglected. We can compare these results, then, with some obtained in fluorescence studies made at a definite temperature.

Acetone has been shown to fluoresce from two excited states, both of which can be quenched by acetone molecules (3). No fluorescence enhancement was reported at any pressure. At 50° C. the quenching occurs appreciably at acetone pressures of about 150 mm. for both states. Studies as detailed as this do not appear to have been reported for 25° C., but the behavior of total fluorescence with pressure is about the same at 25° C. and 50° C. (6). Purely for the present purposes of discussion, it will be assumed that this behavior is also the same for each state at the two temperatures.

From the photolysis studies, in conjunction with those of Herr and Noyes and the foregoing results, it is inferred that the excited state which yields acetyl radicals and is deactivated in the low pressure region of Fig. 1 is probably not responsible for the fluorescence, although the one deactivated in the higher pressure range may be. Carbon monoxide also does not appear to be a product of either fluorescing excited state, unless the fluorescence behavior at 25° C. and 50° C. is rather different.

### *Studies in Progress*

Studies in progress in this laboratory include the effects of added hydrocarbons, of oxygen, and of increased temperature on the lifetime of the excited acetone molecules.

## CONCLUSIONS

The determination of the chemical reaction products of flash photolysis is particularly suited for studying the reactions of electronically-excited molecules. It is shown that the addition of inert gases, for purposes of reducing the possible temperature rise of the flash, has led to misleading information. These gases can deactivate excited molecules and so change the reaction scheme. A preferable procedure, it is suggested, is to test for the effects of any temperature rise, and a diagnostic test is proposed.

Results obtained on the flash photolysis of acetone in several studies in this laboratory are described.

## REFERENCES

1. AUSLOOS, P. and STEACIE, E. W. R. *Can. J. Chem.* **33**, 47 (1955).
2. AYSCOUGH, P. B. and STEACIE, E. W. R. *Proc. Roy. Soc. (London), A* **234**, 476 (1956).
3. GROH, H. J., JR., LUCKEY, G. W., and NOYES, W. A., JR. *J. Chem. Phys.* **21**, 115 (1953).
4. HERR, D. S. and NOYES, W. A., JR. *J. Am. Chem. Soc.* **62**, 2052 (1940).
5. KHAN, M. A., NORRISH, R. G. W., and PORTER, G. *Proc. Roy. Soc. (London), A* **219**, 312 (1953).
6. LUCKEY, G. W. and NOYES, W. A., JR. *J. Chem. Phys.* **21**, 227 (1953).
7. MAINS, G. J., ROEBBER, J. L., and ROLLEFSON, G. K. *J. Am. Chem. Soc.* **59**, 733 (1955).
8. MARCOTTE, F. B. and NOYES, W. A., JR. *Discussions Faraday Soc.* **10**, 236 (1951).
9. MARCOTTE, F. B. and NOYES, W. A., JR. *J. Am. Chem. Soc.* **74**, 783 (1952).
10. MARCUS, R. A. *Ann. N.Y. Acad. Sci.* **67**, 661 (1957).
11. NORRISH, R. G. W. and PORTER, G. *Nature*, **164**, 658 (1949).
12. NORRISH, R. G. W. and THRUSH, B. A. *Quart. Revs. (London)*, **10**, 149 (1956).
13. NOYES, W. A., JR., PORTER, G. B., and JOLLEY, J. E. *Chem. Revs.* **56**, 49 (1956).
14. OSTER, G. K. and MARCUS, R. A. *J. Chem. Phys.* **27**, 189 (1957).
15. OSTER, G. K. and MARCUS, R. A. *J. Chem. Phys.* **27**, 472 (1957).
16. SLAGOWITZ, N. and MARCUS, R. A. Paper presented at Am. Chem. Soc. meeting, New York City, September, 1957.
17. SLAGOWITZ, N. and MARCUS, R. A. Unpublished.
18. STEACIE, E. W. R. *Atomic and free radical reactions*. 2nd ed. Reinhold Publishing Corporation, New York. 1954.
19. THACHER, H. C., JR. (Consulting Editor). *Ann. N.Y. Acad. Sci.* **67**, 449-669 (1957).

# CHEMILUMINESCENCE IN THE SYSTEM ATOMIC SODIUM PLUS ATOMIC HYDROGEN<sup>1</sup>

J. D. MCKINLEY, JR.<sup>2</sup> AND J. C. POLANYI<sup>3</sup>

## ABSTRACT

When atomic sodium is diffused into a mixture of atomic and molecular hydrogen, a weak chemiluminescence is observed in the gas phase. Visible emission consists of the sodium D lines. The total intensity of the emission,  $\sim 5 \times 10^4$  photons/second, indicates that only one in  $5 \times 10^4$  of the sodium atoms entering the reaction vessel is involved in luminescent reaction. In order to account for the rapid fall-off in intensity of the flame away from the nozzle it is necessary to suppose that some non-luminescent reaction is removing sodium atoms in the gas phase. Preliminary experiments suggest that the non-luminescent reaction is  $\text{Na} + \text{H} + \text{H}_2 \rightarrow \text{NaH} + \text{H}_2$ , and the luminescent reaction either  $\text{Na} + \text{Na} + \text{H} \rightarrow \text{NaH} + \text{Na}^*$  with collision yield  $4 \times 10^{-8}$  or  $\text{Na} + \text{H} + \text{H} \rightarrow \text{H}_2 + \text{Na}^*$  with collision yield  $1 \times 10^{-6}$ .

This study of chemiluminescence in the gas phase was undertaken to obtain quantitative information concerning the efficiency of energy transfer into an electronic degree of freedom. It is frequently supposed that "energy matching" is important in processes of this type, although there is little direct experimental evidence for this supposition.

The luminescence of sodium vapor in the presence of atomic hydrogen was observed by Bonhoeffer (4), by Mohler (12), and recently by Aynard (1). The technique in every case was to pass dissociated hydrogen from a Wood's tube over hot sodium. Both Bonhoeffer and Mohler found that the luminescence consisted exclusively of the sodium D lines. Aynard, however, found the 3302–3303 Å sodium lines as well and attributed this discrepancy to the fact that earlier workers used wet hydrogen.

In the above investigations it was not possible to distinguish between surface reactions and gas phase reactions. In the present work we have avoided this ambiguity by operating under diffusion flame (13) conditions. The reaction can be confined in this way to the gas phase, and rates can be calculated from the observed diameter of the luminescent flame. This information was supplemented by measurements of emission intensity.

## EXPERIMENTAL

The apparatus (Fig. 1) consisted of two separately controlled hydrogen flow systems, one carrying sodium vapor from a saturator, *S*, into the reaction vessel through a nozzle (0.05 mm. radius), and the other bringing atomic hydrogen from the discharge tube, *W*, into the reaction vessel.

In each system, cylinder hydrogen flowed through a "Deoxo" catalytic purifier and then through towers of magnesium perchlorate, ascarite, and again magnesium perchlorate. Hydrogen flows were regulated by needle valves and measured with calibrated capillary flow meters.

Prior to an experiment cubes of A.R. sodium, from which the outer layer of oxide had been cut away under benzene, were introduced into the saturator. By moving the sliding furnace, *F*<sub>1</sub>, it was possible to distill the sodium in three stages along the length of the

<sup>1</sup>Manuscript received August 16, 1957.

Contribution from the James Forrestal Research Center, Princeton University, Princeton, New Jersey, U.S.A. This paper was presented at the Symposium on the Structure and Reactivity of Electronically-Excited Species held at the University of Ottawa, Ottawa, Canada, September 5 and 6, 1957.

This research was supported by the United States Air Force under Contract No. AF 33(038)-23976 monitored by the Air Research and Development Command.

<sup>2</sup>Present address: National Bureau of Standards, Washington, D.C.

<sup>3</sup>Present address: Department of Chemistry, University of Toronto, Toronto, Canada.

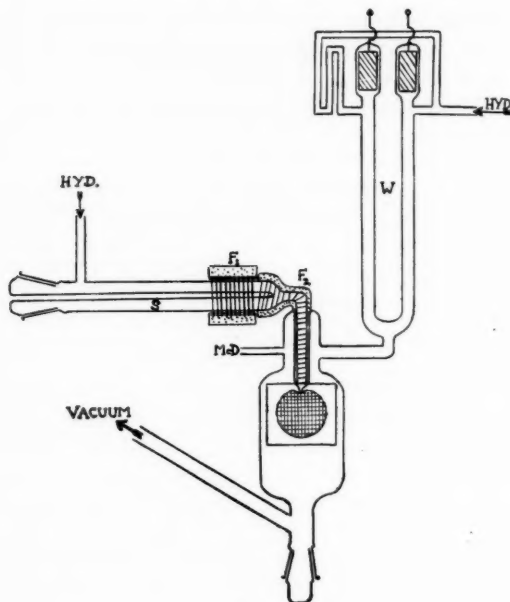


FIG. 1.

saturator. The last distillation resulted in a clean sodium mirror on the walls of the saturator just short of the heating coil  $F_2$ .  $F_2$  was continued between the double walls of the central tube of the reaction vessel as far as the internal seal directly above the nozzle. By means of  $F_2$  the central tube and the nozzle were kept at about  $350^\circ\text{ C}$ . to prevent condensation of sodium.

The pressure of sodium at the nozzle was determined by the temperature of  $F_1$ . Since the total pressure in the saturator could be measured on a McLeod gauge (not shown in Fig. 1) the molar flow of sodium into the reaction vessel was calculable using the relationship

$$\text{molar flow of Na} = (\text{vapor pressure of Na in the saturator}/\text{total pressure in saturator}) \times \text{molar flow of H}_2 \text{ in saturator.}$$

In order to show that the vapor pressure of sodium in the saturator was the equilibrium pressure corresponding to the temperature of  $F_1$ , separate experiments were performed in which a copper gauze cylinder was suspended inside the reaction vessel to catch the sodium issuing from the nozzle in given time at known hydrogen flow rate and known  $F_1$  temperature. The sodium thus collected was washed off the gauze with alcohol, and titrated against standard HCl. The results showed that the hydrogen stream was within 5% of being saturated with sodium. (The copper gauze was found to be necessary since deposition of the sodium on the pyrex vessel resulted in a substantial loss through combination with the glass.)

The hydrogen stream leading to the Wood's tube could be diverted through a water bubbler prior to the flow meter in order to observe the effect of using wet hydrogen.

The current passing through the discharge tube was in the region of 50 ma. at 15,000 volts (0.75 kw.). The percentage decomposition of the hydrogen in the region of the nozzle

was *ca.* 30%; this was determined in separate experiments by a calorimetric method (9, 14). Typical rates of flow through the saturator and Wood's tube were  $3 \times 10^{-5}$  and  $5 \times 10^{-6}$  moles/second respectively; total pressure in the saturator was *ca.* 6 mm. and total pressure in the Wood's tube and reaction vessel 0.4–0.5 mm.

The region of luminescence could be observed through a plane pyrex window in the reaction vessel.

### RESULTS AND DISCUSSION

With pressures of sodium at the nozzle tip from  $2.5 \times 10^{-3}$  to  $1.5 \times 10^{-2}$  mm. ( $F_1$  *ca.* 260°–300° C.), and a rate of inflow of sodium of *ca.*  $5 \times 10^{-8}$  moles/second, an orange-colored luminescent flame was observed centering on the nozzle. The intensity of the emission was such as to be weakly visible in a partially darkened room. The luminescence was weaker at points further from the nozzle, fading into darkness well short of the walls.

After 10 minutes of operation under flame conditions a white deposit began to obscure the window. The deposit was formed in a ring around the reaction vessel along a length corresponding to the flame region. The deposit, a fine powder, could easily be distinguished from the metallic sodium-mirror obtained when the Wood's discharge tube was switched off. This white salt-like deposit is almost certainly sodium hydride.

Concurrently with the appearance of the white deposit a diffuse orange glow was observed at the walls of the reaction vessel. The glow was most intense in its upper region, i.e. at the level of the nozzle, where the deposit of sodium hydride was thickest. This secondary glow obscured the emission from the flame and made photography of the flame impossible. A photograph (*f* 2.5 camera, Eastman Kodak 103aF plates, 25-minute exposure) taken through an interference filter transmitting the sodium D line showed only the secondary luminescence. The flame emission could, however, be weakly detected on the same plate by microdensitometry.

A spectroscopic examination of the luminescence showed only the D line radiation 5890–5896 Å ( $3^2P \rightarrow 3^2S$ ) and the H<sub>a</sub> line at 6560 Å (the latter probably originating in scattered light from the Wood's tube). A glass lens focused the luminescence on the slit of a small Hilger constant deviation glass prism wavelength spectrometer, similar to the D-186 (focal length 286 mm., *f* 11) with camera attachment. The dispersion was *ca.* 70 Å/mm. at 5900 Å. Spectrograms were taken on Eastman Kodak I-F plates with 2 hours' exposure. It now seems unlikely that any light entered the spectrometer after the first 30–40 minutes, owing to the formation of the sodium hydride film on the window. The greater part of the light after the first 10 minutes must have come from the secondary emission. With the spectrometer we used we would have been unable to observe the sodium  $4^2P \rightarrow 3^2S$  emission at 3302–3303 Å had it been present.

In view of the rapid deposition of NaH and consequent secondary luminescence, observations had to be of a kind that could be completed in the first 5 to 10 minutes after the flame had been started in a clean reaction vessel: namely visual observation and photometric observation.

By visual observation it was found that the size of the flame could be increased either by increasing the pressure of sodium at the nozzle or by decreasing the pressure of atomic hydrogen, which suggests that the luminescent reaction, or its rate-determining reaction, involves these two species.

The fact that the flame falls short of the vessel walls is proof that one of the reagents involved in the luminescence, or its rate-determining reaction, is more plentiful at the nozzle than away from it. This reagent is in all probability sodium.

We have therefore to account for an observed chemiluminescence in the gas phase,

and consumption of some (or all) of the atomic sodium in the gas phase. Our further observations lead us to believe that these two effects arise from different reactions.

Experiments made with an R.C.A. 5819 photomultiplier tube calibrated against a 200 watt bulb of known color temperature showed that the total hemispherical emission from the flame was *ca.*  $5 \times 10^{11}$  photons/second when the inflow of sodium was  $2.4 \times 10^{16}$  molecules/second. Thus approximately one sodium atom in  $5 \times 10^4$  is involved in chemiluminescent reaction.

If the luminescent reaction were to account for the total consumption of sodium, then the ratio of the sodium pressure at the nozzle to that at the edge of the flame (ignoring the gradient due to flow) would be  $1/[1 - (5 \times 10^4)^{-1}] = 1/[1 - (2 \times 10^{-5})]$ . In fact (see below) this ratio is *ca.* 1/0.3, from which we conclude that a non-luminescent gas-phase reaction is responsible for the bulk of the sodium consumption.

The true pressure of sodium at the limit of the visible flame can be estimated, since it must be approximately the same as the pressure at the nozzle *when the limit of the flame is at the nozzle*, i.e. when the first trace of flame, right at the nozzle tip, is observed. As already noted, the first luminescence was observed with  $F_1 \approx 260^\circ \text{C.}$ , i.e. *ca.*  $2.5 \times 10^{-3}$  mm. pressure of sodium at the nozzle. We therefore take this to be the pressure,  $p_R$ , of sodium at the edge of the flame.

The flame diameter was found to be 3.8 cm. ( $\pm 10\%$ ) in an experiment carried out under the following conditions:  $\text{H}_2$  flow through the saturator  $3 \times 10^{-6}$  moles/second,  $\text{H}_2$  flow through the Wood's tube  $5 \times 10^{-6}$  moles/second, H flow from Wood's tube  $4 \times 10^{-6}$  moles/second, pressure of  $\text{H}_2$  in the saturator 6.5 mm., pressure of sodium in the saturator and at the nozzle 0.0074 mm. ( $F_1$  at  $284^\circ \text{C.}$ ), pressure of  $\text{H}_2$  in Wood's tube and reaction vessel 0.4 mm., pressure of H in reaction vessel 0.04 mm.

No change in flame diameter was observed when the water saturator was switched into the hydrogen stream supplying the Wood's tube. This indicates that the gas-phase chemiluminescence proceeds at the same rate, and presumably by the same mechanism, whether or not water vapor is present. A faster chemiluminescent reaction, for example, would be expected to give a larger flame since it would have an appreciable rate at lower pressures of sodium. (It is not likely that the switch to wet hydrogen would have any instantaneous effect on the H atom concentration in the reaction vessel—time would be needed for water to be adsorbed on the wall.) Some other explanation must therefore be found for the discrepancy between Aynard's results and those of Bonhoeffer and Mohler.

We propose the following reaction scheme:



in which [1] is the non-luminescent reaction consuming sodium, and either [2] or [3] or both are responsible for the observed luminescence. At a distance  $r$  from the nozzle the stationary state requirement is then

$$\delta d^2 p_{\text{Na}}(r)/dr^2 - k_1 p_{\text{Na}} p_{\text{H}} p_{\text{H}_2} = 0 \quad (i)$$

if we ignore the very small amount of sodium that may be consumed by reaction [2].  $p_{\text{Na}}(r)$  is the sodium pressure within the interval  $dr$ ;  $\delta$  is the diffusion constant of atomic sodium in hydrogen ( $3.14 \text{ cm.}^2/\text{second}$  (8)). This is a termolecular analogue to the well-known diffusion flame equation (Reference 4). Integration gives

$$k_1 = \delta(\ln p_R/p_0)^2 / [p_{\text{H}} p_{\text{H}_2} (R - r_0)^2], \quad (ii)$$

where  $p_R$  is the pressure of sodium at the edge of the flame,  $p_0$  is the pressure of sodium at the nozzle,  $R$  is the radius of the flame, and  $r_0$  is the radius of the nozzle. Inserting the values listed above gives  $k_1 = 1.5 \times 10^{16} \text{ cc.}^2 \text{ moles}^{-2} \text{ seconds}^{-1}$ .

This rate constant is only significant as an order of magnitude for  $k_1$ , in view of the approximate manner in which  $p_R$  was estimated. However,  $k_1 \sim 1 \times 10^{16} \text{ cc.}^2 \text{ moles}^{-2} \text{ seconds}^{-1}$  is in good agreement with rate constants obtained for other atomic combination reactions. Farkas and Sachsse (7) obtained  $k = 3.4 \times 10^{16} \text{ cc.}^2 \text{ moles}^{-2} \text{ seconds}^{-1}$  for  $\text{H} + \text{H} + \text{H}_2$ , in quite good agreement with an earlier value of  $k = 9 \pm 2 \times 10^{16} \text{ cc.}^2 \text{ moles}^{-2} \text{ seconds}^{-1}$  for the same reaction, due to Steiner and Wicke (17). In addition various workers (5, 6, 15, 16) have obtained (with accuracies to  $\pm 5\%$ )  $k \simeq 1 \times 10^{16} \text{ cc.}^2 \text{ moles}^{-2} \text{ seconds}^{-1}$  for  $\text{I} + \text{I} + \text{M}$ , depending on the nature of  $\text{M}$ , which is some inert gas; and for  $\text{Br} + \text{Br} + \text{A}$ ,  $k = 2.5 \times 10^{15} \text{ cc.}^2 \text{ moles}^{-2} \text{ seconds}^{-1}$  (18).

As an alternative to reaction [1] we have considered the bimolecular reaction



$\Delta H = -31 \text{ kcal./mole}$  so that the reaction would be non-luminescent ( $3^2P \rightarrow 3^2S$  for sodium requires 48 kcal./mole). However, in order for this reaction to affect the concentration of atomic sodium appreciably, it would be necessary for molecular sodium to be replenished by a termolecular reaction, most probably (since  $\text{H}_2$  is the most abundant "third body")



The minimum rate constant for [5] can be obtained by setting up a stationary state equation in which [5] determines the rate of consumption of sodium. Integration gives  $k_5 > 3 \times 10^{17} \text{ cc.}^2 \text{ moles}^{-2} \text{ seconds}^{-1}$ , which is improbably high and would seem to rule out this possibility.

Another possible reaction involving sodium consumption,



is endothermic and must be very slow since hydrogen is used as an "inert" carrier gas in sodium flame experiments (2, 13, 19).

We therefore consider that on the present evidence reaction [1] is the most likely non-luminescent reaction responsible for the consumption of sodium.

The luminescent reaction



is energetically possible ( $\Delta H \simeq -56 \text{ kcal./mole}$ ) and may be the explanation of the secondary luminescence at the wall. However, there are two reasons for supposing that it is not of major importance in the gas phase (possibly owing to appreciable activation energy). In cases where luminescence arises from reaction among the products formed in a diffusion flame one would not expect to observe, as we did under all flow conditions, the maximum emission at the tip of, or in, the nozzle. Observations on other low-pressure diffusion flames indicate that it is the initial reaction that occurs in this region. If reaction [7] nonetheless accounts for the luminescence, it must be extremely fast, in which case [1] will be the rate-determining reaction for luminescence. Evidence against this comes from our experiments with a photomultiplier tube. We attempted to vary separately the pressure of atomic sodium, atomic hydrogen, and molecular hydrogen. The luminescent intensity was found to be strongly dependent on the first two variables and only weakly on the third. This would not be the case if reaction [1] was determining the rate of luminescent reaction. We conclude that reaction [7] is not the principal luminescent reaction.

Calculation of the total number of collisions  $\text{Na} + \text{Na} + \text{H}$  in the flame and  $\text{Na} + \text{H} + \text{H}$  in the flame leads to values of the collision yields for the two luminescent reactions, [2] and [3], in the case that either [2] or [3] predominates. Recent experimental evidence (5) indicates that Bodenstein's method (3) of calculating rates of termolecular collision is as good as any at present available. Accordingly we write

$$\frac{\text{rate of bimolecular collision}}{\text{rate of termolecular collision}} = \frac{\text{mean free path}}{\text{mean molecular diameter}}. \quad (\text{iii})$$

The total number of bimolecular collisions  $\text{Na} + \text{H}$  in the flame per second is

$$Z_{\text{Na},\text{H}}^{\text{Tot.}} = Z_{\text{Na},\text{H}} \rho_{\text{H}} 4\pi N_0 \int_{r_0}^R p_{\text{Na}}(r) r^2 dr, \quad (\text{iv})$$

where  $Z_{\text{Na},\text{H}}$  is the rate of collision at a concentration of 1 mole/cc. So that the total numbers of termolecular collisions are

$$Z_{\text{Na},\text{Na},\text{H}}^{\text{Tot.}} = \frac{Z_{\text{Na},\text{H}} Z_{\text{Na},\text{NaH}} \rho_{\text{H}} 4\pi \sigma_{\text{Na},\text{NaH}} N_0}{\bar{c}_{\text{Na}}} \int_{r_0}^R (p_{\text{Na}}(r))^2 r^2 dr \quad (\text{v})$$

$$= 1.3 \times 10^{14} \text{ seconds}^{-1},$$

$$Z_{\text{Na},\text{H},\text{H}}^{\text{Tot.}} = \frac{Z_{\text{Na},\text{H}} Z_{\text{H},\text{NaH}} \rho_{\text{H}}^2 4\pi \sigma_{\text{H},\text{NaH}} N_0}{\bar{c}_{\text{H}}} \int_{r_0}^R p_{\text{Na}}(r) r^2 dr \quad (\text{vi})$$

$$= 4.5 \times 10^{16} \text{ seconds}^{-1}.$$

Since the total luminescence is  $\sim 5 \times 10^{11}$  photons/second, the luminescent collision yield in the case that reaction [2] predominates is  $5 \times 10^{11}/1.3 \times 10^{14} \simeq 4 \times 10^{-3}$ , and in the case that reaction [3] predominates  $5 \times 10^{11}/4.5 \times 10^{16} \simeq 1 \times 10^{-5}$ . If both reactions [2] and [3] contribute appreciably to the luminescence these figures are still substantially correct, and in any case they represent upper limits for the luminescent collision yields of these reactions.

Table I shows the extent of "energy matching" for the two luminescent reactions under discussion (cf. Kaplan (10) and Aynard (1)).

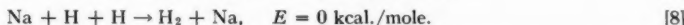
TABLE I

No.	Reaction	$-\Delta H$ , kcal./mole
[2]	$\text{Na} + \text{Na} + \text{H} \rightarrow \text{NaH}(v = 0, J = 0) + \text{Na}^* 3^3P$	$0 \pm 1.5^*$
[3] a.	$\text{Na} + \text{H} + \text{H} \rightarrow \text{H}_2(v = 0, J = 0) + \text{Na}^* 3^3P$	54.5
b.	$\text{Na} + \text{H} + \text{H} \rightarrow \text{H}_2(v = 1, J = 0) + \text{Na}^{**} 4^3P$	5.2
c.	$\text{Na} + \text{H} + \text{H} \rightarrow \text{H}_2(v = 1, J = 5) + \text{Na}^{**} 4^3P$	0.2
d.	$\text{Na} + \text{H} + \text{H} \rightarrow \text{H}_2(v = 5, J = 0) + \text{Na}^* 3^3P$	1.9
e.	$\text{Na} + \text{H} + \text{H} \rightarrow \text{H}_2(v = 5, J = 3) + \text{Na}^* 3^3P$	0.2

\*A. G. Gaydon (*Dissociation energies*, Dover Publications, 1950) gives  $D(\text{Na}-\text{H}) = 47$  kcal. G. Herzberg (*Spectra of diatomic molecules*, D. Van Nostrand, 1950) gives  $D(\text{Na}-\text{H}) = 50.5$  kcal.; spectroscopic constants for  $\text{H}_2$  were taken from Herzberg.

If one considers all the quantized degrees of freedom of the products to be simultaneously equally available, then a case can always be made for perfect energy matching —certainly to the accuracy to which the energy terms are known. Some additional criterion is therefore required, the simplest being to suppose that the greater the number of degrees of freedom among which the energy must be distributed the less likely is the process. On this basis reaction [2] is favored as against reaction [3].

Magee and Ri (11), in a theoretical study of reaction [3] according to the semiempirical method, calculate a potential energy surface across which [3] proceeds adiabatically (activation energy  $E = 6.5$  kcal./mole) in competition with the non-luminescent reaction [8] on a lower surface ( $E = 0$  kcal.),



Making reasonable assumptions about the magnitudes of the transmission coefficients ( $\kappa_3/\kappa_8 = 1/0.1$ ) they calculate that at 200° C. 15 sodium atoms are excited electronically for 1000 which gain only thermal energy. Since  $\kappa_8 = 0.1$ , this leads to a collision yield of  $1.5 \times 10^{-3}$  at 200° C., or  $3 \times 10^{-5}$  at room temperature, for luminescence due to reaction [3], in good agreement with our figure of *ca.*  $1 \times 10^{-5}$ . It is not possible to say how far this agreement is real until the kinetics of the luminescence have been properly elucidated, preferably over a range of temperatures.

#### ACKNOWLEDGMENTS

We are indebted to Mr. C. Sadowski of the University of Toronto for assistance with the calculations. We should also like to thank Professor A. G. Shenstone of the Physics Department, Princeton University, for the loan of a spectrograph.

#### REFERENCES

1. AVNARD, R. Ph.D. Thesis, Sorbonne, Paris (1956).
2. BAUW, C. E. H. Am. Chem. Soc. Repts. **39**, 36 (1943).
3. BODENSTEIN, M. Z. physik. Chem. **100**, 118 (1922).
4. BONHOEFFER, K. F. Z. physik. Chem. **113**, 199 (1924); **116**, 391 (1925).
5. CHRISTIE, M. I., NORRISH, R. G. W., and PORTER, G. Proc. Roy. Soc. A, **216**, 152 (1953).
6. DAVIDSON, N., MARSHALL, R., LARSH, A. E., and CARRINGTON, T. J. Chem. Phys. **19**, 1311 (1951); **21**, 659 (1953).
7. FARKAS, L., and SACHSSE, H. Z. physik. Chem. B, **27**, 111 (1934).
8. HARTEL, V., MEER, N., and POLANYI, M. Z. physik. Chem. B, **19**, 139 (1932).
9. HENKIN, H. and TAYLOR, H. A. J. Chem. Phys. **8**, 1 (1940).
10. KAPLAN, J. Phys. Rev. **31**, 997 (1928).
11. MAGEE, J. L. and RI, T. J. Chem. Phys. **9**, 638 (1941).
12. MOHLER, F. I. Phys. Rev. **29**, 419 (1927).
13. POLANYI, M. Atomic reactions. Williams & Norgate Ltd., London. 1932.
14. POOLE, H. G. Proc. Roy. Soc. (London), A, **163**, 404 (1937).
15. RABINOWITCH, E. and WOOD, W. C. Trans. Faraday Soc. **32**, 907 (1936); J. Chem. Phys. **4**, 497 (1936).
16. RUSSELL, K. E. and SIMONS, J. Proc. Roy. Soc. (London), A, **217**, 271 (1953).
17. STEINER, W. and WICKE, F. W. Z. physik. Chem. Bodenstein-Festband, 817 (1931).
18. STRONG, R. L. and WILLARD, J. E. Abstracts, Am. Chem. Soc. Meeting, New York (Sept. 1954), p. 26R.
19. WARHURST, E. Quart. Revs. (London), **5**, 44 (1951).

# THE QUENCHING OF THE IODINE FLUORESCENCE SPECTRUM<sup>1</sup>

C. ARNOT AND C. A. McDOWELL

## ABSTRACT

The quenching of the iodine fluorescence spectrum by various inert gases and oxygen has been studied with a view to obtaining information on the efficiencies of vibration energy transfer processes in this system. Preliminary results here presented are in agreement with earlier work of Rössler and Eliashevich and indicate that the transfer processes are very efficient. A kinetic scheme is proposed to account for the various possible quenching and transfer processes and it is shown that this is in agreement with experimental results.

## INTRODUCTION

The fluorescence spectrum of iodine vapor excited by the green mercury line 5461 Å was first investigated by Wood (6) (see Fig. 1). It consists of a series of bands stretching from 5461 towards the red. The excited state was shown by Mulliken (2) to be a  $^3\Pi_u$  state which is split into levels by  $\Lambda$  doubling; these two levels behave almost like two independent  $^1\Sigma$  states and only one of them (designated by Mulliken as  $^30_u^+$ ) combines with the ground state.

On excitation with the narrow green line (Hg 5461) the iodine molecules are raised to the 26th vibrational level (6) of this  $^30_u^+$  state and the fluorescence bands are produced by the transitions back to the ground state  $26' \rightarrow 0''$ ,  $26' \rightarrow 1''$ ,  $26' \rightarrow 2''$ ,  $26' \rightarrow 3''$ , etc. The resonance spectrum has been extended as far as the 39th member at 9097 Å (6). The bands under these conditions have only a doublet structure (6).

It has been established that the quenching mechanism by foreign gases is by induced predissociation (3); the iodine molecule is induced by the foreign gas to pass into a repulsion potential energy state.

Transfer of the excited iodine molecule from the 26th vibrational level to other vibrational levels occurs with certain foreign gases, and new fluorescence bands originating from these levels are then observed (see Fig. 2). Rössler (4) showed that the vibrational quantum number only changes by 1 or 2 on these transfer collisions and so molecules are only transferred to the 24th, 25th, 27th, and 28th vibrational levels of the excited state. Change of rotational state also occurs in these transfer collisions and the bands lose their doublet structure and are broadened.

Transfer bands have, in general, only been observed with the rare gases, as the quenching action is much stronger with other gases, and the fluorescence intensity is weakened to a much larger extent.

## EXPERIMENTAL

### Materials

The rare gases were spectroscopically pure samples provided by the British Oxygen Company. The iodine was purified by sublimation.

### Apparatus

The light source was a high intensity low pressure mercury arc with water-cooled electrodes, operated at 25 amp., 180 volts, which was made to a design by Stoicheff (5).

<sup>1</sup>Manuscript received October 7, 1957.

Contribution from the Department of Chemistry, University of British Columbia, Vancouver 8, B.C., Canada, and the Department of Inorganic and Physical Chemistry, University of Liverpool, Liverpool, England. This paper was presented at the Symposium on the Structure and Reactivity of Electronically-Excited Species held at the University of Ottawa, Ottawa, Canada, September 5 and 6, 1957.

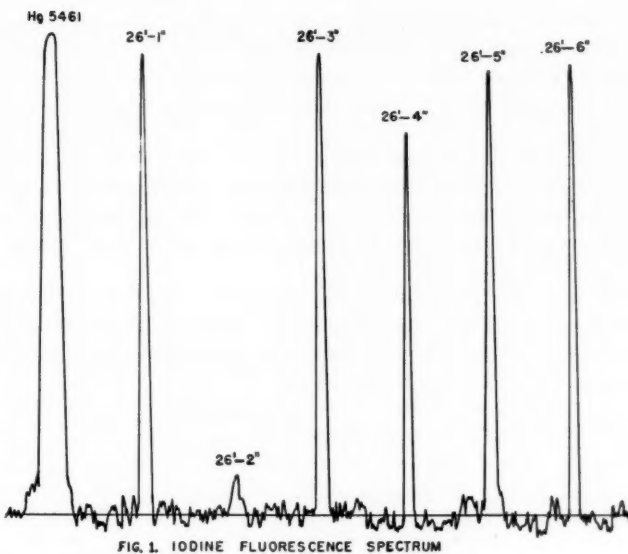


FIG. 1. IODINE FLUORESCENCE SPECTRUM

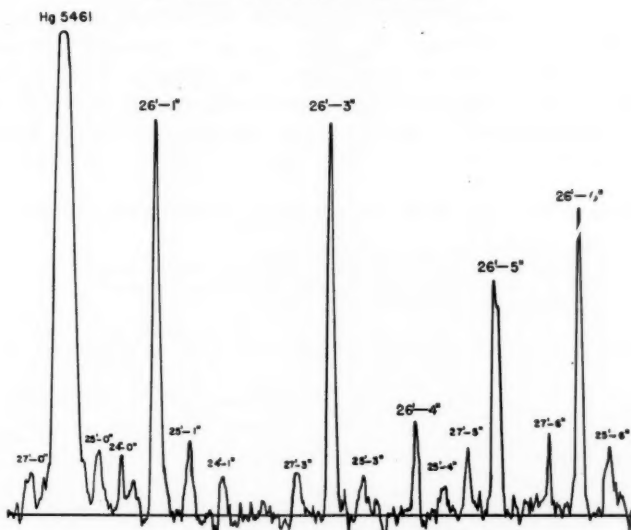


FIG. 2. IODINE FLUORESCENCE 0.5mm NEON PRESENT

FIG. 1. A portion of the fluorescence spectrum of the iodine molecule.

FIG. 2. A portion of the fluorescence spectrum of iodine showing transfer bonds caused by adding 0.5 mm. of neon.

The fluorescence vessel was a glass tube 70 cm. long and 2.5 cm. in diameter with an outer jacket 4.0 cm. in diameter to contain the filter solution. An optical flat at one end of the tube served as a viewing window and the other end of the tube led to a dibutyl phthalate manometer for measuring foreign gas pressure, a gas-introduction apparatus, and vacuum pumps.

The fluorescence was photographed using a prism spectrograph having a dispersion of 33 Å per mm. The photographic plates were Kodak Scientific Plates type IIaF, which are sensitive to 7000 Å, thus allowing the first 19 bands of the resonance series to be studied. The plates were analyzed using a Hilger microphotometer, the blackening of the plates being recorded on a Leeds and Northrup recorder. The filter solution was a 0.5 M  $\text{NdCl}_3$  solution, which eliminated the yellow mercury lines 5770 and 5790 Å.

The fluorescence tube and arc were mounted side by side and surrounded by a magnesium oxide reflector to cut down exposure times. A set of calibration marks was put on each plate by means of a Hilger calibrated step filter. Under these conditions an exposure time of 2 minutes was satisfactory.

Iodine crystals were contained in a small glass bulb. The system was evacuated with the iodine bulb maintained at a temperature of  $-80^\circ\text{C}$ . The iodine was then kept at  $0^\circ\text{C}$ . while the pumping was continued, and then the system was isolated and the iodine allowed to come to equilibrium with its vapor at  $0^\circ\text{C}$ .

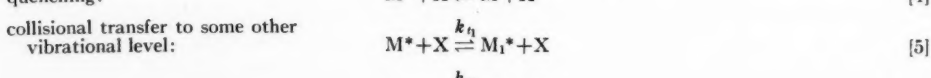
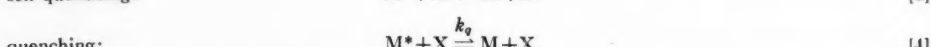
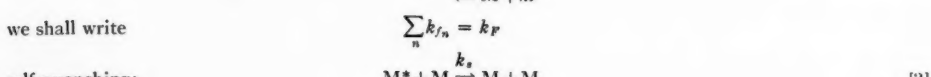
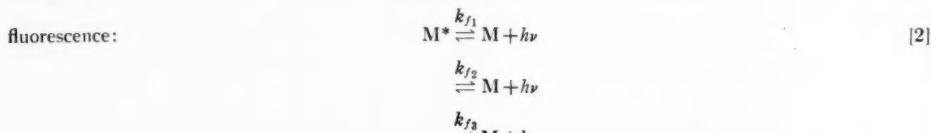
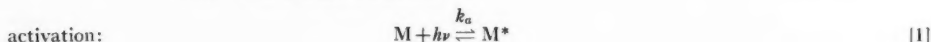
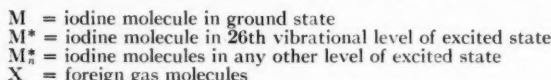
Exposures were made of the fluorescence in the absence of foreign gas and at various pressures of foreign gas, the gas being admitted by expansion from a small volume.

For self-quenching data the iodine was allowed to warm up and exposures were made at various iodine pressures, the pressure being measured on a Pirani gauge.

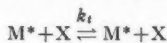
#### RESULTS AND DISCUSSION

Transfer bands were observed only on the plates with helium, neon, argon, hydrogen, and in some cases oxygen as foreign gas. Of these the intensities of the argon ones were very small and difficult to measure accurately. Even with He or Ne as foreign gas the intensities of the transfer bands were small and could not be accurately measured, as their density of blackening fell in the toe of the calibration curve for the photographic emulsion. With the other foreign gases added ( $\text{O}_2$ ,  $\text{N}_2$ , Kr, and Xe) the quenching action was stronger.

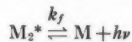
The data obtained were interpreted in the light of the following kinetic scheme:



back-transfer to 26th level:



fluorescence from collisionally excited levels:



self-quenching:



quenching:



Without foreign gas this scheme leads to the following expression for the intensity of the band of the fluorescence spectrum:

$$F_{0n} = k_{fn}[M^*].$$

Since

$$F_0 = \sum_n F_{0n},$$

we get

$$F_0 = k_F k_a [M] / (k_F + k_s [M]) \quad [10]$$

and

$$F_{0n} = k_{fn} k_a [M] / (k_{fn} + k_s [M]); \quad [11]$$

hence

$$1/F_{0n} = k_F/k_a k_{fn} [M] + k_s/k_{fn} k_a. \quad [12]$$

A plot of  $1/F_{0n}$  against  $1/[M]$  yields an intercept/slope ratio equal to  $k_s/k_F$ , and so the self-quenching efficiency of iodine can be determined.

With foreign gas present and where no transfer bands are observed, the above kinetic scheme leads to the following expression for the intensity of the  $n$ th band of the spectrum:

$$\begin{aligned} F_n &= k_{fn}[M^*] \\ &= k_{fn} k_a [M] / (k_F + k_s [M] + k_q [X]) \end{aligned} \quad [13]$$

and

$$F_{0n}/F_n = k_F + k_s [M] + k_q [X] / (k_F + k_s [M]) \quad [14]$$

$$= 1 + (k_q/k_F)[X] / \{1 + (k_s/k_F)[M]\}. \quad [15]$$

From a plot of  $F_{0n}/F_n$  against  $[X]$ ,  $k_q/k_F$  can be calculated for each of the foreign gases studied.

Where transfer bands are observed, all the processes 1-9 have to be considered and we can deduce an expression for the over-all kinetic scheme in the following way:

Let  $R_1$  be the ratio of the total fluorescence intensities before and after the addition of foreign gas at a concentration  $X$ .

Let  $R_2$  be the ratio of intensities of fluorescence originating from the 26th vibrational level before and after the addition of foreign gas at a concentration  $X$ .

Let  $R_3$  be the ratio of intensity of fluorescence from levels other than the 26th level when foreign gas at a concentration  $X$  is present.

At equilibrium,  $d[M^*]/dt = 0$  and  $d[M_n^*]/dt = 0$ .

Hence  $k_a[M] = k_F[M^*] + k_s[M^*][M] + k_q[M^*][X] + k_T[M^*][X] - [X]\sum_n k_{tn'}[M_n^*]$ , [16]

also  $k_T[M^*][X] = [X]\sum_n k_{tn'}[M_n^*] + k_F\sum_n[M_n^*] + k_s[M]\sum_n[M_n^*]$ , [17]

assuming  $\sum k_{fn} = \sum k_{f1} = \sum k_{fn} = k_F$ .

Processes involving collisional transfer of energy between the 24th, 25th, 27th, and

28th vibrational levels have been disregarded since these only lead to the iodine molecule being in a state in which processes identical to those in its previous state can occur and here we are considering the *summation* of intensities originating from these collisionally excited states.

Assuming that

$$k_{t_1'} = k_{t_2'} = k_{t_3'},$$

i.e. assuming

$$\sum_n k_{t_n'} = Z k_{t_n'} = k_{T'},$$

it follows, therefore, that  $k_{t_n'} = k_{T'}/Z$ , where  $Z$  is the number of occupied levels, i.e.  $k_{t'}$  is independent of the vibrational level for back transfer to the original state;

then

$$\begin{aligned} \sum_n k_{t_n'} [M_n^*] &= k_{t_n'} \sum_n [M_n^*] \\ &= (k_{T'}/Z) \sum_n [M_n^*], \end{aligned}$$

then, from [2],

$$\begin{aligned} R_3 &= k_F [M_n^*]/k_F [M^*] \\ &= k_T [X]/([X] k_{t_n'} + k_F + k_s [M] + k_q [X]) \end{aligned} \quad [18]$$

and also, from [2],

$$\begin{aligned} \sum_n [M_n^*] &= k_T [M^*] [X]/([X] k_{t_n'} + k_F + k_s [M] + k_q [X]) \\ &= [M^*] R_3. \end{aligned} \quad [19]$$

Hence

$$\begin{aligned} [X] k_{t_n'} \sum_n [M_n^*] &= k_{t_n'} [X] [M^*] R_3 \\ &= (k_{T'}/Z) [X] [M^*] R_3 \end{aligned}$$

and, substituting in [1], we get

$$k_a [M] = k_F [M^*] + k_s [M^*] [M] + k_q [M^*] [X] + k_T [M^*] [X] - (k_{T'}/Z) [X] [M^*] R_3, \quad [20]$$

and the intensity of fluorescence from the 26th level at the concentration of foreign gas

$$\begin{aligned} [X] &= k_F [M^*] \\ &= k_F k_a [M]/(k_F + k_s [M] + k_q [X] + k_T [X] - (k_{T'}/Z) [X] R_3). \end{aligned} \quad [21]$$

Since

$$F_0 = k_F k_a [M]/(k_F + k_s [M]),$$

therefore

$$R_2 = \{k_F + k_s [M] + k_q [X] + k_T [X] - (k_{T'}/Z) [X] R_3\}/(k_F + k_s [M]). \quad [22]$$

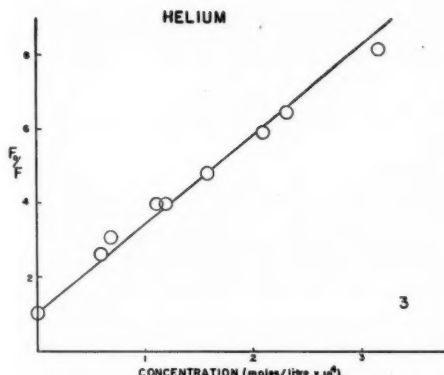
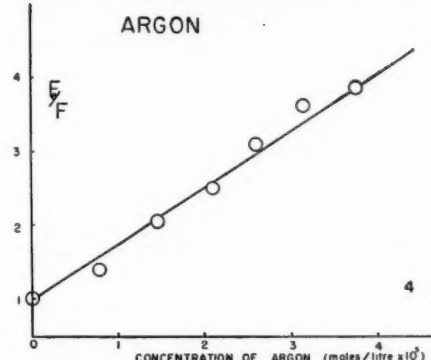
Assuming the probability of back transfer equals the probability of transfer, i.e.  $k_T = k_{T'}$ , then the following expression is obtained for  $R_2$ :

$$R_2 = \frac{1 + (k_s/k_F) [M] + (k_q/k_F) [X] + (k_T/k_F) [X] (1 - R_3/Z)}{1 + (k_s/k_F) [M]}. \quad [23]$$

$k_T/k_F$  can be determined from  $R_1$  in the following manner. If we consider that  $M^*$  is an iodine molecule in any vibrational level of the excited state, then transfer processes may be neglected as they only lead to an excited molecule which undergoes exactly the same processes as in its previous state, i.e. fluorescence, self-quenching, and quenching. We thus obtain the same equation as previously for quenching processes, i.e.

$$R_1 = F_0/F = 1 + (k_q/k_F) [X]/\{1 + (k_s/k_F) [M]\}. \quad [24]$$

It follows from equation [24] that a plot of  $F_0/F$  against the concentration of quenching gas  $X$  should be linear with an intercept of unity on the  $F_0/F$  axis. In Figs. 3 and 4

FIG. 3. Plot of  $F_0/F$  for the quenching of the fluorescence spectrum of iodine by helium.FIG. 4. Plot of  $F_0/F$  for the quenching of the fluorescence spectrum of iodine by argon.

we show graphs of  $F_0/F$  against the concentration of the quenching gas for helium and argon; it will be seen that these are linear and that both intercept the  $F_0/F$  axis at unity in agreement with the requirements of equation [24]. It has been found that equation [24] is also obeyed by the gases listed in Table I.

From the slope of the straight line resulting from plotting equation [24] one can calculate the ratio  $(k_q/k_F)/\{1+(k_s/k_F)[M]\}$ . Knowing the concentration of the iodine in the experiments and having previously determined  $k_s/k_F$  from self-quenching experiments with iodine using self-quenching bands where self-absorption is negligible, one can calculate values for  $k_q/k_F$  for each quenching gas studied.

Similarly, by plotting  $R_2$  against the concentration of quenching gas X, one can determine (see equation [23]) the ratio

$$(1-R_3/Z)(k_q/k_F+k_T/k_F)/\{1+(k_s/k_F)[M]\},$$

and knowing the concentration of iodine in the experiments and having determined  $R_3$  (see definition above),  $k_q/k_F$ , and  $k_s/k_F$ , one can calculate  $k_T/k_F$ , the transfer coefficient, since Z is known, being the number of occupied levels of the excited iodine molecule. The values obtained for the coefficients  $k_T/k_F$  for the different gases studied are given in Table I.

TABLE I  
COEFFICIENTS FOR THE TRANSFER OF VIBRATIONAL ENERGY IN EXCITED IODINE MOLECULES ( $T = 20^\circ \text{ C.}$ )

Gas	$k_T/k_F$ , liters mole $^{-1}$ experimental	$k_T/k_F$ , liters mole $^{-1}$ theoretical
Helium	$5.31 \times 10^4$	$3.23 \times 10^3$
Neon	$2.69 \times 10^4$	$1.66 \times 10^3$
Argon	$1.64 \times 10^4$	$1.39 \times 10^3$
Oxygen	$1.5 \times 10^4$	$1.37 \times 10^3$

The theoretical values quoted for the quenching coefficients in Table I were calculated from the equation

$$k_T/k_F = \frac{\rho \tau N(r_1+r_2)^2}{1000} 8\pi RT \left( \frac{1}{M_1} + \frac{1}{M_2} \right)^{\frac{1}{2}} \quad [25]$$

using the following values for the parameters:

$$\begin{aligned} N &= 6.023 \times 10^{23} \text{ molecules liter}^{-1}, & r_{\text{He}} &= 0.98 \text{ \AA}, \\ r_{I_2} &= 2.72 \text{ \AA}, & r_{\text{Ne}} &= 1.18 \text{ \AA}, \\ r_A &= 1.46 \text{ \AA}, & r_{O_2} &= 0.47 \text{ \AA}; \\ M_1 &= \text{mass of the iodine molecule}; \\ M_2 &= \text{mass of the quenching molecule}. \end{aligned}$$

The value taken for the lifetime of the excited  $^3\Pi_{0a}$  state of the iodine molecule was  $\tau = 10^{-8}$  second and the theoretical values were computed for a pressure of 1 cm.

The experimental data in Table I, which must only be regarded as preliminary, indicate that the transfer of energy in the system studied must be very efficient. Though our data are in agreement with the results of Rössler (4) and Eliashevich (1), there is, of course, still to be explained the discrepancy between the experimental and theoretical values. It could be that the value of  $10^{-8}$  second assumed for the lifetime of the excited iodine molecule is too short and it should be of the order of  $10^{-7}$  second. Were this so, then the experimental values would be more nearly in agreement with the theoretical ones, which would now be 10 times larger.

#### ACKNOWLEDGMENTS

The earlier part of this work was carried out in the Department of Inorganic and Physical Chemistry, University of Liverpool, Liverpool 7, England, and we are grateful to Professor C. E. H. Bawn, C.B.E., F.R.S., for providing laboratory facilities. The remainder of the work and the analysis of the photographic plates was carried out in the Department of Chemistry, University of British Columbia, Vancouver 8, B.C. This latter portion was supported by grants from the National Research Council of Canada whom we should like to thank.

#### REFERENCES

1. ELIASCHEVICH, M. Phys. Rev. **39**, 532 (1932); Physik. Z. Sowjetunion, **1**, 510 (1932).
2. MULLIKEN, R. A. Revs. Modern Phys. **4**, 1 (1932).
3. RABINOVITCH, E. and WOOD, W. C. Trans. Faraday Soc. **31**, 689 (1935).
4. RÖSSLER, F. Z. Physik, **96**, 251 (1935).
5. STOICHEFF, B. P. Can. J. Phys. **32**, 330 (1954).
6. WOOD, R. W. Phil. Mag. **12**, 499 (1906).

# QUENCHING AND VIBRATIONAL-ENERGY TRANSFER OF EXCITED IODINE MOLECULES<sup>1</sup>

J. C. POLANYI<sup>2</sup>

## ABSTRACT

Quenching of  $I_2^*$  ( ${}^3\Pi_{0+}$ ) ( $v' = 26$ ) is shown to take place to the exclusion of vibrational-energy transfer in iodine at pressures up to 19 mm. A possible quenching mechanism involving sensitized predissociation of the collision partner is described. Vibrational transfer in collisions with  $H_2$  and  $D_2$  is found to occur at less than every gas kinetic collision. Arguments on general grounds are put forward to support this result, which conflicts with that of earlier workers. Increase in the mass of the isotope is found to bring about increased efficiency of vibrational transfer.

## INTRODUCTION

Franck and Wood (1) were the first to observe that the resonance spectrum of iodine vapor excited by the mercury green line is transformed into the complete band spectrum when foreign gases are added. Absorption of the narrow green line obtained from a water-cooled mercury discharge gives rise to the electronic transition  ${}^3\Pi_{0+} \leftarrow {}^1\Sigma_g^+$  resulting for the most part in  $I_2^*$  ( $v' = 26$ ;  $J' = 35, 34, 29$ , and  $28$ ) (2, 3). Collisions between  $I_2^*$  and added gas may result either in quenching or in transfer to new vibrational and rotational levels of the excited  ${}^3\Pi$  state.

The latter phenomenon is the origin of the effect observed by Franck and Wood. They were able to show that the changes in vibrational quantum number ( $v'$ ) were restricted to  $\pm 1$  or  $\pm 2$ , with roughly equal probability, the changes in rotational quantum number to  $\pm 2$ . It was clear that if the "transferred spectra" could be compared for a series of foreign gases, relative efficiencies in taking up single vibrational quanta of a known size would be calculable. Eliashevich (4) made use of this method with  $H_2$  and  $N_2$  as the foreign gases. Rössler (5) performed similar experiments using the inert gases. Both workers calculated the probability of vibrational transfer on the assumption that the lifetime of  $I_2^*$  ( ${}^3\Pi$ ) is  $1 \times 10^{-8}$  second. The calculated number of successful collisions was in every case greater (up to  $100\times$ ) than the number of collisions obtained when the collision cross-section from kinetic theory was used. Rössler found that the transfer probability increased with the atomic weight of the inert gas.

It is generally supposed (see for example Pringsheim (6)) that the effect of increasing iodine pressure is the same as that of adding foreign gas, but there is to the writer's knowledge no experimental evidence for this. Wood and Speas (7) and also Pringsheim (8) investigated the self-quenching of iodine fluorescence at elevated pressures, but did not examine the fluorescent spectrum.

The present work was undertaken in the first place to ascertain the probability of vibrational-energy transfer in collisions  $I_2^*$  ( ${}^3\Pi$ ) ( $v' = 26$ ) +  $I_2$ . Secondly it was hoped to obtain an independent check on the large transfer probabilities reported by Eliashevich and Rössler. At the same time information was sought concerning the effect on transfer probability of a change in mass of the colliding partner in a case where other factors (such as polarizability) remained constant. Hydrogen and deuterium were therefore chosen as foreign gases.

<sup>1</sup>Manuscript received October 10, 1957.

Contribution from the James Forrestal Research Center, Princeton University, Princeton, New Jersey, U.S.A. This paper was presented at the Symposium on the Structure and Reactivity of Electronically-Excited Species held at the University of Ottawa, Ottawa, Canada, September 5 and 6, 1957.

This research was supported by the United States Air Force under Contract No. AF 33(038)-23976 monitored by the Air Research and Development Command.

<sup>2</sup>Present address: Department of Chemistry, University of Toronto, Toronto, Canada.

## EXPERIMENTAL

In the early part of this work an attempt was made to observe the fluorescence using a Raman-type apparatus (see for example Stoicheff (9)). A greatly increased fluorescence intensity was obtained in this way but the method was abandoned because of the considerable self-absorption in the important region of the spectrum up to  $v'' = 3$ .

The apparatus used is shown in Fig. 1. At first the source was a water-cooled mercury-discharge lamp but it was found that a sufficiently narrow green line could be obtained

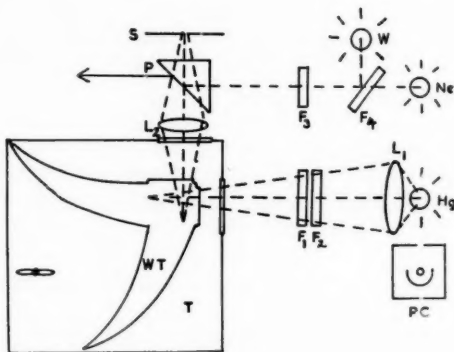


FIG. 1.

using a Mazda medium pressure 250 watt concentrated mercury arc. This lamp was started in a closed container and then operated in the open under an air blower. In this way the discharge was operated at the lowest practicable mercury pressure. The photocell (PC) was a WL930 used to keep a check on the constancy of the mercury lamp intensity.

Condenser lens  $L$  focused the light beam on a point about 1.55 cm. inside the double-horned Wood's fluorescence tube ( $WT$ ), as close as possible to the exit window so as to minimize self-absorption. The Wood's tube shown in the figure was a sealed tube containing only crystals of iodine purified by resublimation. In the experiments where foreign gases were added a Wood's tube was used with a tap which was connected through a fine capillary to minimize absorption of iodine in the tap grease. This tube also differed from the sealed tube in that the ends of the conical limbs were connected to one another by an S shaped length of 6 mm. glass tubing. After the foreign gas had been introduced one limb of the S would be cooled while the other was heated so that the convecting gas would mix with the iodine vapor (for 10–15 minutes). The Wood's tube was immersed in a thermostated water-bath ( $T$ ). The temperature was controllable to  $\pm 0.1^\circ C$ .

The filters  $F_1$  and  $F_2$  consisted of a Baird Multilayer filter with peak transmission at the mercury green line, and a Kodak Wratten No. 77 filter (2% transmission at the yellow line). The fluorescent light was focused by  $L_2$  onto the slit  $S$  of a Steinheil spectrograph with three large glass prisms (*ca. f/10*), dispersion approximately  $40 \text{ \AA/mm}$ . in the yellow. When the fluorescent spectrum was being observed, prism  $P$  was removed in the direction of the arrow (Fig. 1). With  $P$  in front of the slit the neon lamp ( $Ne$ ) or the standard tungsten-filament lamp ( $W$ ) could be photographed for calibration purposes. ( $F_3$  was a sheet of frosted glass,  $F_4$  a half-silvered mirror.) The neon spectrum was used both for wavelength calibration and for density vs. log exposure calibration. In the latter case a rotating sector not shown in Fig. 1 (Jarrel Ash, J.A. 1660;  $I_0/I = 2$ ) was placed in front of the spectrograph slit. The tungsten lamp was a standard lamp of known color

temperature; it was used for calibrating the plates for variation in sensitivity with wavelength.

Hydrogen and deuterium were kindly supplied by Dr. P. M. Gundry, Princeton University. The gases had been purified by passage through a palladium thimble.

#### RESULTS

Fig. 2a is the fluorescent spectrum of iodine at 0.43 mm. pressure, photographed on a Kodak 103 aF plate (used for all spectra of Fig. 2) at a 6.5 minute exposure. Fig. 3a is the microdensitometer trace of this plate. The spectrum corresponds to that reported by Rank (3) for the iodine emission  $^3\Pi_{0u}^+ \rightarrow ^1\Sigma_g^+$ ;  $v' = 26 \rightarrow v'' = 0, 1, (2), 3, \dots$ . Using a sensitized IN plate and 8.75-hour exposure we were able to photograph this spectrum as far as  $v' = 26 \rightarrow v'' = 37$  (8830 Å). The rotational structure of the bands could not be resolved. The possibility that some of the fluorescence originated in  $v' = 27$  and  $v' = 25$  owing to absorption from wings of the mercury green line cannot be ruled out since the positions of the bands and their relative intensities would not be appreciably different if this were the case. However, the mercury green line did not appear significantly broadened in photographs of the source; promotion to 27' and 25' would consequently be expected to be slight.

Fig. 2b is the fluorescent spectrum of iodine at 19.2 mm. pressure (84° C.), with 4 hours'

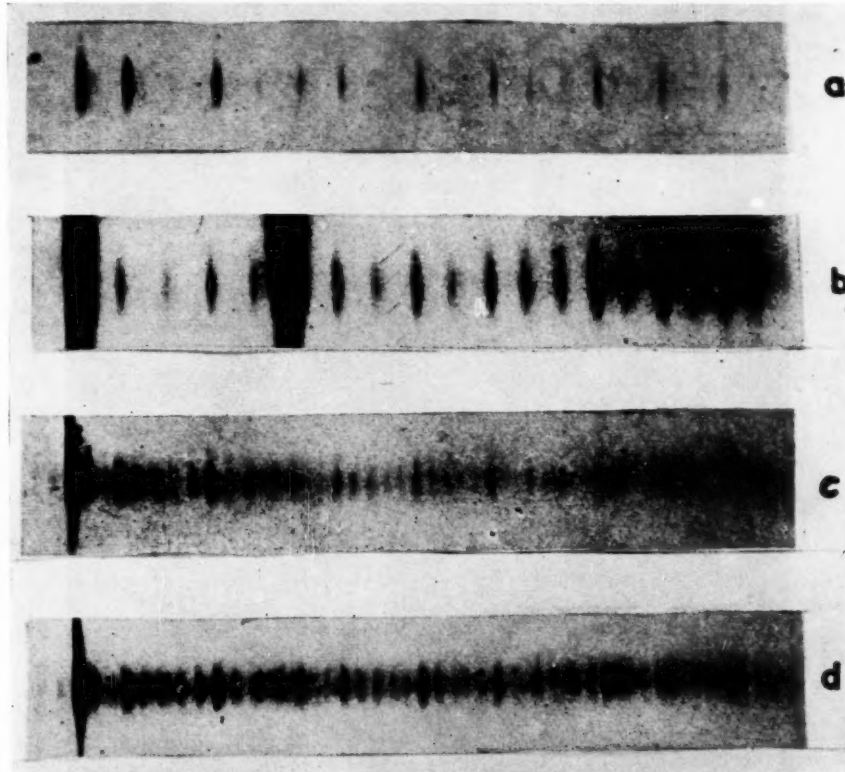
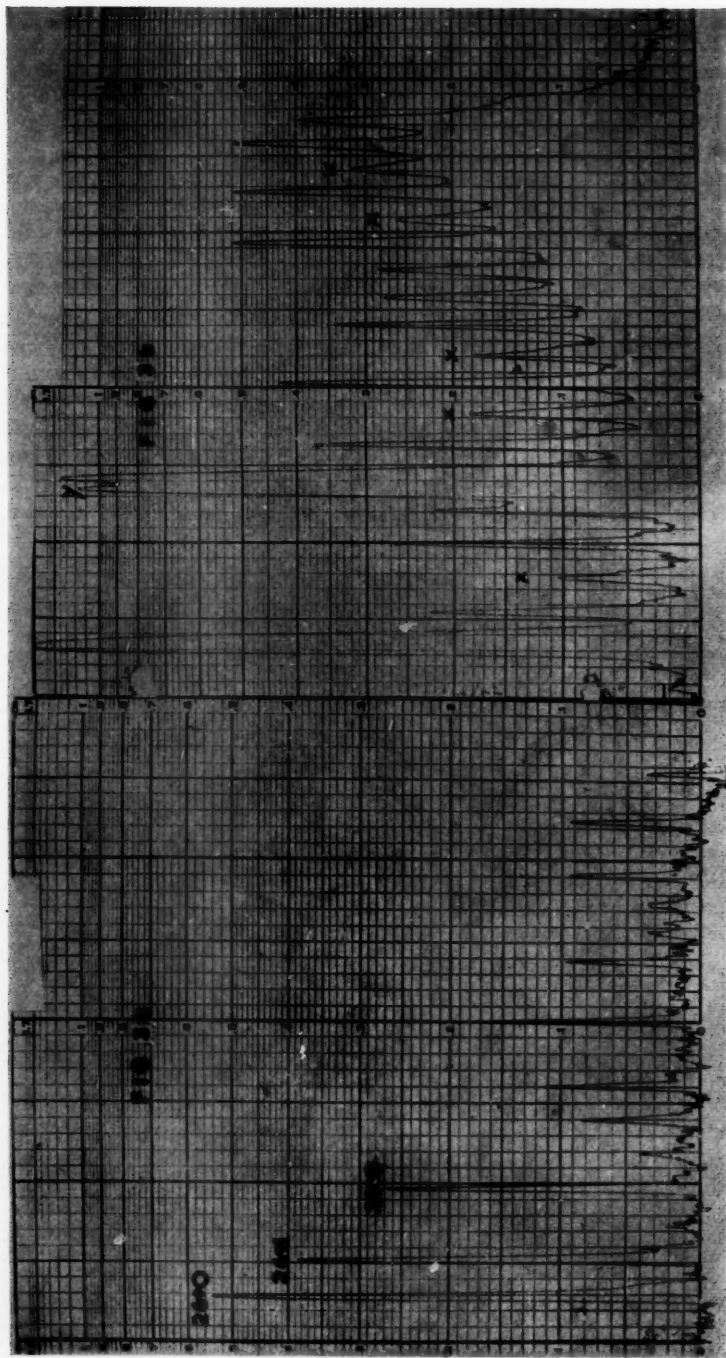
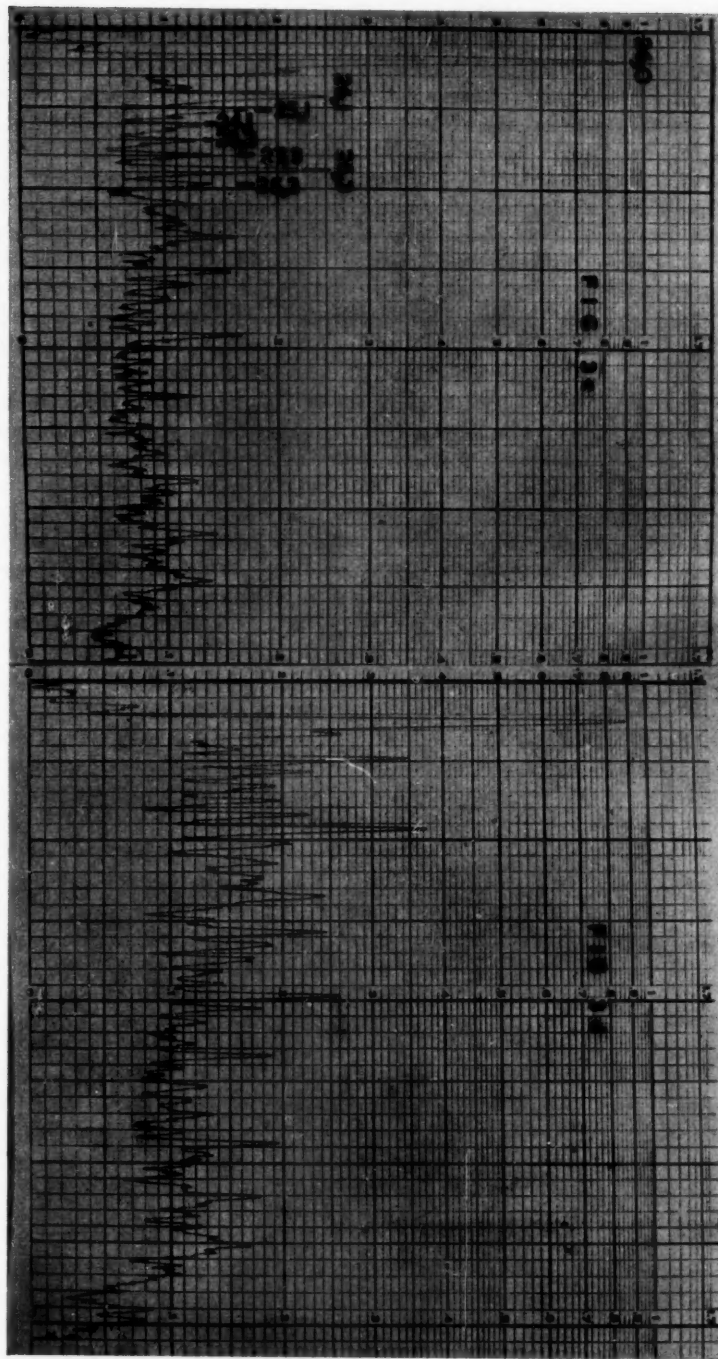


FIG. 2.

FIG. 3 *a* and *b*.

FIG. 3 *c* and *d*.

exposure. The first band, at 5460 Å, as in all these plates, also contains reflected green light from the mercury discharge lamp. In plate 2b the amount of scattered light appears greater relative to the fluorescence since the latter has been much reduced by quenching. Some scattered yellow light (5770 and 5780 Å) from the mercury lamp appears at Y on trace 3b of plate 2b, obscuring the  $v' = 26 \rightarrow v'' = 5$  transition.

Three significant changes have occurred in the fluorescent spectrum. The bands are now broader relative to their height. Five new bands have appeared (marked X in Fig. 3b) at the positions of the missing bands in the low pressure spectrum. Two anti-Stokes bands have appeared, separated from the resonance band by a space approximately equal to the separation between the normal bands,  $26' \rightarrow 0''$ ,  $26' \rightarrow 1''$ , etc. (these anti-Stokes lines are not shown in 2b or 3b).

All three changes can be accounted for by supposing (cf. Loomis' (10) detailed analysis of Wood's low pressure spectrum) that the fundamental series of doublets originates in  $v'' = 0$  and has no anti-Stokes members. At an elevated temperature the series of doublets originating in  $v'' = 1$  and  $v'' = 2$  will become important. With the dispersion used in the present work the various orders of the new series of doublets will almost coincide with the orders of the fundamental series. The slight difference in wavelength between the doublets of the new series and those of the fundamental series will result in the observed broadening of the spectral bands. Thus the origin of the first new series  $29' \rightarrow 1''$  at  $18,341 \text{ cm.}^{-1}$  overlaps heavily with the origin of the fundamental series  $26' \rightarrow 0''$  at  $18,311 \text{ cm.}^{-1}$ . The anti-Stokes doublets of -1 and -2 order are a part of the series originating in  $v'' = 1$  and  $v'' = 2$  respectively.

The appearance of the new bands X can be explained as follows. It is known that the fundamental series  $26' \rightarrow 0'', 1'', 2'' \dots$  has practically identical doublet intensities to the series  $27' \rightarrow 0'', 1'', 2'' \dots$  and  $28' \rightarrow 0'', 1'', 2'' \dots$ . This is probably due (cf. Pringsheim (6), p. 156) to the relatively high values,  $v'$ , of the eigenfunctions for all the upper levels (26, 27, 28) resulting in a great number of maxima near the turning points, which are all at nearly the same internuclear separation. It follows from the Franck-Condon principle that the transition probabilities depend largely on the eigenfunctions of the lower states determined by  $v''$ . This being the case the transitions  $29' \rightarrow 0'', 1'', 3'', 4'' \dots$  (but not  $2'', 7'', 9'', 14'',$  and  $16''$ ) should be observed. Of these,  $29' \rightarrow 3''$  will fall very close to the position of the missing line  $26' \rightarrow 2''$ . The other four new doublets are similarly accounted for by transitions  $29' \rightarrow 8'', 10'', 15'',$  and  $17''$ .

This leaves no lines unaccounted for and leads us to conclude that vibrational-energy transfer (the Wood effect) does not take place as a result of  $I_2^* + I_2$  collisions to any extent even at this high pressure of iodine. The same was found to be true at intermediate pressures of iodine.

Figs. 2c and 2d are the fluorescent spectra of iodine at 0.43 mm. pressure in the presence of 9.6 mm. of hydrogen and 8.3 mm. of deuterium respectively. The exposure time was 35 minutes in each case. Four new bands are visible between the  $v'' = 1$  and  $v'' = 3$  bands of the original series. The positions and relative intensities of these bands identify them as arising from transitions  $25' \rightarrow 1''$ ,  $24' \rightarrow 1''$ ,  $28' \rightarrow 3''$ ,  $27' \rightarrow 3''$  (in order of increasing wavelength). Immediately to the long wavelength side of  $v'' = 3$  of the original series is  $25' \rightarrow 3''$ . It is evident that the addition of hydrogen or deuterium has the effect of bringing about "transferring" collisions in which  $I_2^*(v' = 26) \rightarrow I_2^*(v' = 28, 27, 25, 24)$ , i.e. the iodine molecule may lose or gain either one or two quanta.

To interpret the densitometer traces (Figs. 3c and 3d) it is necessary to assume (see above) that the probability of a transition  $v' \rightarrow v''$  is determined, in this region of high  $v'$ , by  $v''$  alone. The density plot is first converted to an intensity plot making use of the

calibration marks on the plate, and the area under each band is integrated graphically. The areas obtained for bands having the same  $v''$ , but different  $v'$ , should then be in the ratio of the populations of the  $v'$  levels from which they originate. The areas obtained for the bands  $28' \rightarrow 3''$ ,  $27' \rightarrow 3''$ ,  $25' \rightarrow 3''$  were the same to within  $\pm 10\%$ , indicating that a collision results in a change of vibrational quantum number of  $\pm 1$  or  $\pm 2$  with equal probability. This was the case for both  $H_2$  and  $D_2$ .

A closer analysis of the data requires that one take into account that a new vibrational level may be partially converted by further collisions back to the original level. This may be significant for  $H_2$  and  $D_2$  since the quenching probability (which must be distinguished from the vibrational-transfer probability) is low. Rössler (5) (following Eliashevich's (4) extension of the Stern-Volmer (11) treatment of quenching curves) took this "compound transfer" into account and derived the relationship

$$[1] \quad I_0/I_p - 1 - \delta\tau p = \epsilon\tau p(1 - B \cdot I_p'/I_p),$$

where  $I_p$  and  $I_0$  are the fluorescent intensities of a particular band ( $v' \rightarrow v''$ ) with and without the addition of a pressure  $p$  mm. of gas,  $I_p'$  is the intensity of some new band arising from vibrational transfer when gas is added:  $(v'+1) \rightarrow v''$ ,  $(v'-1) \rightarrow v''$ , etc.,  $\delta$  and  $\epsilon$  are quenching and vibrational-transfer constants such that the probabilities of quenching and transfer are given by  $\delta p$  and  $\epsilon p$ ,  $\tau$  is the mean life of  $I_2^*$  ( ${}^3\Pi_{0+}^*$ ) ( $v' = 26$ ) which we take to be  $1 \times 10^{-8}$  second in conformity with earlier workers, and  $B$  is an empirical constant which allows for the fact that the probability of a change in the vibrational quantum number by  $\pm 1$  may not be exactly the same as that by  $\pm 2$ . Rössler found  $B$  to be  $\sim 0.85$ , only weakly dependent on the ratio of double to single jumps. We have adopted the same value.

The quenching constant  $\delta$  comes from the expression

$$[2] \quad Q = 1/(1 + \delta p \tau),$$

where  $Q$  is the over-all quenching, i.e. the total intensity of the fluorescence in the presence of  $p$  mm. of added gas divided by the intensity in the absence of added gas. We have taken  $Q$  from the quenching curve for hydrogen obtained by Wood (12).

$Q$  for deuterium is not known. However, we have provisionally calculated  $\epsilon$  for deuterium on the basis that  $Q$  is the same as for hydrogen. This amounts to the assumption that the factor governing the relative quenching efficiencies of hydrogen and deuterium will be the collision duration. If this is the case, then  $Q$  at any pressure  $p$  must be the same for the two gases since the increased collision duration for  $D_2$  will be exactly offset by the decreased number of collisions. Rössler found that the relative quenching efficiencies of the inert gas series could be accounted for in terms of three variables: collision duration, polarizability, and effective cross section. Polarizability will not vary between  $H_2$  and  $D_2$ . The effective cross section varies by only 10% from one member to the next of the inert gas series, making a negligible contribution to the variation in  $Q$ .

Table I lists the values used for the various quantities in equation [1] ( $I_0/I_p$  and  $I_p'/I_p$  are mean values) and the values obtained for the vibrational-transfer probability per

TABLE I  
For  $\tau = 1 \times 10^{-8}$  second

$p$ , mm.	$I_0/I_p$	$I_p'/I_p$	$Z_p \times 10^{-8}$	$\delta \times 10^{-8}$	$\delta p/Z_p$	$\epsilon \times 10^{-8}$	$\epsilon p/Z_p$
$H_2$	9.6	3.15	0.78	2.78	0.17	0.59	0.16
$D_2$	8.3	3.88	0.80	1.69	(0.17)	(0.83)	(0.55)

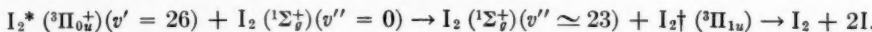
collision,  $\epsilon p/Z_p$ .  $Z_p$  is the number of collisions per second suffered by  $I_2^*$  at a pressure  $p$  of added gas, calculated using  $r_{I_2} = 2.7 \text{ \AA}$  and  $r_{H_2} = r_{D_2} = 1.1 \text{ \AA}$ .

### DISCUSSION

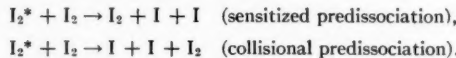
In the previous section it was observed that quenching collisions  $I_2^* + I_2$  take place to the exclusion of vibrational-transfer collisions even up to a pressure of 19.2 mm. of iodine. The question arises as to whether this is a specific effect due to the fact that the colliding partners are both iodine molecules.

It has been established (13) that the quenching of iodine resonance radiation excited by the mercury green line is due almost entirely to predissociation. According to the potential-energy diagram for iodine given by Mathieson and Rees (2) predissociation in normal quenching involves a transition from  ${}^3\Pi_0^+(v' > 24)$  to  ${}^3\Sigma_u^+(0_u^-) \rightarrow {}^2P_{3/2} + {}^2P_{1/2}$ , normal atoms. Mulliken (14) has suggested that the transition may also be to  ${}^1\Sigma_u^-(0_u^-)$ .

In the present case, which involves self-quenching of iodine vapor, it is possible that the process is one in which the  ${}^3\Pi_0^+$  excited iodine molecule transfers its electronic energy to the ground-state  $I_2$  collision partner, which is consequently excited to the lower repulsive state  ${}^3\Pi_{1u}$  and dissociates into normal atoms. This could be characterized as *sensitized predissociation* by analogy with sensitized fluorescence. The transition  ${}^3\Pi_{1u} \leftarrow {}^1\Sigma_g^+$  has actually been observed as a weak absorption in the red. The energy required is about 13 kcal./mole less than that liberated by the Hg-green-line fluorescence of  $I_2$  in falling to the zero vibrational level of the ground state. The 13 kcal. would most probably remain in the quenched iodine molecule as vibrational energy ( $v'' \approx 23$ ):



On the evidence at present available the self-quenching of iodine fluorescence could equally well be due to a collisional transfer of  $I_2^* ({}^3\Pi_0^+)$  into the  ${}^3\Sigma_u^+(0_u^-)$  repulsive state, in precisely the same way that the inert gases quench the fluorescence. However, in view of the high efficiency observed for self-quenching it is of interest to note that this quenching is unique in having two reaction paths open to it:



In view of uncertainty in the value of  $\delta$ , and probable error in obtaining  $I_0/I_p$  and  $I_p'/I_p$ , the value obtained for  $\epsilon p/Z_p$  for hydrogen (vibrational-transfer probability per collision) could be in error by a factor of  $\times 2$ . With these limits of error our conclusion, taking  $\tau = 1 \times 10^{-8}$  for  $I_2^*$ , is that on the average one to four collisions are needed between  $I_2^* (v' = 26)$  and hydrogen molecules to bring about a transfer of one or two quanta of vibrational energy into rotational or kinetic energy of  $H_2$ .

Eliaschevich (4) obtained a transfer efficiency  $25 \times$  our highest figure. Though significant differences in experimental technique exist between the two pieces of work they do not seem to account for the large discrepancy between our results and his. Eliaschevich appears to have used the peak height on an intensity vs.  $\lambda$  plot as a measure of band intensity, whereas we have used the integrated area under the band. Self-absorption would be somewhat greater in his experiments, though he used a lower pressure of  $I_2$  (0.17 mm. compared with 0.43 mm.), owing to a 15 cm. long emission path compared with 1–1.5 cm. in our experiments. Our vibrational-transfer probabilities were measured at almost  $10 \times$  the pressure of  $H_2$  that he used (1.1 mm. compared with 9.6 mm.). It is not expected that

appreciable Lorentz pressure-broadening would occur even at the higher pressure of hydrogen.

As regards the correct lifetime ( $\tau$ ) to be used for  $I_2^* \ ^3\Pi$ , Rabinowitch and Wood (13) point out that there is an analogy between  $^3\Pi \rightarrow ^1\Sigma$  for  $I_2^*$  emission, and  $^3P \rightarrow ^1S$  for  $Hg^*$  emission. The  $Hg^* \ ^3P_1$  lifetime is known to be  $\sim 1 \times 10^{-7}$  second ( $Cd^* \ ^3P_1$  and  $Zn^* \ ^3P_1$  are respectively  $\sim 2 \times 10^{-6}$  and  $1 \times 10^{-5}$  second). The assumption of  $10^{-8}$  for the lifetime of  $I_2^*$  seems therefore to be a poor one. If a value of  $3 \times 10^{-7}$  were taken for the lifetime of  $I_2^*$ , then even for the case of Xe, for which Rössler obtained the highly improbable effective-collision-radius  $r_{I_2} = 20 \text{ \AA}$ , vibrational transfer would not occur at more than every gas kinetic collision. According to our results and using  $\tau = 3 \times 10^{-7}$  seconds  $H_2$  would have a collision efficiency for vibrational transfer of 1 collision in 55, and  $D_2$  of 1 collision in 11. This seems more plausible than Eliashevich and Rössler's collision efficiencies, which are  $\gg 1$ . As is well known, sound-dispersion data, which relate to changes in vibrational quantum number in the region  $v \approx 0$ , give collision efficiencies  $\ll 1$ . "Third-body" data (see for example I + I + argon (15)), which refer to the removal of vibrational quanta in the region  $v \sim \infty$ , i.e. at the point of dissociation, can best be interpreted on the basis that the collision efficiency is 1. It would be remarkable if the intermediate case for which  $v \approx 26$  (approximately halfway to dissociation) were to have a collision efficiency  $\gg 1$ .

The value of  $\epsilon p/Z_p$  for deuterium has been included in order to show that if, as seems likely, the ratio of quenching probabilities per collision for  $D_2$  and  $H_2$  is the same as the ratio of the collision durations,  $\sqrt{(m_{D_2}/m_{H_2})} = 1.4$ , then the ratio of the vibrational-transfer probabilities per collision will be approximately 5:1 (deuterium : hydrogen). Increasing vibrational-transfer efficiency with increasing mass of the colliding partner is in agreement with Rössler's work on  $I_2^* +$  inert gases. However, in the present case the difference is unambiguously associated with a change in mass.

The accuracy of these results could be greatly improved if heterochromatic microdensitometry were replaced by direct photometry. An attempt by the author to do this failed as a result of inadequate technique: the individual lines could be detected using a 10-stage photomultiplier tube, but the signal to noise ratio was too poor for accurate measurement. With a chopped light-beam and 14-stage photomultiplier these difficulties could probably be overcome.

#### ACKNOWLEDGMENTS

The author wishes to thank Dr. G. Herzberg of the Division of Pure Physics, National Research Council, Ottawa, and Prof. A. G. Shenstone of the Department of Physics, Princeton University, for their kindness in providing him with spectrographs and with all possible assistance. He is indebted to the David Sarnoff Research Laboratories, Radio Corporation of America, for the use of their recording microdensitometer.

#### REFERENCES

- FRANCK, J. and WOOD, R. W. Verhandl. deut. physik. Ges. **13**, 78 (1911); Phil. Mag. **21**, 314 (1911).
- MATHIESON, L. and REES, A. L. G. J. Chem. Phys. **25**, 753 (1956).
- RANK, D. H. J. Opt. Soc. Am. **36**, 239 (1946).
- ELIASCHEVICH, M. Phys. Rev. **39**, 532 (1932); Physik. Z. Sowjetunion, **1**, 510 (1932).
- RÖSSLER, F. Z. Physik, **96**, 251 (1935).
- PRINGSHEIM, P. Fluorescence and phosphorescence. Interscience Publishers, Inc., New York. 1949. p. 193.
- WOOD, R. W. and SPEAS, P. A. Phil. Mag. **27**, 531 (1914); Physik. Z. **15**, 317 (1925).
- PRINGSHEIM, P. Z. Physik, **4**, 52 (1921).

9. STOICHEFF, B. P. Can. J. Phys. **32**, 330 (1954).
10. LOOMIS, F. W. Phys. Rev. **27**, 802 (1926); **29**, 112 (1927).
11. STERN, O. and VOLMER, M. Physik. Z. **20**, 184 (1919).
12. WOOD, R. W. Verhandl. deut. physik. Ges. **13**, 72 (1911).
13. RABINOWITCH, E. and WOOD, W. C. J. Chem. Phys. **4**, 358 (1936).
14. MULLIKEN, R. S. Phys. Rev. **46**, 549 (1934); **57**, 500 (1940).
15. (a) DAVIDSON, N., MARSHALL, R., LARSH, A. E., and CARRINGTON, T. J. Chem. Phys. **19**, 1311 (1951);  
**21**, 659 (1953).  
(b) CHRISTIE, M. I., NORRISH, R. G. W., and PORTER, G. Proc. Roy. Soc. A, **216**, 152 (1953).  
(c) RUSSELL, K. E. and SIMONS, J. Proc. Roy. Soc. A, **217**, 271 (1953).

# EXCITED STATES OF ACETYLENE AND THEIR ROLE IN PYROLYSIS<sup>1</sup>

G. J. MINKOFF

## ABSTRACT

Previous theories of acetylene pyrolysis are reviewed in the light of recent work by Minkoff, Newitt, and Rutledge. It is shown that the relatively large rates observed at the beginning of the induction period do not agree with mechanisms involving the intervention of comparatively stable dimers. The required kinetic form is obtained, however, if a triplet diradical is produced on the surface in a bimolecular process, followed by gas phase polymerization, with some chain ending on the surface. The detailed mechanism closely resembles Flory's scheme for liquid phase vinyl polymerization. The shape of the radical is discussed, and it is suggested that the *trans*-configuration leads to polymerization, while the *cis* facilitates dehydrogenation.

There has recently been some interest in the reactions of atoms or molecules in excited states (12, 14), and particularly of unsaturated molecules in triplet states. The purpose of this communication is to examine the role played by acetylene, and its polymers, in triplet states, during the pyrolysis of acetylene at temperatures below 500° C., particularly in view of the failure of mechanisms based on ground state molecules and radicals (21). In fact, there has been considerable controversy not only over the proposed mechanisms, but also over the experimental results. As a consequence of some recent work at temperatures below 525° C. (15), it has been possible to select those results which are most likely to be free of unexpected complications, and to propose a simple mechanism to account for most of the observations.

## 1. REVIEW OF PREVIOUS WORK

The main difficulties indicated in the literature are threefold; the first are concerned with the nature of the products, the second with the effect of surfaces, and the third is related to the effect of nitric oxide and the role of radicals. These will be considered in turn.

Confusion has often arisen regarding the products, since it is frequently stated, for example, that benzene is the main product of pyrolyzing acetylene. The latter result is only obtained under special conditions; the main reaction at low temperatures (i.e. below 500° C.) is polymerization to polycyclic and substituted aromatic compounds (see Ref. 15 for detailed references). Above 7–800° C., this is almost entirely superseded by decomposition to carbon and hydrogen (2). Products in the intervening region vary continuously from hydrogen and methane down to lower aromatics, including benzene, depending mainly on the temperature, but also on other factors. In particular Minkoff, Newitt, and Rutledge have shown that even at low temperatures, polymerization can be replaced by decomposition to carbon and hydrogen when halogen compounds or some metals are added to acetylene.

The elucidation of the mechanism has also been hindered by the differing reports of the effect of packing the reaction vessel with glass or other supposedly inert materials. Schlapfer and Brunner (19), and Frank-Kamenetsky (7), found the rate to be unaffected by increasing the surface-to-volume ratio. Pease (17), however, found the rate to be reduced by *ca.* 30%; Minkoff, Newitt, and Rutledge reported a weaker, but still inhibitory, influence of surface, while Silcocks (20) (who observed reaction to occur at unusually

<sup>1</sup>Manuscript received August 16, 1957.

Contribution from the Chemical Engineering Department, Imperial College, University of London, London, England. This paper was presented at the Symposium on the Structure and Reactivity of Electronically-Excited Species held at the University of Ottawa, Ottawa, Canada, September 5 and 6, 1957.

low temperatures) stated that the rate of reaction was considerably increased by packing the vessel. The treatment of the surface can also influence the rate in some circumstances (15, 24) but not in others (7). The different influences could be explained to some extent if both the chain initiation and chain termination were surface dependent, though to different extents. Any modifications of the surface would then have an over-all effect on the rate, which would depend on the relative activity of the surface to each of the two steps.

Random effects cannot be excluded, but the reported surface effects show some correlation with the amount of permanent gases (mostly hydrogen) detected, this being a possible measure of the decomposition reaction. Thus, in the absence of hydrogen, Pease found packing to inhibit the rate; Minkoff, Newitt, and Rutledge, who found only small inhibition, detected approximately 2–3% hydrogen, while the acceleration observed by Silcocks was associated with the isolation of considerable amounts of hydrogen.

Contradictions also exist regarding the presence of radicals. For example, Paneth and Hofeditz (16) found no positive evidence, so that if any radicals participate in the reaction, they may have unusual properties. On the other hand, Minkoff, Newitt, and Rutledge have confirmed the findings of Burnham and Pease (4) and of Frank-Kamenetzky (7), who observed that nitric oxide can almost completely inhibit the polymerization, and that after the nitric oxide has been used up, the reaction proceeds at the normal rate. While this indicates the presence of radicals, there is a sharp contrast with the normal effect of nitric oxide on hydrocarbon pyrolysis (see Ref. 21), since in the latter case, the rate gradually diminishes as more nitric oxide is added; however, some residual reaction is always observed, which the nitric oxide does not inhibit. A further complication is that exactly this behavior was reported for acetylene pyrolysis by Robertson, Magee, Fain, and Matsen (18); however, their measure of the rate was based on the instantaneous concentration of benzene, which occurred as an intermediate. This clearly was not indicative of the required rate, since the results obtained by this method are the only ones which do not give linear plots of log rate against  $1/T$  (15). In view of the recent work of Jach and Hinshelwood (11), it is not impossible that the uninhibited reaction was induced by the Freon which was present in the system as an internal standard for the infrared absorption. Presumably, these observations will be of value when a deeper understanding of the reaction has been obtained.

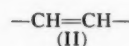
## 2. KINETIC FEATURES

Most workers agree that the polymerization is, essentially, kinetically of the second order, although an induction period is usually observed (7, 15, 20). It has usually been assumed that the induction period represents the formation of a comparatively stable dimeric intermediate, and its accumulation to a steady state concentration when the rate of formation equals the rate of decomposition. The radicals formed by the decomposition are then supposed to catalyze the polymerization. Various suggestions have been made regarding the nature of the dimer, which has been said to be vinyl acetylene, cyclobutadiene, etc. Clearly, this scheme is formally of the Semenoff degenerate branching chain type, and the rate should therefore increase considerably from an initially very small value. This does not agree with the recent observation (15) that the initial rate, instead of being extremely low relative to the maximum value, is usually 30–50% of the latter. Another difficulty is that, while the initial rate and the maximum rate are both proportional to the square of the initial pressure (15), the length of the induction period is independent of the initial pressure (7, 15) below 500° C.

A more satisfactory explanation is provided by a slow, bimolecular initiation, followed by a series of comparatively rapid bimolecular addition steps. The molecularity of the initiation step is indicated not only by the dependence of the initial rate on the square of the initial pressure, but also by the similarity of the initial and maximum rates. The relatively small difference between the latter implies that both sets of reactions contribute to the total rate of disappearance of acetylene, throughout the time during which second order kinetics are observed, and both must therefore be second order reactions. It is in fact shown later that the observed kinetic form closely resembles that of liquid phase polymerizations, which have similar mechanisms.

### 3. IDENTIFICATION OF CHAIN CARRIERS

Only two types of chain carriers can readily be formed from acetylene. One involves the fission of a C—H bond (I), while the other is formed by the "opening" of one of the triple bonds (II):



(No distinction is made at this stage between monomeric and polymeric radicals of each category.) Bimolecular collisions of two acetylene molecules seem at first sight to lead to  $-\text{CH}=\text{CH}-\text{CH}=\text{CH}-$  (II) rather than to  $\text{CH}\equiv\text{C}-\text{CH}=\text{CH}-$  (I), but, once formed, either radical would be able to propagate the polymerization chain. Considerations of the heats of formation (in the absence of activation energies) favor the formation of radical II. Thus, for radical I, the bond energy of the acetylenic C—H has been estimated as being 121 kcal. (25). With regard to II, the energy required to 'open one of the triple bonds' has been variously estimated as being in the region of 30 to 60 kcal. (cf. (5, 26)). A value of 50 kcal. will thus be assumed as being reasonably high. The conversion of the triple C—C bond into a double C—C bond probably implies (see below) a change of bonding orbitals in the C—H bonds from  $sp$  to  $sp^2$ . According to Walsh, the consequent total weakening requires 20–30 kcal. If this value is added to the 50 kcal. deduced previously, the heat of formation of II from acetylene has an upper limit of *ca.* 80 kcal. and a lower limit of 50 kcal. This is at least 40 kcal. less than is required to form I. The conclusion that  $\text{C}_2\text{H}-$  is more difficult to form than  $-\text{C}_2\text{H}_2-$ , in the absence of an excess of energy, is supported by a number of observations. The lack of effect of ethyl radicals when lead tetraethyl is added suggests that the energy of hydrogen abstraction is high, and this agrees with the lack of effect of oxygen, and with the shortness of extra chains produced by acetyl (or methyl) radicals from the pyrolysis of diacetyl, and of methyl radicals from the photolysis of acetone (23). Furthermore, the negative results of Paneth and Hofeditz suggest II rather than I. The results of photochemical experiments are not directly applicable. Nevertheless, it is clear that when sufficient energy is available to form  $\text{C}_2\text{H}-$ , polymerization proceeds readily; this can occur, for example, in the presence of  $\text{Cd}(^1P_1)$  (2288 Å, 124 kcal.) or of  $\text{Hg}(^3P_1)$  (2537 Å, 112 kcal.) (22). However, polymerization is also observed when triplet cadmium atoms (3261 Å, 87 kcal.) are used; Steacie and Le Roy attempted to overcome the difficulty by suggesting that since the heat of formation of cadmium hydride is 15.5 kcal., the reaction

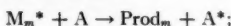


can proceed if  $D_{\text{C}-\text{H}(\text{C}_2\text{H}_2)}$  is not greater than 103 kcal. Since this estimate is much lower than that of other workers, a preferable explanation is that a triplet acetylene diradical is formed, which is responsible for the polymerization.

#### 4. THE MULTIPLICITY AND NATURE OF THE RADICAL

The end of the previous paragraph introduced the possibility that the diradical is in the triplet state; this was necessary in the photochemical system because the multiplicity of the triplet cadmium atoms cannot be lost, but must be passed to another atom or molecule (cf. 14).

Since the triplet state, for any configuration, lies energetically lower than the corresponding singlet, the former would be more readily formed at a given temperature, were it not for the Wigner-Witmer spin conservation rules. These prohibit, in simple systems at least, the direct conversion of a singlet into a triplet. However, this restriction can be overcome by perturbing the fields of the system undergoing transition; this could be effected particularly well by a surface. If the suggestion is correct, then the bimolecular initiation reaction will become a surface process. If the polymerization is now visualized as a successive lengthening of the carbon skeleton of the diradical (II), by incorporation of acetylene molecules, then the formation of stable compounds can occur in two ways (other than by mutual destruction of carriers). One of these consists of passing the triplet multiplicity to an acetylene molecule

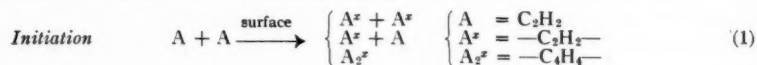


this is exactly parallel to the concept of chain transfer in liquid phase polymerization (3, 6); the regeneration of the chain carriers is thus ensured. The other process represents the spontaneous, unimolecular, conversion of a triplet chain carrier into a stable molecule. Again, this would be very slow in the gas phase, because of spin conservation restrictions, but it will readily occur on the surface.

The mechanism thus introduces a partial dependence on the surface of both chain initiation and termination, as was required by the consideration of the effect of surfaces. The apparent irregularities in the latter may further be explained by the difference in kinetic order of the two processes, in view of the fact that the comparisons are usually carried out under only one set of conditions by each worker.

#### 5. MECHANISM

Formally, the mechanism can be represented as follows:

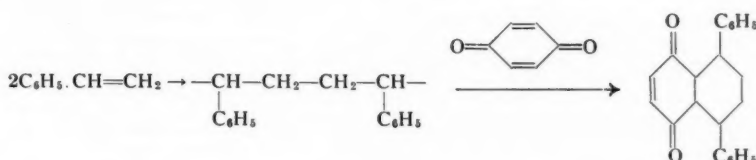


Regarding the initiation reaction, it is not at present possible to decide whether this results in one or more entities, but this does not affect the remainder of the discussion.

Apart from the inherent simplicity, the mechanism is supported by a number of considerations. Thus, it is very similar to the simplified scheme which Flory (6) proposed in 1937 to account for "vinyl" type polymerization in the liquid phase (see Ref. 1, 3 for later refinements). The main steps were: (a) formation of a dimeric divalent radical, (b) comparatively long polymerization chains, (c) chain transfer, similar to reaction (3), and (d) chain termination, involving interaction of two chain carriers. (The order of the

last reaction had little effect on the kinetic form deduced.) With some simplifications, graphs of concentration ( $C$ ) against time have been deduced by the author for various possible ratios of chain termination to chain propagation. In every case, the initial rate is of the same order of magnitude as the maximum rate. From the diagram in Flory's paper, values of  $1/C$  have been deduced, and plotted against time; the resulting graphs are identical in form with those reported for acetylene polymerization by Minkoff, Newitt, and Rutledge.

In the liquid phase system, direct evidence has been obtained of the formation of the dimeric radical, by the isolation of an addition compound with a molecule of benzoquinone inhibitor (13):



Under these conditions, Bamford and Dewar suggested that there was no need to invoke a triplet state. However, this point of view does not necessarily apply to the gas phase, particularly in view of the need for making the reaction mechanism sensitive to surface.

#### 6. THE SHAPE OF THE TRIPLET STATE

The use of  $-\text{CH}=\text{CH}-\text{CH}=\text{CH}-$  as a chain carrier is not new (20), but it is only when this radical is considered as a triplet that the effect of surfaces, and of tests for radicals, can be reasonably explained. A further refinement is to predict the conditions leading to polymerization, and to decomposition. This is made possible by Ingold and King's analysis of the U.V. absorption spectrum of acetylene (10), which indicates that the triplet diradical is likely to have the *trans* configuration in the lower state, and the *cis* in a higher one:



It seems probable that during polymerization the carbon skeleton retains the *trans* shape. To some extent, this is supported by the "staggered" configuration of diacetylene in its upper, singlet, state (Dr. Callomon, private communication). Comparatively long carbon skeletons would then be formed in preference to small cyclic ones. At higher temperatures, however, sufficient energy becomes available for the *cis* configuration to be of importance, thus facilitating both the elimination of molecular hydrogen, and the formation of benzene in considerable amounts (cf. the textbook methods of making benzene by passing acetylene through a red-hot tube).

It is also possible that the effect of halogenated compounds and of metals can be explained in a similar way, by postulating that the change from *trans* to *cis* is facilitated by the free electrons in the metal surfaces, or by the strong electronegativity of the

halogen atoms. Once the C<sub>2</sub> molecules (or radicals) have been formed in the gas phase, they readily react with acetylene and form carbonaceous deposits (9).

This explanation of the role of halogens seems to be at least as probable as mechanisms based on the so-called affinity of halogen atoms for hydrogen. The latter are difficult to reconcile with the relative bond dissociation energies of 121 kcal. for C—H in acetylene and of 102 kcal. for HCl and even lower for HBr (8).

#### CONCLUSION

The mechanism presented in this communication explains the greater part of the effects reported below 500° C., and particularly that of surfaces. It has the advantage of treating the polymerization of acetylene in a manner analogous to that generally accepted for vinyl polymerization reactions, and it provides a simple explanation of the change from polymerization to decomposition at low temperatures. More experimental work on the latter aspect would be desirable.

The author acknowledges valuable discussions with Dr. V. Griffing, Dr. G. W. King, Prof. D. M. Newitt, and Dr. P. V. Rutledge.

#### REFERENCES

1. BAMFORD, C. H. and DEWAR, M. J. S. Proc. Roy. Soc. A, **192**, 309 (1948).
2. BONE, W. A. and COWARD, H. F. J. Chem. Soc. **93**, 1197 (1908).
3. BURNETT, G. M. Quart. Revs. (London), **4**, 292 (1950).
4. BURNHAM, H. D. and PEASE, R. N. J. Am. Chem. Soc. **64**, 1404 (1942).
5. COTTRELL, T. L. The strengths of chemical bonds. Butterworth Scientific Publications, London. 1954.
6. FLORY, P. J. J. Am. Chem. Soc. **59**, 241 (1937).
7. FRANK-KAMENETZKY, D. A. Acta Physicochim. U.R.S.S. **18**, 148 (1943).
8. GAYDON, A. G. Dissociation energies. 2nd. ed. Chapman & Hall, Ltd., London. 1953.
9. GAYDON, A. G. and FAIRBAIRN, A. R. 5th Symposium on Combustion. Reinhold Publishing Corporation, New York. 1955. p. 324.
10. INGOLD, C. K. and KING, G. W. J. Chem. Soc. 2713 (1953).
11. JACH, J. and HINSHELWOOD, C. Proc. Roy. Soc. A, **229**, 143 (1955).
12. KASHA, M. and McGLYNN, S. P. Ann. Rev. Phys. Chem. **7**, 403 (1956).
13. KERN, W. and FEUERSTEIN, K. J. prakt. Chem. **158**, 186 (1941).
14. LAIDLOR, K. J. Chemical kinetics of excited states. Oxford University Press, Oxford. 1955. p. 93.
15. MINKOFF, G. J., NEWITT, D. M., and RUTLEDGE, P. V. J. Appl. Chem. (London), **7**, 412 (1957).
16. PANETH, F. and HOFEDITZ, W. Ber. B, **62**, 1335 (1929).
17. PEASE, R. N. J. Am. Chem. Soc. **51**, 3470 (1929).
18. ROBERTSON, W. W., MAGEE, E. M., FAIN, J., and MATSEN, F. A. 5th Symposium on Flame and Combustion. Reinhold Publishing Corporation, New York. 1955. p. 628.
19. SCHLÄFFER, P. and BRUNNER, M. Helv. Chim. Acta, **13**, 1125 (1930).
20. SILCOCKS, C. G. Ministry of Supply Report 39/R/49 (open).
21. STEACIE, E. W. R. Atomic and free radical reactions. Vol. I. 2nd ed. Reinhold Publishing Corporation, New York. 1954. p. 172.
22. STEACIE, E. W. R. Ref. 21, p. 423.
23. TAYLOR, H. S. and JUNGERS, J. C. Trans. Faraday Soc. **33**, 1353 (1937).
24. TAYLOR, H. A. and VAN HOOK, A. J. Phys. Chem. **39**, 811 (1935).
25. WALSH, A. D. Discussions Faraday Soc. No. **2**, 18 (1947).
26. WESTBROOK, E. A., HELLWIG, K., and ANDERSON, R. C. 5th Symposium on Combustion. Reinhold Publishing Corporation, New York. 1955. p. 631.

# THE FLUORESCENCE AND ITS RELATIONSHIP TO PHOTOLYSIS IN HEXAFLUOROACETONE VAPOR<sup>1</sup>

HIDEO OKABE<sup>2</sup> AND E. W. R. STEACIE

## ABSTRACT

Hexafluoroacetone vapor, when excited at 25° C. by light of wavelength 3130 Å, gives rise to fluorescence. The fluorescence spectrum starts at about 3470 Å and extends to almost 6000 Å with a maximum at about 4200 Å, independent of pressure over the range 3 mm. to 170 mm. No fine structure is observed. Oxygen has almost no effect on the spectrum, contrary to the cases of acetone and biacetyl vapor, where oxygen causes a marked change. The absorption follows Beer's law between 5 mm. and 50 mm. of hexafluoroacetone pressure and the absorption coefficient has been measured.

The fluorescence efficiency decreases slightly with the addition of less than 1 mm. of oxygen and there stays constant up to an oxygen pressure of 30 mm., indicating that the fluorescence may be principally from the short-lived singlet excited state. The fluorescence efficiency increases with pressure of hexafluoroacetone or with the addition of inert gases such as perfluorobutane, perfluoropropene, hexafluoroethane, or carbon dioxide. The present results may be compared with those of the photolysis, where it was found that the quantum yield of the decomposition decreases with increasing pressure and with added inert gases. A close relationship between the fluorescence and the photolysis suggests itself. A mechanism is proposed to explain the results, which assumes that the molecule is raised to the upper vibrational levels of a singlet excited state, and subsequently deactivated to the lowest vibrational levels of the same state, from which it fluoresces. On the basis of this mechanism it seems possible to correlate the photolysis with the fluorescence.

## INTRODUCTION

The photolysis and fluorescence of ketones have been studied extensively for many years (1).

While most photochemical reactions seem to involve principally the dissociation of molecules, in some cases both the dissociation and the fluorescence take place concurrently, when excited species are formed by the absorption of the radiation. In a few cases it seems possible to explain the results in terms of a mechanism which correlates both phenomena (2, 3).

The photolysis of hexafluoroacetone has been studied mainly by Ayscough and Steacie (4). They found that the mechanism of the photolysis by light of wavelength 3130 Å seems to be unusually simple over a wide range of temperatures. By investigating the effect of pressure and of various inert gases on the primary photochemical yields they concluded that the photolysis proceeds by way of an electronically excited species with a considerable lifetime. They found that the photochemical yields decreased with increase of pressure and with the addition of inert gases, which indicates that the excited molecules are deactivated effectively by collision. Since the photochemical yields were always considerably less than unity over the range of pressures studied, the possibility of fluorescence may be suggested as another way of energy dissipation. The study of fluorescence, if it is found, is of interest in order to arrive at a further understanding of the primary process. The present work was undertaken to investigate the hitherto unknown fluorescence of hexafluoroacetone and to correlate it with the photolysis data.

<sup>1</sup>Manuscript received October 7, 1957.

Contribution from the Division of Pure Chemistry, National Research Laboratories, Ottawa, Canada. This paper was presented at the Symposium on the Structure and Reactivity of Electronically-Excited Species held at the University of Ottawa, Ottawa, Canada, September 5 and 6, 1957.

Issued as N.R.C. No. 4648.

<sup>2</sup>National Research Council of Canada Postdoctorate Fellow 1956-58.

## EXPERIMENTAL

Hexafluoroacetone hydrate was supplied by Dr. Leitch of this laboratory, to whom we are greatly indebted. It was dehydrated by phosphorus pentoxide, degassed and stored in a blackened bulb behind a mercury cutoff. The fluorocarbons were supplied by E. I. duPont de Nemours and Company. They were purified by trap to trap distillation in the vacuum line, a middle portion being retained, dried by phosphorus pentoxide, and stored behind a mercury cutoff. Oxygen was prepared by heating potassium permanganate and by passing it through liquid nitrogen traps.

The light source was a Hanovia S-500 lamp operated with a Sorensen regulator. The radiation passing through a 10 mm. hole was collimated by a quartz lens of 100 mm. focal length, and passed through the color filter combination of 3 mm. Corning No. 9863, 50 mm. path length of 0.178 M nickel chloride solution, and 30 mm. path length of 0.0025 M potassium chromate solution. The wavelength of the radiation was mainly 3130 Å. That light transmitted by the cell was focused by another quartz lens of 150 mm. focal length on a G.E. 935 photocell and the light intensity measured by galvanometer deflection. The fluorescent radiation was measured at right angles to the incident radiation. After removal of scattered ultraviolet radiation by a Corning No. 738 filter, the fluorescent radiation was focused by a quartz lens on the 1P21 photomultiplier tube of a Farrand photometer. The photocurrent was measured on a galvanometer. A correction for the background radiation, amounting to less than 3%, was applied. It was found that both the fluorescence and the transmission amplifier circuits were stable and reproducible during the run. The intensity of the light source sometimes fluctuated over a long period of time and it was necessary to correct this occasionally during a run by changing the secondary voltage.

The cell employed was similar to that of Hunt and Noyes (5) except that it was made of Pyrex with quartz windows in order to facilitate the replacement of the windows, which were attached to the cell by Apiezon W cement. The cell was T shaped with an internal diameter of 40 mm. and length of 150 mm. The stem of the T was 40 mm. in diameter and tapered down to 10 mm.

A Toepler-type expansion bulb was used for mixing the reactants. Oxygen was stored in a 5 liter bulb and was dosed into the cell by means of a 20 cc. mercury Toepler pump.

Most spectrograms were taken with a Hilger f/4 quartz spectrograph. Eastman Kodak 103a-B plates were employed with Kodak D-19 developer. The vacuum line, free of stopcocks, followed the customary design used in this laboratory.

The following measurements were carried out for hexafluoroacetone: (1)  $I_t^0$ , the light transmitted by the empty cell; (2)  $I_t$ , the transmitted light with the gas in the cell; (3)  $I_f$ , the intensity of the fluorescence emerging from the center of the cell; and (4)  $I_f^0$ , the intensity of scattered radiation, which was very small and virtually constant so that it was not measured each time.

The fluorescence efficiency,  $Q$ , proportional to the absolute quantum yield of fluorescence, was calculated from the following equation:

$$Q = (I_f - I_f^0) / (I_t^0 - I_t).$$

## RESULTS

It was found that hexafluoroacetone gives strong fluorescence when excited by light of wavelength 3130 Å. The spectrum starts at about 3470 Å and extends to 6000 Å with a maximum at about 4200 Å (Fig. 1). The main features follow:

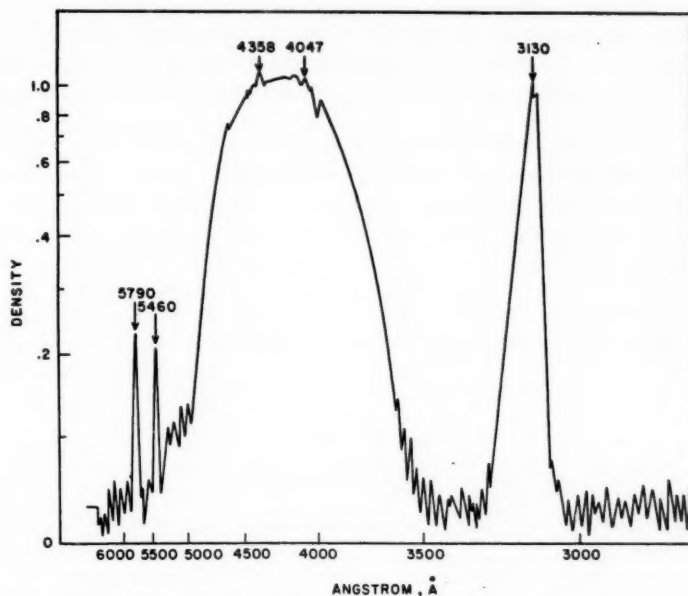


FIG. 1. Microdensitometer tracing of the fluorescence spectrum of hexafluoroacetone vapor excited by light of 3130 Å, using a Kodak 103a-B plate.

- (1) The spectrum was independent of pressure of hexafluoroacetone from 3 mm. to 170 mm. at room temperature.
- (2) No fine structure was observed with a Hilger high aperture glass spectrograph with a reciprocal linear dispersion of 80 Å/mm.
- (3) The same spectrum was also obtained by exciting with light of wavelength 2800 Å or shorter.
- (4) Oxygen had almost no effect on the spectrum.

The absorption followed Beer's law well between 5 mm. and 50 mm. and the calculated absorption coefficient  $k$  from the equation  $I_t = I_t^0 10^{-kd}$ , where  $I_t^0$  is the incident intensity,  $I_t$  the radiation transmitted,  $c$  the concentration in moles per liter, and  $d$  the distance in centimeters, was 6.80. The absorption coefficient is about 2.4 times greater than that of acetone at 3130 Å (6). The fluorescence efficiency  $Q$  was measured at 25° C. with various pressures of hexafluoroacetone and is given in Table I. It may be seen from

TABLE I  
THE VARIATION OF THE FLUORESCENCE  
EFFICIENCY WITH HEXAFLUOROACETONE  
PRESSURE AT 3130 Å

$P$ (mm.)	$Q$	$P$ (mm.)	$Q$
1.75	6.9	17.0	7.81
4.7	7.7	21.5	8.19
7.3	6.51	25.5	8.31
11.9	7.21	30.5	8.91
15.4	7.40	37.5	8.36

the table that  $Q$  increases with pressure and reaches almost a maximum at about 20 mm. of pressure. This is quite contrary to the case of acetone, where  $Q$  decreases with pressure (6, 7), but is similar to biacetyl phosphorescence excited by light of wavelength 3650 Å (8). Fig. 2 shows the effect of oxygen pressure on the fluorescence efficiency  $Q$  of

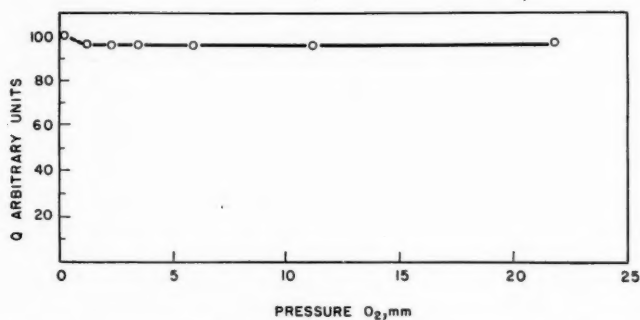


FIG. 2. Variation of fluorescence efficiency of 20 mm. hexafluoroacetone with oxygen pressure at 3130 Å.

20 mm. hexafluoroacetone at 25° C. As is seen from the curve,  $Q$  decreases slightly but definitely somewhere in the region below 1 mm. of oxygen pressure and there stays almost constant with further addition of oxygen. This is in marked contrast to acetone (6, 7) or biacetyl (9, 10, 11), where the emission decreased sharply to an almost negligible value with increasing oxygen pressure. The absorption of hexafluoroacetone was also measured and no change was observed with added oxygen.

In order to correlate the photolysis results with the fluorescence, the same inert gases used in the photolysis experiments were added to hexafluoroacetone and the fluorescence efficiency measured. Fig. 3 illustrates the effects of perfluorobutane, perfluoropropane, hexafluoroethane, and carbon dioxide on the fluorescence efficiency  $Q$  with 10 mm. of

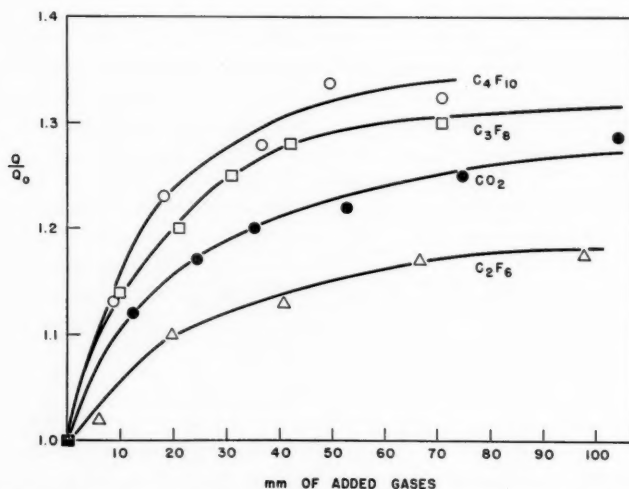


FIG. 3. Variation of fluorescence efficiency of 10 mm. hexafluoroacetone with pressure of added inert gases at 3130 Å.

hexafluoroacetone at 25° C. It can be seen from the curves that in every case there is an increase of  $Q$  with added gases. The order in which the gases increase  $Q$  is as follows: perfluorobutane > perfluoropropane > carbon dioxide > hexafluoroethane. Perfluorobutane increases the fluorescence efficiency by almost 30%, and hexafluoroethane by 17% over the range covered. If smaller pressures of hexafluoroacetone were used, a more pronounced effect of added gas would be expected. Apparently neither of the added gases is as effective as hexafluoroacetone itself in increasing the fluorescence efficiency. The intensity transmitted by the empty cell  $I_0$  was frequently checked by freezing down the mixtures with liquid nitrogen. No change of absorption occurred in the presence of the added gases. The photolysis data (4) show that the decomposition is reduced by the addition of inert gases and that the efficiency of reduction follows the same order as the efficiency of fluorescence increase, except that the order of carbon dioxide and hexafluoroethane is reversed. This suggests related mechanisms for the fluorescence and the photochemical decomposition.

#### DISCUSSION

The striking simplicity of the over-all photochemical process at 3130 Å in hexafluoroacetone was reported by Ayscough and Steacie (4). They found that hexafluoroethane and carbon monoxide are the only products and that the quantum yield of decomposition is always less than unity and strongly dependent on pressure and the addition of inert gases. These facts led them to postulate the formation of a long-lived electronically excited molecule as an intermediate, which decomposes by a first order process unless deactivated by collision. Since the quantum yield of dissociation is always less than unity, the energy must be dissipated by some process other than dissociation. These steps may be the internal conversion or the fluorescence or both. No details of this process are known.

The present work revealed the existence of strong fluorescence extending from 3470 Å to 6000 Å with a maximum at about 4200 Å, independent of pressure studied, with incident radiation of 3130 Å. The fluorescence does not seem to originate from perfluorobiacetyl as acetone fluorescence does from biacetyl, because (1) the CO to  $C_2F_6$  ratio is always unity indicating that no  $CF_3CO$  radical is formed, (2) no perfluorobiacetyl was found mass-spectrometrically after the sample was photolyzed, (3) the fluorescence spectrum starts almost from the end of the absorption band, and has no resemblance to that of biacetyl fluorescence, and (4) the fluorescence intensity does not change with time, whereas the acetone fluorescence does, owing to the accumulation of reaction product (biacetyl) (5).

The absorption band of the vapor lies between 2450 and 3550 Å (4). Since fluorescence and absorption overlap, the 0-0 band would lie in the region of overlap. This band may tentatively be assigned to 28570 cm.<sup>-1</sup> (3500 Å). This would be the 0-0 band for the transition in absorption and presumably for the transition in fluorescence from a singlet excited state. By excitation at 3130 Å the molecule will be raised to high vibrational levels,  $Y_n$ , of a singlet excited state (see Fig. 4). Since no resonance fluorescence was observed, the molecule must be deactivated rapidly to the lowest vibrational levels,  $Y_0$ , of the singlet excited state before it fluoresces. Oxygen has almost no effect on the fluorescence efficiency as well as on the spectrum. By analogy with the cases of acetone and biacetyl, in which the fluorescence from a singlet excited state is not quenched by added oxygen, whereas the phosphorescence from a triplet state is strongly quenched by oxygen (6, 7, 10, 11), it may be assumed that the fluorescence is mainly from the singlet excited state of hexafluoroacetone although no direct evidence has been found.

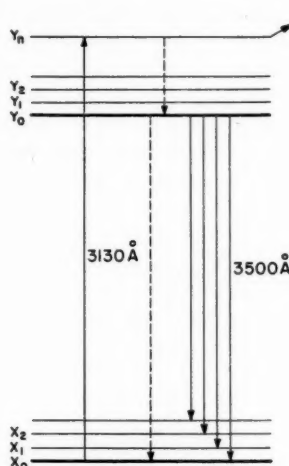


FIG. 4. Energy level diagram of hexafluoroacetone, where  $X_i$  is the  $i$ th vibrational level of the ground state,  $Y_i$  is the  $i$ th vibrational level of the singlet excited state, and  $D$  is the decomposition process. The full line represents the absorption or fluorescence process and the broken line represents the internal conversion or deactivation process.

The measurement of lifetime of hexafluoroacetone fluorescence is highly desirable in this respect.

It may be of interest to compare acetone and hexafluoroacetone with benzene and fluorobenzene. It was found that benzene shows both fluorescence and phosphorescence, whereas fluorobenzene shows only fluorescence at 77° K. (12). This was attributed to the more rapid transition from the singlet excited to the ground state compared to the radiationless transition to the triplet state in fluorobenzene, relative to that in benzene. This may be the case with acetone and hexafluoroacetone, although integrated extinction coefficients have not been compared in both cases.

From the foregoing discussion, the following process may be written:



where  $X$  designates the ground state and  $Y_0$  and  $Y_n$ , 0th and  $n$ th vibrational levels of the singlet excited state of hexafluoroacetone. Either or both steps [3] and [6] may be included. The following equation may be obtained from the above steps:

$$[7] \quad \frac{1}{\phi} = 1 + \frac{k_3}{k_2} + \frac{k_4}{k_2} (X),$$

where  $\phi$  is the quantum yield of decomposition and  $(X)$  is hexafluoroacetone concentration. The validity of equation [7] may be tested by plotting  $1/\phi$  against  $(X)$  from the

photolysis data (4). The plot corresponding to various temperatures gives a series of straight lines with an intercept of unity. This indicates that  $k_3 = 0$ , that is, there is no first order step other than the decomposition. Therefore the following equations will be obtained:

$$[8] \quad \frac{1}{\phi} = 1 + \frac{k_4}{k_2} (X)$$

and

$$[9] \quad \frac{1}{aQ} = \frac{k_5 + k_6}{k_5} + \frac{k_2(k_5 + k_6)}{k_4 k_5} \frac{1}{(X)},$$

where  $Q$  is the fluorescence efficiency and  $a$  is the ratio of quantum yield of fluorescence to the fluorescence efficiency. Since  $a$  is not known, each individual constant can not be obtained. The process may be compared to that for biacetyl when excited by 3650 Å radiation where step [3] should be included since the intercept is always greater than unity (2).

Fig. 5 illustrates the relation between  $1/Q$  and  $1/(X)$ . It may be seen that equation [9] is approximately obeyed. At pressures lower than 5 mm., the plot deviates considerably from linearity, indicating that some other process must be considered. However, the data are not extensive and accurate enough to warrant further discussion of this process.

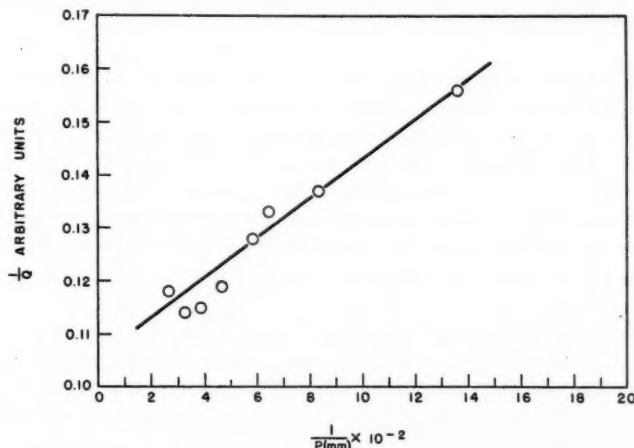


FIG. 5. The dependence of the reciprocal of the fluorescence efficiency on the reciprocal of the hexafluoroacetone pressure at 3130 Å.

The mechanism for hexafluoroacetone fluorescence seems to follow that for biacetyl green phosphorescence excited by light of 3650 Å, but not that for acetone fluorescence excited by light of 3130 Å. It indicates that the self-quenching process  $Y_0 + X = 2X$  is small and relatively unimportant compared to the deactivation process [4]. It also follows from the mechanism that

$$[10] \quad \frac{aQ}{\phi} = \frac{k_4 k_5}{k_2(k_5 + k_6)} (X).$$

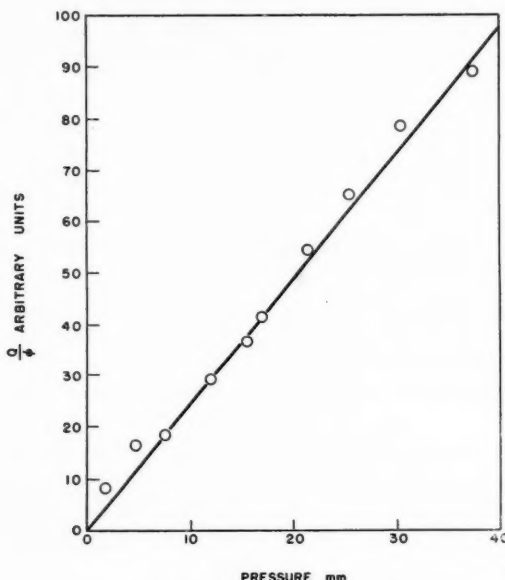


FIG. 6. The dependence of the ratio of the fluorescence efficiency,  $Q$ , and the photochemical yield,  $\phi$ , on the pressure of hexafluoroacetone at 3130 Å.

Fig 6 shows the relation between  $Q/\phi$  and ( $X$ ), the pressure of hexafluoroacetone. The values for photochemical decomposition are taken from Ayscough and Steacie's data (4). As can be seen, a plot of  $Q/\phi$  vs. pressure gives a straight line which passes through the origin. This indicates that the decomposition results almost exclusively from a first order step, and the fluorescence, from a second order step. The positive intercept on the  $Q/\phi$  axis observed with biacetyl (2), indicating that dissociation results from the collision of two excited molecules, does not appear with hexafluoroacetone.

The close relationship between the photolysis and the fluorescence may be seen further from the effect of inert gases.

The hexafluoroacetone has the great advantage that it is possible to compare the effect of inert gas on the photolysis and the fluorescence simultaneously; since firstly it is possible to measure the primary photochemical yields even in the presence of added gas, and secondly the fluorescence yields are large enough to measure, thus making it possible to compare both directly.

In the presence of inert gas, the following step must be added:



where  $M$  designates inert gases. The following equations may be derived:

$$[12] \quad \frac{1}{\phi} = 1 + \frac{k_4}{k_2} (X) + \frac{k_{11}}{k_2} (M),$$

$$[13] \quad \frac{\phi_0}{\phi} = 1 + \frac{k_{11}}{k_2 + k_4(X)} (M),$$

$$[14] \quad \frac{aQ}{\phi} = \frac{k_4 k_5}{k_2(k_5+k_6)} (X) + \frac{k_b k_{11}}{k_2(k_5+k_6)} (M),$$

and

$$[15] \quad \frac{Q}{Q_0} \frac{\phi_0}{\phi} = 1 + \frac{k_{11}}{k_4(X)} (M),$$

where (M) represents added inert gas concentration, and  $\phi_0$  and  $Q_0$ , the quantum yield of decomposition and the fluorescence efficiency, respectively, with 10 mm. hexafluoroacetone without added inert gas in the cell. It was shown (4) that  $\phi_0/\phi$  plotted against (M) gives a series of straight lines. Fig. 7 shows the relation between  $(Q/Q_0)(\phi_0/\phi)$  and

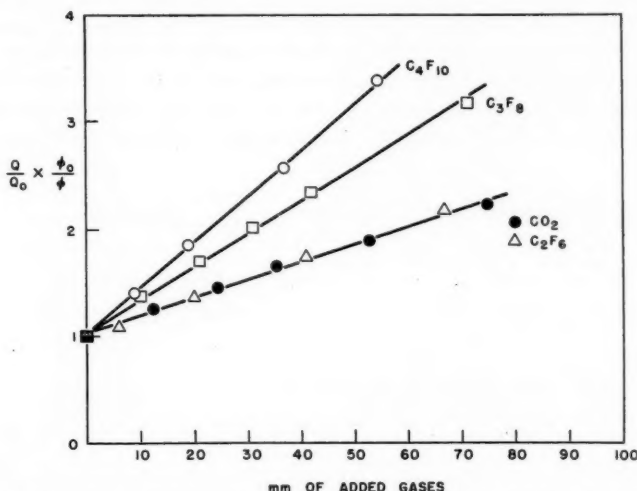


FIG. 7. The dependence of the ratio of the fluorescence efficiency and the primary photochemical yield on the pressure of added inert gases at 3130 Å.

(M). In this figure  $\phi_0/\phi$  values were taken from the points on the straight line corresponding to each pressure of added inert gas at 78° C., the only temperature for which data are available. It may be seen that a series of straight lines is obtained for each added gas. The slopes of the lines give the rates of deactivation by inert gases relative to that by hexafluoroacetone. The relative rates are 1, 0.42, 0.31, 0.17, and 0.17 for  $CF_3COCF_3$ ,  $C_4F_{10}$ ,  $C_3F_8$ ,  $C_2F_6$ , and  $CO_2$  respectively. These values are lower than those obtained from the photolysis data, although their relative orders are the same with the exception of that for  $CO_2$ . This is probably due to the fact that  $\phi_0/\phi$  values are obtained at 78° C. whereas  $Q/Q_0$  values are at 25° C.

The authors wish to thank Mr. G. Ensell for the construction of the cell.

#### REFERENCES

- NOYES, W. A., JR., PORTER, G. B., and JOLLEY, J. E. Chem. Revs. **56**, 49 (1956).
- SHEATS, G. F. and NOYES, W. A., JR. J. Am. Chem. Soc. **77**, 1421 (1955).
- OKABE, H. and NOYES, W. A., JR. J. Am. Chem. Soc. **79**, 801 (1957).
- AVSCOUGH, P. B. and STEACIE, E. W. R. Proc. Roy. Soc. A, **234**, 476 (1956).

5. HUNT, R. E. and NOYES, W. A., JR. *J. Am. Chem. Soc.* **70**, 467 (1948).
6. LUCKEY, G. W. and NOYES, W. A., JR. *J. Chem. Phys.* **19**, 227 (1951).
7. GROH, H. J., JR., LUCKEY, G. W., and NOYES, W. A., JR. *J. Chem. Phys.* **21**, 115 (1953).
8. ALMY, G. M. and GILLETTE, P. R. *J. Chem. Phys.* **11**, 188 (1943).
9. COWARD, N. A. and NOYES, W. A., JR. *J. Chem. Phys.* **22**, 1207 (1954).
10. ALMY, G. M., FULLER, H. Q., and KINZER, G. D. *J. Chem. Phys.* **8**, 37 (1940).
11. GROH, H. J., JR. *J. Chem. Phys.* **21**, 674 (1953).
12. GILMORE, E. H., GIBSON, G. E., and McCLURE, D. S. *J. Chem. Phys.* **20**, 829 (1952).

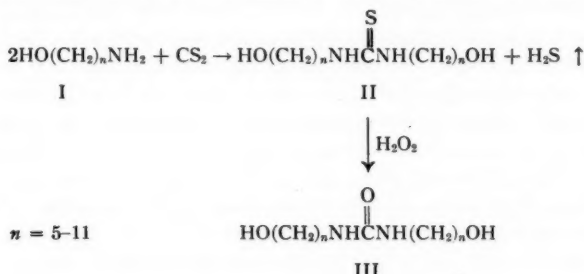
## REACTION OF AMINO ALCOHOLS WITH CARBON DISULPHIDE<sup>1</sup>

A. F. MCKAY, M. SKULSKI, AND D. L. GARMAISE

### ABSTRACT

$\omega$ -Amino alcohols possessing five or more methylene units between the amino and hydroxyl groups on condensation with carbon disulphide gave good yields of 1,3-di-( $\omega$ -hydroxyalkyl) thioureas. These symmetrically disubstituted thioureas on oxidation gave the corresponding 1,3-di-( $\omega$ -hydroxyalkyl) ureas.

The investigation of the reaction of carbon disulphide with amino alcohols (1) has been extended to the longer chain  $\omega$ -amino alcohols. The  $\omega$ -amino alcohols having five or more methylene units between the amino and hydroxy groups combine with carbon disulphide to give 1,3-di-( $\omega$ -hydroxyalkyl) thioureas (II). A series of these symmetrical thiourea derivatives II have been prepared and their properties are listed in Table I. 1,3-Di-(5-hydroxypentyl)-thiourea (II,  $n = 5$ ) was isolated as an oil and it was converted directly into the corresponding urea without further purification. The 1,3-di-(5-hydroxy-



pentyl)-, 1,3-di-(6-hydroxyhexyl)-, and 1,3-di-(7-hydroxyheptyl)-thioureas were oxidized in alkaline solution with hydrogen peroxide into the corresponding symmetrical urea derivatives III. 1,3-Di-(11-hydroxyundecyl)-thiourea was not oxidized under the same conditions but it was converted into 1,3-di-(11-hydroxyundecyl)-urea by refluxing with ethanolic silver nitrate solution (2).

TABLE I  
 $\text{X}$   
 $\text{HO(CH}_2)_n\text{NHCNH(CH}_2)_n\text{OH}$

X	$n$	Yield, %	M.p., °C.	Formula	C		H		N		S	
					Calc.	Found	Calc.	Found	Calc.	Found	Calc.	Found
O	5	73.2	106.5-108.5	C <sub>11</sub> H <sub>24</sub> N <sub>2</sub> O <sub>3</sub>	56.87	57.06	10.41	10.14	12.06	11.96		
S	6	81.5	79.5-80.5	C <sub>12</sub> H <sub>26</sub> N <sub>2</sub> O <sub>3</sub> S	56.48	56.49	10.21	10.23	10.14	10.21	11.60	11.42
O	6	68.9	117-118	C <sub>12</sub> H <sub>26</sub> N <sub>2</sub> O <sub>3</sub>	59.95	59.75	10.84	10.83	10.76	10.96		
S	7	69.0	82.5-83	C <sub>13</sub> H <sub>28</sub> N <sub>2</sub> O <sub>3</sub> S	59.18	59.55	10.59	10.35	9.20	8.96	10.53	9.98
O	7	60.9	122.5	C <sub>13</sub> H <sub>28</sub> N <sub>2</sub> O <sub>3</sub>	62.48	62.58	11.19	11.00	9.72	9.71		
S	11	69.3	97-98.5	C <sub>20</sub> H <sub>46</sub> N <sub>2</sub> O <sub>3</sub> S	66.28	66.45	11.61	11.81	6.72	6.74	7.69	7.81
O	11	88.3	134.5-136	C <sub>22</sub> H <sub>48</sub> N <sub>2</sub> O <sub>3</sub>	68.95	68.80	12.08	12.11	6.99	6.78		

<sup>1</sup>Manuscript received September 19, 1957.

Contribution from the L. G. Ryan Research Laboratories of Monsanto Canada Limited, Ville LaSalle, Quebec.

Other urea derivatives prepared for characterizing the amino alcohols were 1-( $\alpha$ -naphthyl)-3-(6-hydroxyhexyl)-urea, 1-phenyl-3-(7-hydroxyheptyl)-urea, and 1-( $\alpha$ -naphthyl)-3-(11-hydroxyundecyl)-urea.

## EXPERIMENTAL<sup>2</sup>

### 5-Aminopentanol-1

5-Aminopentanol-1 (b.p. 119–120° C. at 17 mm.; m.p. 26–28° C.;  $n_D^{16}$  1.4608) was prepared in 45.5% yield by the method of Putokhin (3). The previously reported (3) physical constants are m.p. 26° C.,  $d_4^{17}$  0.9488, and  $n_D^{17}$  1.4618.

### 6-Aminohexanol-1

6-Aminohexanol-1 was prepared by a modification of Wallach's method (4). Metallic sodium (150 g., 6.52 moles) was added to a refluxing solution of caprolactam (30 g., 0.26 mole) in freshly distilled absolute ethanol (1500 cc.) at a sufficient rate to maintain vigorous reflux. The reaction was complete in 1½ hours. The reaction mixture was steam distilled and the distillates were collected in 1 liter fractions. These fractions were acidified with hydrochloric acid and then evaporated to dryness. The first two fractions gave an impure hydrochloride melting at 215–235° C., yield 5.85 g. (16.25%). These crystals were considered to be impure hexamethylenimine hydrochloride, which Wallach reported (4) to melt at 236–237° C. The remaining distillate fractions gave a yellowish colored hydrochloride melting at 63–64° C., yield 28.91 g. (70.9%). This crude material (23.63 g., 0.15 mole) in absolute methanol (500 cc.) was passed through IRA-400 resin (1000 cc. of resin in the hydroxyl form previously washed with methanol) at a rate of 5 cc. per minute. The column of resin was washed with methanol (2500 cc.) and the eluate and washings were taken to dryness *in vacuo* under nitrogen. The product was distilled *in vacuo* under nitrogen. A crystalline product (b.p. 137–139° C. at 20 mm.) was obtained, yield 13.10 g. (42.1%). This crystalline product appeared to be dimorphous with one form melting at 57–58° C. and the other at 75–78° C. Wallach (4) reported a melting point of 55–56° C. Both forms gave one spot with a  $R_f$  value of 0.54 when chromatographed on Whatman No. 1 paper with butanol: acetic acid: water (4:1:5) solvent.

A sample (0.15 g., 0.001 mole) of 6-amino hexanol-1 was treated with  $\alpha$ -naphthylisocyanate (0.218 g., 0.001 mole) in dry benzene (10 cc.). This suspension was refluxed for 1 hour. The gummy precipitate of 1- $\alpha$ -naphthyl-3-(6-hydroxyhexyl)-urea was removed by filtration and then crystallized from boiling acetone (5 cc.). A crop of colorless needles (m.p. 140–141° C.) was obtained, yield 0.265 g. (71.8%). The melting point was not changed by further crystallization. Anal. Calc. for  $C_{17}H_{22}N_2O_2$ : C, 71.30; H, 7.69; N, 9.78%. Found: C, 71.39; H, 7.83; N, 9.97%.

### 7-Aminoheptanol-1

Cycloheptanone oxime (b.p. 129–130° C. at 23 mm.) was prepared in 94.4% yield by the method of Pearson and Bruton (5). It was then converted into enantholactam (b.p. 148–150° C. at 10 mm.) in 82% yield by the method of Eck and Marvel (6).

Enantholactam (75.95 g., 0.6 mole) was converted into 7-aminoheptanol-1 hydrochloride by the method described above for the preparation of 6-amino hexanol-1. The first two distillates yielded a brownish oil (20 g.), which is probably impure heptamethylenimine hydrochloride. The residue from distillate fractions 3–7 was obtained as

<sup>2</sup>All melting points are uncorrected. Microanalyses were performed by Micro Tech Laboratories, Skokie, Illinois.

brownish needles melting at 67–75° C., yield 25.06 g. This crude 7-aminoheptanol-1 hydrochloride was dissolved in water (500 cc.) and the solution passed through a column of IRA-400 resin (600 cc. of resin in the hydroxyl form) at a rate of 5 cc. per minute. The column was washed with water (3500 cc.) and the eluate and washings were evaporated to dryness *in vacuo* under nitrogen. A crystalline distillate (b.p. 123° C. at 5 mm.; m.p. 48–53° C.) was obtained from the residue, yield 23.5 g. (29.9%). Wallach (4) reported a melting point of 48–50° C. for 7-aminoheptanol-1. A sample of the 7-aminoheptanol-1 (0.67 g., 0.0051 mole) in dry benzene (10 cc.) was treated with phenylisocyanate (0.61 g., 0.0051 mole). The product (m.p. 79.5–83° C.) was recovered by filtration, yield 1.25 g. (97%). One crystallization from acetone raised the melting point to 87–88° C. Anal. Calc. for  $C_{14}H_{22}N_2O_2$ : C, 67.16; H, 8.86; N, 11.20%. Found: C, 67.03; H, 8.71; N, 11.22%.

#### 11-Bromoundecanoic Acid

11-Bromoundecanoic acid (m.p. 48° C.) was prepared in 69.9% yield from 11-undecanoic acid by the method of Ashton and Smith (7). The reported (7) melting point is 49.25° C.

#### 11-Aminoundecanoic Acid

The patent procedure (8) for the preparation of 11-aminoundecanoic acid from 11-bromoundecanoic acid gave a 78.4% yield of product melting at 182–185° C. The reported (9) melting point of 11-aminoundecanoic acid is 186–187° C.

11-Aminoundecanoic acid (47 g., 0.23 mole) in 3.5 N methanolic hydrogen chloride solution was allowed to stand at room temperature for 16 hours. After most of the methanol was removed *in vacuo*, the crude methyl ester hydrochloride (m.p. 158–161° C.) was recovered by filtration, yield 51.1 g. (86.8%). One crystallization from methanol raised the melting point to 159.5–160.5° C. Anal. Calc. for  $C_{12}H_{26}ClNO_2$ : C, 57.24; H, 10.14; Cl, 14.09; N, 5.56%. Found: C, 57.33; H, 10.25; Cl, 14.35; N, 5.50%.

#### 11-Aminoundecanol-1

Methyl 11-aminoundecanoate hydrochloride (m.p. 158–161° C.) (22.2 g., 0.088 mole) in methanol (400 cc.) was passed through a column of IRA-400 (OH) resin (400 cc. of resin previously washed with methanol) at a rate of 5–7 cc. per minute. The eluates and washings were evaporated to dryness *in vacuo* under nitrogen. The residue of crude methyl 11-aminoundecanoate melted at 70–85° C., yield 16.2 g. (85.3%). Pellets of metallic sodium (28 g., 1.2 moles) were added to the crude methyl ester (16.2 g., 0.075 mole) in absolute ethanol (500 cc.) at a rate to maintain the alcoholic solution at gentle reflux. After the solution cooled it was diluted with water (250 cc.) to decompose the excess sodium ethoxide. The methanol was removed *in vacuo* under nitrogen and the residual aqueous solution was extracted with chloroform. The chloroform extract was dried over anhydrous sodium sulphate and evaporated to dryness. A residue (m.p. 74–78° C.) of yellowish crystals was obtained, yield 4.0 g. (28.3%). This crude 11-aminodecanol-1 was purified by solution in warm methanol (13.5 cc./g.), and filtration and dilution of the filtrate with water (10 cc.). The final product melted at 71–73° C.

A sample (0.187 g., 0.001 mole) of 11-aminoundecanol-1 in dry benzene on treatment with  $\alpha$ -naphthylisocyanate (0.169 g., 0.001 mole) gave 0.286 g. (80.2%) of crude 1- $\alpha$ -naphthyl-3-(11-hydroxyundecyl)-urea (m.p. 126–130° C.). Crystallization from acetone-benzene solution raised the melting point to 131° C. Anal. Calc. for  $C_{22}H_{32}N_2O_2$ : C, 74.11; H, 9.05; N, 7.86%. Found: C, 73.73; H, 9.05; N, 7.84%.

The aqueous filtrate from the chloroform extraction gave 16.5 g. of material melting at 197–205° C. This is considered to be the crude sodium salt of 11-aminoundecanoic acid. On treatment with concentrated hydrochloric acid solution it gave 11-aminoundecanoic acid hydrochloride (m.p. 148–149° C.). The latter material did not depress the melting point of a known sample of 11-aminoundecanoic acid hydrochloride (m.p. 148–149° C.).

#### *Reaction of Amino Alcohols with Carbon Disulphide*

The amino alcohol (0.05 mole) in absolute alcohol (25 cc.) was added dropwise over a period of 20 minutes to a stirred solution of carbon disulphide (0.025 mole) at 5° C.

After the reaction mixture had remained at room temperature for several hours, it was refluxed for 9 to 15 hours. The colored alcoholic solution was treated with Norite A and filtered. The product was recovered by evaporating the filtrate to dryness *in vacuo* under nitrogen. The crystals were purified by crystallizing from a suitable solvent such as ethyl acetate. The properties of the symmetrical 1,3-di-( $\omega$ -hydroxyalkyl) thioureas prepared in this manner are given in Table I.

#### *1,3-Di-( $\omega$ -hydroxyalkyl) Ureas*

##### *Method A*

The 1,3-di-( $\omega$ -hydroxyalkyl) ureas with the exception of 1,3-di-(11-hydroxyundecyl)-urea were prepared in the manner described below for 1,3-di-(7-hydroxyheptyl)-urea.

To 1,3-di-(7-hydroxyheptyl)-thiourea (3.04 g., 0.01 mole) in alcoholic sodium hydroxide solution (34 cc. containing 0.8 g. of sodium hydroxide) hydrogen peroxide (5.08 cc. of 7.6 molar solution; 0.03 mole) was added dropwise at a temperature of 25–28° C. After the solution had been left at room temperature for 4 hours, it was diluted with water (250 cc.). The crystals (m.p. 121–122° C.) were recovered by filtration and dried, yield 2.77 g. (86.3%). One crystallization from absolute ethanol raised the melting point to 122–122.5° C.

##### *Method B*

1,3-Di-(11-hydroxyundecyl)-thiourea was converted in 88.3% yield into 1,3-di-(11-hydroxyundecyl)-urea (m.p. 128–129° C.) by the method of Kjaer *et al.* (2). Two crystallizations from ethyl acetate – ethanol (1:1) solution along with one treatment with Norite A raised the melting point to 134.5–136° C.

#### REFERENCES

1. SKULSKI, M., GARMAISE, D. L., and MCKAY, A. F. Can. J. Chem. **34**, 815 (1956).
2. KJAER, A., RUBENSTEIN, K., and JENSEN, K. A. Acta Chem. Scand. **7**, 5181 (1953).
3. PUTOKHIN, N. Trans. Inst. Pure Chem. Reagents (Moscow), No. **6**, 10 (1927).
4. WALLACH, O. Ann. **324**, 292 (1902).
5. PEARSON, D. E. and BRUTON, J. D. J. Org. Chem. **19**, 957 (1954).
6. ECK, J. C. and MARVEL, C. S. Org. Syntheses, Coll. Vol. II, p. 76 (1944).
7. ASHTON, R. and SMITH, J. C. J. Chem. Soc. 435 (1934).
8. Brit. Patent No. 591,027 (August 5, 1947); Chem. Abstr. **42**, 592 (1948).
9. COFFMAN, D. D., COX, N. L., MARTIN, E. L., MOCHEL, W. E., and VAN Natta, F. J. J. Polymer Sci. **3**, 85 (1948).

# THE INFRARED SPECTRA OF MALONATE ESTERS<sup>1</sup>

R. A. ABRAMOVITCH<sup>2</sup>

## ABSTRACT

The infrared spectra of a number of malonate esters have been examined. Most of them exhibit two ester carbonyl stretching bands which have been shown not to be due to enolization and conjugate chelation or to association. The influence of  $\alpha$ -substituents is discussed, as well as the reason for the splitting of the band.

During the course of another investigation diethyl 1-methyl-2-cyanoethylmalonate was prepared and its infrared spectrum examined. Two bands were observed at 1742 and 1730 cm.<sup>-1</sup> respectively which could only be attributed to the carbonyl groups of the ester functions. This was surprising, since Bellamy (5) states that diethyl malonate is essentially normal in its carbonyl frequency. The original authors (24), however, had only measured the spectrum up to 1750 cm.<sup>-1</sup>. Bender and Figueras (7) remarked that diethyl malonate had an unusually broad (25 cm.<sup>-1</sup>) band at 1740 cm.<sup>-1</sup>, and indeed Felton and Orr (10) have recently shown that diethyl malonate exhibits two C=O stretching peaks at 1757 and 1740 cm.<sup>-1</sup> (in carbon tetrachloride solution). These authors ascribe the splitting either to symmetric and antisymmetric coupling of the two C=O stretching vibrations or to their resonance coupling with an overtone. In view of current interest in the splitting of carbonyl stretching frequencies the spectra of the malonate esters were examined in greater detail.

Vibrational coupling between carbonyl groups (16a) has been observed in a number of cases: diacyl and diaroyl peroxides (9), carboxylic acid anhydrides (23), and N,N-diacylamines (1). Recently, it has been suggested that glycidic esters dimerize in non-hydrogen-bonding solvents and that vibrational coupling then occurs between the carbonyl stretching motions of the two ester groups in the dimer (19). It should be pointed out, however, that whereas anhydrides exhibit two Raman bands corresponding to those found in the infrared (16a), the malonates, with one exception, show only one Raman shift in this region (18).

Preliminary examinations of some available malonates seemed to indicate that an  $\alpha$ -hydrogen was necessary for two bands to appear, which would have pointed towards enolization with subsequent hydrogen bonding as the reason for the second peak. Thus, diethyl diethylmalonate and diethyl 2,2-trans-hydrid-5-enylmalonate only showed one band, though the former compound also had a very poorly-defined shoulder on the higher frequency side. Again, Felton and Orr (10) report only one band for diethyl isopropylidene malonate though tetraethyl ethylenetetracarboxylate shows two. There is a large body of chemical evidence indicating that malonate esters have no appreciable enol content (3). In any case, had the second peak been due to a chelated carbonyl group its frequency should have been lower, and not higher, than the normal ester carbonyl stretching frequency. To examine the possibility of enolization and hydrogen bonding, diethyl ethyldeuteromalonate was prepared and compared with diethyl ethylmalonate; if enolization was taking place the position of the hydrogen-bonded carbonyl band would be altered on deuteration. Another possibility considered was that, when

<sup>1</sup>Manuscript received September 9, 1957.

Contribution from King's College, University of London, Strand, London, W.C.2, England.

<sup>2</sup>I.C.I. Research Fellow at King's College. Present address: Chemistry Department, University of Saskatchewan, Saskatoon, Sask., Canada.

the  $\alpha$ -carbon atoms carried two substituents other than hydrogen, steric inhibition of vibrational coupling might occur and this could account for the single band observed in some cases. To investigate this, the spectra of diethyl *tert*-butylmalonate and di-*tert*-butylmalonate were recorded. Finally, a number of  $\alpha$ -mono- and di-substituted malonates were examined in which the substituents varied in size and in electron attracting or repelling character.

### EXPERIMENTAL

Most of the diethyl malonates used in this study were commercial samples purified by repeated fractional distillation when required. The author wishes to acknowledge gratefully the following gifts of specimens: diethyl 2,2-*trans*-hydrind-5-enylmalonate from Dr. H. B. Henbest; a sample of diethyl 1-acenaphthylmalonate from Dr. R. A. Heacock; and a sample of diethyl 1,1-dimethylprop-2-ynylmalonate from Dr. K. MacKenzie.

Di-*tert*-butylmalonate was prepared according to Backer and Homan (4). Diethyl bis-(2-cyanoethyl)-malonate was prepared according to Bruson and Riener (8) and had m.p. 62°. Diethyl *p*-nitrobenzylidene malonate, m.p. 94°, was obtained from *p*-nitrobenzaldehyde and diethyl malonate in the presence of piperidine (17). Diethyl *tert*-butylmalonate was prepared in low yield by the action of *tert*-butylbromide on diethyl sodiomalonate (13). Diethyl 1-methyl-2-cyanoethylmalonate was prepared by the action of diethyl malonate on allyl cyanide in ethanolic sodium ethoxide (2).

#### *Diethyl Ethyldeuteromalonate*

Diethyl ethylmalonate (5 g.,  $n_D^{23}$  1.4150, redistilled, b.p. 212–214°) in absolute ethanol (20 ml.) containing sodium ethoxide (prepared from 0.615 g. sodium) was kept at room temperature overnight and then taken to dryness under vacuum to remove all traces of

TABLE I  
ESTER CARBONYL FREQUENCIES ( $\text{cm}^{-1}$ ) OF MALONATE ESTERS AS LIQUID FILMS OR NUJOL MULLS

Diethyl malonate derivative	$\nu$ ( $\text{cm}^{-1}$ )	Mean $\nu$ ( $\text{cm}^{-1}$ )	$\Delta\nu_{\text{C=O}}$ ( $\text{cm}^{-1}$ )
Dihydrogen	1760 (vs), 1742 (vs)	1751	18
Ethyl	1759 (m), 1742 (s)	1750	17
<i>n</i> -Propyl	1754 (s), 1737 (vs)	1745	17
<i>n</i> -Butyl	1757 (s), 1737 (vs)	1747	17
Ethyldeutero	1758 (sh) (m), 1742 (s)	1750	16
Diethyl	1751†(indistinct sh) (m), 1737 (s)	1744	(14†)
1-Acenaphthyl	1757 (sh) (s), 1745 (vs)	1751	12
Phenyl	1762 (s), 1741 (vs)	1752	21
Ethylphenyl	1754†(indistinct sh) (m), 1736 (s)	1745	(18†)
Chloro	1767 (s), 1754 (vs)	1760	13
Bromo	1771 (sh) (m), 1751 (s)	1761	20
Dibromo	1763 (s), 1752 (sh) (m)	1758	11
1,1-Dimethylprop-2-ynyl	1751 (s), 1730 (vs)	1740	21
2,2- <i>trans</i> -Hydrind-5-enyl	1730 (br) (vs)	—	—
1-Methyl-2-cyanoethyl	1742 (sh) (s), 1730 (vs)	1736	12
Bis-(2-cyanoethyl)*	1754 (s), 1733 (vs), 1705 (sh) (m)	1743	21
<i>tert</i> -Butyl	1767 (s), 1742 (vs)	1754	25
Acetamido*	1761 (vs), 1745 (sh) (s)	1753	16
<i>p</i> -Nitrobenzylidene*	1739 (vs), 1724 (vs)	1731	15
Thiophenacetamido* (21)	1745	—	—
Di- <i>tert</i> -butyl malonate	1751 (sh) (s), 1739 (vs)	1745	12
Ethyl cyanoacetate	1754 (vs)	—	—
Ethyl acetate	1748 (vs)	—	—

\*Nujol mulls.

†Only approximate position can be obtained, though the presence of a shoulder can be readily seen.

TABLE II  
EFFECT OF DILUTION ON ESTER CARBONYL FREQUENCIES (CM.<sup>-1</sup>) OF DIETHYL ETHYLMALONATE IN CHLOROFORM

Concn. (mg./cc.)	Cell thickness (in.)	$\nu$ (cm. <sup>-1</sup> )	% Absorption
50	0.00194	{ 1742 (sh)	81
		{ 1730	90.5
10	0.00970	{ 1742 (sh)	81
		{ 1730	90.5

TABLE III  
ESTER CARBONYL FREQUENCIES OF DIETHYL MALONATE DERIVATIVES IN SOLUTION

Compound	$\nu_{C=O}$ (cm. <sup>-1</sup> )	
	Carbon tetrachloride solution	Chloroform solution
Diethyl malonate <sup>a</sup>		1761 (vs), 1742 (vs), 1706 (sh) (vw)
Diethyl malonate <sup>b</sup>	1757, 1740	1747, 1731
Diethyl ethylmalonate <sup>a</sup>	1760 (vs), 1742 (vs), 1709 (sh) (w)	
Diethyl ethyldeuteromalonate <sup>a</sup>	1760 (vs), 1742 (vs), 1709 (sh) (w)	
Diethyl diethylmalonate <sup>a</sup>	1757 (indistinct sh) (s)†, 1742 (vs) $\Delta\nu_2$ 50 cm. <sup>-1</sup>	
Diethyl bromomalonate <sup>a</sup>	1776 (s), 1754 (vs), 1712 (sh) (w)	
Diethyl dibromomalonate <sup>a</sup>	1767 (vs), 1751 (s), 1712 (sh) (w)	
Diethyl phenylmalonate <sup>a</sup>	1764 (vs), 1743 (vs), 1727 (sh) (s)	
Diethyl ethylphenyl-malonate <sup>a</sup>	1739 (vs), 1730 (sh) (s) $\Delta\nu_2$ 58 cm. <sup>-1</sup>	
Diethyl <i>tert</i> -butylmalonate <sup>a</sup>		1761 (s), 1736 (vs), 1701 (sh) (w)
Tetraethyl ethylenetetra-carboxylate <sup>b</sup>	1750, 1739	1750, 1737
Tetraethyl ethanetetra-carboxylate <sup>b</sup>	1751, 1742	1746, 1737
Diethyl <i>isopropylidene</i> -malonate <sup>b</sup>	1726	1719
Ethyl acetate <sup>b</sup>	1744	1733
Ethyl propionate <sup>b</sup>	1740	1728
Ethyl succinate <sup>b</sup>	1740	1732
Ethyl cyanoacetate <sup>b</sup>	1754	1751

<sup>a</sup>Solutions containing ca. 25 mg./cc. Cell thickness 0.01 in. Average of three determinations.

<sup>b</sup>Values taken from the paper by Felton and Orr (10).

†Only approximate position could be obtained, though the presence of a shoulder could be readily seen.

ethanol. The residual solid was treated with redistilled 99.9% deuterium oxide (5 ml.), the product quickly extracted with AnalalR carbon tetrachloride (previously dried over Na<sub>2</sub>SO<sub>4</sub>), the extract dried (Na<sub>2</sub>SO<sub>4</sub>), evaporated to dryness, and distilled in the absence of moisture, giving diethyl ethyldeuteromalonate, b.p. 211–212°,  $n_D^{25}$  1.4167.

Diethyl ethyldeuteromalonate (0.5 g., twice redistilled, b.p. 211–212°) in absolute ethanol containing an excess of sodium ethoxide (solution got warm on mixing) was kept at room temperature overnight, evaporated to dryness, and treated with water

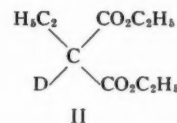
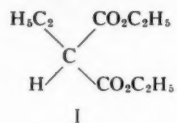
(5 cc.). Extraction with carbon tetrachloride and working up as above gave only a trace of a high boiling product, which proved to be diethyl diethylmalonate, b.p. 222° (I.R. spectrum identical with that of an authentic specimen but different from that of either diethyl ethylmalonate or diethyl ethyldeuteromalonate).

### Infrared Spectra

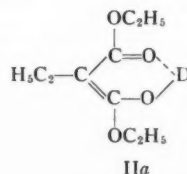
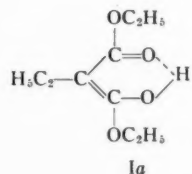
A Grubb-Parsons double-beam spectrometer, type S4, with a sodium chloride prism, was used. The measurements were carried out at slow chart speeds over the  $6\text{ }\mu$  range (at faster chart speeds the second band may be difficult to detect or appears only as a poorly defined shoulder) though they were carried out from 2 to  $15\text{ }\mu$  for some individual compounds. Points of interest other than in the  $6\text{ }\mu$  region are mentioned in the discussion. The frequency scale was calibrated by ammonia vapor bands (accuracy  $\pm 3\text{ cm.}^{-1}$  in the  $6\text{ }\mu$  region). Carbon tetrachloride and chloroform were analytical reagent grade, thoroughly dried before use. The measurements were carried out at a slit schedule of 1.5 mm. A variable-path cell was used to study the effect of dilution so that when the concentration of the solution was halved, for example, the cell thickness was doubled. The results are summarized in Tables I, II, and III. The relative intensities of the spectral bands are shown in parentheses, i.e. (vs) very strong, (m) medium, (w) weak, (sh) shoulder, (br) broad.

### DISCUSSION

Most of the compounds examined exhibit two bands in the  $5.6$ – $5.9\text{ }\mu$  region, with the notable exception of three of these: diethyl diethylmalonate ( $\Delta\nu_1$  46  $\text{cm.}^{-1}$ , liquid film), diethyl ethylphenylmalonate, and diethyl 2,2-trans-hydrid-5-enylmalonate. The first two of these do have an indistinct shoulder, the first on the high and the second on the low frequency side of the peak respectively, whereas the third gives a broad band ( $\Delta\nu_1$  45  $\text{cm.}^{-1}$ ). In agreement with the chemical evidence (3), the presence of double peaks in compounds such as diethyl bis-(2-cyanoethyl)-malonate, diethyl *p*-nitrobenzylidene-malonate, and tetraethyl ethylenetetracarboxylate (10), in which no hydrogen atom is present *alpha* to the carbonyl groups, makes the hypothesis that the double peaks are due to enolization and conjugate chelation untenable. In support of this conclusion is the fact that the replacement of an  $\alpha$ -hydrogen by a deuterium atom makes no apparent difference to the positions of the two bands in this region. This is seen particularly well when the spectra of diethyl ethylmalonate (I) and diethyl ethyldeuteromalonate (II) in carbon tetrachloride solutions are compared:



If enolization with consequent conjugate chelation had occurred, it would be expected that the positions of these carbonyl peaks would be shifted somewhat, which is not the case:



Finally, the positions of the two peaks are not in agreement with those expected for chelated and unchelated carbonyl groups (22). On the other hand, some of the malonates which have an  $\alpha$ -hydrogen atom do show a weak shoulder at  $1700\text{--}1712\text{ cm.}^{-1}$  when in solution, whereas those that do not have an  $\alpha$ -hydrogen atom (with the exception of diethyl dibromomalonate, which is also abnormal in other respects) do not have this shoulder. This may be evidence of a very small extent of enolization, though other explanations are possible. Gordy (12) attributes a very weak band at  $6.12\text{ }\mu$  in the spectrum of ethyl malonate to the presence of a very small quantity of enol.

Dilution has no effect on either the position or the intensity of the double peaks (Table II), which means that end-to-end association of molecules, should it exist in the condensed state, is not the cause of the splitting of the  $\text{C=O}$  band (20). Also, Morris and Young (19) showed that, in a solvent such as chloroform (which was the solvent used in our dilution experiments), their suggested glycidic ester anti-parallel dimers dissociated into single molecules, so that our results indicate the absence also of such an association in the case of malonate esters as the cause of the two carbonyl peaks. It would be interesting to see if the positions and relative intensities of the peaks showed any temperature dependence. There is practically no shift in the positions of the bands on passing from the pure liquid to the solution spectra.

The absence of a second clear-cut peak in the cases of diethyl diethylmalonate and diethyl ethylphenylmalonate does not seem attributable to steric inhibition of vibrational coupling or dipole-dipole interaction between the two carbonyl groups, since when a single large group is present, as in the cases of diethyl *tert*-butylmalonate and diethyl 1-acenaphthylmalonate, as well as in di-*tert*-butylmalonate, the two bands still appear. The positions and the frequency differences between the two bands ( $\Delta\nu = 11\text{--}25\text{ cm.}^{-1}$ ) do, however, vary with the nature of the  $\alpha$ -substituents (the influence of  $\alpha$ -substituents is discussed in greater detail below), and a possible explanation is that, in the cases where only a single band or a band and an indistinct shoulder (only approximate position can be obtained) are observed, the two peaks are insufficiently resolved because  $\Delta\nu$  is too small. The unusually large band widths at half maximal intensity ( $\Delta\nu_{1/2}$ ) observed support this view.

The variation to a greater or lesser extent of the position of the peaks with the nature of the  $\alpha$ -substituent makes it unlikely that resonance coupling of a  $\text{C=O}$  stretching vibration with an overtone should be the cause of the splitting, though it does not eliminate it as a possibility. Also, the absence of a clear-cut steric effect seems to rule out dipole-dipole interaction as the cause, since this would probably necessitate having the dipoles parallel to each other. A likely explanation for the double peaks seems, on the present evidence, to be symmetric and anti-symmetric coupling of the two  $\text{C=O}$  stretching vibrations, which would not, presumably, require such restricted steric conditions as would dipole-dipole interaction. Another possible answer, which would also fit in with some of the effects observed with  $\alpha$ -halogeno substituents, would be some form of rotational isomerism, e.g. III  $\rightleftharpoons$  IV:



Confirmation (or otherwise) of this possibility might be obtained from an examination

of the temperature dependence, if any, of the spectra (14). It is hoped to investigate this soon. The vibrational coupling hypothesis would fit in with the positions of the double peaks rather well. Thus, ethyl acetate absorbs at  $1748\text{ cm}^{-1}$ , and the introduction of an electron-withdrawing substituent *alpha* to the carbonyl group raises the  $\text{C}=\text{O}$  stretching frequency by increasing the double-bond character of the carbonyl group. The ester band in ethyl cyanoacetate is at  $1754\text{ cm}^{-1}$  and a similar (though somewhat lesser) effect to that of the cyano group is to be expected by the introduction of an  $\alpha$ -ethoxy-carbonyl group, as in diethyl malonate, in which the common ester stretching frequency should be *ca.*  $1750$ – $1752\text{ cm}^{-1}$ . Splitting of the  $\text{C}=\text{O}$  band precludes the observation of this effect, though two things can be noted: (i) the mean position of the two components ( $1751\text{ cm}^{-1}$ ) is higher than that of the band for ethyl acetate, and (ii) the  $\text{C}=\text{O}$  band is split into two components, one at a frequency higher, and the other at a frequency lower, than the common value expected had no splitting occurred. Such behavior is typical of groups undergoing vibrational coupling (16a).

In view of the splitting of the  $\text{C}=\text{O}$  band it is rather difficult to correlate the nature of the  $\alpha$ -substituent with its effect on the stretching frequency. It is clearly not justifiable to consider the influence of the substituent on the position of either one of the bands, and the only way is to consider the mean of the two peaks. The use of this frequency in any correlation is of a rather doubtful nature, however, since  $\Delta\nu_{\text{C}=\text{O}}$  varies from one substituent to another and, though vibrational coupling is the most likely explanation of the splitting, other possibilities have not been completely ruled out, as mentioned above. In the case of the monocarboxylic acids and esters, lengthening of the alkyl chain causes a slight fall in the  $\text{C}=\text{O}$  frequency, as in ethyl propionate ( $1740\text{ cm}^{-1}$ ) compared with ethyl acetate ( $1744\text{ cm}^{-1}$ ) (see Table III). This is in line with the electron-repelling character of the methyl group. A similar, though weaker, effect takes place when one of the  $\alpha$ -hydrogen atoms in diethyl malonate ( $1751\text{ cm}^{-1}$ ) is replaced by an ethyl group ( $1750\text{ cm}^{-1}$ ), and a still larger fall (in the mean position) occurs when it is replaced by an *n*-propyl group ( $1745\text{ cm}^{-1}$ ). When both  $\alpha$ -hydrogen atoms are replaced by ethyl groups the mean frequency falls still further to  $1744\text{ cm}^{-1}$ . With a single *n*-butyl substituent the frequency rises slightly to  $1747\text{ cm}^{-1}$  and with a single  $\alpha$ -*tert*-butyl substituent it *rises above* the mean value for diethyl malonate, to  $1754\text{ cm}^{-1}$ . It appears, therefore, that a steric effect *is* in operation with  $\alpha$ -alkyl substituents, and that it acts in opposition to the inductive and hyperconjugative effect of these groups. The nature of this steric effect is not clear (rotational isomerism?), and though it does not inhibit the splitting of the band it seems to raise the mean  $\text{C}=\text{O}$  stretching frequency. (*This, of course, obtains only if the use of the mean of the two frequencies is valid.*) The very slight increase caused by an  $\alpha$ -phenyl group ( $1752\text{ cm}^{-1}$ ) could be due either to its  $-I$  effect or to its steric effect, and in the ethylphenyl derivative the frequency falls to  $1745\text{ cm}^{-1}$ . The  $-I$  effect of the  $\alpha$ -acetamido group is seen in the increase to  $1753\text{ cm}^{-1}$ , whereas the effect of  $\alpha\beta$ -unsaturation in diethyl *p*-nitrobenzylidene malonate ( $1731\text{ cm}^{-1}$ ) and in diethyl *iso*-propylidene malonate ( $1726\text{ cm}^{-1}$ ) is clear. The influence of  $\alpha$ -halogens is not straightforward. As is well established, in general, halogenation of the alkyl group *alpha* to a carbonyl raises the  $\text{C}=\text{O}$  frequency, the magnitude of the shift increasing with the increasing dipole moment of the  $\text{C}-\text{X}$  bond (viz.  $\text{F} > \text{Cl} > \text{Br} > \text{I}$ ) (16b) (Table IV).

Further, Jones *et al.* (15) showed that while an equatorial bromine atom *alpha* to a keto group in steroidal cyclohexanones causes an increase in the  $\text{C}=\text{O}$  frequency of  $13$ – $19\text{ cm}^{-1}$  by virtue of a Coulombic field effect which outweighs its inductive effect, introduction of a second bromine atom at the same  $\alpha$ -carbon atom to form a *gem*-dibromide produces no, or only a slight, further increase, which can be associated with residual

TABLE IV

Compound	$\nu_{C=O}$ (cm. <sup>-1</sup> )
Acetic acid	1721
Moniodoacetic acid	1721
Monobromoacetic acid	1730
Monochloroacetic acid	1736

inductive effects (6). Diethyl chloromalonate shows the expected strong increase in frequency (1760 cm.<sup>-1</sup>); in diethyl bromomalonate the increase is still larger (1761 cm.<sup>-1</sup>), which is the reverse of the order expected on the basis of electronegativity (Table IV) (see also Ref. 16c). Furthermore, the introduction of a second bromine atom to give diethyl dibromomalonate *lowers* the frequency to 1758 cm.<sup>-1</sup>. It seems likely that the governing factor which produces the first increase is connected with the size of the halogen atom ( $Br > Cl$ ) and that the second bromine introduced interferes sterically or otherwise with the first bromine-carbonyl interaction. It may be worth noting in this connection that the ratio of the intensities of the two carbonyl peaks is reversed on passing from the monochloro- and monobromo-malonates, to the dibromo-malonate.

The spectrum of diethyl ethyldeuteromalonate was interesting in that no C—D stretching band could be detected. This is not altogether surprising, for two reasons: (i) in most aliphatic hydrocarbons no peak attributable to the stretching vibration of a tertiary C—H bond can be discerned (16d), especially in this case, where only one such group exists in the molecule so that its contribution to the integrated absorption intensity on the basis of Francis' equation (11) would be very small; (ii) the force constant of the  $\alpha$ -tertiary C—H bond in malonates would be expected to be rather weak and the band would, therefore, be shifted towards the long wave-length region. It may be possible that the additional shift in the same direction caused by substituting deuterium for hydrogen would move the band close to the carbonyl region, where it could not be detected. The presence of the C—D linkage in this compound is readily detected in the 'bending' region of the spectrum, and by a comparison of the spectrum with those of diethyl ethylmalonate and diethyl diethylmalonate over this range. In Table V the abbreviations h = high, l = low, and e = approx. equal intensities have been used to compare very roughly the relative intensities of corresponding peaks in the three compounds.

Some of the peaks present in diethyl ethylmalonate are shifted to lower frequencies

TABLE V  
SPECTRA OF LIQUID FILMS OF DIETHYL MALONATE DERIVATIVES

Ethyl (cm. <sup>-1</sup> )	Ethyldeutero (cm. <sup>-1</sup> )	Diethyl (cm. <sup>-1</sup> )
1339 (h)	1339 (l)	1339 (l)
1259 (l)	1259 (h)	—
1235 (l)	1238 (h)	1239 (h)
1209 (e)	1209 (sh)(e)	1209 (e)
1181 (h)	1174 (l)	1174 (sh)(l)
1156 (e)	1142 (e)	1151 (e)
1117 (l)	1125 (h)	1125 (h)
1098 (l)	—	1098 (l)
1093 (sh)	—	—
—	1075	—
1049	—	—
1026 (e)	1032 (sh)(e)	1024 (e)

in the deutero compound and the ratio of intensities of some peaks is altered considerably. The spectrum of the deutero compound falls in very nicely as a mixture of parts of the ethyl and parts of the diethyl spectra, as expected.

An interesting reaction was observed when diethyl ethyldeuteromalonate was treated with sodium ethoxide in absolute ethanol (slight heat evolved), kept overnight, and the mixture taken to dryness and treated with water. Instead of the expected diethyl ethylmalonate there was obtained a very small amount of diethyl diethylmalonate, identical in boiling point and infrared spectrum with an authentic specimen. In view of the repeated purifications to which the diethyl ethyldeuteromalonate was subjected, it is unlikely that any diethyl compound was present in it before the sodium ethoxide treatment. The reaction probably involves a disproportionation, as *no* diethyl ethylmalonate was isolated from the product. That the ethyl group should have come from the sodium ethoxide or the alcohol used seems unlikely.

#### ACKNOWLEDGMENTS

The author wishes to thank Dr. R. N. Jones for a valuable discussion. This work was carried out during the tenure of an I.C.I. Research Fellowship in the University of London.

#### REFERENCES

1. ABRAMOVITCH, R. A. *J. Chem. Soc.* 1413 (1957).
2. ABRAMOVITCH, R. A. Forthcoming publication.
3. (a) ARNDT, F., LOEWE, L., and GINKÖK, R. *Rev. fac. sci. univ. Istanbul, A*, **11**, 147 (1946); *Chem. Abstr.* **41**, 3761 (1947).  
(b) EISTER, B. and REISS, W. *Chem. Ber.* **87**, 92 (1954).  
(c) MEYER, K. H. *Ber.* **45**, 2864 (1912).
4. BACKER, H. J. and HOMAN, J. D. H. *Rec. trav. chim. Belg.* **58**, 1054 (1939).
5. BELLAMY, L. J. *The infrared spectra of complex molecules*. Methuen & Co., Ltd., London. 1954. p. 157.
6. BELLAMY, L. J., THOMAS, L. C., and WILLIAMS, R. L. *J. Chem. Soc.* 3704 (1956).
7. BENDER, M. L. and FIGUERAS, J. *J. Am. Chem. Soc.* **75**, 6304 (1953).
8. BRUSON, H. A. and RIENER, T. W. *J. Am. Chem. Soc.* **65**, 23 (1943).
9. DAVISON, W. H. T. *J. Chem. Soc.* 2456 (1951).
10. FELTON, D. G. I. and ORR, S. F. D. *J. Chem. Soc.* 2170 (1955).
11. FRANCIS, S. A. *J. Chem. Phys.* **18**, 861 (1951).
12. GORDY, W. *J. Chem. Phys.* **8**, 516 (1940).
13. GRYSZKIEWICZ-TROCHIMOWSKI, E. and GRYSZKIEWICZ-TROCHIMOWSKI, O. *Bull. soc. chim. France*, **18**, 269 (1951).
14. JONES, R. N., FORBES, W. F., and MUELLER, W. A. *Can. J. Chem.* **35**, 504 (1957).
15. JONES, R. N., RAMSAY, D. W., HERLING, F., and DOBRINER, K. *J. Am. Chem. Soc.* **74**, 2828 (1952).
16. JONES, R. N. and SANDORFY, C. *Technique of organic chemistry*. Vol. IX. *Chemical applications of spectroscopy*. Interscience Publishers, Inc., London. 1956. (a) p. 495, (b) p. 474, (c) p. 478, (d) p. 340.
17. KNOEVENAGEL, E. *Ber.* **31**, 2593 (1898).
18. KOHLRAUSCH, K. W. F. and SABATHY, R. *Monatsh.* **72**, 303 (1939).
19. MORRIS, H. H. and YOUNG, R. H. *J. Am. Chem. Soc.* **79**, 3408 (1957).
20. PARTINGTON, J. R. *An advanced treatise on physical chemistry*. Vol. V. Longmans, Green and Co., Ltd., London. 1954. p. 384.
21. RANDALL, H. M., FOWLER, R. G., FUSON, N., and DANGL, J. R. *Infrared determination of organic structures*. D. Van Nostrand Company, Inc., New York. 1949. p. 111.
22. RASMUSSEN, R. S., TUNNICLIFFE, D. D., and BRATTAIN, R. R. *J. Am. Chem. Soc.* **71**, 1068 (1949).
23. THOMPSON, H. W. *J. Chem. Soc.* 328 (1948).
24. THOMPSON, H. W. and TORKINGTON, P. *J. Chem. Soc.* 640 (1945).

## HYDROGEN ABSTRACTION REACTIONS OF DIPHENYLPICRYLHYDRAZYL<sup>1</sup>

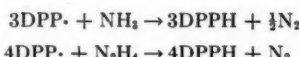
A. G. BROOK, R. J. ANDERSON, AND J. TISSOT VAN PATOT

### ABSTRACT

The stable free radical diphenylpicrylhydrazyl (DPP<sup>·</sup>) has been found to react quantitatively with ammonia and hydrazine forming nitrogen and diphenylpicrylhydrazine, and less cleanly with hydroxylamine forming diphenylpicrylhydrazine and nitrous oxide. The reactions of DPP<sup>·</sup> with a variety of amines are not clean, in part owing to the formation of complexes of the amines with the reaction product diphenylpicrylhydrazine. Preliminary investigations of the reactions of DPP<sup>·</sup> with mercaptans have shown that these otherwise clean reactions have a variable stoichiometry, dependent on the concentration and other reaction conditions.

The stable free radical diphenylpicrylhydrazyl (DPP<sup>·</sup>), while not in general a powerful dehydrogenating agent, nevertheless shows considerable facility in removing hydrogen atoms attached to a nitrogen atom in a variety of compounds (3). In order to study this behavior further we have investigated the reactions of DPP<sup>·</sup> with a number of simple compounds having N—H bonds, and also with some mercaptans.

The ability of the radical to abstract hydrogen atoms from nitrogen is evidently a general reaction but a marked variation in the "cleanliness" of the reactions was noted. It was found that DPP<sup>·</sup> quantitatively converted both ammonia and hydrazine to nitrogen, being itself reduced to diphenylpicrylhydrazine (DPPH), according to the following equations:



These reactions occurred relatively rapidly at room temperature and could be followed by collection of the gas evolved, and also by observing the disappearance of the characteristic intense purple color of the radical. The DPPH formed could be isolated practically quantitatively. Typical results are summarized in Table I. Attempts to partially dehydrogenate ammonia to give hydrazine failed, and the volume of gas collected indicated that complete oxidation of one-third of the ammonia occurred.

TABLE I  
REACTION OF DIPHENYLPICRYLHYDRAZYL WITH HYDRAZINE AND AMMONIA

Run	DPP <sup>·</sup> , mM.	H donor, mM.	Solvent	N <sub>2</sub> , mM.	% N <sub>2</sub>	% DPPH <sup>a</sup>
1	0.80	N <sub>2</sub> H <sub>4</sub> , 0.20	CHCl <sub>3</sub>	0.199	99 <sup>b</sup>	99.5
2	0.40	N <sub>2</sub> H <sub>4</sub> , 0.40	CHCl <sub>3</sub>	0.098	98 <sup>c</sup>	99
3	1.20	N <sub>2</sub> H <sub>4</sub> , 0.20	CHCl <sub>3</sub>	0.197	98.5 <sup>b</sup>	4
4	2.74	NH <sub>3</sub> , 0.913	GMME <sup>e</sup>	0.453	99.2 <sup>c</sup>	98
5	1.81	NH <sub>3</sub> , 0.457	GMME <sup>e</sup>	0.448	98 <sup>b</sup>	4
6	1.37	NH <sub>3</sub> , 0.457	GMME <sup>e</sup>	0.448	98 <sup>b</sup>	99

<sup>a</sup> Yield of DPPH is the % of DPP<sup>·</sup> recovered as DPPH in all cases.

<sup>b</sup> Yield based on hydrogen donor.

<sup>c</sup> Yield based on diphenylpicrylhydrazyl.

<sup>d</sup> Product was a mixture of DPP<sup>·</sup> and DPPH.

<sup>e</sup> GMME = ethylene glycol monomethyl ether.

<sup>1</sup> Manuscript received July 2, 1957.

Contribution from the Department of Chemistry, University of Toronto, Toronto, Ontario.

DPP<sup>·</sup> also reacts rapidly with hydroxylamine but the reaction is not as clean as those above, nor is the stoichiometry as clearly defined. Dilute solutions of the reagents can be "titrated" against one another to a clear orange-brown end point formed as the purple color of the radical disappears. From such experiments the molar ratio of DPP<sup>·</sup> to hydroxylamine was found to lie between 2.88 and 2.98. From larger runs in more concentrated solutions, carried out to afford reasonable quantities of reduction products and gas for examination, the molar ratio varied from 2.5 to 3.1. The major reduction product again was DPPH, isolated in 89% yield, and the gas was shown by its infrared absorption spectrum to be nitrous oxide. The most reasonable equation representing these data is as follows:



However, no product corresponding to 1-hydroxy-1-picryl-2,2-diphenylhydrazine (DPPOH), a known compound (6), was detected although small amounts of other products were isolated by chromatography of the reaction mixture. Since the ratio of DPP<sup>·</sup> to hydroxylamine and the amount of gas evolved in most cases corresponded fairly well to that predicted by the above equation it seems probable either that any DPPOH formed decomposed during the working up of the reaction or that other reactions are also occurring to a small extent. In support of this reasoning is the fact that more DPP<sup>·</sup> was converted to DPPH (89%) than is predicted by the equation (83%). These results are listed in Table II.

TABLE II  
REACTION OF DIPHENYLPICRYLHYDRAZYL WITH HYDROXYLAMINE AND METHYLAMINE

Run	DPP <sup>·</sup> , mM.	H donor, mM.	Gas, mM.	Molar ratios			Products
				DPP/donor	DPP/gas		
7	6.34 <sup>a</sup>	NH <sub>2</sub> OH, <sup>b</sup> 2.31	1.09	2.75	5.8	DPPH, N <sub>2</sub> O	
8	6.34 <sup>a</sup>	NH <sub>2</sub> OH, <sup>b</sup> 2.58	1.16	2.46	5.47	DPPH (89%), N <sub>2</sub> O	
9	6.34 <sup>a</sup>	NH <sub>2</sub> OH, <sup>b</sup> 2.26	0.65	2.81	9.7	DPPH, N <sub>2</sub> O	
10	6.34 <sup>a</sup>	MeNH <sub>2</sub> , <sup>a</sup> 3.40	0.607	1.86	10.4	DPPH, N <sub>2</sub> ?	
11	12.7 <sup>a</sup>	MeNH <sub>2</sub> , <sup>a</sup> 6.24	1.02	2.04	12.4	DPPH (50%), N <sub>2</sub> ?	
12	6.34 <sup>c</sup>	MeNH <sub>2</sub> , <sup>c</sup> 3.19	0.36	1.99	17.6	DPPH (46%), N <sub>2</sub> ?	
13	6.34 <sup>c</sup>	MeNH <sub>2</sub> , <sup>c</sup> 3.28	0.30	1.93	20.8	DPPH, N <sub>2</sub> ?	

<sup>a</sup>Solvent was chloroform.

<sup>b</sup>Solvent was methanol.

<sup>c</sup>Solvent was benzene.

DPP<sup>·</sup> also reacts with a variety of amines but the nature of the reaction is not clear. Titration of very dilute (0.0005 M) solutions of the radical and methylamine to an orange end point indicates a molar ratio of radical to amine of 2.0, and the same ratio seems to hold for isopropylamine and *n*-butylamine also. Of the amines investigated only methylamine evolves significant quantities of gas, which by the absence of any characteristic infrared spectrum appears to be nitrogen. However the volume of gas evolved varied markedly with the solvent (see Table II).

From relatively large scale runs in concentrated chloroform solution the main reduction product isolated from all the amines investigated was DPPH, in amounts corresponding to 50–75% of the DPP<sup>·</sup> originally present. The remaining products were either intractable tars or amorphous solids which had variable and wide melting point ranges which recrystallization failed to improve. All that can be definitely stated about the

reactions of the radical with these primary amines is that one of the amino hydrogens is readily abstracted by DPP· and that the resulting radical then apparently reacts in a variety of ways, in part with a second equivalent of DPP· and perhaps also with the solvent.

We also investigated to some extent the reaction between DPP· and diethylamine but the stoichiometry of the reaction could not be definitely established. In non-polar solvents the reactions were extremely slow while in polar solvents the reaction mixture became a muddy brown-black color as the reaction proceeded instead of the typical clear orange-brown color. Work-up of these reaction mixtures yielded as major products DPPH and a black solid which at about 115°-120° turned red and then melted at 172° as if it were pure diphenylpicrylhydrazine. It was shown that this latter material was a 1:1 complex of diphenylpicrylhydrazine and diethylamine.

The reactions of the radical with amines were much slower than those with the other reagents previously described. This led to the interesting observation that the rates of reduction of DPP· were much more rapid in polar solvents such as methanol or ethanol than in non-polar solvents such as benzene or chloroform, and furthermore, that in the polar solvents the final reaction mixtures were usually an opaque muddy brown color while in the non-polar solvents the reaction mixtures were a clear orange or orange-brown color. It was found that the intensity of this muddy brown color could be markedly changed by dilution, especially with a non-polar solvent, so that the system became clear orange-brown, or that this color could be turned to muddy brown by the addition of more amine solution. These observations are explained if a complex is formed between diphenylpicrylhydrazine and the amine which can dissociate into its components depending on the polarity of the medium and the concentration of the solution.



Such a complex was actually isolated in the case of diethylamine. It is obvious that such complex formation will completely confuse any stoichiometric determinations which may depend on the color of end points.

That the rate of a homopolar reaction should be dependent on the polarity of the medium is not unreasonable, since in these reactions the most probable means for transfer of a hydrogen atom from donor to acceptor is through formation of a complex between the amine and stable free radical (3). Such complexes involving the picryl group of DPP· would be expected to be more readily formed and to be more stable in polar solvents, as are the well-known complexes of amines with polynitroaromatic compounds (8). If hydrogen transfer depends on the formation of such complexes, it is not surprising that dehydrogenation occurs more rapidly in a medium favorable to their formation. Nor is it surprising that DPPH forms similar complexes in polar solvents.

We have also investigated briefly the reactions of DPP· with thiophenol and butyl mercaptan. These reagents react rapidly with the radical but, unlike in the other reactions studied, the molar ratio of DPP· to mercaptan varied markedly, being dependent on the concentration of the solutions and their order of addition. This was particularly noticeable with thiophenol, for in very dilute solution, when the radical was added to the thiophenol, the mole ratio was approximately 1.0 but in concentrated solution with the reverse order of addition the mole ratio was between 1.9 and 2.0. With butyl mercaptan there appeared to be less dependence on the order of addition and the mole ratio varied from 1.0 to 1.15 over a range of concentrations. These results can be explained by assuming the following reactions to be occurring:

- (a)  $DPP \cdot + RSH \rightarrow DPPH + RS \cdot$
- (b)  $2RS \cdot \rightarrow RSSR$
- (c)  $DPP \cdot + RS \cdot \rightarrow DPPSR$

The over-all stoichiometric ratio of the reaction depends on the relative importance of reactions (b) and (c), which depend strongly on concentration and on the various species present in the reaction mixture. In dilute solution, where  $DPP \cdot$  is added to thiophenol, reaction (b) evidently occurs almost to the exclusion of (c), but in concentrated solution, where  $RS \cdot$  radicals are being formed in the presence of  $DPP \cdot$ , coupling of the unlike radicals occurs (reaction c) almost exclusively. When the reactions were worked up it was found that a mixture of compounds was obtained from which DPPH could be separated by chromatography and recrystallization. No success was achieved in isolating the thio derivative DPPSR.

With butyl mercaptan reaction (c) was evidently slower than (b), since the molar ratio varied over a much smaller range and appeared to be less dependent on the concentration of the reagents or the order of addition. In accord with this, relatively high yields (75%) of DPPH were isolated from the reactions. The kinetics of this reaction, in excess butyl mercaptan, have been reported (7).

It is obviously impossible to speculate at this stage as to the nature of the intermediate radicals produced during the dehydrogenation of hydrazine, ammonia, or hydroxylamine, but it is apparent from the last two cases that dimerization occurs at some stage. It is hoped that further insight into these reactions may be gained by kinetic studies on some of the simpler systems. It is obviously desirable to work with these relatively clean systems, since much of the work reported here is disappointing because of the difficulties found in isolating crystalline products in good yield, thus leaving the conclusions as to the processes occurring in many of the reactions rather speculative.

## EXPERIMENTAL

All yields of diphenylpicrylhydrazine (DPPH) are based on the moles of diphenylpicrylhydrazyl ( $DPP \cdot$ ) reduced.

### Materials

$DPP \cdot$  was prepared according to the method of Goldschmidt and Renn (4) as modified by Poirier *et al.* (6). The purple solid was dried *in vacuo* for several hours at 80° to remove the complexed chloroform (5). Anhydrous hydrazine (1) and anhydrous hydroxylamine (2) were prepared by published procedures. All solvents were purified and the liquid amines were distilled. Methylamine solutions were usually prepared by treating a mixture of the appropriate organic solvent and 30% aqueous methylamine solution with sodium hydroxide pellets to remove the bulk of the water. The supernatant liquid was decanted and dried over anhydrous sodium sulphate and then standardized against standard acid using methyl orange indicator. In some cases methylamine was prepared by liberating the amine from methylamine hydrochloride with alkali. Tank ammonia was used. All solutions were freshly prepared and frequently standardized.

### Bulk Reactions of $DPP \cdot$

#### A. Hydrazine

To 25 ml. of methanol containing 0.00125 mole of hydrazine was added 1.97 g. (0.0050 mole) of  $DPP \cdot$  in 25 ml. of chloroform. The violet color of the radical disappeared as the solution successively became violet-red, amber, and finally orange-brown over a

period of about 1 hour. Evaporation of the solution to dryness gave 1.97 g. (100%) of DPPH, m.p. 171°-172° (dec.), identified by mixed melting point with an authentic specimen. Recrystallization from 1:2 chloroform-ethanol failed to raise the melting point. If more than 4 equivalents of DPP<sup>·</sup> were added the solution remained purple and unchanged free radical could be recovered.

#### B. Ammonia

To 25 ml. of methanol containing 0.0013 mole of ammonia was added 1.54 g. (0.0039 mole) of DPP<sup>·</sup> in 25 ml. of chloroform. After 1 hour the solution was orange-brown and 1.54 g. (100%) of red DPPH, m.p. 171°-172° (dec.), was isolated.

#### C. Hydroxylamine

To 5.0 g. (0.00634 mole) of DPP<sup>·</sup> in 35 ml. of chloroform was added in 0.2 ml. aliquots a total of 5.7 ml. (0.00412 mole) of a 0.723 M solution of hydroxylamine in methanol. The reaction mixture was stirred magnetically and the reaction vessel was connected to a mercury-filled gas burette so that any gas evolved could be collected and measured. Gas was steadily evolved and the color changed from purple to orange-brown regularly until about 5.5 or 5.7 ml. of hydroxylamine solution had been added. No significant changes on further additions of hydroxylamine occurred. Toward the end of the addition a red solid precipitated from the reaction mixture. About 20 ml. of gas was evolved, which was shown by its infrared absorption spectrum to be nitrous oxide. This spectrum also contained absorption bands due to chloroform vapor so that a comparison was made with a gas sample made up of chloroform vapor and authentic nitrous oxide, which proved to be identical in every respect. The precipitate was filtered off and shown to be 2.52 g. (50.5%) of DPPH, m.p. 171°-172° (dec.). The filtrate was placed on a 3×25 cm. chromatography column of activated alumina and was eluted with several hundred milliliters of chloroform. Evaporation of this eluate to dryness followed by recrystallization from chloroform-ethanol gave an additional 1.96 g. (39.2%, total 89.7%) of DPPH, m.p. 171°-172° (dec.). A black band remained on the column which was eluted with ethanol to give an intense red colored solution. On evaporation to dryness this yielded 0.24 g. of a green-black solid which appeared to decompose at about 88° and which frothed at 120°. It was insoluble in dry benzene or chloroform but was soluble to give an intensely red solution in ethanol or ethyl acetate. It could not be recrystallized from these solvents or solvent pairs, since only gums were formed.

#### D. Methylamine

To 3.5 g. (0.0089 mole) of DPP<sup>·</sup> in 25 ml. of chloroform was added an excess (0.0087 mole) of methylamine in 5 ml. of chloroform. The color of the solution changed very slowly over 1-1.5 hours until it became orange-brown. About 25 ml. of gas was evolved. The infrared spectra showed absorption characteristic only of chloroform and methylamine vapors, as shown by comparison of a spectrum made up of these two substances; hence it seems likely that the major part of the evolved gas was nitrogen. To guard against the possibility that the excess of methylamine was responsible for the gas evolved, other runs with a deficiency of methylamine were made. Spectra of the gas evolved in these runs showed only the presence of chloroform and a trace of methylamine, neither of which would account for the volume of gas evolved.

The filtrate from this run was chromatographed on alumina and eluted with chloroform. A total of 2.24 g. (64%) of DPPH, m.p. 171°-172° (dec.), was isolated together with small traces of intractable gums and amorphous solids which could not be purified by crystallization.

*E. n-Butylamine and Isopropylamine*

When 14.2 g. (0.036 mole) of DPP· in 100 ml. of ethanol was treated with 1.85 g. (0.025 mole) of *n*-butylamine the color changed from purple to a muddy brown-black color over a period of 1 hour. Only a trace (1–2 ml.) of gas was evolved. A black precipitate weighing 7.75 g. (55%) of crude DPPH, m.p. 164°–172° (dec.), was filtered off and recrystallized from ethanol-chloroform to yield 6.5 g. (46%) of pure DPPH, m.p. 170°–172° (dec.). The filtrate from the original precipitate was evaporated to dryness, dissolved in chloroform, and chromatographed on alumina to yield an additional 0.9 g. (6%) of DPPH, m.p. 170°–172° (dec.), 0.42 g. of a dark solid, m.p. 205°–207° (dec.), which decomposed on attempted recrystallization from chloroform, and some tars which could not be induced to crystallize.

To 39.4 g. (0.1 mole) of DPP· in 300 ml. of diethyl ether was added 2.95 g. (0.05 mole) of isopropylamine. Over a period of several days the reaction mixture became brown. The suspension was filtered and 31.1 g. of solid was collected. Concentration of the filtrate yielded an additional 2.65 g. of solid. Aliquots of this 33.75 g. of solid were chromatographed on alumina. Elution with benzene of a 5-g. sample led to the isolation of 4.15 g. (83% of sample, 71% yield) of DPPH, m.p. 171°–172° (dec.), whose color was red-brown rather than the characteristic red. Elution with ethanol yielded a second fraction, 0.25 g. of brown-black amorphous material which melted at 184°–200° (dec.). Recrystallization from ethanol-petroleum (b.p. 90°–100°) failed to improve the melting range.

*F. Diethylamine*

To 0.5 g. (0.00126 mole) of DPP· in 25 ml. of 95% ethanol was added 0.00069 mole of diethylamine in 5 ml. of ethanol. The solution turned brown over 24 hours and a reddish brown after 48 hours. Red crystals were slowly deposited over 4 weeks and were filtered to yield 0.27 g. (54%) of DPPH, m.p. 171°–172° (dec.), identified by mixed melting point. The filtrate was evaporated to dryness and the resulting red-brown gum was redissolved in benzene and chromatographed on alumina. Two fractions were obtained, one of which was 0.04 g. (8%) of crude DPPH, m.p. 154°–170° (dec.), and the second, 0.02 g., melted at 77°–115° (dec.).

Alternatively, 5.00 g. (0.0127 mole) of solid DPP· was treated with about 10 ml. of diethylamine, the excess amine acting as solvent. There was immediate effervescence, the mixture became warm, and the suspension turned brown. After 1 hour 50 ml. of chloroform was added to dissolve the solid which was present. The solution was concentrated and cooled and a total of 0.58 g. (11%) of black crystalline solid was filtered off. This material started to change color at 90° and by 115° was bright red. It finally melted at 171°–172° (dec.), and a mixed melting point with DPPH was not depressed. This material was identical in behavior to the 1:1 complex of DPPH and diethylamine described below.

The remainder of the filtrate was evaporated to dryness under reduced pressure to yield a red gum. Chromatography on alumina yielded 2.0 g. (40%) of DPPH, m.p. 170°–172° (dec.).

*Preparation and Identification of DPPH-Diethylamine Complex*

To a red solution of 1.00 g. (0.00252 mole) of DPPH in 70 ml. of acetone was added 10 ml. (0.10 mole) of diethylamine. To this dark opaque solution was added 800–900 ml. of water and after it was cooled to 4° for 16 hours, 0.71 g. (61%) of black crystals was filtered off. This material began to change to red at 100° and by 120° was completely bright red. It then melted at 170°–172° (dec.). This material was similar in all respects

to that described above and a mixed melting point was not depressed. This material is the 1:1 complex of DPPH and diethylamine as shown below:

A 0.40-g. (0.00085 mole) sample of the black complex was heated at 120°–140° for 20 minutes while air was passed over the solid and then bubbled into a known amount of standard acid. The acid was then back-titrated with base, which showed that 0.00084 mole of diethylamine had been collected. The residue, which was a light red solid, weighed 0.33 g. (0.00084 mole) and was shown to be DPPH, m.p. 170°–172° (dec.), by its melting point which was not depressed when admixed with authentic DPPH. Thus the black solid is a 1:1 complex of DPPH and diethylamine, and the diethylamine was recovered in 99% yield. A second experiment gave identical results.

When a small sample of the black complex was dissolved in a few milliliters of chloroform an opaque brown solution was obtained. On dilution, the solution gradually became a clear orange-brown color characteristic of solutions of DPPH. Addition of more diethylamine converted the color back to the opaque brown color. Similarly if the opaque brown solution was shaken with concentrated hydrochloric acid, the solution became a clear orange-brown or red color, depending on the concentration.

When solutions of the complex of approximately the same concentration were made up in ethanol, acetone, and chloroform, the more polar solvents produced darker, browner solutions. Addition of a polar solvent, e.g. ethanol, to the chloroform solution produced an even darker solution, indicating that the opaque brown color was intimately associated with the polar medium.

#### *Titration Experiments with DPP.*

##### *A. With Hydroxylamine*

Dilute standard solutions of DPP<sup>·</sup> and hydroxylamine (0.002–0.005 M) in benzene or in ethylene glycol monomethyl ether were prepared. Known volumes of the hydroxylamine solution were titrated with the DPP<sup>·</sup> solution to an end point where a permanent pale purple color persisted. Several runs gave the following values for the molar ratio of DPP<sup>·</sup> to hydroxylamine: 2.97, 2.88, 2.98, 2.96. Evaporation of these solutions to dryness gave impure material melting at 145–170° (dec.).

##### *B. Methylamine*

Similar experiments to those described above carried out in ethanol solution gave the following values for the molar ratio of DPP<sup>·</sup> to methylamine: 1.91, 2.05, 2.07, 1.97.

##### *C. Thiophenol*

To 0.75 g. (0.0019 mole) of DPP<sup>·</sup> in 10 ml. of chloroform was added slowly a 0.374 M solution of thiophenol in ethanol. The color changed rapidly from purple to opaque brown to clear red-brown during the addition of 2.6 ml. (0.00097 mole) (mole ratio 2:1) of the thiophenol solution. Evaporation to dryness and recrystallization from 1:3 chloroform–ethanol yielded 0.30 g. of orange-red solid which appeared to be identical in all respects to DPPH except that the material melted at 132–134° with decomposition. A similar behavior has been previously described (7). Recrystallization failed to improve the melting point markedly. The material was chromatographed on alumina, and elution with benzene and then 1:1 benzene–chloroform yielded the following fractions, with their respective melting points: (1) 0.09 g. (12%), 172–173° (dec.), identified as DPPH by mixed melting point; (2) 0.05 g., 160–164° (dec.); (3) 0.03 g., 150–153° (dec.); (4) 0.05 g., 131–139° (dec.). Recrystallization failed to improve the melting points of the impure fractions.

When an identical run to that above was carried out except that the DPP<sup>·</sup> was dis-

solved in 100 ml. of chloroform and 50 ml. of ethanol, and the thiophenol solution was diluted 20-fold, 72 ml. (0.00133 mole) of thiophenol (mole ratio 1.43:1) was required to produce a clear orange-brown end point. The products isolated were similar to those described above, and DPPH was obtained in 14% yield.

When approximately 0.01 M solutions of the reagents were titrated against one another the mole ratios of radical to mercaptan were 1.09-1.16 when thiophenol was added to DPP<sup>·</sup>, and 1.00 when the DPP<sup>·</sup> was added to the thiophenol solution.

#### D. Butyl Mercaptan

To 0.20 g. (0.0005 mole) of DPP<sup>·</sup> in 25 ml. of chloroform was added 0.00061 mole of butyl mercaptan in 25 ml. of ethanol. The color changed from purple through opaque red-brown to clear orange-red over a few seconds. The solution was concentrated to yield, after recrystallization, 0.15 g. (75%) of DPPH, m.p. 169-172° (dec.), identified by mixed melting point.

When dilute (0.02 M) solutions of DPP<sup>·</sup> and butyl mercaptan were titrated against one another as described above the moles of radical per mole of mercaptan varied between 1.0 and 1.15, depending on the concentration, but the ratio did not seem to depend on the order of addition of the reagents.

#### Gas Evolution Experiments

In experiments in which gas evolution was quantitatively determined, the 50 ml. reaction vessel, equipped with magnetic stirrer and maintained at constant temperature by a water bath, was connected by capillary tubing to a 50-ml. burette filled with mercury which was attached to a mercury levelling bulb. The general procedure was as follows. In experiments in which it was established that nitrogen was evolved, all solutions were presaturated with nitrogen. The DPP<sup>·</sup> dissolved in the major portion of the solvent (concentration approximately 10 ml. per g.) was placed in the reaction flask, the system was closed off, and the solution was stirred and allowed to reach equilibrium. Then the hydrogen donor solution (sufficiently concentrated that the volume added was not more than 20% of the total volume of the system) was admitted from a 5-cc. burette which was attached to the reaction vessel through a ground-glass joint. The mercury levelling bulb was continually adjusted to maintain atmospheric pressure in the reaction flask.

The hydrogen donor solutions were added in arbitrary amounts in the cases of hydrazine and ammonia, after which the volume of gas evolved was measured, or else the hydrogen donor solution was added dropwise until a clear orange-brown end point was obtained, and significant changes in the volume of gas evolved ceased.

Tables I and II summarize the results obtained from a variety of hydrogen donors.

#### REFERENCES

1. AUDRIETH, L. F. and OGG, B. A. *The chemistry of hydrazine*. John Wiley & Sons, Inc., New York, N.Y. 1951. p. 48.
2. BOOTH, H. S. *Inorganic syntheses*. Vol. I. McGraw-Hill Book Company Inc., New York, N.Y. 1939. p. 87.
3. BRAUDE, E. A., BROOK, A. G., and LINSTEAD, R. P. *J. Chem. Soc.* 3574 (1954).
4. GOLDSCHMIDT, S. and RENN, K. *Ber.* **55**, 628 (1922).
5. LYONS, J. A. and WATSON, W. F. *J. Polymer Sci.* **18**, 141 (1955).
6. POIRIER, R. H., KAHLER, E. J., and BENNINGTON, F. *J. Org. Chem.* **17**, 1437 (1952).
7. RUSSELL, K. E. *J. Phys. Chem.* **58**, 437 (1954).
8. WEISS, J. *J. Chem. Soc.* 245 (1942).

## EXCHANGE BETWEEN THALLOUS AND THALLIC IONS IN THE PRESENCE OF SULPHATE ION<sup>1</sup>

D. R. WILES

### ABSTRACT

The rates of the exchange reaction between thallous and thallic ions have been measured as a function of sulphate ion concentration, at constant acidity. At high sulphate concentrations, the results agree with those of Brubaker and Mickel, indicating second- and higher-order dependence of the rate on sulphate ion concentration. At low sulphate concentrations, pure first-order dependence on sulphate is found. The inhibitive effect found in some systems is absent. A bridge-transfer mechanism is suggested.

### INTRODUCTION

The exchange between thallous and thallic ions in aqueous solution has been studied during the past several years by a number of workers, under a variety of conditions (1, 2, 3, 4, 5). It has generally been found that any change in the nature or number of ligands attached to one or other of the exchanging ions has a distinct effect on the rate of the exchange reaction. This effect amounts, in the case of most of the anionic ligands studied (e.g. hydroxyl, nitrate), to a positive catalysis of the reaction. In other cases (e.g. chloride and cyanide) the exchange rate is markedly decreased at low concentrations of the anion and very greatly increased at higher concentrations.

The present work is an investigation of the nature of the kinetics of the thallous-thallic exchange in perchloric acid solutions containing varying small concentrations of sulphate ion. This work is complementary to that of Brubaker and Mickel (1), who have reported recently on this exchange in somewhat stronger sulphate solutions.

### EXPERIMENTAL

Thallous perchlorate was crystallized from a solution of reagent grade thallous nitrate to which had been added a considerable excess of perchloric acid. Crystallization was repeated once from strong perchloric acid, and once from water. Ferric ion was added to the solution of these crystals, and precipitated as hydroxide with ammonia. The thallous perchlorate was twice more crystallized from water, dried for 1 hour at 105°, and dissolved in water to make a stock solution 0.100 molar in thallous ion. This solution showed no darkening on neutralization, which indicated negligible contamination by thallic ion.

The thallic perchlorate solution was prepared from reagent grade thallic oxide which had, in turn, been purified of thallous ion by repeated precipitation with ammonia and redissolution in excess perchloric acid. The purified thallic oxide was dissolved in an excess of perchloric acid, to make a stock solution 0.100 molar in thallic ion, and 4.7 molar in excess acid. Radioactive Tl<sup>204</sup> in the form of a solution of thallic nitrate was added at an early stage in the purification. Failure to show turbidity on addition of iodide to an aliquot of this stock solution set the limiting concentration of thallous ion at <<0.004 molar, i.e. <<4%. In both these preparations, heating of solutions was kept to a low minimum because of the danger that some chloride ion might be formed as a decomposition product of perchloric acid. Analysis of the solutions was done by precipitation of thallous chromate, which was dried and weighed as such. All other reagents were reagent grade, and were used with no further purification.

<sup>1</sup>Manuscript received September 23, 1957.

Contribution from the Department of Mining and Metallurgy, University of British Columbia, Vancouver, B.C. Paper presented at the Annual Conference of the Chemical Institute of Canada, June, 1957.

Exchange measurements were done by using the radioactive tracer as thallium(III) and observing its appearance in the thallous state. Separation of the thallous ion from the reaction mixture was done by the method of Prestwood and Wahl (5) using sodium chromate as precipitating agent, in an alkaline cyanide medium to prevent precipitation of thallic species. The thallous chromate precipitate was filtered onto tared filter disks, dried, weighed, and mounted on cards with cellulose tape. Counting of these radioactive samples was done with an end-window proportional counter, using a flowing methane-argon gas mixture.

Solutions for exchange measurements were made up to 0.010 M in each of thallic and thallous species, and 3.12 M in total acid (i.e.  $[H_2SO_4] + [HClO_4] = 3.12$ ).<sup>a</sup> Solutions were made complete but for the thallous ion, and allowed to come to equilibrium with the constant temperature bath before addition of the thallous solution.

The errors involved in this type of work are very difficult to assess. Constancy in the weights of the samples counted made correction for back-scattering and self-absorption unnecessary. Observed activities in these samples are estimated to be in error by no more than 5%. The standard deviation of the measured specific activities of the "infinite time" samples was  $\pm 2\%$ . It is thus likely that individual rate measurements are, in general, accurate to about  $\pm 10\%$ , and internally consistent to  $\pm 5\%$ .

#### RESULTS AND DISCUSSION

The results of the kinetic studies of the exchange are given in Table I.

Data plotted for the complete range of sulphate concentrations studied are shown in Fig. 1. These data show that the over-all dependence on sulphate concentration is

TABLE I  
THALLOUS-THALLIC EXCHANGE RATES  
 $[Tl(I)] = [Tl(III)] = 0.010 M$

$[SO_4^{2-}]^a$	$[H^+]^a$	$\mu^a$	24.2° C.	37.2° C.	50.0° C.	Rate $\times 10^7$ (moles l. <sup>-1</sup> sec. <sup>-1</sup> ) <sup>b</sup>
0.0000	3.12	3.12	0.064	0.18	0.50	
0.0060	3.13	3.13	0.10		0.70	
0.0067	3.13	3.13		0.28		
0.015	3.14	3.14	0.16	0.44		
0.021	3.14	3.15			1.46	
0.030	3.15	3.17	0.26	0.70		
0.047	3.17	3.19	0.35	0.97	2.7	
0.093	3.21	3.26	0.74	1.7	4.8	
0.158	3.28	3.36	1.1	2.9	5.3	
0.276	3.40	3.56		5.2	12.4	
0.39	3.50	3.72		6.2	19.6	
0.49	3.61	3.86		10.5		

<sup>a</sup>The values of  $[SO_4^{2-}]$ ,  $[H^+]$ , and  $\mu$  were computed using the data of Smith (6) for the dissociation of  $H_2SO_4$ . For values of  $[SO_4^{2-}] < 0.05$  the variations in  $[H^+]$  and  $\mu$  are  $< 2\%$ , and are likely insignificant.

<sup>b</sup>Rate ( $R$ ) =  $[Tl(III)][Tl(I)] / ([Tl(III)] + [Tl(I)]) \cdot 0.693/t_1$ . For the concentrations used in the present work,  $R = 5 \times 10^{-3} \cdot 0.693/t_1$ .

\*Consideration of  $H_2SO_4$  as effectively monobasic, for purposes of determining ionic strength, was based upon widely used but evidently inapplicable dissociation data. The author is very grateful to Dr. C. H. Brubaker for drawing attention to work by Smith (6), who has measured the concentration of the various species in sulphuric acid solutions over a wide range of ionic strength. At the ionic strengths used in the present work, Smith indicates a value of 1.3 for the dissociation constant of the bisulphate ion. The present work was, unfortunately, completed without reference to the more recent values. Values of the sulphate concentration reported in this paper were recalculated in accordance with Smith's data. Only at sulphate concentrations of greater than 0.1 M will the ionic strength and acidity vary significantly from the intended 3.12 M.

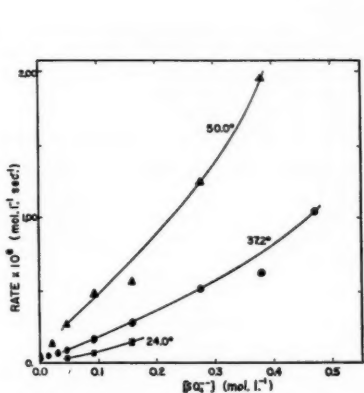


FIG. 1. Thallous-thallic exchange rates.

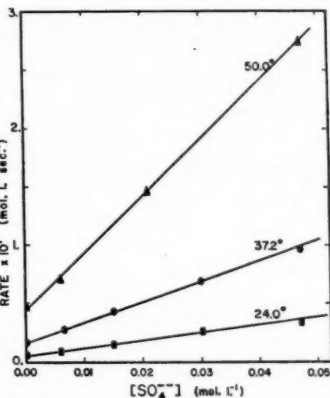


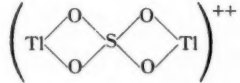
FIG. 2. Thallous-thallic exchange rates at low sulphate concentration.

greater than the first order. This is in agreement with the results of Brubaker and Mickel (1) and indicates that more than one ligand takes part in the rate-determining step.

In Fig. 2 are plotted the exchange data for low values of the sulphate concentration. In this range, the dependence is linear, and the participation of only one sulphate group is indicated at these low sulphate concentrations.

Perhaps the most significant characteristic of the present rate curves is that they do not show the strong negative effect (inhibition) on the exchange found in the chloride (3) and cyanide (4) systems. The sulphate system seems in this respect more to resemble the nitrate (5) system.

From the above results and from the known (1) first-order dependence on each of Tl(III) and Tl(I), it can be inferred that the activated complex contains one ion of each of thallous, thallic, and sulphate. Following the suggestions of Taube (7) and others, in other cases, it seems reasonable that the actual activated complex might well be a bridge type of structure:



in which case the transfer of two electrons arises from the transfer of a sulphate radical from one thallium atom to the other. This same bridge-transfer mechanism would very likely also be applicable in the case of the more highly complexed species at higher sulphate concentrations.

It is important to point out that the above mechanism is not the only one consistent with the kinetics. Others might be: rapid dissociation of the thallic sulphate complex into a thallous ion and a neutral sulphate radical, dissociation of the bridge structure without transfer of sulphate, direct transfer of electrons by barrier penetration, and still others. The bridge-transfer mechanism seems to be the most attractive of these.

#### ACKNOWLEDGMENTS

The author is grateful to Drs. R. W. Dodson and J. Halpern for helpful comments, and to the National Research Council for financial support.

## REFERENCES

1. BRUBAKER, C. H. and MICHEL, J. P. *J. Inorg. & Nuclear Chem.* **4**, 55 (1957).
2. DODSON, R. W. *J. Am. Chem. Soc.* **75**, 1795 (1953).
3. HARBOTTE, G. and DODSON, R. W. *J. Am. Chem. Soc.* **73**, 2442 (1951).
4. PENNA-FRANCA, E. and DODSON, R. W. *J. Am. Chem. Soc.* **77**, 2651 (1955).
5. PRESTWOOD, R. J. and WAHL, A. C. *J. Am. Chem. Soc.* **71**, 3137 (1949).
6. SMITH, H. M. Raman spectral study of the dissociation of sulfuric acid in aqueous solution at 25° C. Ph.D. Thesis, University of Chicago. 1950.
7. TAUBE, H., MYERS, H., and RICH, R. L. *J. Am. Chem. Soc.* **75**, 4118 (1953).

# THE SYSTEMS $\text{Li}_2\text{SO}_4$ - $\text{K}_2\text{SO}_4$ - $\text{H}_2\text{O}$ AND $\text{Li}_2\text{SO}_4$ - $\text{Na}_2\text{SO}_4$ - $\text{H}_2\text{O}$ AT 25° C.<sup>1</sup>

A. N. CAMPBELL AND E. M. KARTZMARK

## ABSTRACT

The 25° isotherm of the system  $\text{Li}_2\text{SO}_4$ - $\text{K}_2\text{SO}_4$ - $\text{H}_2\text{O}$  shows the existence of the double salt,  $\text{Li}_2\text{SO}_4 \cdot \text{K}_2\text{SO}_4$ , whereas that of the system  $\text{Li}_2\text{SO}_4$ - $\text{Na}_2\text{SO}_4$ - $\text{H}_2\text{O}$  yields no double salt but extensive solid solution of lithium sulphate in sodium sulphate. On the other hand, a study at 39.5° C. of the latter system shows that the double salt,  $\text{Li}_2\text{SO}_4 \cdot \text{Na}_2\text{SO}_4$ , does form at this temperature, accompanied as before by solid solution of lithium sulphate in sodium sulphate. The transition temperature for the reaction



is 29.3° C. A further transition, of unknown nature, occurs between 49° and 57°.

This paper is the second stage in our study of the system containing the radicals  $\text{Li}_2$ ,  $\text{Na}_2$ ,  $\text{K}_2$ ,  $\text{Cl}_2$ ,  $\text{SO}_4$ , and water. Our first paper (1) dealt with the system  $\text{LiCl}$ - $\text{NaCl}$ - $\text{KCl}$ - $\text{H}_2\text{O}$  at 25° C. The corresponding system involving the sulphates is  $\text{Li}_2\text{SO}_4$ - $\text{Na}_2\text{SO}_4$ - $\text{K}_2\text{SO}_4$ - $\text{H}_2\text{O}$ . The component ternary systems are  $\text{Li}_2\text{SO}_4$ - $\text{Na}_2\text{SO}_4$ - $\text{H}_2\text{O}$ ,  $\text{Li}_2\text{SO}_4$ - $\text{K}_2\text{SO}_4$ - $\text{H}_2\text{O}$ , and  $\text{Na}_2\text{SO}_4$ - $\text{K}_2\text{SO}_4$ - $\text{H}_2\text{O}$ . The system  $\text{Na}_2\text{SO}_4$ - $\text{K}_2\text{SO}_4$ - $\text{H}_2\text{O}$  has been investigated by various workers. A complete bibliography is given by Hamid (2). A double salt, glaserite or Penny's salt, is formed, having the composition  $3\text{K}_2\text{SO}_4 \cdot \text{Na}_2\text{SO}_4$ . This double salt, however, while it is incapable of forming solid solutions with potassium sulphate, does so, at 25°, to some extent with sodium sulphate. Thus, according to Hamid, the two isothermally invariant ternary solutions, at 25°, are in equilibrium respectively with pure double salt and potassium sulphate and with Glauber's salt and the solid solution of sodium sulphate in double salt.

The systems  $\text{Li}_2\text{SO}_4$ - $\text{K}_2\text{SO}_4$ - $\text{H}_2\text{O}$  and  $\text{Li}_2\text{SO}_4$ - $\text{Na}_2\text{SO}_4$ - $\text{H}_2\text{O}$  have not previously been investigated, although Nacken (3) has investigated the equilibrium diagram of the anhydrous systems  $\text{Li}_2\text{SO}_4$ - $\text{K}_2\text{SO}_4$  and  $\text{Li}_2\text{SO}_4$ - $\text{Na}_2\text{SO}_4$ . He finds that the former system gives rise to the congruently melting compound  $\text{Li}_2\text{SO}_4 \cdot \text{K}_2\text{SO}_4$  and the latter to the compound  $\text{Li}_2\text{SO}_4 \cdot \text{Na}_2\text{SO}_4$ , which cannot exist in equilibrium with the melt. Scacchi (4) and Traube (5) have also obtained  $\text{Li}_2\text{SO}_4 \cdot \text{Na}_2\text{SO}_4$  by crystallization of hot solutions of lithium and sodium sulphates.\*

## EXPERIMENTAL TECHNIQUE

The technique of solubility determinations is too well known to merit description here but something must be said about the methods of analysis. The only really practical method of determining sulphate radical, viz. barium sulphate precipitation, is notoriously unreliable, particularly in solutions containing alkali ions. Although we used this method we thought it necessary to support it by the use of a purely physical method and for this purpose we chose viscosity. All density and viscosity determinations were made on solutions containing 10 or 20 g. total anhydrous salt in 100 ml. of solution.

<sup>1</sup>Manuscript received September 13, 1957.

Contribution from the Chemistry Department, University of Manitoba, Winnipeg, Manitoba.

\*NOTE ADDED IN PROOF.—A paper by L. Cavalca and M. Nardelli (*Gazz. chim. ital.* **82**, 394-405 (1952)) has just come to hand, in which they have studied the system  $\text{Li}_2\text{SO}_4$ - $\text{Na}_2\text{SO}_4$ - $\text{H}_2\text{O}$  at 27° and 45.8° C. They agree with us in finding that the double salt  $\text{Na}_2\text{SO}_4 \cdot \text{Li}_2\text{SO}_4$  does not exist at 27° though it does at 45.8° C. In addition, however, they claim the existence of a double salt  $\text{Na}_2\text{Li}(\text{SO}_4)_2 \cdot 6\text{H}_2\text{O}$ . The existence of such a salt would require that the tie-lines intersect in the body of the diagram and this we feel to be impossible. We point out, in this connection, that prolonged and vigorous stirring is necessary to ensure the attainment of equilibrium.

## EXPERIMENTAL RESULTS

The results for the system  $\text{Li}_2\text{SO}_4\text{-K}_2\text{SO}_4\text{-H}_2\text{O}$  are shown in Tables I and II. Those for the system  $\text{Li}_2\text{SO}_4\text{-Na}_2\text{SO}_4\text{-H}_2\text{O}$  at 25° C. are shown in Tables III, IV, and V.

TABLE I  
DENSITIES AND VISCOSITIES OF SOLUTIONS OF LITHIUM  
SULPHATE AND POTASSIUM SULPHATE, CONTAINING 10 G.  
ANHYDROUS SALT IN 100 ML. SOLUTION, AT 25° C.

Composition	Density, g./ml.	Relative viscosity ( $\text{H}_2\text{O} = 1$ )
10 g. $\text{Li}_2\text{SO}_4$	1.0780	1.6141
10 g. $\text{K}_2\text{SO}_4$	1.0736	1.1316
5 g. $\text{Li}_2\text{SO}_4$ , 5 g. $\text{K}_2\text{SO}_4$	1.0757	1.3460
7 g. $\text{Li}_2\text{SO}_4$ , 3 g. $\text{K}_2\text{SO}_4$	1.0766	1.4347
3 g. $\text{Li}_2\text{SO}_4$ , 7 g. $\text{K}_2\text{SO}_4$	1.0749	1.2602

TABLE II  
COMPOSITIONS OF SOLUTIONS AND "WET" SOLID PHASES AT 25° C.

Liquid phase	Solid phase				Nature of solid phase
Wt. % $\text{Li}_2\text{SO}_4$	Wt. % $\text{K}_2\text{SO}_4$	Wt. % $\text{Li}_2\text{SO}_4$	Wt. % $\text{K}_2\text{SO}_4$		
25.5	—	—	—	—	$\text{Li}_2\text{SO}_4\text{-H}_2\text{O}$
25.8	0.2	—	—	—	$\text{Li}_2\text{SO}_4\text{-H}_2\text{O}$
26.0	0.4	71.2	0.1	—	$\text{Li}_2\text{SO}_4\text{-H}_2\text{O}$
26.7	2.3	61.3	16.8	—	$\text{Li}_2\text{SO}_4\text{-H}_2\text{O}$ + double salt
26.5	2.2	51.7	21.9	—	$\text{Li}_2\text{SO}_4\text{-H}_2\text{O}$ + double salt
26.5	2.4	37.0	45.0	—	Double salt
24.6	2.8	35.8	46.0	—	"
18.1	4.1	34.0	42.8	—	"
12.1	9.2	35.1	55.5	—	"
12.0	9.2	32.0	49.0	—	"
11.9	9.0	31.6	48.1	—	"
11.0	10.3	25.4	61.2	—	Double salt + $\text{K}_2\text{SO}_4$
10.6	10.7	8.8	65.0	—	$\text{K}_2\text{SO}_4$
8.5	10.1	7.4	63.6	—	$\text{K}_2\text{SO}_4$
5.1	10.2	4.1	76.2	—	$\text{K}_2\text{SO}_4$
4.4	9.9	3.7	72.7	—	$\text{K}_2\text{SO}_4$
—	10.7	—	—	—	$\text{K}_2\text{SO}_4$

TABLE III  
DENSITIES AND VISCOSITIES OF SOLUTIONS OF LITHIUM  
SULPHATE AND SODIUM SULPHATE, CONTAINING 20 G.  
ANHYDROUS SALT IN 100 ML. OF SOLUTION, AT 25° C.

Compositions		Density, g./ml.	Relative viscosity ( $\text{H}_2\text{O} = 1$ )
$\text{Li}_2\text{SO}_4$	$\text{Na}_2\text{SO}_4$		
0.0	20	1.1608	1.9057
2	18	1.1600	1.9699
4	16	1.1591	2.0369
8	12	1.1575	2.1817
10	10	1.1567	2.2552
14	6	1.1551	2.4231
16	4	1.1542	2.5163
18	2	1.1534	2.6125
20	0	1.1526	2.7016

## DISCUSSION

The results of Table II are plotted in Fig. 1. It is obvious that the expected double salt,  $\text{Li}_2\text{SO}_4 \cdot \text{K}_2\text{SO}_4$ , is stable at 25° C., although the solution is not congruently saturating; the pure anhydrous double salt decomposes when treated with water to give a mixture of double salt and potassium sulphate. The figure also shows some solid solubility of lithium sulphate in potassium sulphate and of lithium sulphate in double salt.

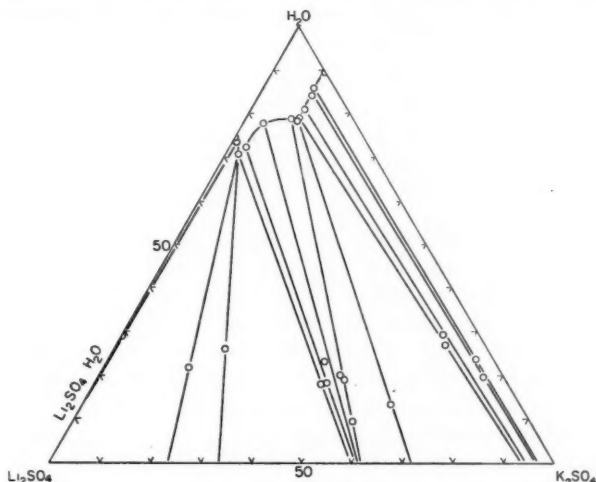


FIG. 1. The system  $\text{Li}_2\text{SO}_4-\text{K}_2\text{SO}_4-\text{H}_2\text{O}$  at 25° C.

The figures of Table IV are plotted in Fig. 2. Rather surprisingly, no double salt forms at 25° C. but there is extensive solid solubility of lithium sulphate in sodium sulphate,

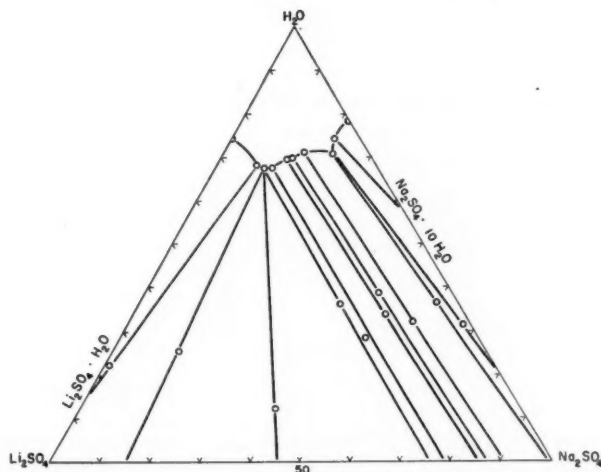


FIG. 2. The system  $\text{Li}_2\text{SO}_4-\text{Na}_2\text{SO}_4-\text{H}_2\text{O}$  at 25° C.

TABLE IV  
COMPOSITIONS OF SOLUTIONS AND "WET" SOLID PHASES IN WT. % AT 25.0° C.

Liquid		"Wet" solid		Nature of solid phase
Na <sub>2</sub> SO <sub>4</sub>	Li <sub>2</sub> SO <sub>4</sub>	Na <sub>2</sub> SO <sub>4</sub>	Li <sub>2</sub> SO <sub>4</sub>	
—	25.5	—	—	Li <sub>2</sub> SO <sub>4</sub> . H <sub>2</sub> O
8.0	23.8	0.9	76.7	"
9.9	22.4	13.2	60.8	Li <sub>2</sub> SO <sub>4</sub> . H <sub>2</sub> O + solid solution
9.7	22.8	39.7	48.7	"
9.2	22.9	40.2	23.7	Homogeneous solid solution
11.3	20.8	49.0	22.5	"
14.2	15.7	47.0	14.5	"
15.9	12.9	56.8	11.0	"
21.9	7.8	59.4	4.0	"
22.0	7.0	67.0	1.3	Na <sub>2</sub> SO <sub>4</sub> + Na <sub>2</sub> SO <sub>4</sub> . 10H <sub>2</sub> O
20.4	5.1	41.7	Trace	Na <sub>2</sub> SO <sub>4</sub> . 10H <sub>2</sub> O
21.7	—	—	—	"

to the extent of, say, 25% lithium sulphate by weight. Because of the difference in crystal structure of lithium sulphate and  $\beta$ -Na<sub>2</sub>SO<sub>4</sub>, and of the difference in ionic radii of the lithium and sodium ions (6), this result surprised us and we verified it with some care. In one case, a very small solid phase was vigorously stirred with solution for 3 weeks, to ensure true equilibrium, before analysis. We have therefore no doubt of the fact, however surprising it may be. According to Nacken (3), solid  $\alpha$ -Na<sub>2</sub>SO<sub>4</sub> dissolves extensively in solid  $\alpha$ -Li<sub>2</sub>SO<sub>4</sub> at temperatures between 600° C. and 850° C., while  $\alpha$ -Li<sub>2</sub>SO<sub>4</sub> does not dissolve at all (in the solid state) in  $\alpha$ -Na<sub>2</sub>SO<sub>4</sub>. We now find that, in the neighborhood of room temperature, Li<sub>2</sub>SO<sub>4</sub> dissolves extensively in  $\beta$ -Na<sub>2</sub>SO<sub>4</sub>. The question of whether  $\beta$ -Na<sub>2</sub>SO<sub>4</sub> dissolves in (anhydrous)  $\beta$ -Li<sub>2</sub>SO<sub>4</sub> cannot be answered by this study, because the equilibrium lithium sulphate solid phase is always the monohydrate.

Since the literature indicated, beyond all reasonable doubt, that the double salt, Li<sub>2</sub>SO<sub>4</sub>. Na<sub>2</sub>SO<sub>4</sub>, does form from hot solution, there must be a transition temperature for the reaction:



Accordingly, a dilatometric experiment was carried out, using a bulb charged with a moist equimolar mixture of lithium and sodium sulphates and *m*-xylene as indicator fluid. A marked expansion was observed at 30.0° C. and a less distinct expansion between 49.6° C. and 56.6° C. This was checked by determination of total solubility of an equimolar mixture of lithium and sodium sulphates. The results were:

Temperature, °C.	Total solubility in wt. %
25	29.0
28.5	32.1
31.4	32.8
39.8	33.3
50.1	34.0
60.3	34.0
67.7	32.3

When the above figures are plotted as total solubility versus temperature, sharp breaks are observed at 29.3° C. and 57.5° C. We did not pursue further the question of the nature of the higher temperature transition.

After determining the transition temperature to be 29.3° C., we undertook the study of the 39.5° C. isotherm. When the data of Table V are plotted (Fig. 3) in the usual

TABLE V  
COMPOSITIONS OF SOLUTIONS AND "WET" SOLID PHASES IN WT. % at 39.5° C.

Liquid		"Wet" solid		Nature of solid phase
Na <sub>2</sub> SO <sub>4</sub>	Li <sub>2</sub> SO <sub>4</sub>	Na <sub>2</sub> SO <sub>4</sub>	Li <sub>2</sub> SO <sub>4</sub>	
—	25.0	—	—	Li <sub>2</sub> SO <sub>4</sub> ·H <sub>2</sub> O
5.8	22.6	1.8	70.0	Li <sub>2</sub> SO <sub>4</sub> ·H <sub>2</sub> O + double salt
9.0	23.4	27.5	43.0	"
9.3	22.7	22.3	50.6	"
12.2	20.1	41.5	38.5	Double salt
14.7	18.3	38.6	35.0	"
17.0	15.7	43.0	34.5	"
17.0	15.5	51.8	28.2	Double salt + solid solution
17.2	15.4	48.5	19.1	Solid solution
20.2	12.3	52.5	14.5	"
27.4	6.7	68.0	9.1	"
32.5	—	—	—	Na <sub>2</sub> SO <sub>4</sub> , anhydrous

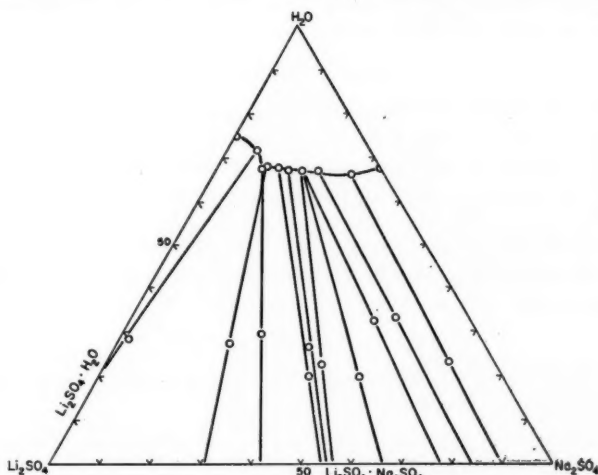


FIG. 3. The system Li<sub>2</sub>SO<sub>4</sub>-Na<sub>2</sub>SO<sub>4</sub>-H<sub>2</sub>O at 39.5° C.

way, it is apparent that the double salt, Li<sub>2</sub>SO<sub>4</sub>·Na<sub>2</sub>SO<sub>4</sub>, does indeed form although the region of its existence in contact with solution is small. Like the corresponding lithium-potassium double salt, it is incongruently saturating. The fact that the double salt of lithium-sodium is not stable at room temperature may account for some of the crystallographic difficulties encountered by Traube (5).

#### REFERENCES

- CAMPBELL, A. N. and KARTZMARK, E. M. Can. J. Chem. **34**, 672 (1956).
- HAMID, M. A. J. Chem. Soc. 201 (1926).
- NACKEN, R. Neues Jahrb. Mineral. Paläontol., Beilage Bd. **24**, 32 (1907).
- SCACCHI, A. Atti Accad. sci. fis. mat. Napoli, **3** (No. 27), 31 (1868).
- TRAUBE, H. Neues Jahrb. Mineral., Geol. u. Paläontol. **II**, 62 (1892).
- WELLS, A. F. Structural inorganic chemistry. 2nd ed. Oxford University Press, London. 1950. pp. 70 and 386.

# PHOTOLYSIS OF ACETONE IN THE PRESENCE OF METHYL-d<sub>3</sub> ACETATE<sup>1</sup>

M. H. J. WIJNEN

## ABSTRACT

The photolysis of acetone in the presence of CH<sub>3</sub>COOCD<sub>3</sub> has been carried out over the temperature range 151° to 274° C., at different ratios of acetone to methyl acetate and at different light intensities. As activation energies for the abstraction reactions



and



were obtained E<sub>a</sub> = 10 ± 0.5 kcal. and E<sub>a</sub> = 14 ± 1 kcal.

## INTRODUCTION

Direct photolysis of CH<sub>3</sub>COOCH<sub>3</sub> (5) and CH<sub>3</sub>COOCD<sub>3</sub> (6), recently undertaken at this laboratory, indicated a considerable difference in activation energy between the abstraction of a hydrogen atom from the acetyl group and the abstraction of a hydrogen or deuterium atom from the methoxy group in methyl acetate by methyl radicals. In order to study these abstraction reactions in a relatively simple system, acetone was photolyzed in the presence of CH<sub>3</sub>COOCD<sub>3</sub>.

## EXPERIMENTAL

The apparatus and technique were mainly the same as described elsewhere (7). The storage vessels containing acetone and methyl acetate were separated from the reaction vessel by mercury cutoffs. In order to prevent absorption by methyl acetate, the light of the S-500 medium pressure arc was filtered through Corning filter 9700, transparent above 2600 Å. The trideuteromethyl acetate was obtained from New England Nuclear Corporation. Mass spectrometric analysis showed it to contain at least 98% of CH<sub>3</sub>COOCD<sub>3</sub>. The acetone was obtained from Celanese Chemcel plant and was distilled once *in vacuo* before use.

## RESULTS AND DISCUSSION

The results of the experiments carried out at various temperatures for various mixtures of acetone and methyl acetate are given in Table I.

The use of acetone as a source of methyl radicals to study hydrogen abstraction reactions is well established. The following reactions are, therefore, proposed to explain the methane and ethane formation when acetone is photolyzed in the presence of CH<sub>3</sub>COOCD<sub>3</sub> at temperatures above 140° C.:



The following equations may be derived from this reaction mechanism:

$$R_{\text{CH}_4}/(R_{\text{C}_2\text{H}_6}^{\frac{1}{2}}[\text{Ac}]) = k_1/k_4^{\frac{1}{2}} + k_2/k_4^{\frac{1}{2}}[\text{MeAc}]/[\text{Ac}] \quad [I]$$

$$R_{\text{CH}_3\text{D}}/(R_{\text{C}_2\text{H}_6}^{\frac{1}{2}}[\text{MeAc}]) = k_3/k_4^{\frac{1}{2}} \quad [II]$$

$$R_{\text{CH}_4}/R_{\text{CH}_3\text{D}} = k_2/k_3 + k_1/k_3[\text{Ac}]/[\text{MeAc}] \quad [III]$$

<sup>1</sup>Manuscript received August 15, 1957.

Contribution from the Chemical Division, Research and Development Laboratories, Celanese Corporation of America, Clarkwood, Texas.

TABLE I  
PHOTOLYSIS OF  $\text{CH}_3\text{COCH}_3$  IN THE PRESENCE OF  $\text{CH}_3\text{COOCD}_3$

Expt. No.	Temp., °C.	$[\text{Ac}]_i$ , $\times 10^{-17}$ molecules/cc.	$[\text{MeAc}]_i$ , $\times 10^{-17}$ molecules/cc.	In molecules/(sec. cc.) $\times 10^{-12}$				
				$R_{\text{CH}_4}$	$R_{\text{CH}_3\text{D}}$	$R_{\text{C}_2\text{H}_6}$	$R_{\text{CO}}$	$10^{14}k_3/k_4^{1/2}$
1	151	13.60	—	5.42	—	13.45	17.93	—
2	"	11.90	9.90	5.02	—	11.69	16.30	—
3	"	13.02	14.58	5.63	—	12.00	17.25	—
4	"	10.20	19.50	4.73	—	10.07	14.12	—
5	"	10.43	23.22	5.10	0.07	10.36	14.32	0.94
14	"	7.98	24.12	0.73	0.01	0.22	0.76	0.98
15	"	10.10	32.10	5.00	0.10	7.77	11.50	1.11
16	"	10.08	31.67	2.08	0.03	1.41	2.88	0.81
19	176	15.70	13.80	1.90	0.01	0.25	1.48	1.63
20	"	10.38	17.37	10.53	0.11	9.85	18.10	2.09
21	"	8.15	28.25	7.08	0.15	5.30	10.90	2.28
22	"	9.20	20.30	7.18	0.11	6.22	11.85	2.23
6	208	7.57	4.72	11.80	0.11	6.40	15.50	9.36
7	"	8.90	10.21	16.60	0.23	6.47	18.40	8.84
8	"	8.20	—	11.32	—	6.95	15.50	—
9	"	5.68	10.98	9.58	0.20	4.10	11.70	9.00
17	"	7.62	19.76	13.80	0.31	4.25	13.82	7.55
18	"	5.35	20.83	3.75	0.10	0.50	2.96	9.06
10	274	9.52	6.78	26.20	0.44	2.16	19.20	44.2
11	"	8.12	16.08	24.65	0.84	1.83	18.35	39.0
12	"	9.40	—	21.20	—	2.05	16.35	—
13	"	8.50	20.00	26.68	1.32	2.41	21.95	42.6
23	"	8.09	23.59	20.22	0.92	1.20	15.15	35.8
24	"	16.38	7.25	36.20	0.42	1.70	23.45	44.4
25	"	6.67	20.58	17.90	0.93	1.14	12.60	42.5

The results obtained for  $k_3/k_4^{1/2}$  via equation [II] are given in Table I. Within experimental error constant values were obtained for  $k_3/k_4^{1/2}$  at constant temperatures. A plot of  $\log k_3/k_4^{1/2}$  against  $1/T$  in Fig. 2 gives an activation energy difference of  $E_3 - \frac{1}{2}E_4 = 14 \pm 1$  kcal.

Equation [I] is plotted in Fig. 1. The data show good agreement with the proposed reaction mechanism. The intercepts of the lines in Fig. 1 give values of  $k_1/k_4^{1/2}$ . These values may also be obtained by photolysis of acetone alone. At three temperatures, runs were carried out photolyzing acetone alone. Values thus obtained are indicated on the ordinate of Fig. 1 and coincide within experimental error with the intercepts obtained by plotting equation [I].

From the slopes of the lines in Fig. 1 we obtain the values of  $k_2/k_4^{1/2}$  reported in Table II. A plot of  $\log k_2/k_4^{1/2}$  against  $1/T$  is shown in Fig. 2, together with data obtained for  $k_2/k_4^{1/2}$  by direct photolysis of  $\text{CH}_3\text{COOCD}_3$  (6). From the slope of this plot an activation energy of  $E_2 = 10 \pm 0.5$  kcal. is obtained, assuming  $E_4 = 0$  kcal. Plots of equation [III] at 208° and 274° C. give the following values for  $k_2/k_3$  and  $k_1/k_3$ :  $k_2/k_3 = 23$  and  $k_1/k_3 = 54$  at 208° C.,  $k_2/k_3 = 8$  and  $k_1/k_3 = 37$  at 274° C. Small errors in the determination of  $R_{\text{CH}_3\text{D}}$  at low temperatures have a large effect on the ratio  $R_{\text{CH}_4}/R_{\text{CH}_3\text{D}}$  and prevent plotting equation [III] at temperatures below 208° C.

Values obtained for the different ratios of rate constants are summarized in Table II.

As activation energy for reaction [2] is obtained  $E_2 = 10 \pm 0.5$  kcal. An activation energy of 10.2 kcal. has been reported by Ausloos and Steacie (1) for the following reaction:



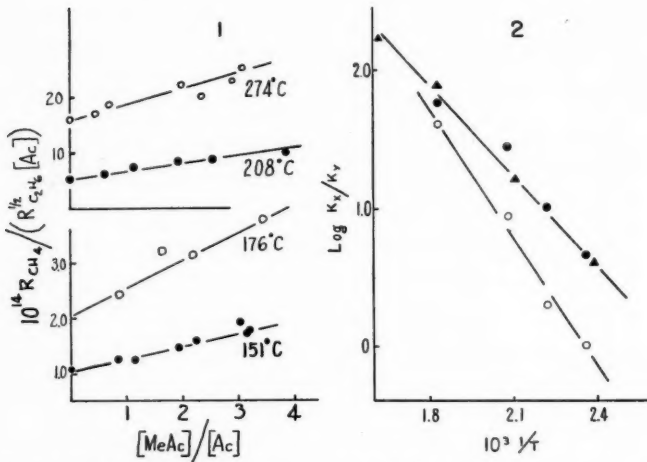


FIG. 1. Plot of  $10^{14} R_{CH_4} / (R_{C_2H_6}^{1/2} [Ac])$  versus  $[MeAc]/[Ac]$  at various temperatures.  
 FIG. 2. Plot of  $14 + \log k_2/k_4^{1/2}$  ( $\circ$ ) and of  $12.7 + \log k_3/k_4^{1/2}$  ( $\bullet$ ,  $\blacktriangle$ ) against  $10^3 1/T$ . Data marked by  $\bullet$  are reported in this work, those marked by  $\blacktriangle$  were obtained by direct photolysis of  $CH_3COOC\bar{D}_3$ .

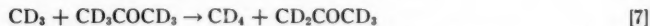
TABLE II  
 RATIOS OF RATE CONSTANTS

Temp., °C.	$10^{13} k_2/k_4^{1/2}$ in molecules $^{1/2}/sec.^{1/2} cc.^{1/2}$	$10^{14} k_3/k_4^{1/2}$ in molecules $^{1/2}/sec.^{1/2} cc.^{1/2}$	$k_1/k_3$	$k_2/k_3$
151	2.3	1.0	—	—
176	5.0	2.0	—	—
208	14.0	8.8	54	23
274	30	41.3	37	8

Since in both reactions, [2] and [5], the hydrogen is abstracted from the acetyl group, these values may be considered to be in good agreement.

The experimentally determined activation energy of  $14 \pm 1$  kcal. for the abstraction of a D-atom from the methoxy group in methyl acetate seems high. A direct comparison of the difference in activation energies between the abstraction of a hydrogen from the acetyl and from the methoxy group in methyl acetate is not possible owing to the different hydrogen isotopes in these groups.

Differences in activation energies between the abstraction reactions of H- and D-atoms by methyl radicals have been observed in the case of acetone, where values of 9.7 kcal. (3) were reported for  $E_6$  and 11.3 kcal. (2) for  $E_7$ .



This difference in activation energies seems mainly caused by the difference in zero point energies between the C—H and C—D bonds, since  $CH_3$  and  $CD_3$  radicals have been suggested (4) to abstract hydrogen atoms with, within experimental error, similar activation energies.

Accepting therefore for the reaction



an activation energy of  $12.5 \pm 1$  kcal., our results indicate that the abstraction of a hydrogen atom from the acetyl group requires less energy than the abstraction of a hydrogen atom from the methoxy group in methyl acetate.

It is interesting to compare these results with results obtained in the direct photolysis of  $\text{CH}_3\text{COOCH}_3$  (5). As activation energy for the hydrogen abstraction by methyl radicals was obtained a value of 10 kcal., in agreement with the value of  $E_2$  obtained in the present work. Among the reaction products were found large amounts of methyl propionate, probably formed by the reaction



No evidence could be obtained for the formation of ethyl acetate, indicating that most hydrogen was abstracted from the acetyl group, rather than from the methoxy group in methyl acetate.

These results confirm the conclusion drawn in this work that less energy is required for the abstraction of a hydrogen atom from the acetyl group than from the methoxy group in methyl acetate by methyl radicals.

In addition to the reaction products given in Table I, trace amounts of  $\text{CD}_3\text{H}$ ,  $\text{CO}_2$ , and occasionally  $\text{CD}_4$  were observed at  $273^\circ \text{C}$ . These products may originate from the thermal decomposition of the  $\text{CH}_2\text{COOCD}_3$  radical.

Accepting as collision diameters of  $\text{CH}_3$  and  $\text{CH}_3\text{COOCD}_3$  3.5 and  $6 \times 10^{-8} \text{ cm.}$ , respectively, we calculated the steric factor ratios and obtained:

$$P_2/P_4^{\frac{1}{2}} = 1.5 \times 10^{-3} \text{ and } P_3/P_4^{\frac{1}{2}} = 5 \times 10^{-3}.$$

These values are of the order of magnitude generally observed in hydrogen abstraction reactions by methyl radicals.

#### ACKNOWLEDGMENTS

The author acknowledges many helpful discussions with Dr. H. D. Medley during the progress of this work. Special thanks are due to Messrs. R. W. Jarrett and R. H. Guedin for calculation and interpretation of the mass spectrometer data.

#### REFERENCES

1. AUSLOOS, P. and STEACIE, E. W. R. *Can. J. Chem.* **33**, 1530 (1955).
2. MCNESBEY, J. R., DAVIS, T. W., and GORDON, A. S. *J. Am. Chem. Soc.* **76**, 823 (1954).
3. TROTMAN-DICKENSON, A. F. and STEACIE, E. W. R. *J. Chem. Phys.* **18**, 1097 (1950).
4. WHITTLE, E. and STEACIE, E. W. R. *J. Chem. Phys.* **21**, 993 (1953).
5. WIJNEN, M. H. J. 131st National Meeting, Am. Chem. Soc., Miami, Florida (April, 1957).
6. WIJNEN, M. H. J. To be published.
7. WIJNEN, M. H. J. and STEACIE, E. W. R. *J. Chem. Phys.* **20**, 205 (1952).

# THE STUDY OF HYDROGEN BONDING AND RELATED PHENOMENA BY ULTRAVIOLET LIGHT ABSORPTION

## PART I. INTRODUCTION<sup>1,2</sup>

W. F. FORBES AND J. F. TEMPLETON

### ABSTRACT

Hydrogen bonding, which is known to give rise to dimer formation in benzoic acids and similar compounds, may affect solution spectra by intermolecular and by intramolecular bond formation. Generally environmental factors affecting absorption spectra can be conveniently divided into three types: intermolecular hydrogen bonding between solute molecules only; intermolecular hydrogen bonding between solute and solvent molecules; and environmental effects not involving the formation of hydrogen bonds.

Distinct evidence for these types of interaction is deduced from ultraviolet spectra, and various implications of the spectral analyses are discussed.

### INTRODUCTION

Hydrogen bonding has been previously mentioned in this series as a possible cause of certain anomalous spectra (13, 14, 15, 17). Intramolecular hydrogen bonding has previously been used to explain certain features of the ultraviolet spectra of *o*-hydroxyacetophenone and salicylic acid (9, 10). Intermolecular hydrogen bonding would be expected to occur in organic compounds like benzoic acid, firstly because dimer formation in benzoic acids is a well-known phenomenon in infrared spectroscopy (2, 11, 22, 26) and secondly because certain changes in ultraviolet absorption spectra on alteration of the solvent have been ascribed to intermolecular hydrogen bonding (5, 6, 7, 30, 31, 33). Further, the dependence of a number of ultraviolet spectra on solution concentration has been noted by several workers (1, 19, 25, 28, 29, 34).

Intermolecular hydrogen bonding, for which there is therefore some evidence, may be conveniently divided into two types. Intermolecular hydrogen bonding may occur between solute molecules only or may occur between solvent and solute molecules. The former, intermolecular hydrogen bonding between solute molecules only, may be a function of the concentration. Consequently, it may be susceptible to independent investigation, particularly since examples can be selected which largely eliminate intramolecular hydrogen bonding and steric effects. Monosubstituted benzenes and especially benzoic acids provide a satisfactory starting point. The latter have also previously been discussed in this series (18) and it was found that although dimer formation was anticipated, the *B*-bands could as a first approximation be satisfactorily related without considering the effect of hydrogen bonding. The present communication may thus be considered as an extension of this previous study.

The effect of intermolecular hydrogen bonding between solvent and solute molecules and other environmental effects may be investigated by choosing examples in which again steric and intramolecular hydrogen bonding effects are small, and which further do not show the concentration changes ascribed to solute-solute hydrogen bonding. Such examples are available and these will be examined separately.

### EXPERIMENTAL

The ultraviolet absorption spectra were determined by standard methods using a Unicam SP 500 spectrophotometer. Intensity readings at different concentrations were

<sup>1</sup>Manuscript received June 24, 1957.

Contribution from the Memorial University of Newfoundland, St John's, Newfoundland.

<sup>2</sup>This paper may also be considered as Part IX of a series of studies on light absorption, Part VIII of which appeared in Can. J. Chem. 35, 1049 (1957).

obtained by using quartz cells of various path length, so that for different concentrations the optical density readings remained similar. For most of the compounds the concentration dependence was determined at least in duplicate over similar concentration ranges and was found to be qualitatively similar.

Compounds were purified by standard methods as described in the literature. Dioxane was purified by the method of Hess and Frahm (24), that is, by refluxing the dioxane with hydrochloric acid in a stream of nitrogen for 12 hours, removing the hydrochloric acid by treatment with potassium hydroxide, and then refluxing the dioxane with sodium for 10 hours. The distilled material, obtained in about 50% yield, was stored under nitrogen. Generally, purification was deemed adequate when additional processing resulted in no further measurable changes in the absorption intensity. Aqueous dioxane solvent mixtures were made up by mixing together the corresponding volume percentages. For example, 75% aqueous dioxane was obtained by mixing 75 volumes of purified dioxane with 25 volumes of distilled water.

The maximal wavelengths and absorption intensities are recorded in Tables I, II, and III. The concentration range was chosen to keep optical density readings between 0.3 and 0.7. Also, since no direct comparison of concentration dependences is intended at present, the reported values are mostly uncorrected. However, care was taken to use well-matched, carefully cleaned, cells, since some pairs of cells gave rise to differences in  $\epsilon$  of up to 6% on interchanging the cells. For each concentration the observed extinction coefficients were within 2%. Band shapes for the benzoic acid spectra were found to be similar and consequently  $\epsilon_{\text{max}}$  values may be used as measures of the actual absorption intensities.

Errors in a number of earlier determinations (cf. 19) were caused by the following:

(i) Solvents, if kept in some polyethylene bottles, frequently deteriorate on standing. Consequently all-glass bottles were used in preparing and storing solutions. The transmission density was checked for each solvent immediately before use. Further, the cells in each calibrated set were checked against each other before use.

(ii) Difficulties in solvent purification did not permit the determination of density readings in the longer cells without altering the sensitivity. This was particularly pronounced for dioxane. To obtain values for the 4 cm. cells at 230 m $\mu$  without altering the sensitivity, about five redistillations were required. As a general rule, the optical density reading in a 1 cm. cell at 250 m $\mu$  was 0.5 or less against air; if not, the dioxane was redistilled.

#### THE DEPENDENCE OF ELECTRONIC ABSORPTION SPECTRA ON CONCENTRATION (INTERMOLECULAR HYDROGEN BONDING BETWEEN SOLUTE MOLECULES ONLY)

For investigating hydrogen bonding and related effects *between solute molecules only*, hexane is a suitable solvent, because of its inactive nature and low dielectric constant. Consequently the main factor influencing the spectra may be the hydrogen bonding between solute molecules, and the intensity change with concentration in hexane as shown in the last examples of Table I may be provisionally assumed to represent a measure of this intermolecular hydrogen bonding.

Using this hypothesis, the data summarized in Table I are in agreement with results deduced by other methods. Thus, diphenyl, aniline, phenol, acetophenone, *p*-methylacetophenone, and methyl benzoate in cyclohexane solution do not show an appreciable intensity increase on increasing the concentration. For diphenyl, acetophenones, and methyl benzoate, this may be related to the inability of these compounds to form a hydrogen bond; and the reported absence of association for acetophenones (27), as

TABLE I  
MAIN ABSORPTION MAXIMA OF COMPOUNDS IN CYCLOHEXANE SOLUTIONS OF VARYING CONCENTRATION\*  
(Concentration,  $c = 6.5 \times 10^{-6}$ – $10^{-4}$  moles/l.; cell lengths in brackets)

Compound	40c (1 mm.)		4c (10 mm.)		c (40 mm.)	
	$\lambda_{\max}$ , $m\mu$	$\epsilon_{\max}$	$\lambda_{\max}$ , $m\mu$	$\epsilon_{\max}$	$\lambda_{\max}$ , $m\mu$	$\epsilon_{\max}$
Diphenyl	246–247	17,400	246	17,200	246–247	17,200
Acetophenone	237–238	12,500	238	12,500	238	12,000
Aniline	233–234	9300	233–234	9200	234	8900
p-Methylacetophenone	246–247	15,000	247	15,200	246–247	14,800
Methyl benzoate	227	12,400	227	12,200	226–227	12,100
Aniline (C-band)	286	1920	286	1890	286	1870
Phenol (C-band)	{ 264 269.5 276	{ 1420 2200 276	{ 263 269.5 276	{ 1400 2200 2050	{ 263 269.5 276	{ 1400 2200 2040
Benzoin acid	231–232	13,700	230	12,900	228	11,900
p-Toluic acid	241	15,500	239	15,000	236–237	13,400
m-Toluic acid	235	12,500	232–233	10,700	232	9700
<i>o</i> -Toluic acid	234–235	10,900	231–232	10,500	230	10,000
Salicylic acid	241	9500	239	8000	238	7200

\*Three concentrations only are reported in this and subsequent tables; intermediate values were obtained at intermediate concentrations.

judged from infrared and Raman spectral studies, may also be noted in this connection. Aniline also does not exhibit any appreciable concentration dependence, which is perhaps surprising, since the presence of association is suggested from infrared data (21). At least two explanations, however, may be proposed for the discrepancy. In the first place, the change in the amount of intermolecular hydrogen bonding may be small or negligible within the concentration range under investigation, but may be more pronounced in a different concentration range. This suggestion receives strong support since pyrrole and related compounds do not show any appreciable stretching vibration changes, which may be ascribed to hydrogen bonding (21), below a concentration of  $10^{-2}$  moles per liter. By contrast, the present concentration range lies between  $10^{-6}$  and  $10^{-2}$  moles per liter. Secondly, the sensitivity of the method may generally not be sufficient to discern a change, which nevertheless actually occurs.

At this stage the significance of the data may be discussed. For all the early examples listed in Table I an intensity change of between 1 and 5% does in fact occur on increasing the concentration by a factor of 40, whereas a similar intensity change does not occur for some of the compounds listed in Table II. Since this change occurs for all the examples in Table I and also frequently occurs independently of the solvent (see, for example, the spectrum of methyl benzoate in ethanol and in cyclohexane as listed in Table II), it is unlikely to be associated with weak intermolecular hydrogen bonding. Moreover, if we take the accuracy of each  $\epsilon$  value to be  $\pm 2\%$  (cf. Experimental), practically all these values are within experimental error. However, the fairly general occurrence of the trend (see Table I) suggests that the slight intensity increase is real. The most probable explanations are therefore that the intensity increase is caused by van der Waal's forces of molecular interaction or merely by errors inherent in the experiments (cf. 3, 4, 12).

Table I also shows that for benzoic acids the situation is different. Apart from the small increase discussed in the previous paragraph, many benzoic acids in cyclohexane solution when the concentration is increased give rise to a more pronounced increase in the observed absorption intensity. Since the changes occur at different wavelengths, they cannot be ascribed to any phenomenon associated with a particular wavelength. Simi-

larly, the previously discussed small intensity increase is not confined to a limited wavelength range; compare the early examples in Table I, which occur between 227 and 286 m $\mu$ . Further, Ugnade and Lamb (34) have noted that similar changes to those described for the *B*-band of benzoic acid occur in the *C*-band of benzoic acid in cyclohexane solution. For example, they report a maximal absorption at 274 m $\mu$ ,  $\epsilon = 1050$  at a concentration of  $0.0805 \times 10^{-3}$  moles per liter, whereas at a concentration of  $10.27 \times 10^{-3}$  moles per liter this absorption occurs at 276 m $\mu$ ,  $\epsilon = 1120$  (34). Lastly, it will be shown in a later section that this intensity decrease is less pronounced for more polar solvents, and this observation again is consistent with the initial assumption which relates these intensity changes to intermolecular hydrogen bonding.

Another example of appreciable intensity change is provided by the concentration dependence of the *C*-band in phenols (28). This dependence has been ascribed to intermolecular hydrogen bonding (28), but possibly for similar reasons as have been mentioned for aniline, no appreciable spectral changes under the conditions of the present experiment are observed.

#### CONCERNING THE INTERPRETATION OF THE INTENSITY DECREASE

The observed intensity changes in Table I are apparently not accompanied by any large wavelength change. With this in mind, the possible factors causing the observed changes may now be briefly discussed at a more fundamental level. One possible explanation is that intermolecular hydrogen bonding (or generally association), by withdrawing part of the electronic cloud from the carboxyl group, increases the planarity of the molecule (cf. 18). The resulting decreased steric hindrance could account for the increased absorption intensity, and would be expected to give rise to a bathochromic shift (cf. 13, 18).

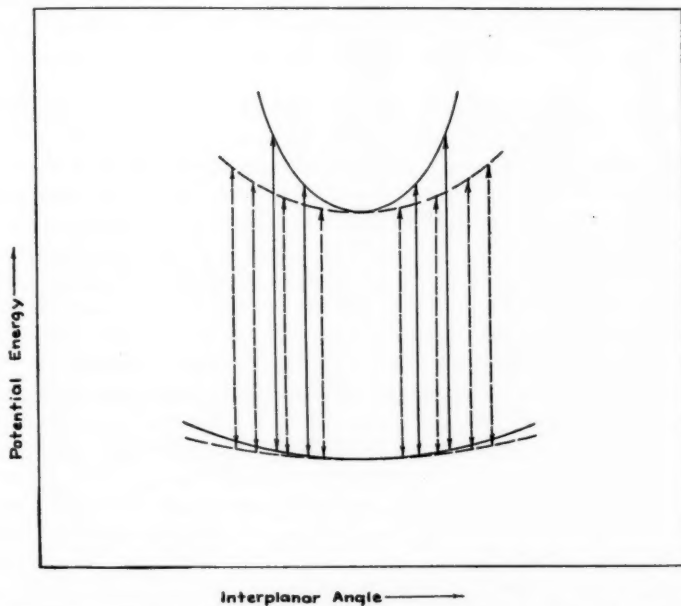


FIG. 1. Schematic representation of potential energy curves and electronic transitions for benzoic acid in the monomeric form (full lines) compared to benzoic acid in the dimeric form (dashed lines).

Another, not necessarily alternative, interpretation is to assume that association decreases the force constant of twist about the bond linking the carboxyl group to the benzene ring. This might be expected to cause an effect as illustrated in Fig. 1. (Fig. 1 is, of course, an idealization since, for example, it is not certain that the energy level minima of ground and excited states occur at similar interplanar angles.) As shown in the diagram, the decreased force constant is assumed to flatten the energy level curves of the ground and excited states and thereby increases the absorption intensity. This follows, because the proportion of molecules in positions favorable for electronic excitation will be increased. At the same time, the wavelength of maximal absorption normally undergoes a bathochromic shift.

A third explanation is that increased association (involving non-bonded electrons of the carbonyl group) increases the energy of excitation, because of the greater amount of energy required to excite partially bound electrons. Since this greater energy would cause a hypsochromic shift, this is probably not the predominant factor for the compounds studied (see Table I).

The hypothesis that association causes the observed changes, chiefly by varying the force constant, receives support from a number of other independent observations. Thus, in the first place, a smaller force constant—assuming the explanation proposed for the *C*-band (17)—would frequently produce similar changes in both *B*- and *C*-bands. This is in fact observed for benzoic acid.

Next, a similarly altered force constant would be anticipated on introduction of an electron-withdrawing substituent in a molecule in a position such that the main mesomeric interaction remains approximately constant. This is found to be correct. For example, *m*-terphenyl ( $\lambda_{\max}$  252 m $\mu$ ,  $\epsilon = 44,000$ ) absorbs at the same maximal wavelength as diphenyl ( $\lambda_{\max}$  252 m $\mu$ ,  $\epsilon = 18,000$ ), but rather surprisingly with more than twice the absorption intensity of diphenyl (23). This suggests that an effect analogous to the above-mentioned association occurs; more precisely, the third phenyl ring may be supposed to weaken the force constant for the central bonds and in this way cause the intensity increase.

Another example may be provided by the previously noted, but unexplained, similarity between the spectra of nitrobenzoic acids and nitrobenzene (18). There, the electron-withdrawing effect of both substituents in nitrobenzoic acids can be supposed to deactivate the benzene nucleus sufficiently to prevent any primary mesomeric interaction. This explains the absence of any appreciable mesomeric interaction between the two substituents in *p*-nitrobenzoic acid as indicated by the lack of any significant wavelength shift. Further, according to the present hypothesis, a secondary effect may now operate which will tend to reduce the force constant of the N-nuclear bond, and thus be responsible for the increased absorption intensity ( $\lambda_{\max}$  258 m $\mu$ ,  $\epsilon = 11,000$ ) in *p*-nitrobenzoic acid. The meta-isomer absorbs with approximately the same intensity ( $\lambda_{\max}$  255 m $\mu$ ,  $\epsilon = 7500$ ) as nitrobenzene ( $\lambda_{\max}$  258 m $\mu$ ,  $\epsilon = 8500$ ), but in this compound a buttressing effect may account for a reduced absorption intensity (16). In the ortho-isomer, steric interactions certainly inhibit the conjugation between the nitro-group and the benzene ring and only an inflection appears at approximately 255 m $\mu$ ,  $\epsilon = 3500$ .

A similar explanation may also be used to explain more fundamentally the increased absorption intensity of phenyl benzoate ( $\lambda_{\max}$  230 m $\mu$ ,  $\epsilon = 15,000$ ) compared with benzoic acid ( $\lambda_{\max}$  227 m $\mu$ ,  $\epsilon = 11,000$ ; cf. (18)), and other "anomalous" spectral changes. These will be discussed in more detail in a separate communication.

THE EFFECT OF INTERMOLECULAR HYDROGEN BONDING BETWEEN SOLUTE AND SOLVENT MOLECULES ON ELECTRONIC ABSORPTION SPECTRA

It has been shown that definite spectral changes, which may be ascribed to association, are observed for benzoic acids in cyclohexane solution. If hydrogen bonding does occur and is responsible for these changes, one would expect that the concentration dependence would normally be greatest in hexane solution. This follows because, in solvents which are able to form a hydrogen bond with the solute molecules, a competitive hydrogen bonding may occur. This in turn presumably reduces the association occurring between solute molecules only, since generally the same substituent of the solute molecule would be involved in both solute-solute and solute-solvent hydrogen bonding. In the limit, as the solute-solvent interaction becomes increasingly more important, no concentration dependence would be observed. Therefore, it might be anticipated that, in the absence of special considerations, concentration dependence varies with the solvent. If concentration dependence occurs in an inert solvent, it may be expected to decrease in the solvent order hexane > ethanol > water.

This hypothesis has been investigated and some of the results are listed in Table II. The data can again be divided into two groups. There are the earlier values in Table II,

TABLE II  
CONCENTRATION DEPENDENCE OF ABSORPTION MAXIMA IN DIFFERENT SOLUTIONS  
(Concentration,  $c = 6.5 \times 10^{-6}$ - $10^{-5}$  moles/l.; cell lengths in brackets)

Compound	Solvent	40c (1 mm.)		4c (10 mm.)		c (40 mm.)	
		$\lambda_{\max}$ , m $\mu$	$\epsilon_{\max}$	$\lambda_{\max}$ , m $\mu$	$\epsilon_{\max}$	$\lambda_{\max}$ , m $\mu$	$\epsilon_{\max}$
Diphenyl	Cyclohexane	246-247	17,400	246	17,200	246-247	17,200
Diphenyl	Ethanol	247	17,300	247	17,200	246	17,300
Aniline	Cyclohexane	233-234	9300	233-234	9200	234	8900
Aniline	Ethanol	234	8200	234	8000	235	7700
Methyl benzoate	Cyclohexane	227	12,400	227	12,200	226-227	12,100
Methyl benzoate	Ethanol	227-228	12,300	227-228	12,100	227	11,700
Benzoic acid	Cyclohexane	231-232	13,700	230	12,900	228	11,900
Benzoic acid	Approx. 0.01 N acidic ethanol HCl	226-227	11,400	227-228	11,400	227	11,700
Benzoic acid	0.01 N aqueous*	229	10,800	229	11,000	229	11,100
Benzoic acid	Ethanol	227	11,600	227	11,500	227	10,800
Benzoic acid	Water	227	9400	224	8700	223	9300

\*Hydrochloric acid has been added to the aqueous solution to avoid ionization, which evidently occurs in the pure aqueous medium as shown by the wavelength displacement to 223 m $\mu$  (cf. 34).

where concentration dependence for both cyclohexane and ethanolic solution is small or absent. As mentioned before, the smallness of these intensity changes renders any conclusions based on them extremely doubtful. However, the indication is, as noted previously, that for some of these compounds changing the solvent does not materially affect the concentration dependence. This in turn indicates that this concentration dependence is not caused by hydrogen bonding. It may also be noted that Raman spectral studies (32) for methyl benzoate in ethanol afford no evidence for hydrogen bonding between methyl benzoate molecules.

For benzoic acid in ethanolic solution the expected decreased concentration dependence is observed. This concentration dependence unfortunately is so small that no decision

can be made concerning its reality. For aqueous solutions of benzoic acid ionization of the acid alters the spectrum (34) and consequently no decision can be made about dimerization. Addition of acid to both aqueous and ethanolic solution apparently inhibits concentration dependence, but the acid—apart from preventing ionization—may clearly also affect the hydrogen bonding. Similar changes are also observed for a number of substituted benzoic acids (20).

These observations are of interest for at least two reasons. First, they support the previous hypothesis, ascribing the spectral changes for benzoic acid in hexane solution to intermolecular hydrogen bonding. If this is so, the smaller concentration dependence or complete absence thereof provides at the same time evidence that hydrogen bonding occurs between solute and solvent molecules. This latter phenomenon is also well established from other physical data. Secondly, the smaller concentration dependence may throw light on the relative strengths of the hydrogen bonding involved. Thus, if no concentration dependence is observed in ethanolic solution, it may be supposed that the monomeric acids are under these conditions preferentially stabilized by hydrogen bonds, which are probably more important than the hydrogen bonds making up the benzoic acid dimer (cf. 34). Unfortunately, on the basis of the present data, remembering their qualitative nature (cf. Experimental), no definite decision can be made. There is, however, some indication that in both ethanolic and aqueous solution intermolecular hydrogen bonding between benzoic acid molecules is entirely inhibited (see Table II for the spectra of benzoic acid in ethanol and water when HCl has been added; cf. also (34)); that is, that any observed concentration dependence in aqueous or ethanolic solution should be ascribed to a changed degree of dissociation for the benzoic acid molecules rather than to dimerization.

#### THE EFFECT OF OTHER ENVIRONMENTAL FACTORS ON ELECTRONIC ABSORPTION SPECTRA

Under this heading we may group together a variety of other environmental factors which by means of a mechanism other than hydrogen bonding affect the absorption spectra. Their existence is almost self-evident from theoretical considerations, but clear-cut examples of their spectral effects are not always available. At present, we shall confine ourselves to discussing only one example, linking this with other spectral phenomena which also point to these environmental factors as a means of affecting spectra. Additional examples will be discussed in other parts of this series as they arise in the course of discussion.

The example chosen is the spectrum of acetophenone in dioxane-water mixtures and the relevant data are recorded in Table III. Dioxane-water mixtures were chosen partly because the dielectric constant of such solutions is known, and it was in this way hoped to find a relation between the dielectric constant of a solution and one of its characteristic spectral properties. The results show that for acetophenone in various solvent mixtures no concentration dependence is observed. This confirms the expectation that acetophenone under these conditions does not associate with itself (cf. 27). On changing the dielectric constant of the solvent, however another type of change is observed, namely a distinct wavelength shift in the *B*-band of acetophenone. This wavelength shift may either be caused by intermolecular hydrogen bonding of the type discussed in the previous section, or it may be caused by other forces acting on the molecule.

The following suggest that "other" factors also contribute to the observed spectral changes:

TABLE III  
ABSORPTION MAXIMA OF COMPOUNDS IN SOLUTIONS OF VARYING DIELECTRIC CONSTANT

Compound	Solvent	Concentration range	$\lambda_{\max}$ , m $\mu$	$\epsilon_{\max}$ and percentage deviation
Acetophenone	Dioxane	$4 \times 10^{-4}$ to $1 \times 10^{-5}$	239	* $12,700 \pm 3\%$
	75% aqueous dioxane	$4 \times 10^{-4}$ to $1 \times 10^{-5}$	241	$12,300 \pm 2\%$
	50% aqueous dioxane	$4 \times 10^{-4}$ to $1 \times 10^{-5}$	243	$12,200 \pm 2\%$
	25% aqueous dioxane	$4 \times 10^{-4}$ to $1 \times 10^{-5}$	244	$12,300 \pm 2\%$
	Water	$4 \times 10^{-4}$ to $1 \times 10^{-5}$	244.5	$12,100 \pm 2\%$
Acetophenone (C-band)	Dioxane	$4 \times 10^{-3}$ to $1 \times 10^{-4}$	277	* $1010 \pm 3\%$
	75% aqueous dioxane	$4 \times 10^{-3}$ to $1 \times 10^{-4}$	277	$1060 \pm 2\%$
	50% aqueous dioxane	$4 \times 10^{-3}$ to $1 \times 10^{-4}$	278	$1120 \pm 2\%$
	25% aqueous dioxane	$4 \times 10^{-3}$ to $1 \times 10^{-4}$	278	$1200 \pm 2\%$
	Water	$4 \times 10^{-3}$ to $1 \times 10^{-4}$	277	$1240 \pm 2\%$
Nitrobenzene	Dioxane	$8 \times 10^{-4}$ to $2 \times 10^{-5}$	258	$8200 \pm 2\%$
	50% aqueous dioxane	$6 \times 10^{-4}$ to $1.5 \times 10^{-5}$	264	$7800 \pm 2\%$
	Water	$8 \times 10^{-4}$ to $2 \times 10^{-5}$	266	$7850 \pm 2\%$

\* $\epsilon$  values within any particular concentration range are  $\pm 2\%$ .

(i) The location of maximal wavelength changes for the *B*-bands of both acetophenone and nitrobenzene with increase of dielectric constant (see Table III). Wavelength displacements of similar magnitude were observed on altering the solvent from ethanol to water by Ungnade (33), who tentatively ascribes these wavelength displacements to hydrogen bonding. However, if hydrogen bonding were exclusively responsible for the spectral change, one would expect almost every dioxane-water solvent mixture to have sufficient water molecules to ensure suitably solvated structures for all the acetophenone molecules present. It would follow that maximal wavelengths would be expected to alter appreciably on addition of a small amount of water to pure dioxane as solvent; after which addition of water to the solvent mixture should not cause any further spectral change. In fact, the addition of water progressively alters the wavelength of maximal absorption, and there is no indication of any break in the curve relating maximal wavelengths and dielectric constant of the solvent mixtures.

(ii) Infrared data (27) for acetophenone in various solutions failed to show any band doubling, such as would be expected if more than one molecular species were present in solution. Such band doubling is observed for various substituted amines and has been ascribed to hydrogen bonding (21).

(iii) It is well known that changing the solvent affects the general shape of an absorption curve in many cases. In one instance at least, an investigation has been carried out to determine whether these changes are due to intermolecular hydrogen bonding. Coggeshall and Lang (8), using the temperature effects in isoctane and ethanolic solutions, conclusively showed that the spectral differences between the two solutions for aniline and phenol do not depend on stable hydrogen bonded complexes.

In concluding this section it should be noted that apart from the existence of other environmental factors, little else can as yet be ascertained about these forces, from electronic absorption spectra. Consequently, no attempt has been made to explain their effects on the *C*-band, which apparently are different from the effect of these forces on the *B*-band (see Table III). For similar reasons steric effects have not been investigated, although steric effects will almost certainly affect such molecular interaction. Finally, the nature of the molecular interaction itself, which probably includes a polar solvent

effect and the possibility of a change in the molecular entity concerned (for example, benzoic acids in different solvent media), has not been fully elucidated, and the problem evidently requires further consideration.

#### ACKNOWLEDGMENTS

The authors gratefully acknowledge the receipt of research grants from the National Research Council of Canada and the Research Corporation of New York.

#### REFERENCES

1. BEINERT, H. J. Am. Chem. Soc. **78**, 5323 (1956).
2. BELLAMY, L. J. *The infra-red spectra of complex molecules*. Methuen and Co., Ltd., London. 1954. p. 139.
3. BLADON, P., HENBEST, H. B., and WOOD, G. W. J. Chem. Soc. 2737 (1952).
4. BRAUDE, E. A. and TIMMONS, C. J. Photoelec. Spectrometry Group Bull. No. 6, 139 (1953).
5. BREALEY, G. J. and KASHA, M. J. Am. Chem. Soc. **77**, 4462 (1955).
6. BURAWOY, A., CAIS, M., CHAMBERLAIN, J. T., LIVERSEDGE, F., and THOMPSON, A. R. J. Chem. Soc. 3721 (1955).
7. BURAWOY, A. and THOMPSON, A. R. J. Chem. Soc. 1443 (1953).
8. COGESHALL, N. D. and LANG, E. M. J. Am. Chem. Soc. **70**, 3283 (1948).
9. CRAM, D. J. and CRANZ, F. W. J. Am. Chem. Soc. **72**, 595 (1950).
10. DANNNENBERG, H. Z. Naturforsch. **4b**, 327 (1949).
11. DAVIES, M. and GRIFFITHS, D. M. L. J. Chem. Soc. 132 (1955).
12. EGLINTON, G., JONES, E. R. H., and WHITING, M. C. J. Chem. Soc. 2873 (1952).
13. FORBES, W. F. and MUELLER, W. A. Can. J. Chem. **34**, 1340 (1956).
14. FORBES, W. F. and MUELLER, W. A. Can. J. Chem. **34**, 1542 (1956).
15. FORBES, W. F. and MUELLER, W. A. Can. J. Chem. **35**, 488 (1957).
16. FORBES, W. F. and MUELLER, W. A. J. Am. Chem. Soc. **79** (In press, 1957).
17. FORBES, W. F., MUELLER, W. A., RALPH, A. S., and TEMPLETON, J. F. Can. J. Chem. **35**, 1049 (1957).
18. FORBES, W. F. and SHERATTE, M. B. Can. J. Chem. **33**, 1829 (1955).
19. FORBES, W. F. and TEMPLETON, J. F. Chem. and Ind. **77**, 600 (1957).
20. FORBES, W. F. *et al.* Unpublished information.
21. FUSON, N., JOSIEN, M. L., POWELL, R. L., and UTTERBACK, E. J. Chem. Phys. **20**, 145 (1952).
22. FUSON, N., JOSIEN, M. L., and SHELTON, E. M. J. Am. Chem. Soc. **76**, 2526 (1954).
23. GILLAM, A. E. and HEY, D. H. J. Chem. Soc. 1170 (1939).
24. HESS, K. and FRAHM, H. Ber. **71**, 2627 (1938).
25. HIRSBERG, Y., KNOTT, E. B., and FISHER, E. J. Chem. Soc. 3313 (1955).
26. JONES, R. N. and SANDORFY, C. In West, W. *Chemical applications of spectroscopy*. Interscience Publishers, Inc., New York. 1956. pp. 424-427.
27. JOSIEN, M. L. and LASCOMBE, J. Compt. rend. **239**, 51 (1954).
28. KEUSSLER, V. v. Z. Elektrochem. **58**, 136 (1954).
29. KOIZUMI, M. and MATAGA, N. Bull. Chem. Soc. Japan, **27**, 194 (1954); cf. Chem. Abstr. **49**, 7382 (1955).
30. KUMLER, W. D. J. Am. Chem. Soc. **68**, 1184 (1946).
31. NAGAKURA, S. and BABA, H. J. Am. Chem. Soc. **74**, 5693 (1952).
32. PURANIK, P. G. J. Chem. Phys. **26**, 601 (1957).
33. UNGNADE, H. E. J. Am. Chem. Soc. **75**, 432 (1953).
34. UNGNADE, H. E. and LAMB, R. W. J. Am. Chem. Soc. **74**, 3789 (1952).

# THE ELECTRIC MOMENTS OF SOME N,N'-DISUBSTITUTED PIPERAZINES<sup>1</sup>

M. V. GEORGE AND GEORGE F WRIGHT

## ABSTRACT

The establishment of significant orientation polarizations for a series of symmetrically N-substituted piperazines including N,N'-dichloro-2,5- $\uparrow\downarrow$ -dimethylpiperazine, which was prepared anew, confirms the report of Partington and contradicts that of Hassel. The existence of these moments is not compatible with the postulation of a favored chair conformation especially in consideration of the proton magnetic resonances of N,N'-dimethylpiperazine and N,N'-diformylpiperazine. On the other hand the experiments favor the postulation of flexible conformation for these piperazines.

According to several reviews (8, 2) the "chair" form of six-membered alicyclic compounds is the expected conformation. The reported zero dipole of N,N'-dichloropiperazine (1) is cited in support of this opinion. This evidence seems to be at variance with the report (14) that piperazine and diphenylpiperazine in benzene have moments of 1.47 D. and 0.85 D. respectively. The experimental data kindly furnished to us by Professor Partington seem to be unequivocal. In order to resolve the apparent contradiction we have examined the polarization of a series of piperazines by methods which have been described previously (15, 16). The results are included in Table I.

The values for solutions in benzene are derived by determination of  $d\epsilon/d\omega$  (lines marked with unprimed letters, Fig. 1) and  $d\bar{V}/d\omega$  (lines marked with primed letters in Fig. 1). Specifically, the dielectric constants ( $\epsilon$ ) and specific volumes ( $\bar{V}$ ) of N,N'-dichloro-2,5- $\uparrow\downarrow$ -dimethylpiperazine are recorded with respect to weight fractions  $\omega$  for a series of solutions along lines A and A', Fig. 1. Extrapolation to zero weight fraction gives values conforming closely with  $\epsilon = 2.2840$  and  $\bar{V} = 1.13795$  for pure benzene at 20°. Therefore calculation for total solute molecular polarization by the method of Halverstadt and Kumler (8) is justified.

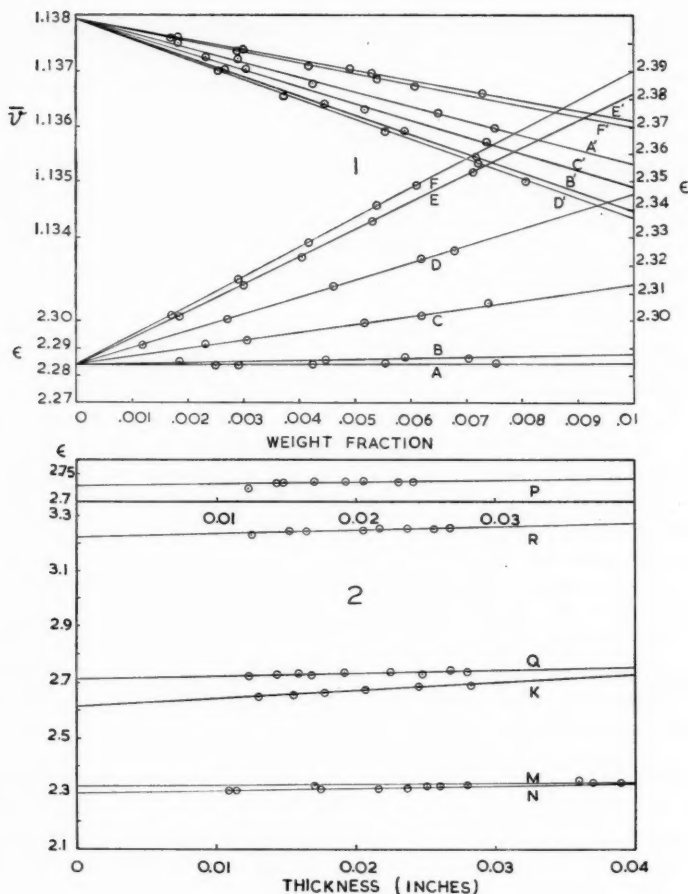
In order to calculate the moment of this substance the distortion polarization must be evaluated. Since the additive group refraction (8.6 cc.) derived from the N-Cl linkage in a few liquid chloramines (17) is probably unreliable we have chosen to determine  $P_{E+A}$  from the dielectric constant of solid dichlorodimethylpiperazine obtained by extrapolation of apparent  $\epsilon$  versus pellet thickness (line M, Fig. 2) to zero thickness where "edge effect" is minimal. The distortion polarization by this method (15, 16) is 40.4 cc. in contrast to 44.9 cc. calculated from group refractions. The electric moment calculated from  $P_T - (P_{E+A})$  is 0.66 D. while that from  $P_T - R_D$  (calc.) is 0.47 D. While the higher value should be considered the more reliable, neither moment conforms with the zero value stipulated for N,N'-dichloropiperazine by Andersen and Hassel (1).

Since these authors did not report experimental details we have redetermined the dielectric constants and specific volumes of benzene solutions containing dichloropiperazine. These values (lines B and B', Fig. 1) justify the calculation of total molecular solute polarization as 46.3 cc. Unfortunately the distortion polarization ( $P_{E+A}$ ) cannot be determined directly because the substance explodes in the pellet press. The damage attests to the energy of the N-Cl linkage.

In the absence of the experimental value we have calculated the moment of dichloropiperazine by use of the additive group refraction, and also by correcting the latter  $R_D$  by a factor derived from the additive versus the experimental distortion polarization of the dimethyl homologue. The moment (Table I) may be 0.85 D. or 0.71 D.,

<sup>1</sup>Manuscript received July 23, 1957.

Contribution from the Department of Chemistry, University of Toronto, Toronto, Ontario.



FIGS. 1 and 2.

depending on whether the corrected or the uncorrected additive refraction is applied. Despite the uncertainty one may affirm that the moment of *N,N'*-dichloropiperazine is not zero, as was reported previously (1). Moreover in view of the low group moment (*ca.* 0.3 D.) which has been assigned to the N-Cl linkage (23, 11) the conformation of atoms in this substance must exist largely in the flexible (so-called boat) form rather than the chair form.

In order to exclude the possibility that the presence of substituent methyl groups might vitiate the comparison between the two dichloropiperazines described above we have determined  $P_T$  and  $P_{E+A}$  for 2,5 $\uparrow\downarrow$ -dimethylpiperazine from  $d\epsilon/d\omega$  (line S, Fig. 3),  $d\bar{V}/d\omega$  (line T, Fig. 3), and  $d\epsilon/d(\text{thickness})$  (line N, Fig. 2). Although we used dioxane solutions the calculated moment (1.55 D.) compares favorably with the 1.47 D. reported by Martin (14) for piperazine in benzene. Furthermore the experimental  $P_{E+A}$  (Table I) is reasonably close to the calculated  $R_D$  for 2,5 $\uparrow\downarrow$ -dimethylpiperazine. A similar comparison (from line P, Fig. 2) justifies Martin's calculated  $R_D$  for diphenylpiperazine. Thus correlations among the distortion polarization of piperazines seem to be reliable.

In view of Martin's small moment (0.85 D.) for N,N'-diphenylpiperazine it seemed worth while to examine an N-alkyl-disubstituted piperazine. Examination of N,N'-dimethylpiperazine in benzene ( $d\epsilon/d\omega$ , line V and  $d\bar{\nu}/d\omega$ , line U, Fig. 3) shows that its

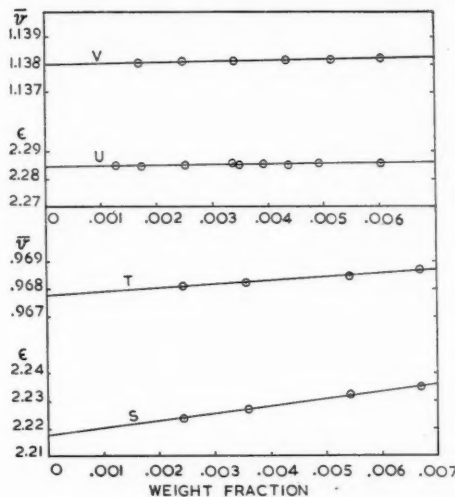


FIG. 3.

moment is low (0.59 D.). The difference between the diphenyl and dimethyl analogues is not unexpected ( $\mu$  for aniline, 1.58 D., versus  $\mu$  for trimethylamine, 0.86 D. in benzene), but closer correlation to define constellar differences is not justified without an elaborate study in which temperature and solvent are varied (15).

However it may be noted that a zero moment would be expected for a symmetrical

TABLE I  
POLARIZATIONS AND MOMENTS OF PIPERAZINES AND RELATED COMPOUNDS AT  $20^\circ \pm 0.05^\circ$  C.

Compound	Solvent	$P_T$ , cc.	$R_D$ , cc. calc.	Pellet $P_{E+A}$ , cc.	$\mu$ , D.
N,N'-Dichloro-2,5- $\downarrow$ -dimethylpiperazine	Benzene	49.6	44.9	40.4	0.47 0.66
N,N'-Dichloropiperazine	Benzene	46.3	35.6		0.71 0.85
Piperazine	Benzene				1.47 (14)
N,N'-Diphenylpiperazine	Benzene		74.3	75.2	0.85 (14)
2,5- $\downarrow$ -Dimethylpiperazine	Dioxane	85.7	34.9	33.1	1.55
N,N'-Diformylpiperazine	Benzene	195	35.6	43.3	$2.72 \pm .03$
N,N'-Bis-cyanoethylpiperazine	Benzene	433	52.7	60.8	$4.23 \pm .02$
N,N'-Bis-cyanoethyl-2,5- $\downarrow$ -dimethylpiperazine	Benzene	470.6	61.5	68.8	$4.32 \pm .01$
Methyldiformamide	Benzene	68.27	20.3 <sup>b</sup>		1.51 <sup>d</sup>
N,N'-Dimethylpiperazine	Benzene	41.8	35.5 <sup>b</sup>		0.59
Dimethylformamide	Benzene	327	19.9 <sup>b</sup>		3.82 <sup>c</sup>
			20.0 <sup>a</sup>		

<sup>a</sup> $R_D$  by additive refraction values.

<sup>b</sup> $R_D$  from density and refractive index.

<sup>c</sup>Confirms S. Suzuki, Kagaku, **23**, 535 (1953); Chem. Abstr. **47**, 11892 (1953).

<sup>d</sup>Kindly furnished by Dr. Rae of Stanford University. The proton magnetic resonance spectrum of this liquid at  $25^\circ$  consists of two simple peaks with areas corresponding to an intensity ratio of 2:3. The lesser peak at -140 c.p.s. (relative to water) should be due to the formyl protons while the larger peak at +88 c.p.s. may be attributed to the methyl protons.

conformation since the methyl groups would be opposed either in axial or equatorial positions. Since their algebraic sum ought then to be zero, the existence of a real moment belies the postulation of a crown conformation.

Inherent in arguments of this sort is the assumption that a chair conformation, because of its essential stability, contributes so largely to the state of atomic arrangement in a six-membered cyclic molecule that the latter may be described as a static chair form. Such a form, if it is centrosymmetrical, will not be oriented in the electrical field. However, any activated deviation from this centrosymmetry will be observable by fields of frequency higher than those of atomic motion within the molecule. Undoubtedly for this reason Partington has suggested (14) that the observed moments of piperazines are due to axial-equatorial disposition of N,N'-substituents of chair conformations. The *e-a* constellation in IV (Fig. 4) would contribute to orientation polarization while the symmetrical *e-e* conformation, V, or the alternative *a-a* form would not make a contribution.

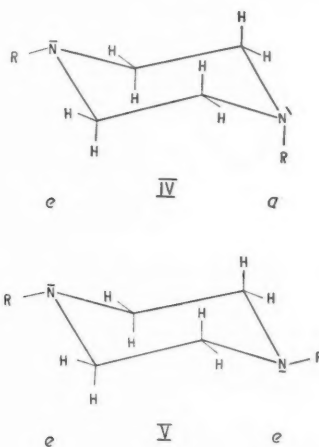


FIG. 4.

The transition from V *e-e* to V *a-a* may be expected to involve an activation energy which is not much less than the 3.6 kcal. specified (3) for the free energy difference between the *a-a* and *e-e* forms of 1,4-dimethylcyclohexane, and this activation energy should not be very different from the free energy difference between Partington's unsymmetrical form, IV, and his symmetrical V *e-e*. In these circumstances the amount of IV should not be great enough to account for the moments observed by Partington and ourselves. Moreover the transition rate from V to IV ought to be of the order of 0.0005 c.p.s. at ordinary temperatures, according to the energies that are involved. For our evaluation of transition rates we are greatly indebted to Dr. H. W. Patton and Mr. J. H. Chaudet of the Tennessee Eastman Company (Division of Eastman Kodak Co.), who determined proton magnetic resonances at 40 Mc. for several of these piperazines.

These workers have reported to us the information that N,N'-dimethylpiperazine shows two simple peaks about 6 cycles apart in the vicinity of 98 c.p.s. relative to water,

at 25°. They attribute the peak at the higher field position to the protons of the two N-methyl groups, which therefore are equivalent. The peak at the lower field position must be due to the methylene protons. Since these methylene protons in a static six-membered ring ought to be non-equivalent, Patton and Chaudet have cooled the sample to -5° C. in an attempt to separate the peak at lower field position, but without success. Therefore the transition rate must be faster by several orders of magnitude than the modulatory frequency at which resonance is measured. It follows that a chair conformation does not describe N,N'-dimethylpiperazine adequately.

For further variation in the piperazine substituents we have included N,N'-diformylpiperazine as a typical amide. The dielectric constants and specific volumes of its benzene solution are shown as D and D', Fig. 1. The distortion polarization has been evaluated by the pellet technique (R, Fig. 2). Calculation of  $P_{E+A}$  discloses the presence of a high (7.7 cc.) atom polarization if the bond additivity calculation of  $P_E$  is reliable. The reliability of the calculated electronic polarization is attested in this instance by the close agreement (Table I) between calculated and observed molecular refractions of the analogous dimethylformamide.

Therefore the atom polarization of diformylpiperazine, specified by pellet measurement, probably is genuine, but one may doubt that it is related to the piperazine ring. More likely this distortion by the external electric field involves the formyl groups. It may be seen in Table I that substances like 2,5-dimethylpiperazine and N,N'-diphenylpiperazine do not display appreciable atom polarization. On the other hand *bis*-N,N'- $\beta$ -cyanoethylpiperazine (moment calculations from F; F', Fig. 1, and K, Fig. 2) and *bis*-N,N'-cyanoethyl-2,5- $\uparrow\downarrow$ -dimethylpiperazine (calculations from E, E', Fig. 1, and Q, Fig. 2) both seem to have atom polarizations comparable in magnitude with that of diformylpiperazine. Presumably the cyano groups, like the formyl group, can be distorted appreciably by a weak electric field at 500 kc. The phenomenon should and will be investigated more thoroughly. At present it is relatively unimportant because it does not affect appreciably the moment (2.72 D.) of diformylpiperazine.

The moment angle of the formylamino group is not known, but it is probably low. Indeed a low formylamino moment angle is exemplified by the value of 1.51 D. found (Table I) for methylidiformamide. Now if N,N'-diformylpiperazine is considered in the sense of two opposed units of dimethylformamide (Table I, 3.82 D.) in which the formyl moment angles are low, then the observed moment (2.72 D.) seems to be high if a symmetrical chair conformation is assumed. In such a structure the formyl groups would be opposed either in axial or equatorial positions. Thus they would largely cancel each other unless random rotation of the formyl group were restricted. Evidence that this restriction does not exist is presented below in order to confirm that the chair conformation for diformylpiperazine is improbable.

The proton magnetic resonance spectrum of N,N'-diformylpiperazine in water at 25° shows the same simplicity as that of N,N'-dimethylpiperazine. The weaker (-115 c.p.s. with respect to water) of two simple peaks has been attributed to the formyl protons, so the stronger peak, at +1.5 c.p.s., must be due to the methylene protons. There is no tendency toward splitting of the peak when the solution of diformylpiperazine is chilled almost to its freezing point. This behavior is different from that of dimethylformamide (19, 24). If the spectrum reported for this latter substance is revised to compare with a 40 Mc. field, a formyl-proton peak exists at -120 c.p.s. and two methyl-proton peaks occur at +80 and +88 c.p.s. relative to water, the respective areas being

1:3:3. However the rigidity is lost when the sample in the field is heated to 117°, at which temperature only a single peak at about 84 c.p.s. is observed.

It is apparent that the spectrum of diformylpiperazine at 25° resembles that of dimethylformamide at 117°, where the latter is presumed to have free, rapidly rotating methyl groups. Of course diformylpiperazine cannot have this generalized positioning of protons because of its cyclic structure. However an oscillatory motion of the six-membered ring would account for the single methylene peak that Patton and Chaudet observed if this oscillation were more rapid than that of the proton resonance frequency.

But in this circumstance the ring oscillation frequency ought to exceed 100 c.p.s. by at least an order of magnitude. Clearly this rate is incompatible with the oscillation of a "chair" ring for which the transition rate should not exceed 0.01 c.p.s., assuming a rather low transition energy of 2 kcal. The transition rate from "chair" to rigid "boat" is even more unfavorable according to the calculated energies (3). Consideration of Patton and Chaudet's results suggests that the transition energy must not exceed 300 cal. in order to attain a rate of about 1000 c.p.s., at which the substituent proton positions would not be discernible by the N.M.R. modulatory frequency.

It is widely accepted that the crown form of cyclohexane is more stable than is the flexible form (13), although some refinement of calculation suggests that the higher free energy attributed to the flexible form may be exaggerated (9). In fact the electron diffraction patterns of 1,2-dichlorocyclohexane and 1,1,2-trichlorocyclohexane have been interpreted in favor of the flexible form at not-too-elevated temperatures (5). Actually it might be expected that substituent groups would affect profoundly the shape of the ring to which they are attached, and Oosterhof (18, 9) has shown that the dipole moment of 1,4-cyclohexanenedione is best explained in terms of a flexible form. This opinion is supported by solid dielectric studies to be reported from the Toronto laboratory, which show that this substance does not have an abnormal atom polarization.

Recently Kumler and Huitric have classified those cyclic types which may be expected to be flexible (12). The inclusion of piperazines among these classes is reasonable. A flattened tetrahedral aspect for the nitrogen atoms should permit the flexibility that is indicated for 1,4-cyclohexanenedione. The potential energy barrier due to methylene hydrogen interaction should be significantly less than that postulated for cyclohexane. In this circumstance a transition energy of 300 cal., largely involving compensated bond rotations, may indeed account satisfactorily for the absence of axial and equatorial proton positions in the N.M.R. spectrum. Therefore piperazines are thought to be in flexible conformation.

Within this definition we question whether the term "conformation" is an appropriate description of the saturated six-membered ring of atoms when it is considered in its flexible aspect. These terms imply the existence, during time intervals greater than those of molecular collision rate, of definite static structures. But the flexible ring will assume an infinity of forms and certainly cannot be defined in less than six static structures. None of these six will be equivalent when substituents of different complexity are present. In such circumstances the difficulties of "conformational analysis" are apparent. Perhaps they are not unsurmountable if the use of a static model is abandoned in favor of a dynamic one.

The authors wish to thank the National Research Council and the Defence Research Board of Canada for funds in support of this research and Mrs. Westland, Mr. Podleschka,

and the Tennessee Eastman Company, Division of Eastman Kodak Company, for extensive experimental aid.

#### EXPERIMENTAL\*

##### *Purification of Solvents*

Benzene was washed with concentrated sulphuric acid until the acid layer was colorless and then was dried and distilled by the sodium benzophenone technique (15). The specific volume and dielectric constant were 1.13795 and 2.284 at 20° C. respectively. Dioxane was refluxed with concentrated hydrochloric acid (5 ml./l.) for 6 hours, then neutralized, dried with sodium hydroxide, then refluxed, and finally distilled by the sodium benzophenone technique. The specific volume and dielectric constant at 20° C. were 0.96770 and 2.2175 respectively.

##### *N,N'-Dichloro-2,5-↑↓-dimethylpiperazine*

Repeated vacuum sublimation of commercial 2,5-↑↓-dimethylpiperazine gave flakes, m.p. 117–117.5° C. A solution of 5 g. (0.044 mole) in 20 ml. of water was added slowly with stirring to an excess of fresh sodium hypochlorite solution at 0° C. The white precipitate was filtered off, washed with cold water, and dried, 5.8 g. (72%), m.p. 81.5–82° C. Vacuum sublimation raised the melting point to 83.8° C. with 64% recovery. The density at 20° C. was found by flotation to be 1.394. Calc. for  $C_6H_{12}Cl_2$ : C, 39.4; H, 6.61; N, 15.3. Found: C, 39.7; H, 6.61; N, 15.8.

##### *N,N'-Dichloropiperazine*

This compound, prepared in 68% yield, m.p. 71–71.5° C. (21), was crystallized from ether–ethanol (2: 1, 15 ml./g.) and this was vacuum sublimed, m.p. 72° C.

##### *N,N'-Diformylpiperazine*

The reported procedure (20) gave a 91.5% yield, m.p. 125–126° C. Repeated crystallization from absolute ethanol (10 ml./g.) raised the melting point to 127.5° C. The density was determined by air displacement to be 1.391.

##### *N,N'-Bis-[2-cyanoethyl]-2,5-↑↓-dimethylpiperazine (25)*

To a suspension of 5.71 g. (0.05 mole) of 2,5-↑↓-dimethylpiperazine in 10 ml. of dioxane was added 0.25 cc. of benzyltrimethylammonium hydroxide (40% aq., Triton B) and then 7.18 g. (0.135 mole) of pure acrylonitrile with stirring during 1 hour. The temperature was maintained below 30° C. After subsequent stirring for 8 hours the system was diluted with 20 ml. of water and was extracted with methylene chloride. The methylene chloride extract was dried by magnesium sulphate and then evaporated, leaving 4.1 g. (38%), m.p. 140° C. Crystallization from absolute ethanol (50 ml./g.) using decolorizing charcoal raised the melting point to 147° C. The density (air displacement) was 1.163. Calc. for  $C_{12}H_{20}N_4$ : C, 65.4; H, 9.16; N, 25.4. Found: C, 65.5; H, 9.05; N, 25.7.

##### *N,N'-Bis-[2-cyanoethyl]piperazine*

The detail for preparation of the substance was not reported (6) so it was synthesized essentially as described above, yielding a brown mass which was distilled under reduced pressure. The fraction boiling at 174–176° C. at 6–7 mm. pressure solidified on cooling, and was purified by crystallization from ether (25 ml./g.), m.p. 62–63° C., 59.9% yield. Density determined by air displacement was 1.119.

\*Melting points have been corrected against reliable standards (see Wright, G. F. *Can. J. Technol.* **34**, 89 (1956)).

*N,N'-Dimethylpiperazine*

The substance was prepared (22) in 40% yield, b.p. 131–132° C. (758 mm.),  $D_4^{20}$  0.861,  $n_D^{20}$  1.4477.

*Polarizations of Solutions*

Dielectric constants and specific volumes were determined as described previously (16) except that a matching signal of 60 c.p.s. or 120 c.p.s. was read from an oscilloscope instead of a zero beat between V.F.O. and F.F.O. The polarization was calculated by the method of Halverstadt and Kumler (8).

*Polarization of the Solids*

The method outlined previously (15) was used, the only alteration being the use of a gold amalgam (4.0 g. Hg + 1.5 g. Au). The densities have been determined either by the flotation method (4) or by an air-displacement method. The density of N,N'-diphenylpiperazine by the latter method was 1.158 at 20° C.

*Density of Solids by Air Displacement*

In order to avoid the errors due to solubility and chemical reactions which are likely to occur when density is determined by flotation an apparatus has been redesigned (shown cross-sectionally in front and top elevations in Fig. 5) for greater precision than

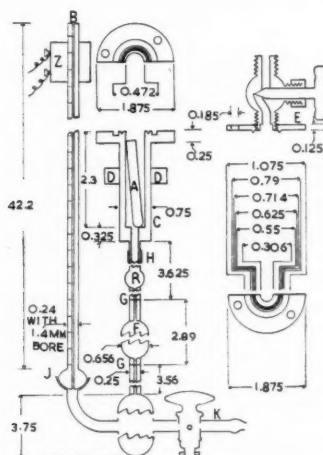


FIG. 5.

was required in the original one (7). The displacement of air by a finely-ground 0.3–1.0 g. sample in weighing tube A is measured by the change in pressure measured in manometer B after a 6-volt buzzer has reduced the column of mercury to a constant height. The brass chamber C, held by clamping block D, is equipped with a flange in which a seating V groove and a sealing square groove (containing a Parker O ring, 0.125 in. width, 0.8125 in. I.D., and 1.0625 in. O.D.) are cut. The V groove matches a V tongue in the flange E which is mated to C by three 10-32 machine screws. This flange, which is equipped for closure by a  $\frac{1}{4}$  inch 1 PS Hoke valve, must be seated carefully with repeated symmetry tests by insertion of feeler stock between the flanges. When properly seated the volume of C, containing the empty sample tube, can be measured to a precision of

0.04% by compressing air (by means of a levelling bulb, not shown) in front of mercury which fills the bulb F, the volume of which between two fiduciary marks G, G is previously known. A glass-metal seal H connects C and F, via a 2 cc. bulb R above the fiduciary mark. This bulb may be reduced in size to obtain proper volume relationship in the system. With attention to barometric pressure the change in manometric height is determined upon compression when the sample is included inside of C.

Thereupon the density is determined according to the relationship  $d = W/L$ , where  $L$  is the volume occupied by weight  $W$  of the sample. Then  $L = M - PN/dp_2$ , where  $P$  is the barometric pressure,  $dp_2$  is the pressure difference (cm. Hg) observed when volume  $N$  of bulb F is filled with mercury, after brass chamber C containing the sample is rendered airtight.  $M$  is the volume of C containing the empty sample tube and is defined as  $M = PN/dp_1$ , where  $dp_1$  is the observed pressure difference when mercury fills F without a sample in airtight chamber C.

Both the 12/2 ball joint J attaching the manometer and the stopcock K leading to the levelling bulb must be clamped tightly during the determination. The O ring but not the tongue and groove should be lightly greased in order to ensure airtightness when the flanges are connected. In order to avoid strain on the glass-metal seal during the closure operation the massive brass clamp D must secure C rigidly to the retort stand. Ordinary burette clamps suffice for the remainder of the apparatus.

The method is more arduous than a determination of density by flotation, but it is less subject to error than is the flotation method. For example the flotation of ferric acetylacetone in aqueous calcium chloride has led to an erroneous value of 1.41 (15). The density by air displacement is  $1.382 \pm 0.002$ . A revised flotation in which the medium was hexane plus 1,2-dibromoethane saturated with the ferric compound gave a value of  $1.381 \pm 0.008$ . The value is decreased by either method when a crystal contains impenetrable faults, so the sample should be ground finely before analysis.

#### *Polarization Values*

Experimentally determined values for  $d\epsilon/d\omega$  ( $\alpha$ ) and  $d\bar{V}/d\omega$  ( $\beta$ ) for the various piperazine derivatives are recorded as follows: N,N'-dichloro-2,5- $\uparrow\downarrow$ -dimethylpiperazine,  $\alpha = 0.05$ ,  $\beta = 0.265$ ; N,N'-dichloropiperazine,  $\alpha = 0.35$ ,  $\beta = 0.355$ ; methyldiformamide,  $\alpha = 2.88$ ,  $\beta = 0.307$ ; N,N'-diformylpiperazine,  $\alpha = 6.14$ ,  $\beta = 0.368$ ; N,N'-bis-cyanoethyl-2,5- $\uparrow\downarrow$ -dimethylpiperazine,  $\alpha = 9.62$ ,  $\beta = 0.180$ ; N,N'-bis-cyanoethylpiperazine,  $\alpha = 10.61$ ,  $\beta = 0.205$ ; 2,5- $\uparrow\downarrow$ -dimethylpiperazine,  $\alpha = 2.65$ ,  $\beta = 0.140$ ; N,N'-dimethylpiperazine,  $\alpha = 0.11$ ,  $\beta = 0.034$ .

The extrapolated values for  $\epsilon$  from pellet measurements are listed as follows: N,N'-dichloro-2,5- $\uparrow\downarrow$ -dimethylpiperazine, 2.325; N,N'-diformylpiperazine, 3.22; N,N'-bis-cyanoethyl-2,5- $\uparrow\downarrow$ -dimethylpiperazine, 2.714; N,N'-bis-cyanoethylpiperazine, 2.615; 2,5- $\uparrow\downarrow$ -dimethylpiperazine, 2.306; and N,N'-diphenylpiperazine, 2.730.

#### REFERENCES

1. ANDERSEN, P. and HASSEL, O. *Acta Chem. Scand.* **3**, 1180 (1949).
2. BARTON, D. H. R. and COOKSON, R. C. *Quart. Revs.* **10**, 44 (1956).
3. BECKETT, C. W., PITZER, K. S., and SPITZER, R. *J. Am. Chem. Soc.* **69**, 2488 (1947).
4. BERNAL, J. D. and CROWFOOT, D. *Nature*, **134**, 809 (1934).
5. DALLINGA, G. *Thesis*, Leyden. 1951.
6. FARBENIND., I.G., A.-G. German patent 641,597 (1937); *Chem. Abstr.* **31**, 5813 (1937).
7. GALLAY, W. and TAPP, J. S. *J. Am. Leather Chemists Assoc.* **37**, 140 (1942); *Chem. Abstr.* **36**, 3387 (1942).
8. HALVERSTADT, I. F. and KUMLER, W. D. *J. Am. Chem. Soc.* **64**, 2988 (1942).
9. HASELBROCK, P. and OOSTERHOF, L. J. *Trans. Faraday Soc.* **10**, 87 (1951).
10. HASSEL, O. *Quart. Revs. (London)*, **7**, 221 (1953).

11. KETELAAR, J. A. A. Rec. trav. chim. **62**, 289 (1943).
12. KUMLER, W. D. and HUITRIC, A. C. J. Am. Chem. Soc. **78**, 3369 (1956).
13. KWESTROO, W., MEIJER, F. A., and HARINGA, E. Rec. trav. chim. **73**, 717 (1954).
14. MARTIN, G. T. O. Thesis, London. 1936. pp. 134, 180. PARTINGTON, J. R. An advanced treatise on physical chemistry. Vol. 5. Longmans, Green and Co., London. 1954. p. 538.
15. MEREDITH, C. C., WESTLAND, L. and WRIGHT, G. F. J. Am. Chem. Soc. **79**, 2385 (1957).
16. MEREDITH, C. C. and WRIGHT, G. F. Can. J. Technol. **33**, 182 (1955).
17. MYERS, G. S. and WRIGHT, G. F. Can. J. Research, B, **26**, 257 (1948).
18. OOSTERHOF, L. J. Thesis, Leyden. 1949.
19. PHILIPS, W. D. J. Chem. Phys. **23**, 1363 (1955).
20. ROBSON, J. H. and REINHART, J. J. Am. Chem. Soc. **77**, 2453 (1955).
21. SCHMIDT, A. and WICHMAN, G. Ber. **24**, 3237 (1891).
22. STEWART, H. W. *et al.* J. Org. Chem. **13**, 134 (1948).
23. THEILACKER, W. and FAUSER, K. Ann. **539**, 103 (1939).
24. VARIAN ASSOCIATES. Anal. Chem. **28**, 25A (Aug., 1956).
25. WAGNER, W. F. and KAUFFMAN, W. B. Anal. Chem. **25**, 538 (1953).

# CRITICAL CONCENTRATION EFFECTS IN POLYMER-POLYMER-SOLVENT SYSTEMS<sup>1</sup>

C. C. BIGELOW AND L. H. CRAGG

## ABSTRACT

In various ternary systems of the type polymer A - polymer B - solvent S, a dip or peak has been observed in the  $[\eta]-c_B$  curve at the critical concentration of polymer B. ( $[\eta]$  is the intrinsic viscosity of A in mixed solvent consisting of B and S, and  $c_B$  is the concentration of B in this mixed solvent.) It is shown that such a critical concentration effect is most likely to occur when the solvent is poor for polymer B, and will be the larger the poorer the solvent.

Evidence is also presented in support of the hypothesis that if, as is usual, the two polymers repel each other, the effect is a dip if the solvent is good for polymer A and is a peak if the solvent is sufficiently poor for polymer A.

Critical concentrations of polystyrene, polyvinyl acetate, and polymethyl methacrylate (five different samples) have been measured in this way in 12 different ternary systems. These observed critical concentrations are in good agreement with values calculated using the equation previously described, according to which the critical concentration of a polymer is inversely proportional to its intrinsic viscosity in the solution.

## INTRODUCTION

In a recent paper (1) we presented evidence to show that a critical concentration can be determined in suitable viscometric experiments with ternary systems of the type polymer A - polymer B - solvent S. ("Critical concentration" here means the concentration of polymer at which the equivalent sphere of a given polymer molecule just touches the equivalent spheres of all of its nearest neighbor molecules of like kind.) If the intrinsic viscosity  $[\eta]$  of Polymer A is measured first in pure S and then in a series of mixed solvents (solutions of polymer B in S) successively richer in polymer B, and if these intrinsic viscosities are plotted against  $c_B$ , the concentration of polymer B in the mixed solvent, then the resulting curve may exhibit a discontinuity at or very near the concentration calculated to be the critical concentration ( $c_{crit}$ ) of polymer B in the solution. In four of the five experiments of this type that were reported, the discontinuity took the form of a dip, the curve having the general shape indicated in Fig. 1.

A qualitative explanation of this behavior was proposed, and an equation for calculating critical concentrations was developed with the aid of the Flory-Fox treatment of intrinsic viscosity. According to this equation, the critical concentration of polymer B should be inversely proportional to its intrinsic viscosity in pure solvent S (more strictly, to its reduced viscosity at  $c_B = c_{crit}$ , but since  $c_{crit}$  is very small, this reduced viscosity will differ little from the intrinsic viscosity). This conclusion was tested in experiments with the ternary system polystyrene - polymethyl methacrylate - solvent in which the intrinsic viscosity of polymer B (polymethyl methacrylate in this system) was varied, first by using samples of different molecular weight with the same solvent (*m*-xylene), and then by using two different solvents with the same sample of polymer. The observed critical concentration varied as predicted, and the values agreed remarkably well with the calculated values. (The observed critical concentration is taken to be the concentration  $c_B$  at which the discontinuity occurs or, more precisely, the concentration corresponding to the bottom of the dip or the top of the peak.)

In this paper we report and discuss the results of further study of this critical concentration phenomenon.

<sup>1</sup>Manuscript received September 16, 1957.

Contribution from the Department of Chemistry, McMaster University, Hamilton, Ontario. This work was done as part of the requirements for the Ph.D. degree, and was financially supported by the National Research Council of Canada.

## PROCEDURE

In the experiments to be reported here, we have (with a few exceptions noted in Table III) used the first of the two methods for determining critical concentrations that were described in the earlier paper (1). This was partly because this "intrinsic viscosity method" is more trustworthy (though much more time-consuming) than the other, but mainly because we were interested in the nature, as well as in the location, of the discontinuity in the  $[\eta]$  vs.  $c_B$  curve.

Special care was taken in determining intrinsic viscosities. Both  $\eta_{sp}/c$  and  $(\ln \eta_r)/c$  were plotted against  $c_A$  on a common plot and the curves were extrapolated to a common point at  $c_A = 0$  to obtain  $[\eta]$ . When, as in almost all cases, these curves were straight lines,  $[\eta]$  was evaluated by the method of least squares.

## RESULTS AND DISCUSSION

*I. The Nature of the Discontinuity*

(a) In all of the experiments reported in the earlier paper, the solvent S was a poor one for polymer B. (By a "poor" solvent we mean here one in which the polymer has a relatively low intrinsic viscosity.) If the explanation of the critical concentration "dip" proposed in the previous paper is correct, a system in which the solvent S is poor for polymer B (and good for polymer A) should give a greater effect than one in which the solvent is good for polymer B (and good for polymer A). In a solvent that is good for it, the molecules of polymer A will be loosely coiled and the effective volume of an isolated molecule will be relatively large. As the critical concentration of polymer A is approached, molecules of polymer B will begin to crowd in on the molecule on all sides; and further increase in concentration will cause contraction of the polymer A molecule or of the polymer B molecules or both (assuming that the two polymers repel each other, as is true of most polymer pairs). If the solvent is poor for polymer B, its molecules will be more tightly coiled, and the density of segments of B in the immediate neighborhood of the A molecule will be higher than if the solvent is good for polymer B. The repulsive forces causing the molecule of A to shrink (and hence its intrinsic viscosity to decrease) will therefore be greater. Conversely, if the solvent is good for polymer B the contraction in volume of the molecule of polymer A (and therefore the decrease in  $[\eta]$ ) might well be so slight as to be undetectable, partly because of the much lower density of B segments at the critical concentration, and partly because such contracting as would occur would be shared by the B molecules.

The validity of these speculations was tested in experiments with the systems listed in Table I. The results are shown graphically in Fig. 3. Toluene and benzene are both *poor* solvents for polyvinyl acetate; experiments 6 and 8 should therefore give measurable effects. Toluene and *m*-xylene are both *good* solvents for polystyrene; in experiments 7 and 9, therefore, the discontinuity should be very small or undetectable. As

TABLE I  
TERNARY SYSTEMS IN EXPERIMENTS 6 TO 9  
(For identification of polymer samples see Table V)

Experiment	Polymer A	Polymer B	Solvent S
6	PS-3	PV-1	Toluene
7	PV-1	PS-3	Toluene
8	PS-3	PV-1	Benzene
9	PM-4	PS-3	<i>m</i> -Xylene

can be seen, unmistakable "dips" do occur in the  $[\eta]$ - $c_B$  curves for experiments 6 and 8 (and they occur at the calculated critical concentrations, indicated by the arrow) but there is no sign of a "dip" in the curves for experiments 7 and 9.

(b) In experiment 5 of the earlier paper (1) the discontinuity in the  $[\eta]$ - $c_B$  curve was a peak rather than a dip (see Fig. 2 of this paper). In this experiment polymer A was

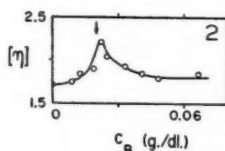
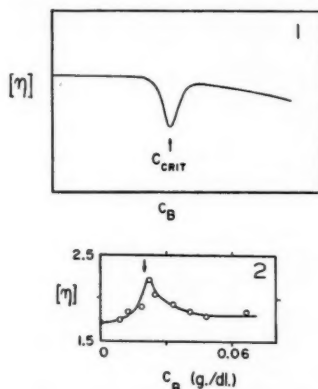


FIG. 1. Viscometric critical concentration effect: idealized curve.

FIG. 2. A critical concentration peak. (System: polystyrene - polymethyl methacrylate - butanone.)

polystyrene, polymer B was polymethyl methacrylate, and the solvent was butanone. This solvent is a poor one for *both* polymers. The shape of the discontinuity was a surprise, but it can be plausibly accounted for in terms of our molecular explanation. If the solvent is a very poor one for the A polymer (as butanone is for polystyrene in experiment 5) the segments of a polymer A molecule will much prefer one another's company to that of solvent molecules, and the polymer molecule will coil up tightly. If the dislike of polymer A for polymer B is less than its dislike of the solvent S, then the fairly uniform environment, consisting of solvent molecules and polymer B segments, that is attained near the critical concentration will be a more favorable environment for the polymer A molecule than pure solvent S. The molecule will therefore expand and  $[\eta]$  will increase. Further, as  $c_B$  is increased,  $[\eta]$  will continue to increase until the critical concentration is reached, after which interpenetration of the two kinds of polymer molecules begins to make the environment within and without the polymer A molecule more nearly the same. Then the molecule of polymer A will begin to contract again, for the mixed solvent is still a poor solvent for the polymer.

One might therefore expect to find a peak with systems in which the solvent S is poor for both polymers and is so poor for polymer A that the mutual repulsion of polymer A segments and solvent S molecules would exceed that of polymer A segments and polymer B segments.

We therefore investigated three additional systems, in which the solvent was at the same time poor for both polymers. These systems are described in Table II and the results obtained with them are shown graphically in Fig. 4. In two of the three experiments (10 and 11) a peak was indeed obtained—and at or very near the concentration calculated to be the critical concentration. In the third (experiment 12) no discontinuity of any kind was observed. This may be because the polymer A - solvent repulsion was not appreciably greater than the polymer A - polymer B repulsion.

TABLE II  
SYSTEMS IN WHICH THE SOLVENT IS POOR FOR BOTH POLYMERS

Experiment	Polymer A	Polymer B	Solvents
10	PS-3	PV-1	Butanone
11	PS-3	PM-5	Ethyl acetate
12	PM-5	PS-3	Ethyl acetate

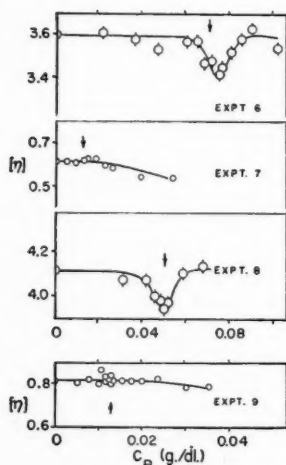


FIG. 3. Effect of goodness of solvent for polymer B. The solvent is poor for B in experiments 6 and 8 and good for B in experiments 7 and 9. (The arrows point to the calculated critical concentrations.)

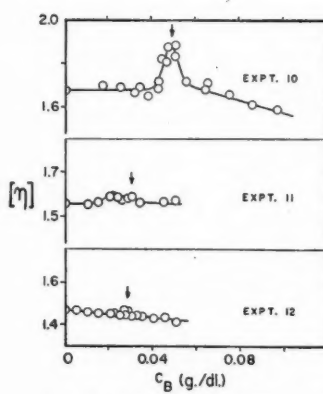


FIG. 4. Critical concentration effects with systems in which the solvent is poor for both polymers. (Arrows indicate calculated critical concentrations.)

(c) The success that our hypothesis has had in explaining and predicting experimental findings makes it seem highly probable that the critical concentration effects we have been studying are due to polymer-polymer and polymer-solvent interactions and to their relative magnitudes. So far we have dealt with systems in which the two polymers would be expected to repel each other (see for example the polymer incompatibility studies of Dobry and Boyer-Kawenoki (2) and of Kern and Slocombe (3)). The magnitude of the dip should be greatest when the solvent is good for polymer A and poor for polymer B and when the two polymers repel each other strongly. The magnitude of the effect should be less when the two polymers are more alike than are polystyrene and polyvinyl acetate, or polystyrene and polymethyl methacrylate. A number of experiments have been done which seem to support this idea. The systems investigated are listed in Table III. In all of them the solvent is a poor one for the solvent polymer (polymer B).

In five of the eight experiments (13, 14, 15, 21, and 22) the critical concentration effect, if any, was too small to manifest itself by an unmistakable discontinuity. In each of the other three experiments (16, 19, and 20) a dip was indicated, each time at or near the concentration calculated to be the critical concentration (see Fig. 5). These dips were, however, very small ones, definitely smaller than those observed in systems in which the two polymers were more different chemically. (It is interesting to note

TABLE III  
SYSTEMS IN WHICH THE POLYMERS ARE SIMILAR

Experiment*	Polymer A	Polymer B	Solvent S	Relationship of polymers
13	PM-5	PV-1	Toluene	Both esters
14f	PV-1	PM-5	Toluene	Both esters
15	PM-5	PV-1	Butanone	Both esters
16	PV-1	PM-5	Butanone	Both esters
19	PS-4	PS-5	Butanone	Homologues
20	PM-6	PM-7	Ethyl acetate	Homologues
21f	PpMeS	PmMeS	Butanone	Isomers
22f	PmMeS	PpMeS	Butanone	Isomers

\*f indicates that the experiment was done using the flow time method only.

that with two quite different systems—see experiments 19 and 20—critical concentration effects were observed when the two polymers were two different samples of the same polymer. These experiments provide direct evidence that molecules of the same polymer repel each other and, when crowded close together, cause each other to shrink. Such behavior was postulated on theoretical grounds and some of its consequences discussed by Weissberg, Simha, and Rothman (4). Indeed, they derived an expression for the concentration at which this shrinkage should occur (in a binary system)—though they did not call it a critical concentration—and their expression has the same form as ours.)

#### II. The Location of the Discontinuity: The Critical Concentration

Although these experiments have been concerned primarily with the nature (shape and magnitude) of the discontinuity, they contribute further evidence that the discontinuity does indeed occur at a critical concentration. In the first paper, proof that a critical concentration effect was being observed was provided by the excellent agreement between observed and calculated values of the critical concentration. The equation for calculating the critical concentration ( $c_{\text{crit}}$ ) was shown to be

$$c_{\text{crit}} = 0.0436k^3/[\eta]_B,$$

where  $k$  is a (dimensionless) proportionality constant whose value is apparently very close to unity. The constant should have substantially the same value for all the polymers used as polymer A in the systems we have studied, for all of them are flexible linear vinyl polymers. The same equation, viz.  $c_{\text{crit}} = 0.0436k^3/[\eta]_B$ , should therefore apply to all the systems.

The value of  $c_{\text{crit}}$ , the critical concentration, obtained from the equation is marked on each of the plots by means of an arrow; any dip or peak in the  $[\eta]-c_B$  curve invariably occurs at or near this point. In Table IV are listed values of the product of the observed critical concentration and the intrinsic viscosity of polymer B. The essential constancy of this product is strong evidence for the validity of our assumptions. Visual evidence of

TABLE IV  
OBSERVED VALUES OF THE PRODUCT  $[\eta]_B c_{\text{crit}}$

Experiment	$[\eta]_B c_{\text{crit}}$	Experiment	$[\eta]_B c_{\text{crit}}$
1	0.046	8	0.044
2	0.047	10	0.046
3	0.042	11	0.034
4	0.046	16	0.040
5	0.048	19	0.034
6	0.047	20	0.044

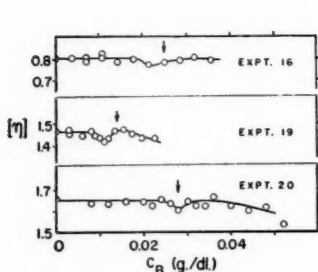


FIG. 5. Critical concentration effects. (Experiment 16, polyvinyl acetate - polymethyl methacrylate - butanone; Experiment 19, polystyrene-polystyrene-butanone; Experiment 20, polymethyl methacrylate - polymethyl methacrylate - ethyl acetate.)

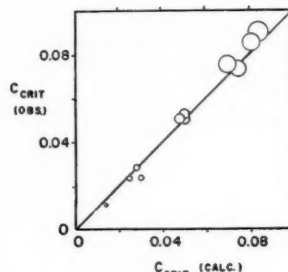


FIG. 6. Plot of observed vs. calculated critical concentrations.

the good agreement between calculated and observed values is afforded in Fig. 6, in which  $c_{\text{crit}}(\text{observed})$  is plotted against  $c_{\text{crit}}(\text{calculated})$  for all systems in which a discontinuity has been observed. The agreement would be perfect if the points fell on the  $45^\circ$  line; it is not perfect, but it is surprisingly good.

#### EXPERIMENTAL

The apparatus and experimental methods were those used previously (1). The intrinsic viscosities of the various polymers used are given in Table V.

TABLE V  
INTRINSIC VISCOSITIES OF POLYMER SAMPLES USED

Polymer	Solvent	$[\eta]$ (dl./g.)
Polystyrene PS-3	Benzene	4.13
	Butanone	1.67
	Ethyl acetate	1.55
	Toluene	3.60
	<i>m</i> -Xylene	3.44
PS-4	Butanone	1.67
PS-5	Butanone	3.07
Polymethyl methacrylate PM-4	<i>m</i> -Xylene	0.81
PM-5	Butanone	1.74
	Ethyl acetate	1.47
	Toluene	1.75
PM-6	Ethyl acetate	1.65
PM-7	Ethyl acetate	1.57
Polyvinyl acetate*	Benzene	0.88
PV-1	Butanone	0.80
	Toluene	0.62
Poly( <i>m</i> -methylstyrene) and poly( <i>p</i> -methylstyrene)* PmMeS PpMeS	Butanone	1.55
	Butanone	1.28

\*We are grateful to Shawinigan Chemicals Ltd., Shawinigan Falls, Que., for providing us with the sample of polyvinyl acetate (Gelva, V-27) and to Dr. R. J. Kern (3), Monsanto Chemical Co., Dayton, Ohio, for the samples of poly(*m*-methylstyrene) and poly(*p*-methylstyrene).

## REFERENCES

1. CRAGG, L. H. and BIGELOW, C. C. *J. Polymer Sci.* **24**, 429 (1957).
2. DOBRY, A. and BOYER-KAWENOKI, F. *J. Polymer Sci.* **2**, 90 (1947).
3. KERN, R. J. and SLOCOMBE, R. J. *J. Polymer Sci.* **15**, 183 (1955).
4. WEISSBERG, S. G., SIMHA, R., and ROTMAN, S. *J. Research Natl. Bur. Standards*, **47**, 298 (1951).

# THE SYNTHESIS OF $\omega$ -DEOXY- $\omega$ -S-ETHYL-POLYOLS<sup>1</sup>

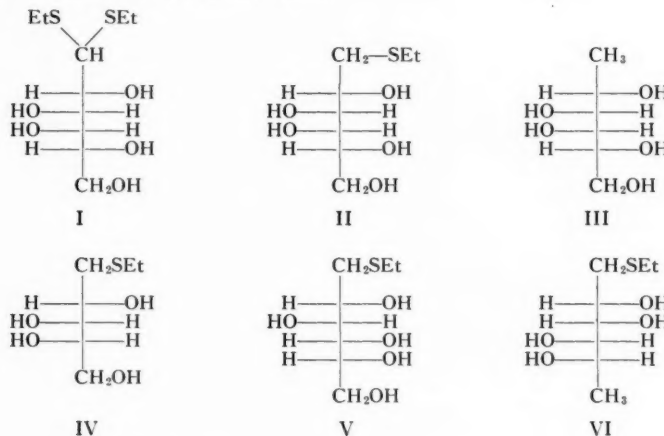
J. K. N. JONES AND D. L. MITCHELL<sup>2</sup>

## ABSTRACT

Treatment of an aldose diethyl thioacetal with a limited amount of aged Raney nickel catalyst resulted in the reductive cleavage of one thioethyl group. 1-Deoxy-1-S-ethyl derivatives of D-galactitol, L-arabitol, L-rhamnitol, and D-glucitol have thus been synthesized and their structures proved. 1-Deoxy-1-S-ethyl-L-galactitol has been prepared by the borohydride reduction of 6-deoxy-6-S-ethyl-D-galactose.

## INTRODUCTION

Reductive desulphurization of aldose thioacetals (1, 2, 3, 4, 5, 6) and aldose thioacetal acetates (1, 7) using an excess of Raney nickel catalyst provides a simple method of preparing 1-deoxy sugar alcohols. In a review, Fletcher and Richtmyer (8) questioned the value of using as high catalyst ratios as have been reported in the literature. They tabulate examples of ratios from 9:1 to 15:1 (grams of Raney nickel catalyst to grams of thioacetal derivative). Generally, the yield of 1-deoxy-polyol or 1-deoxy-polyol acetate varied inversely with the catalyst ratio. The decrease in yield was probably due to adsorption of product on the catalyst. We found that when a catalyst with a low hydrogen content (e.g. W-2 catalyst) was used, and a low catalyst ratio was chosen (*ca.* 5:1), a mixture of three compounds resulted. When D-galactose diethyl thioacetal was thus treated, paper chromatographic examination of the product indicated the presence of a fast-moving compound, D-galactose diethyl thioacetal; a slow-moving compound, 1-deoxy-D-galactitol (L-fucitol); and a second sulphur-containing compound (II) which was between these two compounds on the chromatogram. A catalyst ratio was determined, by means of trial experiments in which compound II was the main product of the reaction. In this reaction one thioethyl group of the aldose diethyl thioacetal (I) was replaced by a hydrogen atom to give the monothioethyl derivative (II). Compound II on reductive desulphurization gave 1-deoxy-D-galactitol (L-fucitol) (III).



<sup>1</sup>Manuscript received September 9, 1957.

Contribution from the Department of Chemistry, Queen's University, Kingston, Ontario.

<sup>2</sup>Present address: Department of Organic Chemistry, University of Bristol, Bristol 8, England.

The diethyl thioacetals of D-galactose, L-arabinose, D-glucose, and L-rhamnose were also partially desulphurized, and respectively yielded 1-deoxy-1-S-ethyl-(D-galactitol) (II), -(L-arabitol) (IV), -(D-glucitol) (V), and -(L-rhamnitol) (VI). Crystalline acetates of compounds II, IV, and V were also prepared. The yields were not appreciably reduced when large scale experiments were carried out. This result corresponded with the observations of Richtmyer and co-workers (2, 3, 4, 5, 6). Complete reductive desulphurization of compounds II, IV, V, and VI yielded the known  $\omega$ -deoxy sugar alcohols, which are 1-deoxy-D-galactitol (L-fucitol), 1-deoxy-L-arabitol (L-lyxomethylitol), 1-deoxy-D-glucitol (L-gulomethylitol), and 1,6-dideoxy-L-mannitol respectively.

$\omega$ -Deoxy- $\omega$ -S-alkyl polyols can also be synthesized by the reduction of the corresponding aldose (9). In this manner 6-deoxy-6-S-ethyl-D-galactose (6-deoxy-6-thioethyl-D-galactose) (10) was reduced with potassium borohydride to 1-deoxy-1-S-ethyl-L-galactitol (6-deoxy-6-S-ethyl-D-galactitol). This compound had about the same melting point and magnitude of optical rotation (but in the opposite direction) as the D-isomer. The D- and L-isomers had identical rates of movement on paper chromatograms. The racemate melted at about 10° C. lower than the isomers.

#### EXPERIMENTAL

Solutions were concentrated under reduced pressure (*ca.* 15 mm.) at a bath temperature of 50° C. or less. Melting points were uncorrected and optical rotations were determined in water unless otherwise stated. Paper chromatography was carried out by the descending method (11) on Whatman No. 1 filter paper using the following solvent systems (v: v): (a) ethyl acetate - acetic acid - water (9: 2: 2), (b) ethyl acetate - acetic acid - formic acid - water (18: 3: 1: 4), (c) n-butanol-ethanol-water (3: 1: 1), (d) n-butanol-pyridine-water (10: 3: 3). Non-reducing compounds were detected on paper chromatograms with a silver nitrate spray reagent (12). The rate of movement of the compound on paper chromatograms is quoted relative to that of the solvent front ( $R_f$  value) or relative to that of rhamnose ( $R_{Rh}$  value).

A standard method of preparing Raney nickel catalyst W-2 (13) was followed exactly. It was stored in ethanol at 0-5° C. This catalyst will be referred to as catalyst (a) in these experiments. A catalyst of slightly lower hydrogen content was obtained from the Aldrich Chemical Company.\* It was washed free from traces of alkali and was stored in ethanol at 0-5° C. This catalyst will be referred to as catalyst (b). The activity of catalysts (a) and (b) did not change appreciably over a storage period of 4 months.

#### Preliminary Experiments

Weighed samples (*ca.* 0.5 g.) of D-galactose diethyl thioacetal (14) were dissolved in 75% isopropanol (50 ml.). A range of catalyst ratios was chosen (*ca.* 3:1 to 8:1) and the appropriate volume of Raney nickel catalyst (a) was added to the flasks. The mixture was boiled under reflux for 2 hours and cooled. The solutions were filtered from the catalyst and examined by paper chromatography. The catalyst ratio that produced the maximum amount of component with a rate of movement between galactose diethyl thioacetal and fucitol was used in subsequent experiments. Catalyst ratios are expressed in liters of settled volume of nickel per mole of aldose thioacetal.

#### Preparation of 1-Deoxy-1-S-ethyl-D-galactitol

(i) D-Galactose diethyl thioacetal (3.73 g., 0.013 mole) and Raney nickel catalyst (a)

\*Aldrich Chemical Co., Inc., Milwaukee 12, Wisconsin.

(settled volume 30 ml. equivalent to 2.3 liters/mole) in 75% *isopropanol* (200 ml.) were shaken in a hydrogen atmosphere (pressure *ca.* 800 mm.) for 2 hours at 60° C. and then boiled under reflux on the water bath (100° C.) for an additional 3 hours. The filtered solution was concentrated to a crystalline mass, which was recrystallized from methanol and acetone (5 : 1) to give 1.24 g. (57.5%) of product melting at 151–153° C. (The catalyst was lost accidentally before it could be washed.) The rate of movement on a paper chromatogram ((a)  $R_f$  0.47,  $R_{Rh}$  1.70; (b)  $R_f$  0.52,  $R_{Rh}$  1.29) was intermediate between galactose diethyl thioacetal and fucitol, and the compound on treatment with silver nitrate spray reagent gave an intense spot which appeared immediately, whereas the spot due to fucitol appeared slowly. The product on recrystallization from methanol gave a chromatographically pure product that had m.p. 149–151° C. and  $[\alpha]_D^{25} -9^\circ \pm 2^\circ$  ( $c$ , 0.95). Anal. Calc. for  $C_8H_{18}O_5S$ : C, 42.6; H, 8.1; S, 14.2. Found: C, 42.5; H, 8.1; S, 14.0.

(ii) *Large scale experiment.*—*D*-Galactose diethyl thioacetal (11.0 g., 0.038 mole) and Raney nickel catalyst (a) (83.5 ml. settled volume equivalent to 2.2. liters/mole) in 75% *isopropanol* (1 liter) were boiled under reflux on the water bath (100° C.) for 3 hours. The solution was decanted from the catalyst, which was washed twice with ethanol and separated by centrifugation. The catalyst was digested with ethanol (3 times with 300 ml.) and then with water (2 times with 200 ml.), and the combined washings and decanted solution were filtered through a pad of Celite and evaporated to dryness. Recrystallization from methanol and acetone (5 : 1) gave 5.80 g. (67%) of product in three crops of crystals, m.p. 148–149° C. Duplicate readings gave  $[\alpha]_D^{21} -8.2^\circ$  ( $c$ , 2.24);  $[\alpha]_D^{24} -8.9^\circ$  ( $c$ , 2.33).

#### *1-Deoxy-1-S-ethyl-D-galactitol Pentaacetate*

1-Deoxy-1-S-ethyl-D-galactitol (88 mg.) in pyridine (1 ml.) was acetylated for 24 hours with acetic anhydride (1 ml.). The product crystallized when it was poured into a slurry of chipped ice and water, and it was collected by filtration. It was dissolved in hot methanol, and the solution was purified with a little charcoal and filtered through a pad of Celite. The filtrate was warmed and an equal volume of hot water was added. After cooling, the crystals in the form of flakes were collected by filtration and washed with cold water. Yield: 117 mg. (60%), m.p. 150.5–151.0° C.  $[\alpha]_D^{22} 8^\circ \pm 1^\circ$  ( $c$ , 1.1, chloroform). Anal. Calc. for  $C_{18}H_{24}O_{10}S$ : C, 49.5; H, 6.5; S, 7.3. Found: C, 49.8; H, 6.7; S, 7.1.

#### *Conversion of 1-Deoxy-1-S-ethyl-D-galactitol to L-Fucitol*

1-Deoxy-1-S-ethyl-D-galactitol (120 mg.) was dissolved in 70% ethanol (10 ml.) containing Raney nickel W-2 catalyst (3 ml. settled volume) and the suspension was boiled under reflux on the water bath (100° C.) for 3 hours. The catalyst was removed by filtration through a pad of Celite, and the filtrate was concentrated to a crystalline mass. The product moved as a single spot on paper chromatograms developed in solvents (a), (b), (c), and (d) and had a rate of movement identical with that of L-fucitol prepared by the borohydride reduction of L-fucose. The following  $R_f$  and  $R_{Rh}$  values were obtained:  $R_f$  0.37,  $R_{Rh}$  1.12 (a);  $R_f$  0.39,  $R_{Rh}$  1.07 (b);  $R_f$  0.31,  $R_{Rh}$  1.00 (c);  $R_f$  0.30,  $R_{Rh}$  0.93 (d). Recrystallization from ethanol (3 ml.) gave 33.4 mg. (38%) of fine needles melting at 156.0–156.5° C. The mixed melting point with an authentic specimen was 156.0–156.5° C.

#### *1-Deoxy-1-S-ethyl-L-arabitol*

(i) L-Arabinose diethyl thioacetal (1.50 g., 0.008 mole) (15, 16) and freshly prepared Raney nickel catalyst (a) (settled volume 12 ml., 1.5 liters/mole) in 75% *isopropanol* (80 ml.) were boiled under reflux on the water bath (100° C.) for 3 hours. The cooled solution was decanted and the catalyst was washed with ethanol and separated by centrifugation. The catalyst was then digested with ethanol (2×100 ml.) and the combined

washings and decanted solution were filtered through a pad of Celite and evaporated to dryness. The crystalline mass was examined by paper chromatography, which indicated the presence of two compounds. The main constituent had a rate of movement of  $R_f$  0.61,  $R_{RH}$  1.79 (a) and the second component had a rate of movement of  $R_f$  0.43,  $R_{RH}$  1.27 (a). The ratio of the two components was visually estimated to be 20:1. The crude product was dissolved in hot acetone (40 ml.), filtered, and chilled in the refrigerator. The crystals were collected by filtration and the mother liquors were concentrated to yield a second crop. Yield: 0.71 g. (68%), m.p. 118.5–119.5° C.,  $[\alpha]_D^{25} -12^\circ \pm 1^\circ$  (c, 2.59). Anal. Calc. for  $C_7H_{16}O_4S$ : C, 42.8; H, 8.2; S, 16.3. Found: C, 43.1; H, 8.5; S, 16.1.

(ii) L-Arabinose diethyl thioacetal (19.0 g., 0.074 mole) and 75% isopropanol (3 liters) were stirred mechanically with aged Raney nickel catalyst of a low hydrogen content (settled volume 250 ml., 3.3 liters/mole) and boiled under reflux on the water bath (100° C.) for 3.5–4 hours. The cooled solution was decanted and the catalyst was treated in the manner described above. Examination of the product by paper chromatography revealed only a single spot ( $R_f$  0.69,  $R_{RH}$  1.83 (a)). The product was recrystallized from acetone–ethanol (3:1) to give a total yield of 8.43 g. (58%) in four crops, m.p. 119–120° C.,  $[\alpha]_D^{26} -12^\circ \pm 1^\circ$  (c, 1.75). Recrystallization from isopropanol gave fine needles, m.p. 118.5–119.5° C. When tested in high concentration, a trace of L-lyxomethylitol was revealed on the chromatogram and this impurity was removed by repeated recrystallizations from isopropanol, but the melting point remained unchanged (118.5–119.5° C.).

#### 1-Deoxy-1-S-ethyl-L-arabitol Tetraacetate

The tetraacetate was prepared in the manner previously described for the acetylation of 1-deoxy-1-S-ethyl-D-galactitol. Recrystallization from ethanol and water (3:1) gave white plates (40%) melting at 58.0–58.5° C.,  $[\alpha]_D^{26} -35^\circ \pm 1^\circ$  (c, 1.64, chloroform). Anal. Calc. for  $C_{15}H_{24}O_8S$ : C, 49.4; H, 6.6; S, 8.8. Found: C, 49.5; H, 6.5; S, 8.9.

#### 1-Deoxy-L-arabitol (L-Lyxomethylitol)

1-Deoxy-L-arabitol (7) was prepared in 70% yield by the desulphurization of 1-deoxy-1-S-ethyl-L-arabitol in the same fashion as is described for the desulphurization of L-fucitol. The product (0.19 g.) was recrystallized from ethyl acetate (40 ml.), m.p. 128–129° C.,  $[\alpha]_D^{25} -1.8^\circ$  (c, 1.70), (lit. m.p. 129–131° C.,  $[\alpha]_D^{30} -1.46^\circ$  (water) (9)). 1-Deoxy-D-arabitol has a reported m.p. 129–131° C. and a  $[\alpha]_D^{20} +0.7^\circ$  (6).

#### 1-Deoxy-1-S-ethyl-D-glucitol

D-Glucose diethyl thioacetal (15) (5.0 g., 0.017 mole) in 75% isopropanol (600 ml.) was boiled under reflux with aged Raney nickel catalyst (b) (50 ml. settled volume, 2.9 liters/mole) in exactly the same manner as is described for the preparation of 1-deoxy-1-S-ethyl-D-galactitol in experiment (ii). The crude product, 1.94 g. (51%), contained a trace of 1-deoxy-D-glucitol (paper chromatography), and was recrystallized four times from isopropanol. The pure compound had a rate of movement on a paper chromatogram of  $R_f$  0.59,  $R_{RH}$  1.70 (a);  $R_f$  0.61,  $R_{RH}$  1.53 (b);  $R_f$  0.52,  $R_{RH}$  1.61 (c);  $R_f$  0.53,  $R_{RH}$  1.48 (d); a m.p. 107.5–108° C.; and  $[\alpha]_D^{26} -29^\circ \pm 1^\circ$  (c, 1.85). Anal. Calc. for  $C_8H_{18}O_6S$ : C, 42.7; H, 8.1; S, 14.2. Found: C, 42.9; H, 8.2; S, 14.0.

When the experiment was repeated on a larger scale (D-glucose diethyl thioacetal, 23.6 g., Raney nickel catalyst (b), 215 ml. settled volume, and isopropanol, 3 liters) in the manner previously described for the preparation of 1-deoxy-1-S-ethyl-L-arabitol, part (ii), a yield of 9.87 g. (49%) of crude product was obtained. Repeated recrystallizations from isopropanol gave 6.9 g. (34%) of pure compound, m.p. 107.5–108° C.,  $[\alpha]_D^{24} -30^\circ$  (c, 1.89).

*1-Deoxy-1-S-ethyl-d-glucitol Pentaacetate*

The pentaacetate was prepared in the manner previously described and was crystallized from methanol and water (1:1) in a 59% yield, m.p. 82° C.,  $[\alpha]_D^{26} 5^\circ \pm 1^\circ$  (*c*, 1.1, chloroform). Anal. Calc. for  $C_{18}H_{28}O_{10}S$ : C, 49.5; H, 6.5; S, 7.4. Found: C, 49.7; H, 6.5; S, 7.4.

*1-Deoxy-d-glucitol Pentaacetate*

Reductive desulphurization of 1-deoxy-1-S-ethyl-d-glucitol in ethanol with an excess of Raney nickel catalyst (*a*) in the usual manner gave a non-crystalline product which appeared to be chromatographically pure ( $R_f$  0.60,  $R_{Rh}$  1.52 (*a*);  $R_f$  0.28,  $R_{Rh}$  0.95 (*c*);  $R_f$  0.29,  $R_{Rh}$  0.88 (*d*)). It was therefore acetylated and the pentaacetate was recrystallized from ethanol, m.p. 105.5–107° C.,  $[\alpha]_D^{26} 21^\circ \pm 1^\circ$  (*c*, 1.26, methanol) (lit. m.p. 105–106° C.,  $[\alpha]_D^{21} 21^\circ$  (methanol) (7, 17)).

*1-Deoxy-1-S-ethyl-L-rhamnitol*

L-Rhamnose diethyl thioacetal (15) (4.0 g., 0.015 mole) was dissolved in 75% *iso*-propanol (600 ml.) and was boiled under reflux with Raney nickel catalyst (*a*) (33 ml. settled volume equivalent to 2.2 liters/mole) for 4 hours. The crude product (1.0 g. (32%)), m.p. 118–119.5° C., was isolated in the usual way. This compound was readily soluble in water, ethanol, and *iso*-propanol but it could be recrystallized from a small volume of ethyl acetate. Repeated recrystallizations from ethyl acetate gave flat plates melting at 120.5–121° C. and with  $[\alpha]_D^{26} -21.2^\circ$  (*c*, 1.36). The rates of movement on paper chromatograms were  $R_f$  0.76 (*a*) and  $R_f$  0.73 (*b*). Anal. Calc. for  $C_8H_{18}O_4S$ : C, 45.7; H, 8.6; S, 15.2. Found: C, 46.1; H, 8.9; S, 15.1.

Reductive desulphurization of this compound in the usual way gave 1,6-dideoxy-L-mannitol. Recrystallization from a small volume of ethyl acetate gave clusters of crystals melting at 146–147° C. and with  $[\alpha]_D^{24} 23^\circ$  (*c*, 1.02) (lit. m.p. 145–146° C.,  $[\alpha]_D^{20} 22.8^\circ$  (3)).

*1-Deoxy-1-S-ethyl-L-galactitol*

The preparation of 6-deoxy-6-S-ethyl-d-galactose described by Baker (10) was followed except that 1,2,3,4-diisopropylidene-6-O-methanesulphonyl-d-galactose (18) was used as the starting compound. 1,2,3,4-Diisopropylidene-6-deoxy-6-S-ethyl-d-galactose,  $[\alpha]_D^{29} 1.4765$ ,  $[\alpha]_D^{26} -85.8^\circ$  (*c*, 5.90, chloroform), was obtained in 92% yield after purification by high vacuum distillation. The reported constants are:  $[\alpha]_D^{24} 1.4795$ ,  $[\alpha]_D^{22} -85.7^\circ$  (chloroform) (10). Mild acid hydrolysis gave a reducing sirup that moved as a single spot on a paper chromatogram ( $R_f$  0.53,  $R_{Rh}$  1.35 (*b*)) (*p*-anisidine spray reagent).

A solution of this sirup (2.6 g. in 25 ml. of water) was added dropwise to a stirred solution of potassium borohydride (0.85 g. in 20 ml. of water). After 2 hours a test portion was neutralized with acetic acid and it gave a negative test with Fehling's solution. The solution was acidified with acetic acid, then percolated through a column of IR-120 (H form) ion exchange resin. The solution and washings were filtered and concentrated to dryness. After six codistillations with methanol, the residue was dissolved in a solution of methanol-acetone (5:1)(15 ml.). Crystals (1.0 g. (39%)) were deposited when the solution was chilled to –20° C. A second recrystallization from methanol-acetone gave a chromatographically pure compound which had a rate of movement on a paper chromatogram identical with that of 1-deoxy-1-S-ethyl-d-galactitol in solvents (*a*), (*b*), and (*c*), m.p. 151–153° C.,  $[\alpha]_D^{24} 8.6$  (*c*, 4.18). The racemate melted at 141.5–142.0° C. Anal. Calc. for  $C_8H_{18}O_5S$ : C, 42.6; H, 8.1; S, 14.2. Found: C, 42.8; H, 8.1; S, 13.9.

The pentaacetate was prepared in 57% yield in the usual way. Recrystallization from methanol-water (5:1) gave flakes melting at 151.0–151.5° C.,  $[\alpha]_D^{24} -9^\circ \pm 1^\circ$  (*c*, 1.31

chloroform). Anal. Calc. for  $C_{18}H_{24}O_{10}S$ : C, 49.5; H, 6.5; S, 7.3. Found: C, 49.7, H, 6.7; S, 7.2.

#### ACKNOWLEDGMENTS

The authors thank Dr. W. B. Reid of the Upjohn Company, Kalamazoo, Michigan, for a gift of nickel-aluminum alloy. One of us (D. L. M.) thanks the Ontario Research Foundation for grants which made this investigation possible.

#### REFERENCES

1. KARABINOS, J. V. and WOLFROM, M. L. *J. Am. Chem. Soc.* **66**, 909 (1944).
2. HUDSON, C. S. and RICHTMYER, N. K. *J. Am. Chem. Soc.* **72**, 3880 (1950).
3. RICHTMYER, N. K. and ZISSIS, E. *J. Am. Chem. Soc.* **74**, 4373 (1952).
4. HUDSON, C. S., RICHTMYER, N. K., and ZISSIS, E. *J. Am. Chem. Soc.* **73**, 4714 (1951).
5. RICHTMYER, N. K. and ZISSIS, E. *J. Am. Chem. Soc.* **72**, 129 (1950).
6. RICHTMYER, N. K. and ZISSIS, E. *J. Am. Chem. Soc.* **76**, 5515 (1954).
7. BOLLENBACK, G. N. and UNDERKOFLER, L. A. *J. Am. Chem. Soc.* **72**, 741 (1950).
8. FLETCHER, H. G., JR. and RICHTMYER, N. K. *Advances in carbohydrate chemistry*. Vol. 5. Academic Press, Inc., New York, 1950. p. 1.
9. OVEREND, W. G. and PARKER, L. F. J. *Nature*, **167**, 527 (1951).
10. BAKER, S. B. *Can. J. Chem.* **33**, 1102 (1955).
11. PARTRIDGE, S. M. *Biochem. J.* **51**, 238 (1948).
12. TREVELYAN, W. E., PROCTOR, D. P., and HARRISON, J. S. *Nature*, **166**, 444 (1950).
13. ORGANIC SYNTHESES. Vol. 21. John Wiley & Sons, Inc., New York. 1941. p. 15.
14. WOLFROM, M. L. *J. Am. Chem. Soc.* **52**, 2464 (1930).
15. FISCHER, E. *Ber.* **27**, 673 (1894).
16. WOLFROM, M. L. *J. Am. Chem. Soc.* **52**, 2464 (1930).
17. GATZI, K. and REICHSTEIN, T. *Helv. Chim. Acta*, **21**, 914 (1938).
18. HELFERICH, B. and DRESSLER, R. *J. prakt. Chem.* **153**, 285 (1939).

# THE RELATION BETWEEN THE SULPHATE AND NITROGEN CONTENT OF UNSTABILIZED CELLULOSE NITRATE<sup>1</sup>

PAUL E. GAGNON, KARL F. KEIRSTEAD,<sup>2</sup> AND BRIAN T. NEWBOLD<sup>3</sup>

## ABSTRACT

The sulphate and nitrogen contents of cellulose nitrates prepared from mixed acids containing different amounts of sulphuric acid were compared. The sulphate content showed a tendency to decrease with increasing nitrogen, for instance it was 1.96% for 10.54% and 0.44% for 13.31%. Similar results were obtained with a series of wood cellulose nitrates, for instance 2.40% for 11.01% and 0.91% for 12.47%. With practically the same amount of sulphuric acid in the mixed acid, cellulose nitrates were prepared and the sulphate and nitrogen contents were compared. For unstabilized cotton cellulose nitrates, the sulphate content decreased steadily with increasing nitrogen content. Similar results were obtained with wood cellulose nitrates.

## INTRODUCTION

In a recent publication (1) the degree of nitration of cotton linters and wood cellulose was determined when the same mixed acid was used. The sulphate content of the unstabilized cellulose nitrates obtained was shown to be dependent upon the sulphuric acid content of the mixed acid.

Miles (4) has stated that the total sulphate content of cellulose nitrate tends to increase with decreasing nitrogen content. The object of the present work was to determine the relation between the total sulphate and nitrogen contents of both cotton and wood unstabilized cellulose nitrates.

## EXPERIMENTAL

### *Cellulose Nitrate*

The procedure for the nitration of cotton linters and wood cellulose was given in a recent publication (2). The methods used to analyze the mixed acids and to determine the sulphate and nitrogen contents of the unstabilized cellulose nitrates were also described in previous papers (1, 3).

## RESULTS AND DISCUSSION

In general the total sulphate content of unstabilized cellulose nitrate depends upon several factors, namely, the composition of the mixed acid used to nitrate the cellulose, the nitration conditions, the degree of washing, and the nitrogen content of the cellulose nitrate. The sulphate content has been shown to increase when the proportion of sulphuric acid in the mixed acid increased (1).

In the present work, the sulphate and nitrogen contents of unstabilized cotton and wood cellulose nitrates were determined by good precision methods (1) and compared. The nitrogen contents of the cellulose nitrates varied from 13.3 to 7.7% for cotton, and 13.0 to 7.3% for wood cellulose nitrate.

The sulphate and nitrogen contents of cotton cellulose nitrates prepared from mixed acids containing different amounts of sulphuric acid are compared in Table I. The sulphate content showed a tendency to decrease with increasing nitrogen, for instance

<sup>1</sup>Manuscript received September 27, 1957.

Contribution from the Department of Chemistry, Laval University, Quebec, Que., with financial assistance from the Defence Research Board of Canada.

<sup>2</sup>Present address: Lignosol Chemicals Limited, Quebec, Que.

<sup>3</sup>Research assistant, Department of Chemistry, Laval University.

TABLE I  
COMPARISON OF SULPHATE AND NITROGEN CONTENTS OF COTTON AND OF WOOD CELLULOSE NITRATES  
PREPARED FROM A VARIETY OF MIXED ACIDS

Cotton cellulose nitrates				Wood cellulose nitrates			
Expt. No.	Sulphuric acid in mixed acid, %	Total sulphate, %H <sub>2</sub> SO <sub>4</sub>	Nitrogen, %	Expt. No.	Sulphuric acid in mixed acid, %	Total sulphate, %H <sub>2</sub> SO <sub>4</sub>	Nitrogen, %
1	68.25	1.96	10.54	1	73.31	2.40	11.01
2	70.67	1.55	11.66	2	72.50	2.32	11.43
3	"	1.53	11.66	3	"	2.17	11.36
4	71.20	1.17	11.71	4	71.20	2.13	11.44
5	65.40	1.00	11.40	5	72.83	2.12	11.74
6	72.50	0.95	11.60	6	70.67	2.02	10.86
7	"	0.95	11.73	7	71.30	2.01	12.01
8	65.40	0.89	11.35	8	65.40	1.71	10.80
9	65.99	0.85	11.28	9	"	1.62	10.75
10	65.71	0.85	11.52	10	"	1.33	11.67
11	65.40	0.69	11.91	11	70.35	1.30	12.75
12	65.00	0.63	12.14	12	65.40	1.23	11.80
13	65.40	0.58	12.07	13	71.23	1.04	13.00
14	70.35	0.47	13.21	14	65.00	0.93	11.91
15	65.66	0.44	13.31	15	65.66	0.91	12.47

it was 1.96% for 10.54% and 0.44% for 13.31%, but no definite curve can be drawn. Similar results were obtained with a series of wood cellulose nitrates, as shown also in Table I, for instance 2.40% for 11.01% and 0.91% for 12.47%.

The nitrogen contents of the cellulose nitrates given in Table I varied from 13.3% to 10.5%, which is the range for cellulose nitrates used in industry. In the present work, cellulose nitrates containing less than 10.0% nitrogen did not give satisfactory results because they were either swollen or gelatinized to such an extent that it was not possible to attain a reproducible degree of washing.

The nitration conditions and the degree of washing with water for the preparation of the two types of cellulose nitrates mentioned in Table I were very similar; therefore any effects on sulphate content due to the latter can be discounted. The fact that no precise curve could be drawn to show the relation between the sulphate and nitrogen contents of the cellulose nitrates prepared from various mixed acids was thought to be due to the effects of the proportion of sulphuric acid in the mixed acid and that of the nitrogen in the cellulose nitrate. Since it has been shown that the sulphuric acid content of the mixed acid has a profound effect upon the sulphate content (1), it was essential

TABLE II  
COMPARISON OF SULPHATE AND NITROGEN CONTENTS OF CELLULOSE NITRATES  
PREPARED FROM MIXED ACIDS CONTAINING SIMILAR AMOUNTS OF SULPHURIC  
ACID

Expt. No.	Sulphuric acid in mixed acid, %	Cotton cellulose nitrate		Wood cellulose nitrate	
		Sulphate, %H <sub>2</sub> SO <sub>4</sub>	Nitrogen, %	Sulphate, %H <sub>2</sub> SO <sub>4</sub>	Nitrogen, %
1	65.40	1.00	11.40	1.62	10.75
2	"	0.89	11.35	1.71	10.80
3	"	0.69	11.91	1.33	11.67
4	"	0.58	12.07	1.23	11.80
5	65.66	0.44	13.31	0.93	12.47

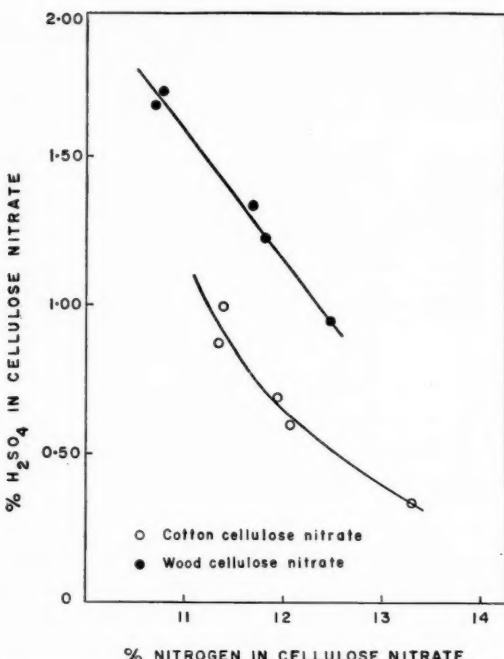


FIG. 1. Relation between sulphate and nitrogen contents of cellulose nitrates prepared from mixed acids containing similar amounts of sulphuric acid.

to remove this factor before determining the sulphate-nitrogen relation. Accordingly, cellulose nitrates were prepared using mixed acids containing an almost constant amount of sulphuric acid, and their sulphate and nitrogen contents were compared. The results for cotton and wood cellulose nitrates are given in Table II and Fig. 1.

For unstabilized cotton cellulose nitrates, the sulphate content decreased steadily with increasing nitrogen content. Furthermore, similar results were obtained for wood cellulose nitrates.

#### REFERENCES

1. GAGNON, P. E., KEIRSTEAD, K. F., and NEWBOLD, B. T. Can. J. Chem. **36**, 215 (1958).
2. GAGNON, P. E., KEIRSTEAD, K. F., and YAMASAKI, D. Can. J. Technol. **34**, 477 (1957).
3. KEIRSTEAD, K. F. and MYERS, J. Can. J. Chem. **32**, 566 (1954).
4. MILES, F. D. Cellulose nitrate. Clarke, Irwin & Co. Ltd., Toronto. 1955.

# A CONTRIBUTION TO THE CHEMISTRY OF UNSTABILIZED CELLULOSE NITRATE<sup>1</sup>

PAUL E. GAGNON, KARL F. KEIRSTEAD,<sup>2</sup> AND BRIAN T. NEWBOLD<sup>3</sup>

## ABSTRACT

Cotton linters and wood cellulose were nitrated in parallel experiments with a series of mixed acids and the products examined for nitrogen and sulphate content. A higher degree of nitration was obtained with the cotton cellulose, and the sulphate content of the nitrated cotton increased steadily with increasing concentration of sulphuric acid in the nitration medium while the sulphate content of the wood cellulose passed through a maximum value which depended on the degree of nitration. The sulphate content of the cotton cellulose nitrates was higher than that of the wood cellulose nitrates when the nitrations were performed under similar conditions.

## INTRODUCTION

The sulphate content of crude, but well washed, cellulose nitrate prepared from mixed acid varies from about 0.2 to 3.0%, expressed as sulphuric acid, according to the composition of the nitric-sulphuric acid mixture. The total sulphate and the proportion of sulphate ester tend to increase with decreasing nitrogen content (2, 4).

The object of the present work was to compare the degree of nitration of cotton linters and wood cellulose obtained when the composition of the mixed acid used was the same, and to establish the relation between the sulphate content of unstabilized cellulose nitrate and the sulphuric acid content of the mixed acid.

## EXPERIMENTAL

### *Cellulose Nitrate*

Cotton linters and wood cellulose were nitrated with mixed acids, using the method given in a previous publication (2). The mixed acids were analyzed by standard methods. The total sulphate content in the cellulose nitrates was determined as barium sulphate (3). The nitrogen content was obtained by the Devarda method.

## RESULTS AND DISCUSSION

### *Degree of Nitration*

Many nitrations of cotton linters and wood cellulose were carried out using a variety of mixed acids, in order to determine the relation between mixed acid constitution and nitrogen content. Miles (4) states that "the degree of nitration possible in any mixed acid is chiefly a function of acid composition". In the present work, the results obtained were in accord with this statement. The range of mixed acids varied from 65.0 to 73.6% for the sulphuric acid, from 9.0 to 25.5% for the nitric acid, and from 8.4 to 20.4% for the water. The composition of the mixed acids and the corresponding nitrogen contents for the cotton cellulose nitrates together with a few results reported by Miles and Milbourn for ramie fiber cellulose nitrates are given in Table I.

Miles and Milbourn (5) nitrated ramie fiber with a wide range of mixed acids, and expressed their results for the relation between "composition and degree of nitration" in the form of a triangular chart. The results obtained for the nitration of cotton linters

<sup>1</sup>Manuscript received August 29, 1957.

Contribution from the Department of Chemistry, Laval University, Quebec, Que., with financial assistance from the Defence Research Board of Canada.

<sup>2</sup>Present address: Lignosol Chemicals Limited, Quebec, Que.

<sup>3</sup>Research Assistant, Department of Chemistry, Laval University.

TABLE I  
MIXED ACID COMPOSITIONS AND NITROGEN CONTENTS  
OF COTTON CELLULOSE NITRATES

Expt. No.	% $H_2SO_4$	% $HNO_3$	% $H_2O$	% N
1	71.2	20.4	8.4	—*
2	65.7	22.1	12.2	13.3
3	70.4	19.0	10.6	13.2
4	71.3	13.3	15.4	12.8
5	72.8	12.6	14.6	12.2
6	65.0	18.7	16.3	12.1
7	70.7	13.4	15.9	11.7
8	65.7	16.8	17.5	11.5
9	73.3	10.8	15.9	11.4
10†	67.9	13.6	18.5	10.9
11	68.3	12.3	19.4	10.5
12	62.0	25.5	12.5	—*
13	65.0	14.6	20.4	9.7
14†	73.6	9.0	17.4	10.5
15	73.1	9.0	17.9	9.7
16†	70.1	10.0	19.9	9.4
17	70.1	10.0	19.9	9.0

\*Product dissolved.

†Results of Miles and Milbourn (5).

in the present work are given in Fig. 1, which is a portion of the triangular chart used by Miles (4), but drawn on a larger scale. Miles's constant nitrogen lines are shown by broken lines and the results of the present work are plotted as individual points over the nitrogen range 9.0 to 13.3%.

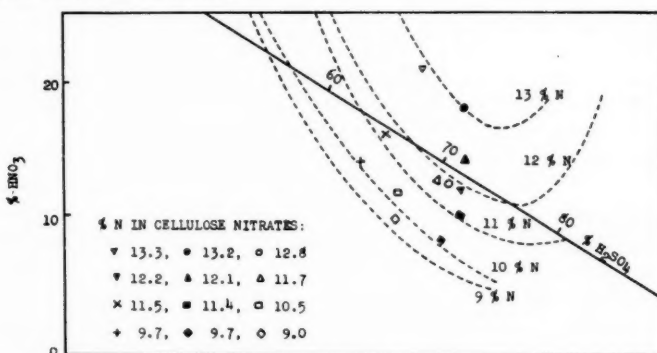


FIG. 1. Mixed acid chart.

Part of the difference in the nitrogen content of cellulose nitrate prepared from ramie fiber and from cotton linters with the same nitric-sulphuric acid, as shown in Table I, experiments 16 and 17, can be attributed to structural differences in the fibers employed. In two experiments, the cellulose nitrate dissolved, a phenomenon encountered by Miles and Milbourn (5).

In order to assess the experimental error involved in attempts to prepare identical cellulose nitrates from the same nitric-sulphuric acid, several duplicate experiments were carried out and the nitrogen determined on each sample. The results are shown in Table II. The mean difference in the nitrogen content of the duplicates was 0.08%.

TABLE II  
NITROGEN CONTENTS IN CELLULOSE NITRATES PREPARED BY  
DUPLICATE NITRATIONS

Expt. No.	Cotton cellulose nitrate, %N		Wood cellulose nitrate, %N	
	Original	Duplicate	Original	Duplicate
1	12.1	11.9	11.7	11.8
2	11.7	11.6	11.4	11.4
3	11.4	11.4	10.8	10.8
4	8.9	9.0	8.5	8.4

and the standard deviation was 0.07. The confidence limits for the difference calculated by the method of Dean and Dixon (1) were  $0.08\% \pm 0.08$ , 95% confidence. This difference for duplicates is significantly less than the difference in nitrogen content, 0.4%, found between ramie and cotton cellulose nitrate prepared from the same mixed acid (Table I, expts. 16 and 17).

Further evidence for varying degrees of nitration of different fibers nitrated with the same mixed acid is shown in Table III. A series of mixed acids were used to nitrate

TABLE III  
NITROGEN CONTENTS OF CELLULOSE  
NITRATES

Expt. No.	Cotton cellulose nitrate, %N	Wood cellulose nitrate, %N
1	13.3	12.8
2	13.2	12.8
3	12.8	12.0
4	12.2	11.7
5	12.1	11.9
6	11.7	10.9
7	11.5	10.8
8	11.4	11.0
9	10.5	9.9
10	10.2	10.0
11	9.7	9.7
12	9.4	9.3
13	9.0	8.4
14	8.9	8.5

cotton linters and wood cellulose. The cotton cellulose nitrate almost invariably had a greater nitrogen content than the corresponding wood cellulose. The average difference was 0.4% and the standard deviation was 0.29. The confidence limits for the difference were  $0.46\% \pm 0.17$ , 95% confidence.

Assuming the same conditions for nitration, it appears that the percentage of nitrogen obtained from the same mixed acid varies with the nature of the fibers as follows:

ramie, 9.4; cotton linters, 9.0; wood cellulose, 8.4.

Cotton cellulose was nitrated to a higher degree than wood cellulose when the same conditions were employed. The sulphate content of both was dependent upon the composition of the mixed acid. The sulphate content of wood cellulose nitrate was almost always

higher than that of cotton cellulose nitrate. The different behavior exhibited by cotton and wood cellulose during nitration could be attributed to the different structures. These results agree with the experience of Schur and McMurtrie (6), who found that cotton linters, when nitrated with mixed acid containing 26.0% nitric acid, yielded cellulose nitrate of higher nitrogen content, under the conditions of nitration employed, than did most of the wood pulp samples used. These authors concluded that the behavior of the wood pulps during nitration depended partly on the gross physical form and partly on differences in the physical characteristics of the fibers undergoing nitration.

#### Sulphate Content

In order to establish the relation between the sulphuric acid content of the mixed acid and the total sulphate content of the cellulose nitrates, many experiments were carried out with cotton linters and wood cellulose, using mixed acids containing amounts of sulphuric acid varying from 65.0 to 73.3%. The sulphate contents of the cellulose nitrates are given in Table IV.

TABLE IV  
SULPHURIC ACID IN MIXED ACID AND TOTAL SULPHATE IN CELLULOSE NITRATES

Expt. No.	%H <sub>2</sub> SO <sub>4</sub> in mixed acid	Cotton cellulose nitrate		Wood cellulose nitrate	
		%H <sub>2</sub> SO <sub>4</sub>	%N	%H <sub>2</sub> SO <sub>4</sub>	%N
1	65.0	1.54	9.7	2.17	9.7
2	68.3	1.86	10.5	2.36	9.9
3	73.3	2.30	11.0	2.40	11.0
4	65.7	0.79	11.5	1.13	10.8
5	70.7	1.53	11.7	1.46	10.9
6	65.0	0.63	12.1	0.93	11.9
7	72.8	2.26	12.2	2.12	12.0
8	71.3	1.13	12.8	2.09	12.0
9	70.4	0.47	13.2	1.30	12.8
10	65.7	0.44	13.3	0.91	12.5

It was found that the sulphate content of wood cellulose nitrate was almost always higher than that of cotton cellulose nitrate, when products prepared from the same mixed acid and containing about the same amount of nitrogen were compared. The mean difference was 0.38% and the standard deviation was 0.29. The confidence limits for the difference were  $0.38\% \pm 0.21$ , 95% confidence.

To test the reproducibility of the sulphate determinations, several duplicate experiments were performed and typical results are given in Table V. The mean difference

TABLE V  
SULPHATE DETERMINATIONS ON COTTON CELLULOSE NITRATES PREPARED BY  
DUPLICATE NITRATIONS

Expt. No.	%H <sub>2</sub> SO <sub>4</sub> in mixed acid	Total sulphate, %H <sub>2</sub> SO <sub>4</sub>		Nitrogen, %	
		Original	Duplicate	Original	Duplicate
1	68.3	1.91	1.86	10.8	10.5
2	70.1	1.76	1.62	8.9	8.9
3	70.7	1.53	1.55	11.7	11.6
4	71.3	1.13	1.17	12.0	11.8
5	65.4	1.00	0.89	11.4	11.4
6	65.3	0.69	0.58	11.9	12.1

in the duplicate sulphate contents was 0.09% and the standard deviation was 0.05. The confidence limits for the difference were  $0.09\% \pm 0.05$ , 95% confidence. Similar results were obtained from sulphate analyses of wood cellulose nitrates.

The relation between the sulphuric acid content of the mixed acid and the sulphate content of the cellulose nitrates is shown in Figs. 2 and 3. In Fig. 2, three curves are given for cotton cellulose nitrates of average nitrogen content of 9.4, 11.5, and 12.4%. The sulphate content increases with increasing concentration of sulphuric acid.

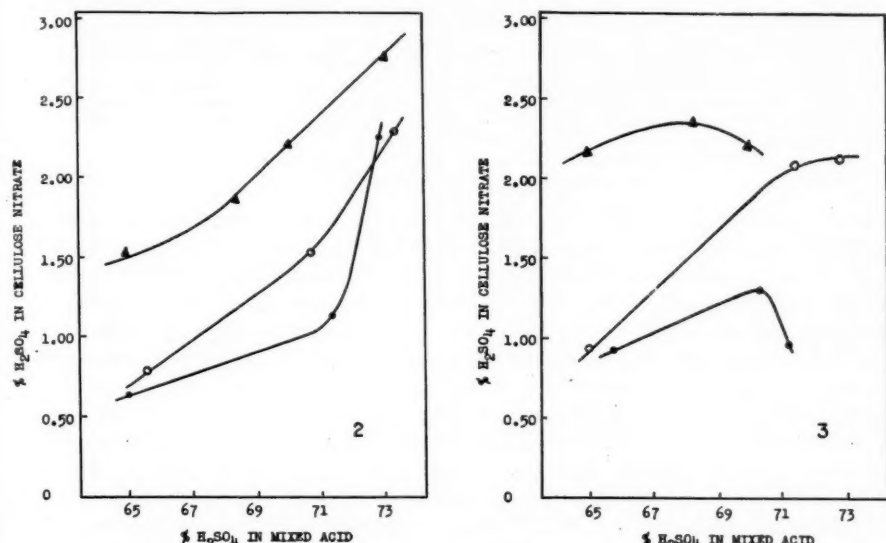


FIG. 2. Relation between  $\% \text{H}_2\text{SO}_4$  in mixed acid and the sulphate content of cotton cellulose nitrates. Av. %N in cellulose nitrate: ● 12.4%, ○ 11.5%, ▲ 9.4%.

FIG. 3. Relation between  $\% \text{H}_2\text{SO}_4$  in mixed acid and the sulphate content of wood cellulose nitrates. Av. %N in cellulose nitrate: ● 12.8%, ○ 11.9%, ▲ 9.4%.

The curves for wood cellulose nitrates (Fig. 3) possess a maximum indicating the optimum concentration of sulphuric acid for the highest sulphate content. For instance, 70.3% sulphuric acid was the optimum concentration for 1.30% sulphate in a wood cellulose nitrate containing 12.8% nitrogen.

#### Conclusion

The nitrogen and sulphate contents of both cotton and wood cellulose nitrates are shown to be intimately related. The sulphate content of the cellulose nitrates depends upon the formation of sulphate ester, which will be discussed in a forthcoming publication.

#### REFERENCES

1. DEAN, R. B. and DIXON, W. J. *Anal. Chem.* **23**, 636 (1951).
2. GAGNON, P. E., KEIRSTEAD, K. F., and YAMASAKI, D. *Can. J. Technol.* **34**, 477 (1957).
3. KEIRSTEAD, K. F. and MYERS, J. *Can. J. Chem.* **32**, 566 (1954).
4. MILES, F. D. *Cellulose nitrate*. Clarke, Irwin & Co. Ltd., Toronto. 1955.
5. MILES, F. D. and MILBOURN, M. *J. Phys. Chem.* **34**, 2598 (1930).
6. SCHUR, M. O. and MCMURTRIE, J. *Paper Trade. J.* **16**, 2 (Sept. 23, 1948).

## AMMONOLYSIS OF 1,2-EPOXYCYCLOHEXANE AND TRANS-2-BROMOCYCLOHEXANOL<sup>1</sup>

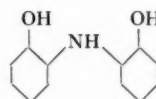
L. R. HAWKINS AND R. A. B. BANNARD

### ABSTRACT

Optimum conditions for the preparation of *trans*-2-aminocyclohexanol by ammonolysis of 1,2-epoxycyclohexane or *trans*-2-bromocyclohexanol are realized by use of a 20-fold excess of aqueous alcoholic ammonia at 100°. Under these conditions formation of secondary amines is minimized. Lower ammonia-reactant ratios, or the use of absolute methanolic ammonia or aqueous ammonia, lead to lower yields of primary amine and higher yields of secondary amines. 1,2-Epoxyhexane has been isolated from the interaction of *trans*-2-bromocyclohexanol with aqueous ammonia. The oxide reacts more rapidly with aqueous alcoholic ammonia than the bromohydrin and the rate of conversion of the latter to amine is thus controlled by the rate of conversion of bromohydrin to oxide.

### INTRODUCTION

Winstein and Henderson (31) have emphasized that reactions involving *trans*-1,2-halohydrins under basic conditions can proceed via the corresponding oxide as intermediate. If such is the case, approximately equal yields of primary amine should be obtainable from either reactant, and the preferred starting material for preparation of 1,2-aminocyclanols would be the halohydrin rather than the oxide, a synthetic step thereby being eliminated. For the synthesis of a 1,2-aminocyclanol, practical considerations demand that attention be given to the possible intervention of side reactions. Mousseron and Granger (16), for example, found in a number of instances that ammonolysis of alicyclic epoxides or 1,2-chlorohydrins led to formation of considerable quantities of secondary amines together with the desired primary amine. Brunel (4) prepared *trans*-2-aminocyclohexanol by heating 1,2-epoxycyclohexane with a sixfold excess of aqueous ethanolic ammonia at 110–115°. When a twofold excess of ammonia was used, however, the main products were two diastereoisomeric bis-2-hydroxycyclohexylamines (I) of m.p. 114° and 153°, subsequently shown by Mousseron and Granger (16) to be *dl* and *meso* forms respectively.



Godchot and Mousseron (9), however, studying the same reaction, obtained cyclohexadiene as by-product. Osterberg and Kendall (17) obtained a 61% yield of *trans*-2-aminocyclohexanol by heating *trans*-2-chlorocyclohexanol at 100° with an unspecified excess of aqueous alcoholic ammonia, and reported that omission of the alcohol resulted in formation of secondary and tertiary amines as the main products. They failed, however, to characterize these substances. Wilson and Read (32) studied the same reaction at room temperature, and did not note formation of by-products. Our purpose was to determine whether the halohydrin is the preferred starting material and to establish experimental conditions leading to maximum yield of primary amine, since we required

<sup>1</sup>Manuscript received July 15, 1957.

Contribution from Defence Research Chemical Laboratories, Ottawa, Canada. Issued as D.R.C.L. Report No. 220.

certain more complex aminocyclanols in connection with other studies to be described later.

The ammonolysis of 1,2-epoxycyclohexane and *trans*-2-bromocyclohexanol with aqueous alcoholic, aqueous, and absolute methanolic ammonia has been studied at 100° and at room temperature. The influence of these and other variables, such as molar ratio of ammonia to reactant and time of contact, on the yield of primary and secondary amines has been determined.

### RESULTS AND DISCUSSION

From Table I it is clear that, within the limits of the variables examined, optimum conditions for conversion of 1,2-epoxycyclohexane and *trans*-2-bromocyclohexanol to

TABLE I  
AMMONOLYSIS OF 1,2-EPOXYCYCLOHEXANE AND *trans*-2-BROMOCYCLOHEXANOL

Run number	Reactant*	Medium†	Molar ratio NH <sub>3</sub> :reactant	% Yield primary amine	% Yield secondary amine			Experimental conditions
					m.p. 154°	m.p. 126°	Total	
1	Oxide	1	20	86.5	2.0	1.5	3.5	1 hr. 100°
2	Oxide	1	20	85.5	1.9	1.3	3.2	4 hr. 100°
3	Bromohydrin	1	20	76.4			1.7	1 hr. 100°
4	Bromohydrin	1	20	75.6			1.9	4 hr. 100°
5	Oxide	1	5	71.7	10.1	5.3	15.4	1 hr. 100°
6	Oxide	1	5	68.2	11.4	6.1	17.5	2 hr. 100°
7	Bromohydrin	1	5	65.2	7.2	3.1	10.3	1 hr. 100°
8	Bromohydrin	1	5	62.2	8.0	3.3	11.3	2 hr. 100°
9	Oxide	1	20	68.3			Trace	16 hr. R.T.‡
10	Bromohydrin	1	20	56.7			Trace	16 hr. R.T.
11	Oxide	1	20	26.6			Nil	4 hr. R.T.
12	Bromohydrin	1	20	4.4			Nil	4 hr. R.T.
13	Oxide	1	5	64.0	7.0	6.6	13.6	48 hr. R.T.
14	Bromohydrin	1	5	63.9	7.7	6.5	14.2	72 hr. R.T.
15	Oxide	2	20	75.3	2.9	2.4	5.3	1 hr. 100°
16	Oxide	2	20	72.3	2.9	4.6	7.5	24 hr. 100°
17	Oxide	2	2	31.7	25.4	11.7	50.7§	2 hr. 100°
18	Bromohydrin	2	20	47.8	2.8	3.3	6.1	1 hr. 100°

\*0.200 mole per run.

†1, aqueous ethanolic ammonia; 2, aqueous ammonia.

‡Room temperature.

§13.6% of mixed secondary amines was not further purified.

*trans*-2-aminocyclohexanol are realized by ammonolysis for 1 hour at 100° with aqueous ethanolic ammonia in which the ammonia-reactant ratio is 20:1. Under these conditions the oxide and bromohydrin furnish the primary amine in 85% and 75% yield respectively and formation of secondary amines is limited to 3.5% (runs 1 and 3). In spite of the slightly higher yield of *trans*-2-aminocyclohexanol obtained by the one-step ammonolysis of the bromohydrin (75% vs. 68%), the two-step method, involving prior preparation of the oxide, is preferred because of greater ease of isolation of the product. Prolonging the time of heating has no significant effect on the yield of amines (runs 2 and 4). Use of only a fivefold excess of ammonia, however, causes a marked drop in the yield of primary amine and a corresponding increase in yield of secondary amines (runs 5-8). This result follows from the Law of Mass Action.

The effect of temperature on yield and rate of reaction is illustrated by comparing

the results of runs 9 to 14 at room temperature with runs 1 to 8 at 100°. It is evident that ammonolysis is much slower at room temperature, as would be expected. However, the results described here for the oxide contrast with Brunel's observation (4) that 1,2-epoxycyclohexane requires several weeks to react with aqueous alcoholic ammonia at room temperature. At room temperature the bromohydrin reacts more slowly than the oxide at both high and low ammonia-reactant ratios. It is thus clear that in the case of bromohydrin, the rate of formation of the intermediate oxide (see below) at room temperature becomes the governing factor.

Aqueous ammonia is a less satisfactory medium for ammonolysis of 1,2-epoxycyclohexane or *trans*-2-bromocyclohexanol than aqueous alcoholic ammonia (runs 15, 16, and 18), presumably because two-phase systems are formed and there is an increased tendency toward formation of 1,2-cyclohexanediol as by-product (4, 20). The especially poor yield from the bromohydrin is to be expected because the intermediate oxide is readily soluble in the bromohydrin. The result reported in run 18 contrasts with Osterberg and Kendall's claim (17) that ammonolysis of *trans*-2-chlorocyclohexanol with aqueous ammonia produces secondary and tertiary amines as the main products. We did not obtain tertiary amines under any of the conditions studied, in agreement with Brunel's (4) results on ammonolysis of 1,2-epoxycyclohexane. Normally, ammonolysis of a 1,2-epoxide or halohydrin in aqueous solution leads to formation of primary, secondary, and tertiary amine together with quaternary ammonium salt (19), but in the present case formation of the last two may be prevented by steric factors. Brunel's (4) observation that treatment of the oxide with a twofold excess of ammonia produces the diastereoisomeric secondary amines as major product has been verified (run 17). Ammonolysis with anhydrous methanolic ammonia causes the yield of primary amine to fall approximately 30% from maximum. This result was not unexpected since water exerts a catalytic effect on the ammonolysis reaction (6, 3, 22) and, moreover, reaction of 1,2-epoxides or 1,2-halohydribs with alcohols under basic conditions leads to formation of glycol monoethers (4, 13, 14). We did not attempt to isolate glycol or glycol monoethers from the ammonolyses but these compounds would undoubtedly be present in small amounts in the distillate collected prior to sublimation of the primary amine.

The reaction of ammonia or amines with 1,2-epoxides in aqueous solution is considered to proceed by an  $S_N2$  mechanism (31, p. 27; 12; 23; 7). The stereochemical course of the reaction of 1,2-epoxycyclohexane with ammonia (15) and the fact that the reaction rate increases (runs 9 and 13) when the concentration of nucleophile is increased (12, p. 321) are in agreement with such a mechanism.

Ammonolysis of *trans*-2-bromocyclohexanol proceeds with over-all retention of stereochemical configuration, and this suggests that 1,2-epoxycyclohexane is an intermediate (27; 30; 31, pp. 11 and 27). The conversion of 1,2-halohydrin to oxide in the presence of a strong base is rapid and almost quantitative (31, p. 8) but there does not appear to be any definite evidence for formation of oxide in the presence of a weak base such as ammonia, other than the kinetic data of Smith and Nilsson (23). On the other hand Elderfield *et al.* (8) and Petrov and Lagucheva (18) have published data which indicate that amination of 1-chloropentanol-2 with diethylamine or ethylene chlorohydrin with 2,5-dichloroaniline does not proceed via an intermediate oxide stage. Therefore, although oxide can intervene (31), this is not always the case and proof must be sought in each instance. In the present study, we treated *trans*-2-bromocyclohexanol with 28% aqueous ammonia at room temperature, obtained 1,2-epoxycyclohexane and ammonium bromide in 38.8% and 41.8% yield respectively, and recovered 43.3% of the bromohydrin. This is the first time to our knowledge than an oxide has actually been isolated from inter-

action of a halohydrin and ammonia. This observation, together with the fact that the rate of formation of amine from oxide is greater than from bromohydrin at both high and low ammonia-reactant ratios (runs 9 to 14), leads to the conclusion that the oxide is an intermediate in ammonolysis of *trans*-2-bromocyclohexanol.

The bis-2-hydroxycyclohexylamine of m.p. 126° was reported by Brunel (4) to have m.p. 114°, and it presumably contained a trace of the higher melting diastereoisomer. *meso*-Bis-2-hydroxycyclohexylamine hydrochloride was reported (4) to have m.p. 264°, whereas the *dl*-isomer exhibited a double melting point, the first at 192° and the second at 264°. Brunel (4) suggested that the *dl*-isomer was converted to the *meso*-isomer above its first melting point, melting again at 264°. We have found *dl*-bis-2-hydroxycyclohexylamine to possess a single melting point, 194–195°, and conclude that Brunel's suggestion regarding interconversion of the isomers is incorrect. The hydrobromides of *meso*- and *dl*-bis-2-hydroxycyclohexylamine were prepared and have m.p. 257–258° and 180–182° respectively.

Recently, Guss and Rosenthal (10) reported the preparation of *trans*-2-bromocyclohexanol by bromination of cyclohexene with *N*-bromosuccinimide. We used their method and found that the liquid product frequently darkens rapidly either during distillation or on storage. Similar observations regarding the rapid discoloration of *trans*-2-bromocyclohexanol have been made independently by Schmidt, Schumacher, and Asmus (21), Bedos (1), and Hunter and Marriott (11), all of whom used different methods of preparation. Swarts' observation (25) that *trans*-2-bromocyclohexanol is a solid of m.p. 27° seems to have been overlooked by subsequent workers (10, 26, 28, 29). Guss and Rosenthal's (10) procedure was modified by using a 5 mole % excess of olefin over bromoimide, and *trans*-2-bromocyclohexanol was obtained in 89% yield as a colorless solid of m.p. 27°, after purification by recrystallization from heptane rather than distillation. This product does not discolor on standing in contact with light and air. The colorless solid, if distilled *in vacuo*, discolors much more slowly than preparations made by Guss and Rosenthal's method. This observation suggests that *trans*-2-bromocyclohexanol decomposes slightly on distillation (cf. Swarts (25)) and that the excess of olefin used in our method of preparation is beneficial, possibly in preventing the presence of excess hypobromous acid, which could either cause slight oxidation of the product or lead to formation of *trans*-1,2-dibromocyclohexane as observed by Coffey (5). The latter substance is difficult to obtain in a colorless condition because it undergoes oxidation readily in the presence of air (24). During several ammonolysis experiments in which discolored *trans*-2-bromocyclohexanol was used, explosions occurred. Explosions were not experienced when colorless bromohydrin was used. Boon (2) found the reaction of alkylene dibromides with certain amines to be very exothermic during the initial stage, and it is possible that a trace of *trans*-1,2-dibromocyclohexane present in the bromohydrin is responsible for the observed explosions.

#### EXPERIMENTAL

All melting points are uncorrected. Microanalyses are by Micro-Tech Labs., Skokie, Ill., and C. E. Reynolds of these Laboratories.

#### *trans*-2-Bromocyclohexanol

Guss and Rosenthal's (10) procedure was modified as follows. Cyclohexene (86.2 g., 1.05 moles), water (400 ml.), and *N*-bromosuccinimide (178 g., 1.00 mole) were placed in a 1-liter three-necked flask equipped with a "trubore" stirrer and thermometer. The mixture was stirred mechanically until the *N*-bromosuccinimide dissolved and a colorless heavy layer of bromohydrin separated (15 minutes), during which time the

temperature rose to 75°. The two-phase system was allowed to cool to room temperature, the bromohydrin layer was separated, and the aqueous phase extracted with ether ( $2 \times 100$  ml.). The extracts and bromohydrin were combined and the ether removed *in vacuo*. The residue was diluted with heptane (1 liter) and kept at 4° overnight. The precipitated succinimide was removed and the filtrate was allowed to stand overnight at -20°. The colorless crystals of *trans*-2-bromocyclohexanol which separated were collected by suction filtration and washed with ice-cold heptane. Concentration of the mother liquor gave further crops. Yield, 160 g. (89.0%), m.p. 27°. Swarts (25) reports m.p. 27.5°. Calc. for  $C_6H_{11}OBr$ : C, 40.24; H, 6.19; Br, 44.63%. Found: C, 40.20; H, 6.10; Br, 44.58%. *trans*-2-Bromocyclohexanol prepared as described above has remained colorless for more than 4 months on storage in clear bottles not protected from daylight.

#### *Ammonolysis of trans-2-Bromocyclohexanol*

The bromohydrin was treated with aqueous, aqueous ethanolic, or absolute methanolic ammonia in glass or stainless steel pressure vessels at room temperature or 100° for varying lengths of time. Experimental conditions required for maximum yield of *trans*-2-aminocyclohexanol are as follows. *trans*-2-Bromocyclohexanol (35.8 g., 0.200 mole) was heated for 1 hour at 100° with an aqueous ethanolic ammonia solution prepared from 28% aqueous ammonia (270 ml., 4.00 moles) and absolute ethanol (120 ml.). The pale yellow solution was evaporated to dryness *in vacuo* at room temperature. The residual solid was treated with a boiling solution of sodium hydroxide (8.0 g.) in absolute ethanol (100 ml.) for 20 minutes with stirring. The insoluble salt was collected and washed with anhydrous ether (50 ml.). The combined filtrate and washings were evaporated to dryness *in vacuo* at room temperature, and the primary amine (17.6 g., 76.4%) was obtained as a colorless sublimate, m.p. 67-68°, by heating the residue at 80-100° at 1 mm. (McCasland *et al.* (15) report m.p. 68°). *trans*-2-Aminocyclohexanol is hygroscopic and carbonates rapidly. Complete separation of primary amine from the mixture of secondary amines and inorganic salt is not effected and the residue still possesses the characteristic piperidine-like odor of the primary amine. The water-insoluble *meso*-bis-2-hydroxycyclohexylamine (m.p. 154°) was isolated by filtration after the residue from the sublimation was treated with boiling water (100 ml.) and allowed to cool. The *dl*-secondary amine (m.p. 126°) was isolated by evaporation of the filtrate to dryness. The experiment under consideration yielded only 0.36 g. (1.7%) of a mixture of the two secondary amines, m.p. 114-116°. Calc. for  $C_{12}H_{23}NO_2$ : C, 67.56; H, 10.86%. Found: C, 68.00; H, 11.10%.

#### *1,2-Epoxyhexane from Ammonolysis of trans-2-Bromocyclohexanol*

*trans*-2-Bromocyclohexanol (35.8 g., 0.200 mole) was stirred at room temperature for 6 hours in a stoppered flask with 28% aqueous ammonia (20 ml., 0.297 mole). The lower layer was decanted and the aqueous layer extracted with ether ( $3 \times 10$  ml.) and combined with the non-aqueous layer. The ether solution was dried and distilled, yielding 7.6 g. (38.8%) of cyclohexene oxide, b.p. 130°,  $n_D^{25}$  1.4497, and 15.5 g. (43.3%) of *trans*-2-bromocyclohexanol, b.p. 50-52° at 1.5 mm.,  $n_D^{25}$  1.5185. Evaporation of the aqueous solution to dryness yielded 8.2 g. (41.8%) of ammonium bromide which contained only a trace of *trans*-2-aminocyclohexanol as revealed by paper chromatography using *n*-butanol - acetic acid - water (25:6:25) as developer and bromcresol green as detector.

#### *1,2-Epoxyhexane*

1,2-Epoxyhexane was prepared in 80% yield from *trans*-2-bromocyclohexanol by the method of Guss and Rosenthal (10), b.p. 130°,  $n_D^{25}$  1.4498.

### *Ammonolysis of 1,2-Epoxycyclohexane*

1,2-Epoxycyclohexane was ammonolyzed with aqueous, aqueous alcoholic, or absolute methanolic ammonia in glass or stainless steel pressure vessels at room temperature or 100° for varying lengths of time. Experimental conditions which produce maximum yield of *trans*-2-aminocyclohexanol are as follows. 1,2-Epoxycyclohexane (19.6 g., 0.200 mole) was heated for 1 hour at 100° with aqueous ethanolic ammonia solution as described for *trans*-2-bromocyclohexanol. The pale yellow solution was evaporated to dryness *in vacuo* at room temperature. The residue was heated at 80–100° at 1 mm. and *trans*-2-aminocyclohexanol (19.9 g., 86.5%) was obtained as a colorless sublimate, m.p. 67–68°. The two secondary amines were recovered by the method described under ammonolysis of *trans*-2-bromocyclohexanol. More complete recovery and separation of the amines was effected because the process is uncomplicated by the presence of inorganic salt. The *meso*-secondary amine (m.p. 154°) was obtained in 2.0% yield and the *dl*-isomer (m.p. 126°) in 1.5% yield.

### *trans*-2-Aminocyclohexanol Hydrochloride

*trans*-2-Aminocyclohexanol (23.0 g., 0.200 mole) was dissolved in hot anhydrous benzene (250 ml.) and hydrogen chloride gas was passed into the solution until precipitation was complete. The colorless hydrochloride was collected, washed with anhydrous ether (2×100 ml.), and recrystallized from absolute ethanol (180 ml.), yielding 26.5 g. (87.2%) of colorless *trans*-2-aminocyclohexanol hydrochloride as clusters of fine prisms, m.p. 180–181°. McCasland *et al.* (15) report m.p. 176–177°.

### *trans*-2-Aminocyclohexanol Hydrobromide

*trans*-2-Aminocyclohexanol (2.88 g., 0.025 mole) was dissolved in anhydrous ether and treated with hydrogen bromide gas as described above. The salt was collected, washed with anhydrous ether, and recrystallized from absolute ethanol (20 ml.), yielding 4.28 g. (92.2%) of fine colorless clusters of needles, m.p. 191–192°. Osterberg and Kendall (17) report m.p. 191°.

### *trans*-2-Acetamidocyclohexanol

*trans*-2-Aminocyclohexanol (1.00 g., 0.0878 mole) was dissolved in acetic anhydride (5.0 ml.) and a very exothermic reaction occurred. Water (3.0 ml.) was added and the mixture was evaporated to dryness *in vacuo*. The amide was collected and washed with cold anhydrous ether. Yield 1.14 g. (82.4%), m.p. 126–127°. McCasland *et al.* (15) report m.p. 126–127°. Calc. for C<sub>8</sub>H<sub>15</sub>O<sub>2</sub>N: C, 61.12; H, 9.62; N, 8.91%. Found: C, 61.22, 61.36; H, 9.55, 9.55; N, 8.98, 8.82%.

### *meso*-Bis-2-hydroxycyclohexylamine

This substance had m.p. 145–150° when first obtained from the ammonolysis reactions. Recrystallization from benzene (17 ml./g.) gave colorless platelets, m.p. 154°. Brunel (4) reports m.p. 153°.

### *meso*-Bis-2-hydroxycyclohexylamine Hydrochloride

*meso*-Bis-2-hydroxycyclohexylamine (1.07 g., 0.005 mole) was dissolved in anhydrous ether (250 ml.) and treated with hydrogen chloride gas as described above. The precipitate was collected, washed with anhydrous ether (3×25 ml.), and recrystallized from absolute ethanol (100 ml.), yielding 1.14 g. (91.2%) of *meso*-bis-2-hydroxycyclohexylamine hydrochloride, m.p. 270–271°, as colorless clusters of prisms. Calc. for C<sub>12</sub>H<sub>24</sub>NO<sub>2</sub>Cl: N, 5.61; Cl, 14.19%. Found: N, 5.68, 5.79; Cl, 14.50, 14.56%. Brunel (4) reports m.p. 264°. This substance sublimes below its melting point.

*meso-Bis-2-hydroxycyclohexylamine Hydrobromide*

The hydrobromide was prepared in the same manner as the hydrochloride and recrystallized from absolute ethanol (70 ml.), yielding 1.89 g. (95.5%) of fine colorless needles, m.p. 257–258°. Calc. for  $C_{12}H_{24}NO_2Br$ : N, 4.76; Br, 27.16%. Found: N, 4.85, 4.91; Br, 27.05, 26.75%.

*dl-Bis-2-hydroxycyclohexylamine*

This substance usually had m.p. 114–116° when obtained from the ammonolysis reactions. Recrystallization from ethanol–ether or benzene gave colorless needles, m.p. 126°. Brunel (4) previously reported m.p. 114° for this substance. Calc. for  $C_{12}H_{22}NO_2$ : C, 67.56; H, 10.87; N, 6.57%. Found: C, 67.76; H, 11.20; N, 6.39%. Recrystallization did not effect recovery of all the lower melting isomer in a pure condition. A small portion always remained contaminated with the higher-melting isomer. Such residues usually melted over a 1° range within the region 110–118° and analyzed satisfactorily for secondary amine.

*dl-Bis-2-hydroxycyclohexylamine Hydrochloride*

*dl*-Bis-2-hydroxycyclohexylamine (200 mg., 0.000935 mole) was dissolved in anhydrous ether (40 ml.) and the solution treated with hydrogen chloride gas. The precipitate was collected and washed with anhydrous ether ( $2 \times 10$  ml.) yielding 213 mg. (91.0%) of colorless substance, m.p. 193–194°. Calc. for  $C_{12}H_{24}NO_2Cl$ : N, 5.61; Cl, 14.19%. Found: N, 5.45, 5.59; Cl, 14.34, 14.46%. The double melting point phenomenon previously reported by Brunel (4) for this substance was not observed.

*dl-Bis-2-hydroxycyclohexylamine Hydrobromide*

*dl*-Bis-2-hydroxycyclohexylamine (2.00 g., 0.00935 mole) was dissolved in ethanol–ether and treated with hydrogen bromide gas as above. The salt was collected and recrystallized from ethanol–ether yielding 2.1 g. (76.1%) of colorless needles, m.p. 180–182°. Calc. for  $C_{12}H_{24}O_2NBr$ : C, 48.98; H, 8.22; N, 4.76; Br, 27.16%. Found: C, 48.93, 48.99; H, 8.07, 8.37; N, 5.04, 5.00; Br, 27.10, 27.00%.

## REFERENCES

1. BEDOS, P. Bull. soc. chim. France, **39**, 292 (1926).
2. BOON, W. R. J. Chem. Soc. 307 (1947).
3. BORTNICK, N., LUSKIN, L. S., HURWITZ, M. D., CRAIG, W. E., EXNER, L. J., and MIRZA, J. J. Am. Chem. Soc. **78**, 4039 (1956).
4. BRUNEL, L. Ann. chim. (Paris) [8], **6**, 200 (1905).
5. COFFEY, S. Rec. trav. chim. **42**, 387 (1923).
6. EASTHAM, A. M. J. Chem. Soc. 1936 (1952).
7. EASTHAM, A. M., DARWENT, B. DE B., and BEAUBIEN, P. E. Can. J. Chem. **29**, 575 (1951).
8. ELDERFIELD, R. C., CRAIG, L. C., LAUER, W. M., ARNOLD, R. T., GENSLER, W. J., HEAD, J. D., BEMBRY, T. H., MIGHTON, H. R., TINKER, J., GALBREATH, J., HOLLEY, A. D., GOLDMAN, L., MAYNARD, J. T., and PICUS, N. J. Am. Chem. Soc. **68**, 1516 (1946).
9. GODCHOT, M. and MOUSERON, M. Bull. soc. chim. France, **51**, 1277 (1932).
10. GUSS, C. O. and ROSENTHAL, R. J. Am. Chem. Soc. **77**, 2549 (1955).
11. HUNTER, L. and MARRIOTT, J. A. J. Chem. Soc. 285 (1936).
12. INGOLD, C. K. Structure and mechanism in organic chemistry. Cornell University Press, Ithaca, N.Y. 1953. p. 342.
13. KOTZ, A. and BUSCH, G. J. prakt. Chem. [2], **119**, 1 (1928).
14. KOTZ, A. and HOFFMANN, W. J. prakt. Chem. [2], **110**, 101 (1925).
15. McCASLAND, G. E., CLARK, R. K., and CARTER, H. E. J. Am. Chem. Soc. **71**, 637 (1949).
16. MOUSERON, M. and GRANGER, R. Bull. soc. chim. France, **14**, 850 (1947).
17. OSTERBERG, A. E. and KENDALL, E. C. J. Am. Chem. Soc. **42**, 2616 (1920).
18. PETROV, K. D. and LAGACHEVA, E. S. Zhur. Obscheshch. Khim. **23**, 403 (1953).
19. POTTER, C. and McLAUGHLIN, R. R. Can. J. Research, **B**, **25**, 405 (1947).
20. ROTHSTEIN, B. Ann. chim. (Paris), **14**, 461 (1930).
21. SCHMIDT, E., SCHUMACHER, R., and ASMUS, R. Ber. **56B**, 1239 (1923).
22. SHECHTER, L., WYNSTRA, J., and KURKJIV, R. P. Ind. Eng. Chem. **48**, 94 (1956).

23. SMITH, L. and NILSSON, T. *J. prakt. Chem.* **162**, 63 (1943).
24. SNYDER, H. R. and BROOKS, L. A. *Organic syntheses. Collective Vol. 2.* John Wiley and Sons, Inc., New York. 1943. p. 171.
25. SWARTS, F. *Bull. soc. chim. Belg.* **46**, 13 (1937).
26. WINSTEIN, S. *J. Am. Chem. Soc.* **64**, 2792 (1942).
27. WINSTEIN, S. and LUCAS, H. J. *J. Am. Chem. Soc.* **61**, 1576 (1939).
28. WINSTEIN, S. *J. Am. Chem. Soc.* **61**, 1610 (1939).
29. WINSTEIN, S. and BUCKLES, R. E. *J. Am. Chem. Soc.* **64**, 2780 (1942).
30. WINSTEIN, S., GRUNWALD, E., BUCKLES, R. E., and HANSON, C. *J. Am. Chem. Soc.* **70**, 816 (1948).
31. WINSTEIN, S. and HENDERSON, R. B. *In Heterocyclic compounds. Vol. I.* John Wiley and Sons, Inc., New York. 1950. p. 39.
32. WILSON, N. A. B. and READ, J. *J. Chem. Soc.* 1269 (1935).

# CONFORMATIONAL EFFECTS AND THE INFLUENCE OF PRESSURE ON REACTION RATES<sup>1</sup>

E. WHALLEY

## ABSTRACT

It has been suggested that the pressure coefficient of the rate constant of some reactions may be influenced by the formation of intermolecular or intramolecular conformations prior to reaction. This has been examined theoretically and the relevant experimental evidence has been discussed. No examples of an effect in which the conformations are at equilibrium are known with certainty, but the effect of pressure on termination in the polymerization of styrene appears to be an example of a conformational effect when the conformations are not at equilibrium.

The pressure coefficient of the rate constant for the isomerization of citraldehyde to 3,8-carvomenthenediol is not consistent with a unimolecular slow step, but it is consistent with either a bimolecular or a termolecular slow step. It is pointed out that the pressure coefficient of rate constants may be very useful in determining the molecularity of some reactions.

## 1. INTRODUCTION

According to the theory of absolute reaction rates (4) the rate constant  $k$  for a chemical reaction in dilute solution which goes via an activated complex is given by

$$[1.1] \quad k = \kappa (kT/h) \exp(-\Delta F^\ddagger / RT),$$

where  $\kappa$  is the transmission coefficient,  $k$  is Boltzmann's constant,  $h$  is Planck's constant, and  $\Delta F^\ddagger$  is the partial free energy of activation in the solution under discussion. The pressure coefficient of  $k$  is obtained by taking logarithms of equation [1.1], differentiating with respect to pressure, and using the identity

$$\partial F / \partial p = V,$$

where  $V$  is the molar volume. One finds

$$[1.2] \quad d \ln k / dp = -\Delta V^\ddagger / RT + d \ln \kappa / dp,$$

where  $\Delta V^\ddagger$  is the partial volume of activation. If  $\ln \kappa$  is effectively independent of pressure—and no other assumption is fruitful at present—equation [1.2] reduces to the well-known equation

$$[1.3] \quad d \ln k / dp = -\Delta V^\ddagger / RT.$$

This derivation has of course been given many times; it is included to emphasize that the variation of  $\ln \kappa$  with pressure is quite unknown and introduces an uncertainty into all discussions of the pressure coefficient of reaction rate constants in terms of the activated state theory.

There are some reactions which either can or must occur in at least two stages, the first stage of which is the formation of an intermolecular or intramolecular conformation which is favorable to the reaction. For example, the reaction



may need or be helped by the formation of a conformation  $A'$  of  $A$  thus



<sup>1</sup>Manuscript received September 26, 1957.

Contribution from the Division of Applied Chemistry, National Research Council, Ottawa, Canada.  
Issued as N.R.C. No. 4552.

where the products of reactions (1.1) and (1.3) are identical. The term conformational effects is used in this paper to denote the effects of the conformation A'. It has been suggested several times (2, 5, 11), though without detailed examination, that the acceleration of some reactions by pressure is due to the increase in concentration with pressure of a favorable conformation. This is a very interesting suggestion and it deserves quantitative investigation, not least because the pressure coefficient of reaction rate constants can be very valuable in elucidating reaction mechanisms, and it is important to know all that may influence the pressure coefficient. The purpose of this paper is to discuss the pressure coefficients of the rate constants of reactions in which a conformational effect may occur, and in particular to examine the effect of the conformational change (1.2). The theory is discussed in Section 2 and the experimental evidence in Section 3.

## 2. THEORY OF CONFORMATIONAL EFFECTS

We consider the simple reaction



with a rate constant  $k_1$ , and assume either that it can go in one step as above or that A can take up an intramolecular or intermolecular conformation A' which can also react with B to give the same activated state and same products as reaction (2.1). Thus the reactions



with rate constants  $k_2$ ,  $k_3$ , and  $k_4$  respectively, are also possible. We note that

$$[2.1] \quad k_2/k_3 = K_2,$$

where  $K_2$  is the equilibrium constant for the formation of A', the standard state being such that the molar extensive properties are equal to the partial molar properties in the (dilute) solution under discussion. We assume that reactions (2.1) and (2.4) give the same activated complexes; if they do not, then two different reactions occur simultaneously and the analysis of the effect of pressure must take account of this. Hence the partial volumes of activation of (2.1) and (2.4),  $\Delta V_1^\ddagger$  and  $\Delta V_4^\ddagger$  respectively, are related to the partial volume change  $\Delta V_2$  of reaction (2.2) thus

$$[2.2] \quad \Delta V_1^\ddagger = \Delta V_2 + \Delta V_4^\ddagger.$$

Also

$$[2.3] \quad d \ln K_2/dP = -\Delta V_2/RT.$$

We have chosen a simple bimolecular reaction for consideration and assume that A can take up only two conformations; if the reaction is of different molecularity, or if it occurs in a number of steps, and if there are many conformations of A each with its different rate constant for reaction with B, simple modifications of the treatment will lead to results similar to those below.

The rate constant usually measured is  $k$ , where

$$[2.4] \quad \begin{aligned} \text{rate of reaction} &= k(c_A + c_{A'})c_B \\ &= kc_A c_B (1 + c_{A'}/c_A), \end{aligned}$$

and  $c_A$ ,  $c_{A'}$ , and  $c_B$  represent the concentrations of A, A', and B. By considering reactions (2.1)–(2.4) the rate of reaction is given by

$$\begin{aligned} \text{rate of reaction} &= k_1 c_A c_B + k_4 c_{A'} c_B \\ [2.5] \quad &= k_1 c_A c_B \{1 + (k_4/k_1)(c_{A'}/c_A)\}. \end{aligned}$$

By equating [2.4] and [2.5] we have

$$[2.6] \quad k = k_1 \{1 + (k_4/k_1)(c_{A'}/c_A)\} / \{1 + (c_{A'}/c_A)\}.$$

It is convenient to let  $c_{A'}/c_A$  be the fraction  $\alpha$  of its equilibrium value  $K_2$ , so that

$$[2.7] \quad c_{A'}/c_A = \alpha K_2.$$

If  $c_{A'}$  is the same as if it were independent of time a simple kinetic analysis shows that

$$[2.8] \quad \alpha = (1 + c_B k_4 / k_3)^{-1}.$$

By taking logarithms of [2.6], differentiating, inserting [2.7], using equation [1.3] for  $k_1$  and  $k_4$ , and using [2.2], which is equivalent to

$$[2.9] \quad d \ln(K_2 k_4 / k_1) / dp = 0,$$

we find

$$[2.10] \quad \frac{d \ln k}{dp} = \frac{d \ln k_1}{dp} + \frac{\alpha K_2 k_4 / k_1}{1 + \alpha K_2 k_4 / k_1} \frac{d \ln \alpha}{dp} - \frac{d \ln(1 + \alpha K_2)}{dp}.$$

This is a rather complicated equation but it simplifies quite considerably under some extreme conditions as follows.

(a) If A and A' are always at equilibrium with one another,  $\alpha = 1$  and [2.10] becomes

$$[2.11] \quad d \ln k / dp = d \ln k_1 / dp - d \ln(1 + K_2) / dp.$$

There is therefore a conformational effect contained in the second term of [2.11]. The direction of the effect is at first sight unexpected. If A' is favored by pressure,  $K_2$  is increased by pressure and consequently  $d \ln(1 + K_2) / dp$  is positive. The effect of this term in equation [2.11] is therefore to reduce or to make more negative  $d \ln k / dp$ . The effect of a conformation favored by pressure is therefore to reduce the pressure coefficient below that which would otherwise occur. A conformational effect of this kind, in which the conformations are at equilibrium with one another, cannot therefore be invoked to explain an apparently anomalously large pressure coefficient of  $k$  unless it is assumed that the conformations are disfavored by pressure.

If the concentration of A' is small so that  $K_2 \ll 1$ , equation [2.11] becomes

$$\begin{aligned} [2.12] \quad d \ln k / dp &= d \ln k_1 / dp - d K_2 / dp \\ &= -\Delta V_1^\ddagger / RT + K_2 \Delta V_2 / RT. \end{aligned}$$

The conformational effect, though present, is small unless

$$|\Delta V_2 / \Delta V_1^\ddagger| \gg 1.$$

If the concentration of A is small so that  $K_2 \gg 1$ , equation [2.11] becomes

$$\begin{aligned} [2.13] \quad d \ln k / dp &= d \ln k_1 / dp - d \ln K_2 / dp - d K_2^{-1} / dp \\ &= -\Delta V_4^\ddagger / RT + (1/K_2) \Delta V_2 / RT, \end{aligned}$$

where we have used equation [2.2]. Again the conformational effect is very small unless  $|\Delta V_2/\Delta V_4^\ddagger| \gg 1$ .

Even when  $K_2$  is at its most effective value the effect will usually be rather small because

$$d \ln(1+K_2)/dp < d \ln K_2/dp = -\Delta V_2/RT;$$

since  $\Delta V_2$  is the difference in volume between two orientations, either mutual or intramolecular, of the molecules it will usually be less than the volume of melting, which is rarely more than a few  $\text{cm}^3 \text{mole}^{-1}$  except perhaps for very large molecules. It will consequently not be easy to distinguish it from the volume of activation, though a conformational effect probably occurs frequently since a reaction between two molecules, of which at least one is not spherically symmetrical, necessitates some prior orientation which may occur with a change of volume. No certain examples are known at present, as we shall show in Section 3.

(b) If A and A' are always at equilibrium and  $k_1 = 0$ , the reaction will not go unless a particular conformation is first formed, and it is formed at equilibrium. Then equation [2.6] becomes, when differentiated and with the substitutions as above,

$$\begin{aligned} d \ln k/dp &= d \ln k_4/dp + d \ln K_2/dp - d \ln(1+K_2)/dp \\ &= -\Delta V_1^\ddagger/RT - d \ln(1+K_2)/dp. \end{aligned}$$

This is identical with equation [2.11], so the discussion which follows that equation applies to this. Even when the conformation is necessary for the reaction to go, the effect of the conformation on the pressure coefficient will usually be rather small if the conformations are present at equilibrium.

(c) If the reaction will not go unless a particular conformation is first formed, and the rate of formation of the conformation is the rate determining step, then

$$[2.14] \quad k_1 = 0, \quad k_4 \gg k_3,$$

and so

$$\alpha \sim (k_3/k_4)c_B \ll 1.$$

An example of this appears to be the diffusion into proximity of the live ends of polymer chains in the termination step in the polymerization of styrene (see Section 3). Inserting [2.14] in [2.6], differentiating, and making the usual substitutions, we find

$$k = k_2/c_B,$$

which could be obtained directly much more easily. The pressure coefficient of  $k$  is very nearly that of  $k_2$ . For this example the conformational effect may be quite large.

### 3. EXPERIMENTAL EVIDENCE FOR CONFORMATIONAL EFFECTS

In this section the experimental evidence for the occurrence of the conformational effects which we are discussing is reviewed.

The first suggestion that conformational effects alter the pressure coefficient of chemical reactions was made by Conant and Peterson (2) to explain the qualitative observation that aliphatic aldehydes and isoprene could be polymerized to products of high molecular weight by subjecting them to pressures of several kilobars, but no reaction took place under the same conditions at normal pressure. In their own words, "the accelerating effect of great pressures is due to the orientation of the molecules of the isoprene or the

aldehyde into a more compact bundle in which longer reaction chains would be propagated". It was realized by Conant (3) in an earlier paper that aliphatic aldehydes do not polymerize at ordinary temperatures and pressures because the chemical equilibrium between monomer and polymer is well on the side of the monomer; under pressures of several kilobars the free energy of polymerization is altered, because of the large contraction which occurs in polymerization, enough to shift the equilibrium to the side of the polymer. This is shown by the fact that the polymer depolymerizes to monomer at atmospheric pressure. Any conformational effect on the rate is secondary to the equilibrium effect, and cannot at present be distinguished from it.

The effect of pressure on the polymerization of isoprene is probably similar to its effect on the polymerization of styrene, which has recently been investigated in some detail by Nicholson and Norrish (8). The rate constants for both the propagation and termination steps are altered by pressure, but for quite different reasons. The rate constant for the propagation step,



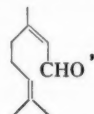
where  $M_n$  is a free radical  $n$ -mer and  $M$  is the monomer, is increased by pressure by an amount which corresponds to an apparent volume of activation of  $-13.4 \text{ cm.}^3 \text{ mole}^{-1}$  (12). This is an altogether reasonable value, being about 60% of the total decrease in volume of the propagation step (10, 12), and it is not necessary to invoke conformational effects to explain it.

The rate constant for the termination step,



is reduced by increasing pressure and it was shown (8) that this is probably caused by a reduction, consequent on the decrease in diffusion coefficients with increasing pressure, in the rate at which the live polymer ends can diffuse to one another. This then is an example of a conformational effect of the kind discussed in Section 2(c), in which the necessary conformation is the juxtaposition of two live polymer ends and the rate of formation of this conformation is the rate of reaction. The effect of pressure on the polymerization of isoprene is probably caused in part by a combination of these two effects, with the second one perhaps predominant. Hence a conformational effect probably occurs, but of a type quite different from that envisaged by Conant and Peterson.

The pressure coefficient of the rate of isomerization of citraldehyde to 3,8-carvomenthenediol (5) corresponds to a volume of activation of  $-24.5 \text{ cm.}^3 \text{ mole}^{-1}$  at atmospheric pressure. This was not explicable by the mechanism proposed by Price and Dickman (9) and consequently conformational effects were invoked. In order to cyclize, citraldehyde,



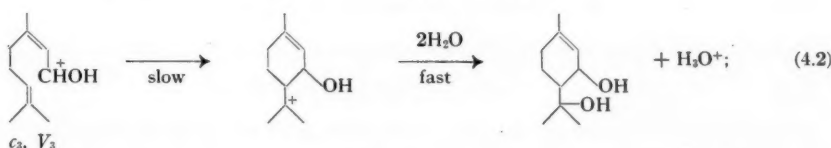
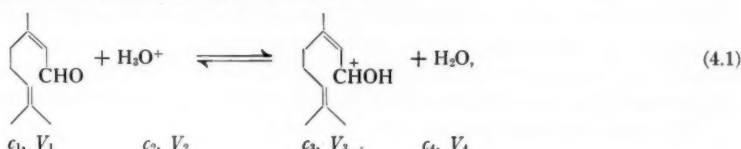
must undoubtedly take up a conformation in which the 1 and 6 carbon atoms are very close. The conformations are almost certainly in equilibrium with one another because the energy differences between them will be smaller than the activation energy for cyclization, which is 12.5 kcal. mole<sup>-1</sup> (5). The arguments of Section 2(b) apply and show that a conformation which is favored by pressure would tend to reduce the apparent volume of activation. It is possible that conformations in which the 1 and 6 carbon atoms are

close together may be disfavored by pressure, and so contribute a little negatively to the apparent volume of activation. This is unlikely to be more than a few  $\text{cm}^3 \text{mole}^{-1}$  and is probably much less than this because the equilibrium constant for the formation of the cyclic conformation is probably much less than unity because of the relatively high steric hindrance in this conformation. The observed volume of activation cannot be explained as the result of conformational effects, and another explanation must be sought; it is shown in Section 4 that a slight change in mechanism is enough.

We conclude therefore that the only reaction in which conformational effects influence the pressure coefficient of the rate constant by an appreciable amount is the termination step in the polymerization of styrene. Pressure acts by reducing the rate at which the live polymer ends diffuse into juxtaposition.

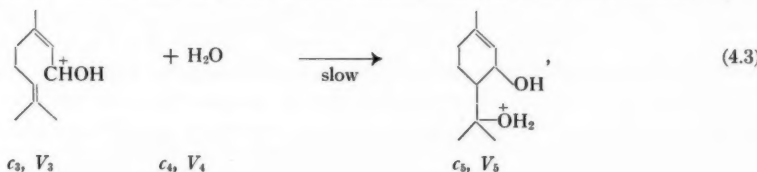
#### 4. THE EFFECT OF PRESSURE ON THE RATE OF ISOMERIZATION OF CITRALDEHYDE

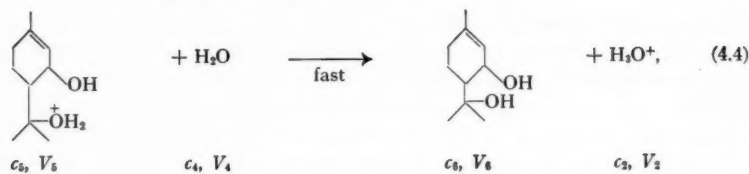
Citraldehyde isomerizes in the presence of aqueous acid to 3,8-carvomenthenediol, and Price and Dickman (9) have proposed that the slow step is the unimolecular cyclization of the conjugate acid of citraldehyde as follows:



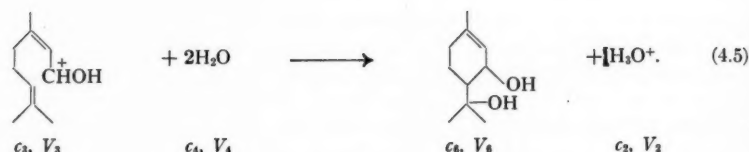
The concentrations and standard molar volumes are written under compounds for which they are required. The effect of pressure on the rate constant was investigated by Harris and Weale (5). They found an unexpectedly high pressure coefficient of  $\ln k / 24.5 \text{ cm}^3 \text{mole}^{-1}/RT$  at  $25.2^\circ \text{C}$ . and 1 atm., and this is not consistent with the above mechanism. The arguments are summarized thus: the volume change in reaction (4.1) will be rather small; the volume change in the slow step of reaction (4.2) should be very roughly  $10 \text{ cm}^3 \text{mole}^{-1}$  since this is about the volume lost in converting a van der Waals to a C-C valence interaction and the volume of activation will be smaller than this; the change of volume of the solvent during the reactions will be small. Consequently it is not possible to explain the measured volume of activation by a simple unimolecular slow step. Harris and Weale (5) suggested that an unspecified conformational effect was responsible. I have shown in the preceding section that this is unlikely to be correct.

There are two other likely mechanisms by which the conjugate acid of citraldehyde might be cyclized, a bimolecular reaction and a termolecular reaction, as follows:





and



It will be shown below that both the bimolecular and the termolecular mechanisms are consistent with the measured pressure coefficient. It is less easy to distinguish between the two multimolecular mechanisms than to distinguish between these and the unimolecular mechanism. It is indeed possible that there is no formal distinction; reaction (4.4) may be so fast that the proton may leave the activated complex or may leave later depending upon the availability of a water molecule suitably oriented to accept it.

The measured rate constant  $k$  is defined by

$$[4.1] \quad \text{rate of cyclization} = k(c_1 + c_3)c_2,$$

If the reaction goes via reactions (4.3) and (4.4), then

$$[4.2] \quad \text{rate of cyclization} = K_1 k_3 c_1 c_2,$$

where  $K_1$  is the equilibrium constant of reaction (4.1) and  $k_3$  the rate constant of reaction (4.3). From equations [4.1] and [4.2] we find

$$[4.3] \quad k = K_1 k_3 / (1 + c_3/c_1), \quad \text{bimolecular.}$$

If the reaction goes via reaction (4.5), then

$$[4.4] \quad \text{rate of cyclization} = K_1 k_5 c_1 c_2 c_4,$$

and from [4.1] and [4.4] we find

$$[4.5] \quad k = K_1 k_5 c_4 / (1 + c_3/c_1), \quad \text{termolecular.}$$

In order to reduce repetition we discuss equation [4.5] in detail and later state the results of considering in a similar manner the bimolecular equation [4.3].

Taking logarithms of [4.5] and differentiating with respect to pressure, we obtain

$$[4.6] \quad d \ln k/dp = d \ln K_1/dp + d \ln k_5/dp + d \ln c_4/dp - d \ln(1 + c_3/c_1)/dp.$$

Now

$$[4.7] \quad d \ln K_1/dp = -\Delta V_1/RT, \quad d \ln k_5/dp = -\Delta V_5^\pm/RT,$$

where  $\Delta V_1$  is the partial volume change of reaction (4.1) and  $\Delta V_5^\pm$  the partial volume of activation of reaction (4.5).  $K_1$  is probably very small, so

$$[4.8] \quad d \ln(1 + c_3/c_1)/dp = 0 \quad \text{very nearly.}$$

The value of  $d \ln c_4/dp$  depends upon the compressibility of the solution; assuming that

it is the same as that of the pure solvent (44.1% w/w ethanol in water) and using the measurements of Moesveld (7) we find

$$[4.9] \quad d \ln c_4/dp = -49 \times 10^{-6} \text{ atm.}^{-1} \text{ at } p = 0.$$

From [4.6]–[4.9] we obtain

$$[4.10] \quad d \ln k/dp = -(\Delta V_1 + \Delta V_5^\ddagger + 1.2 \text{ cm.}^3 \text{ mole}^{-1})/RT \text{ at } p = 0.$$

Let  $\Delta V_5^*$  be the change in partial volume between the activated complex of reaction (4.5) and the final products and  $\Delta V_5$  be the change in partial volume of reaction (4.5) so that

$$[4.11] \quad \Delta V_5 = \Delta V_5^\ddagger + \Delta V_5^*.$$

Now

$$\Delta V_1 = V_3 + V_4 - V_1 - V_2,$$

and

$$\Delta V_5 = V_6 + V_2 - V_3 - 2V_4,$$

so by addition

$$[4.12] \quad \Delta V_1 + \Delta V_5 = V_6 - V_1 - V_4, = \Delta V,$$

where  $\Delta V$  is the partial volume change of the whole reaction. From equations [4.10], [4.11], and [4.12] we have

$$[4.13] \quad d \ln k/dp = -(\Delta V - \Delta V_5^* + 1.2 \text{ cm.}^3 \text{ mole}^{-1})/RT.$$

The density of citraldehyde at 20° C. is 0.887 g. cm.<sup>-3</sup> (6) and hence

$$V_1 = 171 \text{ cm.}^3 \text{ mole}^{-1}$$

if the solution is perfect. Also

$$V_4 = 18 \text{ cm.}^3 \text{ mole}^{-1}.$$

The density of 3,8-carvomenthenediol has not, apparently, been recorded but if we assume that it is the same as that of the 6,8-diol, 1.13 g. cm.<sup>-3</sup> (1), we find

$$V_6 = 168 \text{ cm.}^3 \text{ mole}^{-1}.$$

Hence

$$\Delta V = -21 \text{ cm.}^3 \text{ mole}^{-1},$$

and

$$d \ln k/dp = (\Delta V_5^* + 19.8 \text{ cm.}^3 \text{ mole}^{-1})/RT.$$

Experimentally  $d \ln k/dp = 24.5 \text{ cm.}^3 \text{ mole}^{-1}/RT$  at zero pressure; hence

$$\Delta V_5^* = 4.7 \text{ cm.}^3 \text{ mole}^{-1} \text{ at } p = 0.$$

If the termolecular mechanism is correct the final products of reaction (4.5), the 3,8-diol and H<sub>3</sub>O<sup>+</sup>, have a slightly higher volume than the activated complex. The value of  $\Delta V_5^*$  may be somewhat in error because partial molar volumes differ from molar volumes, and the molar volume of 3,8-carvomenthenediol will differ from that of 6,8-carvomenthenediol. However, it seems safe to conclude that if reaction (4.5) is correct, the bond lengths in the activated state are close to those in the products.

If the bimolecular mechanism is correct, a similar treatment of equation [4.3] results in

$$\Delta V_4 + \Delta V_3^* = 3.5 \text{ cm.}^3 \text{ mole}^{-1},$$

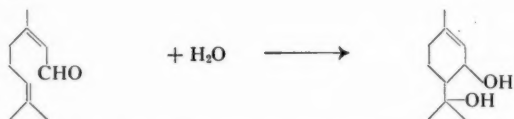
where  $\Delta V_4$  is the partial volume change of reaction (4.4) and  $\Delta V_5^*$  is the difference in partial volume between the products and the activated complex of reaction (4.3).  $\Delta V_4$  is probably close to zero and the remarks of the preceding paragraph apply here also; if reactions (4.3) and (4.4) are correct the bond lengths in the activated state are close to those in the products.

We may note in passing that the pressure coefficient for the complete reaction is independent of the pressure coefficient of  $K_1$ . This is shown by the absence of  $\Delta V_1$  from equation [4.13] and its counterpart in the bimolecular mechanism and is due to the fact that because  $K_1$  is small a change of  $\Delta V_1$  is exactly balanced by an equal and opposite change of  $\Delta V_3$  or  $\Delta V_5$ .

The apparent volume of activation decreases rapidly with pressure from  $-24.5 \text{ cm}^3 \text{ mole}^{-1}$  at 1 atm. and  $25.2^\circ \text{ C.}$  to  $-1.3 \text{ cm}^3 \text{ mole}^{-1}$  at 5000 atm. and the same temperature (5). If the reaction is termolecular, then by differentiating [4.13] with respect to pressure we obtain

$$[4.14] \quad d^2 \ln k / dp^2 = -(1/RT)(d \Delta V / dp - d \Delta V_5^* / dp + d^2 \ln c_4 / dp^2).$$

It seems unlikely that  $\Delta V_5^*$  will change much with pressure because it is already small, and  $d^2 \ln c_4 / dp^2$  is negligible, so the major part of  $d^2 \ln k / dp^2$  is  $d \Delta V / dp$ .  $\Delta V$  is the volume change of the reaction



and  $d \Delta V / dp$  depends upon the difference in compressibilities of the reactants and products. The reactants will be much more compressible than the products because two van der Waals interactions in the reactants, the intramolecular interaction between carbon atoms 1 and 6 and the intermolecular interaction between the water and the aldehyde, are converted into valence interactions which are much less compressible. Consequently  $-\Delta V$  will decrease fairly rapidly with pressure, in agreement with the kinetic results. Very similar arguments hold if the slow step is bimolecular.

We conclude therefore that the kinetics of the isomerization of citraldehyde at 1 atm. together with the effect of pressure on the rate constant show that the elementary steps of the reaction are (4.1), and (4.3) and (4.4), or (4.1) and (4.5) in which the rate-controlling step is either bimolecular or termolecular. The unimolecular step (4.2) is excluded. It is likely that in the activated complex the bond lengths are close to those in the products. We note also that the effect of pressure on reaction rates may help to determine in other similar reactions whether or not the solvent is incorporated into the activated complex.

#### SUMMARY

1. The effect of a change of intermolecular or intramolecular conformation prior to reaction on the pressure coefficient of a reaction rate constant has been examined theoretically and the pertinent experimental evidence has been discussed.
2. If the conformations involved are at thermodynamic equilibrium with one another and if one conformation is present in much higher concentrations than the others, no effect will occur. If the concentrations of the conformations involved are of the same order of magnitude, an effect is present but it will usually be rather small.

3. If the conformations are far from equilibrium and a particular conformation is necessary for reaction to occur, the rate of formation of the necessary conformation is rate controlling and a well-defined conformational effect may occur.

4. The experimental evidence for the existence of conformational effects is reviewed and it is concluded that the only authentic example is that on the termination rate constant in the polymerization of styrene, which falls into class 3 above.

5. The apparent volume of activation for the cyclization of citraldehyde to 3,8-carvomenthenediol can be explained if the slow step is either bimolecular or termolecular but not if it is unimolecular. The bond lengths in the activated complex are close to those in the products. It is pointed out that the molecularity of other reactions may be determinable by measuring volumes of activation.

#### REFERENCES

1. BEILSTEINS HANDBUCH DER ORGANISCHEN CHEMIE. Vol. 6. *Edited by* B. Prager, P. Jacobsen, P. Schmidt, and D. Stern. Springer-Verlag, Berlin. 1923. p. 752.
2. CONANT, J. B. and PETERSON, W. R. J. Am. Chem. Soc. **57**, 628 (1932).
3. CONANT, J. B. and TONBERG, C. O. J. Am. Chem. Soc. **52**, 1659 (1930).
4. GLASSTONE, S., LAIDLER, K. J., and EYRING, H. Theory of rate processes. McGraw-Hill Book Company, Inc., New York. 1941.
5. HARRIS, R. T. and WEALE, K. E. J. Chem. Soc. 953 (1956).
6. HEILBRON, SIR I. and BUNBURY, H. M. Dictionary of organic compounds. Vol I. Eyre & Spottiswoode Ltd., London. 1953. p. 589.
7. MOESVELD, A. L. Th. Z. physik. Chem. **105**, 450 (1923).
8. NICHOLSON, A. E. and NORRISH, R. G. W. Discussions Faraday Soc. **22**, 104 (1956).
9. PRICE, C. C. and DICKMAN, M. L. Ind. Eng. Chem. **40**, 257 (1948).
10. STERN, A. E. and EYRING, H. Chem. Revs. **29**, 509 (1941).
11. WEALE, K. E. Discussions Faraday Soc. **22**, 145 (1956).
12. WHALLEY, E. Discussions Faraday Soc. **22**, 146 (1956).

# THE PREPARATION OF AMINES AND HYDRAZO COMPOUNDS USING HYDRAZINE AND PALLADIZED CHARCOAL<sup>1</sup>

P. M. G. BAVIN<sup>2</sup>

## ABSTRACT

The reduction of nitro compounds to amines by ethanolic hydrazine and palladized charcoal probably proceeds through the nitroso and hydroxylamine derivatives. This reagent is shown to be useful for the reduction of azo to hydrazo compounds.

The reduction of nitro compounds to amines using ethanolic hydrazine and Raney nickel (2, 3) or palladized charcoal (10, 24) as catalyst offers many advantages over classical reducing agents. In particular, the catalyzed hydrazine reductions are very rapid and give high yields of easily isolable amines without the use of special apparatus.

The earlier work showed that hydrazine-palladium was useful for the preparation of aniline, the toluidines, phenylenediamines, *p*-aminobenzoic acid, and aminofluorescein (24), and the amino derivatives of polynuclear hydrocarbons (10). The present work, most of which is summarized in Table I in the Experimental section, extends the usefulness of the method and points out some limitations.

The reduction of 2,2'-dinitrodiphenyl proceeded erratically, the products obtained depending on the activity of the catalyst. A highly active palladium-on-charcoal catalyst gave 2,2'-diaminodiphenyl in good yield, but a less active one gave a mixture of the diamine with benz-[c]-cinnoline. The latter compound could be obtained pure in 92% yield using Raney nickel of low activity<sup>3</sup> as catalyst.

Ortho- and *p*-chloronitrobenzene and *p*-nitrophenylacetonitrile did not give pure amines. 2,5-Dichloronitrobenzene gave, very rapidly, an excellent yield of  $\beta$ -(2,5-dichlorophenyl)-hydroxylamine and, more slowly, 2,5-dichloroaniline. 2-Chloro-5-nitroterephthalic acid (11) and 2-fluoro-5-nitrotoluene gave good yields of the amines.

The reduction of nitrobenzene, which has been reviewed by Sidgwick (25), is known to proceed through nitrosobenzene and  $\beta$ -phenylhydroxylamine to aniline, much of our knowledge being due to Haber (17) and Brand (4, 5, 6). Goldschmidt showed (13, 14, 15, 16) that the relative rates of reduction were in the order nitrosobenzene >  $\beta$ -phenylhydroxylamine > nitrobenzene, explaining the difficulty encountered in isolating nitrosobenzene as a reduction product except under rigorously controlled conditions. In alkaline media nitrosobenzene and  $\beta$ -phenylhydroxylamine condense to form azoxybenzene, giving rise to another series of reduction products.

The hydrazine-palladium reagent reduces nitro- and nitroso-benzene and  $\beta$ -phenylhydroxylamine to aniline, but azo- and azoxy-benzene are reduced to hydrazobenzene.<sup>4</sup> These facts suggest that the reduction of nitro compounds to amines by this reagent proceeds through monomeric compounds, as shown below in route I. The isolation of

<sup>1</sup>Manuscript received September 5, 1957.

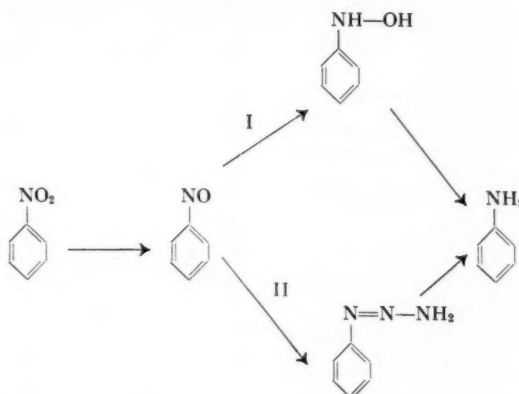
Contribution from the Departments of Chemistry of the University of Ottawa, Ottawa, Canada, and (present address) the Ohio State University, Columbus 10, Ohio, U.S.A.

<sup>2</sup>National Research Council of Canada Postdoctorate Fellow at the University of Ottawa, 1954-1956.

<sup>3</sup>The Raney nickel catalyst was W1 (1, 8), which had been stored for several months at 0° under absolute methanol.

<sup>4</sup>It is interesting to note that fermenting yeast will reduce nitro- and nitroso-benzene and  $\beta$ -phenylhydroxylamine but not azo- or azoxy-benzene, to aniline (23).

$\beta$ -(2,5-dichlorophenyl)-hydroxylamine as a reduction product of 2,5-dichloronitrobenzene lends strong support to this mechanism.



An alternative mechanism is shown, route II, based on the known easy condensation of nitrosobenzene with many amines and phenylhydrazine. Hydrazine was found to react rapidly with nitrosobenzene but the red oil obtained appeared to be stable to hydrazine-palladium, making route II improbable.

The reduction of azobenzene to hydrazobenzene by hydrazine-palladium is a considerable improvement on the usual zinc - alcoholic potash method. An excess of hydrazine is advantageous since it appears to protect the hydrazobenzene during crystallization. Hydrazo-*o*-diphenyl was also prepared in good yield, and the method may prove to be generally useful for the preparation of hydrazo compounds.

#### EXPERIMENTAL

Melting points are uncorrected. The active palladium-on-charcoal catalyst was 10%, supplied by Baker and Co., Newark, New Jersey; the less active catalyst was an old sample.

The reductions were carried out essentially as described by Pietra (24). Most of the results are presented in Table I. Wherever possible the identity of a product was confirmed by taking the melting point of a mixture with an authentic sample, and by taking the infrared spectrum. Many of the amines were acetylated to aid isolation.

*o*-Chloronitrobenzene did not give a pure product. *p*-Chloronitrobenzene gave, after several crystallizations from benzene, impure *p*-chloroacetanilide (27%), m.p. 171–175° (lit. m.p. 178° (19)).

#### $\beta$ -(2,5-Dichlorophenyl)-hydroxylamine

Hydrazine hydrate (4 ml.) was added to a suspension of 2,5-dichloronitrobenzene (5 g.) and active 10% palladium-on-charcoal (0.1 g.) in ethanol (100 ml.). The vigorous exothermic reaction was over in 2 minutes, as shown by a pronounced slackening in the rate of nitrogen evolution. After the catalyst was removed by filtration, the solution was poured into ice water (500 ml.). A white solid separated and was collected, washed, and dried by suction. The yield was almost quantitative.

Recrystallization was achieved by dissolving the product in hot benzene (100 ml.),

TABLE I<sup>1</sup>

Compound	Isolated as:	%	M.p.	Lit. m.p.
Nitrobenzene	Acetanilide	91	110-112	113-114 (19)
Nitrosobenzene	Acetanilide	93	109-111	113-114 (19)
$\beta$ -Phenylhydroxylamine	Acetanilide	89	112-113	113-114 (19)
Azobenzene	Hydrazobenzene	84 <sup>2</sup>	125-126	126-127 (19)
Azoxybenzene	Hydrazobenzene	79 <sup>2</sup>	125-126	126-127 (19)
Azoxo- <i>o</i> -diphenyl	Hydrazo- <i>o</i> -diphenyl	70 <sup>2</sup>	172-176 <sup>3</sup>	182 (12)
4,6-Dinitro- <i>m</i> -xylene	N,N'-Diacetyl-4,6-diamino- <i>m</i> -xylene	87	290-292	295 (19)
1-Nitro-2-naphthylamine	1,2-Diaminonaphthalene <sup>4</sup>	85	96-98	98.5 (19)
5-Nitro-6-amino-2-methyl-pyridine	5,6-Diamino-2-methyl-pyridine	82	64-67	69-70 (20)
<i>o</i> -Nitrophenol	<i>o</i> -Aminophenol	88	171-173	174 (19)
2-Nitrofluorene <sup>7</sup>	2-Aminofluorene	97	127-128	129 (19)
2-Fluoro-5-nitrotoluene	6-Fluoroaceto- <i>m</i> -toluidide	88	76-77	74 (7)
2-Nitrodiphenyl	2-Aminodiphenyl	89	47-49	49-50 (19)
4-Nitrodiphenyl	4-Aminodiphenyl	92	51-53	50-52 (19)
2,2'-Dinitrodiphenyl <sup>6</sup>	N,N'-Diacetyl-2,2'-diamino-diphenyl	88	162-164	161 (19)
6,6'-Dimethyl-2,2'-dinitrodi-phenyl	6,6'-Dimethyl-2,2'-diamino-diphenyl	63 <sup>6</sup>	133-135	136 (19)

<sup>1</sup> Yield and melting point refer to crude dried product unless otherwise indicated.<sup>2</sup> Crystallized from ethanol containing hydrazine.<sup>3</sup> Melting point with decomposition and dependent on the rate of heating.<sup>4</sup> Characterized by condensation with phenanthraquinone to give 1,2;3,4;5,6-tribenzphenazine, yellow prisms from xylene, m.p. 272-273° (lit. m.p. 273° (21)).<sup>5</sup> Using a catalyst of low activity, a mixture of the diamine with benz-[c]-cinnoline, m.p. 155-156°, was obtained.<sup>6</sup> The low yield is probably due to the use of only 0.1 g. of nitro compound.<sup>7</sup> Raney nickel has been used as the catalyst for this reduction, a yield of 100% being claimed (22).

adding a little anhydrous magnesium sulphate to remove traces of water, and decanting off the supernatant solution. Addition of hot heptane gave, on cooling, long white needles, m.p. 95-96° with decomposition to a black tar. The melting point depended on both the rate of heating and the crystal size, powdered samples having m.p. 93-94° (lit. m.p. 93° (9)). The melting point was not depressed when the product was mixed with an authentic sample, prepared by Lapworth's general method (18). The identity was confirmed by oxidation to 2,5-dichloronitrosobenzene, m.p. 99-100° (lit. m.p. 101° (9)), and by comparison of infrared spectra. Sharp peaks at 3600 and 3340 cm.<sup>-1</sup> in the spectra of dilute chloroform solutions were probably O—H and N—H stretching bands since the spectrum of  $\beta$ -phenylhydroxylamine was identical in that region.

Recrystallized  $\beta$ -(2,5-dichlorophenyl)-hydroxylamine is stable at 0° but heating a benzene solution on the steam bath for a few minutes causes extensive decomposition to a brown tar.

When the reduction was carried out for 24 hours, 2,5-dichloroaniline was obtained, m.p. and mixed m.p. 49-50° (lit. m.p. 50° (9)).

#### Benz-[c]-cinnoline

2,2'-Dinitrodiphenyl was reduced using the general method described by Balcom and Furst (2). After the catalyst was removed by filtration, the filtrate was concentrated to give, on cooling, benz-[c]-cinnoline as yellow prisms, m.p. 155-156° (lit. m.p. 156° (19)). The yield was consistently greater than 90% when a weakly active Raney nickel catalyst was used.

Benz-[c]-cinnoline picrate crystallized from benzene as dark yellow prisms, m.p. 194-195° (lit. m.p. 194° (19)).

## NOTE ADDED IN PROOF

Since this paper was accepted for publication, two more articles have become available (26, 27) which deal with some uses of hydrazine as a reducing agent in the presence of metal catalysts.

## ACKNOWLEDGMENT

The author is grateful to Doctors F. A. L. Anet, M. P. Cava, and M. S. Newman for their interest and encouragement.

## REFERENCES

1. ADKINS, H. and PAVLIC, A. A. *J. Am. Chem. Soc.* **69**, 3039 (1947).
2. BALCOM, D. and FURST, A. *J. Am. Chem. Soc.* **75**, 4334 (1953).
3. BAVIN, P. M. G. and DEWAR, M. J. S. *J. Chem. Soc.* 164 (1956).
4. BRAND, K. *Die elektrochemische Reduktion organischer Nitrokörper*. F. Enke, Stuttgart. 1908.
5. BRAND, K. and MAHR, J. *J. prakt. Chem.* **131**, 97 (1931); **142**, 153 (1935).
6. BRAND, K. and MODERSON, A. *J. prakt. Chem.* **120**, 160 (1928-1929).
7. BUU-HOÏ, N. P. and JACQUIGNON, P. *J. Chem. Soc.* 4173 (1952).
8. COVERT, L. W. and ADKINS, H. *J. Am. Chem. Soc.* **54**, 4116 (1932).
9. de CRAUW, T. *Rec. trav. chim.* **50**, 753 (1931).
10. DEWAR, M. J. S. and MOLE, T. *J. Chem. Soc.* 2556 (1956).
11. FISHEL, D. L. Unpublished data.
12. FRIEBEL, G. and RASSOW, B. *J. prakt. Chem.* **63**, 459 (1901).
13. GOLDSCHMIDT, H. and ECKARDT, M. *Z. physik. Chem.* **56**, 385 (1906).
14. GOLDSCHMIDT, H. and INGEBRECHSTEN, K. *Z. physik. Chem.* **48**, 435 (1904).
15. GOLDSCHMIDT, H. and LARSEN, H. *Z. physik. Chem.* **71**, 437 (1910).
16. GOLDSCHMIDT, H. and SUNDE, E. *Z. physik. Chem.* **56**, 1 (1906).
17. HABER, F. *Angew. Chem.* **13**, 435 (1900); *Z. physik. Chem.* **32**, 193 (1900).
18. HAWORTH, R. D. and LAPWORTH, A. *J. Chem. Soc.* **119**, 768 (1921).
19. HEILBRON, SIR I. *Dictionary of organic compounds*. Oxford University Press, New York. 1953.
20. LAPPIN, G. R. and SLEZAK, F. B. *J. Am. Chem. Soc.* **72**, 2806 (1950).
21. LAWSON, T. A. *Ber.* **18**, 2426 (1885).
22. LITVNEK, L. M. and GREKOV, A. P. *Zhur. Obshchei Khim.* **27**, 234 (1957); *Chem. Abstr.* **51**, 12866e (1957).
23. NEUBERG, C. and WELDE, E. *Biochem. Z.* **60**, 474 (1914); **67**, 18, (1914). *See also* Advances in carbohydrate chemistry. Vol. 4. Academic Press, Inc., New York. 1949. p. 98.
24. PIETRA, S. *Ann. chim. (Rome)*, **45**, 850 (1955).
25. SIDGWICK, N. V. *The organic chemistry of nitrogen*. Oxford University Press, London. 1937.
26. PIETRA, S. *Ann. chim. (Rome)*, **47**, 410 (1957).
27. FURST, A. and MOORE, R. E. *J. Am. Chem. Soc.* **79**, 5492 (1957).

# TRIARYLMETHANE COMPOUNDS AS REDOX INDICATORS IN THE SCHOENEMANN REACTION

## III. THE DYES AND THEIR SPECTRA<sup>1</sup>

G. A. GRANT, R. BLANCHFIELD, AND D. MORISON SMITH

### ABSTRACT

A series of triarylmethane dyes were made by varying the substituents in the thiophene ring of the dye [4-(*p*-dimethylamino- $\alpha$ -2-thienylbenzylidene)-2,5-cyclohexadiene-1-ylidene]-dimethylammonium chloride. The spectra of the zinc salts of these dyes were shown to be similar to that of the dye formed in the Schoenemann reaction when the parent triarylmethane compound was used as an indicator. Neither of the absorption bands occurring in the 475 m $\mu$  or 625 m $\mu$  regions is affected by pH or buffer salts in the pH range 2.4 to 6.4 but both bands are hypsochromically shifted when the pH is lowered to 0.5. The substitution of 5-nitro and 5-acetamido groups in the thiophene ring results in the largest bathochromic and hypsochromic shifts respectively. Interpretation of the effect of substitution and pH was attempted employing existing theories on the relation between color and constitution.

### INTRODUCTION

The preceding papers in this series (4, 14) described the preparation and use of some triarylmethane compounds as indicators in the Schoenemann reaction with a view to improving the method for detecting the phosphonofluoridate type of anticholinesterase compounds. As the success of the method depended greatly on the color of the dye produced it was of interest to ascertain the effect of various substituents attached to the thiophene ring on the spectra of the dyes. The effect of the replacement of the benzene nucleus by thiophene and a number of 5-substituted thiophene nuclei on triarylmethane dyes has been reported by Mason and Nord (11, 12). However, the present investigation enlarges on the previous studies by including a number of new mono- and di-substituted thiophenyl derivatives. The effect of pH on the spectra is also reported.

It was of interest to check the assumption that the oxidized compound produced in the Schoenemann reaction was the same as that of an authentic dye cation. Therefore spectral comparisons have been made of a number of zinc chloride salts of prepared dyes with the dyes formed in the Schoenemann reaction.

### EXPERIMENTAL

#### *Preparation of Dyes*

The preparation and purification of the triarylmethane compounds from which the dyes were made have been described previously (4).

The zinc chloride salts of the dyes were prepared from the corresponding triarylmethane compounds according to the procedure of Mason and Nord (11) except that identical molar concentrations of the solutions were always used in an attempt to produce salts of the same composition. The method of Davies and Hodgson (2) was investigated but was not found to be superior to the method outlined by Mason and Nord (11) or Levi (7).

Briefly, the leuco compounds (0.04 mole) were dissolved in 2 N HCl (80 ml.) and the solutions were diluted with 800 ml. of water. Freshly prepared lead dioxide (0.04 mole) was added with stirring and cooling. After 2 hours sodium sulphate (0.05 mole) was

<sup>1</sup>Manuscript received July 24, 1957.

Contribution from Defence Research Board, Defence Research Chemical Laboratories, Ottawa, Ontario. Issued as D.R.C.L. Report 135C. Presented at the Annual Conference of the Chemical Institute of Canada at Vancouver in June, 1957.

added and the solution filtered. To 400 ml. of solution were added saturated zinc chloride solution (0.03 mole) and saturated brine solution (800 ml.). The precipitated dye was filtered off and the dye crystals were washed with ice water. The average yields were approximately 80%. An exception to the above procedure was the case of the dye with a nitro group in the 5-position in the thiophene ring. This leuco compound could not be made satisfactorily by the usual condensation of the nitrothiophenealdehyde with dimethylaniline (11). However, removal of the excess dimethylaniline and the oxidation of the reaction mixture by the above procedure gave the dye salt. The nitrothiophene-aldehyde mentioned above was prepared from thiophenealdehyde by nitration of the aldehyde diacetate and subsequent hydrolysis according to the procedure of Patrick and Emerson (13).

The composition of some of these dyes is given in Table I.

TABLE I  
ANALYSIS OF DYE SALTS

Zinc chloride salt of formula I with:			Found			Calculation (based on these analyses) for:		
R	R'	R''	% C	% H	% N	Moles ZnCl <sub>2</sub>	Moles H <sub>2</sub> O	Mol. wt.
H	H	H	45.00	4.55	—	1.24	1.15	560.5
CH <sub>3</sub>	H	H	47.33	4.89	—	1.13	1.04	558.2
C <sub>2</sub> H <sub>7</sub>	H	H	58.02	5.94	5.62	0.59	0.22	497.0
CH <sub>3</sub>	CH <sub>3</sub>	H	52.57	5.40	5.21	0.85	0.57	525.4
CH <sub>3</sub>	C <sub>2</sub> H <sub>5</sub>	H	52.60	5.95	—	0.77	1.68	547.9
C <sub>6</sub> H <sub>5</sub>	H	H	51.32	5.23	—	0.98	2.88	631.9
Br	CH <sub>3</sub>	H	44.02	4.70	4.65	0.74	2.00	600.2

#### Spectral Measurements

On the basis of the analysis of the dyes, solutions of a definite molarity were made up in distilled water or in the appropriate Clark and Lubs buffer and the spectra were determined on a Beckman Model DU Spectrophotometer between 320 and 700 m $\mu$ . Spectra were also taken of known dyes, e.g. malachite green, for comparison purposes. Absorption spectra of the dyes produced in the Schoenemann reaction were obtained employing a test procedure as outlined previously (4). The spectra were scanned from 320 to 700 m $\mu$  in 20 m $\mu$  steps 10 minutes after the addition of all the reagents.

#### RESULTS AND DISCUSSION

##### Composition of Dyes

The analyses for the dye salts given in Table I showed that the zinc chloride salts as prepared do not have a definite composition. Mason and Nord (11) on the basis of nitrogen analyses suggested a formula with 2 moles of zinc chloride and 3 moles of water.

##### Spectra of Dyes Formed in the Schoenemann Reaction

A comparison was made between the spectra of the dye solutions obtained in the Schoenemann reaction and the spectra of the corresponding solutions of the zinc chloride salts of the dyes. Fig. 1 is an example of this comparison for the 4,5-dimethylthienylidene dye. Along with similar plots obtained for other compounds this supports the assumption that I is the dye formula responsible for the color in the Schoenemann reaction.

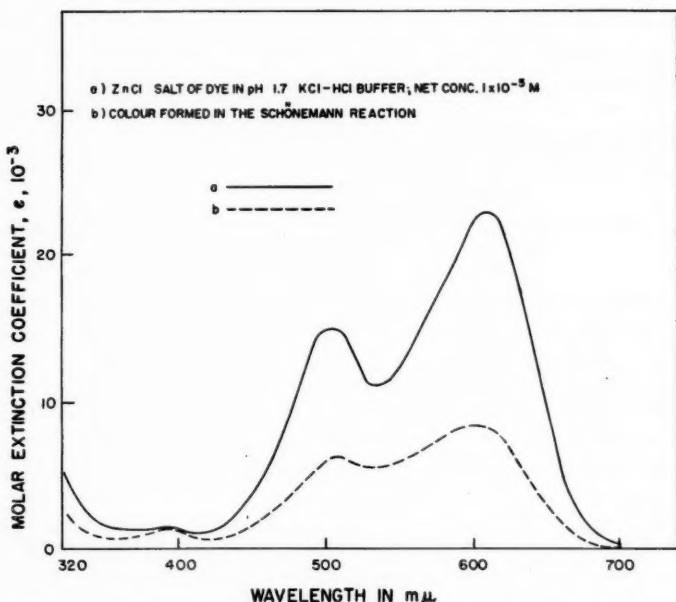
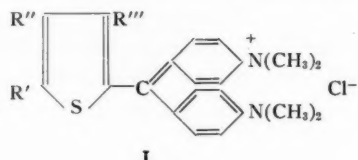


FIG. 1. Comparison of color formed in Schoenemann reaction with that of a solution of zinc chloride salt of the 4,5-dimethylthienyl substituted dye.

#### *Effect of pH on Dye Spectra*

Although a pH of approximately 2.2 or lower is necessary for the formation of the dye from the leuco compound, the pH for optimum color intensity may occur at a different pH. However, only under acid conditions would the results be of significance in the Schoenemann reaction, because the dyes are rapidly destroyed by alkaline peroxide, an excess of which is always present in this reaction.

The effect of pH was investigated over the range 0.5 to 6.4 in buffered solution. The results are reported in Table II. Neither the *y* band nor the *x* band is affected by pH or buffer salts in the pH range 2.4 to 6.4, but both bands are hypsochromically shifted for all the compounds studied except the 3-methyl and 5-acetamido derivatives when the pH is lowered to 0.5. At pH 0.5 the absorption intensity of some of the dyes decreased, and it was thought that decomposition might be taking place. The system was found to be only partially reversible, for although on the addition of alkali the color reappeared the original absorption bands were not entirely restored in intensity. All the dyes studied showed the same reversible reaction except the 3-methyl substituted compound which gave an irreversible bathochromic shift from 469 to 474 mμ when the pH was dropped from 1.60 to 0.5. Fig. 2 illustrates this decrease in intensity and shift in the absorption

TABLE II  
EFFECT OF pH ON ABSORPTION BANDS

Substituent	Absorption maximum ( $m\mu$ )				
	pH 0.5	pH 1.6	pH 2.4	pH 4.4	pH 6.4
y-Absorption bands					
5-Acetamido	460	460	536		
4,5-Dimethyl-2-thienyl	392	504	499	499	499
4-Ethyl-5-methyl-2-thienyl	392	500	500	500	500
5-Methyl-2-thienyl	386	490	486	486	486
5-Ethyl-2-thienyl	386	488	486	486	486
5-Propyl-2-thienyl	386	486	486	486	484
5-Chloro-2-thienyl	F	476	476	476	476
5-Bromo-2-thienyl	385	474	476	476	476
5-Methyl-5-bromo-2-thienyl	F	F	476	476	476
3-Methyl-2-thienyl	474	469	469	469	469
2-Thienyl	F	F	465	465	465
x-Absorption bands					
5-Bromo-2-thienyl	568	635	637	634	632
5-Chloro-2-thienyl	F	F	634	634	632
2-Thienyl	F	F	623	623	623
4-Methyl-5-bromo-2-thienyl	F	F	624	624	624
3-Methyl-2-thienyl	618	620	620	620	620
4-Ethyl-5-methyl-2-thienyl	552	603	620	620	620
5-Methyl-2-thienyl	534	614	616	616	616
5-Ethyl-2-thienyl	534	608	616	614	616
5-Propyl-2-thienyl	534	604	614	614	614
4,5-Dimethyl-2-thienyl	552	603	614	614	614
5-Acetamido	607	607	605		Insoluble

F—Unstable solution.

curve of the 3-methyl compound when the pH value is decreased from 6.4 to 0.5. At pH 1.6 an inflection appears in the absorption curve at  $555 m\mu$ , which becomes a distinct band when the pH value is lowered to 0.5.

From pH 2.54 to 6.45 dyes with alkyl substitution in the 5-position absorb similarly to those with 3-methyl substitution, while from pH 1.6 to 2.54 they are markedly different. The appearance of the band at  $540 m\mu$  at pH 0.5 was more pronounced in the case of 5-substitution (e.g., 5-methylthienyl, Fig. 3), than with 3-substitution. The dialkyl substituted dyes responded to pH change in a similar manner to the unsubstituted and monosubstituted compounds.

The examination of the effect of pH on triarylmethane dyes containing a thienyl or substituted thienyl group showed that they were behaving as acid-base indicators similar to crystal violet. Adams and Rosenstein (1) examined the color changes of crystal violet in acid solution and showed that the absorption spectra corresponded to successive addition of positive charge to the cation. However, it is of interest to compare spectra obtained in the present investigation with those of the triphenylmethane dyes because of the difference in resonance structure between thienyl and phenyl groups. The hetero-sulphur atom in the thienyl group changes the electronic distribution and makes it impossible for the thienyl group to contribute quinoidal resonance hybrids as postulated for other triphenylmethane dyes.

In the case of crystal violet, the addition of a proton to one dimethylamino group results in the loss of the contribution of that dimethylaminophenyl group to the resonance of the molecule. The electron cloud is then redistributed between the other two dimethyl-anilino groups and the absorption spectrum becomes similar to that of malachite green.

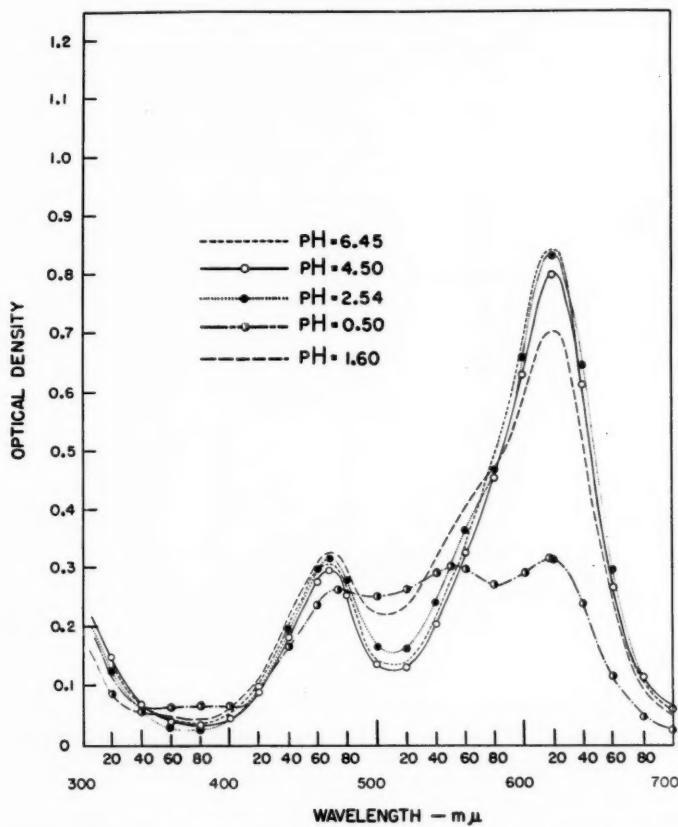
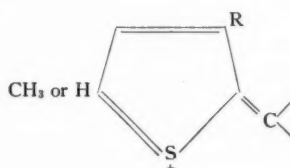


FIG. 2. Spectra at various acidities for 3-methylthienyl substituted dye.

In the case of thiophene malachite green a proton attack on one of the dimethylaminophenyl groups would substantially change the picture since the electron cloud would either be concentrated in the remaining dimethylaminophenyl group or shared between it and the 2-thienyl group. However, when the 2-thienyl group is unsubstituted or substituted only in the 3-position the resonance form showing a continuous conjugated system has a high probability.



II

This structure is less likely to be subject to a proton attachment but the  $\text{S}=\text{C}$  bond may be attacked and split. This in part may account for some of the decomposition of the unsubstituted and 3-methyl substituted dyes at the lower pH. In all cases that

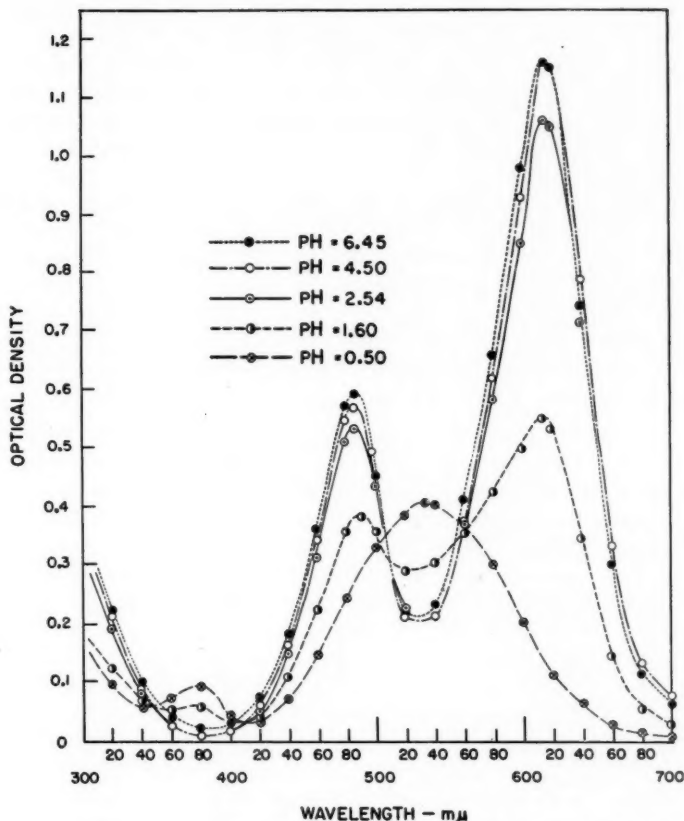


FIG. 3. Spectra at various acidities for 5-methylthienyl substituted dye.

were studied, except that of the 3-methyl-2-thienyl dye, a proton attack caused a general hypsochromic shift. The resonance hybrid of the 3-methyl substituted thienyl dye is therefore different from that obtained by disubstitution in the 4,5-positions or mono-substitution in the 5-position. That there is no shift with a proton attack on the 3-methyl substituted dye may be explained by the fact that when a methyl group is substituted in the 3-position of the thiophene ring, a larger proportion of the resonance hybrid is in the conjugated form (Formula II).

#### *Effect of Substitution*

Because of the variable composition of the zinc chloride salts the values of extinction coefficients are not reported. The wavelengths of the absorption maxima are comparable since it has been shown that the salt forming Lewis acid has little or no effect on wavelength maxima of the dye spectra (10).

For those dyes which are the same as those made previously (11, 12), the spectra and wavelength shifts obtained in this study in aqueous solution exhibit the same tendencies but are not identical in magnitude to those obtained by Mason and Nord in acetic acid solutions (12).

The relation between color and chemical constitution has been explored by Lewis (9), Knott (6), and Dewar (3). According to Lewis (9) the change from the single  $x$  absorption band of crystal violet to the  $x$  and  $y$  absorption bands of malachite green indicates the introduction of the second mode of electronic oscillation involving the unsubstituted phenyl ring. The wavelength of the  $x$  absorption of malachite green is higher than that of crystal violet because, in the malachite green case, the positive charge is distributed mainly between the two dimethylaniline rings, whereas it is distributed between three equivalent rings in the crystal violet case (8). In this degenerate case the  $x$  and  $y$  bands coincide. It would seem that the wavelength difference between the  $x$  and  $y$  bands could be used as a measure of the degree of participation of the resonance forms of the aryl portion in the aryl bis(dimethylaniline) dyes. That is, it would indicate qualitatively how close they were to the crystal violet case when there is equal participation of all three groups attached to the central carbon atom, and as well might provide a way of ranking substituted aryl rings according to their positive nature when involved in this kind of attachment. These differences are given in Table III.

TABLE III  
ABSORPTION MAXIMA OF  $x$  AND  $y$  BANDS

Zinc chloride salt of ( <i>p</i> -dimethylamino-aryl-benzylidene)-2,5-cyclohexadiene-1-ylidene dimethylammonium chloride where aryl is	$\lambda_x$ , $m\mu$	$\lambda_y$ , $m\mu$	$\lambda_x - \lambda_y$ , $m\mu$
5-Acetamido-2-thienyl	605*	532*	73
4-Methyl-5-ethyl-2-thienyl	614	500	114
4,5-Dimethyl-2-thienyl	614	499	115
4-Ethyl-5-methyl-2-thienyl	614	499	115
5-Methyl-2-thienyl	616	486	130
5-Ethyl-2-thienyl	616	486	130
5-Propyl-2-thienyl	614	484	130
4-Methyl-5-bromo-2-thienyl	624	476	148
3-Methyl-2-thienyl	620	468	152
5-Chloro-2-thienyl	634	476	158
5-Bromo-2-thienyl	634	476	158
<i>p</i> -Tolyl	600	442	158
2-Thienyl	625	465	160
2-Furyl	637	475	162
5-Phenyl-2-thienyl	632	518	174
Phenyl	617	428	189
5-Nitro-2-thienyl	662	456	216

\* Taken in distilled water solution.

Table III also includes a comparison of the wavelengths of the  $x$  and  $y$  bands of some of the triarylmethane dyes. Substitution in the 5-position, with nitro, halo, or phenyl groups, produces bathochromic shifts while alkyl or acetamido substitution produces a hypsochromic shift in the  $x$  band. The largest bathochromic and hypsochromic shifts (37 and 23  $m\mu$  respectively) result from 5-nitro and 5-acetamido substitution. The effect of substitution on  $y$  band absorption is also appreciable. Substitution of a phenyl or nitro group in the 5-position results in hypsochromic shifts of 7 and 9  $m\mu$  respectively while substitution of alkyl, acetamido, halogen groups or both alkyl and halogen groups produced bathochromic shifts.

Mason and Nord (12) reported that the hypsochromic influence exerted on the  $x$  band increased with the size of the alkyl group. The total shift was 3  $m\mu$  when the group size was increased from methyl to propyl. Our data indicate that 5-propyl thiophene

malachite green absorbs at a shorter wavelength than the 5-methyl and 5-ethyl compounds. However, there is no strong evidence to indicate that the magnitude of the hypsochromic shift increases significantly with the size of the alkyl group.

It was reported (12) that substitution of the electronegative chlorine and bromine atoms in the 2-position of the thiophene ring causes bathochromic shifts of the  $x$  and  $y$  bands. Larger bathochromic shifts of the  $x$  band were reported for the chloro compound than for the bromo compound, while the reverse was true for the  $y$  bands. The present investigation confirms that bathochromic shifts occur for the  $x$  and  $y$  bands. However, no difference in the magnitude of the shifts was noted when the less electronegative bromine atom was substituted for a chlorine atom.

It is also of interest to note that if both electron attracting and donating groups are substituted in the thiophene nucleus no appreciable shift occurs. When a methyl group is placed in the 4-position and a bromine atom in the 5-position, it is evident from the absence of wavelength shift that most of the electrons attracted by the halogen are obtained at the expense of the methyl group in the 4-position. Thus the net electronic distribution approaches that of the unsubstituted 2-thienyl nucleus.

The new members of the series are the 4,5-dialkyl, and acetamido-, nitro-, and phenyl-substituted thiophene dyes. The spectra of the 4,5-dialkyl dyes show an enhancement of the effects observed for the 5-monoalkyl dyes. These compounds possess more resonance forms with a positive charge in the thiophene ring. The 5-acetamidothienyl dye approaches most closely to the situation in crystal violet where all rings are equivalent, thus indicating possible participation of positively charged nitrogen in the amide group in the resonance of the dye. In the case of 5-nitrothienyl dye the difference between  $x$  and  $y$  peaks is much greater because the electron-attracting nitro group makes the thiophene ring system even less positive than usual. A similar effect is observed with the 5-phenylthienyl dye where the charge is dissipated over two aromatic rings, although the effect is less pronounced than in the nitro compound, because the phenyl ring, in itself, is only slightly more negative than the thiophene ring ( $\lambda_x - \lambda_y = 189 \text{ m}\mu$  for malachite green vs.  $160 \text{ m}\mu$  for the thiophene analogue). With respect to this difference in  $x$  and  $y$  peaks, "furan malachite green" appears to be quite similar to the thiophene derivative. The effect of a para-methyl group in the phenyl ring (8) is about the same as the effect of a 5-methyl group in the thiophene ring, that is,  $\lambda_x - \lambda_y$  is decreased by  $30 \text{ m}\mu$ .

In summary, it may be noted that the leuco compounds effective as indicators in the Schoenemann reaction (14) have a wavelength difference between the absorption maxima of 110 to  $150 \text{ m}\mu$ , and the order of their effectiveness increases as the wavelength difference decreases. It may also be noted that this order of substituents given in Table III corresponds to the order to be expected for Hammett's  $\sigma$  constants, going from negative to positive values (5), allowing for the difference to be expected between the phenyl and thienyl ring systems.

#### REFERENCES

1. ADAMS, E. Q. and ROSENSTEIN, L. J. Am. Chem. Soc. **36**, 1452 (1914).
2. DAVIES, R. R. and HODGSON, H. H. J. Soc. Dyers Colourists, **59**, 196 (1943).
3. DEWAR, M. J. S. J. Chem. Soc. 2329 (1950).
4. GRANT, G. A., BLANCHFIELD, R., and SMITH, D. M. Can. J. Chem. **35**, 40 (1957).
5. JAFFÉ, H. H. Chem. Revs. **53**, 191 (1953).
6. KNOTT, E. B. J. Chem. Soc. 1024 (1951).
7. LEVI, L. E. Ber. **20**, 517 (1887).
8. LEWIS, G. N. J. Am. Chem. Soc. **67**, 770 (1945).
9. LEWIS, G. N. and BIGELEISEN, J. J. Am. Chem. Soc. **65**, 2102 (1943).

10. LEWIS, G. N. and BIGELEISEN, J. *J. Am. Chem. Soc.* **65**, 1144 (1943).
11. MASON, C. D. and NORD, F. F. *J. Org. Chem.* **16**, 722 (1951).
12. MASON, C. D. and NORD, F. F. *J. Org. Chem.* **17**, 778 (1952).
13. PATRICK, T. M. and EMERSON, W. S. *J. Am. Chem. Soc.* **74**, 1356 (1952).
14. SMITH, D. M., BLANCHFIELD, R., THOMPSON, J. L., and GRANT, G. A. *Can. J. Chem.* **35**, 156 (1957).

# THE PHOTOCHEMICAL OXIDATION OF ALDEHYDES IN THE GASEOUS PHASE

## PART I. THE KINETICS OF THE PHOTOCHEMICAL OXIDATION OF ACETALDEHYDE<sup>1</sup>

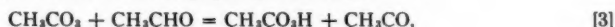
C. A. McDOWELL AND L. K. SHARPLES

### ABSTRACT

The photochemical oxidation of acetaldehyde has been studied in the gaseous phase at 20° C. and a wavelength of 3130 Å. It has been established that when the pressure of oxygen is between 0.5 mm. and 150 mm. the reaction obeys the kinetic law:

$$-\frac{d[\text{CH}_3\text{CHO}]}{dt} = (k_1/k_2^{\frac{1}{2}})(\phi_2 I_a)^{\frac{1}{2}}[\text{CH}_3\text{CHO}],$$

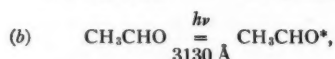
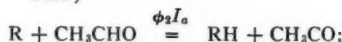
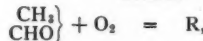
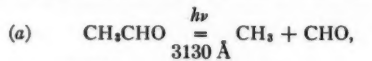
where  $k_1$  is the velocity constant for the propagating reaction [3]:



$k_2$  is the velocity constant for the terminating reaction [6]:



and  $\phi_2 I_a$  is the rate of initiation of the photooxidation, i.e. the rate of formation of acetyl radicals, which are thought to be produced in one or both of the following ways:



### INTRODUCTION

Considerable progress has been made during the past decade in our knowledge of the mechanisms of the oxidation of hydrocarbons and related compounds. It has been well established that aldehydes are produced early in all hydrocarbon combustion reactions (15). Evidence has been produced which indicates that the decomposition of primary products such as peroxide radicals leads to the production of these aldehydes. It has also been shown that various aldehydes are capable of eliminating the induction periods which are observed in certain slow oxidation reactions (2, 15). Thus evidence has accumulated showing that the main course of the combustion of many hydrocarbons is largely controlled by the way aldehydes react with oxygen. In many cases it is evident that the hydrocarbon acts as a precursor of aldehyde and the combustion is largely that of the aldehyde formed early in the reaction between the hydrocarbon and oxygen (19).

It is, therefore, of considerable importance that the mechanism of the reactions between aldehydes and oxygen be thoroughly understood. There is general agreement as to the main features of the mechanism of the thermal oxidation of acetaldehyde (9, 13), and doubtless a similar mechanism is applicable to the cases of the oxidation of higher aldehydes though there have been rather few detailed studies of these latter reactions.

<sup>1</sup>Manuscript received July 22, 1957.

Contribution from the Department of Inorganic and Physical Chemistry, University of Liverpool, Liverpool 7, England, and the Department of Chemistry, University of British Columbia, Vancouver 8, B.C., Canada.

(9, 17). It is, for example, generally accepted that the thermal oxidation of acetaldehyde is a chain reaction in which the acetyl radical ( $\text{CH}_3\text{CO}$ ) and the peracetic radical ( $\text{CH}_3\text{CO}_3$ ) play important parts. There are, however, certain details of the reactions of these radicals which have not been elucidated.

It was the aim of the work here described to discover the mechanism of the photochemical oxidation of acetaldehyde, for it is obvious that this is a very direct way to investigate the reactions of the acetyl and peracetic radicals. Furthermore, as will be seen later in Part III of this series, it is desirable to know the absolute values of the velocity constants for the propagating and terminating steps in the oxidation chain involving the acetyl and peracetic radicals, and photochemical techniques present a ready means of evaluating these constants.

The photochemical oxidation of acetaldehyde in the gaseous phase was first studied by Bowen and Tietz (6) using a flow method. It was later investigated briefly by Carruthers and Norrish (8). Bowen and Tietz found that the rate of the reaction at about 20° C. was independent of the oxygen concentration and directly proportional to the aldehyde concentration. It was also found that the rate was proportional to the square root of the light intensity. A brief investigation was also carried out later by Mignolet (14) and some preliminary studies were more recently reported briefly by McDowell and Farmer (13). The present study, which covers much of the earlier work of McDowell and Farmer, was preliminary to that reported in Part III, in which is described the determination of the absolute values of the velocity constants for the propagating and terminating steps in the photooxidation of acetaldehyde.

#### EXPERIMENTAL

The acetaldehyde and oxygen were prepared by the methods described previously (13). The same photochemical apparatus was used except that a "Mazda" high pressure mercury arc was used as a light source. This was supplied with power from a d.c. generator, which was driven by an a-c. synchronous motor. Calibrated fine mesh wire gauzes were used to vary the intensity of the illumination. The rate of the reaction was determined by measuring the amount of peracetic acid produced in a known time, the analytical method being that previously described (13). To obtain reproducible results it was necessary to evacuate and bake the reaction vessel at above 200° C. for more than 4 hours between runs. These precautions made it possible to obtain results reproducible to  $\pm 7\%$ , and any thermal or induced thermal reaction was kept to a minimum. For experiments up to  $\frac{1}{2}$  hour in duration the reaction rate was accurately proportional to time.

#### RESULTS

The main product of the photooxidation of acetaldehyde is peracetic acid and the rate of the reaction was determined by measuring the amount of this compound formed in a given time on illuminating the reaction vessel with light of wavelength 3130 Å.

##### *Dependence of Rate of Reaction on Acetaldehyde Concentration*

The dependence of the rate of the reaction,  $d[\text{CH}_3\text{CO}_3\text{H}]/dt$ , on the concentration of acetaldehyde was measured at a fixed light intensity for mixtures containing 5 mm. pressure of oxygen at 20° C.; the results are given in Table I and shown graphically in Fig. 1, where we have plotted the logarithm of the corrected rate against the logarithm of the concentration of acetaldehyde. The straight line shown in Fig. 1 has a slope of 0.98. Thus it is apparent that the rate of formation of peracetic acid in the photooxidation of acetal-

TABLE I  
DEPENDENCE OF RATE OF PHOTOOXIDATION OF ACETALDEHYDE ON CONCENTRATION OF ALDEHYDE

All data refer to corrected absorption of 100% and mixtures containing 5 mm. Hg pressure of oxygen at 20° C.

Acetaldehyde, mm. Hg	Duration of experiment, minutes	Corrected rate, mole l. <sup>-1</sup> sec. <sup>-1</sup> × 10 <sup>8</sup>
50	15	0.51
100	15	1.02
150	15	1.57
200	15	2.03
300	75	4.15

dehyde is directly proportional to the concentration of acetaldehyde over the sixfold variation in the concentration of the aldehyde indicated in Table I.

#### Dependence of the Rate of Reaction on Oxygen Concentration

The data in Table II show clearly that the rate of formation of peracetic acid in this reaction is independent of the concentration of oxygen over a 30-fold variation in concentration from 5 mm. to 150 mm. Hg.

TABLE II  
DEPENDENCE OF THE RATE OF THE PHOTOOXIDATION OF ACETALDEHYDE ON THE CONCENTRATION OF OXYGEN

All data refer to mixtures containing 150 mm. Hg of acetaldehyde and were carried out at a constant light intensity at 20° C.

Oxygen, mm. Hg	Rate, mole l. <sup>-1</sup> sec. <sup>-1</sup> × 10 <sup>9</sup>
5	8.57
25	8.50
50	8.17
100	7.90
150	8.68

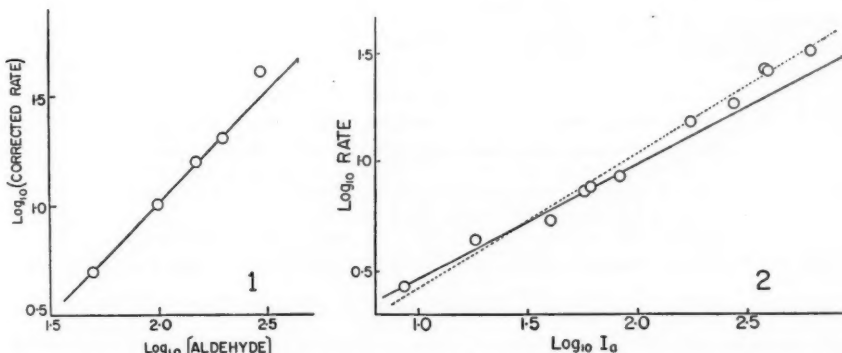


FIG. 1. Dependence of rate of photochemical oxidation of acetaldehyde on concentration of aldehyde.

FIG. 2. Dependence of rate of photochemical oxidation of acetaldehyde on intensity of absorbed radiation.

*Dependence of the Rate of Reaction on the Intensity of Illumination*

In Table III are given the rates of reaction observed for a mixture of 150 mm. Hg of acetaldehyde and 5 mm. Hg of oxygen at 20° C. and for different intensities of the incident radiation. In column three of this table is shown the value of the ratio "rate/square root of intensity absorbed". These data show clearly that the rate of formation of peracetic acid in this photooxidation is proportional to  $I_a^{\frac{1}{2}}$ . This conclusion is also demonstrated by Fig. 2, where the logarithm of the rate of reaction has been plotted against the logarithm of the absorbed intensity. The slope of the dotted line is 0.55 and that of the continuous line 0.51. It is important to note that in the experimental data listed in Table II the light intensity has been varied over a 73-fold range.

TABLE III  
DEPENDENCE OF THE RATE OF THE PHOTOOXIDATION OF ACETALDEHYDE  
ON THE INTENSITY OF THE ILLUMINATION

All data refer to a mixture containing 150 mm. Hg of acetaldehyde and 5 mm. Hg of oxygen at 20° C.

$I_a$ , percentage	Rate, mole l. <sup>-1</sup> sec. <sup>-1</sup> × 10 <sup>9</sup>	Rate/ $I_a^{\frac{1}{2}}$
0.086	2.7	9.2
0.185	4.4	10.2
0.40	5.4	8.6
0.58	7.4	9.7
0.62	7.8	9.9
0.83	8.6	9.5
1.74	15.6	11.8
2.74	18.8	11.4
3.82	27.4	14.0
3.94	27.1	13.7
6.21	33.6	13.5

*Over-all Activation Energy*

It was difficult to obtain an extremely accurate value for the over-all activation energy for this reaction because above 30° C. there intervenes a troublesome thermal reaction. A value for the activation energy was, however, obtained by taking a mean of seven experiments carried out at 20° C. and a mean of a similar number carried out at 30° C. These data are set out in Table IV and there is also given the value for the activation energy  $E$  calculated from the equation  $E = [RT_1T_2/(T_1 - T_2)] \ln(R_1/R_2)$ , where  $R_1$  and  $R_2$  are relative rates of the reaction at temperatures  $T_1$  and  $T_2$ .

TABLE IV  
ACTIVATION ENERGY FOR THE PHOTOOXIDATION OF ACETALDEHYDE  
Data refer to a mixture of 150 mm. Hg of acetaldehyde and 5 mm. Hg of oxygen and a light intensity of 2.05% of the total intensity

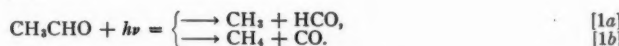
Rate at 293° K.	$30.6 \pm 0.7$	Arbitrary units,
Rate at 303° K.	$45.7 \pm 1.8$	mean of seven experiments
$E$	$7.16 \pm 1.0$	kcal. mole <sup>-1</sup>

**DISCUSSION**

The above experimental results show that the photochemical oxidation of acetaldehyde at 20° C. is governed by the kinetic equation:

$$d[\text{CH}_3\text{CO}_3\text{H}]/dt = K I_a^{\frac{1}{2}}[\text{CH}_3\text{CHO}].$$

There has been considerable discussion as to the nature of the primary process which occurs when acetaldehyde absorbs a quantum of radiation. Steacie (16) gives a detailed discussion of the relevant facts. Suffice it to say that Volman *et al.* (18) have shown that free radicals are produced in the direct photolysis of acetaldehyde at a wavelength of 3130 Å. There has been considerable controversy as to the primary quantum efficiencies of the two processes [1a] and [1b]:



Early work (2, 3, 10) led to the view that at 3130 Å and moderate temperatures reaction [1a] predominated but the quantum yield was low. More recent studies by Calvert, Pitts, and Thompson (7) have shown that at low light intensities of 3130 Å radiation and at temperatures in excess of 250° C. the sum of all the primary efficiencies of free radical formation at 3130 Å is equal to 0.8. This conclusion is based on careful measurements of the quantum efficiencies for the formation of hydrogen at different temperatures. In this connection it is interesting to note that Lossing (12) has shown recently that in the mercury ( $\text{Hg } ^3P_1$ ) photosensitized decomposition of acetaldehyde at 55° C. the primary step is at least 95% to form methyl and formyl radicals.

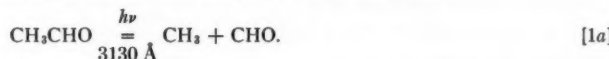
The work of Leermakers (11) on the low temperature photolysis of acetaldehyde gave a quantum yield of 0.2 to 0.3. This could represent either a molecular rearrangement or a free radical non-chain reaction. Blacet and Volman's (4) results, however, indicate that at 3130 Å the primary process is entirely a free radical one.

In the case of acetaldehyde mixed with oxygen there is no reason a priori for assuming that entirely the same process or processes will occur as those which take place when pure acetaldehyde absorbs a quantum of radiation of wavelength 3130 Å. In view of the difficulties in understanding the results obtained by the photolysis of acetaldehyde in the presence of iodine (2, 3, 10), it would be unwise to assume that the presence of oxygen in the acetaldehyde would not give rise to some difficulties of interpretation.

It is to be expected that on the absorption of radiation of wavelength 3130 Å, acetaldehyde will be excited to several different states. One or more of these may dissociate to yield free radicals as in reaction [1a]. Energy transfer processes will probably occur from the other states; fluorescence may also occur; and by collisions with other acetaldehyde molecules some of those in excited states will be quenched. In the presence of oxygen some of these excited states may also be preferentially quenched.

The work reported in this paper does demonstrate, however, that a photolytic oxidation of acetaldehyde at a wavelength of 3130 Å does occur at 20° C. We shall, therefore, assume that this photochemical oxidation is initiated by one, or both, of the following processes:

(a) By the absorption of a quantum of radiation of wavelength 3130 Å the acetaldehyde, even in the presence of oxygen, undergoes the primary process [1a],



The two radicals produced can then react with oxygen as indicated in equation [1d],



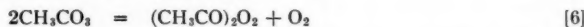
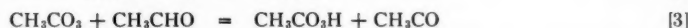
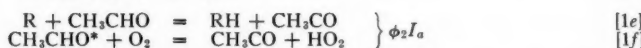
It is assumed that the radical R can then abstract a hydrogen atom from acetaldehyde to form an acetyl radical which is regarded as being the chain initiator in the thermal oxidation of acetaldehyde (13).

(b) The absorption of a quantum of radiation of wavelength 3130 Å can lead to excited states of acetaldehyde which may not dissociate to form radicals by reaction [1a]. Nevertheless, though it is possible that in the presence of oxygen some or all of these excited states may be quenched, it is at least likely that the excited acetaldehyde molecules may react with oxygen to yield free radicals which can start the oxidation chain. There is no reason why, for example, one or more of these excited states of acetaldehyde, here denoted in [1c] simply by  $\text{CH}_3\text{CHO}^*$ , may not react with oxygen by a process [1f] analogous to that thought (13) to be the mode of initiation of the thermal oxidation between ground state acetaldehyde molecules and oxygen:



Reaction [1f] would, of course, be expected to occur at a much lower temperature than that at which the corresponding reaction between ground state acetaldehyde molecules and oxygen has a reasonable rate.

Whatever the means whereby acetyl radicals are produced following the initial absorption of radiation at 3130 Å by the acetaldehyde this radical is regarded as being the initiator of the oxidation chain and we may then write the following mechanism for the photooxidation of acetaldehyde at 3130 Å and at low temperatures ( $20\text{--}40^\circ \text{C}$ ):



Since it has been shown that the rate of the photochemical oxidation is proportional to  $I_a^{\frac{1}{2}}$ , and independent of the oxygen pressure, it is probable that reaction [2] is rather fast and it is also likely that at the oxygen pressures used reactions [4] and [5] are negligible compared with reaction [6].

The application of the stationary state hypothesis to the above reaction mechanism leads to the equation

$$\frac{d[\text{CH}_3\text{CO}_3\text{H}]}{dt} = \frac{k_3(\phi_2 I_a)^{\frac{1}{2}} [\text{CH}_3\text{CHO}]}{(k_4\beta^2 + k_5\beta + k_6)^{\frac{1}{2}}},$$

where  $\beta = k_3[\text{CH}_3\text{CHO}]/k_2[\text{O}_2]$ . When  $\beta \ll 1$ , as is likely to be the case in our experiments (see above), this equation reduces to

$$d[\text{CH}_3\text{CO}_3\text{H}]/dt = (k_3/k_6^{\frac{1}{2}})(\phi_2 I_a^{\frac{1}{2}})[\text{CH}_3\text{CHO}]. \quad [A]$$

This equation is in agreement with the experimental results reported above and it, therefore, follows that the proposed mechanism is a satisfactory one. It is, of course, similar to that shown to govern the rates of oxidation of olefins and other organic compounds in solution (5) and for aldehyde oxidations in the gas phase (9, 13).

Equation [A] and our results are in accord with the view that the main terminating step in the oxidation is the interaction of two peracetic radicals ( $\text{CH}_3\text{CO}_2\cdot$ ). Thus it follows from [A] that the over-all activation energy for the photo-oxidation is  $E = E_2 - \frac{1}{2}E_0$ . It is in general thought that reaction [6] requires little or no activation energy. If this is so, then the value which we have obtained for the activation energy, namely,  $7.16 \pm 1.0$  kilocalories mole<sup>-1</sup> refers to  $E_2$ . It is interesting to compare this with the value of  $7.5 \pm 0.3$  kilocalories mole<sup>-1</sup> (19) for the activation energy of the corresponding reaction for the methyl radicals, namely:



#### ACKNOWLEDGMENT

Most of the experimental work described in this paper was carried out in the Department of Inorganic and Physical Chemistry, University of Liverpool, and we wish to thank Professor C. E. H. Bawn, C.B.E., F.R.S., for laboratory facilities and for his interest in the work.

#### REFERENCES

1. BARDWELL, J. and HINSHELWOOD, Sir Cyril N. Proc. Roy. Soc. A, **205**, 375 (1951).
2. BLACET, F. E. and HELDMAN, J. D. J. Am. Chem. Soc. **64**, 889 (1942).
3. BLACET, F. E. and HOEFFER, D. E. J. Am. Chem. Soc. **64**, 893 (1942).
4. BLACET, F. E. and VOLMAN, D. A. J. Am. Chem. Soc. **60**, 1243 (1938).
5. BOLLAND, J. L. Quart. Revs. (London), **3**, 1 (1949).
6. BOWEN, E. G. and TIETZ, E. L. J. Chem. Soc. **234** (1930).
7. CALVERT, J. G., PITTS, J. N., and THOMPSON, D. D. J. Am. Chem. Soc. **78**, 4239 (1956).
8. CARRUTHERS, J. L. and NORRISH, R. G. W. J. Chem. Soc. **1036** (1936).
9. COMBE, A., NICLAUSE, M., and LETORT, M. Rev. inst. frang. pétrole, **10**, 786, 929 (1955).
10. GORIN, E. Acta Physiochim. U.R.S.S. **9**, 681 (1938); J. Chem. Phys. **7**, 256 (1939).
11. LEERMAKERS, J. A. J. Am. Chem. Soc. **56**, 1537 (1934).
12. LOSSING, F. P. Can. J. Chem. **35**, 305 (1957).
13. McDOWELL, C. A. and FARMER, J. B. Fifth Symposium (International) on Combustion. Reinhold Publishing Corp., New York, 1955, p. 453.
14. MIGNOLET, J. Bull. soc. roy. sci. Liège, **10**, 343 (1941).
15. NORRISH, R. G. W. Discussions Faraday Soc. **10**, 269 (1951).
16. STEACIE, E. W. R. Atomic and free radical reactions. 2nd ed. Reinhold Publishing Corp., New York, 1954.
17. STEACIE, E. W. R., HATCHER, W. H., and ROSENBERG, J. J. Phys. Chem. **38**, 1190 (1934).
18. VOLMAN, D. H., LEIGHTON, P. A., BLACET, F. E., and BRINTON, R. K. J. Chem. Phys. **18**, 203 (1950).
19. VOLMAN, D. H. and BRINTON, R. J. Chem. Phys. **20**, 1053 (1952).

## THE PHOTOCHEMICAL OXIDATION OF ALDEHYDES IN THE GASEOUS PHASE

### PART II. THE KINETICS OF THE PHOTOCHEMICAL OXIDATION OF PROPIONALDEHYDE<sup>1</sup>

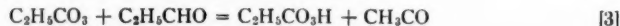
C. A. McDOWELL AND L. K. SHARPLES

#### ABSTRACT

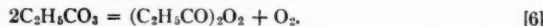
The photochemical oxidation of propionaldehyde has been studied in the gaseous phase at 23° C. and a wavelength of 3130 Å. With pressures of oxygen varying from 0.3 mm. to 100 mm. Hg it has been established that the reaction obeys the same kinetic law as that found for the corresponding reaction with acetaldehyde, namely:

$$d[C_2H_5CO_3H]/dt = (k_3/k_6)^{\frac{1}{2}} (\phi_2 I_a)^{\frac{1}{2}} [C_2H_5CHO],$$

where  $k_3$  is the velocity constant for the propagating reaction [3]:



and  $k_6$  is the velocity constant for the terminating reaction [6]:



$\phi_2 I_a$  is the rate of initiation and it is regarded as being a composite quantity representing the rate of formation of propionyl radicals, which are thought to be the initiators of the oxidation chain. The propionyl radicals are thought to be formed by two processes: (a) from the subsequent reactions of free radicals produced in the primary free radical process which occurs when propionaldehyde absorbs a quantum of radiation at 3130 Å, and (b) from the subsequent reactions, with oxygen, of excited states of propionaldehyde, which are also thought to be formed by the absorption of light of wavelength 3130 Å.

#### INTRODUCTION

Following the study of the photooxidation of acetaldehyde (Part I) reported in the preceding paper, it seemed desirable to study other higher aldehydes. It is important to know if the derived mechanism was of general application. It was also necessary to establish this mechanism for several aldehydes, for one of our main aims was to determine the absolute values for the propagating and terminating steps in the oxidation chain. A knowledge of the velocity constant for these oxygen-containing radicals is most important if the general features of the rates of combustion processes of hydrocarbons and other organic compounds are to be understood. Such results would also add to our available information of the factors influencing the interactions of large radicals in the gaseous phase.

Few studies have been made of the kinetics of the oxidation of aldehydes higher than acetaldehyde. Steacie *et al.* (8) investigated the gas phase thermal oxidation of propionaldehyde and showed that its kinetics were similar to those found for acetaldehyde. More recently a similar investigation (4) has largely substantiated the earlier work. Both of these studies were carried out at temperatures between 100° and 200° C. and the rates were determined by measuring pressure-time curves. It was found that the main product was perpropionic acid. Blacet and Volman (2) reported a study of the photooxidation of crotonaldehyde, but their results were not detailed enough to yield much information about the mechanism and kinetics of the reaction.

#### EXPERIMENTAL

Eastman-Kodak white label propionaldehyde was dried three times over anhydrous  $CaSO_4$  and distilled, at a reflux ratio of 20: 1, through an efficient column in an atmosphere

<sup>1</sup>Manuscript received July 22, 1957.

Contribution from the Department of Chemistry, University of British Columbia, Vancouver 8, B.C., Canada.

of cylinder "purified" grade nitrogen. A fraction boiling at 47.9° C., comprising half of the sample, was collected. This sample was redistilled and finally bulb-to-bulb distilled 10 times on the vacuum line, each time a middle fraction being taken.

Oxygen was prepared by heating A.R. grade potassium permanganate. A trap plugged with glass wool and immersed in liquid oxygen was interposed between the oxygen reservoir and the potassium permanganate.

A sample of ethanol from a freshly opened can of "absolute" was dried over anhydrous magnesium sulphate and bulb-to-bulb distilled on the vacuum line. A sample of A.R. isopropyl alcohol was similarly purified.

A sample of A.R. acetone was dried over anhydrous potassium carbonate, refluxed with potassium permanganate, and bulb-to-bulb distilled on the vacuum line.

The apparatus was a conventional high vacuum system utilizing stopcocks lubricated with Apiezon L grease. A cylindrical quartz reaction vessel (volume 76 ml., 4 ml. of which was dead space) having optically flat ends was housed in a block aluminum furnace, the temperature of which could be readily adjusted and accurately maintained. The gases were metered into the vessel using either a calibrated, sensitive spiral gauge, or, for lower pressures, the same gauge in conjunction with a calibrated expansion volume. The reaction products were trapped in a series of cold traps, which could be plugged with glass wool, the last of which was removable to facilitate analysis of the normally liquid reaction products. A copper oxide furnace was incorporated to analyze for CO and H<sub>2</sub>, and means was incorporated for measuring small quantities of gas, and for collecting small samples of gaseous products for analysis by mass spectrometry.

A water-cooled, General Electric AH6 mercury arc, housed in a small, water-cooled box with a 3 mm. diameter hole in one side, gave a "point" source of illumination. The input voltage to the 1000 volt transformer for the arc was stabilized at 100 volts by a Sorensen a-c. voltage regulator. The arc had a short-term stability within 5%. Liquid filters were used to isolate a fairly narrow wavelength band in the 3200 Å region. Neutral density filters made by evaporating aluminum on quartz plates were used to vary the intensity incident upon the reaction vessel. Quartz lenses were arranged so that light from the "point" source was collimated through a 5 mm. diameter hole and then into a 50 mm. diameter, very nearly parallel, beam which uniformly filled the reaction vessel. The intensity of the radiation was monitored by an electronic photometer unit utilizing a QVA39 quartz photocell as a light detector. The linearity of the response of this unit was checked occasionally and found to be good.

Perpropionic acid was estimated by the ferrous thiocyanate method, a Bausch and Lomb "Spectronic 20" absorptiometer being used to assess the intensity of the color developed by the various concentrations of peroxide. The absorptiometer was calibrated using a solution of perpropionic acid, the actual strength of which was determined iodometrically by the method of Sully (9).

The light intensity was estimated by measuring the amount of CO formed when gaseous acetone was illuminated under identical conditions to those prevailing during runs, at temperatures from 100° to 120° C. for a given length of time. The quantum yield of CO formation was found to be very nearly constant over the region 100–120° C. In calculating the intensity of our source, the quantum yield of CO from acetone was taken as being 1 (7). The estimated intensity may be in error owing to the fact that an unknown, but presumably appreciable, fraction of the light used was in the 3130–3300 Å region of the spectrum (owing to lack of sharpness of the filters and the continuous background delivered by the arc) and the precise CO quantum yield in this region is not known.

## RESULTS

Initial runs showed that the main product of the reaction was perpropionic acid, with a quantum yield proportional to the square root of the absorbed intensity,  $I_a^{\frac{1}{2}}$ , and of the order of 50 for a medium intensity. The oxygen uptake was found to be equal to the perpropionic acid formation within experimental error. A complete analysis of the products was not carried out, but  $\text{CO}_2$  and CO were formed in approximately equal amounts with a quantum yield of the order of 1. A very small quantity of ethane was formed, but the quantum yield was not estimated.

The reaction rate was estimated by measuring the amount of peracid formed in a given time. In all runs, except those for the determination of  $\text{CO}_2$  and CO formation and  $\text{O}_2$  uptake, the reaction was confined to <0.5% conversion of aldehyde.

There was found to be no measurable thermal reaction at all in a range from 20° to 40° C. and the absence of this was frequently checked. However, after about 70 runs, quite suddenly an appreciable thermal reaction became apparent and built up to a rate which was about 2% of the photochemical rate. This was only appreciable because the reactants were allowed to mix for 1 hour prior to photolysis. When the cell was removed, cleaned, and replaced, no thermal reaction took place.

No cell aging effect was noticed and runs were generally reproducible within  $\pm 7\%$ . A colorless, transparent polymeric substance of unknown composition was gradually deposited upon the cell walls. On being heated to 300° C. the polymer did not simply decompose and evaporate, but charred. When propionaldehyde is photolyzed, a certain amount of polymerization does take place (6); hence the polymer on the wall may be polypropionaldehyde with physically absorbed reaction products, or a polyoxypolymer formed by reaction of polypropionaldehyde with perpropionyl radicals.

*Dependence of Rate of Reaction on Time*

The rate of reaction remained constant up to a conversion of 0.7% of the aldehyde during a 10 minute run, indicating that there was no induction period or photochemical growth effect and no autocatalysis. See Fig. 1.

Later on in this study the apparent rate for certain runs of <0.5% conversion, but of longer duration than usual, was lower than had been anticipated. This was due to the slow decomposition or removal of perpropionic acid, and the rate of this reaction was therefore investigated.

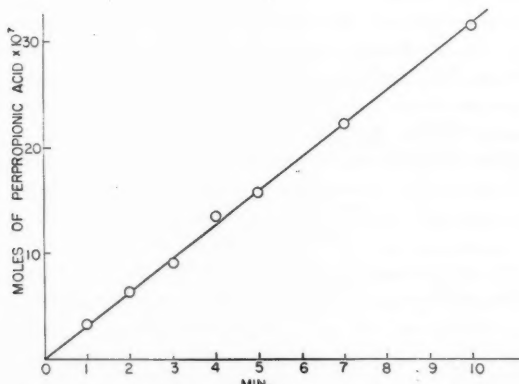


FIG. 1. Dependence of rate of photochemical oxidation of propionaldehyde on time.

### *Effect of Decomposition of Perpropionic Acid on Rate*

The rate of peracid decomposition was not very reproducible, but it was found to be proportional to the concentration of the peracid within experimental error and roughly proportional to the reciprocal of the aldehyde pressure. It was initially thought that removal of peracid may have been due to the reaction



either homogeneously or at the wall, but this was obviated by the  $1/[\text{aldehyde}]$  dependence of the rate. The rate is too slow for diffusion to be the rate-controlling step. A possible explanation is that the peracid is removed by physical absorption at the wall and the aldehyde deactivates absorption sites.

In a system where peracid is formed at a constant rate and is removed at a rate proportional to [peracid], then if  $P$  is the amount of peracid measured after  $t$  seconds, and  $P_1$  is the amount of peracid that would have been formed in  $t$  seconds if the peracid was not being removed at all, then  $P/P_1 = 1 - e^{-k_p t}/k_p t$  where  $k_p$  is the rate constant of the removal step; hence the ratio of the measured rate of formation of peracid to the real rate of formation is a function of time only for a given  $k_p$ . The values of  $k_p$  were calculated for 100 mm. Hg and 35 mm. Hg of aldehyde, and the ratios  $P/P_1$  were calculated for various times. The results are shown in Table I. The results are probably correct within  $\pm 20\%$ .

TABLE I  
EFFECT OF TIME ON RATIO OF OBSERVED RATE  
TO ACTUAL RATE

Time, min.	$k_p$ , sec. $^{-1}$	$P/P_1$
1	0.0011	1.00
10	0.0011	0.97
30	0.0011	0.91
60	0.0011	0.80
1	0.0023	0.99
10	0.0023	0.92
30	0.0023	0.79
60	0.0023	0.68

It is seen that the error, due to removal of peracid, in the measured rate for a 10 minute run with 100 mm. aldehyde, is about 2%; hence the only runs in this study which require correction in this respect are runs 53, 54, and 60.

### *Dependence of Rate of Reaction on Intensity of Absorbed Radiation*

The dependence of the rate of oxidation on the light intensity was studied over a 10,000-fold range of absorbed intensity for a mixture of 100 mm. Hg of propionaldehyde and 3 mm. of  $\text{O}_2$ . It was found that over a range of  $I_a$  from  $10^{-10}$  to  $2.5 \times 10^{-8}$  einstein  $\text{l.}^{-1} \text{sec.}^{-1}$  the rate was accurately proportional to  $I_a^{\frac{1}{2}}$ , but at  $I_a < 10^{-10}$  einstein  $\text{l.}^{-1} \text{sec.}^{-1}$  this  $I_a^{\frac{1}{2}}$  dependence falls off. The results are shown in Fig. 2 and Table II.

### *Dependence of Rate of Reaction on Pressure of Propionaldehyde*

The dependence of the rate on the aldehyde pressure was studied by maintaining the oxygen pressure at 3 mm. Hg and varying the aldehyde pressure from 10 to 200 mm. Hg. As the aldehyde pressure was varied, the absorbed intensity also varied, so all these runs were carried out in the intensity region where rate is accurately proportional to  $I_a^{\frac{1}{2}}$ , and the tabulated results are corrected to 100% absorption of a given constant intensity (Table III). The plot of rate against aldehyde pressure was a straight line passing through

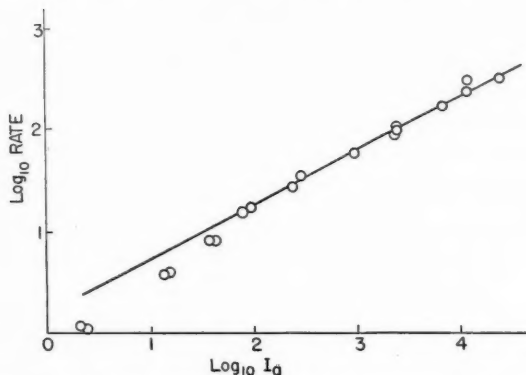


FIG. 2. Dependence of rate of photochemical oxidation of propionaldehyde on intensity of absorbed radiation.

TABLE II  
DEPENDENCE OF RATE ON ABSORBED INTENSITY  
These experiments were all carried out with a mixture of 100 mm. Hg  
of propionaldehyde, 3 mm. Hg oxygen, and at 23° C.

Run No.	$I_a$ ein. l. <sup>-1</sup> sec. <sup>-1</sup> $\times 10^{+12}$	Rate, mole l. <sup>-1</sup> sec. <sup>-1</sup> $\times 10^{+9}$
32	$2.39 \times 10^3$	$8.32 \times 10$
33	$2.42 \times 10^4$	$2.50 \times 10^3$
34	$9.34 \times 10^2$	$4.48 \times 10$
35	$2.32 \times 10^3$	$2.14 \times 10$
36	$4.20 \times 10$	6.40
37	$1.35 \times 10$	3.07
38	$1.18 \times 10^4$	$2.40 \times 10^2$
39	$2.37 \times 10^3$	$7.68 \times 10$
40	$6.76 \times 10^3$	$1.31 \times 10^2$
41	$2.35 \times 10^3$	$7.04 \times 10$
42	$2.82 \times 10^2$	$2.78 \times 10$
43	$8.01 \times 10$	$1.25 \times 10$
44	2.06	0.93
45	$1.53 \times 10$	3.20
46	2.32	0.82
47	$9.25 \times 10$	$1.34 \times 10$
48	$3.73 \times 10$	6.60
49	$1.18 \times 10^4$	$1.86 \times 10^2$
50	$2.29 \times 10^3$	$8.00 \times 10$

the origin, Fig. 3, but the apparent rates for low aldehyde pressure runs fall well below the straight line. This is probably due to the peracid removal step mentioned earlier, and if a correction is applied, these points fit more closely to the line.

#### Dependence of the Rate of Reaction on Pressure of Oxygen

The rate of oxidation was found to be independent of oxygen pressure over a range of 0.3–100 mm. Hg, in a system in which the aldehyde pressure and  $I_a$  were maintained constant. The results are shown in Table IV.

#### Over-all Activation Energy

In Table V are given the values of the over-all rate of the reaction at observed different temperatures for a mixture containing 3 mm. of oxygen and  $5.87 \times 10^{-3}$  mole l.<sup>-1</sup> of

TABLE III

## DEPENDENCE OF RATE ON PRESSURE OF PROPIONALDEHYDE

These experiments were carried out at 23° C. with a mixture of 3.0 mm. Hg of oxygen, and the rates were corrected to an  $I_a$  of  $2.14 \times 10^{-9}$  einstein l.<sup>-1</sup> sec.<sup>-1</sup>

Run No.	Aldehyde pressure, mm. Hg	Rate, mole l. <sup>-1</sup> sec. <sup>-1</sup> $\times 10^{18}$
51	33	3.68
52	70	8.0
53	22.5	2.24*
54	16.2	1.84*
55	100	13.2
56	200	26.7
57	41.5	5.6
58	100	13.3
59	150	20.3
60	10	1.11*

\*These experiments corrected for decomposition of perpropionic acid as they exceeded 12 minutes in duration.

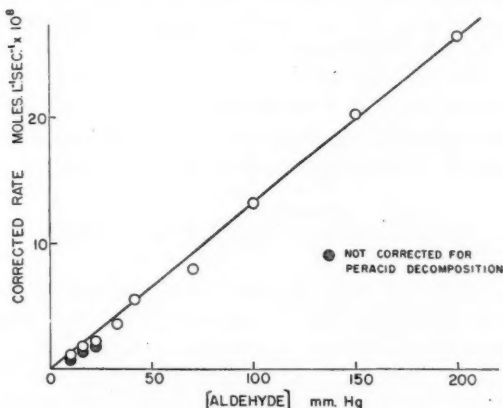


FIG. 3. Dependence of rate of photochemical oxidation of propionaldehyde on pressure of aldehyde.

TABLE IV

## DEPENDENCE OF RATE ON OXYGEN PRESSURE

All experiments carried out on a mixture of 100 mm. Hg of aldehyde at 22° C., and at an  $I_a$  of  $2.14 \times 10^{-9}$  einstein l.<sup>-1</sup> sec.<sup>-1</sup>

Run No.	Oxygen, mm. Hg	Rate, mole l. <sup>-1</sup> sec. <sup>-1</sup> $\times 10^8$
25	10	9.6
26	40	10.4
27	2	12.0
28	0.36	10.9
29	100	9.3
30	5	9.6
31	10	8.5

TABLE V

## DEPENDENCE OF RATE ON TEMPERATURE

All experiments carried out with a mixture of 3 mm. Hg of oxygen,  $5.87 \times 10^{-3}$  mole l.<sup>-1</sup> of propionaldehyde, and at an  $I_a$  of  $1.11 \times 10^{-9}$  einstein l.<sup>-1</sup> sec.<sup>-1</sup>

Run No.	Temp., °C	Rate, mole l. <sup>-1</sup> sec. <sup>-1</sup> $\times 10^8$
129	19.5	5.28
130	22.6	6.08
131	27.0	8.00
132	37.5	10.6
133	21.3	6.56
134	20.0	5.92
135	39.0	11.7
136	46.5	15.0
137	34.0	9.60
138	19.5	5.75

propionaldehyde. These experiments were performed using a value of  $I_a$  of  $1.11 \times 10^{-9}$  einstein l.<sup>-1</sup> sec.<sup>-1</sup>.

These data have been plotted in Fig. 4. From these data we have calculated by the method of least squares that the activation energy for the photooxidation of propionaldehyde is 6.75 ( $\pm 0.5$ ) kilocalories mole<sup>-1</sup>.

## DISCUSSION

The above experimental results indicate that the gas-phase photooxidation of propionaldehyde at about 23° C. is a chain process and the initial stage is governed by the kinetic equation

$$d[C_2H_5CO_3H]/dt = kI_a^{1/2}[C_2H_5CHO]^n[O_2]^0.$$

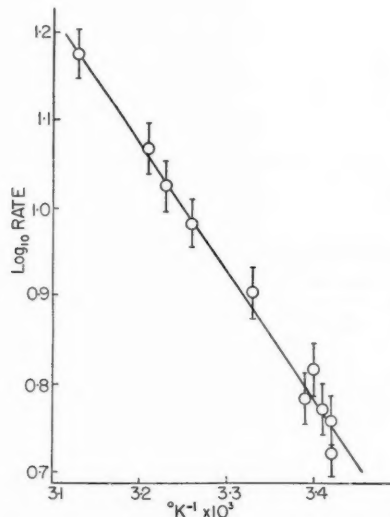
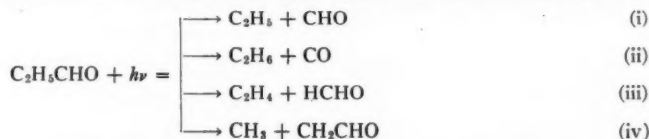


Fig. 4. Activation energy curve for the photochemical oxidation of propionaldehyde.

At low intensities this expression ceases to apply because the  $I_a^{\frac{1}{2}}$  dependence falls off. Also in later stages of the oxidation, removal of the peracid becomes a significant part of the process. The  $I_a^{\frac{1}{2}}$  dependence is undoubtedly due to a radical initiation process which is proportional to  $I_a$  and a chain termination process which is bimolecular. Deviation from  $I_a^{\frac{1}{2}}$  dependence at low intensities indicates that the termination process is no longer solely bimolecular, but that a first-order termination starts to become important. Such a first order termination could be at the wall; which is inherently feasible, because the concentration of radicals at low  $I_a$  is small, and hence the bimolecular termination would be similarly small, thus giving radicals more chance to reach the wall.

The too low rates observed for runs at low aldehyde concentration may be due entirely to the removal of peracid at the wall, but even when a correction is applied, these rates are still somewhat low. There are two possible explanations which could account for this. At low concentrations of aldehyde and consequent low absorbed intensities, the rate of initiation of chain propagating radicals may have an aldehyde pressure dependence if there is a possible fate of the radical R other than reacting with aldehyde to yield  $C_2H_5CO$ . The radical R could react at the wall, and if it did, the wall reaction would be favored by low aldehyde pressure and low intensity, and hence under these conditions the rate would be reduced. The other possible explanation is that at low aldehyde pressure and low intensity, first-order termination of propagating radicals at the wall may become appreciable, thus reducing the observed rate.

The photolysis of propionaldehyde at a wavelength of 3130 Å has been studied by several workers (3, 5, 6). A recent detailed investigation has been made by Blacet and Pitts (1). These authors conclude that there are four separate primary processes involved:

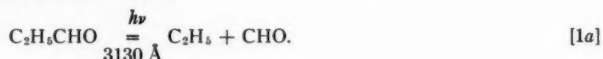


From this work it is apparent that the ratio of the primary process (ii) to primary process (i) at 3130 Å is 0.046. This result and most of the conclusions of Blacet and Pitts are based on experiments performed on mixtures of propionaldehyde and iodine. There have been some doubts expressed (see preceding paper, Part I) about the validity of some of the deductions regarding free radical mechanisms based on the use of iodine "to fix" the radical. It is to be expected that at 3130 Å propionaldehyde will form several excited states, and only some of these may dissociate to form free radicals. Further, the presence of iodine will undoubtedly quench some of these excited states of propionaldehyde by energy transfer processes (see Part I).

Our view is that it is best to regard the photolysis of propionaldehyde-oxygen mixtures as following the same processes as suggested in Part I for the case of acetaldehyde-oxygen mixtures. Namely, that the primary process (i) will undoubtedly occur, but that excited states of propionaldehyde will be formed. Some of these will undoubtedly be quenched by the oxygen, but some may react with oxygen molecules to form free radicals which should be capable of initiating the propionaldehyde oxidation chain. Thus we think that the photochemical oxidation of propionaldehyde, since it evidently obeys the same kinetic law as that of acetaldehyde as shown by our experiments, should also follow the same mechanism.

It is, therefore, assumed that the photochemical oxidation of propionaldehyde is initiated by one, or both, of the following processes:

(1) By the absorption of a quantum of radiation of wavelength 3130 Å, the primary process (i) occurs even in the presence of oxygen,

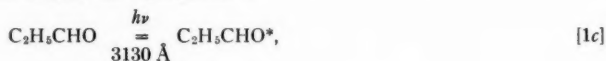


These two radicals can then react with oxygen as follows:

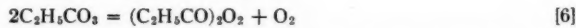
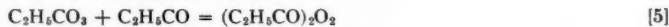


The radical R can then abstract a hydrogen atom from propionaldehyde to form a propionyl radical,  $\text{C}_2\text{H}_5\text{CO}$ , which is regarded as being the initiation of the oxidation chain (4).

(2) Besides primary process (i) occurring, it is possible that excited states are also formed when propionaldehyde absorbs radiation of wavelength 3130 Å (equation [1c]). One or more of these excited states may react with oxygen molecules to form propionyl radicals as indicated in equation [1f] where in both [1c] and [1f] the excited states of propionaldehyde are denoted simply as  $\text{C}_2\text{H}_5\text{CHO}^*$ :



The succeeding steps in the mechanism of the photooxidation of propionaldehyde at low temperatures are regarded as being analogous to those shown (Part I) to lead, on the application of the stationary state hypothesis, to a satisfactory explanation of the kinetics of the photochemical oxidation of acetaldehyde:<sup>†</sup>



The application of the stationary state treatment to the above mechanism leads to the equation [A], when it is assumed (see Part I) that  $k_3[\text{C}_2\text{H}_5\text{CHO}]/k_2[\text{O}_2] \ll 1$ , which is likely to be the case in our experiments,

$$d[\text{C}_2\text{H}_5\text{CO}_3\text{H}]/dt = (k_3/k_6^{\frac{1}{2}})(\phi_2 I_a)^{\frac{1}{2}}[\text{C}_2\text{H}_5\text{CHO}]. \quad [A]$$

Equation [A] agrees with the experimentally determined kinetic equation for the photochemical oxidation of propionaldehyde.

It follows from the above results and equation [A] that the over-all activation energy  $E = E_3 - \frac{1}{2}E_6$ .  $E_6$ , which is the activation energy for the mutual interaction of perpropionic radicals, is likely to be zero. Thus the value which we obtained for the over-all activation energy, namely 6.75 ( $\pm 0.5$ ) kilocalories mole.<sup>-1</sup>, must equal  $E_3$ . There are no reliable values for the reaction analogous to [3] but involving the ethyl radical. Comparison of the value of  $E_3$  for the abstraction of a hydrogen atom from propionaldehyde by

<sup>†</sup>From the data given in the following paper (Part III) we calculate  $\phi = 1.6$ . Blacet and Pitts (1) found  $\phi_{\text{C}_2\text{H}_5\text{I}}$  and  $\phi_{\text{HI}}$  in their experiments on propionaldehyde-iodine mixtures to be  $\approx 0.45$ . Since we regard both the  $\text{C}_2\text{H}_5$  and  $\text{HCO}$  radicals as being capable of reacting with oxygen to form a radical which can abstract a hydrogen atom from propionaldehyde to form a propionyl radical it follows that the portion of the quantum yield  $\phi_2$  which arises from the reaction of excited states of propionaldehyde [1f] is approximately  $1.6 - 0.9 = 0.7$ .

the perpropionic radical with those found for the corresponding metathetical reactions with methyl ( $7.5 \pm 0.3$  kilocalories mole $^{-1}$ ) and peracetic ( $7.16 \pm 1.0$  kilocalories mole $^{-1}$ ) radical shows that it is a realistic value.

#### ACKNOWLEDGMENT

We are indebted to the National Research Council of Canada for a grant in aid of this work.

#### REFERENCES

1. BLACET, F. E. and PITTS, J. N. *J. Am. Chem. Soc.* **74**, 3382 (1952).
2. BLACET, F. E. and VOLMAN, D. H. *J. Am. Chem. Soc.* **61**, 582 (1939).
3. BLAEDEL, W. J. and BLACET, F. E. *J. Am. Chem. Soc.* **74**, 3382 (1952).
4. COMBE, A., NICLAUSE, M., and LETORT, M. *Rev. inst. franc. pétrole*, **10**, 786, 929 (1955).
5. GARRISON, W. M. and BURTON, M. *J. Chem. Phys.* **10**, 730 (1942).
6. LEIGHTON, P. A. and BLACET, F. E. *J. Am. Chem. Soc.* **54**, 3165 (1932).
7. NOYES, W. A., Jr. and HERR, D. S. *J. Am. Chem. Soc.* **62**, 2052 (1940).
8. STEACIE, E. W. R., HATCHER, W. H., and ROSENBERG, J. *J. Phys. Chem.* **38**, 1190 (1934).
9. SULLY, B. D. *Analyst*, **79**, 86 (1954).

## THE PHOTOCHEMICAL OXIDATION OF ALDEHYDES IN THE GASEOUS PHASE

### PART III. THE ABSOLUTE VALUES OF THE VELOCITY CONSTANTS FOR THE PROPAGATING AND TERMINATING STEPS IN THE PHOTOCHEMICAL OXIDATION OF ACETALDEHYDE AND PROPIONALDEHYDE<sup>1</sup>

C. A. McDOWELL AND L. K. SHARPLES

#### ABSTRACT

It has been established (Parts I and II) that the photochemical oxidation of acetaldehyde and propionaldehyde obeys the kinetic expression

$$d[RCO_3H]/dt = (k_3/k_6)^{1/2}(\phi_2 I_a)^{1/2}[RCHO],$$

where RCHO represents the aldehyde and RCO<sub>3</sub>H the corresponding peracid.  $k_3$  is the velocity constant for the propagating reaction, and  $k_6$  that for the terminating reaction involving the mutual interaction of two RCO<sub>3</sub> radicals.  $\phi_2 I_a$  represents the rate of initiation of the photooxidation.

Alcohols have been found to retard the photooxidation and it has been shown that the retarded reaction obeys the kinetic expression:

$$d[RCO_3H]/dt = R_i \{1 + k_3[RCHO]/k_7[ROH]\}.$$

It has thus been possible to determine the rates of initiation  $R_i = \phi_2 I_a$  for each of the photooxidations. Application of the rotating sector technique has enabled the lifetime of the oxidation chains to be measured. These data together with the information given in Parts I and II have been used to calculate the absolute values for the velocity constants for the propagating and terminating reactions,  $k_3$  and  $k_6$ :



in the gas-phase photooxidations of acetaldehyde and propionaldehyde.

The values of the respective velocity constants are: acetaldehyde at 20°,  $k_3 = 8.05(\pm 2.04) \times 10^8 \text{ l. mole}^{-1} \text{ sec.}^{-1}$ ,  $k_6 = 8.93(\pm 4.20) \times 10^{10} \text{ l. mole}^{-1} \text{ sec.}^{-1}$ ; propionaldehyde at 22°,  $k_3 = 4.35(\pm 0.9) \times 10^8 \text{ l. mole}^{-1} \text{ sec.}^{-1}$ ,  $k_6 = 2.69(\pm 1.35) \times 10^{10} \text{ l. mole}^{-1} \text{ sec.}^{-1}$ . These values for the velocity constants for the "recombination" reactions of the peracetic and perpropionic radicals indicate that for these radicals reaction [6] is very efficient.

#### INTRODUCTION

The study of the combustion of hydrocarbons and related compounds has now reached a point where the main features of the over-all kinetics are apparent. It remains, however, to discover the details of the mechanisms of many of the radical reactions which control the over-all processes. It is also desirable to determine the absolute values for the velocity constants for the various radical reactions known to proceed during combustion processes.

The determination of the absolute values of the velocity constants for many radical reactions in oxidation processes has been retarded because of the need to develop sufficiently accurate experimental methods. This has been especially the case for gaseous-phase reactions. In the case of the liquid-phase oxidation of aldehydes (5), olefins (2), and some other compounds (11), it has been possible to apply photochemical techniques to determine the absolute values for the velocity constants for the propagating and terminating steps in the oxidation chains.

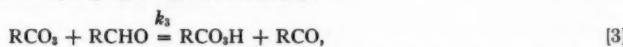
<sup>1</sup>Manuscript received July 22, 1957.

Contribution from the Department of Inorganic and Physical Chemistry, University of Liverpool, Liverpool 7, England, and the Department of Chemistry, University of British Columbia, Vancouver 8, B.C., Canada.

In the preceding papers, Parts I and II, we have elucidated the mechanisms of the photochemical oxidations of acetaldehyde and propionaldehyde. Both of these oxidation reactions have been shown to obey the kinetic expression:

$$d[RCO_3H]/dt = (k_3/k_6^{\frac{1}{2}})(\phi_2 I_a)^{\frac{1}{2}}[RCHO], \quad [A]$$

in which  $RCO_3H$  represents the peracid which is the main product of the oxidation,  $k_3$  is the velocity constant for the propagating reaction [3]:



$k_6$  is the velocity constant for the interaction of two  $RCO_3$  radicals in the terminating reaction [6]:



and  $\phi_2 I_a = R_i$  is the rate of initiation of the photochemical oxidation at 3130 Å, the wavelength of the radiation used. Equation [A] is of the same general form as that found to be obeyed by the liquid-phase oxidation of aldehydes (5) and olefins (2), and so the application of the rotating sector technique in the present cases should enable us to determine the absolute value of the velocity constants for the reactions [3] and [6].

#### EXPERIMENTAL

The acetaldehyde and propionaldehyde were purified as described in Parts I and II. The alcohols were carefully purified by repeated distillations.

The photochemical apparatus was essentially the same as that employed previously. Two different sectors were used. One had two apertures of  $\pi/2$  and the other had two of  $\pi/4$ . The former was used for the experiments with acetaldehyde and the latter in those with propionaldehyde. The light beam was focused at the sector plane so that at the point of interruption the time taken by the edge of the sector to scan the beam was less than 1/30th of the light period. Oscillographic studies showed that the light pulse was quite square. At low speeds the rotation of the sector was timed using a stop watch. An accurate gear enabled the intermediate speeds to be measured. High rotational speeds were measured accurately on a cathode ray oscilloscope.

#### RESULTS

In a chain reaction obeying the kinetic expression [A] in which steady state conditions are quickly established (see Part I), the velocity constant for the termination step,  $k_6$ , is given by the equation

$$k_6 = 1/\tau^2 R_i, \quad [B]$$

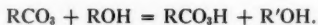
where  $R_i$  is the rate of initiation and  $\tau$  is the lifetime of the kinetic chain. This quantity  $\tau$  may in the case of the oxidation of acetaldehyde be expressed as:

$$\tau = \frac{\text{concentration of peracetic radicals}}{\text{rate of removal of peracetic radicals}}$$

with a similar expression for the lifetime of the kinetic chain in the oxidation of propionaldehyde. Thus it is seen that if  $R_i$  and  $\tau$  can be determined, then the absolute value of the velocity constant,  $k_6$ , can be calculated from equation [B]. The ratio  $k_3/k_6^{\frac{1}{2}}$  is readily obtainable from equation [A] once the rate of initiation  $\phi_2 I_a$  is known; hence once  $k_6$  has been determined,  $k_3$ , the absolute value of the velocity constant for the propagating step in the oxidation chain, may also be calculated.

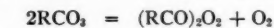
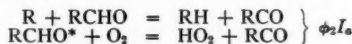
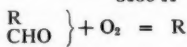
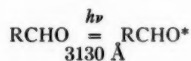
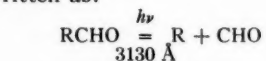
*Determination of the Rate of Initiation*  $R_i = \phi_2 I_a$

It is known that the oxidation of aldehydes is retarded by alcohols (3, 7) and the mechanism of this process is fairly well established. It is thought that when an alcohol, ROH, is added to a mixture of aldehyde and oxygen the ensuing retarding effect is caused by the reaction:



The radical R'OH may react with a similar radical by addition or disproportionation reactions to form stable products faster than it can abstract a hydrogen atom from an aldehyde molecule. Thus the chain length of the oxidation is shortened and the reaction is retarded.

The mechanism for the retarded photochemical oxidation of acetaldehyde and propionaldehyde would then be written as:



When stationary state kinetics are applied to this mechanism the following expression results if it is assumed that  $k_7[\text{ROH}][\text{RCO}_3] > k_6[\text{RCO}_3]^2$ :

$$d[\text{RCO}_3\text{H}]/dt = R_i \{1 + k_3[\text{RCHO}]/k_7[\text{ROH}]\}. \quad [C]$$

In equation [C] we have written  $R_i = \phi_2 I_a$ . This expression implies that if the alcohol-retarded oxidation obeys the mechanism given, the rate of the retarded reaction at a constant concentration of alcohol should be directly proportional to the intensity of illumination. Furthermore, at a constant intensity of illumination the rate of the retarded oxidation is required to be directly proportional to the reciprocal of the concentration of the retarding alcohol. Thus a graph of the rate of the retarded reaction against  $[\text{ROH}]^{-1}$  should be a straight line with slope  $k_3[\text{RCHO}]/k_7$  and an intercept equal to the rate of initiation  $\phi_2 I_a$ .

*Dependence of Rate of Retarded Reaction on Intensity*

In Table I are given the results of experiments carried out at 20° C. on a mixture of 150 mm. Hg pressure of acetaldehyde, 5 mm. Hg pressure of oxygen, a constant concentration of ethanol (30 mm. Hg pressure), and varying intensity of illumination.

These data have been plotted in Fig. 1 and it is seen that the required dependence of the rate of retarded reaction on the intensity of illumination is found, thus substantiating the above mechanism for the retarded reaction.

*Dependence of Rate of Reaction on Concentration of Retarder*

In Table II are given the results of experiments carried out at 20° C. with a mixture of 150 mm. Hg pressure of acetaldehyde, 5 mm. Hg of oxygen, a constant intensity of

TABLE I  
DEPENDENCE OF RATE OF RETARDED REACTION  
ON INTENSITY

All data refer to a mixture containing 150 mm. Hg pressure of acetaldehyde, 5 mm. Hg of oxygen, and 30 mm. Hg of ethanol at 20° C.

Absorbed intensity, percentage	Rate, mole l. <sup>-1</sup> sec. <sup>-1</sup> × 10 <sup>9</sup>
0.080	0.326
0.234	0.912
0.590	2.20
0.598	1.98
1.000	3.53
1.310	4.16
1.480	3.93

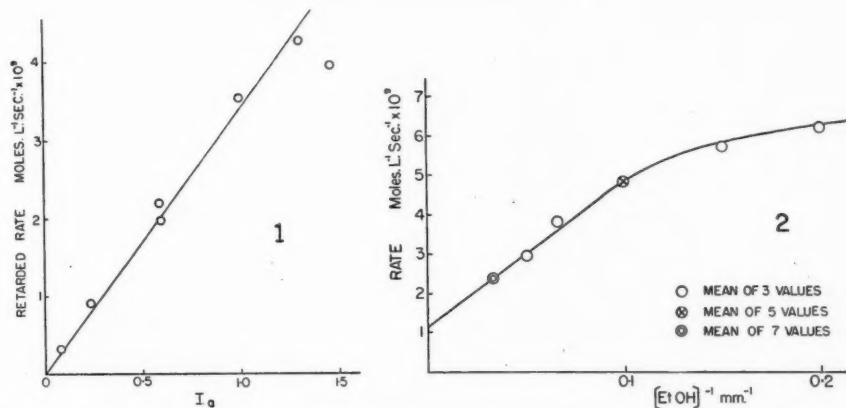


FIG. 1. Dependence of the rate of the ethanol-retarded photochemical oxidation of acetaldehyde on the intensity of the absorbed radiation.

FIG. 2. Dependence of the rate of the ethanol-retarded photochemical oxidation of acetaldehyde on the concentration of ethanol.

TABLE II  
DEPENDENCE OF RATE OF ETHANOL RETARDED  
OXIDATION OF ACETALDEHYDE ON  
CONCENTRATION OF ETHANOL

All data refer to mixtures containing 150 mm. Hg pressure of acetaldehyde, 5 mm. Hg of oxygen at 20° C.; the absorbed light intensity was 0.59% of the total intensity

Ethanol concentration, mm. Hg	Rate, mole l. <sup>-1</sup> sec. <sup>-1</sup> × 10 <sup>9</sup>
0	7.93
3	7.15
5	6.50
7.5	5.85
10	4.93
15	3.92
20	3.00
30	2.39

illumination, and varying concentrations of ethanol. These data are shown graphically in Fig. 2, where the rate of the ethanol-retarded reaction is plotted against the reciprocal of the concentration of the ethanol. The linear relation at higher alcohol concentrations confirms the deductions from equation [C]. The intercept of the straight line in Fig. 2 on the rate axis gives the rate of initiation at the intensity used in these experiments as  $1.12 \times 10^{-9}$  mole l.<sup>-1</sup> sec.<sup>-1</sup>.

Experiments were carried out to see if equation [C] was also obeyed by the alcohol-retarded photochemical oxidation of propionaldehyde. In Table III are given the results

TABLE III  
DEPENDENCE OF RATE OF ETHANOL AND ISOPROPANOL RETARDED OXIDATION OF PROPIONALDEHYDE ON CONCENTRATION OF ALCOHOL

All data refer to mixtures containing 100 mm. Hg pressure of propionaldehyde, 3 mm. Hg of oxygen at 22° C., and a value of  $I_a$  of  $1.12 \times 10^{-9}$  einstein l.<sup>-1</sup> sec.<sup>-1</sup>

Run No.	Alcohol	Alcohol pressure, mm.	Rate, mole l. <sup>-1</sup> sec. <sup>-1</sup> $\times 10^9$
79	Ethyl	37.5	13.0
80	"	18.5	22.7
81	"	12.5	27.2
82	"	36.0	11.9
83	"	8.0	44.8
84	Isopropyl	10.0	15.4
85	"	4.5	32.0
86	"	30.0	6.08
87	"	28.5	6.34
88	"	6.0	21.6

of experiments carried out at 22° C. with a mixture of 100 mm. Hg pressure of propionaldehyde, 3 mm. Hg of oxygen, and varying concentrations of ethanol and isopropanol. These experiments were all performed with a light absorption of  $1.12 \times 10^{-9}$  einstein l.<sup>-1</sup> sec.<sup>-1</sup>. The data in Table III are plotted in Fig. 3, where the rate of the alcohol-retarded reaction is again plotted against the reciprocal of the concentration of the alcohol. It is evident from the straight lines obtained that equation [C] is obeyed by the reaction. Further, it is obvious that isopropanol is a much more efficient retarder than is ethanol.

To obtain an accurate value for the rate of initiation in the case of the oxidation of propionaldehyde a series of experiments were carried out at a somewhat higher value of  $I_a$ . These results are recorded in Table IV. The data there refer to a mixture of 100 mm. Hg of propionaldehyde and 3 mm. Hg of oxygen at 22° C. The value of  $I_a$  was  $1.16 \times 10^{-8}$  einstein l.<sup>-1</sup> sec.<sup>-1</sup>. The data are plotted in Fig. 4. The intercept of the straight line in Fig. 4 was calculated by the method of least squares using weighted means to be  $1.98 \times 10^{-8}$  mole l.<sup>-1</sup> sec.<sup>-1</sup>, which is of course the value of the rate of initiation  $\phi_2 I_a$ . This value is probably correct to  $\pm 10\%$ .

The results quoted in the above paragraphs leave little doubt that the mechanisms proposed for the alcohol-retarded photooxidation of acetaldehyde and propionaldehyde are correct. This in turn is evidence in favor of the correctness of the proposed mechanisms for the over-all photooxidations of acetaldehyde and propionaldehyde.

#### Measurement of the Chain Lifetimes

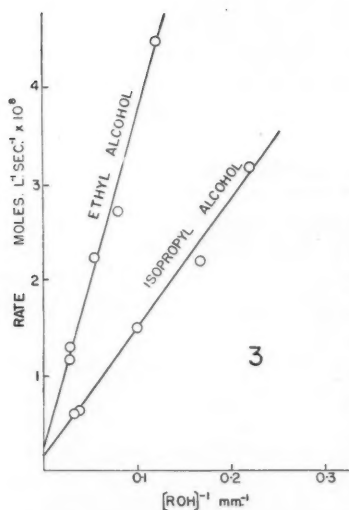
To measure the lifetimes of the chains in the photooxidation of acetaldehyde and propionaldehyde the usual (6) photochemical sector technique was employed. It was

TABLE IV

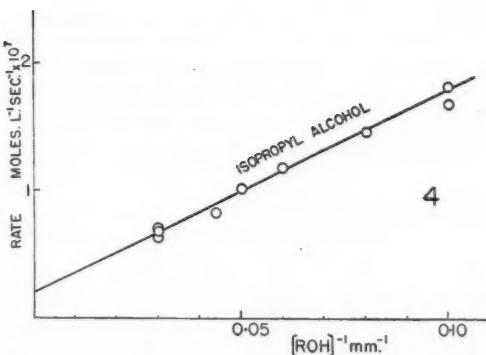
## DEPENDENCE OF RATE OF ISOPROPANOL RETARDED OXIDATION OF PROPIONALDEHYDE ON CONCENTRATION OF ISOPROPANOL

All data refer to mixtures containing 100 mm. Hg pressure of propionaldehyde, 3 mm. Hg of oxygen at 22°C., and a value of  $I_a$  of  $1.16 \times 10^{-8}$  einstein l.<sup>-1</sup> sec.<sup>-1</sup>

Run No.	Alcohol pressure, mm.	Rate, mole l. <sup>-1</sup> sec. <sup>-1</sup> $\times 10^8$
89	32.5	7.26
90	30.0	7.26
91	16.7	11.80
92	12.6	14.4
93	20.0	10.25
94	10.0	16.6
95	5.0	19.9
96	0	20.5
97	32.0	6.88
98	32.0	6.40
99	10.0	18.2



3



4

FIG. 3. Dependence of the rate of the ethanol and isopropanol retarded photochemical oxidation of propionaldehyde on the concentration of alcohol.

FIG. 4. Dependence of the rate of the isopropanol-retarded photochemical oxidation of propionaldehyde on the concentration of isopropanol. The determination of the rate of initiation of the photooxidation reaction.

confirmed experimentally that under the conditions of our studies there was no appreciable thermal oxidation and so the normal sector theory is applicable.

Series of experiments were performed for various values of the time of a single flash,  $t$ . Before and after each intermittent illumination experiment one was done under the same conditions but with continuous illumination. For each value of  $t$ , the ratio of the "intermittent" rate to the "continuous" rate,  $\gamma$ , was taken as ratio of the intermittent illumination rate to the average value of the continuous illumination rates of the experi-

TABLE V  
ROTATING SECTOR EXPERIMENTS IN PHOTOCHEMICAL  
OXIDATION OF ACETALDEHYDE\*

All data refer to a mixture of 150 mm. Hg pressure of acetaldehyde and 5 mm. Hg of oxygen at 20° C.; the incident intensity was 2.2% of the total intensity and  $I_a$  equal to 0.62% of total intensity

Rate, mole l. <sup>-1</sup> sec. <sup>-1</sup> × 10 <sup>3</sup>	R. intermittent R. continuous	Flash time <i>t</i> , sec.
5.47	0.690	0.00174
7.93	—	—
5.52	0.696	0.0125
7.93	—	—
4.72	0.595	0.45
7.93	—	—
5.39	0.679	0.112
7.93	—	—
5.09	0.642	0.20
7.93	—	—
5.60	0.705	0.0625
7.93	—	—
4.66	0.588	0.875
7.93	—	—

\*The values for the "intermittent" rates quoted are mean values computed from the results of eight identical experiments. The value for the "continuous" rate quoted is a mean value of 12 identical experiments carried out between sets of eight "intermittent" experiments during the whole series of experiments.

TABLE VI  
ROTATING SECTOR EXPERIMENTS IN PHOTOCHEMICAL  
OXIDATION OF PROPIONALDEHYDE

All data refer to a mixture of 100 mm. Hg of propionaldehyde and 3 mm. Hg pressure of oxygen at 22° C.; the intensity of the illumination was  $1.12 \times 10^{-9}$  einstein l.<sup>-1</sup> sec.<sup>-1</sup>

Run No.	Rate, mole l. <sup>-1</sup> sec. <sup>-1</sup> × 10 <sup>3</sup>	R. intermittent R. continuous	Flash time <i>t</i> , sec.
100	2.56	0.308	1.50
101	8.32	—	—
102	3.62	0.452	0.125
103	7.68	—	—
104	3.64	0.500	0.022
105	6.88	—	—
106	3.52	0.498	0.081
107	2.68	0.380	0.55
108	7.24	—	—
109	2.84	0.412	0.83
110	7.04	—	—
111	3.12	0.456	0.24
112	6.66	—	—
113	1.92	0.287	10.0
114	6.712	—	—
115	1.92	0.284	3.40
116	6.78	—	—
117	3.36	0.492	0.081
118	6.88	—	—
119	1.89	0.290	3.4
120	6.17	—	—
121	2.80	0.447	0.175
122	6.50	—	—
123	2.03	0.312	1.00

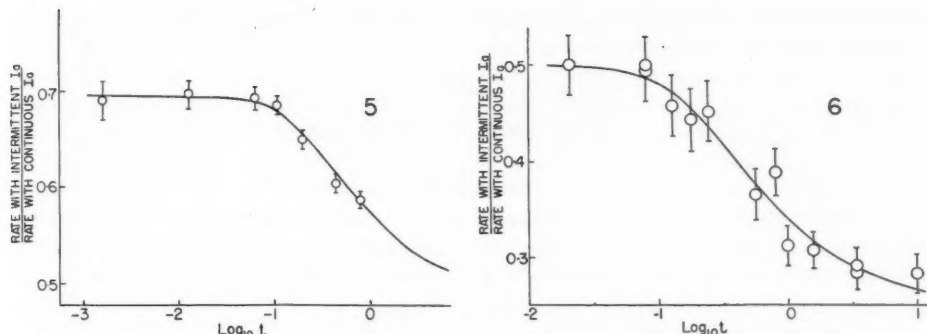


FIG. 5. Rotating sector experiment in the photochemical oxidation of acetaldehyde. Determination of the lifetime of the oxidation chain.

FIG. 6. Rotating sector experiments in the photochemical oxidation of propionaldehyde. Determination of the lifetime of the oxidation chain.

ments before and after the "intermittent" rate experiment. These data are given in Table V for the acetaldehyde oxidation, and in Table VI for the propionaldehyde.

Following the usual procedure a graph of  $\log_{10}t$  against  $\gamma$  was plotted. Fig. 5 refers to the case of the acetaldehyde oxidation and Fig. 6 to the oxidation of propionaldehyde. In the former case a  $\pi/2$  sector was used so the values of  $\gamma$  range from 0.5 to 0.7. In the case of the propionaldehyde oxidation a  $\pi/4$  sector was used and here  $\gamma$  varies from 0.25 to 0.5.

Using the relevant mathematical equations given by Dickinson (6), a theoretical curve of  $\gamma$  against  $\log_{10}b$ , where  $b = t/\tau$ , was fitted to the experimental points. It was then possible to determine  $\tau$  in each case. For the photochemical oxidation of acetaldehyde at 20° C. the data in Fig. 5 give the lifetime of the chain,  $\tau$ , as 0.10 second. The data in Fig. 6 give a value of 0.14 second for the lifetime of the chain,  $\tau$ , in the photochemical oxidation of propionaldehyde. These values could be in error by  $\pm 0.05$  second.

#### ABSOLUTE VALUES FOR THE VELOCITY CONSTANTS $k_3$ AND $k_6$ IN THE PHOTOCHEMICAL OXIDATION OF ACETALDEHYDE AND PROPIONALDEHYDE

##### *Acetaldehyde*

Using the above experimentally determined values for  $R_t = \phi_2 I_a$ , and  $\tau$ , it is possible to calculate the absolute value of the velocity constant for the terminating reaction [6], i.e.  $k_6$ , from equations [A] and [B]. The values of  $1.12 \times 10^{-9}$  mole l.<sup>-1</sup> sec.<sup>-1</sup> for the rate of initiation ( $= \phi_2 I_a$ ) and 0.10 second for  $\tau$  obtained from the experiments with acetaldehyde lead to the following values for  $k_3$  and  $k_6$  at 20° C. in the photochemical oxidation of acetaldehyde:

$$k_3 = 8.05 (\pm 2.40) \times 10^3 \text{ l. mole}^{-1} \text{ sec.}^{-1},$$

$$k_6 = 8.93 (\pm 4.20) \times 10^{10} \text{ l. mole}^{-1} \text{ sec.}^{-1}.$$

##### *Propionaldehyde*

Our experiments lead to the values of  $1.90 \times 10^{-9}$  mole l.<sup>-1</sup> sec.<sup>-1</sup> for the rate of initiation ( $= \phi_2 I_a$ ) at the light intensity of  $1.12 \times 10^{-9}$  einstein l.<sup>-1</sup> sec.<sup>-1</sup> used in the sector experiments, and 0.14 second for  $\tau$  for the photochemical oxidation of propionaldehyde.

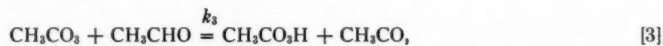
The substitution of these data in equations [A] and [B] leads to the following values for  $k_3$  and  $k_6$  at 22° C. for this reaction:

$$k_3 = 4.35(\pm 0.91) \times 10^4 \text{ l. mole}^{-1} \text{ sec.}^{-1},$$

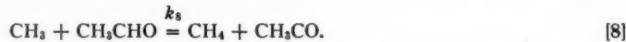
$$k_6 = 2.69(\pm 1.35) \times 10^{10} \text{ l. mole}^{-1} \text{ sec.}^{-1}.$$

#### DISCUSSION

It is of considerable interest to compare these values for the velocity constants for the propagating ( $k_3$ ) and terminating ( $k_6$ ) steps involving peroxidic radicals derived from acetaldehyde and propionaldehyde with those for other radicals. It seems appropriate to compare the value for the velocity constant for the propagating step in the photochemical oxidation of acetaldehyde, i.e. equation [3]:



for which we obtained the value of  $8.05 (\pm 2.40) \times 10^3 \text{ l. mole}^{-1} \text{ sec.}^{-1}$  at 20° C., with the velocity constant for the reaction [8] of the methyl radical:



From Volman and Brinton's experiments (14) we calculate the value of  $2.7 \times 10^3 \text{ l. mole}^{-1} \text{ sec.}^{-1}$  for  $k_3$  in reaction [8] at 20° C. These data indicate that at equal concentration reaction [3] is more rapid. This must be attributed to the higher reactivity of the peracetic radical over the methyl radical. The absolute values for the velocity constant for the terminating reactions,  $k_6$ , in the photooxidation of acetaldehyde and propionaldehyde, namely  $8.93(\pm 4.2) \times 10^{10} \text{ l. mole}^{-1} \text{ sec.}^{-1}$  at 20° (acetaldehyde) and  $2.89(\pm 1.35) \times 10^{10} \text{ l. mole}^{-1} \text{ sec.}^{-1}$  at 22° C. (propionaldehyde), may be compared with the values of  $2.2 \times 10^{10} \text{ l. mole}^{-1} \text{ sec.}^{-1}$  for the recombination of methyl radicals (12), and about  $2.0 \times 10^{10} \text{ l. mole}^{-1} \text{ sec.}^{-1}$  (9, 4, 13) for the recombination of ethyl radicals (at 20° C.). These data indicate that the peracetic radicals "recombine" (see below) more rapidly than do methyl or ethyl radicals, and that perpropionic radicals "recombine" at about the same rate as do the hydrocarbon radicals.

It is instructive to compare the collision efficiencies for the mutual interaction of the methyl, ethyl, peracetic, and perpropionic radicals. To do this it is necessary to have the absolute values for the velocity constants for the recombination reactions and also to know the collision numbers of the radicals. It is further necessary to know if the recombination reactions require any activation energy. In nearly all the investigations of the recombination of methyl (10), trifluoromethyl (1), and ethyl radicals (4, 9, 13) there has been but little reliable evidence to show whether or not these reactions do require an activation energy. In the study of the recombination of methyl radicals by mass spectrometry (8) it has been claimed that there is a net activation energy of  $-1.5$  kilocalories mole $^{-1}$  and this was attributed to a third-body effect. Shepp and Kutschke (13) have recently claimed that their studies on the recombination of ethyl radicals indicate an activation energy for this process of  $2.0 \pm 1$  kilocalories mole $^{-1}$ . Such small activation energies as these are difficult to establish unambiguously and as the assumption that the recombination reactions require but little or zero activation energy introduces little error into our discussion, we shall therefore adopt this commonly-made assumption.

Using Shepp's (12) recalculated value for the velocity constant for the recombination of methyl radicals and the value of 3.5 Å for the collision diameter one obtained a value of about 0.3 for the collision efficiency at 125° C. In the case of trifluoromethyl radicals Ayscough (1) used a collision diameter of 4 Å and calculated a value of 0.16 for the collision efficiency of these radicals at 127° C. These values are comparable with those of 0.12 for the collision efficiency of the recombination of two ethyl radicals found by Shepp and Kutschke (13), and 0.15 for the same process obtained by Bradley, Melville, and Robb (4). We have used a value of 5.4 Å for the collision diameters of both the peracetic and perpropionic radicals—this value seemed to be the most reasonable one as judged from Courtauld models of the radicals. This leads to a collision efficiency for the mutual interaction of the peracetic radicals of 0.8 and a value of 0.29 for the collision efficiency for the mutual interaction of two perpropionic radicals. These values suggest that the mutual interactions of these peroxidic radicals are somewhat more efficient than those of comparable hydrocarbon radicals.

#### *Chemistry of the Recombination Reaction of Peroxide Radicals*

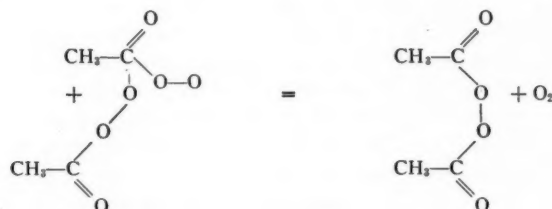
The data described in the above paragraphs show that the "recombination" reactions of peracetic and perpropionic radicals are relatively efficient. It will be recalled that the recombination or terminating step in the photooxidations is the process:



It is not easy to see why this process should be so very efficient, for it is evident from our data that one in every two collisions is effective in the case of the peracetic radical and one in every three or four is effective in the case of the perpropionic radicals. One might have thought that a rather special orientation would have been necessary before two radicals with structures like the peracetic or the perpropionic ones could have reacted.

The chemistry of process [6] is not clear. It could be that when the two peroxide radicals interact the oxygen molecule which is formed is produced by the elimination of an oxygen atom from each of the interacting radicals. This would probably be a rather complicated process and entropy considerations make us believe that it is not the mechanism of process [6].

A more likely mechanism is that the oxygen molecule which is eliminated comes wholly from one of the interacting radicals. This could be understood if the mechanism were as shown below:



Here it is assumed that the peroxide oxygen atoms of one radical attack the second radical at the acyl carbon atom causing the attacked radical to lose two oxygen atoms to form an oxygen molecule. It is thought that the use of isotopically enriched oxygen may enable the chemistry of this process to be elucidated and we are planning to carry out such experiments.

## ACKNOWLEDGMENTS

The experiments on acetaldehyde were carried out in the Department of Inorganic and Physical Chemistry, University of Liverpool, Liverpool 7, England, and we are indebted to Professor C. E. H. Bawn, C.B.E., F.R.S., for laboratory facilities and for his interest in the work. The remainder of the work was supported by a grant from the National Research Council of Canada to whom we tender our thanks.

## REFERENCES

1. AYSCOUGH, P. B. *J. Chem. Phys.* **24**, 944 (1956).
2. BATEMAN, L. H. and GEE, G. *Proc. Roy. Soc. (London)*, A, **195**, 376 (1948).
3. BOWEN, E. G. and TIETZ, E. L. *J. Chem. Soc.* **234** (1930).
4. BRADLEY, J. N., MELVILLE, H. W., and ROBB, J. C. *Proc. Roy. Soc. (London)*, A, **236**, 333 (1956).
5. COOPER, H. R. and MELVILLE, H. W. *J. Chem. Soc.* **1984**, 1994 (1951).
6. DICKINSON, R. G. *In* Noyes and Leighton, *The photochemistry of gases*. Reinhold Publishing Corp., New York. 1941.
7. FARMER, J. B. and McDOWELL, C. A. *Trans. Faraday Soc.* **48**, 624 (1952).
8. INGOLD, K. U., HENDERSON, I. H. S., and LOSSING, F. P. *J. Chem. Phys.* **21**, 2239 (1953).
9. IVIN, K. J. and STEACIE, E. W. R. *Proc. Roy. Soc. (London)*, A, **208**, 25 (1951).
10. KISTIAKOWSKY, G. B. and ROBERTS, E. R. *J. Chem. Phys.* **21**, 1637 (1953).
11. MELVILLE, H. W. and RICHARDS, S. *J. Chem. Soc.* **944** (1954).
12. SHEPP, A. *J. Chem. Phys.* **24**, 939 (1956).
13. SHEPP, A. and KUTSCHKE, K. O. *J. Chem. Phys.* **26**, 1020 (1957).
14. VOLMAN, D. H. and BKINTON, R. *J. Chem. Phys.* **20**, 1053 (1952).

---

## NOTES

---

### LONG-WAVELENGTH LIMIT OF PHOTOOXIDATION OF BUTENE-1 BY NITROGEN DIOXIDE<sup>1</sup>

S. SATO<sup>2</sup> AND R. J. CVETANOVIĆ

Photolysis of nitrogen dioxide is of importance as a source of oxygen atoms and a process which appears to play a vital role in "smog" formation (1). It is believed (2) that dissociation into nitric oxide and ground state oxygen atoms occurs in the spectral region 3700–2450 Å.

The type of product formed in the reaction of oxygen atoms with olefins has been recently established (3). Oxygen atoms were produced by mercury photosensitized decomposition of nitrous oxide and were probably in their ground state. With butene-1, for example, two principal products were formed,  $\alpha$ -butene oxide and *n*-butanal, the former in slight excess, and minor amounts of methyl ethyl ketone and of some fragmentation products. It was thought of interest to study the photochemical reaction of nitrogen dioxide and butene-1 in order to determine more precisely its long-wavelength limit and to compare the two sources of oxygen atoms.

The products were analyzed by gas liquid chromatography using a 7 ft. column of dinonyl phthalate on glass beads (4). Subsequently, use was made of infrared and mass spectroscopy to confirm the identity of the compounds formed. At low conversions the reaction was identical with the one observed in the nitrous oxide work. Two main products were formed,  $\alpha$ -butene oxide and *n*-butanal, the former in slight excess. The minor products amounted to about 15% and consisted of methyl ethyl ketone, propanal, acetaldehyde, and three unidentified compounds. Some of the last appeared to contain nitrogen and, as expected, were absent in the nitrous oxide reaction. No difficulty was experienced with the thermal reaction, which was much slower and led to entirely different products (5).

The light from a medium pressure mercury arc (Hanovia S 500) was used unfiltered or with one of the following Corning glass filters in turn: 0-51, 3-75, 3-73, and 3-74. The reactants, 30 mm. butene-1 and 3 mm. NO<sub>2</sub>, were circulated through a 300 ml. cylindrical quartz reaction cell. The results are shown in Fig. 1 and the corresponding spectra of the incident radiation in Fig. 2 (A, B, C, and D). It is evident that with the light of 4047 Å (70.6 kcal./mole) the reaction still proceeds but not with the very intense line at 4358 Å (65.6 kcal./mole). The former value is comparable with the bond dissociation energy of NO<sub>2</sub> to give NO and O(<sup>3</sup>P) ( $71.861 \pm 0.411$ ,  $71.179 \pm 0.253$ , or  $71.381 \pm 0.013$ , depending on the value of  $\Delta H_0^{\circ}$  for the reaction  $\text{NO} + \frac{1}{2}\text{O}_2 = \text{NO}_2$  (6)). It is of interest that Dickinson and Baxter (7) and Norrish (8) have found exactly the same long-wavelength threshold for the photolysis of NO<sub>2</sub> itself.

The difference in the reaction rates given in Fig. 1, curves A, B, and C, appears to be due to the difference in light intensity. By combining Corning filter 7-54 with the previous ones virtually only the relevant spectral lines were retained (A', B', C', and D', Fig. 2). The ratio of the light intensities was roughly determined by means of a phototube circuit and by applying an approximate correction for the small amount of the longer wavelengths present (taken equal to the transmission of the filter combination D' in

<sup>1</sup>Issued as N.R.C. No. 4559.

<sup>2</sup>National Research Council Postdoctorate Fellow 1956-58.

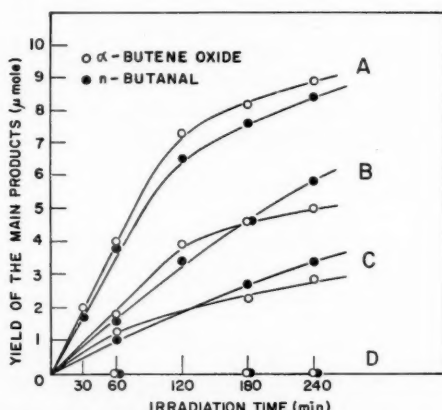


FIG. 1. Yield of the principal products as a function of the spectral structure of incident radiation.

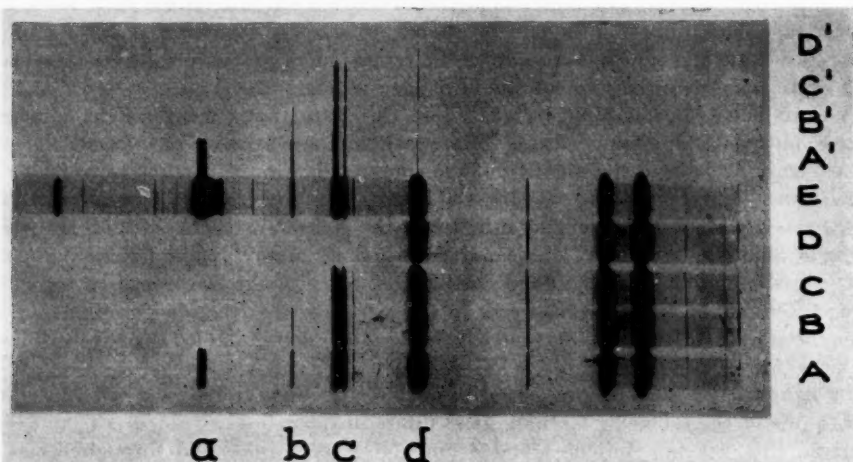


FIG. 2. Spectra of the filtered radiation from a medium pressure mercury arc used for the photooxidation of butene-1 with nitrogen dioxide. (Taken with medium quartz Hilger spectrograph.) The wavelengths of the lines *a*, *b*, *c*, *d* are 3660, 3906, 4047, and 4358 Å, respectively. *E* is unfiltered radiation, and *A*, *B*, *C*, *D*, *A'*, *B'*, *C'*, and *D'* are the spectra of filtered radiation as explained in the text.

Fig. 2). When irradiation times were taken in an inverse ratio, roughly equal amounts of products were obtained (Table I). This result is only semiquantitative.

Further extensions of this work are in progress.

TABLE I  
THE EFFECT OF LIGHT INTENSITY WITH DIFFERENT FILTER COMBINATIONS  
ON THE YIELD OF PRINCIPAL PRODUCTS

Run No.	Incident radiation	Ratio of intensities	Irradiation time, hours	<i>n</i> -Butanal, $\mu$ mole	$\alpha$ -Butene oxide, $\mu$ mole
112	A'	10	1	0.7	0.7
114	B'	3	3	0.6	0.5
113	C'	1	10	0.9	1.0

The authors are thankful to Dr. A. W. Tickner for mass spectrometer analyses and to the analytical section of this division for infrared analyses and the spectrograms in Fig. 2.

1. HAAGEN-SMIT, A. J. *Ind. Eng. Chem.* **48**, 65 (1956).
2. NOYES, W. A., Jr. and LEIGHTON, P. A. *The photochemistry of gases*. Reinhold Publishing Co., New York, 1941. p. 400.
3. CVETANOVIĆ, R. J. *J. Chem. Phys.* **25**, 376 (1956); a more detailed account to be published.
4. CALLEAR, A. B. and CVETANOVIĆ, R. J. *Can. J. Chem.* **33**, 1256 (1955).
5. LEVY, N. and SCAIFE, C. W. *J. Chem. Soc.* 1093 (1946). BROWN, J. F., Jr. *J. Am. Chem. Soc.* **79**, 2480 (1957).
6. GIAUQUE, W. F. and KEMP, J. D. *J. Chem. Phys.* **6**, 40 (1938).
7. DICKINSON, R. G. and BAXTER, W. P. *J. Am. Chem. Soc.* **50**, 774 (1928).
8. NORRISH, R. G. W. *J. Chem. Soc.* 1604 (1929).

RECEIVED SEPTEMBER 13, 1957.  
DIVISION OF APPLIED CHEMISTRY,  
NATIONAL RESEARCH COUNCIL,  
OTTAWA, CANADA.

**ULTRAVIOLET IRRADIATION OF PYRIMIDINE DERIVATIVES  
II. NOTE ON THE SYNTHESIS OF THE PRODUCT OF  
REVERSIBLE PHOTOLYSIS OF URACIL\***

A. M. MOORE

Solutions of uracil, when irradiated with ultraviolet light (2537 Å), undergo photolysis to yield a product that lacks the absorption band (max. 2590 Å) typical of uracil but which regenerates uracil on treatment with acid (4). Several derivatives of uracil, such as uridine, uridylic acid (4, 5), and 1,3-dimethyluracil (2), exhibit a similar "reversible" photolysis.

Using 1,3-dimethyluracil as a model, Moore and Thomson (3) showed that the product of irradiation is 1,3-dimethyl-6-hydroxy-hydouracil, resulting from the addition of a molecule of water to the 5,6 double bond. This compound has also been synthesized by reduction of 5,5-dibromo-1,3-dimethyl-6-hydroxy-hydouracil (3) and of the 5-monobromo compound (6).

The analogous derivative of uracil has now been synthesized and compared with the "reversible" product of ultraviolet irradiation of uracil.

5,5-Dibromo-6-hydroxy-hydouracil (I) (m.p. 136°) synthesized by the method of Wheeler and Johnson (7) was reduced with zinc dust and acetic acid (pH 4–5) using the same technique as that used for the reduction of 1,3-dimethyl-5,5-dibromo-6-hydroxy-hydouracil (3). The product of reduction was then compared chromatographically and spectroscopically with the product of irradiation of uracil. Although the latter has not been isolated in the pure state it can readily be separated on paper chromatograms, the position of the "reversible" product on the developed chromatogram being found by exposing a test strip to HCl vapor to promote conversion of the product to uracil, which is then easily located by the ultraviolet print method of Markham and Smith (1) (Fig. 1).

Accordingly, the product of reduction was chromatographed on paper in parallel with the product of irradiation using four different solvent systems. The observed *R*<sub>f</sub> values are given in Table I.

In Fig. 2 are plotted the respective relative changes in optical density that occurred when a photolyzed solution of uracil and the product of reduction of the dibromo com-

\*Issued as A.E.C.L. No. 523.

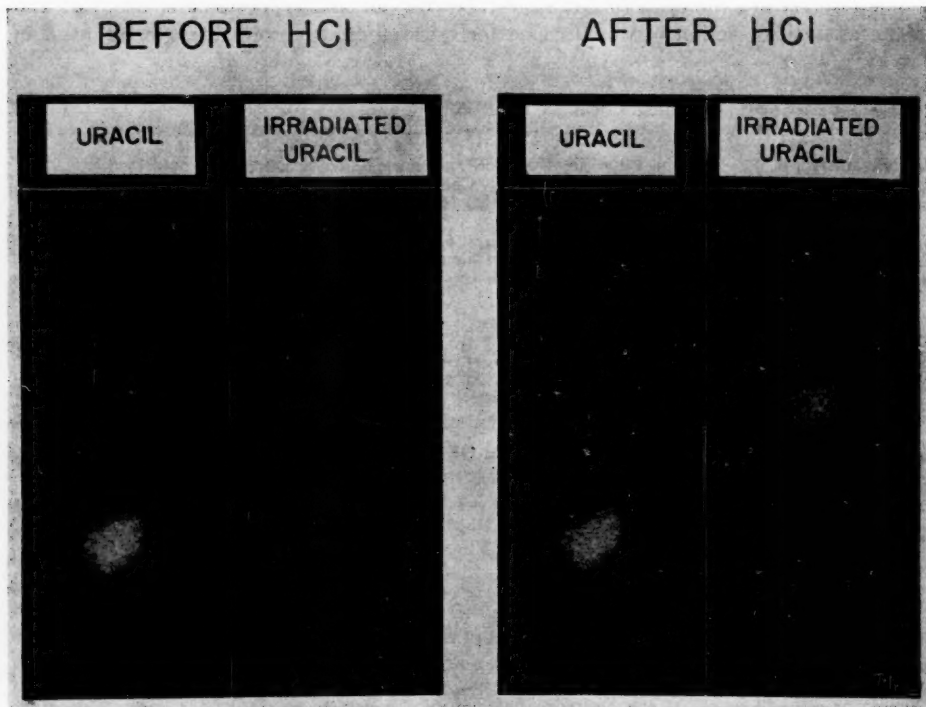


FIG. 1. Paper chromatographic separation of the "reversible" product of ultraviolet-irradiated uracil. (*n*-Butanol: water.)

TABLE I  
COMPARISON OF IRRADIATION PRODUCT\* WITH SYNTHETIC MATERIAL

Solvent†	Observed $R_f$ values (mean)		
	Synthetic 6-hydroxy-hydouracil	Product of irradiation	Uracil
(a)	0.22	0.22	0.35
(b)	0.78	0.78	0.73
(c)	0.42	0.42	0.50
(d)	0.67	0.69	0.68

\*Uracil ( $10^{-2} M$ ) irradiated with ultraviolet light (2537 Å) for 5 hours in the apparatus previously described (3).

†(a) *n*-Butanol saturated with water. (b) Water saturated with *n*-butanol. (c) *n*-Propanol:water, 70:30 by volume. (d) Isopropanol:water, 70:50 by volume.

pound were heated with acid (100°, 5 minutes, pH 1). The agreement is good apart from the points at the three shortest wavelengths where the errors of measurement are at a maximum.

The product of reduction of 5,5-dibromo-6-hydroxy-hydouracil presumably has the OH group at position 6. Its identity with the product of irradiation of uracil, as indicated by the very close agreement in  $R_f$  values and in spectroscopic properties of the two prepara-

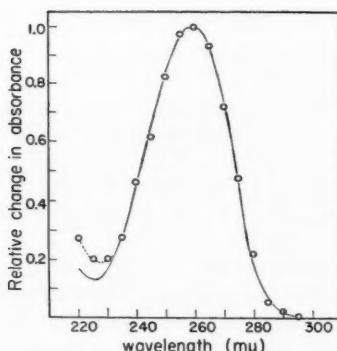


FIG. 2. Plot of  $\Delta D / \Delta D_{260}$ , where  $\Delta D$  is the change in optical density at any wavelength and  $\Delta D_{260}$  is the corresponding change at  $260\text{ m}\mu$  that occurs when the product of irradiation of uracil (solid line) or the product of the reduction of 5,5-dibromo-6-hydroxy-hydouracil (open circles) is treated with HCl ( $100^\circ$ , 5 minutes, pH 1). This method of presentation was chosen because the concentrations obtained in the two preparations were arbitrary.

tions, adds strong support to the suggestion made earlier (2) that the product of irradiation of uracil responsible for the acid-catalyzed regeneration phenomenon is 6-hydroxy-hydouracil.

1. MARKHAM, R. and SMITH, J. D. *Biochem. J.* **45**, 294 (1949).
2. MOORE, A. M. and THOMSON, C. H. *Science*, **122**, 594 (1955).
3. MOORE, A. M. and THOMSON, C. H. *Can. J. Chem.* **35**, 163 (1957).
4. SINSHEIMER, R. L. and HASTINGS, R. *Science*, **110**, 525 (1949).
5. SINSHEIMER, R. L. *Radiation Research*, **1**, 505 (1954).
6. WANG, S. Y., APICELLA, M., and STONE, B. R. *J. Am. Chem. Soc.* **78**, 4180 (1956).
7. WHEELER, H. L. and JOHNSON, T. B. *J. Biol. Chem.* **3**, 183 (1907).

RECEIVED SEPTEMBER 13, 1957.  
BIOLOGY DIVISION,  
ATOMIC ENERGY OF CANADA LIMITED,  
CHALK RIVER, ONTARIO.

#### AN ALTERNATIVE SYNTHESIS OF 2-O-METHYL-D-XYLOSE

W. D. S. BOWERING AND T. E. TIMELL

In studying the structure of a xylan the need arose for 2-*O*- and 3-*O*-methyl-D-xylose as reference compounds. The latter was synthesized from 1,2-*O*-isopropylidene-D-xylofuranose (1) and it was preferable to prepare the former from the same starting material if possible. Such a procedure would also obviate the necessity of using the acid-labile methyl 3,5-*O*-isopropylidene- $\alpha,\beta$ -D-xylofuranoside as described in a previous synthesis of 2-*O*-methyl-D-xylose (2).

1,2-*O*-Isopropylidene-D-xylofuranose was benzylated to give the corresponding 3,5-di-*O*-benzyl derivative, which was converted to methyl 3,5-di-*O*-benzyl- $\alpha,\beta$ -D-xylofuranoside by methanolysis. Methylation (3) of this compound yielded the 2-*O*-methyl derivative, which was then reductively debenzylated to methyl 2-*O*-methyl- $\alpha,\beta$ -D-xylofuranoside. Hydrolysis of this compound gave crystalline 2-*O*-methyl-D-xylose.

## EXPERIMENTAL

*3,5-Di-O-benzyl-1,2-O-isopropylidene-D-xylofuranose*

1,2-O-Isopropylidene-D-xylofuranose,  $[\alpha]_D^{21} - 19.2^\circ$  (*c*, 2.1 in water), (46.4 g.) (1) was treated with benzyl chloride (230 ml.) and powdered potassium hydroxide (57 g.) at 100° C. for 5 hours. The solution was poured into water and the sirupy material obtained on concentration was extracted with boiling ethanol. Evaporation yielded a sirup (103.2 g.) which could not be induced to crystallize,  $[\alpha]_D^{22} + 9.2^\circ$  (*c*, 2.5 in ethanol). Anal.: Calc. for  $C_{22}H_{36}O_5$ : C, 71.3%; H, 7.1%. Found: C, 72.3%; H, 7.5%.

*Methyl 3,5-Di-O-benzyl- $\alpha$ , $\beta$ -D-xylofuranoside*

A portion of the above sirup (40.0 g.) was boiled under reflux with anhydrous methanol (200 ml.) containing 1.5% hydrogen chloride. Neutralization (silver carbonate) and evaporation yielded a sirup,  $[\alpha]_D^{22} + 17.6^\circ$  (*c*, 5.3 in ethanol), (37.5 g., 100.8%). Anal.: Calc. for  $C_{20}H_{24}O_5$ : OCH<sub>3</sub>, 9.0%. Found: OCH<sub>3</sub>, 8.8%.

*Methyl 3,5-Di-O-benzyl-2-O-methyl- $\alpha$ , $\beta$ -D-xylofuranoside*

The above sirupy compound (37.0 g.) was dissolved in a mixture of dimethyl formamide (54 ml.) and methyl iodide (20.4 ml.). Silver oxide (20.4 g.) was added in small portions over a period of 1 hour and the mixture was shaken for 24 hours. The methylated material was recovered (3) to yield a sirup,  $[\alpha]_D^{22} + 23.7^\circ$  (*c*, 3.2 in ethanol), (33.3 g., 86.5%). Anal.: Calc. for  $C_{21}H_{26}O_5$ : C, 70.4%; H, 7.3%; OCH<sub>3</sub>, 17.3%. Found: C, 71.5%; H, 8.1%; OCH<sub>3</sub>, 17.6%. An infrared spectrum of the material indicated the presence of only a trace of hydroxyl groups.

*Methyl 2-O-Methyl- $\alpha$ , $\beta$ -D-xylofuranoside*

The above sirup (33.0 g.) was reductively debenzylated (4). The aqueous solution obtained was passed through a column of Amberlite IRC 50 exchange resin and the eluate was concentrated and extracted with ethanol to yield a sirup,  $[\alpha]_D^{22} + 35.4^\circ$  (*c*, 2.9 in ethanol), (22.1 g.).

*2-O-Methyl-D-xylose*

The above material (22.0 g.) was hydrolyzed with 0.5 N sulphuric acid (150 ml.) by boiling under reflux for 14 hours. After neutralization with barium hydroxide and filtration through Celite, concentration of the filtrate gave a sirup (7.5 g.). Examination by paper chromatography using a system of methyl ethyl ketone - ethanol - water (20:5:2) indicated the presence of 2-O-methyl-D-xylose and a trace of xylose.

The crude material was added to the top of a column containing cocoanut charcoal and was eluted with 2% ethanol until the eluate gave a negative Molisch test. Evaporation yielded a white, crystalline compound, which was recrystallized from ethanol, m.p. 132-133° C. (corrected),  $[\alpha]_D^{21} + 35.1^\circ$  (*c*, 3.5 in water), (3.1 g., 15.3%). Anal.: Calc. for  $C_6H_{12}O_5$ : OCH<sub>3</sub>, 18.9%. Found: OCH<sub>3</sub>, 18.9%.

1. LEVENE, P. A. and RAYMOND, A. L. *J. Biol. Chem.* **102**, 331 (1933).
2. ROBERTSON, G. J. and SPEEDIE, T. H. *J. Chem. Soc.* 824 (1934).
3. KUHN, R., TRISCHMANN, H., and LÖW, I. *Angew. Chem.* **67**, 32 (1955).
4. FREUDENBERG, K. and PLANKENHORN, E. *Ann.* **536**, 257 (1938).

RECEIVED SEPTEMBER 17, 1957.

MCGILL UNIVERSITY AND

PULP AND PAPER RESEARCH INSTITUTE OF CANADA,  
MONTREAL, QUEBEC.

## THE INFRARED AND RAMAN SPECTRUM OF DIMETHOXYMETHANE

J. K. WILMSHURST\*

Infrared spectra of solutions of dimethoxymethane ( $\text{CH}_3\text{OCH}_2\text{OCH}_3$ ) in  $\text{CCl}_4$  and  $\text{CS}_2$  have been obtained over the  $3-7 \mu$  and  $7-33 \mu$  regions respectively (Fig. 1) using a Perkin-Elmer model 112S double pass spectrometer equipped with  $\text{LiF}$ ,  $\text{CaF}_2$ ,  $\text{NaCl}$ , and  $\text{CsBr}$  optics. The infrared spectrum of the vapor has also been obtained around  $3 \mu$  and from  $6.5$  to  $33 \mu$  (Fig. 2). Although the Raman spectrum of the liquid had been recorded previously (4) a better resolved spectrum was obtained here (Fig. 3) using a White grating Raman spectrometer (7) with photoelectric recording.† Depolarization

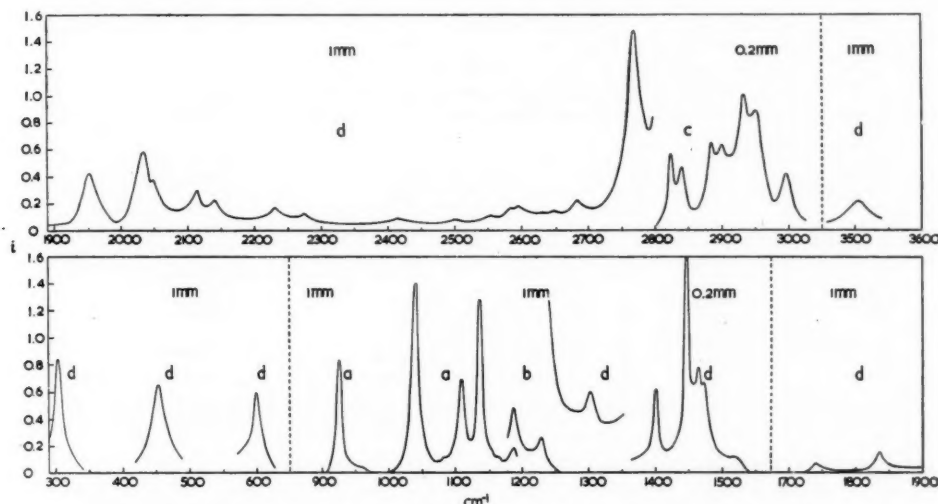


FIG. 1. The infrared spectrum of a solution of dimethoxymethane in  $\text{CCl}_4$  ( $3600-1400 \text{ cm}^{-1}$ ) and in  $\text{CS}_2$  ( $1400-300 \text{ cm}^{-1}$ ). The cell length is as shown and the concentrations (in volume) are  $a = 1:400$ ,  $b = 1:150$ ,  $c = 1:25$ ,  $d = 2:25$ .

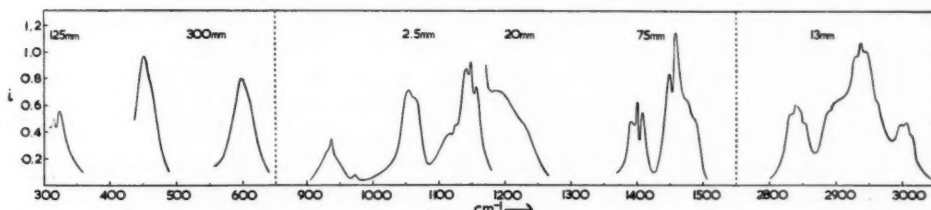


FIG. 2. The infrared spectrum of dimethoxymethane vapor in a 10-cm. cell at the pressure shown.

ratios were measured by the method of Edsall and Wilson (2) and corrected for convergence error by the method of Rank and Kagarise (6).

\*New Zealand University Research Fund Senior Fellow 1957.

†The author wishes to thank Dr. H. J. Bernstein, of the National Research Council Laboratories, for the use of this instrument.

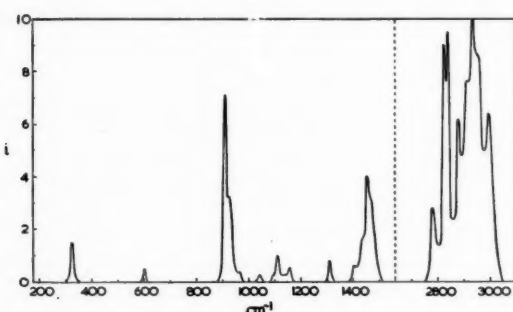


FIG. 3. The Raman spectrum of liquid dimethoxymethane.

TABLE I  
THE INFRARED AND RAMAN SPECTRUM OF DIMETHOXYMETHANE

Infrared spectrum			Raman spectrum				Assignment	
Solution	Vapor		Cm. <sup>-1</sup>	Rel. int.	Depol. ratio	Species	Approximate description	
Cm. <sup>-1</sup>	Int.	Cm. <sup>-1</sup>	Band contour					
304	m	315 324}	?	325	2	0.14	a	COC bending
454	m	452 ~462}	⊥				a	OCO bending
600	m	598 ~611}	⊥	602	1	0.86	b	COC bending
				912	7	0.17	a	Sym. H <sub>3</sub> C—O stretching
		~931 937 ~946}						
927	vs	973	⊥?	925	3	0.56	a	Sym. OCO stretching
~960	w	1054 1064}	⊥ +    hybrid	963	0	p?		?
1042	vs			1042	0		b	Asym. H <sub>3</sub> C—O stretching
~1084	w			~1094	0			1401—304 = 1097 (B)?
1110	vs	1116 ~1125 1141}	?	1111	1	0.80	b	CH <sub>2</sub> rocking
1138	vs	1148 1156}		~1136	0		b	Asym. OCO stretching
~1154	w			1157	1	0.70	a	CH <sub>3</sub> rocking
~1165	w						b	CH <sub>3</sub> rocking
1188	s	~1188					b	CH <sub>3</sub> rocking
1229	s	~1230					a	CH <sub>3</sub> rocking
1303	w	1390}		1310	1	0.86	a	CH <sub>2</sub> twisting
1401	m	1400 1408}		1403	1	dp	b	CH <sub>2</sub> wagging
				~1436	2	~0.70	a	CH <sub>2</sub> sym. bending
1448	m	1449 1458 —}		1455	4	~0.80	a+b	CH <sub>2</sub> sym. bending
1465	m	1464		1469	3	~0.80	a+b	CH <sub>2</sub> asym. bending
1473	m	1487		1483	1	~0.80	a+b	CH <sub>2</sub> asym. bending
1519	w							600+927 = 1527 (B)
1741	w							304+1448 = 1752 (A+B)
1836	w							912+927 = 1839 (A)
1954	m							927+1042 = 1869 (B)
2035	m							912+1138 = 2050 (B)
2049	w							927+1138 = 2065 (B)
2115	w							927+1188 = 2115 (B),
2141	w							1042+1110 = 2152 (A)

TABLE I (concluded)

Infrared spectrum							Assignment	
Solution		Vapor		Raman spectrum				
Cm. <sup>-1</sup>	Int.	Cm. <sup>-1</sup>	Band contour	Cm. <sup>-1</sup>	Rel. int.	Depol. ratio		
2231	w						1110 + 1138 = 2248 (A)	
2275	w						2 × 1138 = 2276 (A)	
2415	w						1110 + 1303 = 2413 (B)	
2502	w						1042 + 1465 = 2507 (A+B)	
2554	w						1110 + 1448 = 2558 (A+B)	
2585	w						1138 + 1448 = 2586 (A+B)	
2596	w						1138 + 1465 = 2603 (A+B)	
2632	vw						1188 + 1448 = 2636 (A+B)	
2650	vw						1188 + 1465 = 2653 (A+B)	
2684	w						1229 + 1465 = 2694 (A+B)	
2770	m	~2831		2780	3	dp	1303 + 1473 = 2776 (A+B)	
2825	m	~2831 2840	⊥	2826	9	0.16	a CH <sub>2</sub> sym. stretching	
2841	m	~2846 ~2853	⊥	2841	9	0.15	2 × 1436 = 2872 (A)	
2885	m	2897 2905	?	2880	6	0.21	2 × 1448 = 2896 (A)	
2901	m			~2914	7	0.30	1448 + 1465 = 2913 (A+B)	
2934	m	2930 2938 2945		2935	10	0.33	a+b CH <sub>3</sub> sym. stretching	
2951	m	~2964 2998		~2956	8	0.36	a+b CH <sub>3</sub> asym. stretching	
2997	m	3005 3013		2996	6	0.53	a+b b {CH <sub>3</sub> asym. stretching CH <sub>2</sub> asym. stretching 2934 + 600 = 3534 (A+B)	
3514	w							

From dipole moment studies (5) it has been concluded that the molecule has point symmetry  $C_2$ , the two O—CH<sub>3</sub> bonds making angles of  $\sim 60^\circ$  with the OCO plane. Electron diffraction data (1) support this model. Thus, of the 33 fundamental vibrations, 17 should be symmetric (type *a*) and 16 antisymmetric (type *b*) with respect to rotation about the symmetry axis. Calculation of the moments of inertia of the molecule\* shows that it is an approximate symmetric top, the Gerhard and Dennison (3) parameter being  $\beta = 2.17$ . Thus, two types of bands are expected: perpendicular-type bands having a prominent *Q* branch with weaker unresolved *P* and *R* branches, and parallel-type bands having three nearly equal maxima with *PR* separation of  $\sim 17$  cm.<sup>-1</sup>. The vapor band contours observed (Fig. 2) can be seen to be essentially consistent with this, the average *PR* separation of the parallel bands being 16 cm.<sup>-1</sup>, in agreement with the previously proposed configuration (5) for the molecule.

The type *a* modes should give rise to polarized bands in the Raman and perpendicular-type bands in the infrared, while the type *b* modes should give rise to depolarized Raman bands and either parallel or perpendicular type bands in the infrared, depending on whether the change of dipole moment is parallel to the minor axis, 0x, or to the major axis, 0y (Fig. 4). Since the two methyl groups are sufficiently far apart, the internal vibrations of one group should be independent of those of the other and, thus, the six *a*-type internal modes should have the same frequency as the corresponding six *b*-type modes. With this in mind the vibrational assignment is fairly straightforward.

\*The moments of inertia were calculated (assuming r<sub>CO</sub> = 1.44 Å, r<sub>CH</sub> = 1.09 Å,  $\angle$  COC = 104°, and all other angles tetrahedral) to be:  $I_x = 75.6$ ,  $I_y = 245.2$ , and  $I_z = 230.5 \times 10^{-40}$  g. cm.<sup>2</sup>, where z is the symmetry axis of the molecule and x and y axes are as shown in Fig. 4.

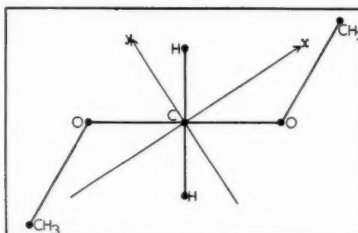


FIG. 4. Projection of the dimethoxymethane molecule on a plane perpendicular to the symmetry axis.

The polarized bands at 2996 and 2935  $\text{cm}^{-1}$ , having corresponding parallel-type infrared bands, are taken as the superimposed *a*- and *b*-type asymmetrical and symmetrical methyl stretchings respectively. The polarized band at 2956  $\text{cm}^{-1}$  is taken as the remaining superimposed *a*- and *b*-type asymmetrical methyl stretching mode. Of the pair of intense polarized bands at 2826 and 2841  $\text{cm}^{-1}$ , the former is assigned to the symmetrical  $\text{CH}_2$  stretching mode while the latter is assigned as  $2 \times 1436 \text{ cm}^{-1}$ , the high intensity arising from Fermi resonance with the fundamental. The asymmetrical  $\text{CH}_2$  stretching mode is not obvious but is assigned to the infrared band at 2997  $\text{cm}^{-1}$  coincident with the *a*- and *b*-type methyl asymmetric stretching mode.

The infrared bands at 1473 and 1465  $\text{cm}^{-1}$  are assigned to the two superimposed *a*- and *b*-type asymmetrical methyl bending modes, while the parallel-type band at 1458  $\text{cm}^{-1}$  is taken as the superimposed *a*- and *b*-type symmetrical methyl bending mode. The polarized band at  $\sim 1436 \text{ cm}^{-1}$  is taken as the symmetrical methylene deformation mode while the parallel-type infrared, depolarized Raman band at 1400  $\text{cm}^{-1}$  is assigned to the methylene wagging mode. The Raman band at 1310  $\text{cm}^{-1}$ , though depolarized, is assigned to the methylene twisting vibration. From electronegativity considerations (8), the four methyl rocking modes would be expected to occur around 1150–1240  $\text{cm}^{-1}$  and the four infrared bands observed in this region are assigned accordingly.

The intense parallel-type infrared band at 1148  $\text{cm}^{-1}$  is assigned to the OCO asymmetric stretching mode, and the perpendicular-type infrared band at 937  $\text{cm}^{-1}$  corresponding to a medium intensity polarized Raman band to the symmetric OCO stretching mode. The strong polarized Raman band at 912  $\text{cm}^{-1}$ , having no infrared counterpart, is taken as the symmetric  $\text{CH}_3\text{—O}$  stretching mode. From the geometry of the molecule, this latter vibration can be seen to give rise to only a small change in dipole moment and, hence, only a weak infrared band would be expected, in contrast to the stronger infrared band expected from the OCO symmetrical stretching mode at 937  $\text{cm}^{-1}$ . Of the two strong infrared bands at 1110 and 1042  $\text{cm}^{-1}$ , the former, though it appears to have a possible parallel-type band contour, is taken as the methylene rocking mode from electronegativity considerations (9), while the latter has a hybrid-type contour and is taken as the asymmetrical O— $\text{CH}_3$  stretching mode. The smaller difference in frequency between the two OCO stretching vibrations, as compared with the difference between the two OCO stretching modes, is consistent with the expected smaller coupling constant between the two OCH<sub>3</sub> bonds.

The polarized band at 325  $\text{cm}^{-1}$  is assigned to the type *a* COC bending mode, and the depolarized band at 602  $\text{cm}^{-1}$ , corresponding to a perpendicular-type infrared band, to the type *b* COC bending mode. The perpendicular-type band at 454  $\text{cm}^{-1}$  is taken as the type *a* OCO bending mode. The four torsional vibrations would be expected to have low frequencies ( $< 300 \text{ cm}^{-1}$ ) and were not observed.

1. AOKI, K. J. Chem. Soc. Japan (Pure Chem. Sect.), **74**, 110 (1953); Chem. Abstr. **47**, 5191 (1953).
2. EDSALL, J. T. and WILSON, E. B. J. Chem. Phys. **6**, 124 (1938).
3. GERHARD, S. L. and DENNISON, D. M. Phys. Rev. **43**, 197 (1933).
4. KOHLRAUSCH, K. W. F. and YPSILANTI, P. Z. physik. Chem. B, **32**, 407 (1936).
5. MIZUSHIMA, S., MORINO, Y., and KUBO, M. Physik. Z. **38**, 459 (1937).
6. RANK, D. H. and KAGARISE, R. E. J. Opt. Soc. Am. **40**, 89 (1950).
7. WHITE, J. U., ALPERT, N., and DEBELL, A. G. J. Opt. Soc. Am. **45**, 154 (1955).
8. WILMSHURST, J. K. J. Chem. Phys. **26**, 426 (1957).
9. WILMSHURST, J. K. Can. J. Chem. **35**, 937 (1957).

RECEIVED SEPTEMBER 30, 1957.

DEPARTMENT OF CHEMISTRY,  
AUCKLAND UNIVERSITY COLLEGE,  
AUCKLAND, NEW ZEALAND.



# HELVETICA CHIMICA ACTA

SCHWEIZERISCHE  
CHEMISCHE GESELLSCHAFT  
Verlag Helvetica Chimica Acta  
Basel 7 (Schweiz)

40  
Seit 1918 Jahre

Abonnement: Jahrgang 1958, Vol. XLI \$22.10 incl. Porto

Es sind noch

Neudruck ab Lager

lieferbar:

Vol. I-XIV (1918-1931)

Vol. XVII-XX (1934-1937)

Vol. XV, XVI, XXI-XXV (1932, 1933, 1938-1942) in Vorbereitung.

Originalausgaben, druckfrisch und antiquarisch.

Vol. XXVI-XL (1943-1957)

Diverse Einzelhefte ab Vol. XXI

Preise auf Anfrage. Nur solange Vorrat

Das wissenschaftliche Organ der

SCHWEIZERISCHEN  
CHEMISCHEN  
GESELLSCHAFT

## Recueil des travaux chimiques des Pays-Bas

FONDÉ EN 1882 PAR

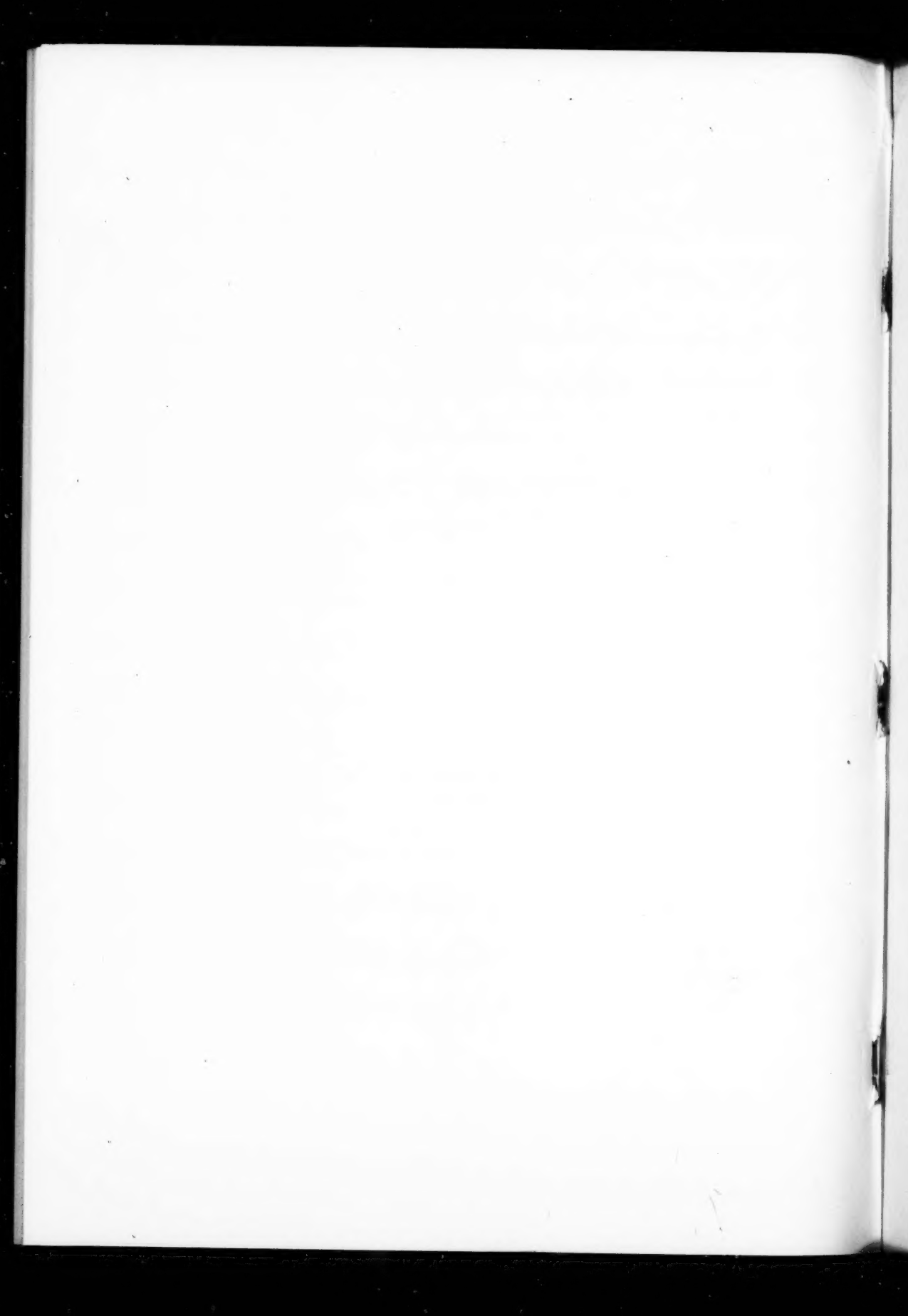
W. A. VAN DORP, A. P. N. FRANCHIMONT, S. HOOGEWERFF,  
E. MULDER ET A. C. OUDEMANS

EDITED BY THE NETHERLANDS CHEMICAL SOCIETY

Generally the "Recueil des travaux chimiques des Pays-Bas" only accepts papers for publication from members of the Dutch Chemical Society who are also subscribers to the Recueil. Applications for membership of this society should be sent to The Secretariate, Lange Voorhout 5, The Hague.

The Recueil contains papers written in English, French or German and appears if possible monthly (the 15th of each month) except in August and September, in issues of varying size. It is obtainable from D. B. Centen's Uitgeversmaatschappij, 1<sup>e</sup> Weteringplantsoen 8, Amsterdam, or through any bookseller in Holland or abroad. The subscription is 30.— guilders for Holland and 32.50 guilders abroad. Authors receive 75 reprints of their papers free of charge.

Editorial Office: Lange Voorhout 5, The Hague.



Hydrogen abstraction reactions of diphenylpicrylhydrazyl— <i>A. G. Brook, R. J. Anderson, and J. Tissot Van Patot</i>	159
The study of hydrogen bonding and related phenomena by ultraviolet light absorption. Part I. Introduction— <i>W. F. Forbes and J. F. Templeton</i>	180
The electric moments of some N,N'-disubstituted piperazines— <i>M. V. George and George F Wright</i>	189
The synthesis of $\omega$ -deoxy- $\omega$ -S-ethyl-polyols— <i>J. K. N. Jones and D. L. Mitchell</i>	206
The relation between the sulphate and nitrogen content of unstabilized cellulose nitrate— <i>Paul E. Gagnon, Karl F. Keirstead, and Brian T. Newbold</i>	212
A contribution to the chemistry of unstabilized cellulose nitrate— <i>Paul E. Gagnon, Karl F. Keirstead, and Brian T. Newbold</i>	215
Ammonolysis of 1,2-epoxycyclohexane and <i>trans</i> -2-bromocyclohexanol— <i>L. R. Hawkins and R. A. B. Bannard</i>	228
The preparation of amines and hydrazo compounds using hydrazine and palladized charcoal— <i>P. M. G. Bavin</i>	238
Triarylmethane compounds as redox indicators in the Schoenemann reaction. III. The dyes and their spectra— <i>G. A. Grant, R. Blanchfield, and D. Morison Smith</i>	242
NOTES	
Long-wavelength limit of photooxidation of butene-1 by nitrogen dioxide— <i>S. Sato and R. J. Cvetanović</i>	279
Ultraviolet irradiation of pyrimidine derivatives. II. Note on the synthesis of the product of reversible photolysis of uracil— <i>A. M. Moore</i>	281
An alternative synthesis of 2-O-methyl-D-xylose— <i>W. D. S. Bowering and T. E. Timell</i>	283
The infrared and Raman spectrum of dimethoxymethane— <i>J. K. Wilmshurst</i>	285

## CONTENTS

	Page
<b>SYMPORIUM ON THE STRUCTURE AND REACTIVITY OF ELECTRONICALLY-EXCITED SPECIES</b>	
A report on a symposium held by the Physical Chemistry Division of the Chemical Institute of Canada— <i>K. J. Laidler and D. A. Ramsay</i>	1
The lower excited states of some simple molecules— <i>R. S. Mulliken</i>	10
Equivalent orbitals and the shapes of excited species— <i>J. W. Linnett</i>	24
The nature of formaldehyde in its low-lying excited states— <i>G. W. Robinson and V. Erdmanis DiGiorgio</i>	31
Excited states of the molecular ions of hydrogen fluoride, hydrogen iodide, water, hydrogen sulphide, and ammonia— <i>D. C. Frost and C. A. McDowell</i>	39
The electronic spectra of crystalline toluene, dibenzyl, diphenylmethane, and biphenyl in the near ultraviolet— <i>Robert Coffman and Donald S. McClure</i>	48
Energy transfer in molecular crystals and in double molecules— <i>Donald S. McClure</i>	59
Diabatic reactions— <i>Henry Eyring, George Stewart, and Ransom B. Partin</i>	72
Reactions involving electronically-excited oxygen— <i>E. Kerry Gill and K. J. Laidler</i>	79
Primary processes in reactions initiated by photoexcited mercury isotopes— <i>Harry E. Gunning</i>	89
Some effects of intramolecular vibrational energy transfer in complex fluorescent molecules— <i>B. Stevens</i>	96
Studies of chemical reactions of excited species using intense light sources— <i>R. A. Marcus</i>	102
Chemiluminescence in the system atomic sodium plus atomic hydrogen— <i>J. D. McKinley, Jr., and J. C. Polanyi</i>	107
The quenching of the iodine fluorescence spectrum— <i>C. Arnot and C. A. McDowell</i>	114
Quenching and vibrational-energy transfer of excited iodine molecules— <i>J. C. Polanyi</i>	121
Excited states of acetylene and their role in pyrolysis— <i>G. J. Minkoff</i>	131
The fluorescence and its relationship to photolysis in hexafluoroacetone vapor— <i>Hideyo Okabe and E. W. R. Steacie</i>	137
<b>PHYSICAL CHEMISTRY</b>	
Exchange between thallous and thallic ions in the presence of sulphate ion— <i>D. R. Wiles</i>	167
The systems $\text{Li}_2\text{SO}_4\text{-K}_2\text{SO}_4\text{-H}_2\text{O}$ and $\text{Li}_2\text{SO}_4\text{-Na}_2\text{SO}_4\text{-H}_2\text{O}$ at 25° C.— <i>A. N. Campbell and E. M. Kartzmark</i>	171
Photolysis of acetone in the presence of methyl-d <sub>4</sub> acetate— <i>M. H. J. Wijnen</i>	176
Critical concentration effects in polymer-polymer-solvent systems— <i>C. G. Bigelow and L. H. Cragg</i>	199
Conformational effects and the influence of pressure on reaction rates— <i>E. Whalley</i>	228
The photochemical oxidation of aldehydes in the gaseous phase. Part I. The kinetics of the photochemical oxidation of acetaldehyde— <i>C. A. McDowell and L. K. Sharples</i>	251
The photochemical oxidation of aldehydes in the gaseous phase. Part II. The kinetics of the photochemical oxidation of propionaldehyde— <i>C. A. McDowell and L. K. Sharples</i>	258
The photochemical oxidation of aldehydes in the gaseous phase. Part III. The absolute values of the velocity constants for the propagating and terminating steps in the photochemical oxidation of acetaldehyde and propionaldehyde— <i>C. A. McDowell and L. K. Sharples</i>	268
<b>ORGANIC CHEMISTRY</b>	
Reaction of amino alcohols with carbon disulphide— <i>A. F. McKay, M. Skulski, and D. L. Garmaise</i>	147
The infrared spectra of malonate esters— <i>R. A. Abramovitch</i>	151

*(Continued on inside)*

